NASA Technical Memorandum 81286

# Experimental Aerodynamic Characteristics of Two V/STOL Fighter/Attack Aircraft Configurations at Mach Numbers From 1.6 to 2.0

Walter P. Nelms, Donald A. Durston, and
J. R. Lummus

May 1981

NASA
National Aeronautics and
Space Administration

NASA Technical Memorandum 81286

# Experimental Aerodynamic Characteristics of Two V/STOL Fighter/Attack Aircraft Configurations at Mach Numbers From 1.6 to 2.0

Walter P. Nelms
Donald A. Durston, Ames Research Center, Moffett Field, California
J. R. Lummus, General Dynamics, Fort Worth Division, Fort Worth, Texas

National Aeronautics and
Space Administration

**Ames Research Center**
Moffett Field, California 94035

TABLE OF CONTENTS


| | Page |
|---|---|
| LIST OF TABLES | v |
| LIST OF FIGURES | vii |
| NOMENCLATURE | xi |
| SUMMARY | 1 |
| INTRODUCTION | 2 |
| TEST FACILITY | 2 |
| MODEL DESCRIPTION | 3 |
| Configuration E205 | 3 |
| Configuration R104 | 3 |
| TEST CONDITIONS AND PROCEDURES | 3 |
| RESULTS AND DISCUSSION | 4 |
| Baseline E205 Configuration | 5 |
| Effects of Alternative Components | 6 |
| Baseline R104 Configuration | 7 |
| Effects of Canard Location | 8 |
| CONCLUDING REMARKS | 8 |
| REFERENCES | 10 |
| TABLES | 11 |
| FIGURES | 16 |

TABULATED DATA (on microfiche — inside back cover)

LIST OF TABLES


| Table | | Page |
|---|---|---|
| 1 | Geometry of the E205 Configuration | 11 |
| 2 | Geometry of the R104 Configuration | 12 |
| 3 | Internal-Force Coefficients of the E205 Configuration | 13 |
| 4 | Internal-Force Coefficients of the R104 Configuration | 13 |
| 5 | Configuration/Run Number Summary | 14 |

LIST OF FIGURES


| Figure | | Page |
|---|---|---|
| 1 | Axis system and sign conventions. | 16 |
| 2 | Details of E205 wind-tunnel model. | 17 |
| | (a) Three-view drawing. | 17 |
| | (b) Wing, canard, and vertical-tail detail. | 18 |
| | (c) Strake options. | 19 |
| | (d) Cross-sectional area distribution. | 20 |
| 3 | Views of E205 model. | 21 |
| | (a) E205 model, R104 body, and components. | 21 |
| | (b) E205 model; top view. | 22 |
| | (c) E205 model; bottom view. | 23 |
| 4 | Details of R104 wind-tunnel model. | 24 |
| | (a) Three-view drawing. | 24 |
| | (b) Wing, canard, and vertical-tail detail. | 25 |
| | (c) Cross-sectional area distribution. | 26 |
| 5 | Views of R104 model. | 27 |
| | (a) R104 model; top view. | 27 |
| | (b) R104 model installed in wind tunnel (front view). | 28 |
| | (c) R104 model installed in wind tunnel (aft view). | 29 |
| 6 | Duct-exit rake installation on E205 model (shown in Ames 11-Foot Wind Tunnel). | 30 |
| 7 | Basic longitudinal characteristics for various Mach numbers. | 31 |
| 8 | Summary of basic longitudinal characteristics with Mach number. | 35 |
| 9-11 | Component buildup, longitudinal characteristics, M = 1.6, 1.8, 2.0. | 41 |
| 12 | Summary of component buildup with Mach number. | 53 |

| Figure | | Page |
|---|---|---|
| 13,14 | Basic lateral/directional characteristics for various alpha, M = 1.6, 2.0. | 59 |
| 15 | Summary of basic lateral/directional characteristics with alpha. | 65 |
| 16 | Lateral/directional characteristics, canard on/off, M = 1.6. | 68 |
| 17-20 | Canard incidence effects, TE-W = 0, 10°, M = 1.6, 2.0. | 71 |
| 21,22 | Flap-deflection effects, canard = 0°, M = 1.6, 2.0. | 87 |
| 23,24 | Vertical-tail deflection effects, longitudinal characteristics, M = 1.6, 2.0. | 95 |
| 25-28 | Vertical-tail deflection effects, lateral/directional characteristics, alpha = 0, 8°, M = 1.6, 2.0. | 103 |
| 29-34 | Canard location effects, longitudinal characteristics, canard = 0°; Strakes $S_1$, $S_2$, $S_3$; M = 1.6, 2.0. | 115 |
| 35-38 | Canard location effects, lateral/directional characteristics, alpha = 0, 8°, M = 1.6, 2.0. | 139 |
| 39,40 | Strake variations, longitudinal characteristics, M = 1.6, 2.0. | 151 |
| 41-44 | Strake variations, lateral/directional characteristics, alpha = 0, 8°, M = 1.6, 2.0. | 159 |
| 45 | Basic longitudinal characteristics for various Mach numbers. | 171 |
| 46 | Summary of basic longitudinal characteristics with Mach numbers. | 175 |
| 47-49 | Component buildup, longitudinal characteristics, M = 1.6, 1.8, 2.0. | 181 |
| 50 | Summary of component buildup with Mach number. | 193 |
| 51,52 | Basic lateral/directional characteristics for various alpha, M = 1.6, 2.0. | 199 |
| 53 | Summary of basic lateral/directional characteristics with alpha. | 205 |
| 54-57 | Vertical tail on/off, lateral/directional characteristics, alpha = 0, 8°, M = 1.6, 2.0. | 208 |

| Figure | | Page |
|---|---|---|
| 58,59 | Lateral/directional characteristics, canard on/off, M = 1.6, 2.0. | 220 |
| 60-65 | Canard incidence effects, TE-W = 0, 10°, M = 1.6, 1.8, 2.0. | 226 |
| 66-68 | Flap deflection effects, canard = 0°, M = 1.6, 1.8, 2.0. | 250 |
| 69,70 | Canard location effects, longitudinal characteristics, M = 1.6, 2.0. | 262 |
| 71-74 | Canard location effects, lateral/directional characteristics, alpha = 0, 8°, M = 1.6, 2.0. | 270 |

## NOMENCLATURE

The axis system and sign conventions are shown in figure 1. The longitudinal characteristics are presented in the stability-axis coordinate system and the lateral/directional characteristics are presented in the body-axis coordinate system. Dimensional units are given in the geometry tables and figures where appropriate.

| | |
|---|---|
| A | aspect ratio |
| A.C. | aerodynamic center |
| B.L. | buttockline, spanwise distance from model centerline |
| b | wing span |
| $C_A$ | axial-force coefficient |
| $C_{A_{INT}}$ | internal (duct) axial-force coefficient |
| $C_C$ | side-force coefficient, wind axes |
| $C_D$ | drag coefficient, drag/qS |
| $C_L$ | lift coefficient, lift/qS |
| $C_{L_\alpha}$ | lift-curve slope |
| $C_\ell$ | rolling-moment coefficient, rolling moment/qSb |
| $C_{\ell_\beta}$ | lateral stability derivative |
| $C_m$ | pitching-moment coefficient, pitching moment/$qS\bar{c}$ |
| $C_{m_{CL=0}}$ | zero-lift pitching moment |
| $C_N$ | normal-force coefficient |
| $C_{N_{INT}}$ | internal (duct) normal-force coefficient |
| $C_n$ | yawing-moment coefficient, yawing moment/qSb |
| $C_{n_\beta}$ | directional-stability derivative |
| $C_R$ | root chord |
| $C_T$ | tip chord |
| $C_Y$ | side-force coefficient, side force/qS |

$C_{Y_\beta}$ side-force derivative

$\bar{c}$ wing mean aerodynamic chord

F.S. fuselage station

H.L. hinge line

L/D lift-drag ratio

M free-stream Mach number

q dynamic pressure

Re/$\ell$ unit Reynolds number

S wing area

S.S. span station

W.L. waterline, vertical distance from model centerline

$\alpha$ angle of attack

$\beta$ angle of sideslip

$\Lambda$ sweep angle

$\psi$ angle of yaw

Subscripts:

MAX maximum

MIN minimum

## Configuration Code

Note: Since there were no strake options on the RALS configuration, body $B_2$ includes both body and strake.

| Component | Ejector | RALS |
|---|---|---|
| Body | $B_1$ | $B_2$ |
| Strake | | |
| Baseline | $S_1$ | |
| High sweep | $S_2$ | |
| Off | $S_3$ | |
| Nacelles | N | N |
| Wing | $W_1$ | $W_2$ |
| Canard | | |
| Mid (baseline) | $C_1$ | $C_1$ |
| Forward | $C_2$ | $C_2$ |
| Aft | $C_3$ | $C_3$ |
| Vertical tail and dorsal | V | V |

Flap deflection and incidence of all movable surfaces (common to both configurations):

| | Wing | Canard | Vertical tail |
|---|---|---|---|
| Leading-edge flap | LE-W | LE-C | --- |
| Trailing-edge flap | TE-W | TE-C | --- |
| Incidence (of all movable surfaces) | --- | Canard | Vertical |

# EXPERIMENTAL AERODYNAMIC CHARACTERISTICS OF TWO V/STOL FIGHTER/ATTACK AIRCRAFT CONFIGURATIONS AT MACH NUMBERS FROM 1.6 TO 2.0

Walter P. Nelms and Donald A. Durston
Ames Research Center

and

J. R. Lummus
General Dynamics, Fort Worth Division

## SUMMARY

A wind-tunnel test was conducted at Ames Research Center to measure the aerodynamic characteristics of two horizontal-attitude takeoff and landing V/STOL fighter/attack aircraft concepts. The concepts were developed by the General Dynamics Corporation, Fort Worth Division, during a contract study for Ames and the David Taylor Naval Ship Research and Development Center (DTNSRDC). One aircraft concept used an ejector to provide propulsive lift; the other concept used separately ducted and heated fan air to provide propulsive lift (remote-augmentation-lift system (RALS)). Neither of these propulsive-lift devices was simulated during the tests reported herein. The tests did investigate the aerodynamic uncertainties for these concepts for a Mach number range from 0.2 to 2.0. The present report covers tests conducted in the Ames 9- by 7-Foot Supersonic Wind Tunnel for Mach numbers from 1.6 to 2.0.

The test results show the effects of varying the angle of attack (-4° to 17°), angle of sideslip (-4° to +8°), Mach number, and configuration buildup. In addition, the effects of wing trailing-edge flap deflections, canard incidence, and vertical-tail deflections are presented. The effects of varying the canard longitudinal location and the shapes of the inboard nacelle-body strakes were also investigated.

For the supersonic Mach numbers of the test, both configurations generated good lift characteristics (values of $C_L$ from 0.8 to over 1.0) for the test angle-of-attack limits (about 15° to 17°). The canard was instrumental in achieving these high lift coefficients, and from this standpoint, the forward canard was the best of the three longitudinal locations. Within the range of canard and wing trailing-edge flap deflections considered in the test, the ejector configuration could be trimmed to angles of attack of about 11° to 15° (depending on Mach number), with the maximum trimmed angles of the RALS model being somewhat less.

The ejector configuration was essentially neutrally stable at these supersonic speeds, with the aerodynamic center varying from about +0.2 to -2.6 percent of the mean aerodynamic chord; the variation depended on Mach number.

In comparison, the RALS configuration was about 5 to 7 percent less stable at these same conditions. Longitudinal stability was increased for the ejector concept by an aft movement of the canard and by a reduction in the planform size of the inboard strakes. As for the ejector configuration, the aft canard position was the most stable for the RALS configuration.

## INTRODUCTION

Ames Research Center has a number of research programs under way to develop aerodynamic and aerodynamic-propulsion integration technology for V/STOL fighter/attack aircraft of the post-1990 time period. One of these programs was a contract study that was jointly sponsored with the David Taylor Naval Ship Research and Development Center and the Naval Air Systems Command. In Phase I of the program, four contractors provided conceptual designs, estimated the aerodynamics of the designs, identified aerodynamic uncertainties of the concepts, and proposed a wind-tunnel program to explore these uncertainties. References 1 through 5 give the detailed results of this Phase I effort, and reference 6 presents a summary of these studies and of several other related programs at Ames. In Phase II of the program, two contractors designed and built wind-tunnel models for tests in the Ames Unitary and 12-Foot Wind Tunnels; the tests covered a Mach number range from 0.2 to 2.0.

This report presents the results of supersonic tests of two models designed and built in Phase II of the contracted program by the General Dynamics Corporation (ref. 1). Both configurations investigated were horizontal-attitude takeoff and landing V/STOL fighter/attack aircraft. One model is a representation of a V/STOL fighter aircraft employing a jet diffuser ejector for its propulsive lift system (identified as configuration E205); the other model (configuration R104) represents an aircraft featuring engine air ducting to a forward combustor and nozzles (remote-augmentation-lift system (RALS)).

The experimental investigation documented in this report was conducted in the Ames 9- by 7-Foot Supersonic Wind Tunnel for a Mach number range from 1.6 to 2.0. The Reynolds number was held constant at $9.84\times10^6$/m ($3.0\times10^6$/ft). The angle of attack was varied up to approximately 17°, and angles of sideslip ranged from -4° to +8°. Model variations investigated included component buildup, canard longitudinal location, inboard-strake shape, and deflections of the canard, wing trailing-edge flaps, and vertical tail.

## TEST FACILITY

The tests were conducted in the Ames 9- by 7-Foot Supersonic Wind Tunnel, which is a variable-density, closed-circuit, continuous-flow facility. This tunnel has an asymmetric, sliding-block nozzle that translates in the streamwise direction to permit testing over a Mach number range that is continuously variable from 1.55 to 2.5. Models are sting-supported in a wings-vertical attitude in this tunnel.

## MODEL DESCRIPTION

Both models tested represent 9.39-percent scaled versions of the conceptual aircraft described in reference 1.

### Configuration E205

A three-view drawing of the wind-tunnel model simulating a V/STOL fighter with a jet-diffuser ejector vertical-lift system (model E205) is shown in figure 2(a). Pertinent dimensions, areas, and other parameters are presented in table 1 and in figures 2(b) and 2(c). Figure 2(d) gives a cross-sectional area distribution of the wind-tunnel model. Photographs of the model and its installation in the wind tunnel are shown in figure 3.

Parametric variations available on the model (not all were investigated in the present test) included: component buildup, variable-wing outboard and inboard trailing-edge flaps, variable-wing leading-edge flaps, a variable incidence canard with variable leading- and trailing-edge flaps, three longitudinal canard locations, three inboard nacelle-body-strake shapes, and an all-movable vertical tail. The term "baseline configuration" as used herein refers to the model with the mid-canard location (fig. 2(a)) and the baseline strake ($S_1$ in fig. 2(c)).

### Configuration R104

Figure 4(a) presents a three-view drawing of the wind-tunnel model representing a V/STOL fighter employing a RALS for vertical lift. Pertinent dimensions, areas, and other parameters are given in table 2 and figure 4(b). Figure 4(c) gives a cross-sectional area distribution of the wind-tunnel model. Photographs of the model and the model installed in the wind tunnel are presented in figure 5.

The parametric variations on the R104 configuration were the same as on the E205 model except that only one inboard nacelle-body-strake shape was available. The baseline configuration again has the mid-canard location (fig. 4(a)).

## TEST CONDITIONS AND PROCEDURES

Tests were conducted at Mach numbers 1.6, 1.8, and 2.0 at a constant unit Reynolds number of $9.84\times10^6$/m ($3.0\times10^6$/ft). The angle of attack was varied up to approximately 17°, and angle of sideslip ranged from -4° to +8°. The angle of attack was corrected for wind-tunnel flow misalignment and for balance and sting deflections caused by aerodynamic loads.

The models were sting-supported through the base of the fuselage body on a 6.35-cm (2.5 in.) six-component strain-gage balance. The moment reference center for both models was located longitudinally at 3 percent of the mean aerodynamic chord, which represents a fuselage station of 0.737 m (29.002 in.) on the E205 model and a fuselage station of 0.748 m (29.463 in.) on the R104 model. Measured axial forces have been adjusted to a condition corresponding to that of having free-stream static pressure acting on the fuselage cavity and on the base areas of the two nacelle choke plugs.

The data presented in this report have been adjusted for internal forces acting in the flow-through nacelles. These internal axial and normal forces were derived from a series of runs employing a duct-exit rake in both nacelles. These rakes, each with 20 total head tubes, were calibrated prior to the test against known mass flows measured by standard ASME nozzles. The duct-exit static pressures were measured during the internal flow survey by using a series of orifices located around the periphery of the nacelle choke plugs. For these tests in the 9- by 7-Foot Wind Tunnel, the rake installation was similar to that shown in figure 6, which is a photograph from the 11-Foot Wind-Tunnel tests. The resulting internal-force coefficients that have been applied to the data are presented in table 3 (E205) and table 4 (R104) as a function of Mach number and angle of attack.

In order to assure an all-turbulent boundary layer, transition strips consisting of a random distribution of 0.0246- to 0.0295-cm (0.0097- to 0.0116-in.) sieved glass spheres were placed near the leading edges of the wing, canard, and vertical tail, around the fuselage nose, and around the nacelle leading edges. Past experience in the 9- by 7-Foot Wind Tunnel indicated that this grit size was appropriate to provide a turbulent boundary layer on the model at the conditions of the test while not producing drag associated with the grit.

## RESULTS AND DISCUSSION

Experimental aerodynamic data for the two models are presented in figures 7 through 74. The results for the E205 model are shown in figures 7 through 44 and the results for the R104 model are presented in figures 45 through 74.

In addition, complete tabulated data are provided on microfiche (affixed to the inside back cover), and a run-number summary is provided in table 5 to correlate the plotted figures with the data listings.

In order to expedite publication of the data, a minimal description of the test results is presented in the following sections. An in-depth analysis of the data and comparisons with theoretical estimates are reported in reference 7. Experimental results for these models at Mach numbers from 0.4 to 1.4 are given in reference 8. Reference 9 presents a summary of some selected results over the complete Mach number range.

## Baseline E205 Configuration

*Longitudinal characteristics (zero deflection on all control surfaces)*- The effect of Mach number on the longitudinal characteristics of the baseline configuration is presented in figure 7 for Mach numbers 1.6, 1.8, and 2.0. These data are summarized in figure 8. As may be expected, the results show that with increasing supersonic Mach number there is a reduction in minimum drag and lift-curve slope and a forward movement of the aerodynamic center. The configuration is essentially neutrally stable at these speeds, with the aerodynamic center varying from about +0.2 to -2.6 percent of the mean aerodynamic chord.

Longitudinal aerodynamic characteristics resulting from model component buildup are presented in figures 9 through 11 for Mach numbers 1.6, 1.8, and 2.0; a summary with Mach number is given in figure 12. The complete baseline configuration generated relatively high lift coefficients (values of $C_L$ up to 1.2 at $M = 1.6$), and even the body/nacelle alone produced values of about half that amount ($C_L = 0.6$ at $M = 1.6$). Adding the canard improved the lift and the drag due to lift. The effects of component buildup on the pitching-moment coefficient were essentially as would be expected when lifting areas are located fore and aft of the moment reference center.

*Lateral/directional characteristics*- Figures 13 and 14 show the lateral/directional aerodynamic characteristics at various angles of attack for the baseline configuration; a summary with angle of attack is given in figure 15. The model produced positive directional stability ($+C_{n_\beta}$) at angles of attack up to about 6.5° for $M = 1.6$ and 10.5° for $M = 2.0$. The effective dihedral is positive ($-C_{\ell_\beta}$) at essentially all angles of attack, as shown in figure 15. Canard on-and-off effects on the lateral/directional characteristics of the baseline configuration are shown in figure 16 for Mach number 1.6 at two angles of attack.

*Trim characteristics*- Figures 17 through 20 present the trim characteristics of the baseline configuration. Canard-incidence variations (0°, ±10°) and canard-off are shown for two wing trailing-edge flap deflections (0°, 10°) at Mach numbers 1.6 and 2.0. For these runs, the wing outboard and inboard trailing-edge flaps were deflected as a unit. Although possible, tests were not run for a canard incidence of +20° and wing trailing-edge flap deflections of 20° and 25°. Likewise, the effects on trim of canard leading- and trailing-edge flap deflections and wing leading-edge flap deflections (all available on the model) were not investigated during this tunnel entry because of time limitations.

Figures 21 and 22 present some of the previous data replotted to show the effectiveness of the trailing-edge flap as a trimming device. The longitudinal aerodynamic characteristics are shown for two flap deflections (0°, 10°) with zero canard incidence at Mach numbers 1.6 and 2.0.

The results of the trim investigation indicate that the configuration could be trimmed over a wide range of angle of attack by using a combination of wing trailing-edge flap deflection and canard incidence.

*Vertical-tail effects*- The longitudinal and lateral/directional aerodynamic characteristics resulting from deflection of the vertical tail are presented in figures 23 through 28 for Mach numbers 1.6 and 2.0. The 5° vertical-tail deflection had essentially no effect on the longitudinal characteristics (figs. 23 and 24), but the 15° deflection produced a significant increase in drag, a reduction in L/D, and a nose-up pitching moment.

The lateral/directional characteristics are shown in figures 25 through 28 for vertical tail off and deflections of 0°, 5°, and 15° at two angles of attack for each Mach number. The results indicate that deflecting the vertical tail was effective in producing significant control forces over the angle-of-attack and angle-of-sideslip ranges of the test.

It should be noted that when the angle of attack is given in a figure title the value given is nominal; more accurate values (to within ±0.5°) are in the headers at the top of each plot page.

## Effects of Alternative Components

*Canard-location effects*- The effect on the longitudinal aerodynamic characteristics of varying the canard longitudinal location (see fig. 2(a) for positions) is given in figures 29 through 34. Data are presented for zero canard deflection at Mach numbers 1.6 and 2.0 for each of the three strake options (baseline, high-sweep, and "off," as shown in fig. 2(c)). For all strakes at both Mach numbers, the forward canard ($C_2$) gave the highest values of $C_L$ at the higher angles of attack and the lowest values of $C_D$ at a given $C_L$. However, this same canard position accounted for the greater instability in all cases. The aft canard produced the lower lift, but it gave the better longitudinal stability.

Lateral/directional characteristics are shown in figures 35 through 38 at two angles of attack for Mach numbers 1.6 and 2.0. At Mach 1.6, the aft canard ($C_3$) generally gives the greater directional stability up to $\alpha = 8°$, and it also gives a slightly higher lateral stability. However, at Mach 2.0, the three canard positions exhibit differences in the lateral/directional characteristics that vary with Mach number and angle of attack.

*Strake effects*- The longitudinal aerodynamic characteristics due to the strake variations on the model (fig. 2(c)) are presented in figures 39 and 40 for Mach numbers of 1.6 and 2.0. The canard was held at the mid-position at an incidence of 0° for these plots. The model with the baseline strake has a greater L/D than the models with high-sweep strake or strake "off," but this model also experiences more longitudinal instability, primarily because the forward planform area of the baseline strake is greater (see fig. 2(c)). Thus the model with the baseline strake incurs a penalty in pitching moment.

The lateral/directional characteristics for the strake variations are plotted in figures 41 through 44 in a sequence similar to that for the canard-location effects. At these Mach numbers and angles of attack there are some slight differences in the lateral/directional characteristics, but no particular trends are evident among the three strake options.

## Baseline R104 Configuration

*Longitudinal characteristics (zero deflection on all control surfaces)*- The effect of Mach number (1.6, 1.8, and 2.0) on the longitudinal characteristics of the baseline configuration is presented in figure 45 and summary data are given in figure 46. In general, the results are similar to those previously discussed for the E205 configuration with the following notable differences: The E205 model has a slightly higher lift-curve slope, a lower minimum drag, and a somewhat higher maximum L/D. (Compare figs. 8 and 46.) Also, the aerodynamic center tends to be about 5- to 7-percent farther forward on the R104 configuration, depending on the Mach number.

Longitudinal aerodynamic characteristics resulting from model-component buildup are shown in figures 47 through 49, and figure 50 presents a summary of these data with Mach number. A canard-on with wing-off configuration was added to this series of runs; this configuration was not tested on the E205 model. The results are similar to those for the E205 configuration except for the aforementioned differences. (Compare figs. 47-49 with figs. 9-12.)

*Lateral/directional characteristics*- Figures 51 and 52 show the lateral/directional aerodynamic characteristics at various angles of attack for the baseline configuration at Mach numbers 1.6 and 2.0; figure 53 presents a summary of these data with angle of attack. The results are similar to those for the E205 configuration (figs. 13-15) except that at both Mach numbers the E205 model exhibited positive directional stability to a higher angle of attack. However, the R104 configuration gave slightly larger values of positive effective dihedral ($-C_{\ell_\beta}$) at both Mach numbers. (Compare figs. 53 and 15.)

The lateral/directional characteristics for vertical-tail on and off are shown in figures 54 through 57 for two angles of attack at Mach numbers 1.6 and 2.0. Canard-off effects on the lateral/directional characteristics of the baseline R104 configuration are shown in figures 58 and 59 for Mach numbers 1.6 and 2.0, respectively, for two angles of attack.

*Trim characteristics*- Figures 60 through 65 present the trim characteristics of the baseline R104 configuration using canard incidence and wing trailing-edge flap deflections. Results are shown for three canard incidences (0°, ±10°) and canard off for two wing trailing-edge flap deflections (0° and 10°) at Mach numbers 1.6, 1.8, and 2.0. It should be noted that results for Mach 1.8 were not obtained during tests of the E205 model. With the exception of the results for zero-trailing-edge flap deflection at $M = 2.0$, test results show that the E205 model could generally be trimmed to higher values of $C_L$ than could the R104 model. (Compare figs. 60-65 with figs. 17-20.) Of the two models, the R104 model had the greater level of instability, as previously indicated.

Figures 66 through 68 show the effectiveness of the wing trailing-edge flap as a trimming surface with canard incidence of zero. The results are for Mach numbers 1.6, 1.8, and 2.0. (Again results for $M = 1.8$ were not obtained on the E205 model.) Comparing these figures with figures 21 and 22

reveals that the E205 model can be trimmed to a higher $C_L$ than the R104 model with the same flap setting.

### Effects of Canard Location

Figures 69 and 70 present the longitudinal aerodynamic effects of moving the canard forward and aft of the baseline mid-location (see fig. 4(a) for positions). The results are shown for Mach numbers 1.6 and 2.0 with all control surfaces at zero deflection. For both Mach numbers, the forward canard ($C_2$) gave the highest values of $C_L$ at the higher angles of attack and the aft canard ($C_3$) produced the lowest values. This result is consistent with the results from the E205 configuration (see figs. 29 and 32). The most notable effect of canard longitudinal location was the effect on stability: An aft movement of the canard increased the stability of the model at all Mach numbers. This result also is consistent with the results for the E205 model.

The effect of canard location on the lateral/directional characteristics is shown in figures 71 through 74 for Mach numbers 1.6 and 2.0 at two angles of attack. The trends shown are similar to those obtained on the E205 configuration (see figs. 35-38).

## CONCLUDING REMARKS

Tests were conducted in the Ames 9- by 7-Foot Supersonic Wind Tunnel for Mach numbers from 1.6 to 2.0 on two models representative of V/STOL fighter/attack aircraft configurations. Both were horizontal-attitude takeoff and landing concepts developed under contract by the General Dynamics Corporation. The concepts differed in their approach to propulsive lift, one featuring a jet-diffuser ejector system for vertical lift and the other employing a remote-augmentation-lift system (RALS).

Detailed effects of varying angle of attack (up to 17°), angle of sideslip (-4° to +8°), Mach number, and configuration buildup were investigated. In addition, the effects of wing trailing-edge flap deflections, canard incidence, and vertical-tail deflections were explored. Three canard longitudinal locations and different shapes of the inboard nacelle-body strakes were also investigated. Results from these tests indicated the following:

1. Both configurations produced high lift coefficients (values of $C_L$ from 0.8 to over 1.0 depending on Mach number) at the test angle-of-attack limits of about 15° to 17°.

2. Addition of the canard increased lift coefficients and improved the drag polars at high angles of attack, but it also increased the instability of both configurations.

3. The forward-canard location produced the higher lift coefficients and the aft position gave the lower values.

4. Within the range of canard and wing trailing-edge flap deflections considered in the test, the ejector concept could be trimmed to an angle of attack of about 11° at Mach 1.6 and 15° at Mach 2.0. These trimmed angles of attack were somewhat less for the RALS configuration.

5. The ejector configuration was essentially neutrally stable with the aerodynamic center varying from about +0.2 percent of the mean aerodynamic chord at Mach 1.6 to -2.6 percent at Mach 2.0. In comparison, the RALS model was about 5 to 7 percent less stable for these same conditions.

6. For the ejector configuration, longitudinal stability was increased by an aft movement of the canard and by a reduction in the planform size of the inboard strakes. The aft-canard location also produced the greater longitudinal stability on the RALS model.

7. The ejector configuration had a positive directional stability to an angle of attack of about 6.5° at Mach 1.6 and about 10.5° at Mach 2.0. These angles were slightly less for the RALS configuration.

## REFERENCES


1. Lummus, J. R.: Study of Aerodynamic Technology for VSTOL Fighter/Attack Aircraft. NASA CR-152128, May 1978.

2. Burhans, W. R.: Study of Aerodynamic Technology for VSTOL Fighter/Attack Aircraft. NASA CR-152129, May 1978.

3. Brown, S. H.: Study of Aerodynamic Technology for VSTOL Fighter/Attack Aircraft — Horizontal Attitude Concept. NASA CR-152130, May 1978.

4. Gerhardt, H. A.; and Chen, W. S.: Study of Aerodynamic Technology for VSTOL Fighter/Attack Aircraft — Vertical Attitude Concept. NASA CR-152131, May 1978.

5. Driggers, H. H.: Study of Aerodynamic Technology for VSTOL Fighter/Attack Aircraft. NASA CR-152132, May 1978.

6. Nelms, W. P.: Studies of Aerodynamic Technology for V/STOL Fighter/Attack Aircraft. AIAA Paper 78-1511, Aug. 1978.

7. Lummus, J. R.; Joyce, G. T.; and O'Malley, C. D.: Analysis of Wind Tunnel Test Results for a 9.39-Percent Scale Model of a V/STOL Fighter/Attack Aircraft. NASA CR-152391, Vols. 1-4, Jan. 1981.

8. Nelms, W. P.; Durston, D. A.; and Lummus, J. R.: Experimental Aerodynamic Characteristics of Two V/STOL Fighter/Attack Aircraft Configurations at Mach Numbers From 0.4 to 1.4. NASA TM-81234, Dec. 1980.

9. Nelms, W. P.; and Durston, D. A.: Preliminary Aerodynamic Characteristics of Several Advanced V/STOL Fighter/Attack Aircraft Concepts. SAE Paper 801178, Oct. 1980.

TABLE 1.- GEOMETRY OF E205 CONFIGURATION

| | Wing | Horizontal canard (mid-position) | Vertical tail |
|---|---|---|---|
| Airfoil at | | | |
| $C_R$ | NACA-64A204 | NACA-64A005 | 5.3% biconvex |
| $C_T$ | NACA-64A204 | NACA-64A003 | 4.0% biconvex |
| Theoretical area, $m^2$ ($ft^2$) | 0.315 (3.3858) | 0.0315 (0.3390)[a] | 0.0389 (0.4188) |
| MAC,[b] m (in.) | 0.340 (13.398) | 0.183 (7.197) | 0.184 (7.256) |
| Aspect ratio | 3.62 | 1.08[a] | 1.27 |
| Taper ratio | 0.190 | 0.37 | 0.43 |
| Root chord, m (in.) | 0.495 (19.505) | 0.249 (9.815) | 0.245 (9.638) |
| Tip chord, m (in.) | 0.094 (3.706) | 0.092 (3.631) | 0.105 (4.144) |
| Span, m (in.) | 1.067 (42.010) | 0.184 (7.261) | 0.222 (8.751) |
| Dihedral, deg | 0 | 0 | — |
| Incidence, deg | 0 | — | — |
| Hinge line at | | | |
| B.L. | — | 0.228 (8.996) | 0 |
| F.S. | — | 0.620 (24.414) | 1.252 (49.297) |
| W.L. | — | 0.396 (15.587) | 0.403 (15.869) |
| Hinge-line sweep, deg | — | -1°46' | 0 |
| Leading-edge sweep, deg | 40 | 45 | 47°30' |
| Trailing-edge sweep, deg | 4°58' | 8°26' | 24°52' |
| Body length, m (in.) | | | |
| 1.526 (60.096) | | | |

[a]Area of one panel.
[b]Mean aerodynamic chord.

TABLE 2.- GEOMETRY OF R104 CONFIGURATION

| | Wing | Horizontal canard (mid-position) | Vertical tail |
|---|---|---|---|
| Airfoil at | | | |
| $C_R$ | NACA-64A204 | NACA-64A005 | 5.3% biconvex |
| $C_T$ | NACA-64A204 | NACA-64A003 | 4.0% biconvex |
| Theoretical area, $m^2$ ($ft^2$) | 0.293 (3.154) | 0.0315 (0.3390)[a] | 0.0389 (0.4188) |
| MAC, m (in.) | 0.330 (12.973) | 0.183 (7.197) | 0.184 (7.256) |
| Aspect ratio | 3.57 | 1.08[a] | 1.27 |
| Taper ratio | 0.1966 | 0.37 | 0.43 |
| Root chord, m (in.) | 0.479 (18.851) | 0.249 (9.815) | 0.254 (9.638) |
| Tip chord, m (in.) | 0.094 (3.706) | 0.092 (3.631) | 0.105 (4.144) |
| Span, m (in.) | 1.023 (40.270) | 0.184 (7.261) | 0.222 (8.751) |
| Dihedral, deg | 0 | 0 | — |
| Incidence, deg | 0 | — | — |
| Hinge line at | | | |
| B.L. | — | 0.206 (8.126) | — |
| F.S. | — | 0.620 (24.414) | 1.247 (49.110) |
| W.L. | — | 0.396 (15.587) | 0.377 (14.836) |
| Hinge-line sweep, deg | — | -1°46' | 0 |
| Leading-edge sweep, deg | 40 | 45 | 47°30' |
| Trailing-edge sweep, deg | 4°58' | 8°26' | 24°52' |
| Body length, m (in.) 1.471 (57.902) | | | |

[a]Area of one panel.

TABLE 3.- INTERNAL-FORCE COEFFICIENTS OF THE E205 CONFIGURATION
(Values are totals of both ducts)

| $\alpha$, deg | M = 1.6 | | M = 1.8 | | M = 2.0 | |
|---|---|---|---|---|---|---|
| | $C_{N_{INT}}$ | $C_{A_{INT}}$ | $C_{N_{INT}}$ | $C_{A_{INT}}$ | $C_{N_{INT}}$ | $C_{A_{INT}}$ |
| -6 | -0.0039 | 0.0022 | -0.0041 | 0.0036 | -0.0044 | 0.0047 |
| -3 | -.0018 | .0021 | -.0019 | .0034 | -.0020 | .0047 |
| 0 | .0005 | .0020 | .0006 | .0032 | .0006 | .0046 |
| 3 | .0030 | .0018 | .0033 | .0030 | .0034 | .0045 |
| 6 | .0054 | .0015 | .0059 | .0028 | .0061 | .0043 |
| 9 | .0078 | .0013 | .0083 | .0025 | .0087 | .0040 |
| 12 | .0100 | .0010 | .0105 | .0022 | .0112 | .0034 |
| 15 | .0117 | .0007 | .0127 | .0017 | .0138 | .0028 |
| 18 | .0123 | .0004 | .0150 | .0010 | .0159 | .0022 |

TABLE 4.- INTERNAL-FORCE COEFFICIENTS OF THE R104 CONFIGURATION
(Values are totals of both ducts)

| $\alpha$, deg | M = 1.6 | | M = 1.8 | | M = 2.0 | |
|---|---|---|---|---|---|---|
| | $C_{N_{INT}}$ | $C_{A_{INT}}$ | $C_{N_{INT}}$ | $C_{A_{INT}}$ | $C_{N_{INT}}$ | $C_{A_{INT}}$ |
| -6 | -0.0042 | 0.0024 | -0.0044 | 0.0039 | -0.0047 | 0.0051 |
| -3 | -.0019 | .0023 | -.0020 | .0037 | -.0022 | .0051 |
| 0 | .0005 | .0022 | .0006 | .0034 | .0006 | .0049 |
| 3 | .0032 | .0019 | .0035 | .0032 | .0037 | .0048 |
| 6 | .0058 | .0016 | .0063 | .0030 | .0066 | .0046 |
| 9 | .0084 | .0014 | .0089 | .0027 | .0093 | .0043 |
| 12 | .0107 | .0011 | .0113 | .0024 | .0120 | .0037 |
| 15 | .0126 | .0008 | .0136 | .0018 | .0148 | .0030 |
| 18 | .0132 | .0004 | .0161 | .0011 | .0171 | .0024 |

TABLE 5.- CONFIGURATION/RUN NUMBER SUMMARY

| Configuration | Wing TE[a] flaps, deg | Canard, deg | Vertical tail, deg | Model | | | Mach numbers | | |
|---|---|---|---|---|---|---|---|---|---|
| | | | | $\alpha$,[b] deg | $\beta$,[b] deg | Re/L | 1.6 | 1.8 | 2.0 |
| Ejector (E205) | | | | | | | | | |
| $B_1S_1NW_1C_1V$ | 0 | 0 | 0 | A | 0 | 3.0 | 630 | 635 | 636 |
| | ↓ | 0 | ↓ | 0 | A | $\times 10^6$ | 631 | | 637 |
| | | 0 | | 4 | A | ↓ | 632 | | 638 |
| | | 0 | | 8 | A | | 633 | | 639 |
| | | 0 | | 12 | A | | 634 | | 640 |
| | | -10 | | A | 0 | | 648 | | 647 |
| | | 10 | | A | 0 | | 646 | | 645 |
| | 10 | 0 | | A | 0 | | 654 | | 653 |
| | 10 | -10 | | A | 0 | | 650 | | 649 |
| | 10 | 10 | | A | 0 | | 652 | | 651 |
| $B_1S_1NW_1C_2V$ | 0 | 0 | | A | 0 | | 660 | | 657 |
| | | | | 0 | A | | 661 | | 658 |
| | | | | 8 | A | | 662 | | 659 |
| $B_1S_1NW_1C_3V$ | | | | A | 0 | | 667 | | 664 |
| | | | | 0 | A | | 668 | | 665 |
| | | | | 8 | A | | 669 | | 666 |
| $B_1S_2NW_1C_1V$ | | | | A | 0 | | 675 | | 672 |
| | | | | 0 | A | | 676 | | 673 |
| | | | | 8 | A | | 677 | | 674 |
| $B_1S_2NW_1C_2V$ | | | | A | 0 | | 679 | | 678 |
| $B_1S_2NW_1C_3V$ | | | | A | 0 | | 671 | | 670 |
| $B_1S_3NW_1C_1V$ | | | | A | 0 | | 701 | | 698 |
| | | | | 0 | A | | 702 | | 699 |
| | | | | 8 | A | | 703 | | 700 |
| $B_1S_3NW_1C_2V$ | | | | A | 0 | | 707 | | 706 |
| $B_1S_3NW_1C_3V$ | | | ↓ | A | 0 | | 705 | | 704 |
| $B_1S_1NW_1C_1V$ | | | 5 | A | 0 | | 687 | | 682 |
| | | | 5 | 0 | A | | 688 | | 683 |
| | | | 5 | 4 | A | | 689 | | 684 |
| | | | 5 | 8 | A | | 690 | | 685 |
| | | | 5 | 12 | A | | 691 | | 686 |
| | | | 15 | A | 0 | | 695 | | 692 |
| | | | 15 | 0 | A | | 696 | | 693 |
| | | ↓ | 15 | 8 | A | | 697 | | 694 |
| $B_1S_1NW_1V$ | | — | 0 | A | 0 | | 623 | 626 | 627 |
| | | — | 0 | 0 | A | | 624 | | |
| | ↓ | — | 0 | 8 | A | | 625 | | |
| | 10 | — | 0 | A | 0 | | 656 | | 655 |
| $B_1S_1NW_1C_1$ | 0 | 0 | — | 0 | A | | 641 | | 643 |
| | 0 | 0 | — | 8 | A | | 642 | | 644 |
| $B_1S_1NC_1V$ | — | 0 | 0 | A | 0 | | 712 | 711 | 710 |
| $B_1S_1NV$ | — | — | 0 | A | 0 | | 715 | 714 | 713 |
| $B_1S_1N$ | — | — | — | A | 0 | ↓ | 718 | 717 | 716 |

TABLE 5.- CONCLUDED

| Configuration | Wing TE[a] flaps, deg | Canard, deg | Vertical tail, deg | Model | | | Mach numbers | | |
|---|---|---|---|---|---|---|---|---|---|
| | | | | $\alpha$,[b] deg | $\beta$,[b] deg | Re/L | 1.6 | 1.8 | 2.0 |
| RALS (R104) | | | | | | | | | |
| $B_2NW_2C_1V$ | 0 | 0 | 0 | B | 0 | 3.0 | 741 | 740 | 735 |
| | ↓ | 0 | ↓ | 0 | A | $\times 10^6$ | 742 | | 736 |
| | | 0 | | 4 | A | ↓ | 743 | | 737 |
| | | 0 | | 8 | A | | 744 | | 738 |
| | | 0 | | 10 | A | | 745 | | 739 |
| | | -10 | | B | 0 | | 756 | 755 | 754 |
| | | 10 | | B | 0 | | 753 | 752 | 751 |
| $B_2NW_2C_1V$ | 10 | -10 | | B | 0 | | 759 | 758 | 757 |
| | 10 | 0 | | B | 0 | | 765 | 764 | 763 |
| | 10 | 10 | | B | 0 | | 762 | 761 | 760 |
| $B_2NW_2C_2V$ | 0 | 0 | | B | 0 | | 772 | | 769 |
| | ↓ | 0 | | 0 | A | | 773 | | 770 |
| | | 0 | | 8 | A | | 774 | | 771 |
| | | -10 | | B | 0 | | 778 | | 777 |
| | | 10 | | B | 0 | | 776 | | 775 |
| $B_2NW_2C_3V$ | | 0 | | B | 0 | | 782 | | 779 |
| | | 0 | | 0 | A | | 783 | | 780 |
| | | 0 | | 8 | A | | 784 | | 781 |
| | | -10 | | B | 0 | | 788 | | 787 |
| | | 10 | | B | 0 | | 786 | | 785 |
| $B_2NW_2V$ | | — | | B | 0 | | 732 | 731 | 728 |
| | | — | | 0 | A | | 733 | | 729 |
| | ↓ | — | | 8 | A | | 734 | | 730 |
| | 10 | — | ↓ | B | 0 | | 768 | 767 | 766 |
| $B_2NW_2C_1$ | 0 | 0 | — | 0 | A | | 749 | | 747 |
| | 0 | 0 | — | 8 | A | | 750 | | 748 |
| $B_2NC_1V$ | — | 0 | 0 | B | 0 | | 727 | 726 | 725 |
| $B_2NV$ | — | — | 0 | B | 0 | | 724 | 723 | 722 |
| $B_2N$ | — | — | — | B | 0 | ↓ | 721 | 720 | 719 |

[a]Trailing edge.
[b]Schedules A: $-4° \leq \alpha \leq 15°$ at 2° increments; $-4° \leq \beta \leq 8°$ at 2° increments.
Schedules B: $-4° \leq \alpha \leq 13°$ at 2° increments.

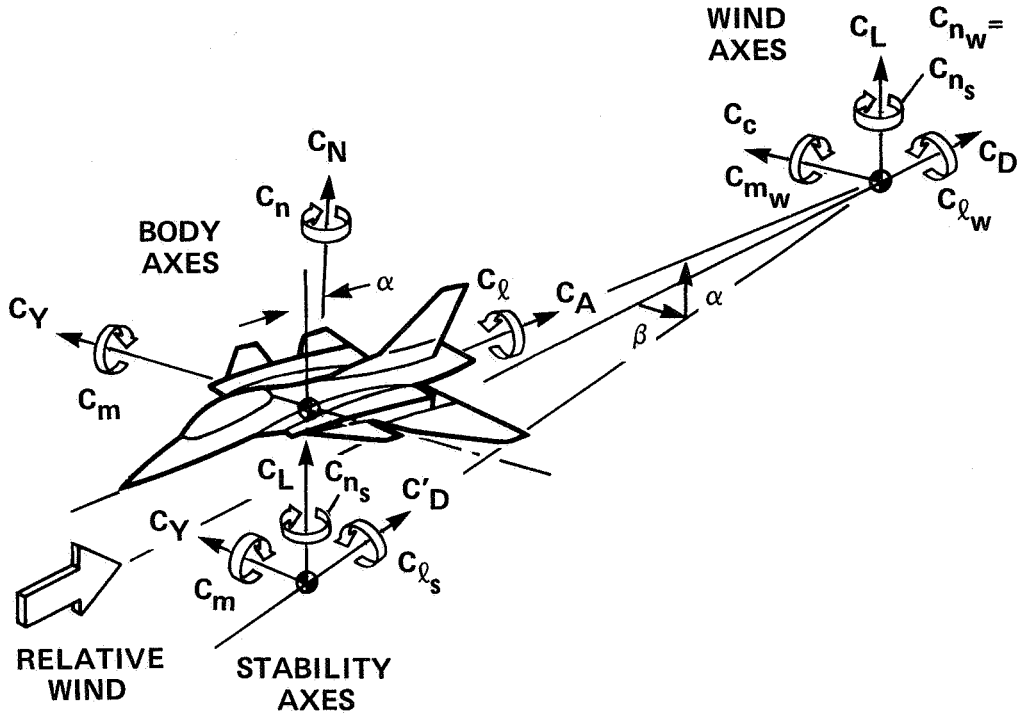


NOTE:

1. POSITIVE VALUES OF FORCE AND MOMENT COEFFICIENTS AND ANGLES ARE INDICATED.
2. ORIGINS OF WIND AND STABILITY AXES HAVE BEEN DISPLACED FROM CENTER OF GRAVITY FOR CLARITY.

$+\beta$ (SIDESLIP) = $-\psi$ (YAW)

Figure 1.- Axis system and sign conventions.

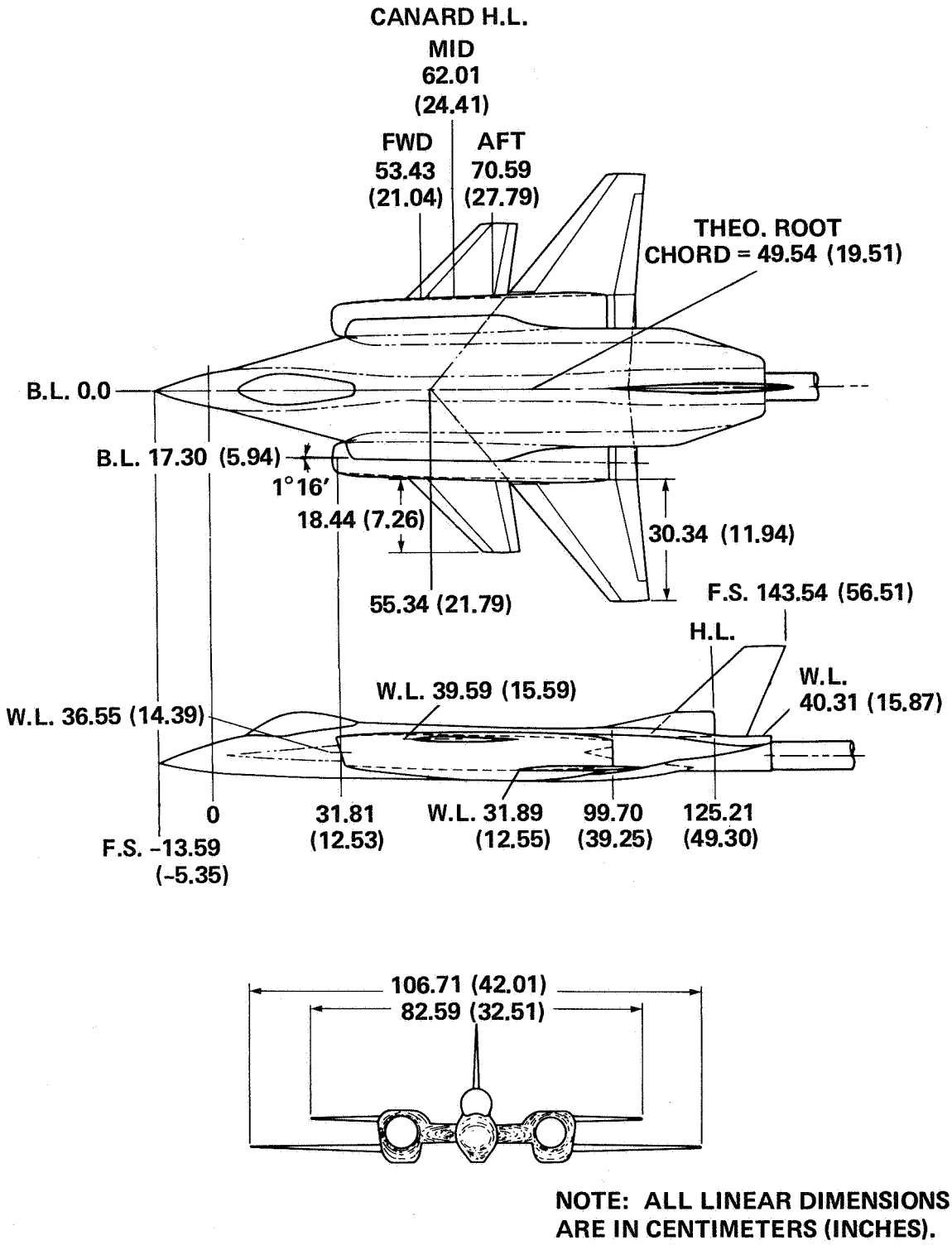


(a) Three-view drawing.

Figure 2.- Details of the E205 wind-tunnel model.

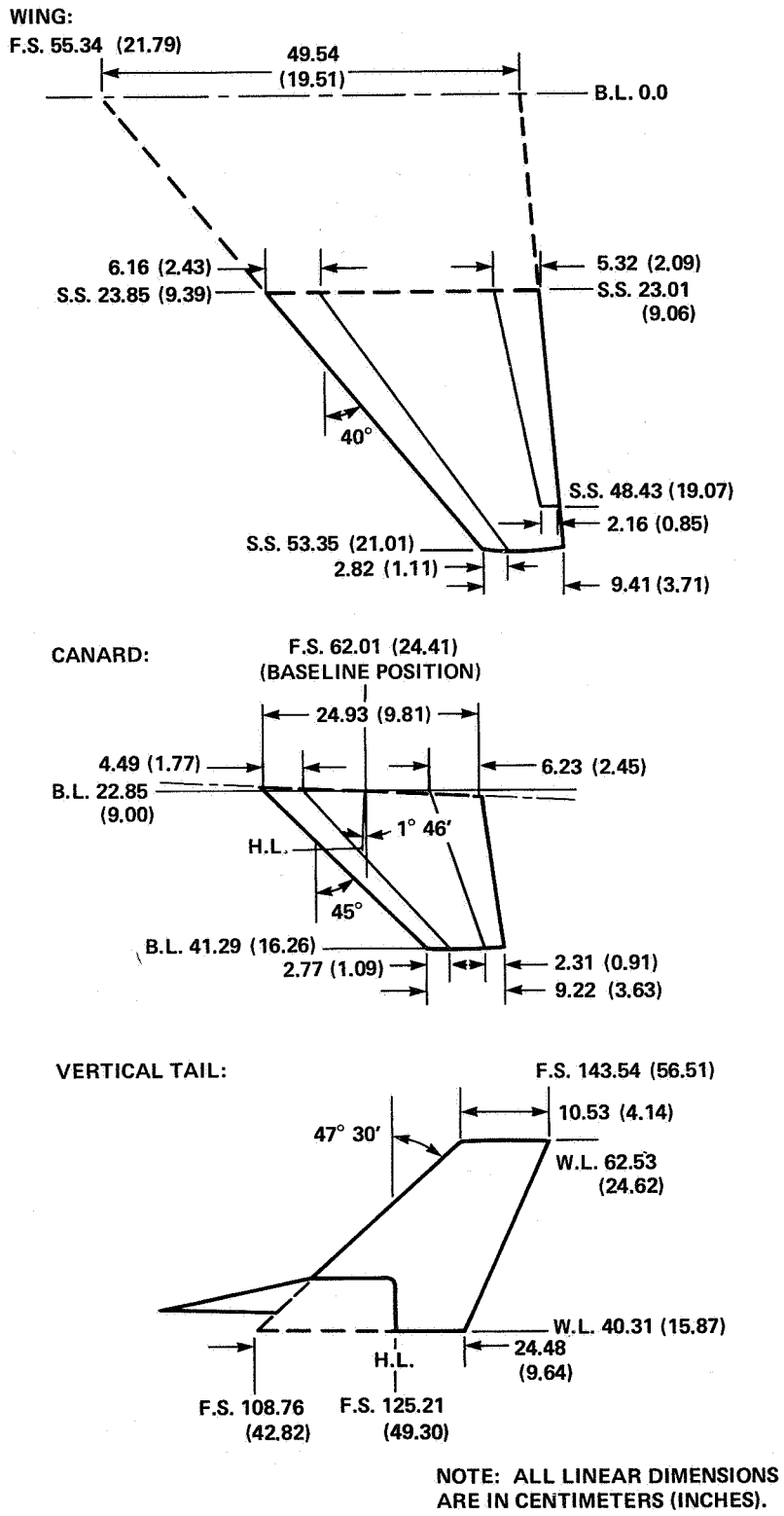


(b) Wing, canard, and vertical-tail detail.

Figure 2.- Continued.

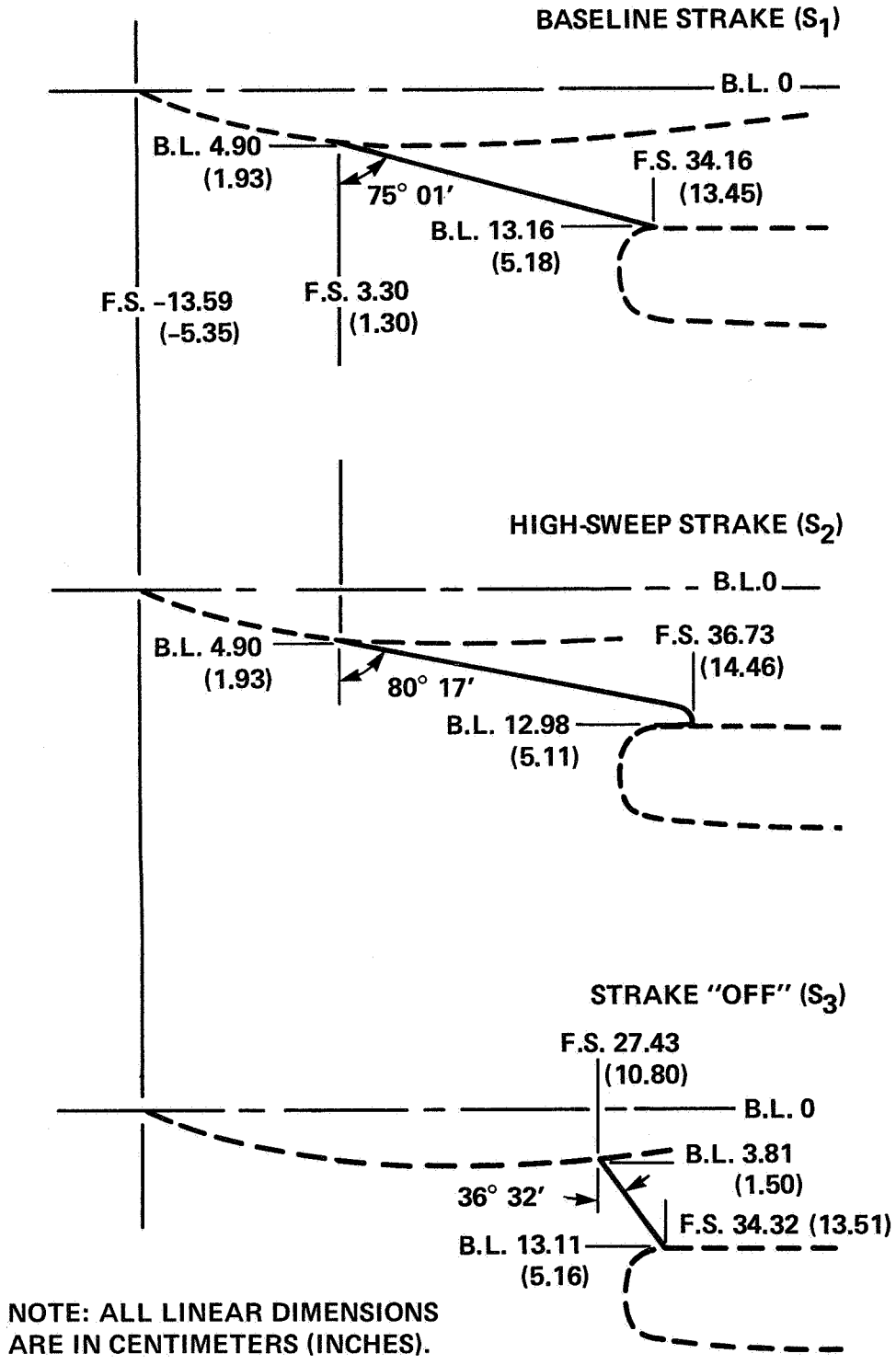


(c) Strake options.

Figure 2.- Continued.

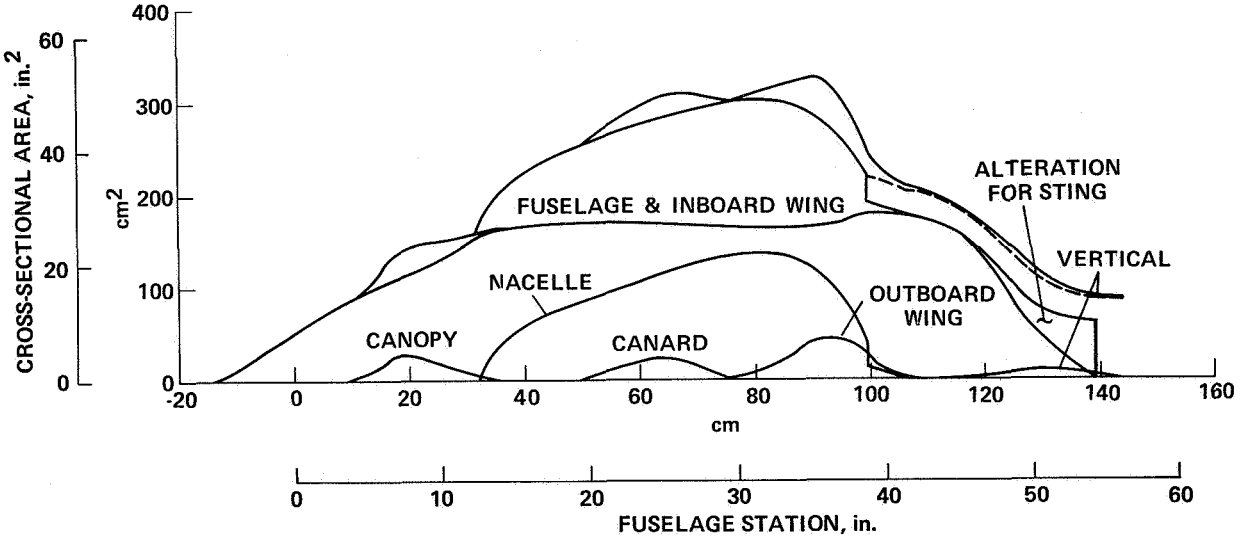


(d) Cross-sectional area distribution.

Figure 2.- Concluded.

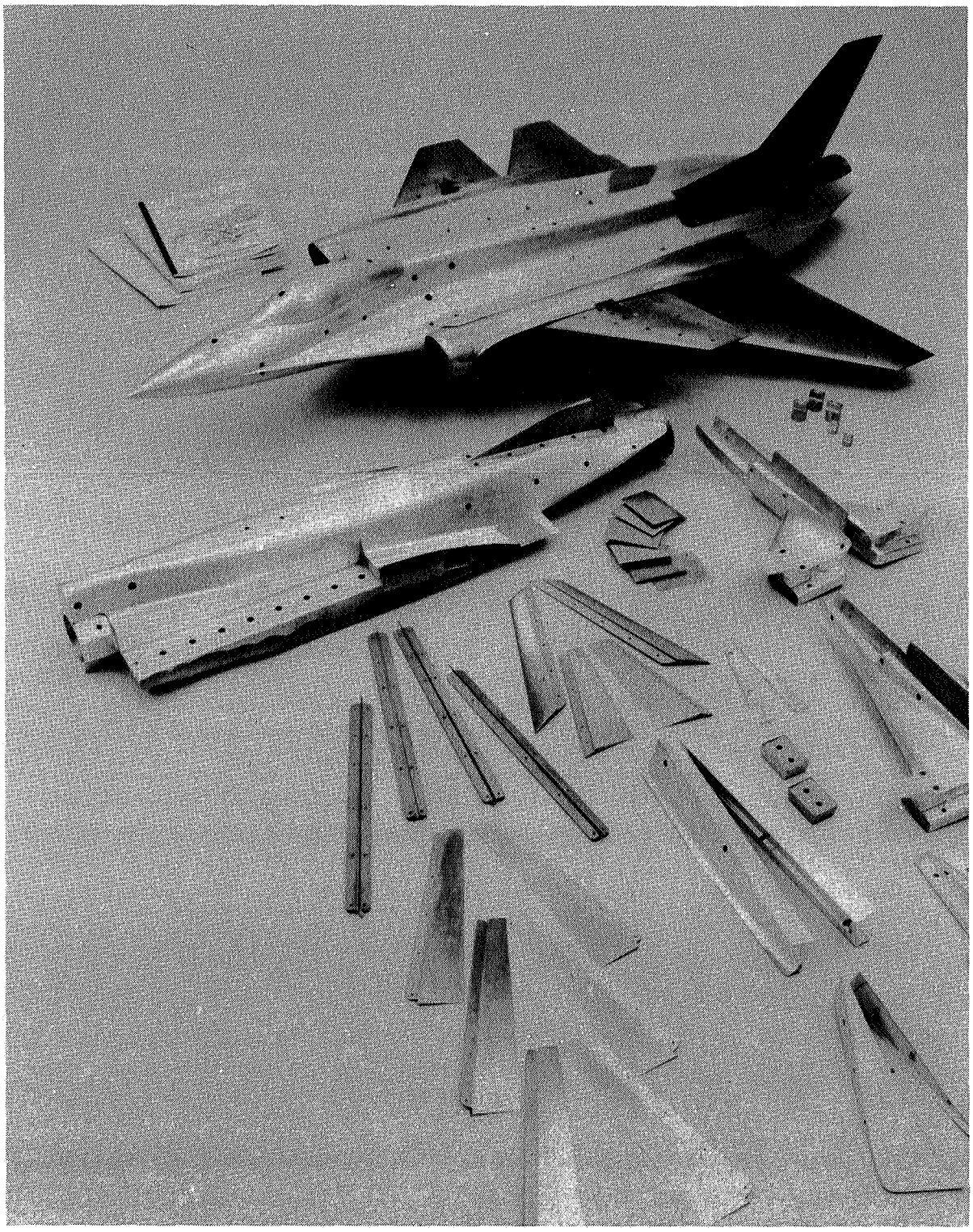

(a) E205 model, R104 body, and components.

Figure 3.- Views of E205 model in Ames 9- by 7-Foot Supersonic Wind Tunnel.

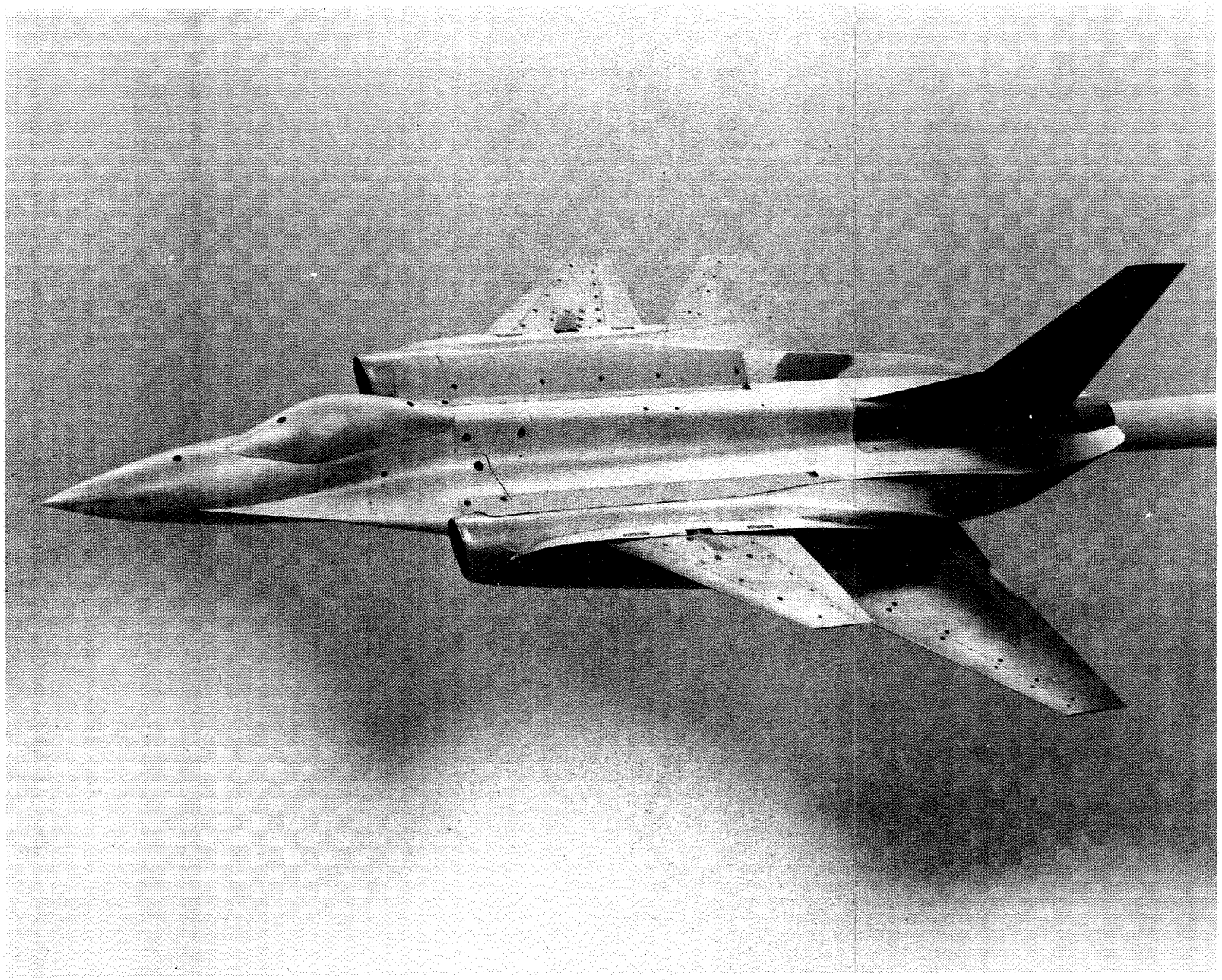

(b) E205 model; top view.

Figure 3.- Continued.

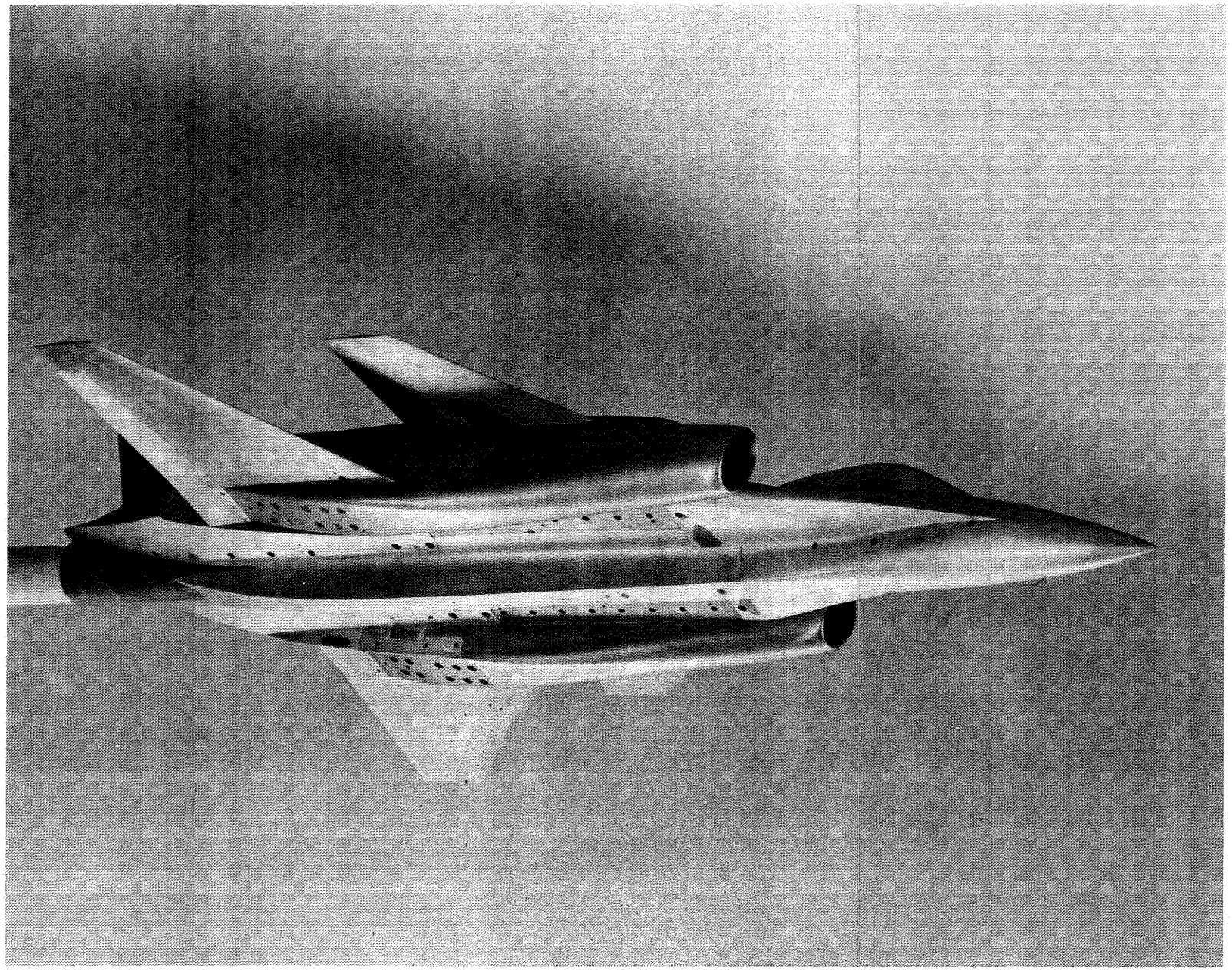

(c) E205 model; bottom view.

Figure 3.- Concluded.

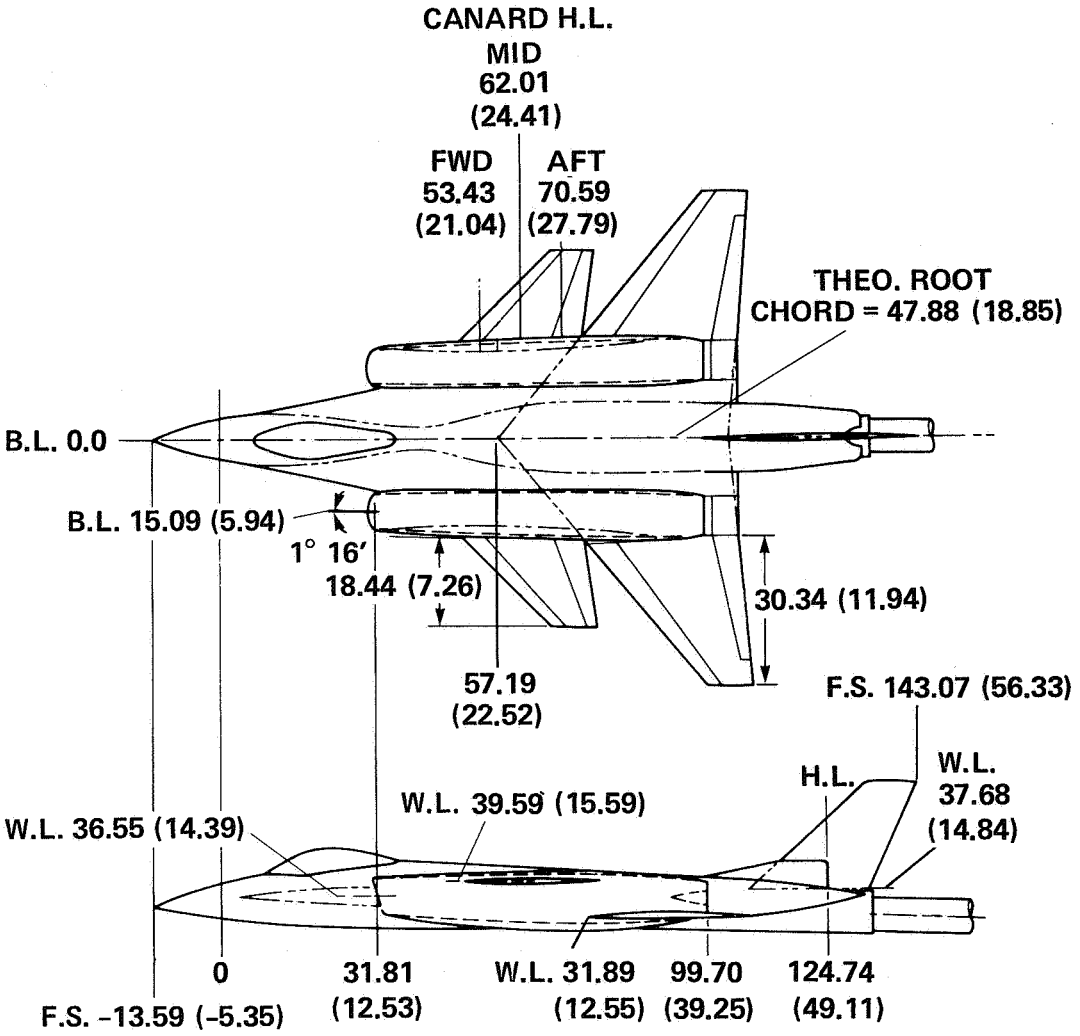


(a) Three-view drawing.

Figure 4.- Details of R104 wind-tunnel model.

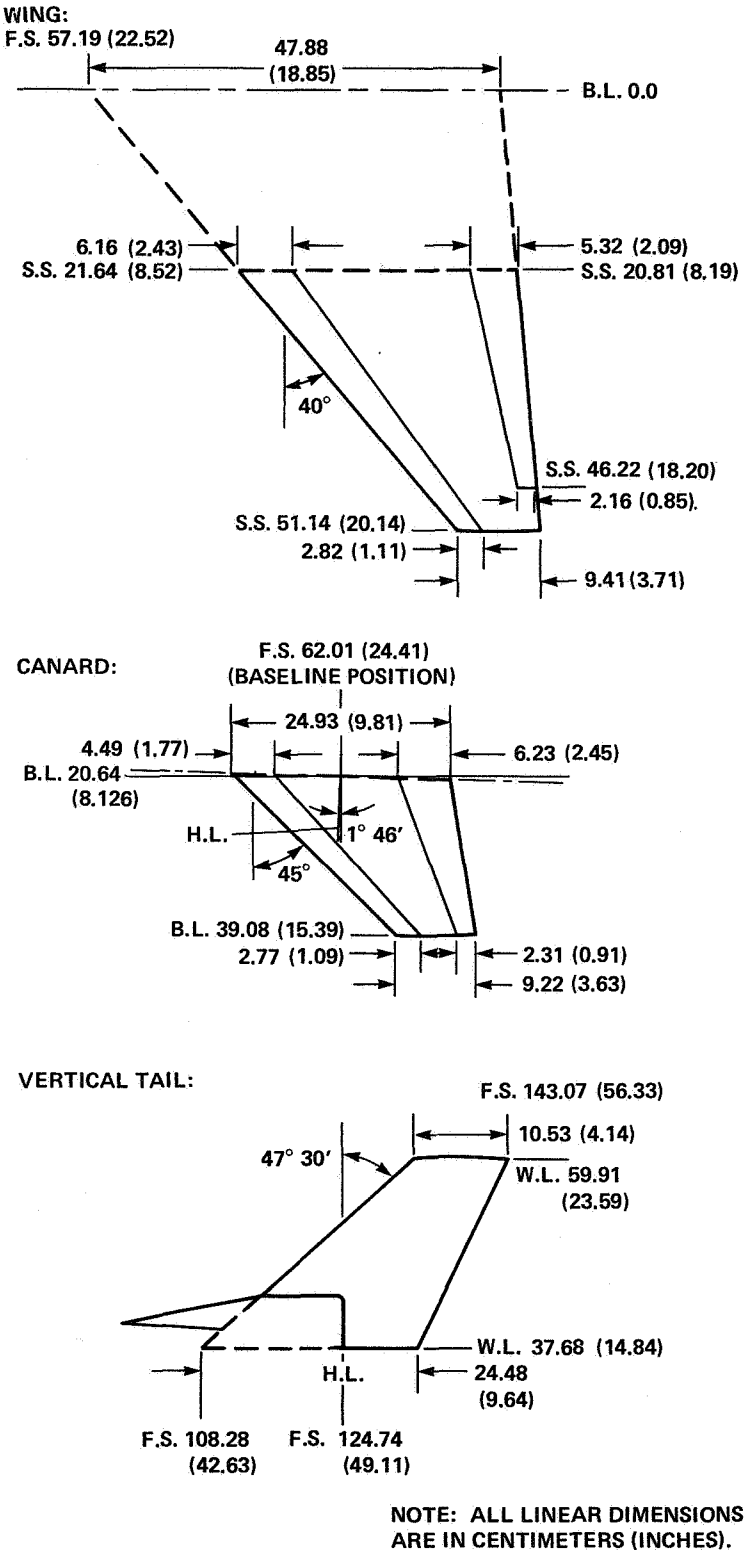


(b) Wing, canard, and vertical-tail detail.

Figure 4.- Continued.

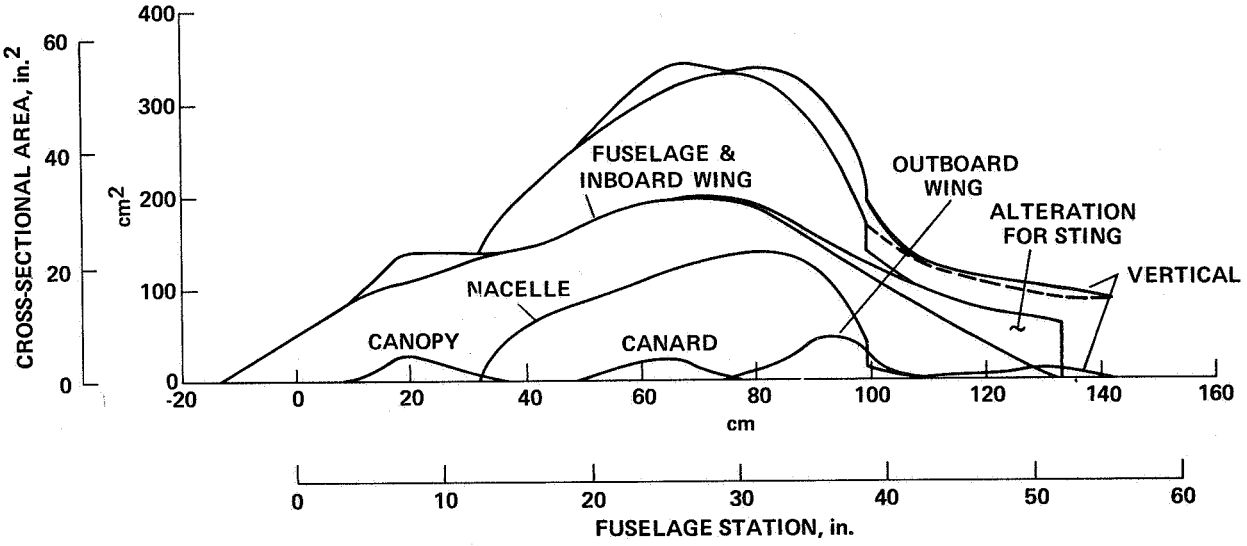


(c) Cross-sectional area distribution.

Figure 4.- Concluded.

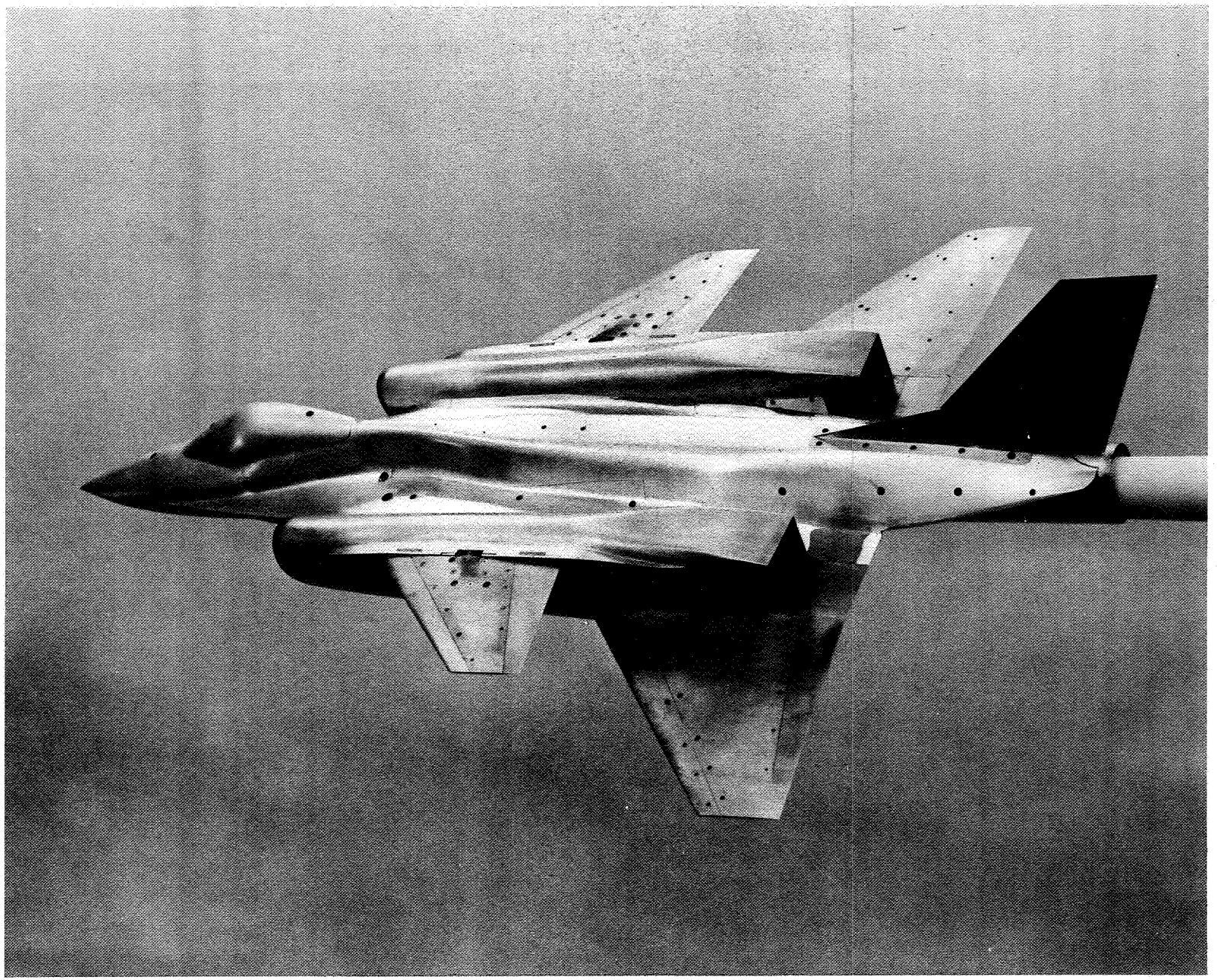

(a) R104 model; top view.

Figure 5.- Views of R104 model.

(b) R104 model installed in wind tunnel; front view.

Figure 5.- Continued.

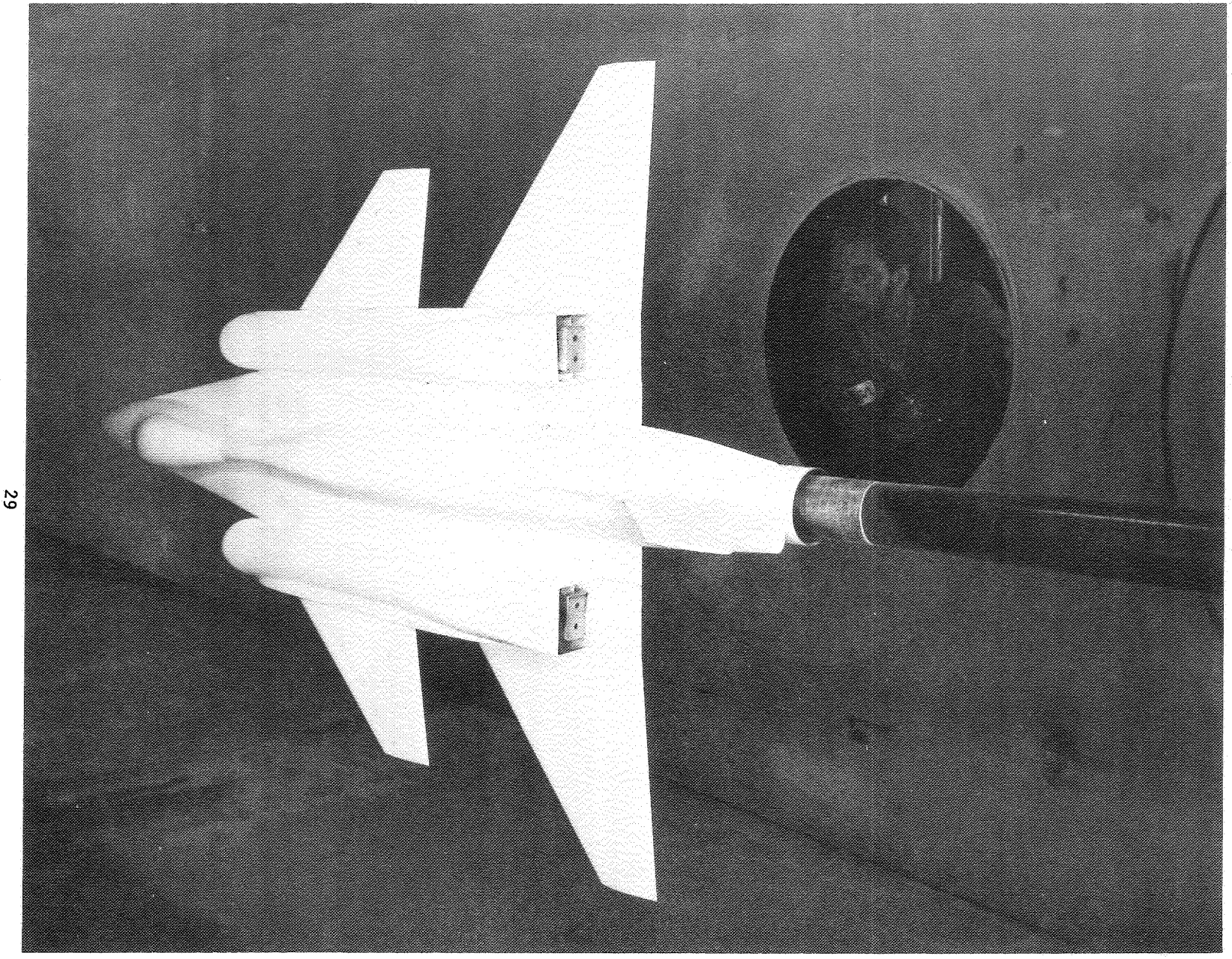

(c) R104 model installed in wind tunnel; aft view.

Figure 5.- Concluded.

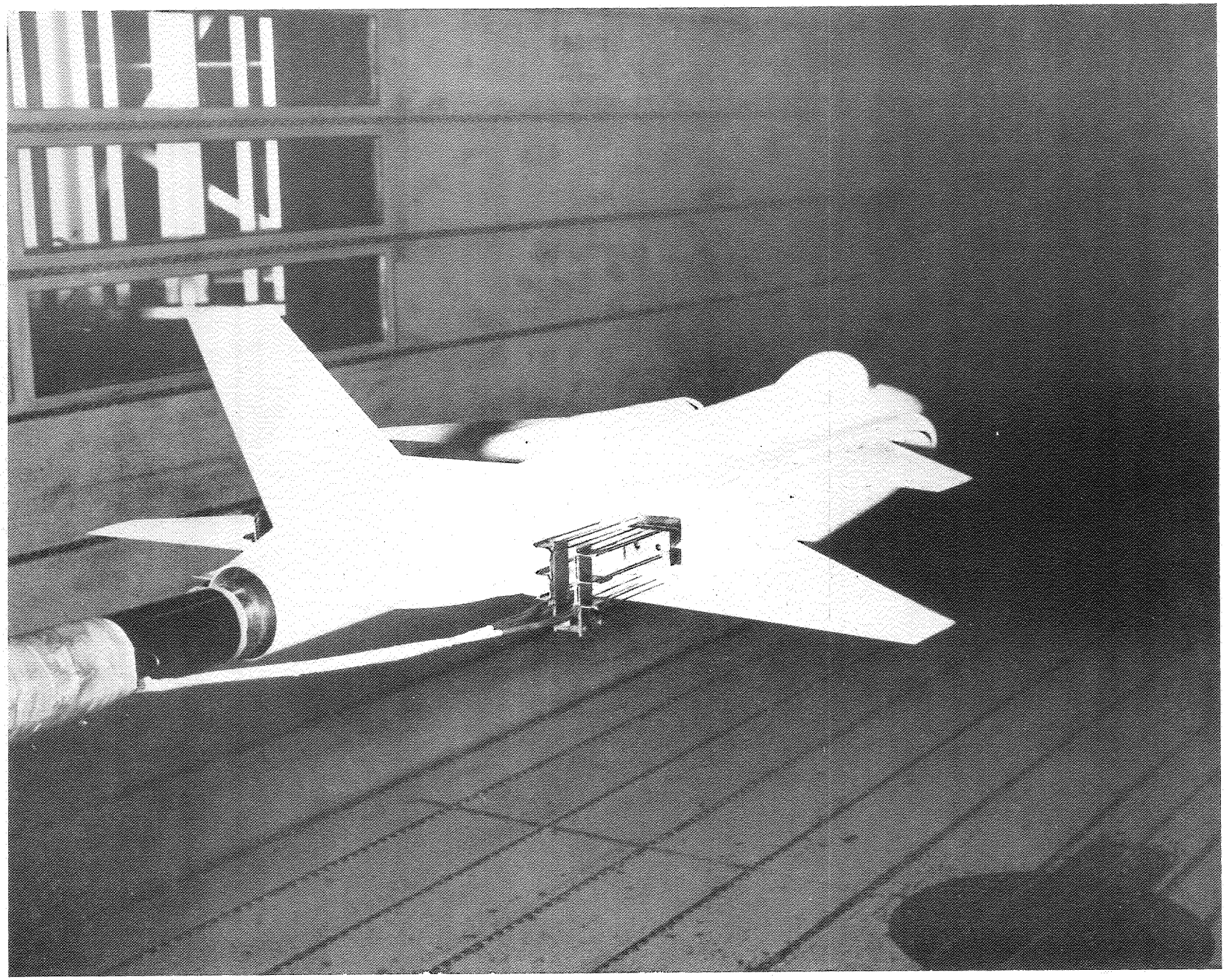

Figure 6.- Duct-exit rake installation on E205 model (shown in Ames 11-Foot Wind Tunnel).

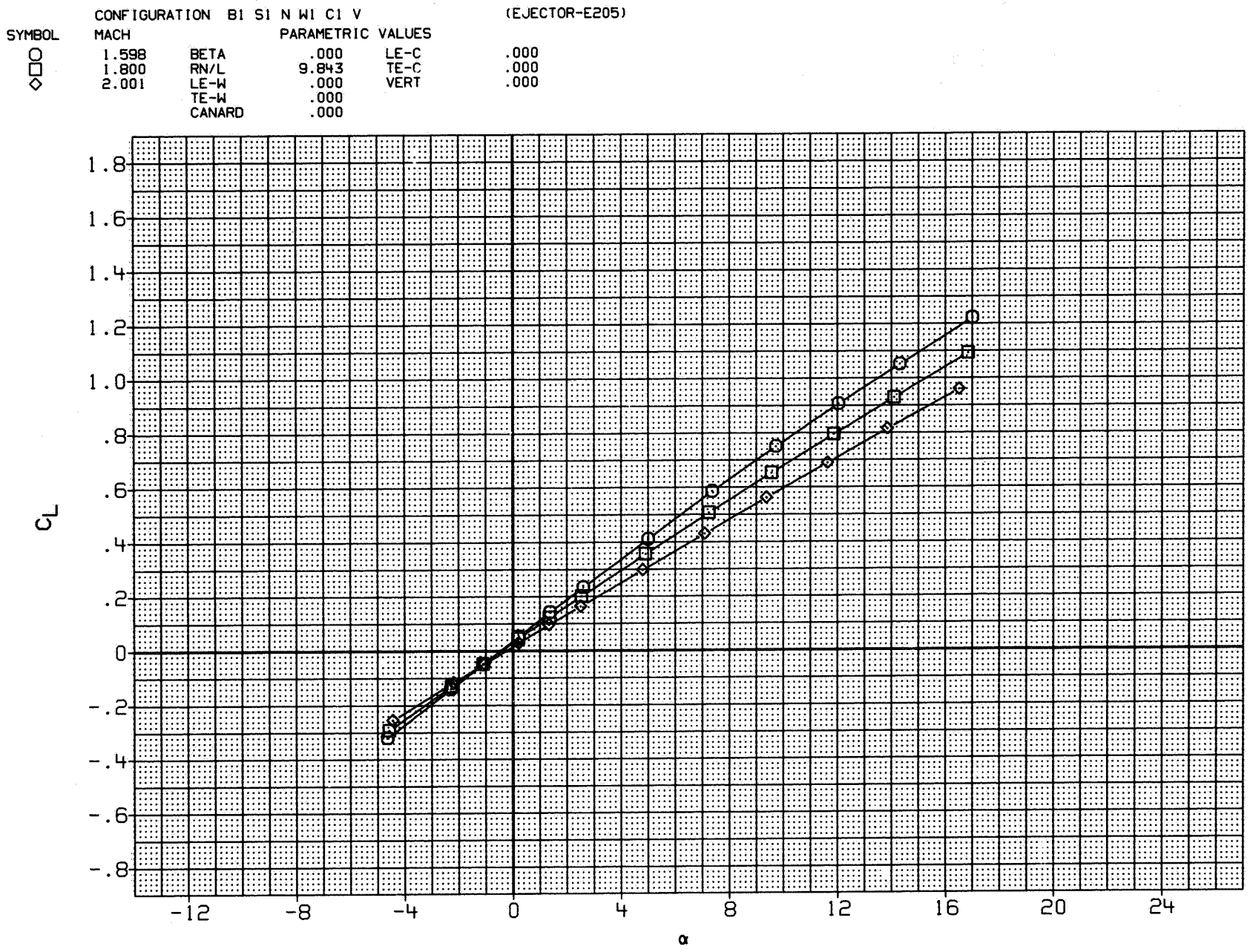


FIG. 7 BASIC LONGITUDINAL CHARACTERISTICS FOR VARIOUS MACH NUMBERS

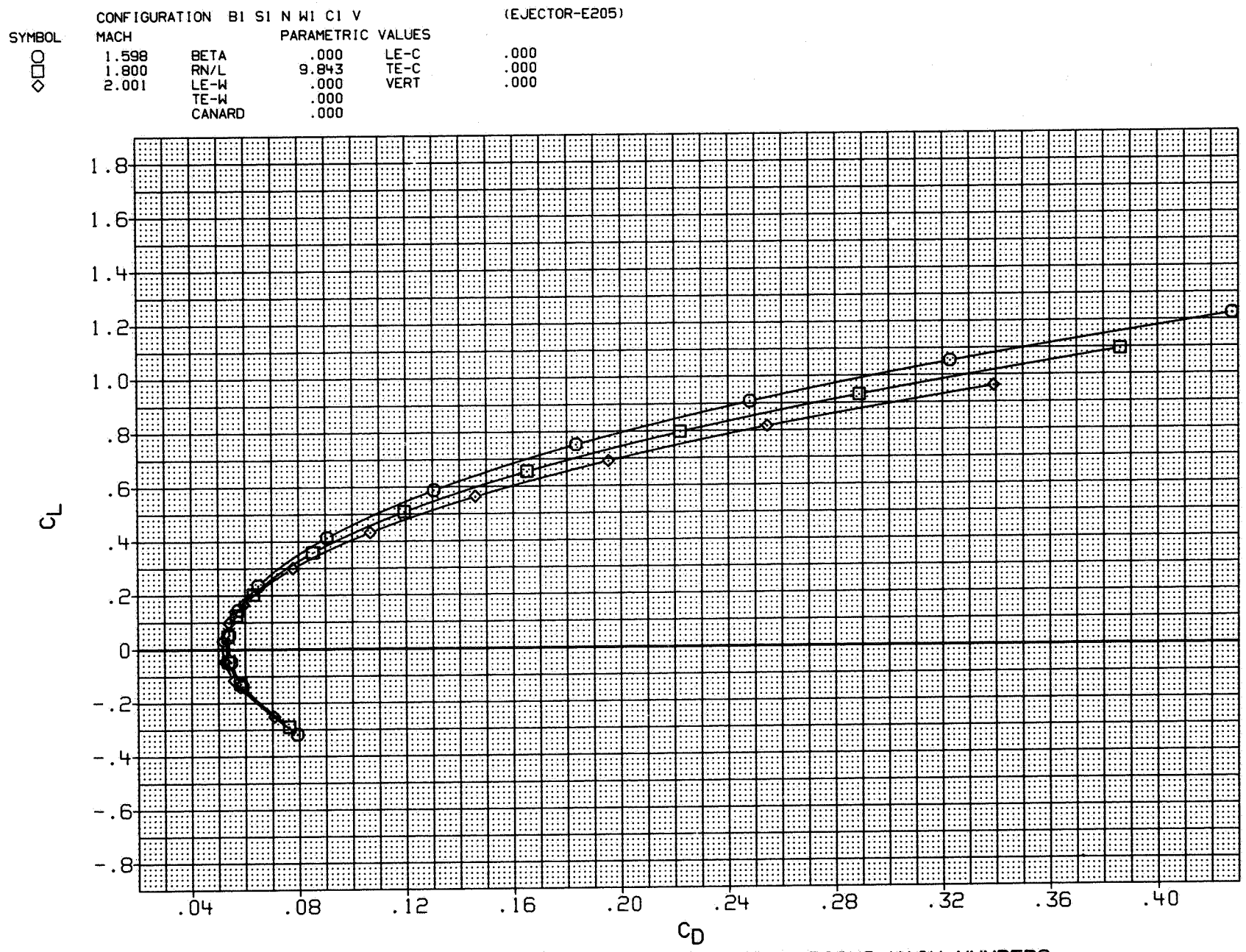


FIG. 7 BASIC LONGITUDINAL CHARACTERISTICS FOR VARIOUS MACH NUMBERS

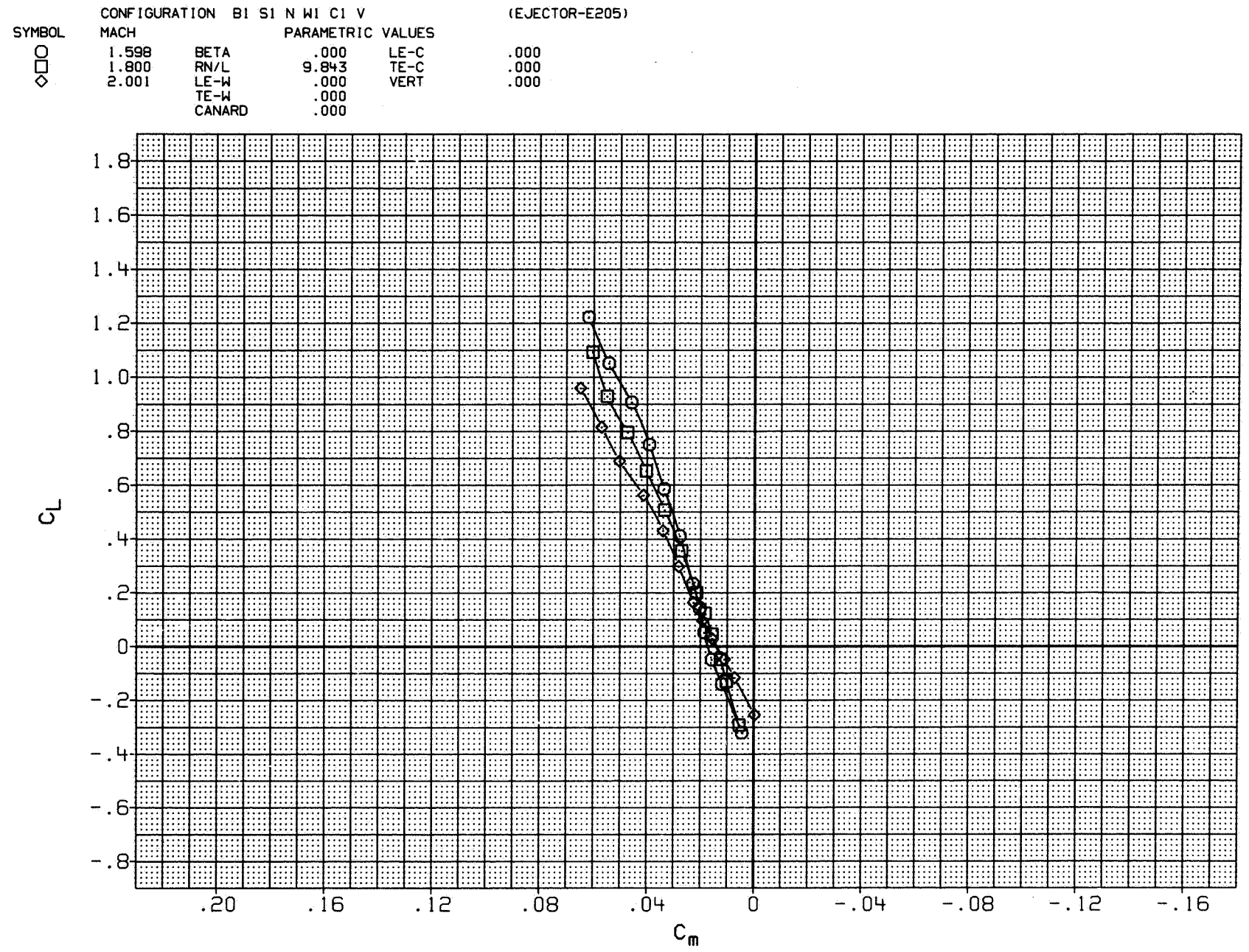


FIG. 7 BASIC LONGITUDINAL CHARACTERISTICS FOR VARIOUS MACH NUMBERS

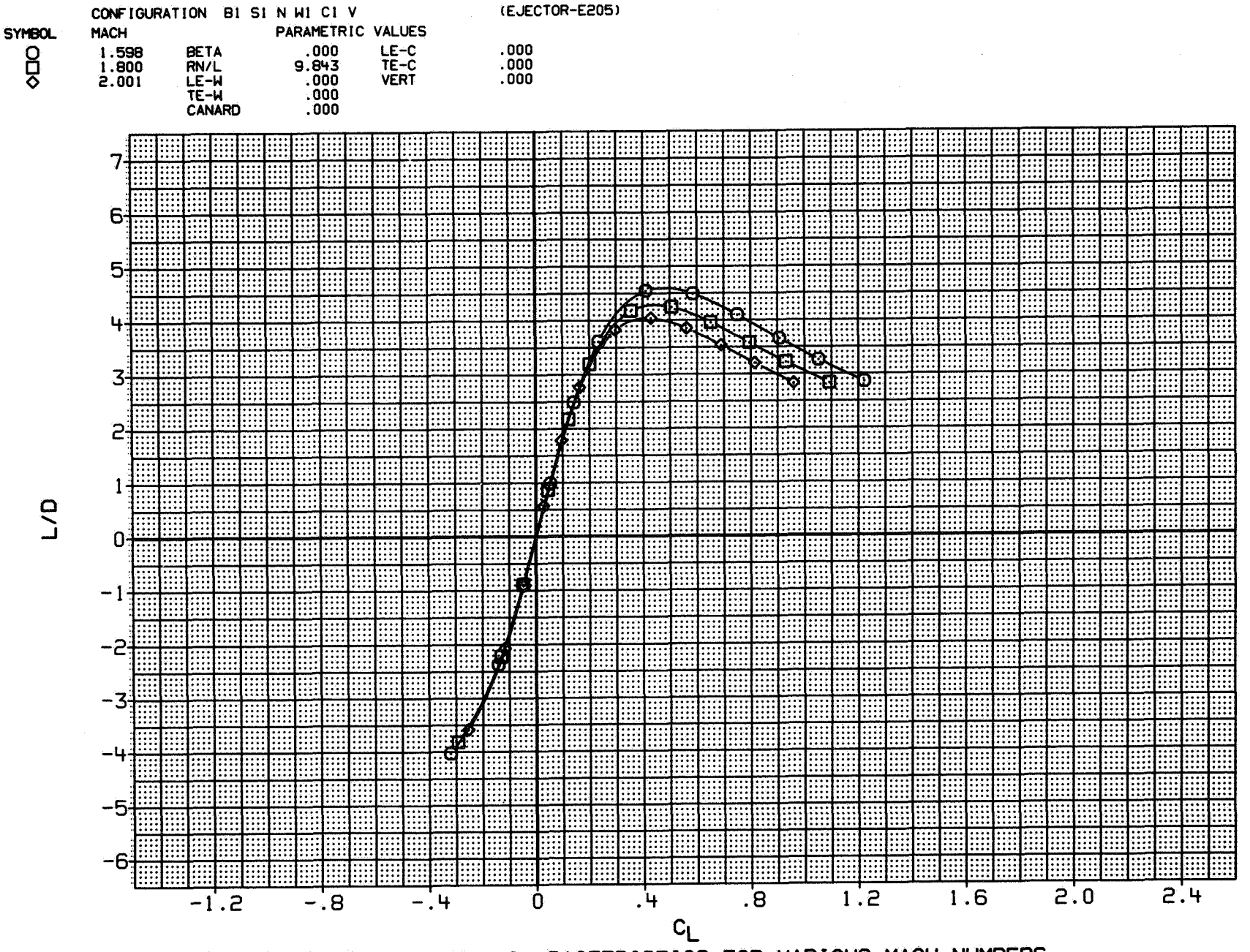


FIG. 7 BASIC LONGITUDINAL CHARACTERISTICS FOR VARIOUS MACH NUMBERS

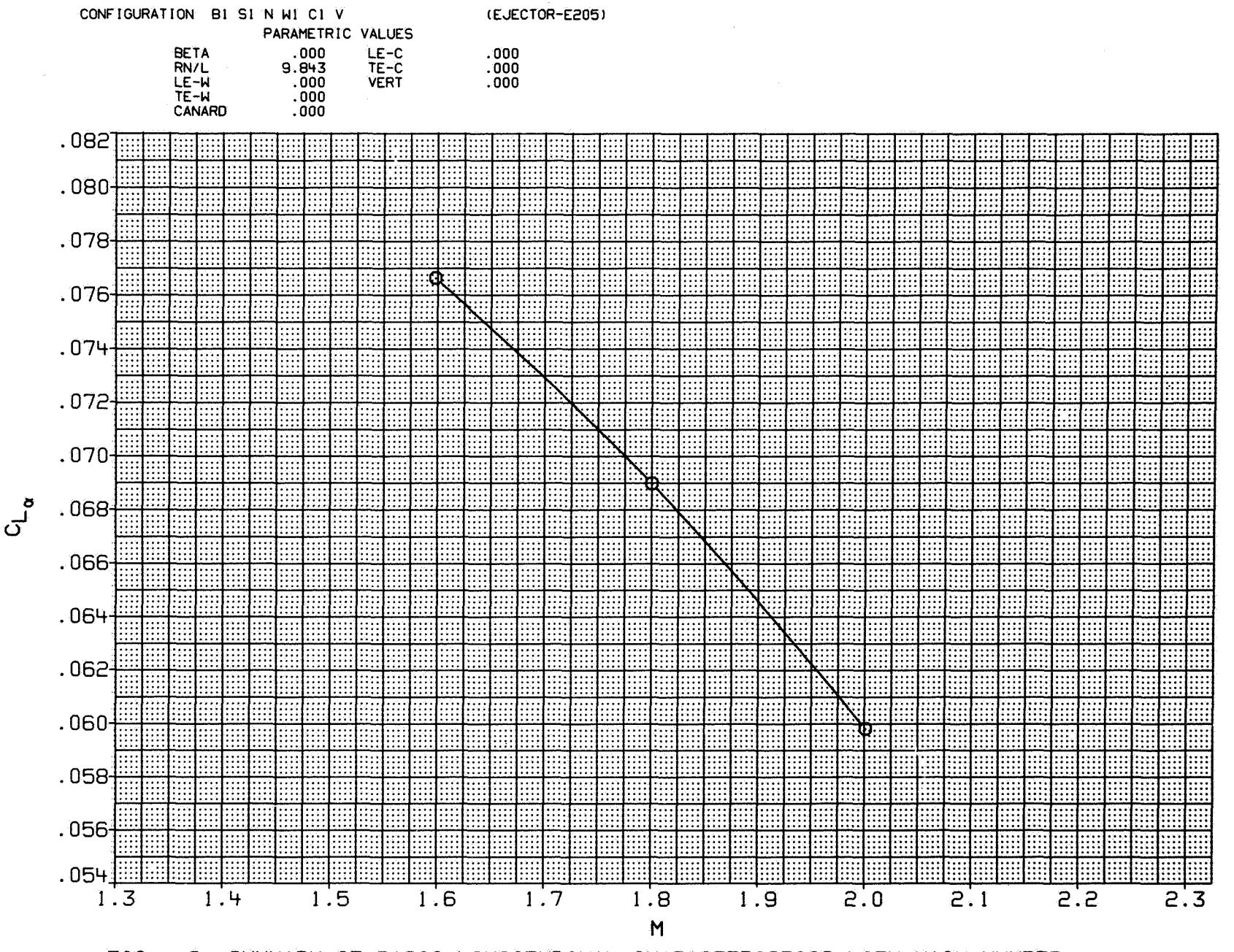


FIG. 8 SUMMARY OF BASIC LONGITUDINAL CHARACTERISTICS WITH MACH NUMBER

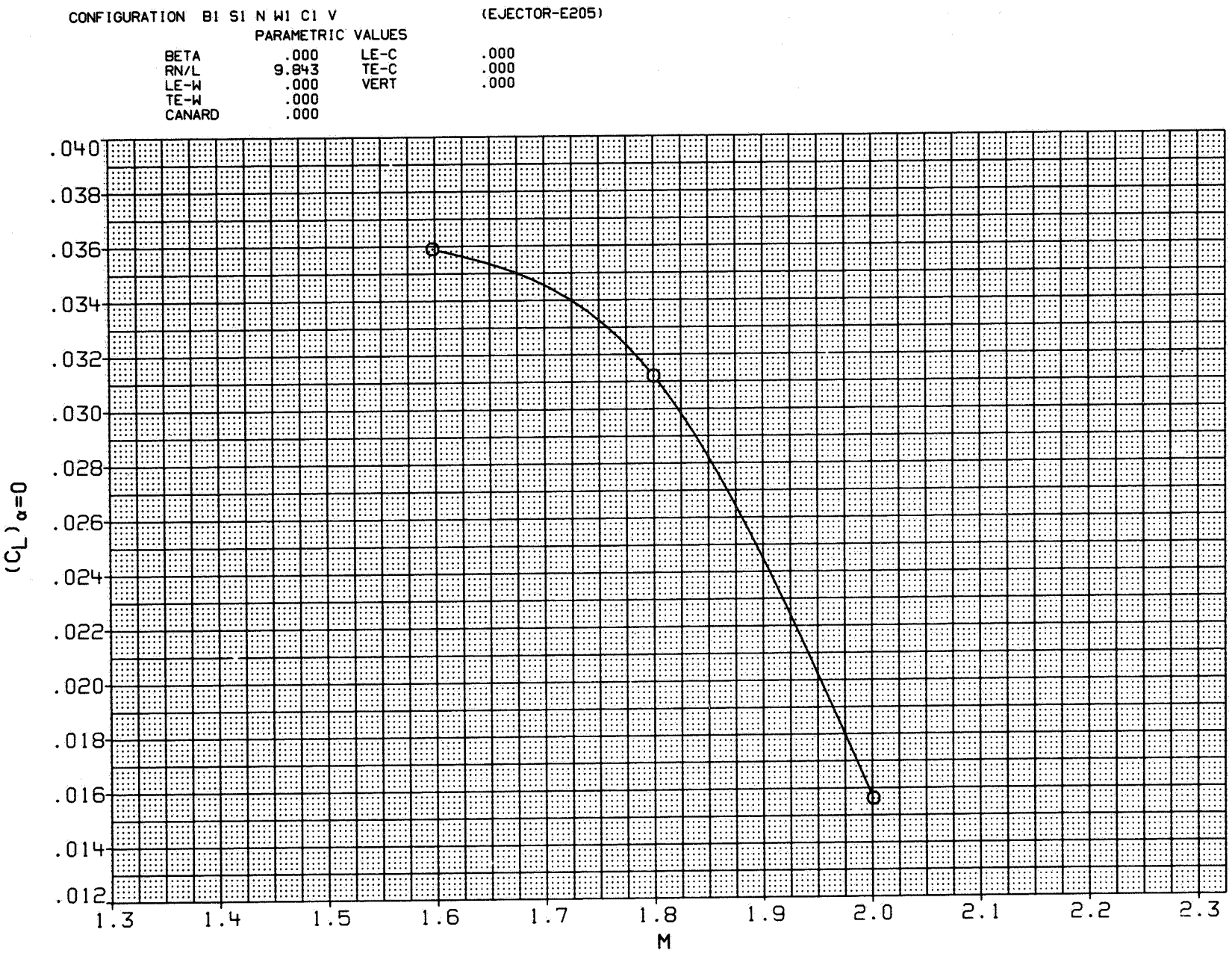


FIG. 8 SUMMARY OF BASIC LONGITUDINAL CHARACTERISTICS WITH MACH NUMBER

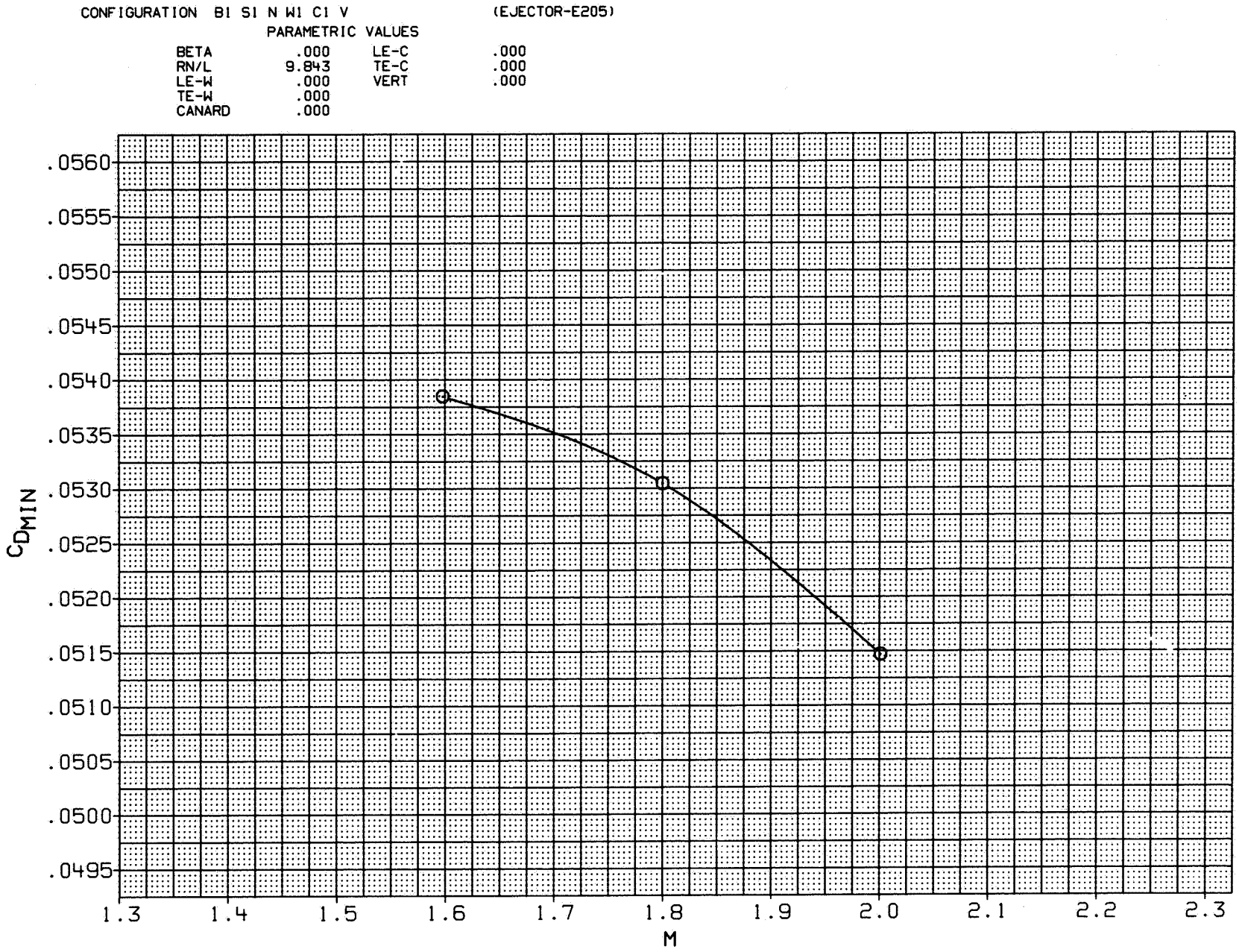


FIG. 8 SUMMARY OF BASIC LONGITUDINAL CHARACTERISTICS WITH MACH NUMBER

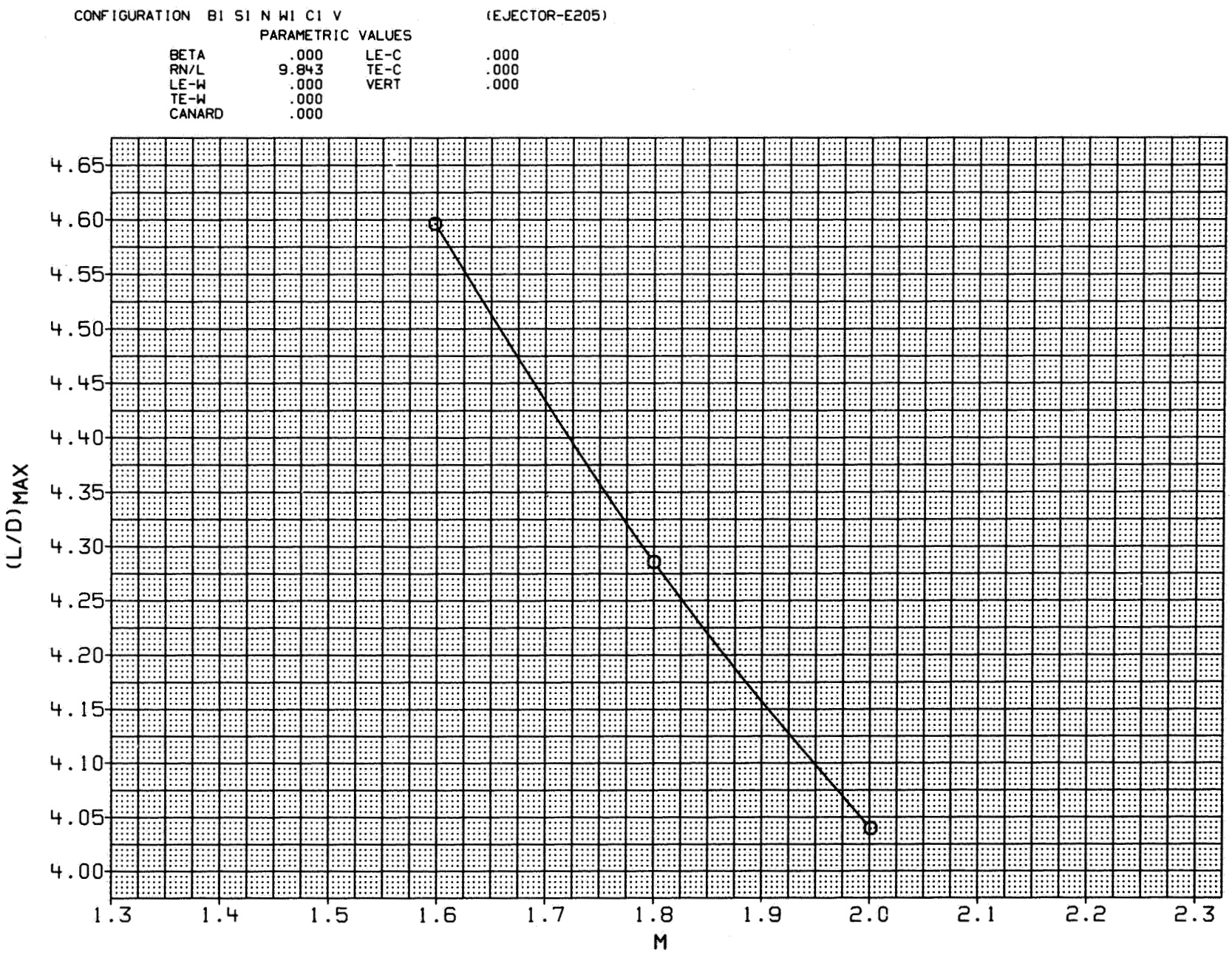


FIG. 8 SUMMARY OF BASIC LONGITUDINAL CHARACTERISTICS WITH MACH NUMBER

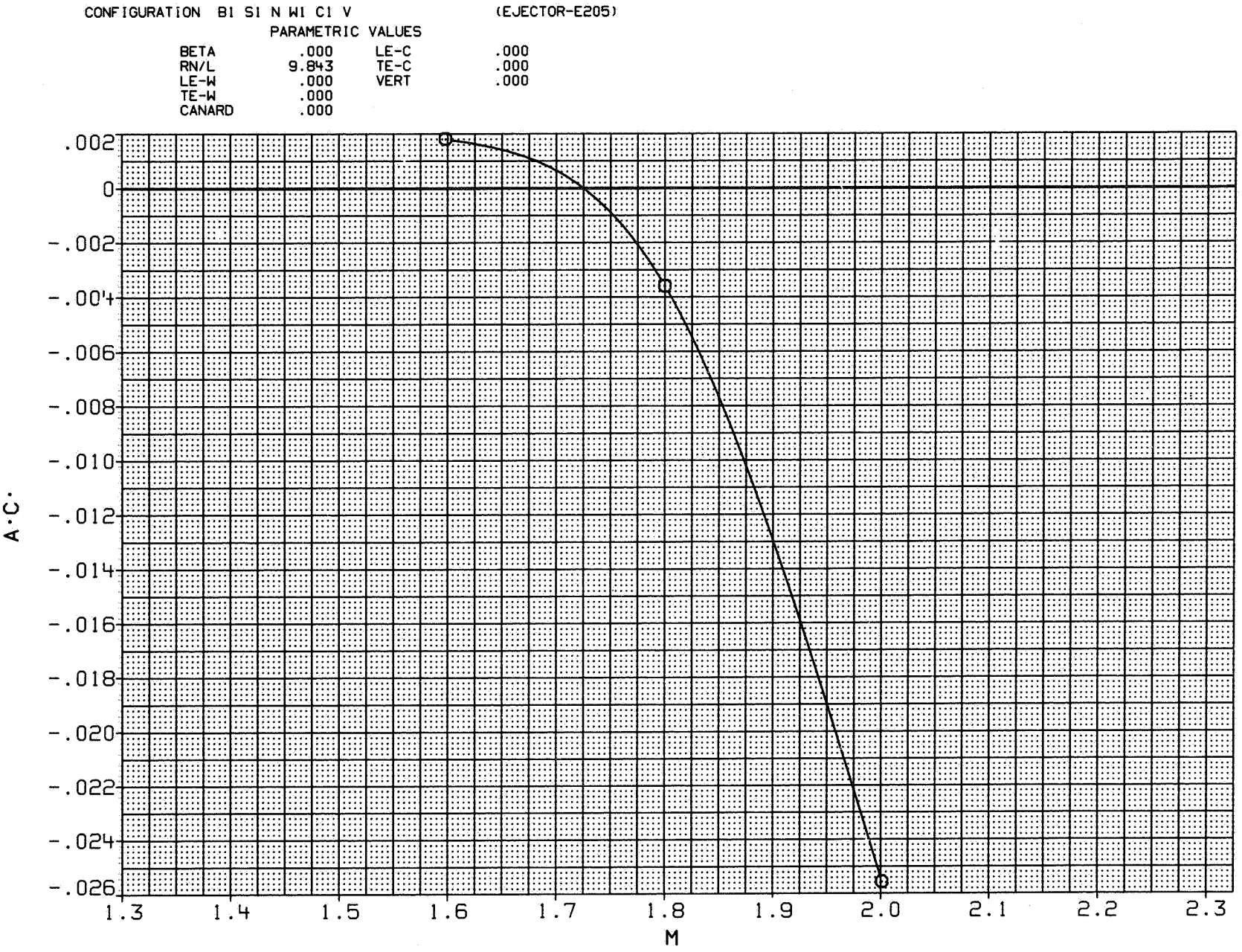


FIG. 8 SUMMARY OF BASIC LONGITUDINAL CHARACTERISTICS WITH MACH NUMBER

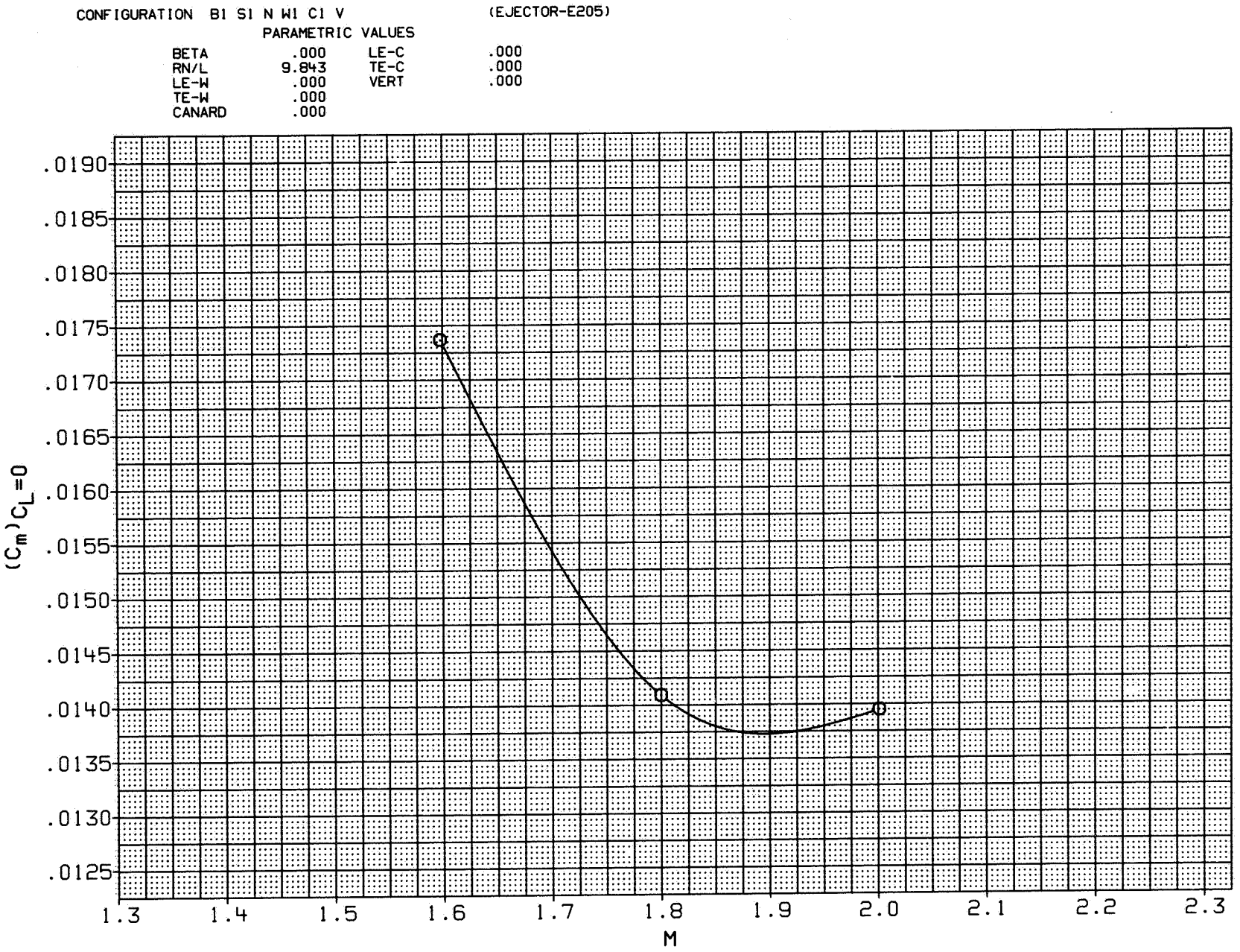


FIG. 8 SUMMARY OF BASIC LONGITUDINAL CHARACTERISTICS WITH MACH NUMBER

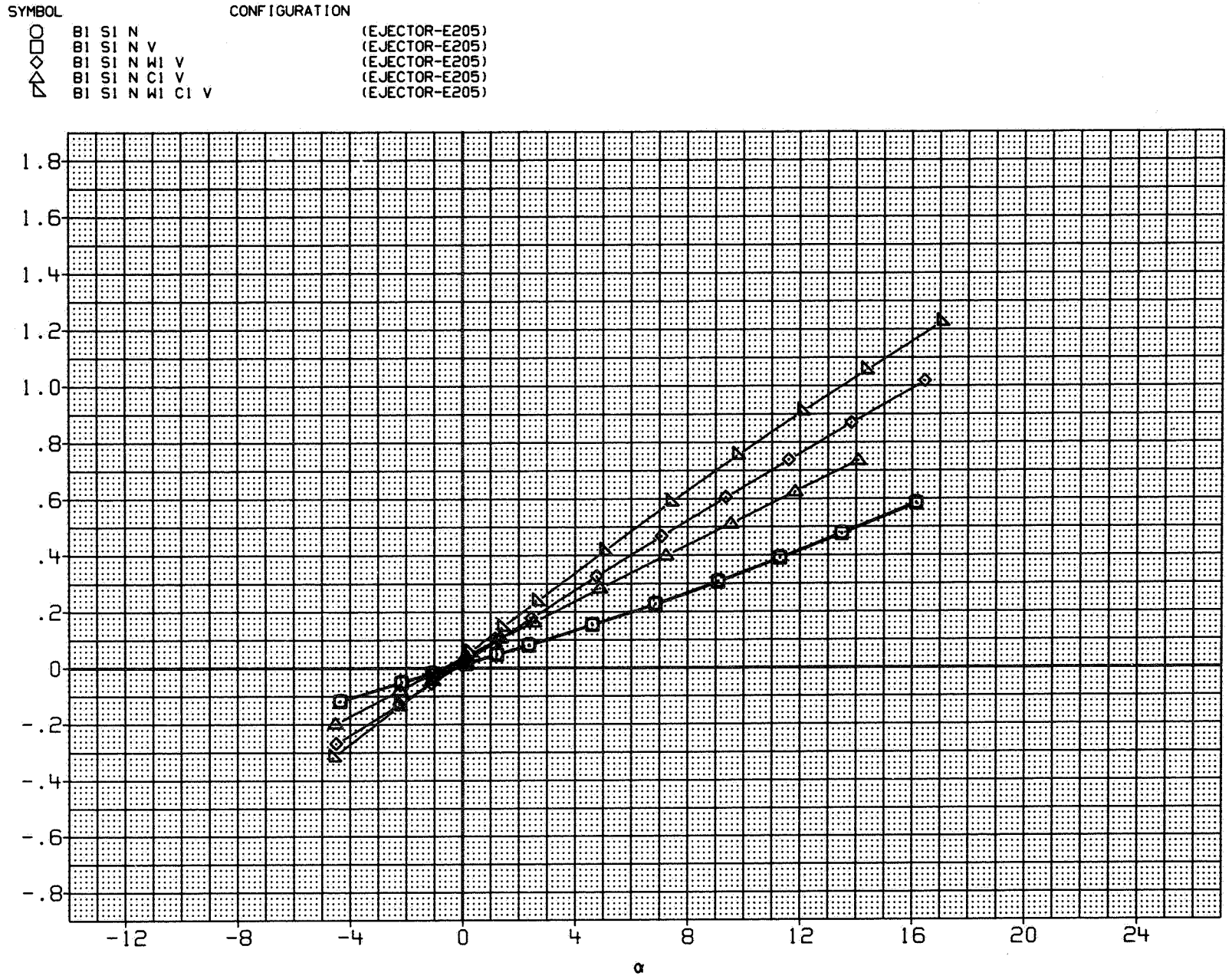


FIG. 9 COMPONENT BUILDUP, LONGITUDINAL CHARACTERISTICS

MACH = 1.60

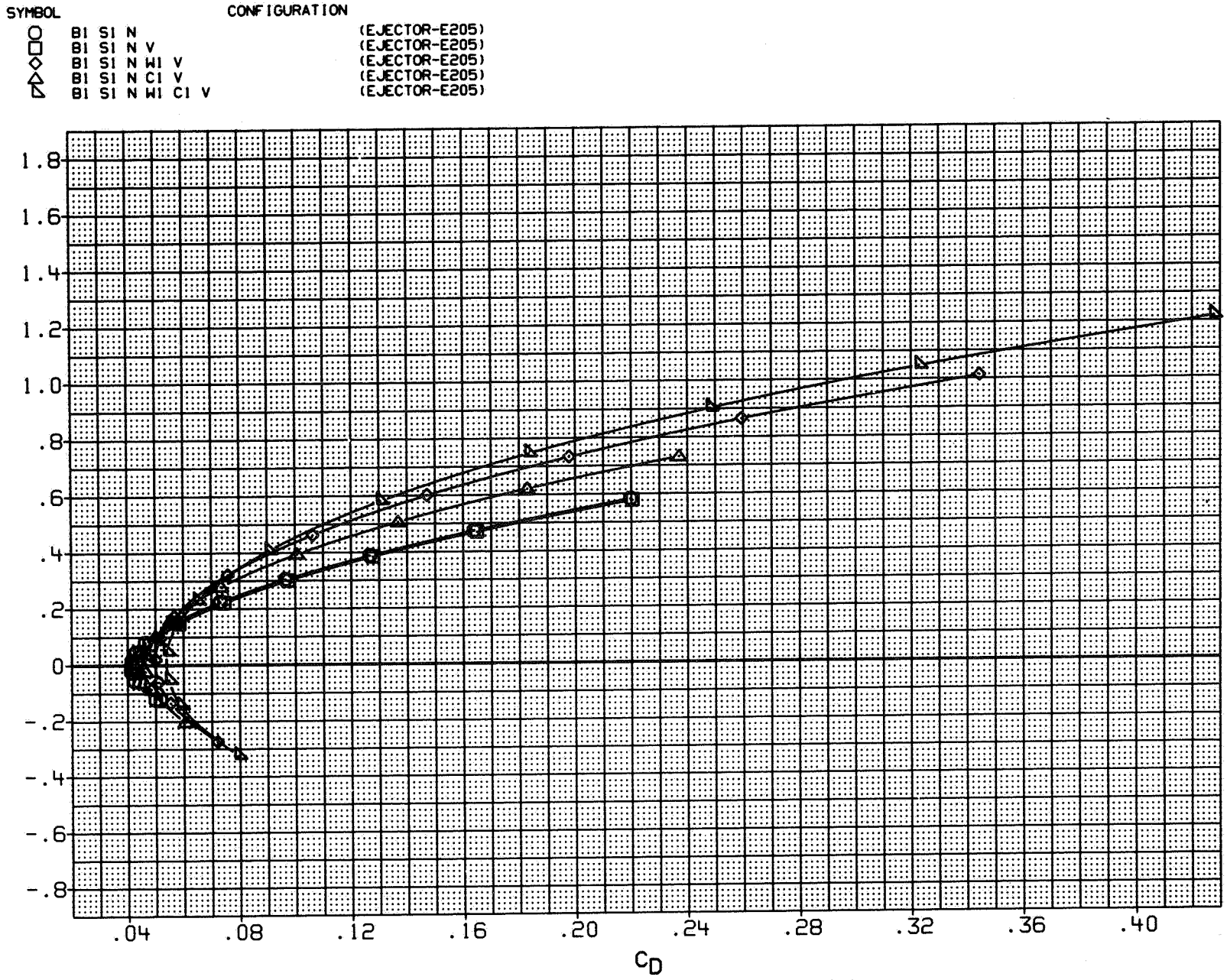


FIG. 9 COMPONENT BUILDUP, LONGITUDINAL CHARACTERISTICS

MACH = 1.60

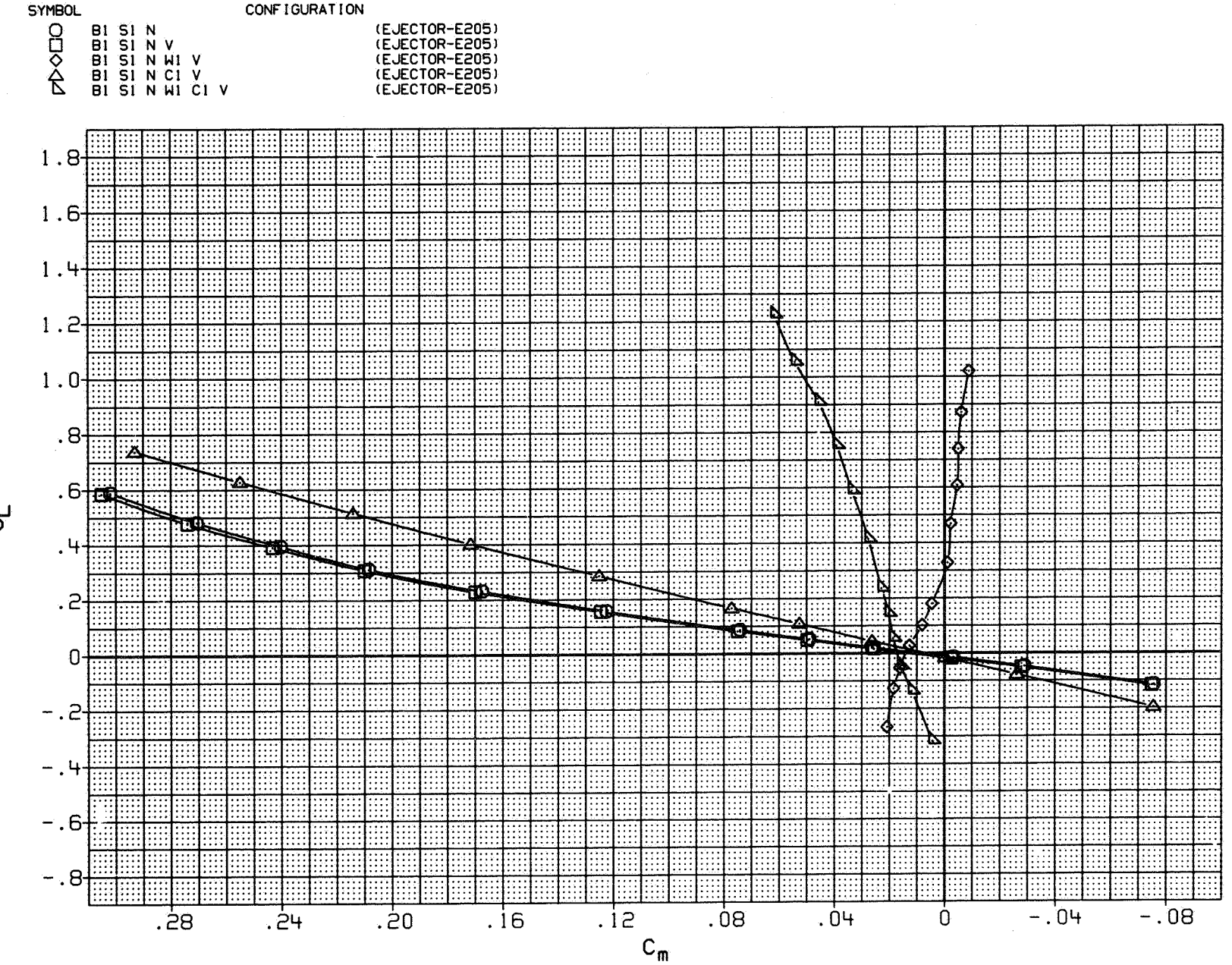


FIG. 9 COMPONENT BUILDUP, LONGITUDINAL CHARACTERISTICS

MACH = 1.60

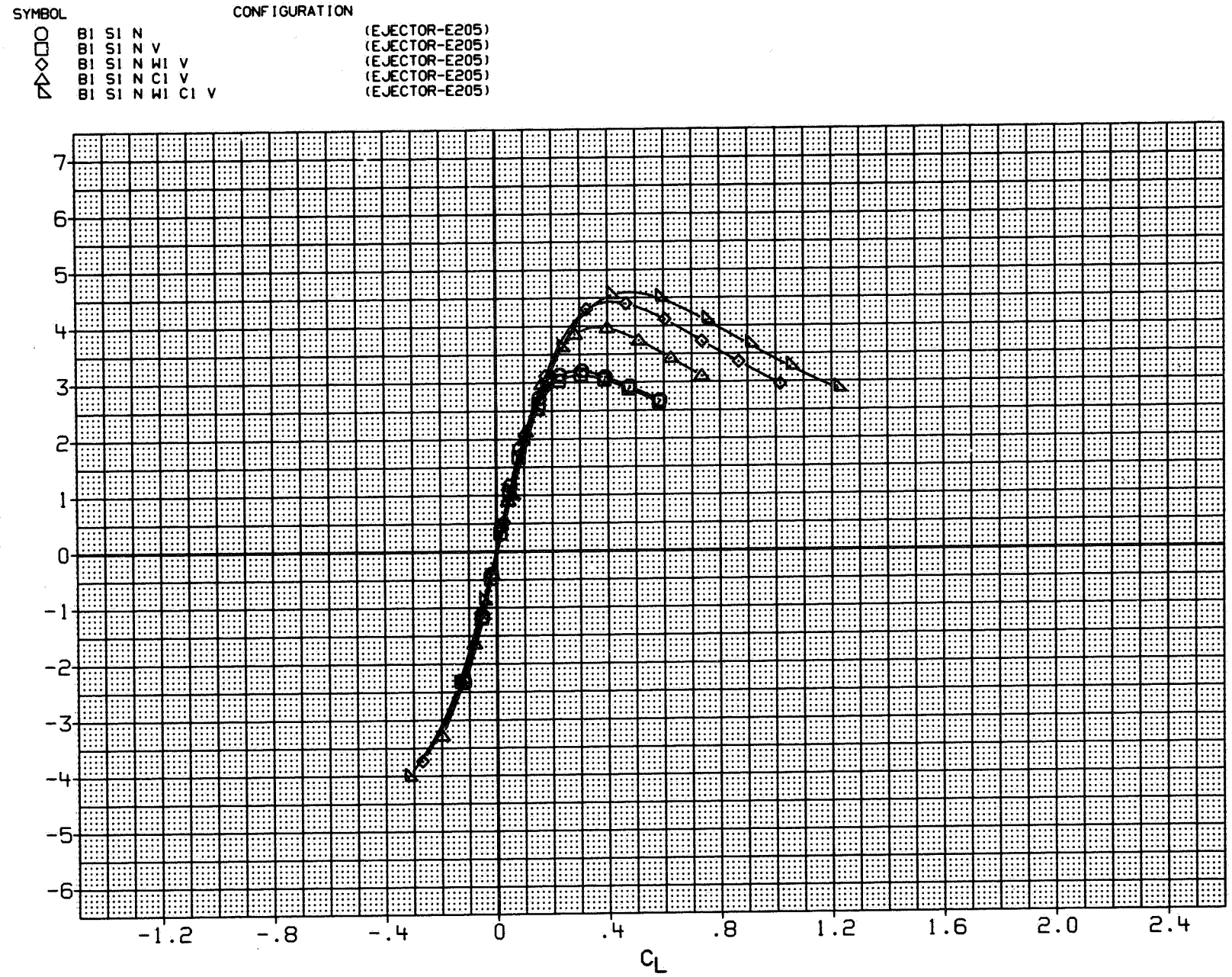


FIG. 9 COMPONENT BUILDUP, LONGITUDINAL CHARACTERISTICS

MACH = 1.60

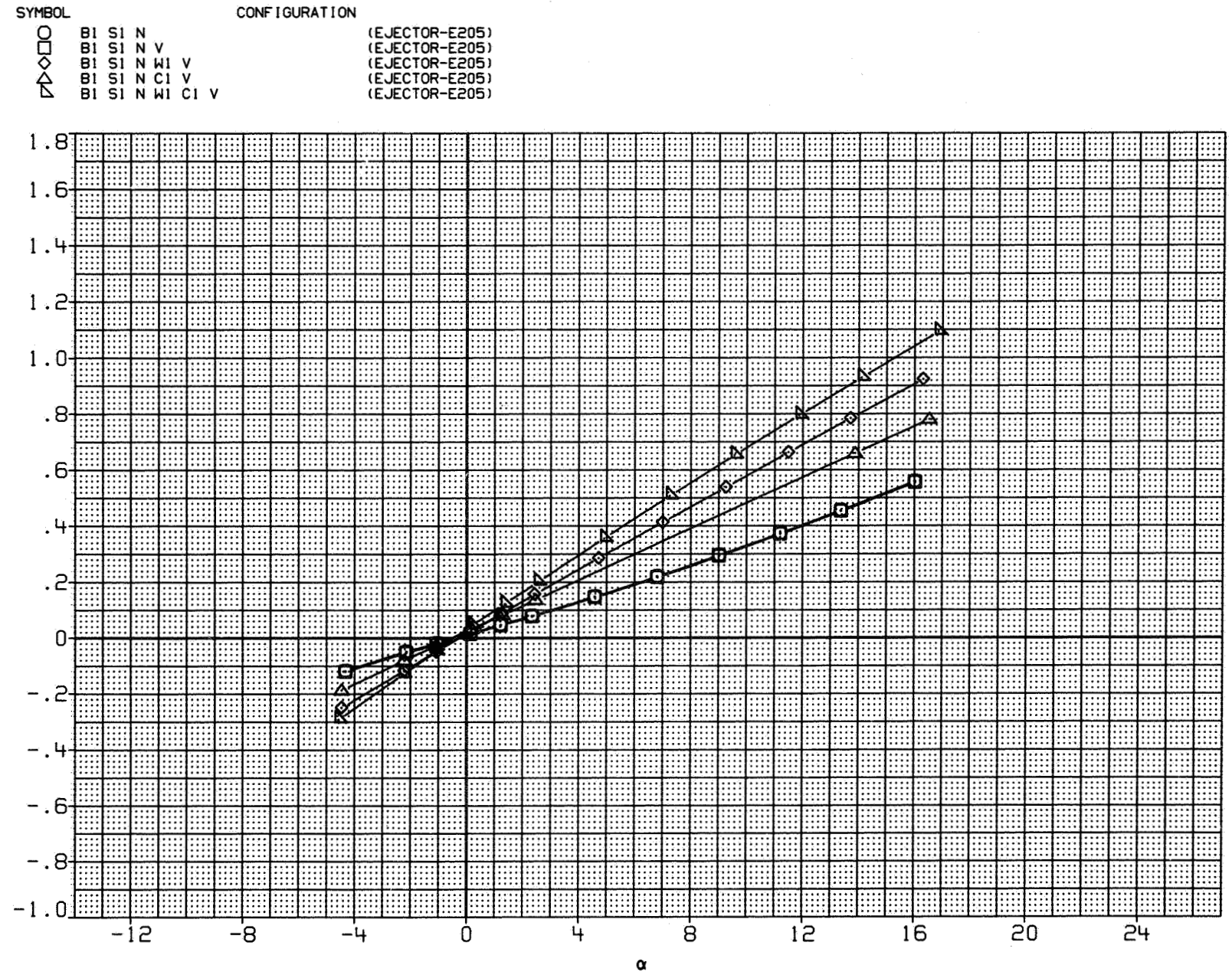


FIG. 10 COMPONENT BUILDUP, LONGITUDINAL CHARACTERISTICS

MACH = 1.80

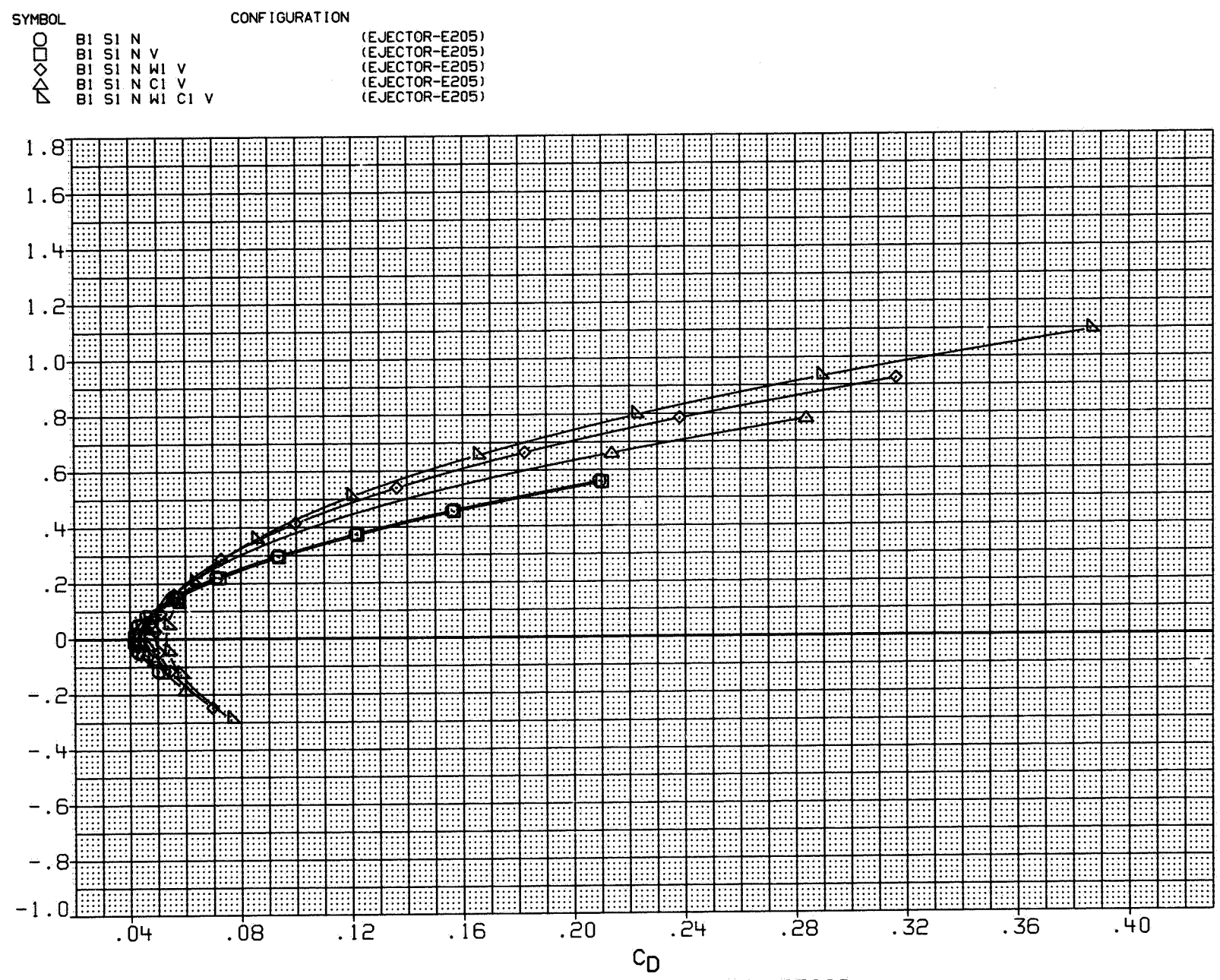


FIG. 10 COMPONENT BUILDUP, LONGITUDINAL CHARACTERISTICS

MACH = 1.80

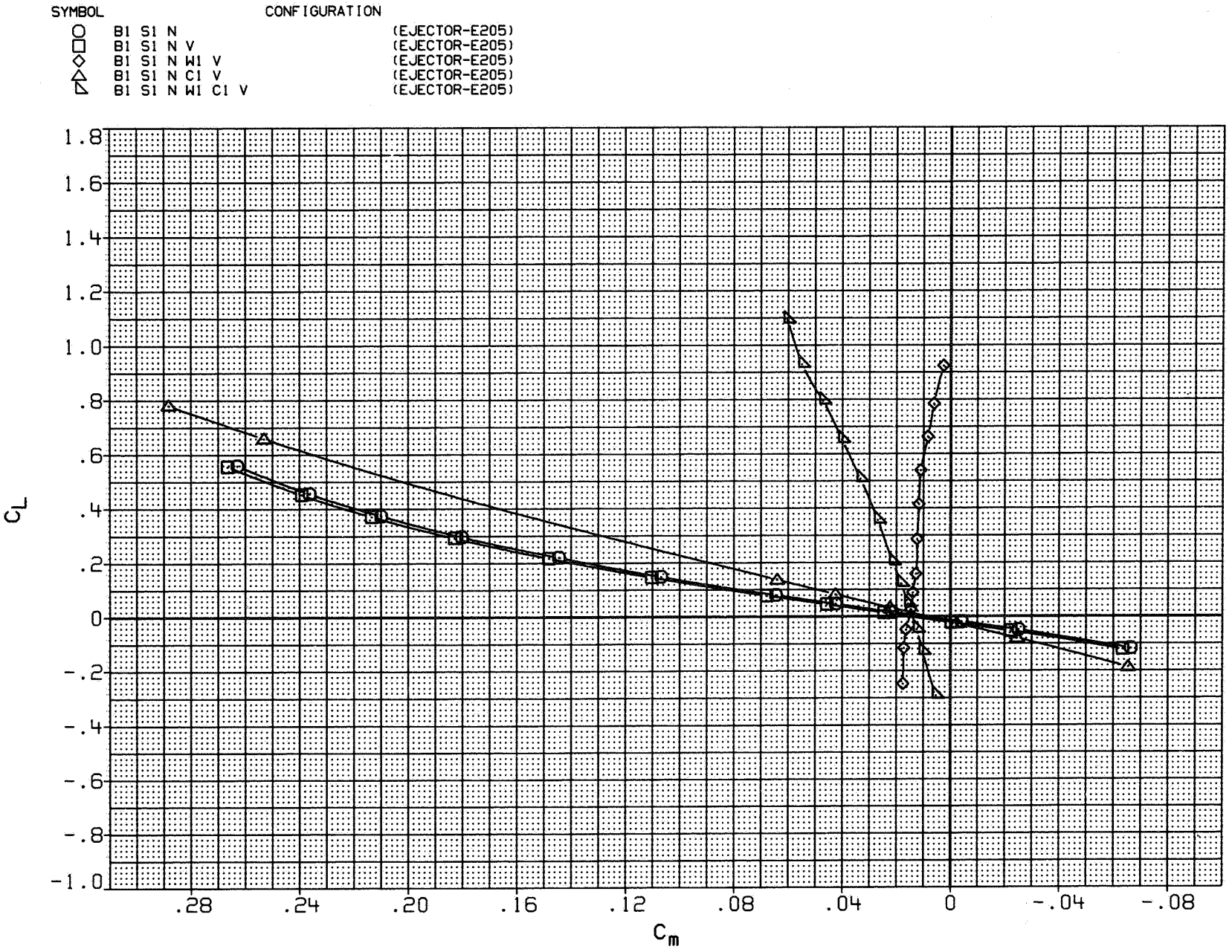


FIG. 10 COMPONENT BUILDUP, LONGITUDINAL CHARACTERISTICS

MACH = 1.80

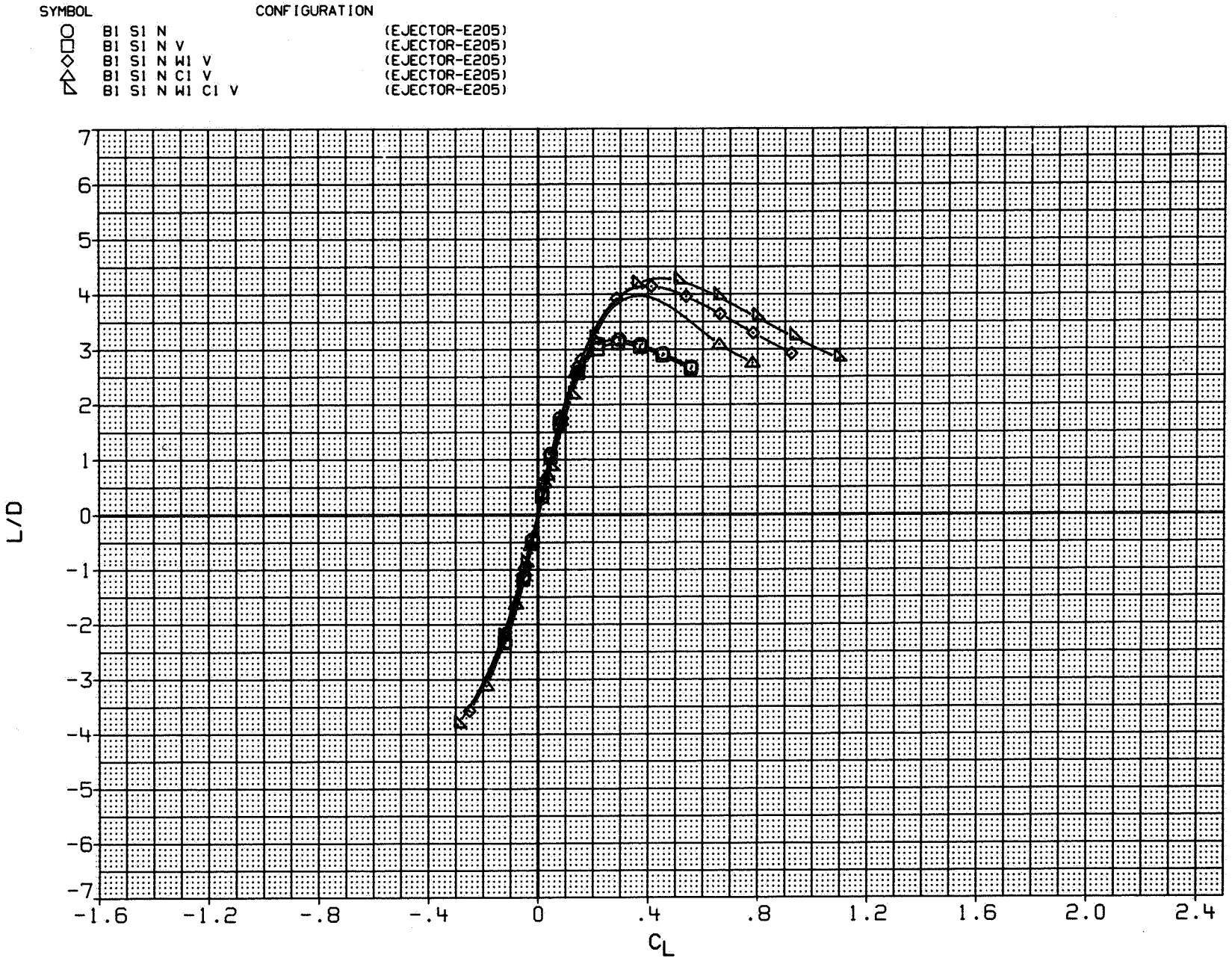


FIG. 10 COMPONENT BUILDUP, LONGITUDINAL CHARACTERISTICS

MACH = 1.80

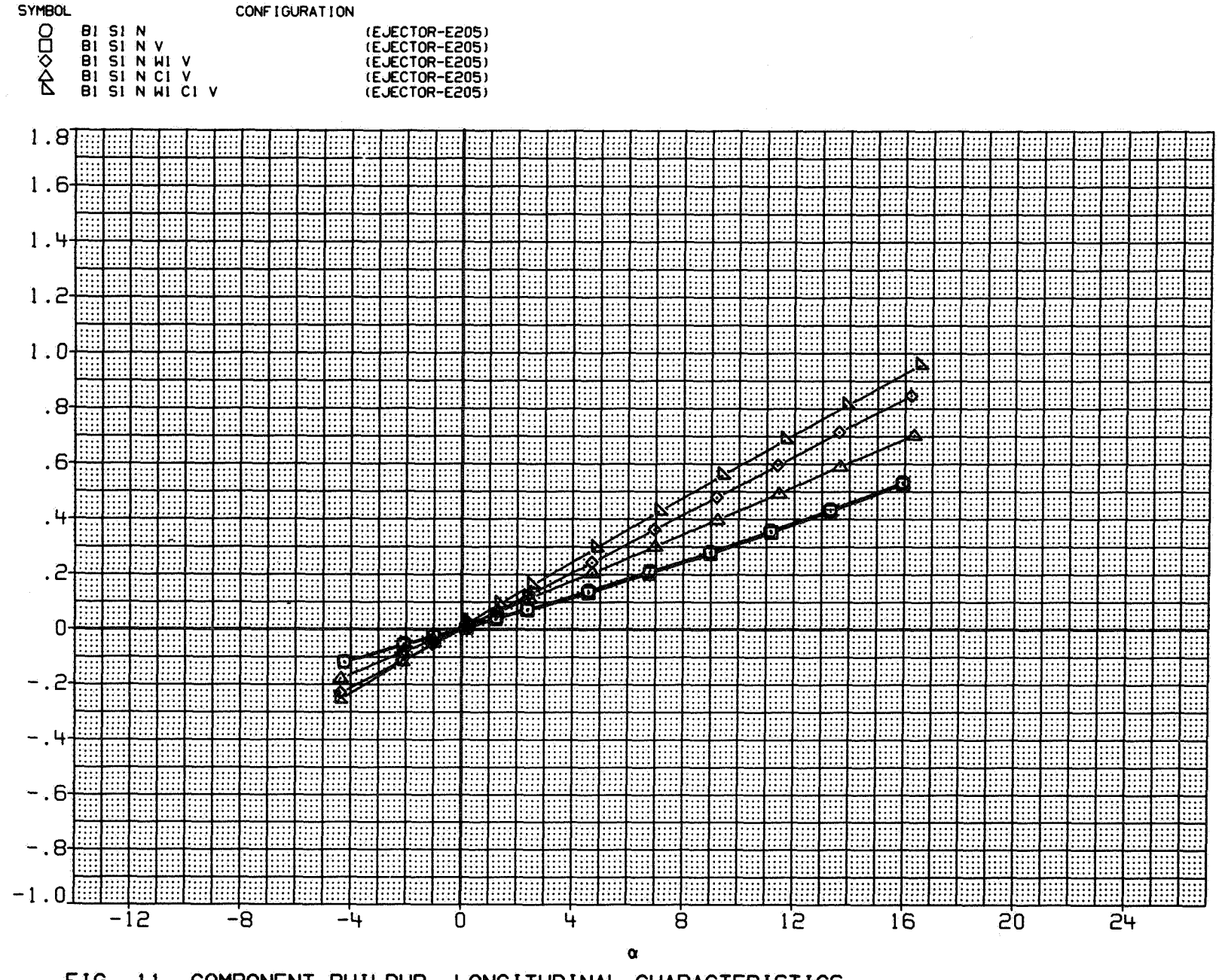


FIG. 11 COMPONENT BUILDUP, LONGITUDINAL CHARACTERISTICS

MACH = 2.00

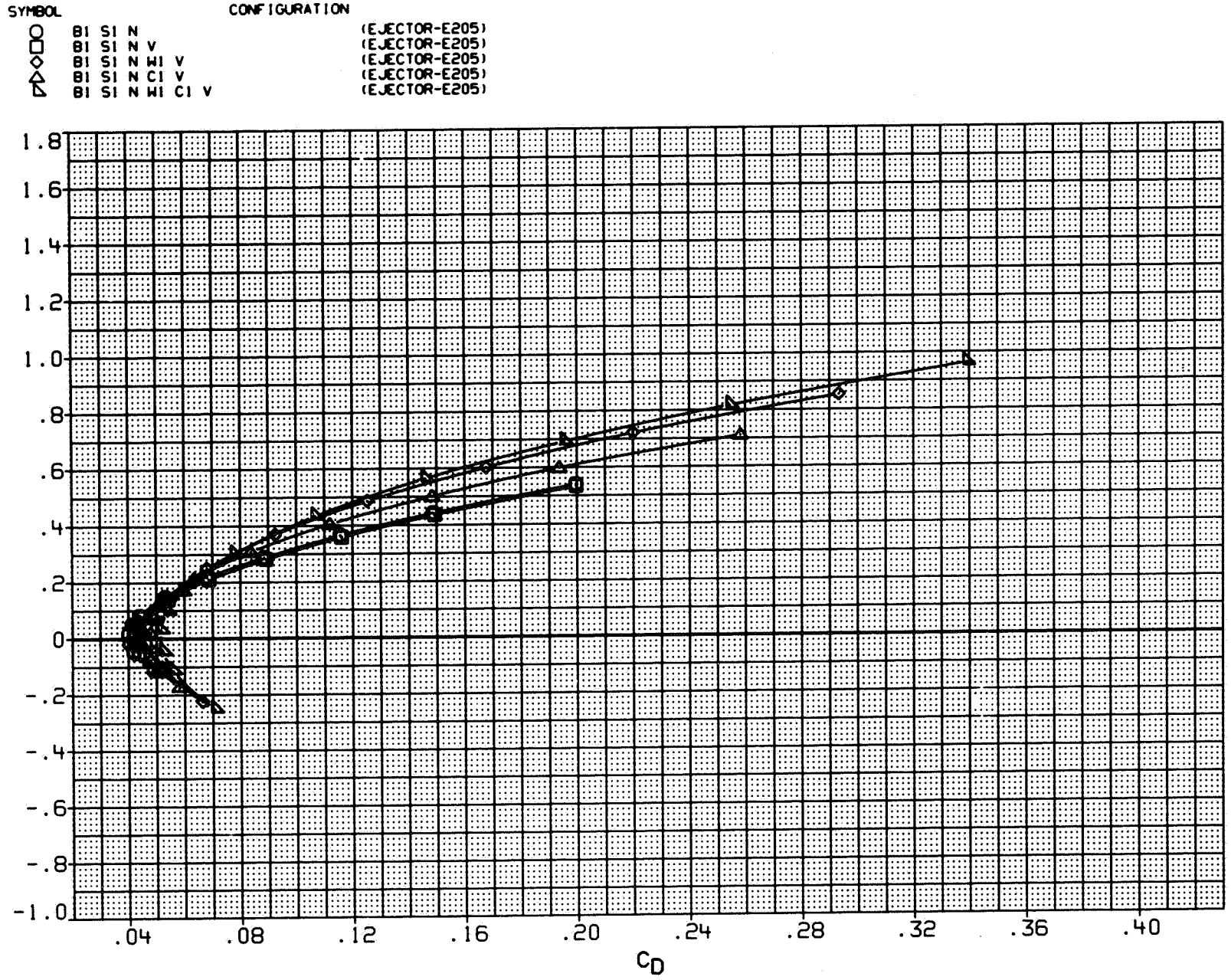


FIG. 11 COMPONENT BUILDUP, LONGITUDINAL CHARACTERISTICS

MACH = 2.00

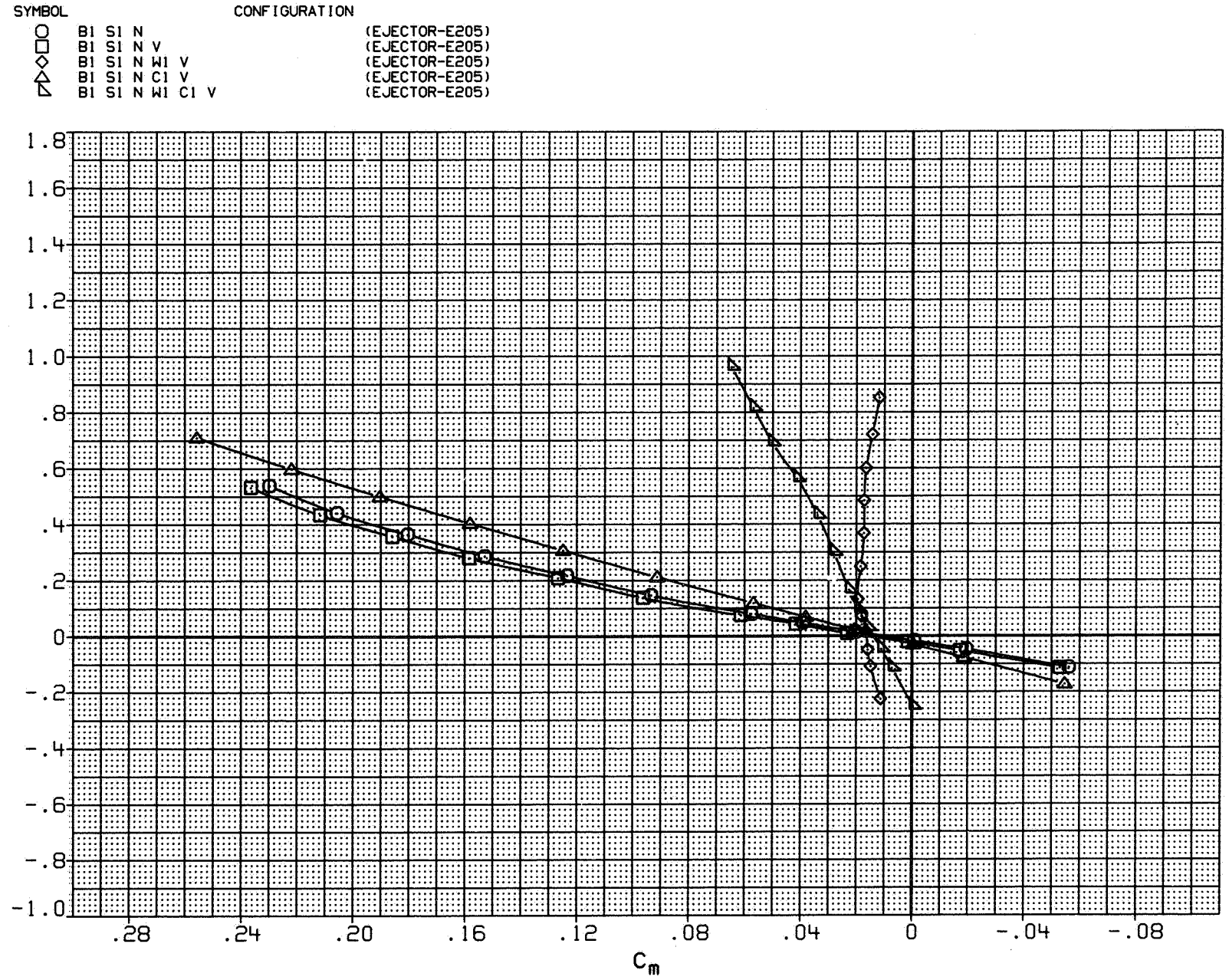


FIG. 11 COMPONENT BUILDUP, LONGITUDINAL CHARACTERISTICS

MACH = 2.00

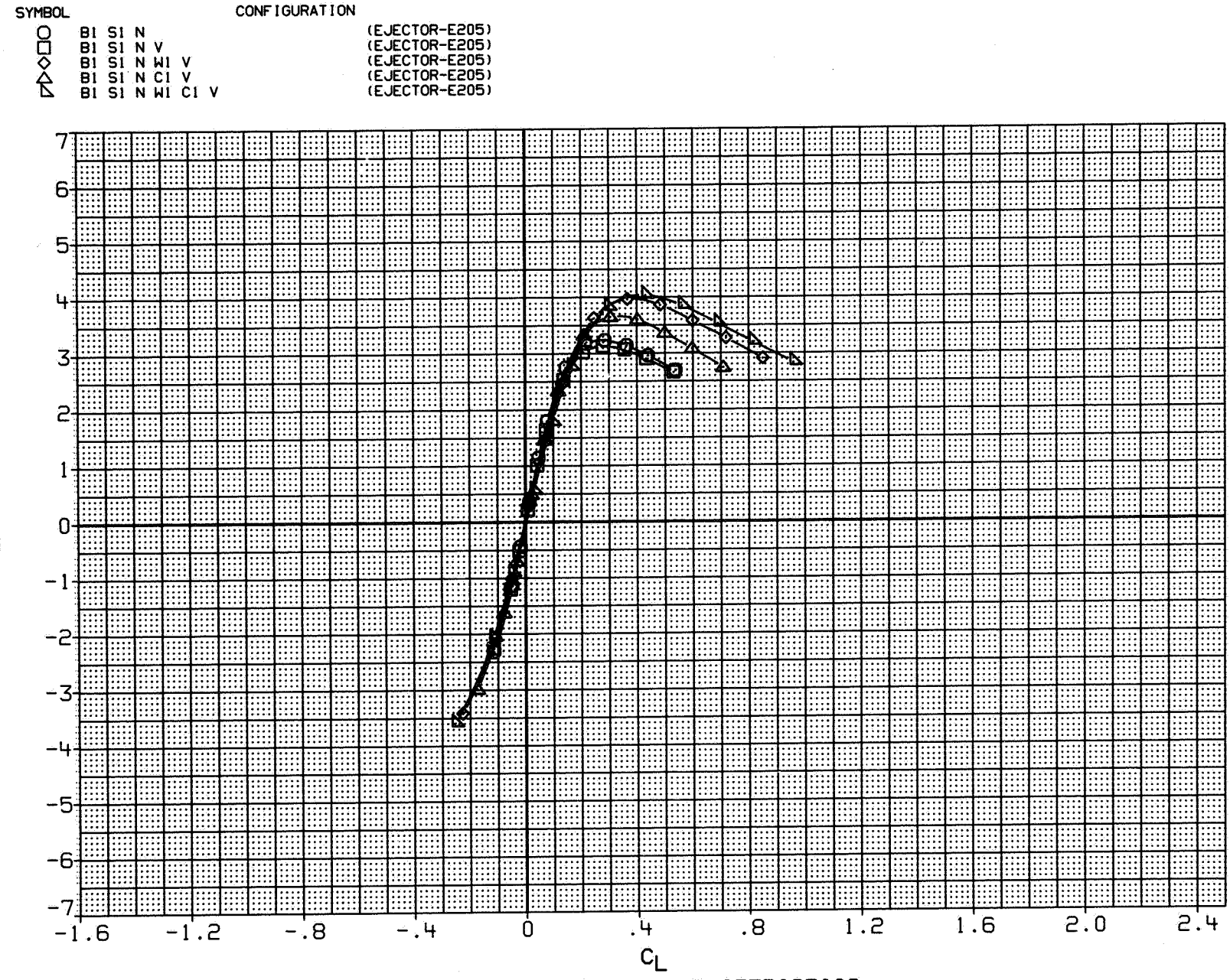


FIG. 11 COMPONENT BUILDUP, LONGITUDINAL CHARACTERISTICS

MACH = 2.00

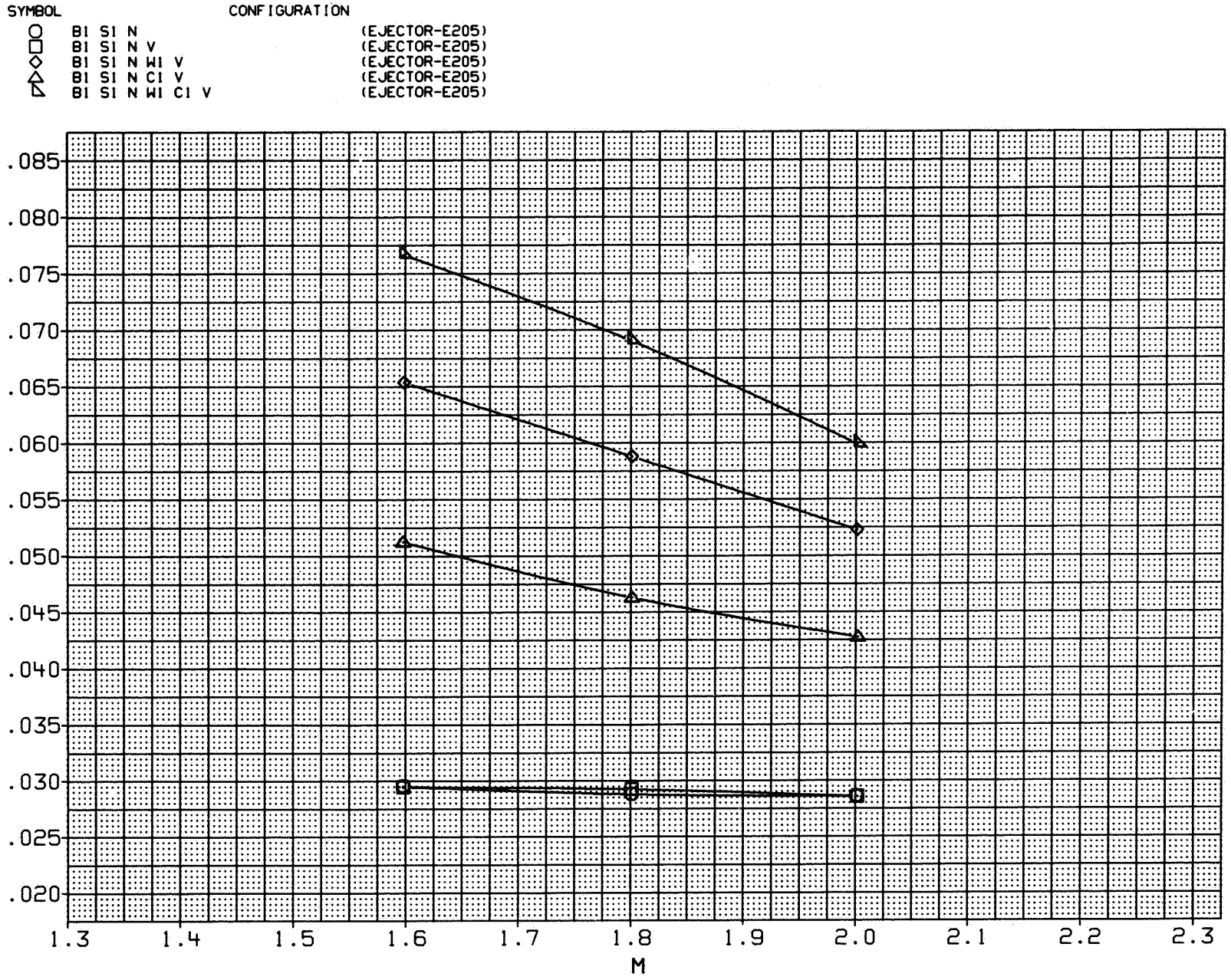


FIG. 12 SUMMARY OF COMPONENT BUILDUP WITH MACH NUMBER

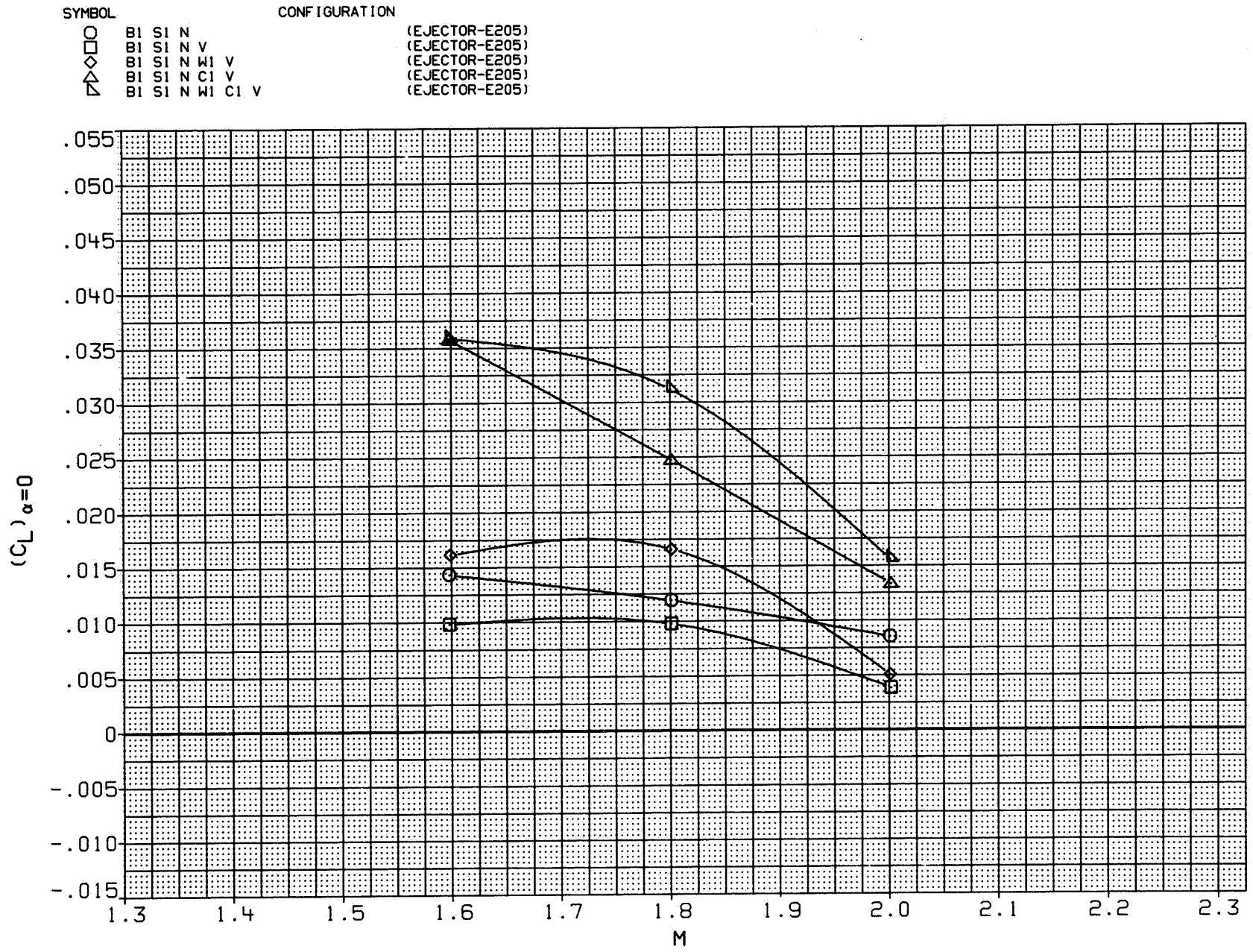


FIG. 12 SUMMARY OF COMPONENT BUILDUP WITH MACH NUMBER

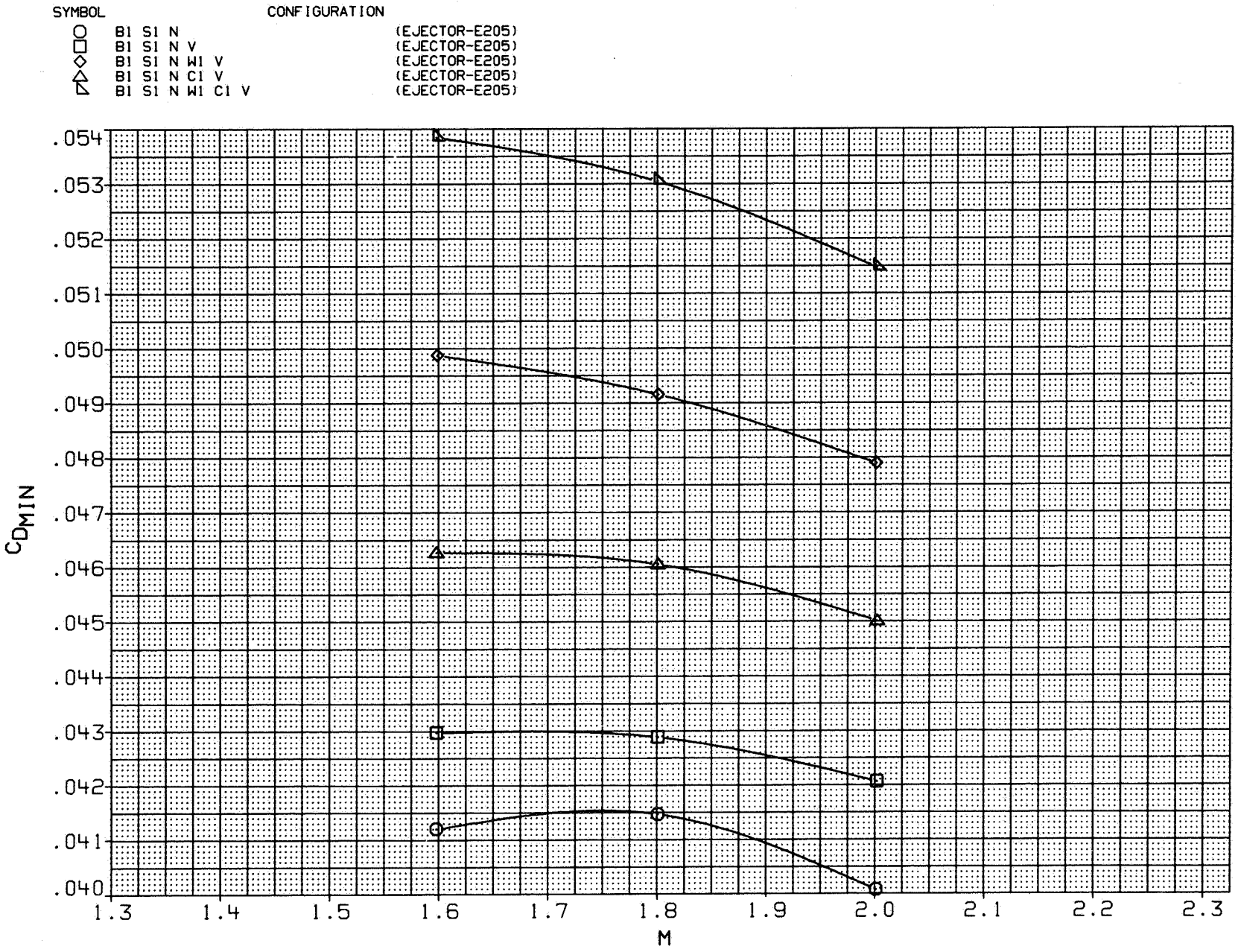


FIG. 12 SUMMARY OF COMPONENT BUILDUP WITH MACH NUMBER

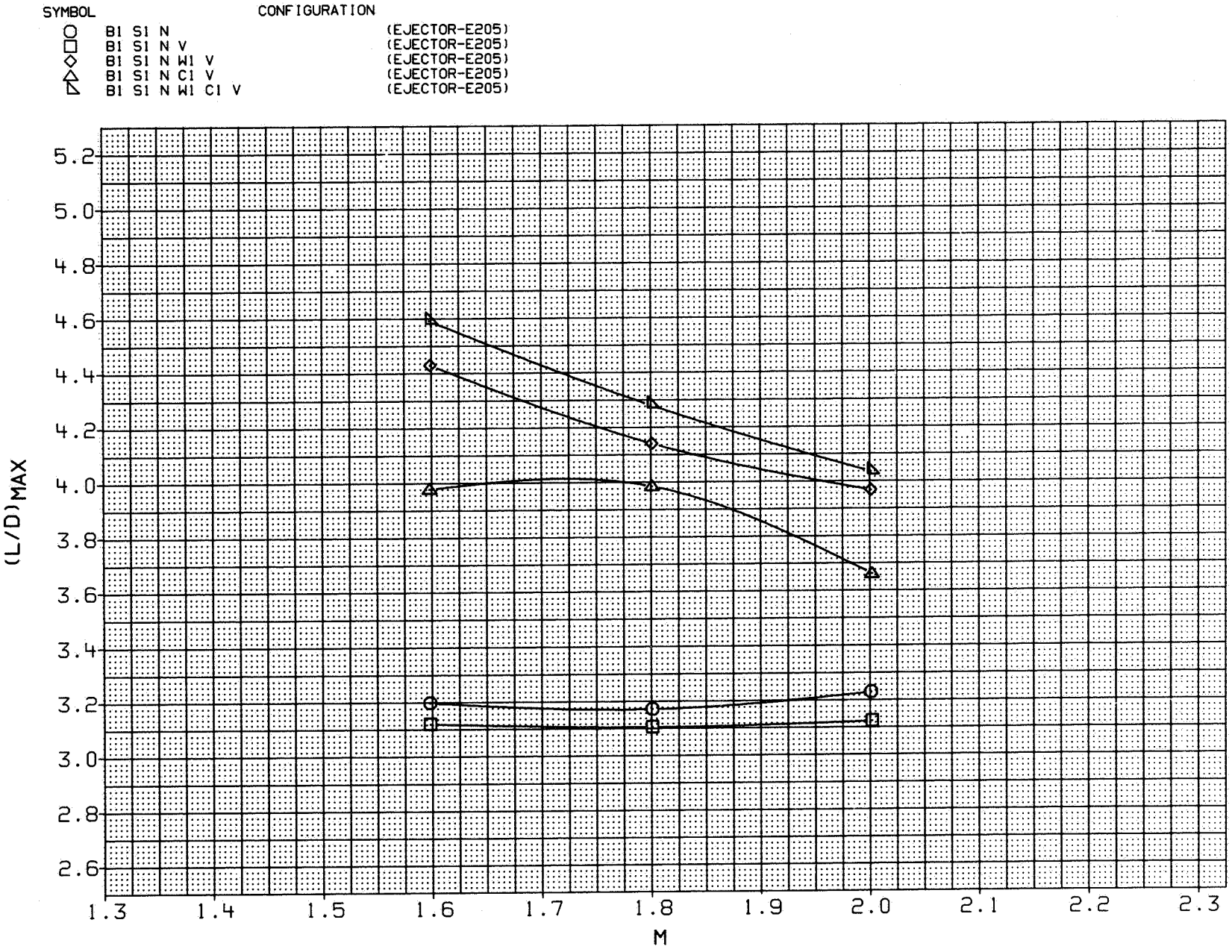


FIG. 12 SUMMARY OF COMPONENT BUILDUP WITH MACH NUMBER

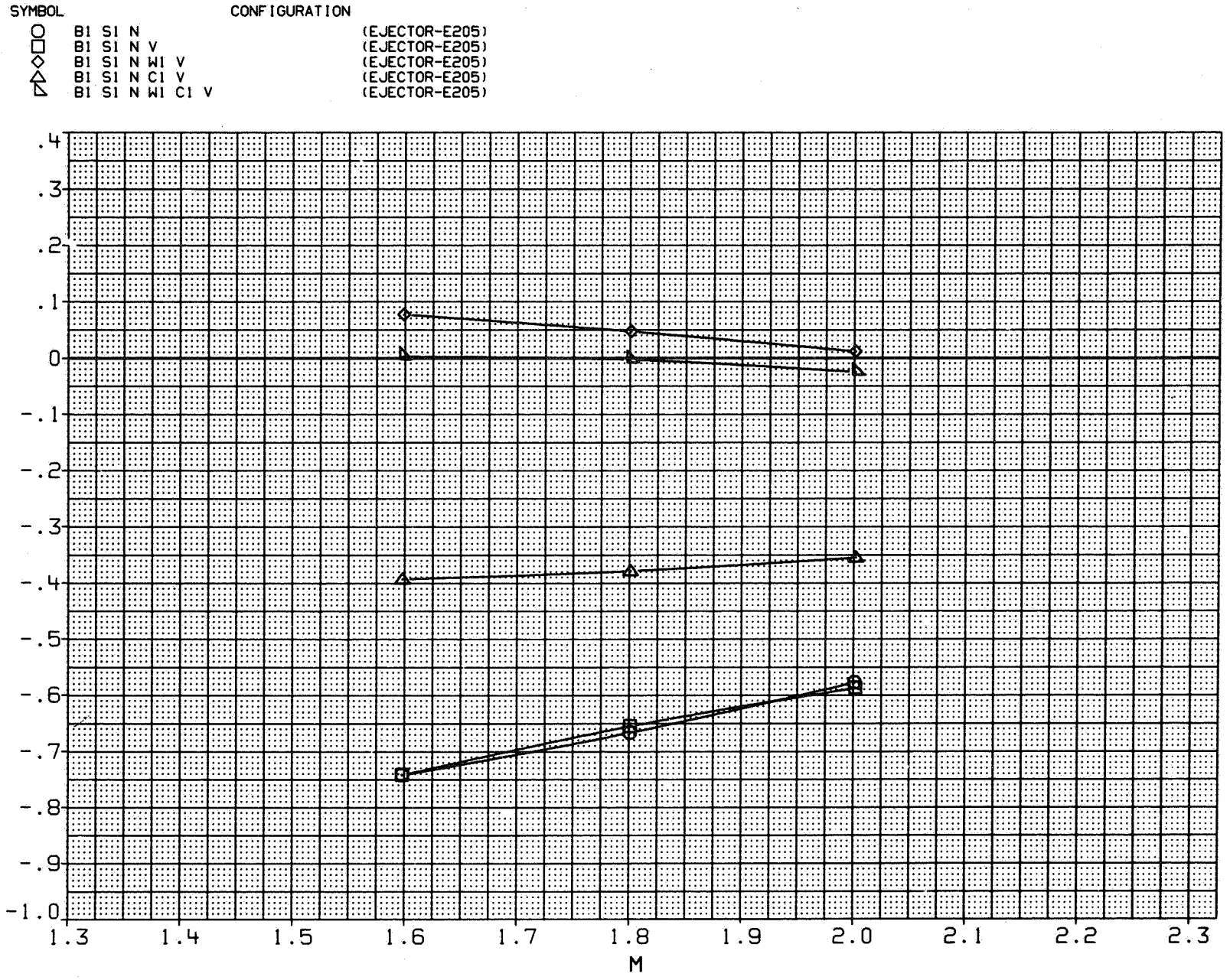


FIG. 12 SUMMARY OF COMPONENT BUILDUP WITH MACH NUMBER

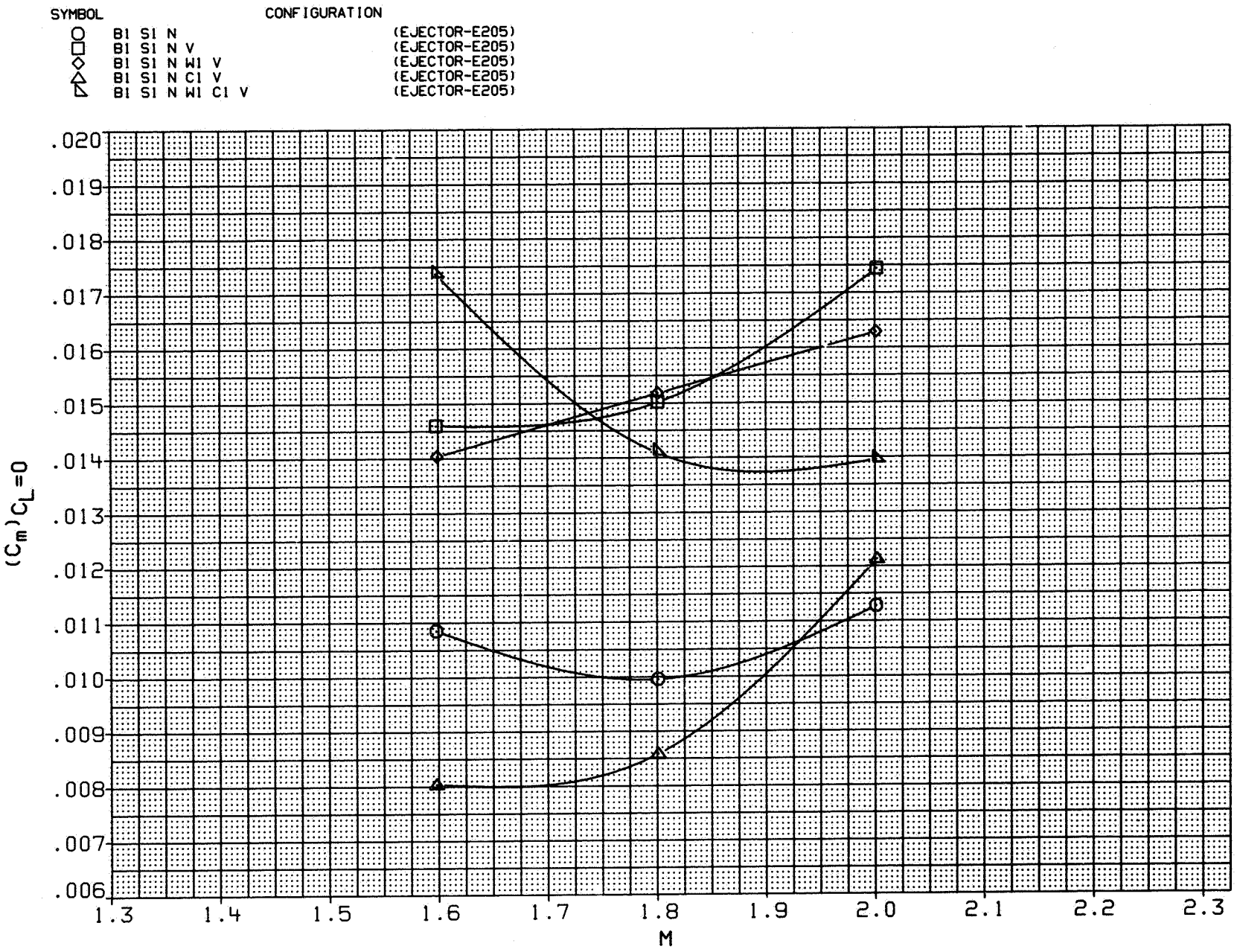


FIG. 12 SUMMARY OF COMPONENT BUILDUP WITH MACH NUMBER

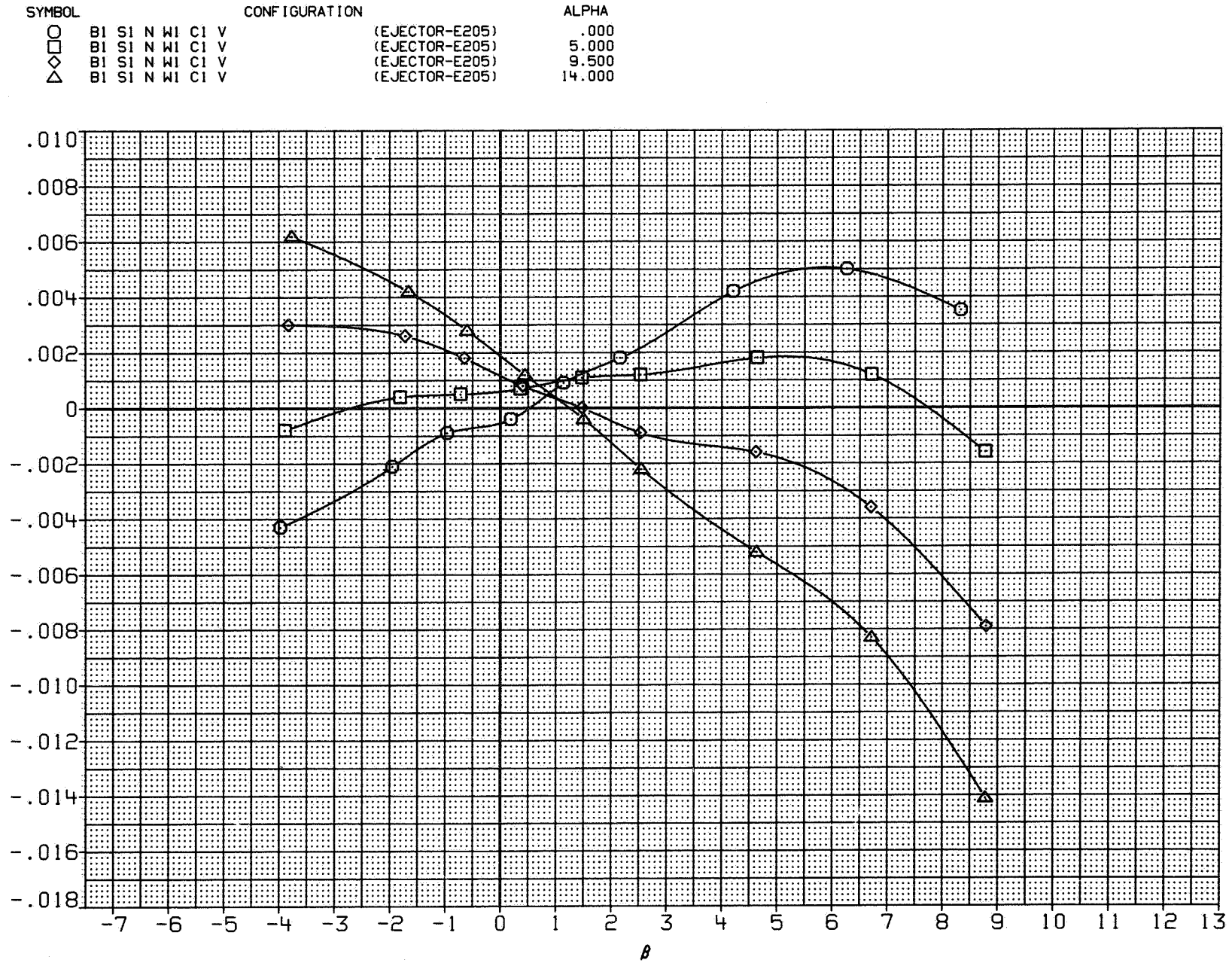


FIG. 13 BASIC LATERAL/DIRECTIONAL CHARACTERISTICS FOR VARIOUS ALPHA

MACH = 1.60

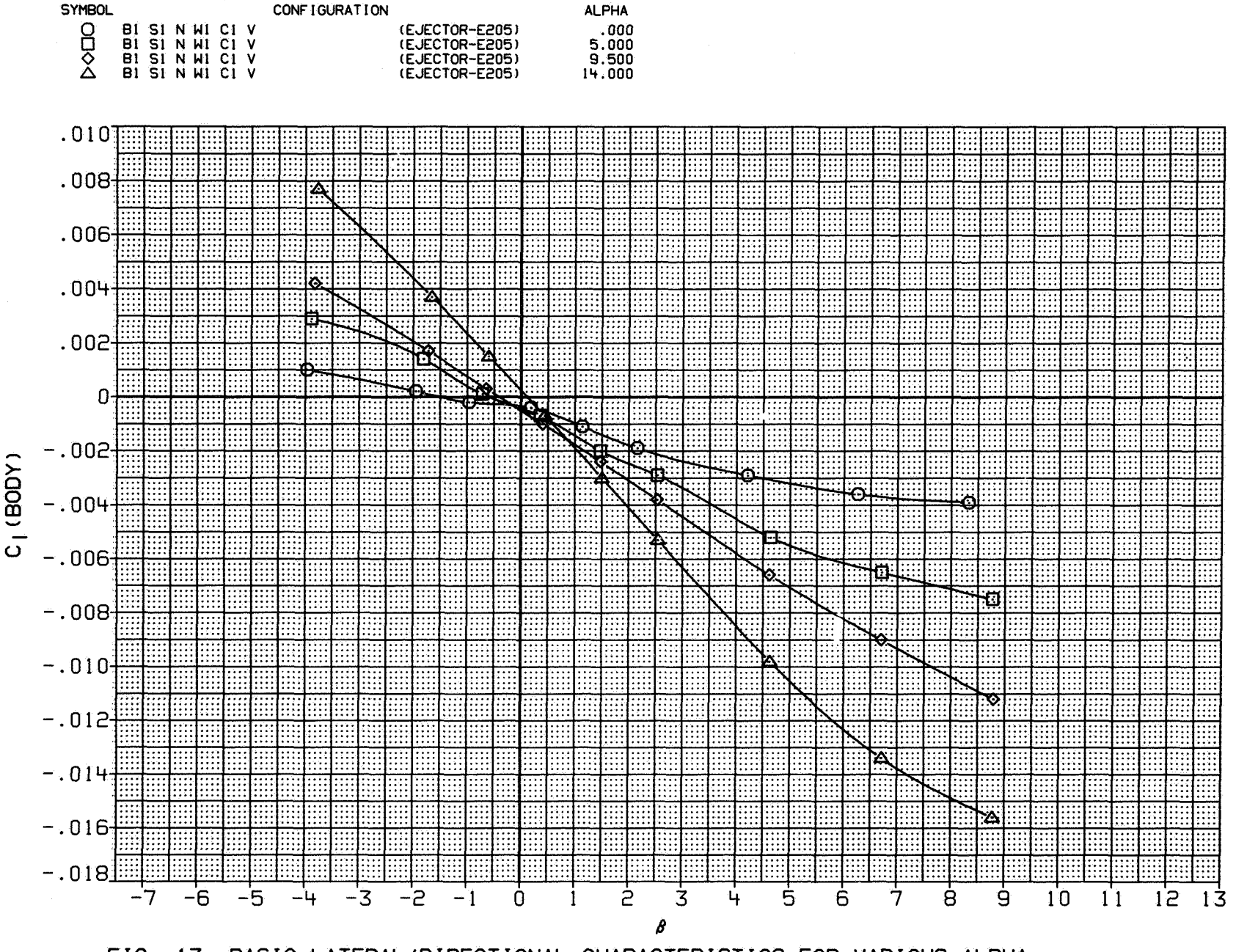


FIG. 13 BASIC LATERAL/DIRECTIONAL CHARACTERISTICS FOR VARIOUS ALPHA

MACH = 1.60

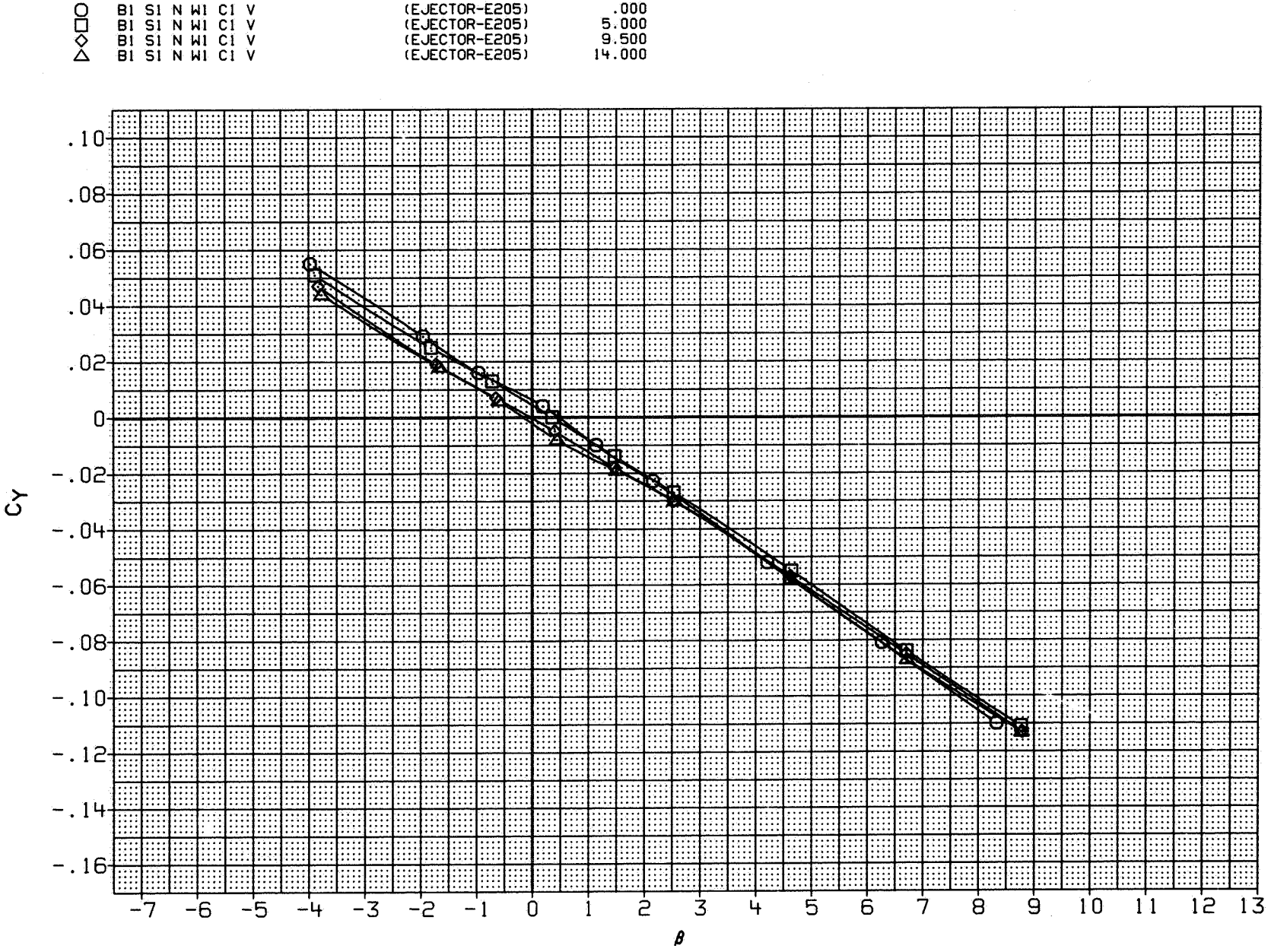


FIG. 13 BASIC LATERAL/DIRECTIONAL CHARACTERISTICS FOR VARIOUS ALPHA

MACH = 1.60

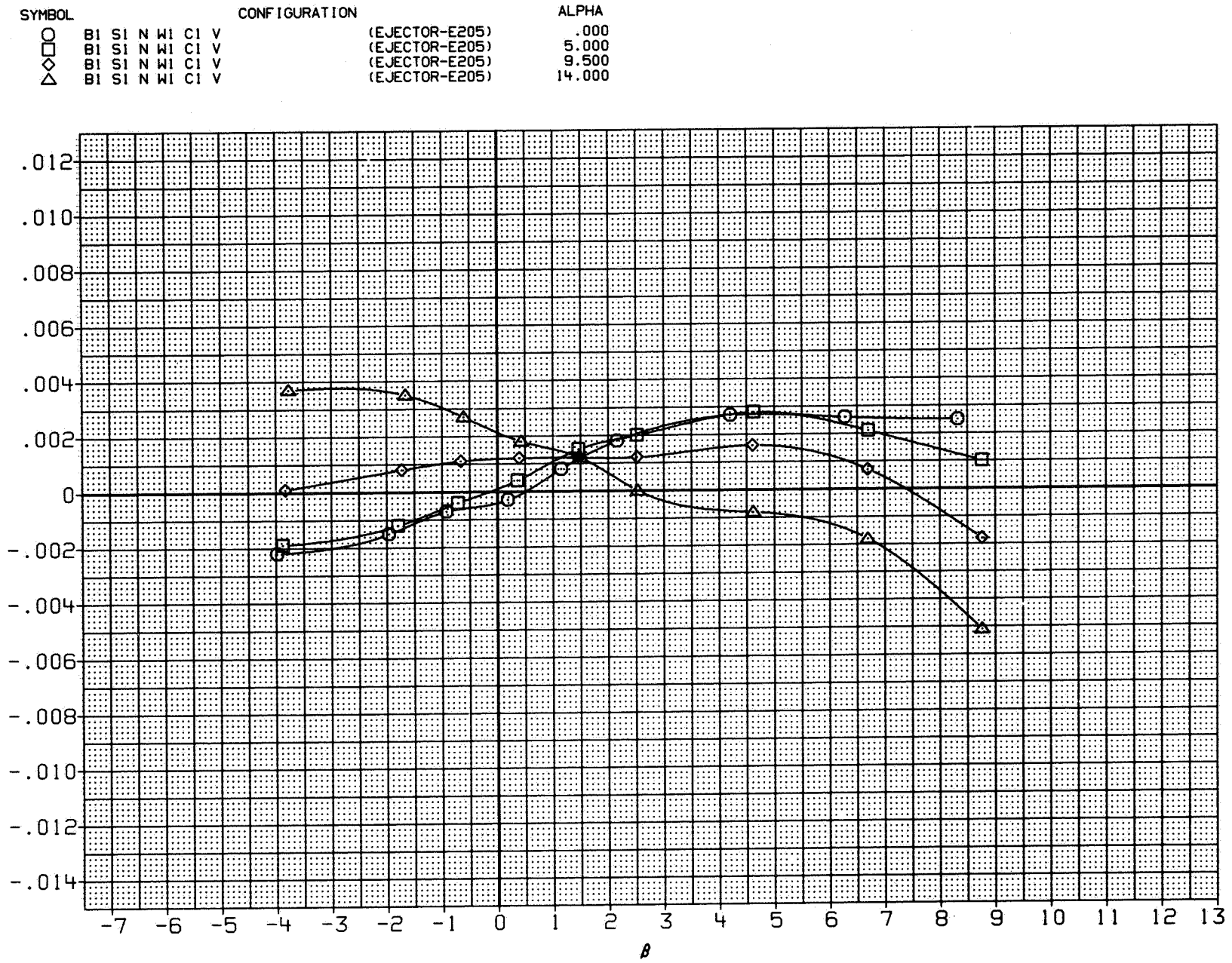


FIG. 14 BASIC LATERAL/DIRECTIONAL CHARACTERISTICS FOR VARIOUS ALPHA

MACH = 2.00

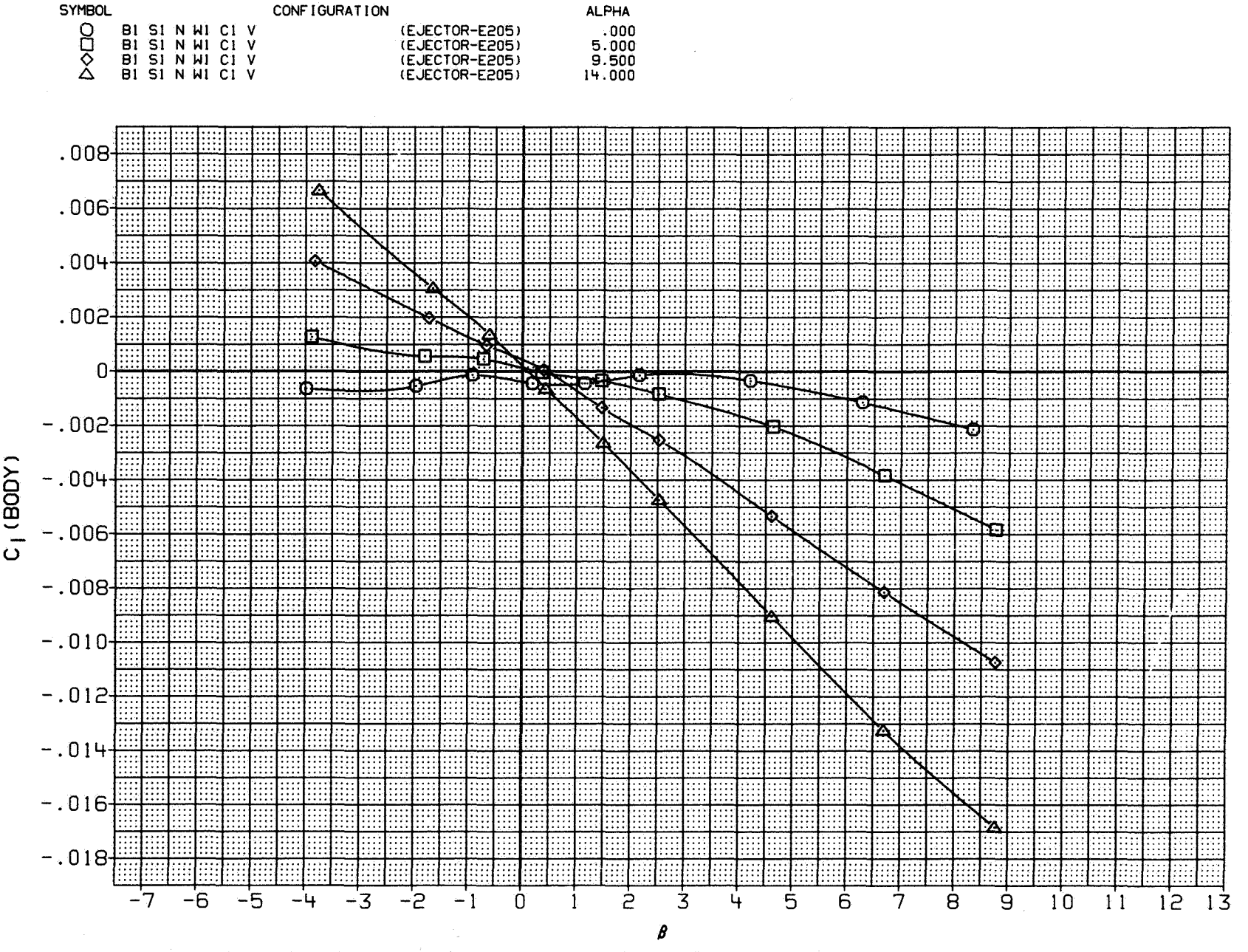


FIG. 14 BASIC LATERAL/DIRECTIONAL CHARACTERISTICS FOR VARIOUS ALPHA

MACH = 2.00

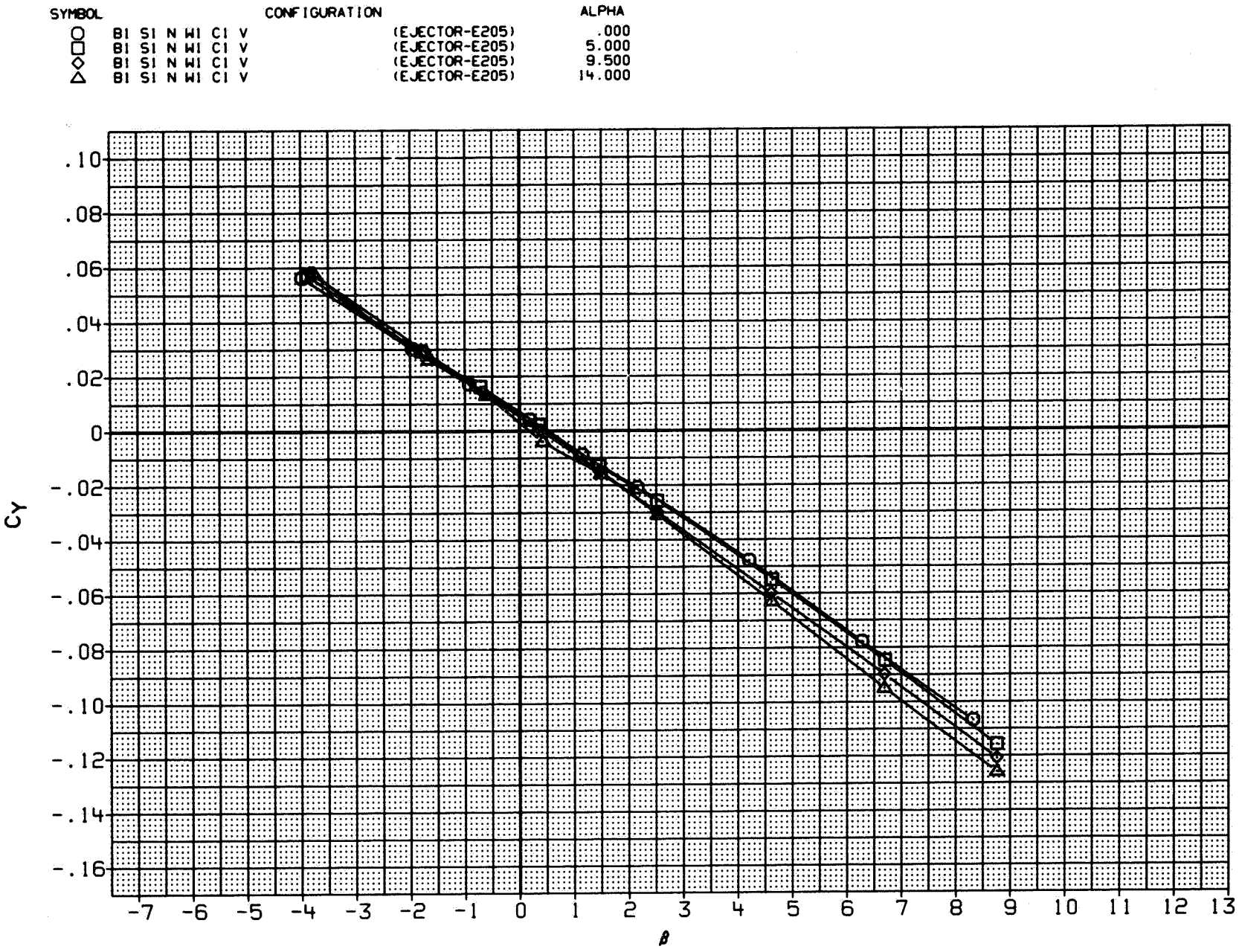


FIG. 14 BASIC LATERAL/DIRECTIONAL CHARACTERISTICS FOR VARIOUS ALPHA

MACH = 2.00

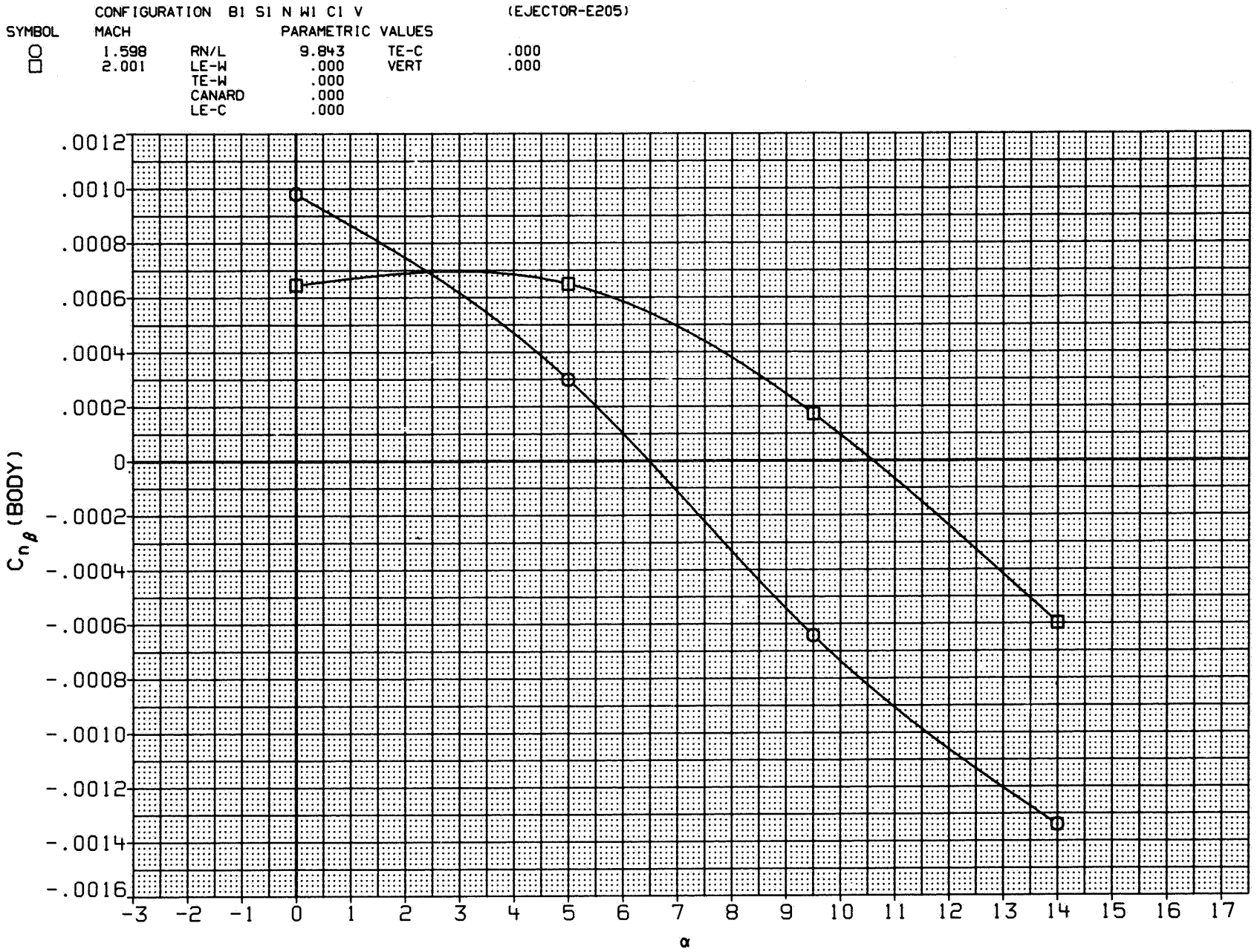


FIG. 15 SUMMARY OF BASIC LATERAL/DIRECTIONAL CHARACTERISTICS WITH ALPHA

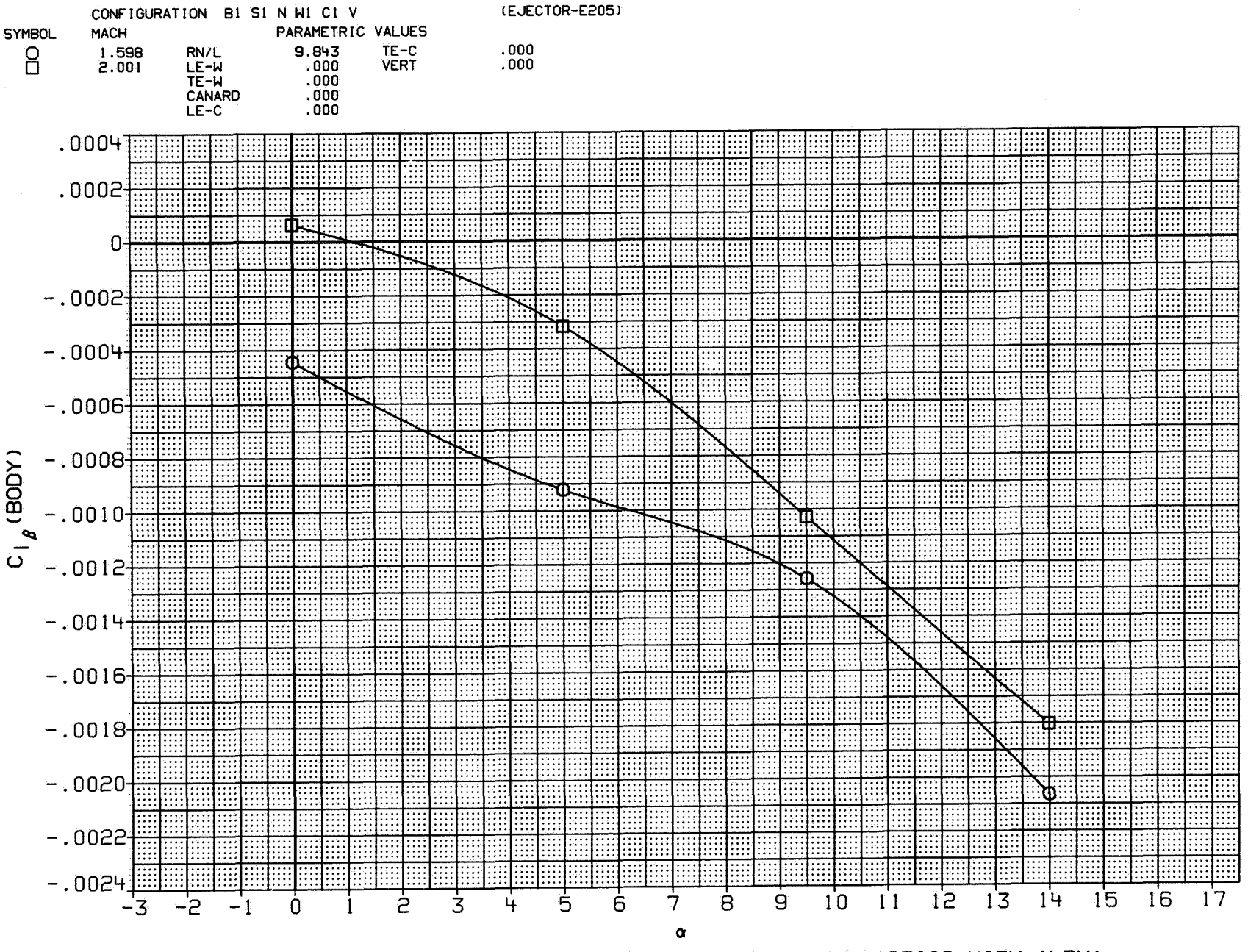


FIG. 15 SUMMARY OF BASIC LATERAL/DIRECTIONAL CHARACTERISTICS WITH ALPHA

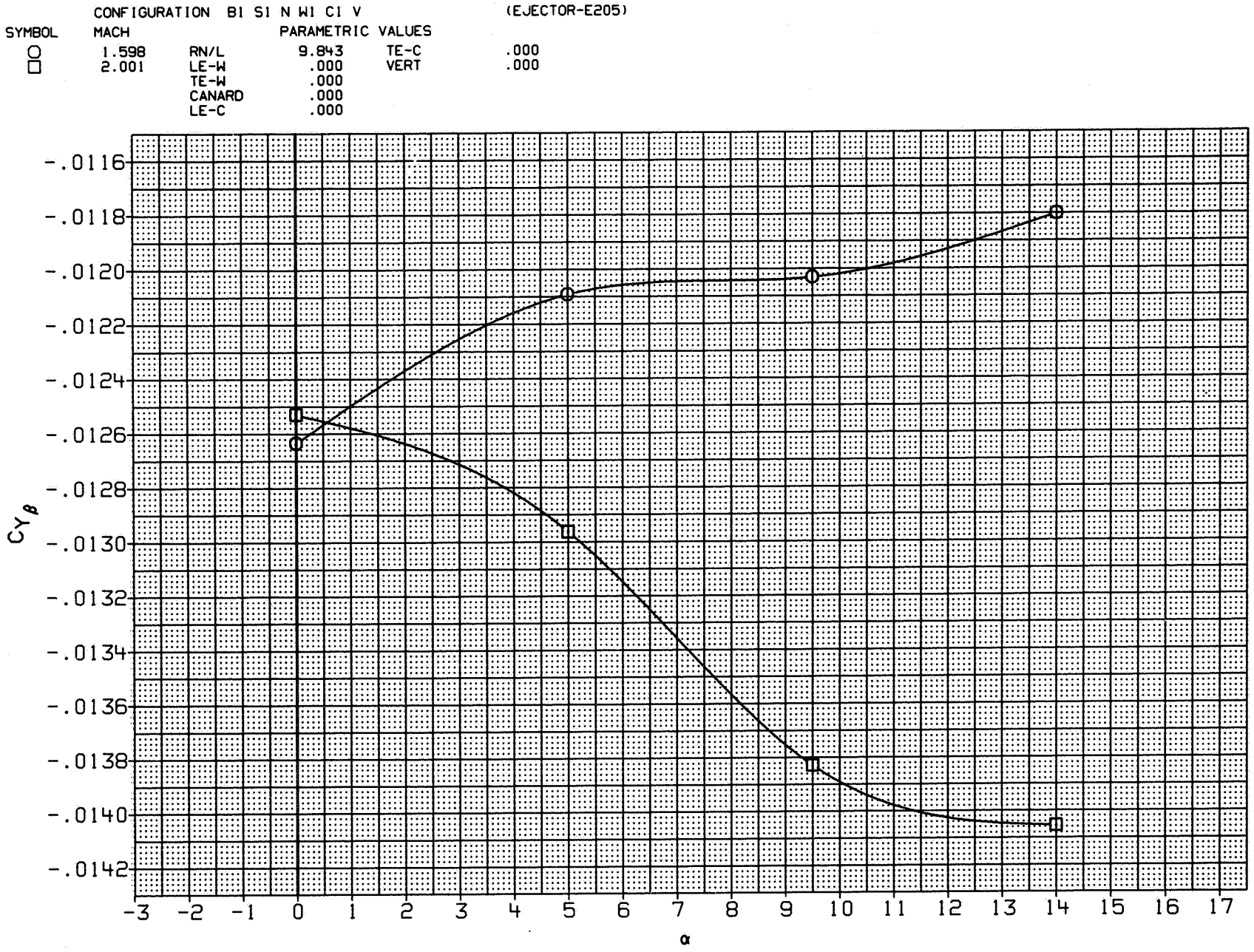


FIG. 15 SUMMARY OF BASIC LATERAL/DIRECTIONAL CHARACTERISTICS WITH ALPHA

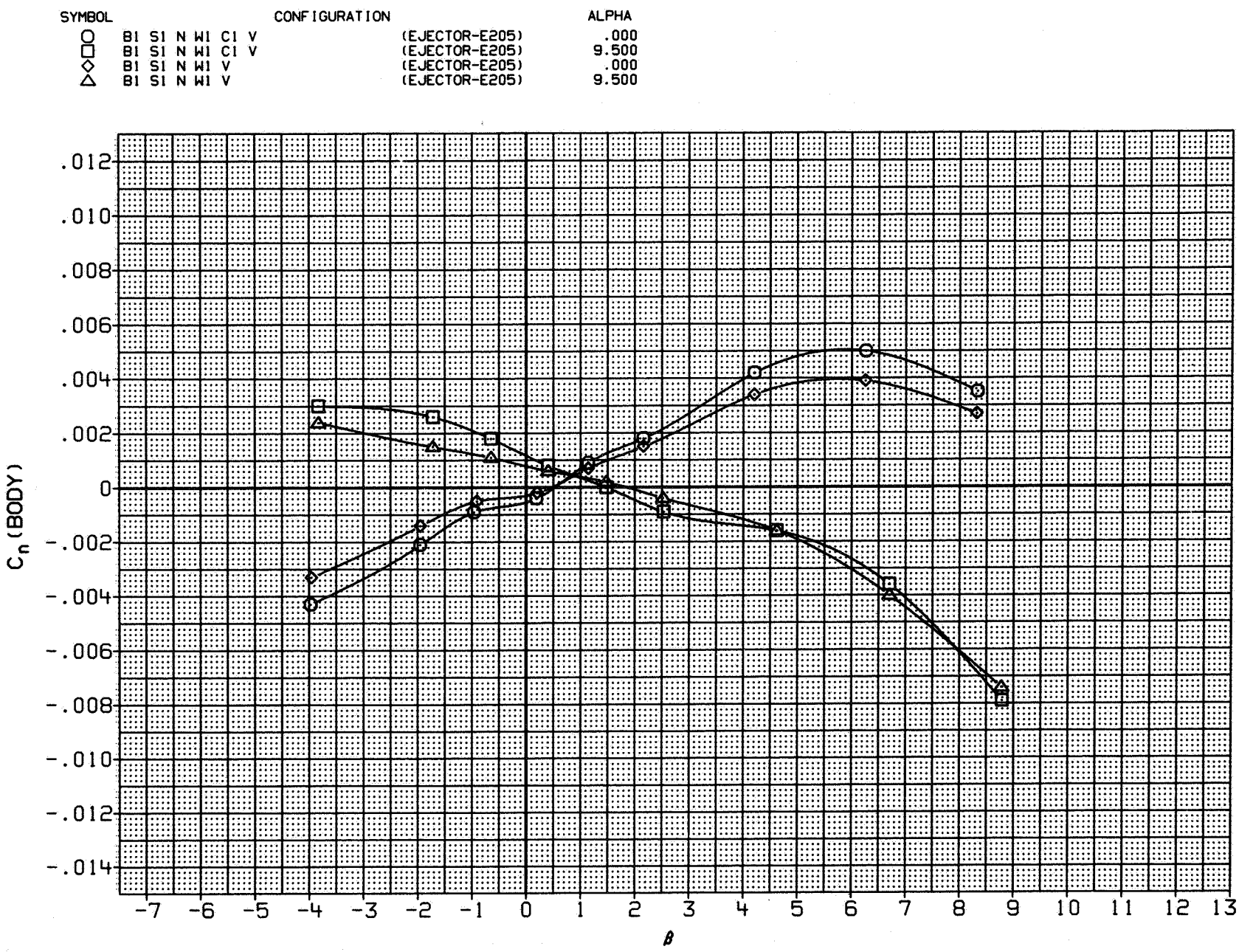


FIG. 16 LATERAL/DIRECTIONAL CHARACTERISTICS, CANARD ON/OFF

MACH = 1.60

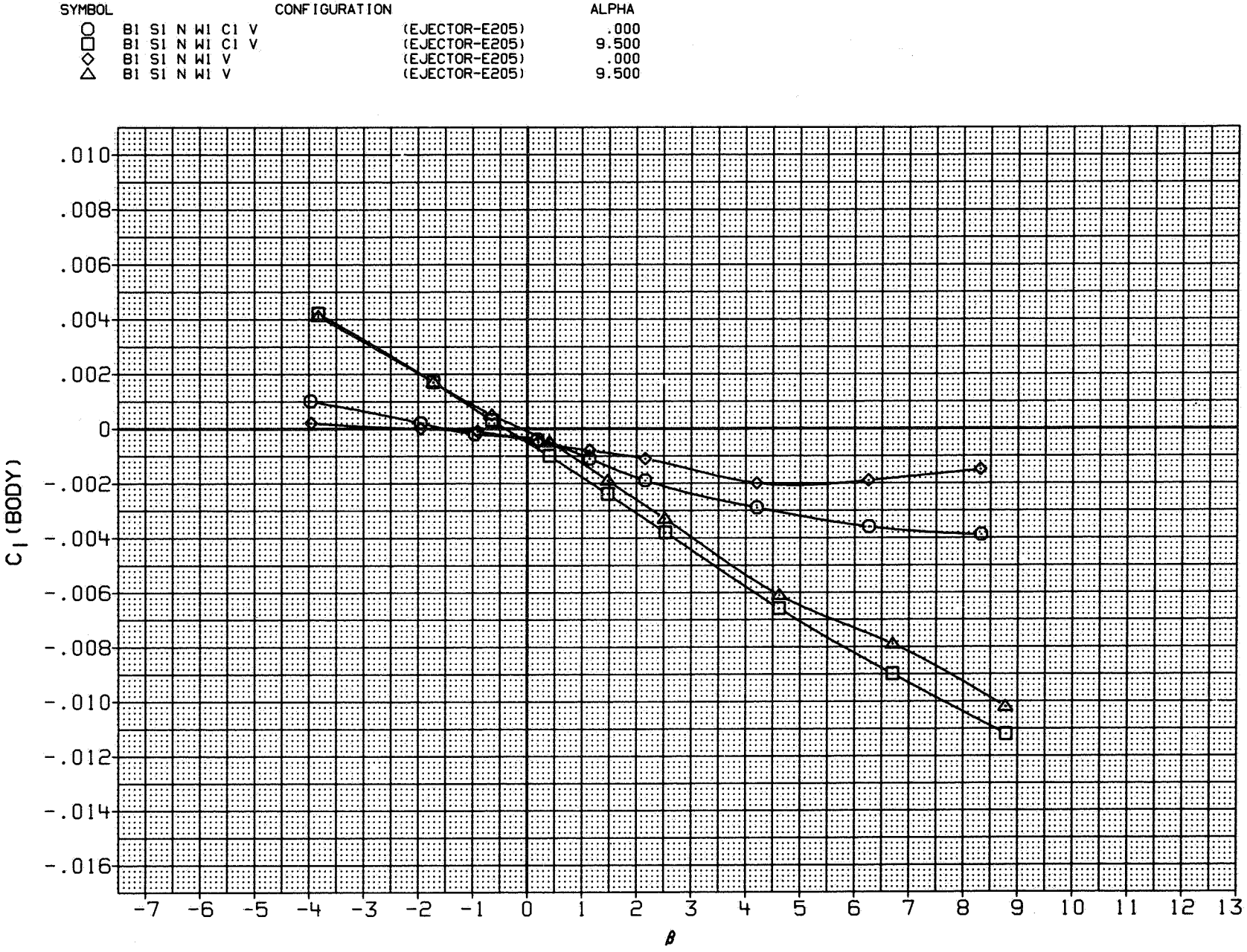


FIG. 16 LATERAL/DIRECTIONAL CHARACTERISTICS, CANARD ON/OFF

MACH = 1.60

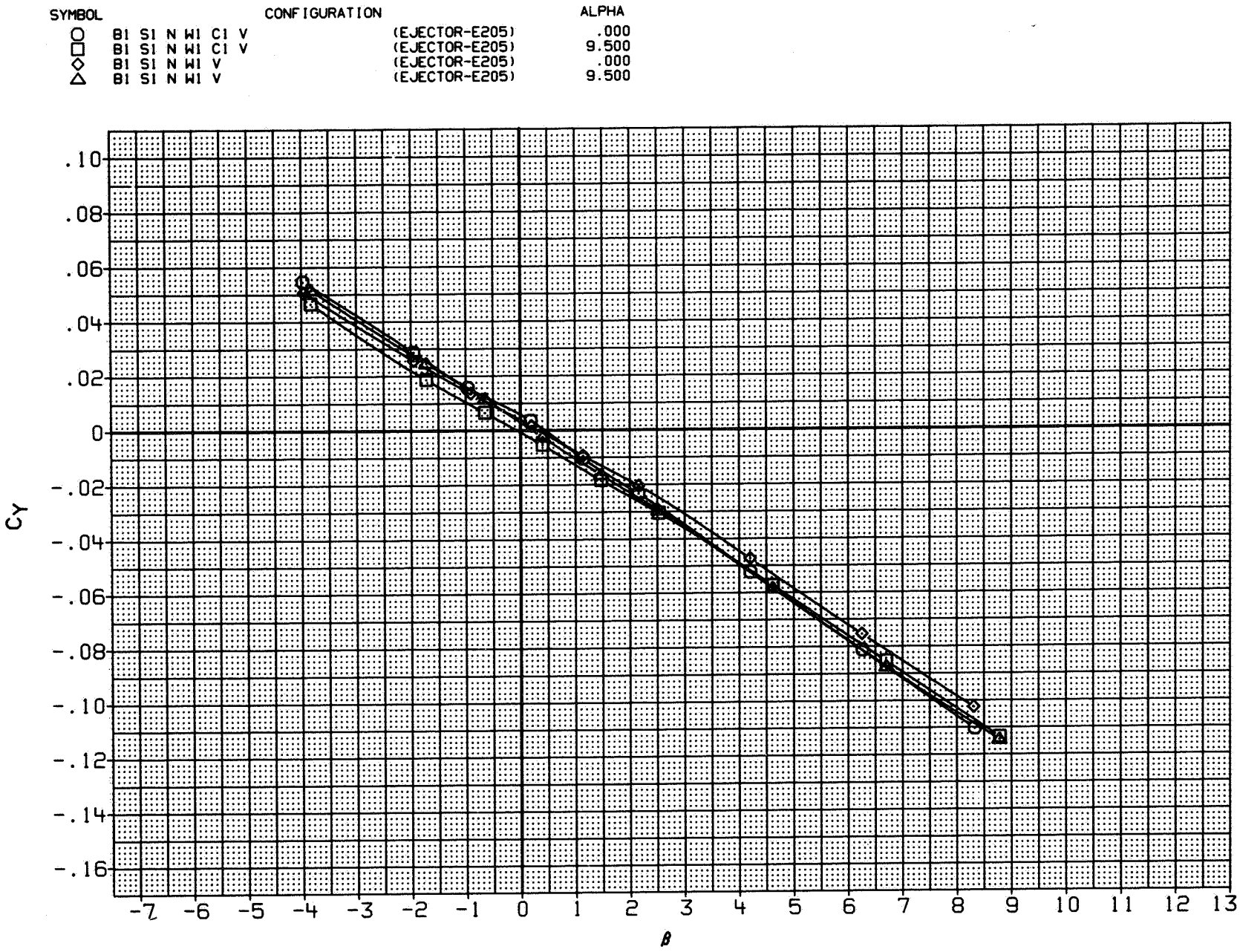


FIG. 16 LATERAL/DIRECTIONAL CHARACTERISTICS, CANARD ON/OFF

MACH = 1.60

| SYMBOL | CONFIGURATION | CANARD |
|---|---|---|
| ○ | B1 S1 N W1 V (EJECTOR-E205) | |
| □ | B1 S1 N W1 C1 V (EJECTOR-E205) | 10.000 |
| ◇ | B1 S1 N W1 C1 V (EJECTOR-E205) | .000 |
| △ | B1 S1 N W1 C1 V (EJECTOR-E205) | -10.000 |

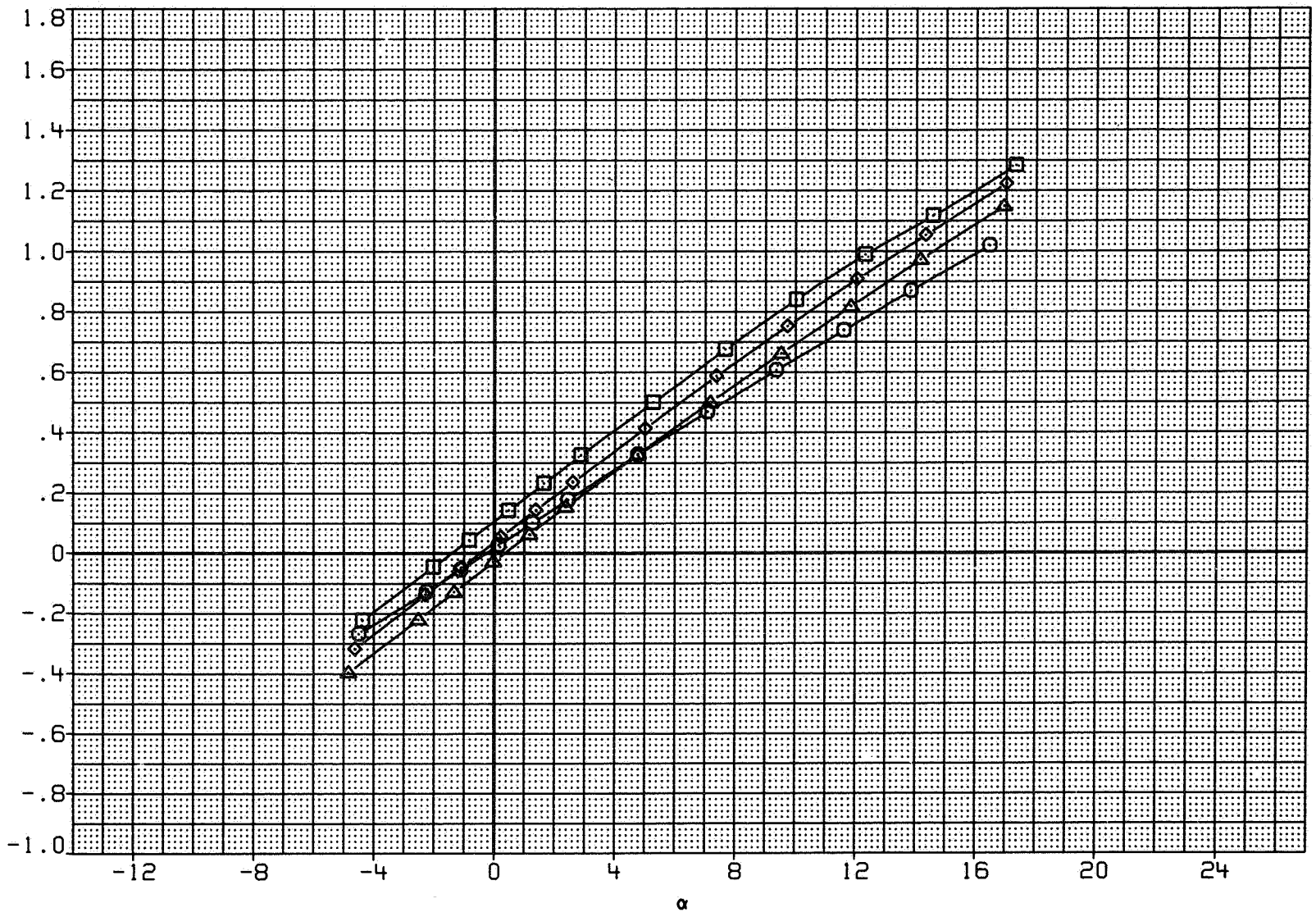


FIG. 17 CANARD INCIDENCE EFFECTS, TE-W = 0 DEGREES

MACH = 1.60

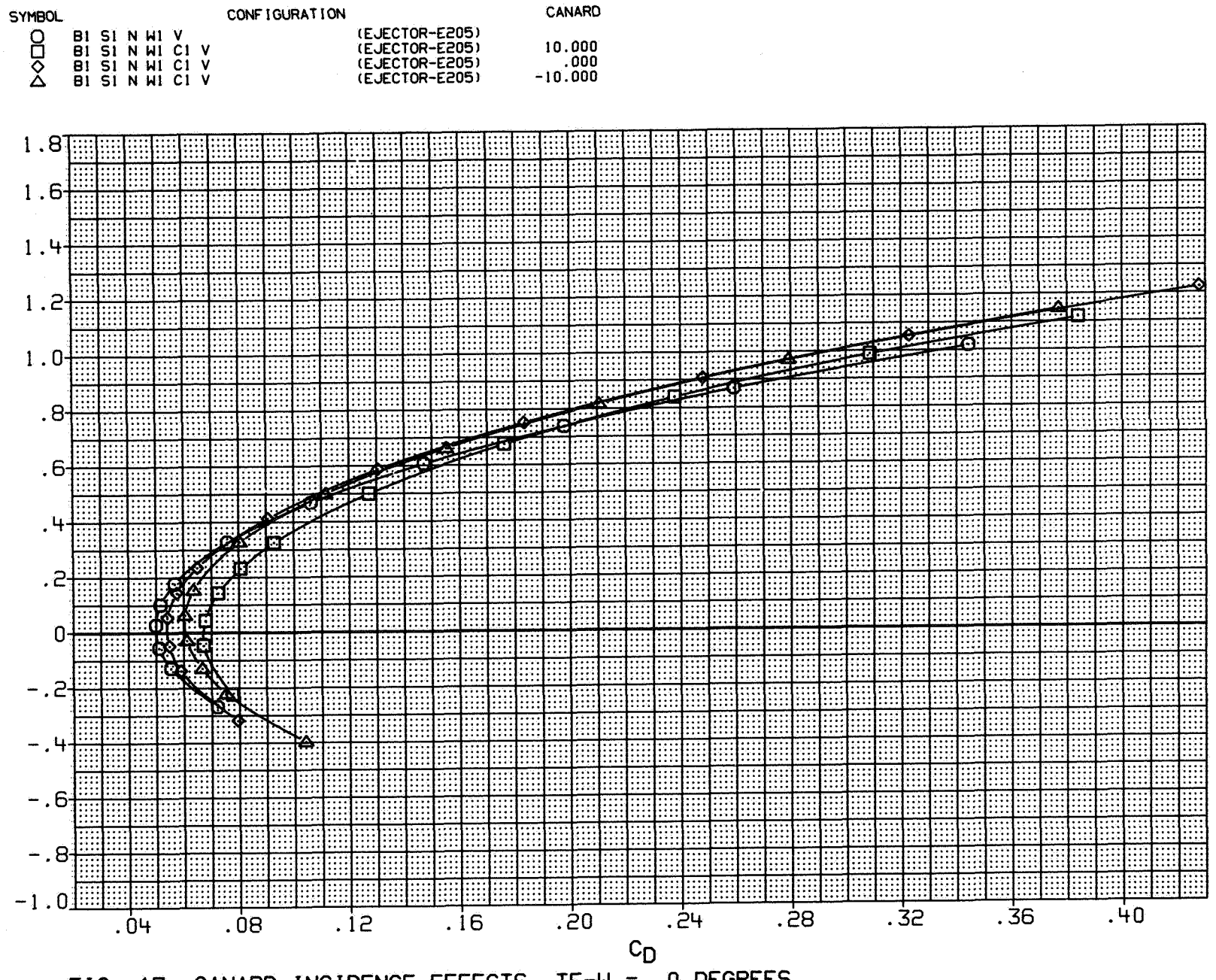


FIG. 17 CANARD INCIDENCE EFFECTS, TE-W = 0 DEGREES

MACH = 1.60

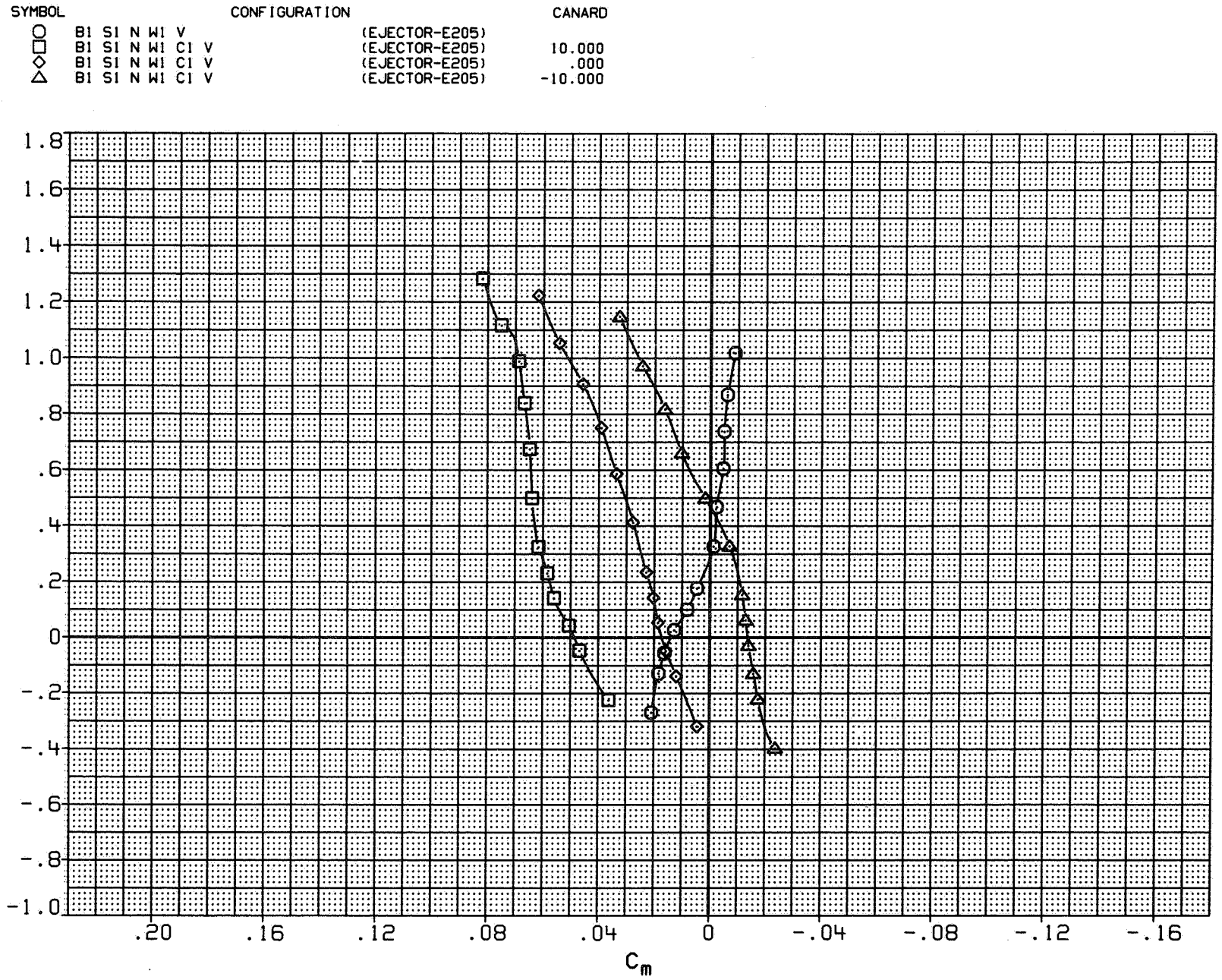


FIG. 17 CANARD INCIDENCE EFFECTS, TE-W = 0 DEGREES

MACH = 1.60

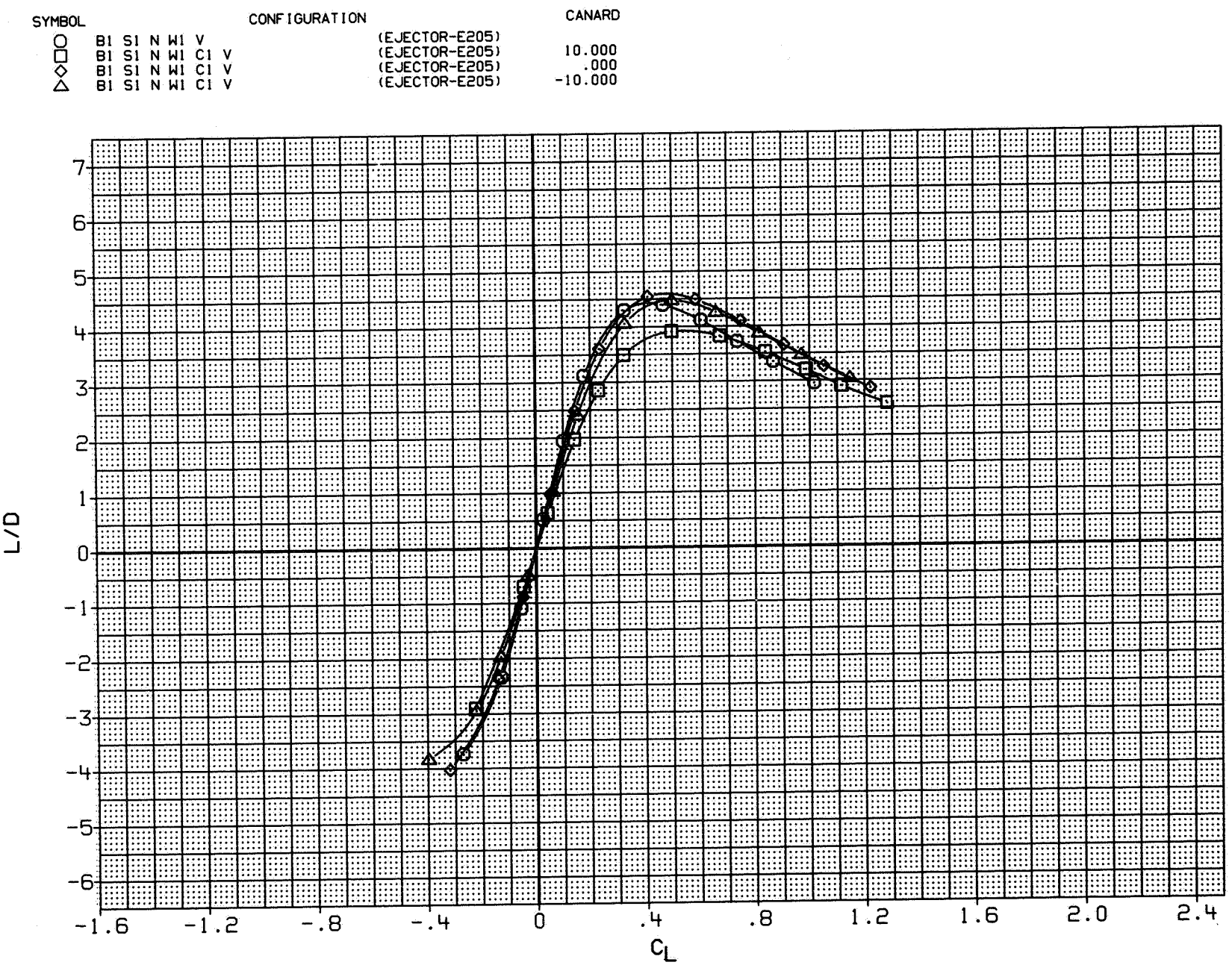


FIG. 17 CANARD INCIDENCE EFFECTS, TE-W = 0 DEGREES

MACH = 1.60

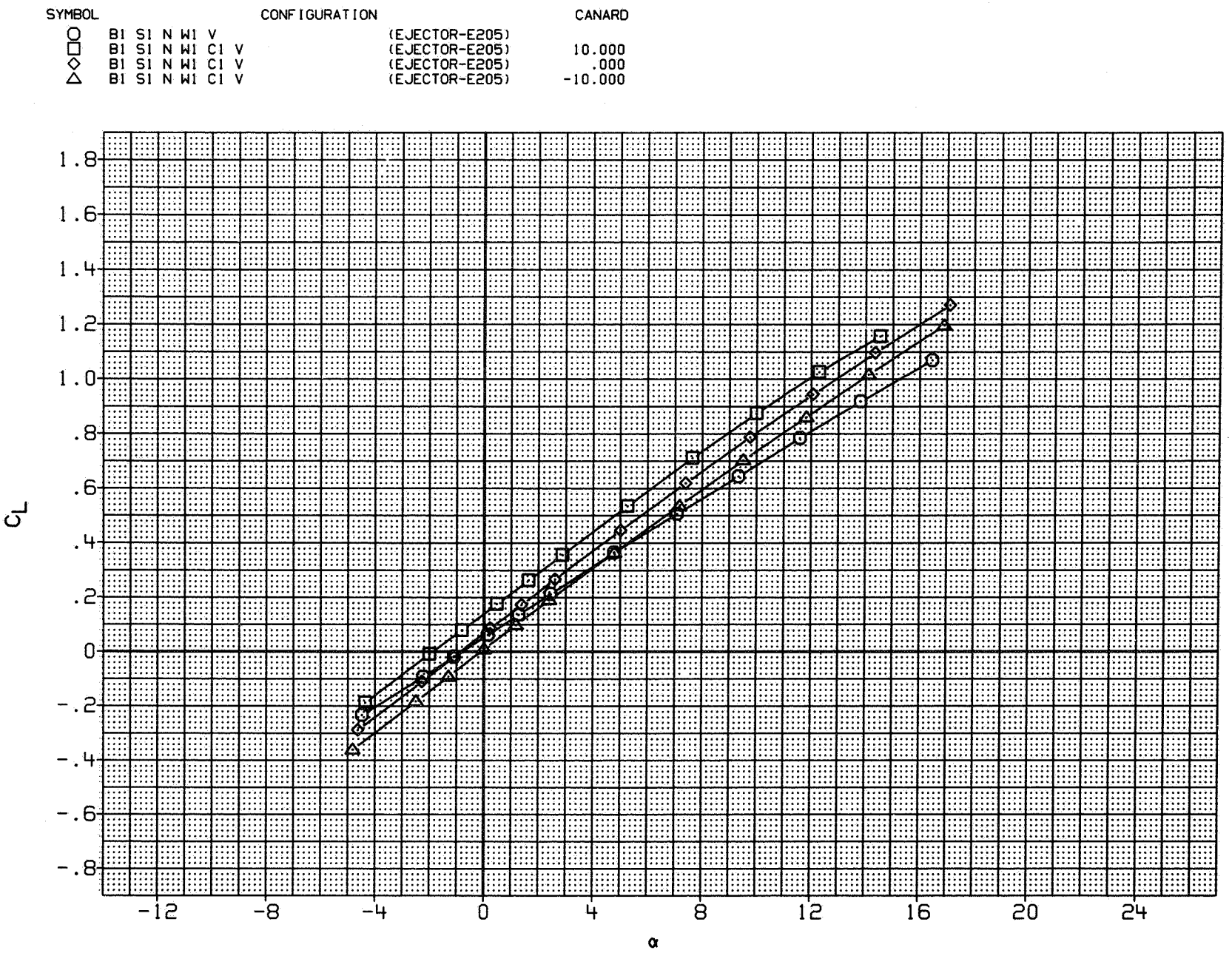


FIG. 18 CANARD INCIDENCE EFFECTS, TE-W = 10 DEGREES

MACH = 1.60

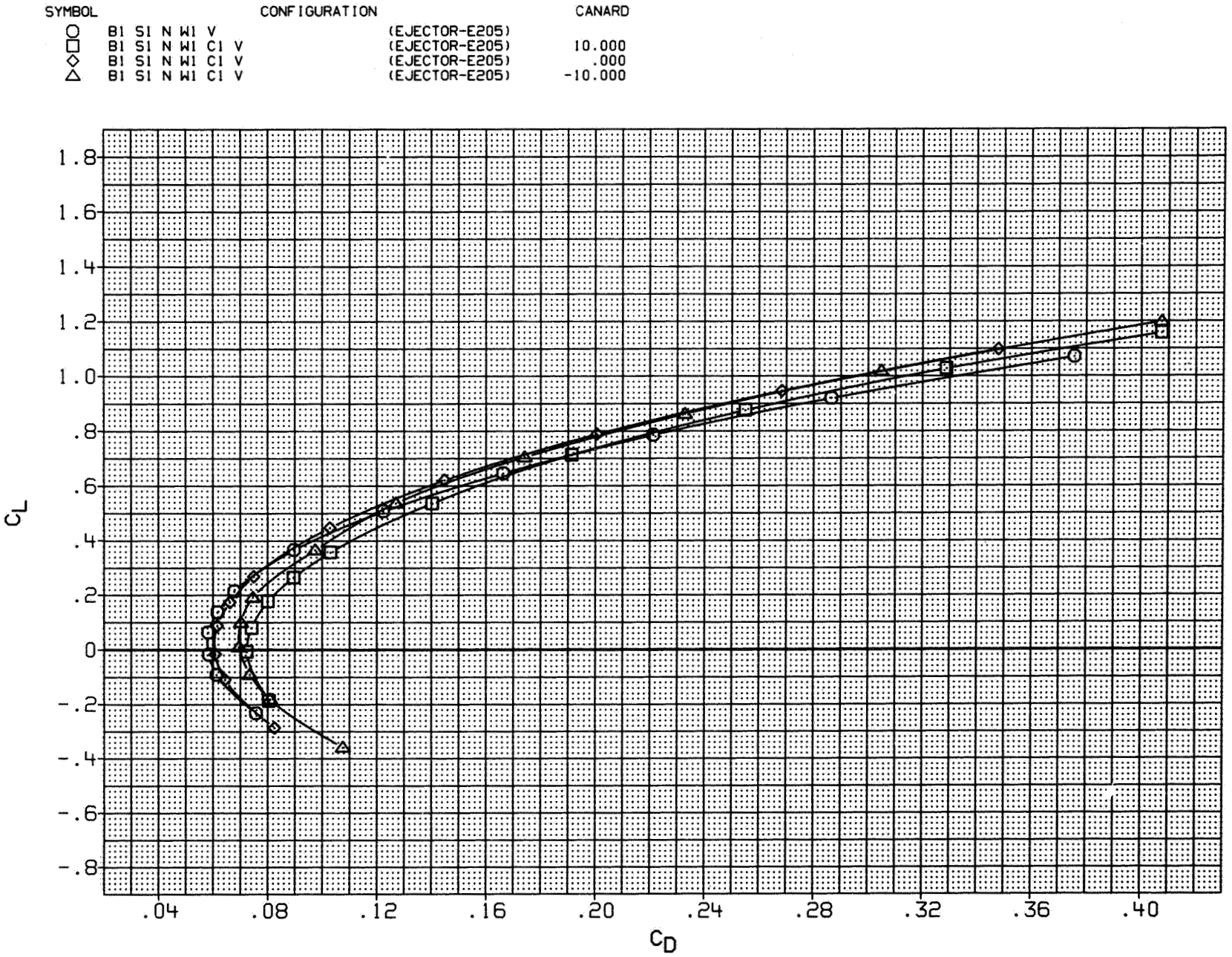


FIG. 18 CANARD INCIDENCE EFFECTS, TE-W = 10 DEGREES

MACH = 1.60

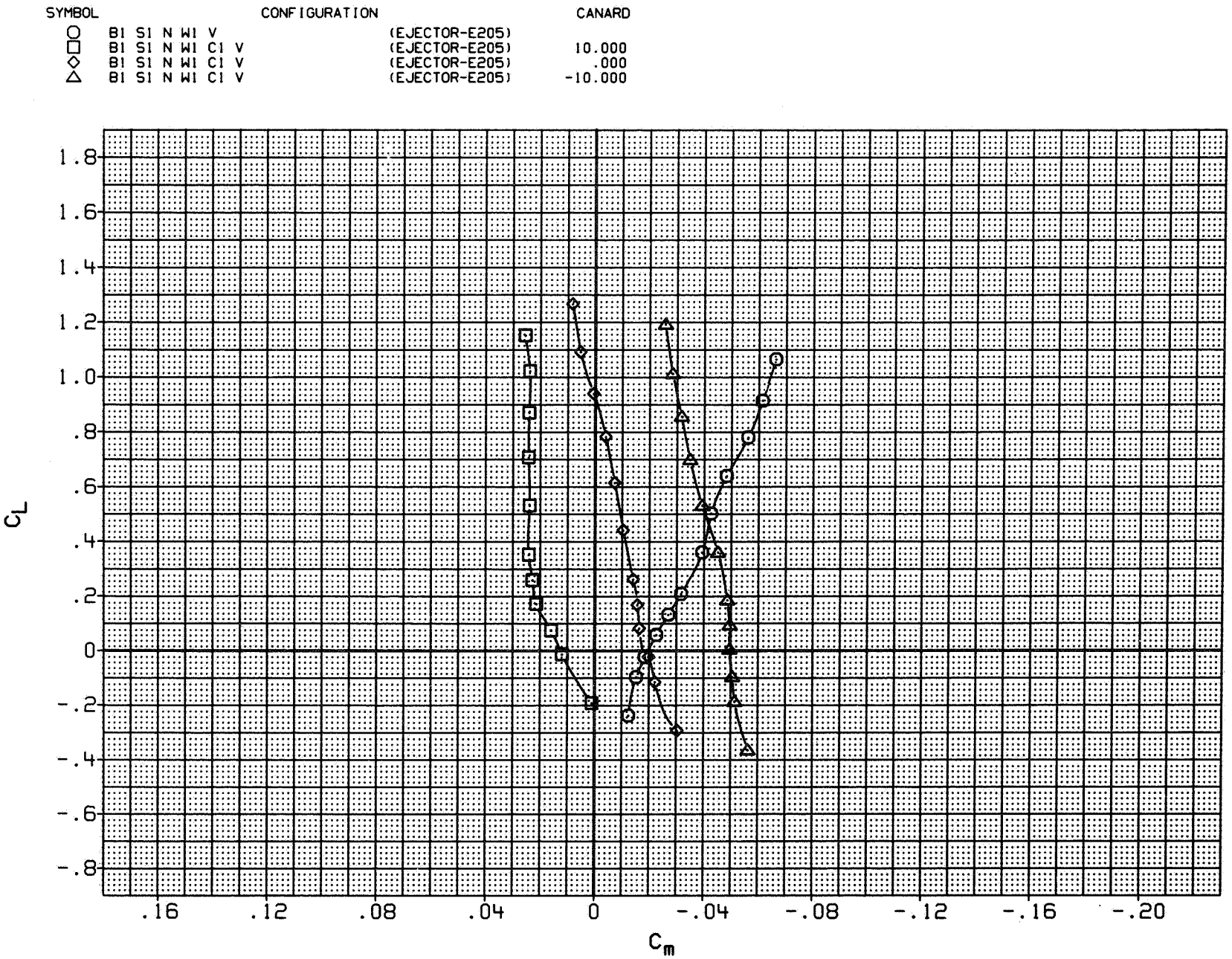


FIG. 18 CANARD INCIDENCE EFFECTS, TE-W = 10 DEGREES

MACH = 1.60

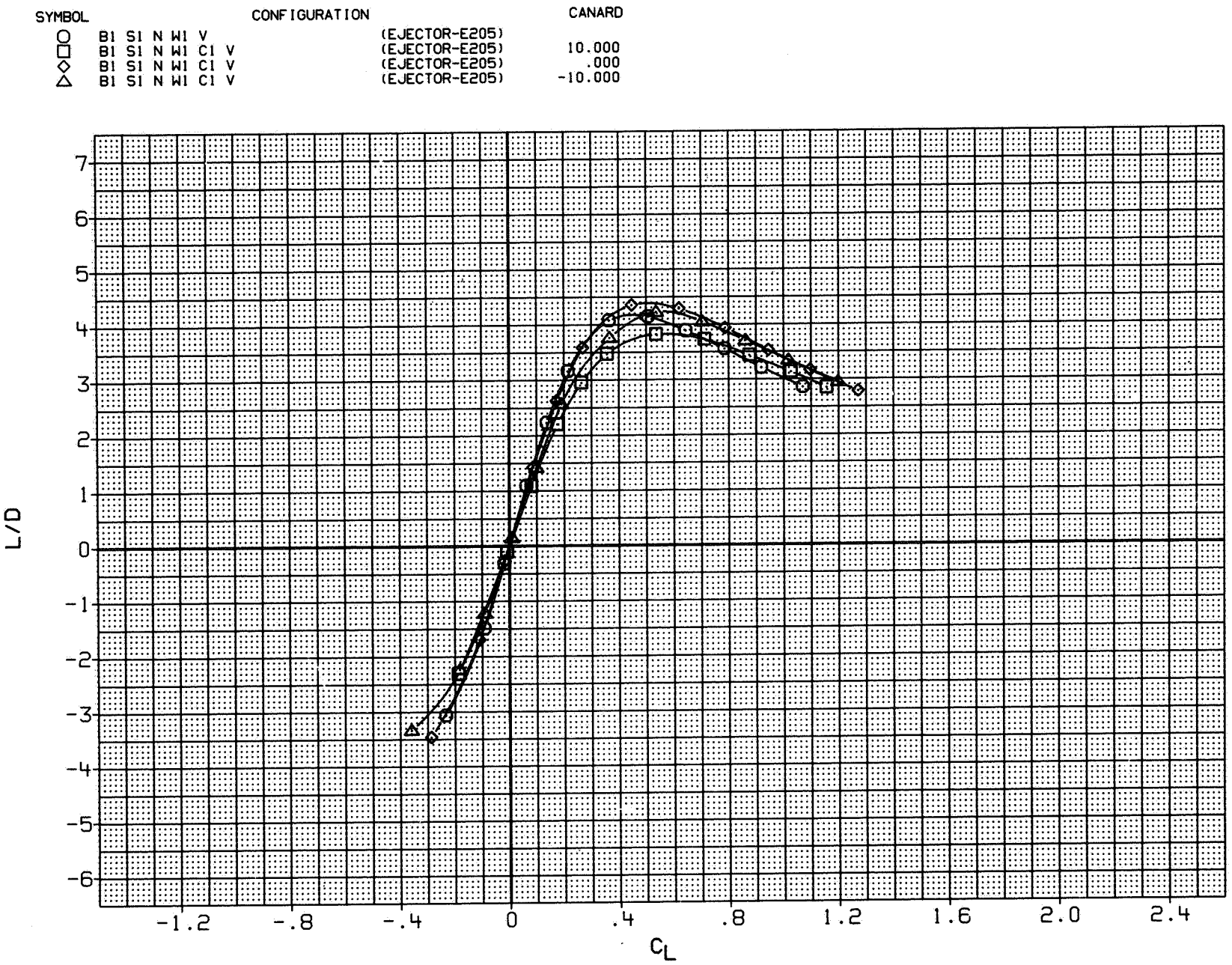


FIG. 18 CANARD INCIDENCE EFFECTS, TE-W = 10 DEGREES

MACH = 1.60

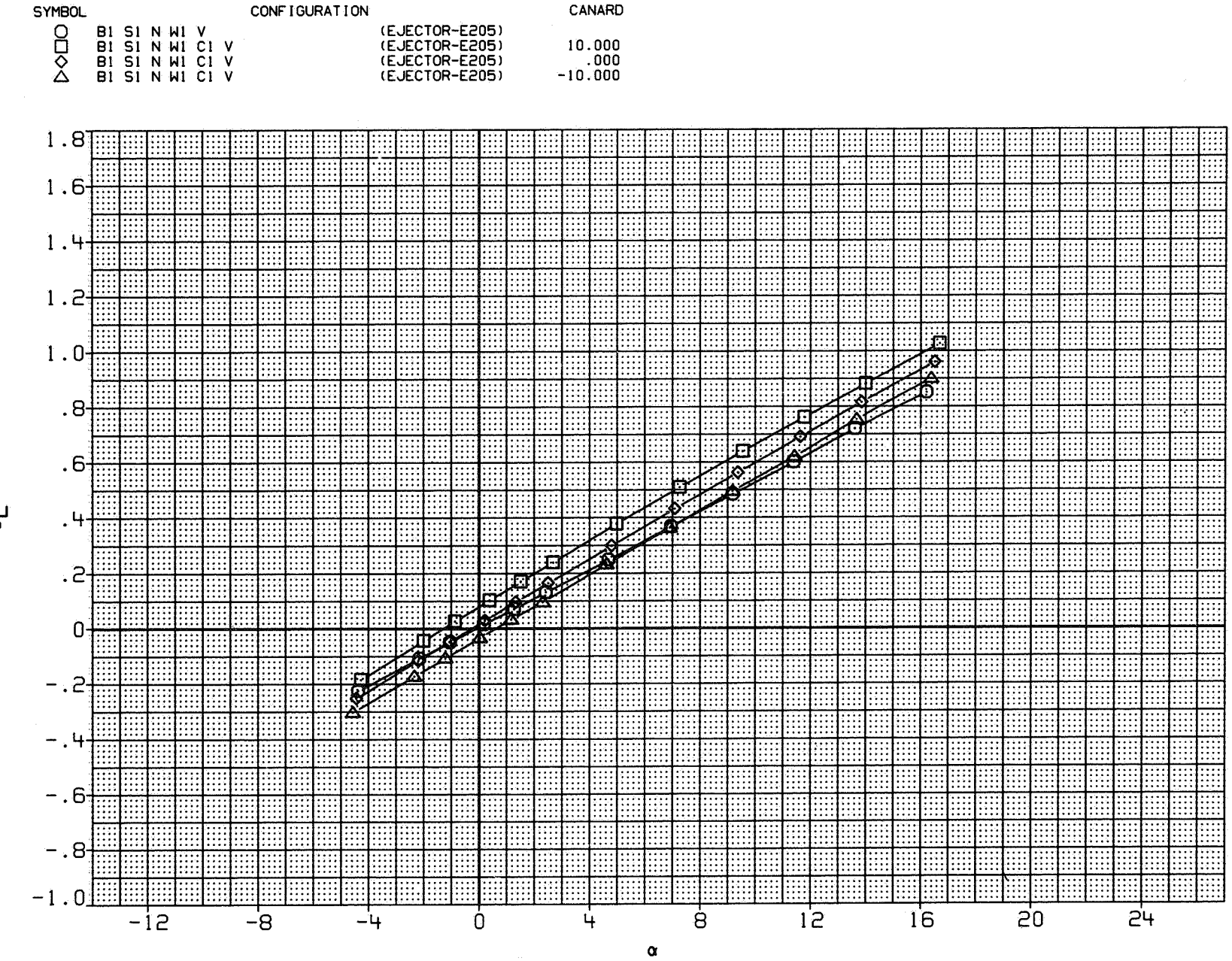


FIG. 19 CANARD INCIDENCE EFFECTS, TE-W = 0 DEGREES

MACH = 2.00

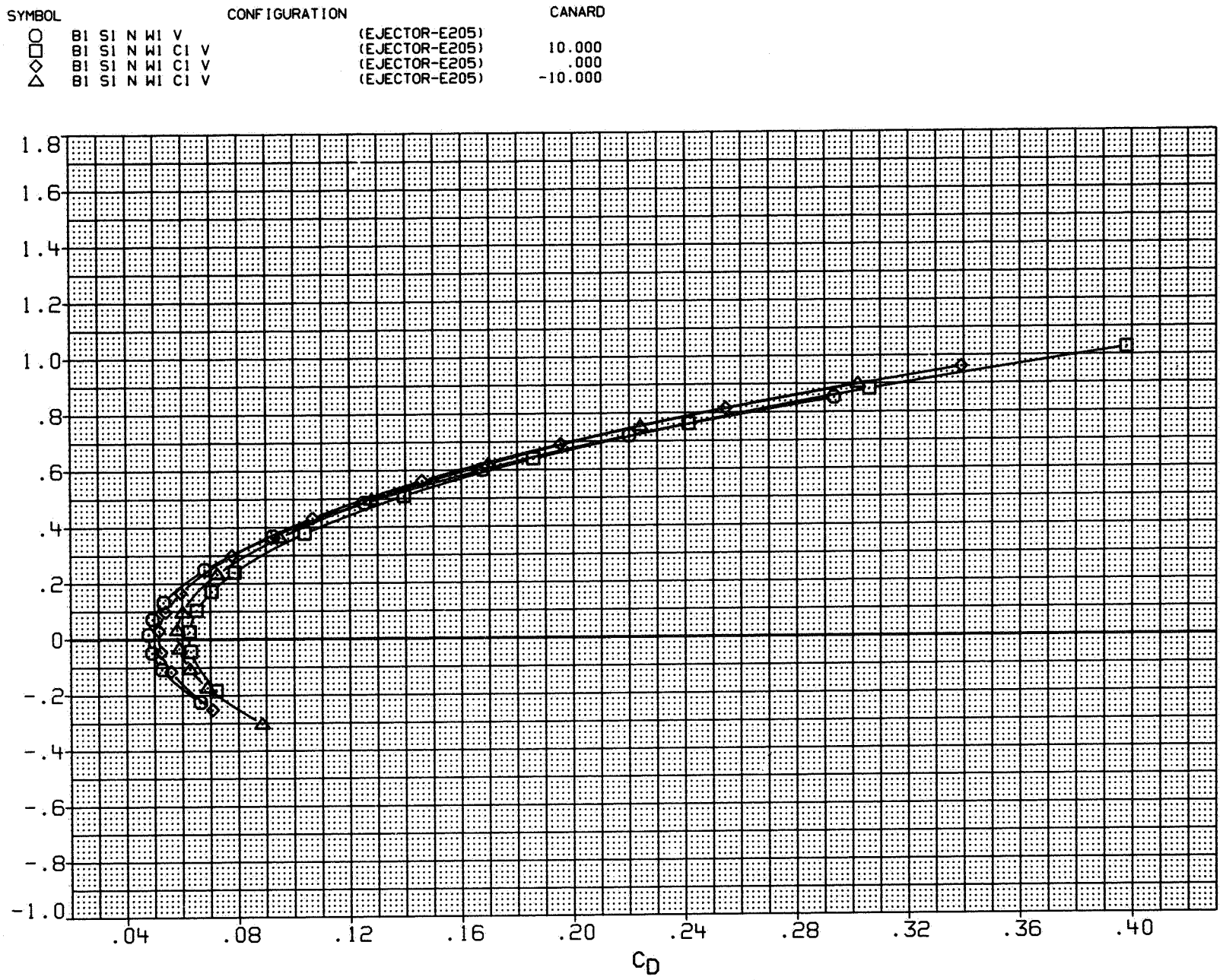


FIG. 19 CANARD INCIDENCE EFFECTS, TE-W = 0 DEGREES

MACH = 2.00

| SYMBOL | CONFIGURATION | | CANARD |
|---|---|---|---|
| ○ | B1 S1 N W1 V | (EJECTOR-E205) | |
| □ | B1 S1 N W1 C1 V | (EJECTOR-E205) | 10.000 |
| ◇ | B1 S1 N W1 C1 V | (EJECTOR-E205) | .000 |
| △ | B1 S1 N W1 C1 V | (EJECTOR-E205) | -10.000 |

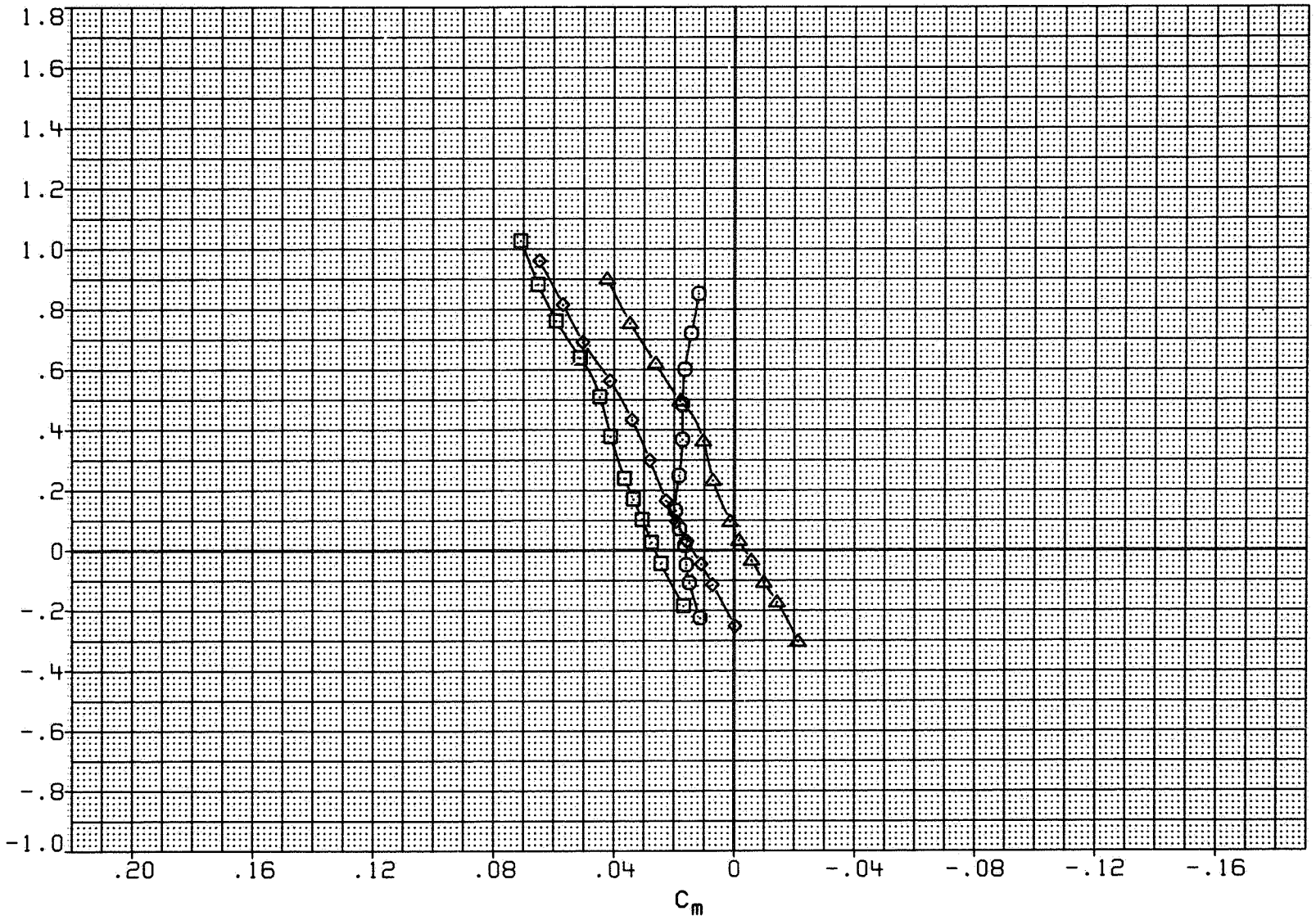


FIG. 19 CANARD INCIDENCE EFFECTS, TE-W = 0 DEGREES

MACH = 2.00

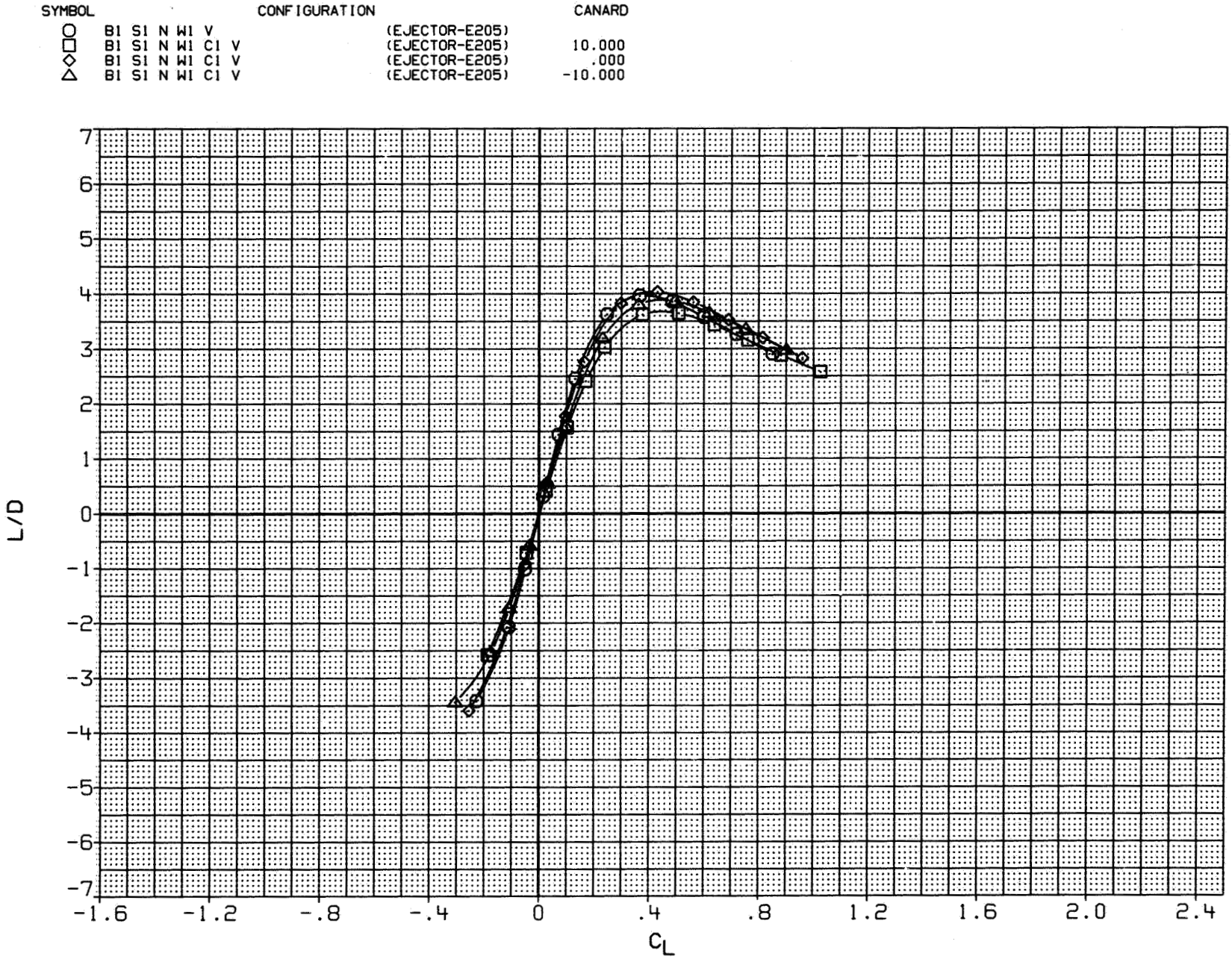


FIG. 19 CANARD INCIDENCE EFFECTS, TE-W = 0 DEGREES

MACH = 2.00

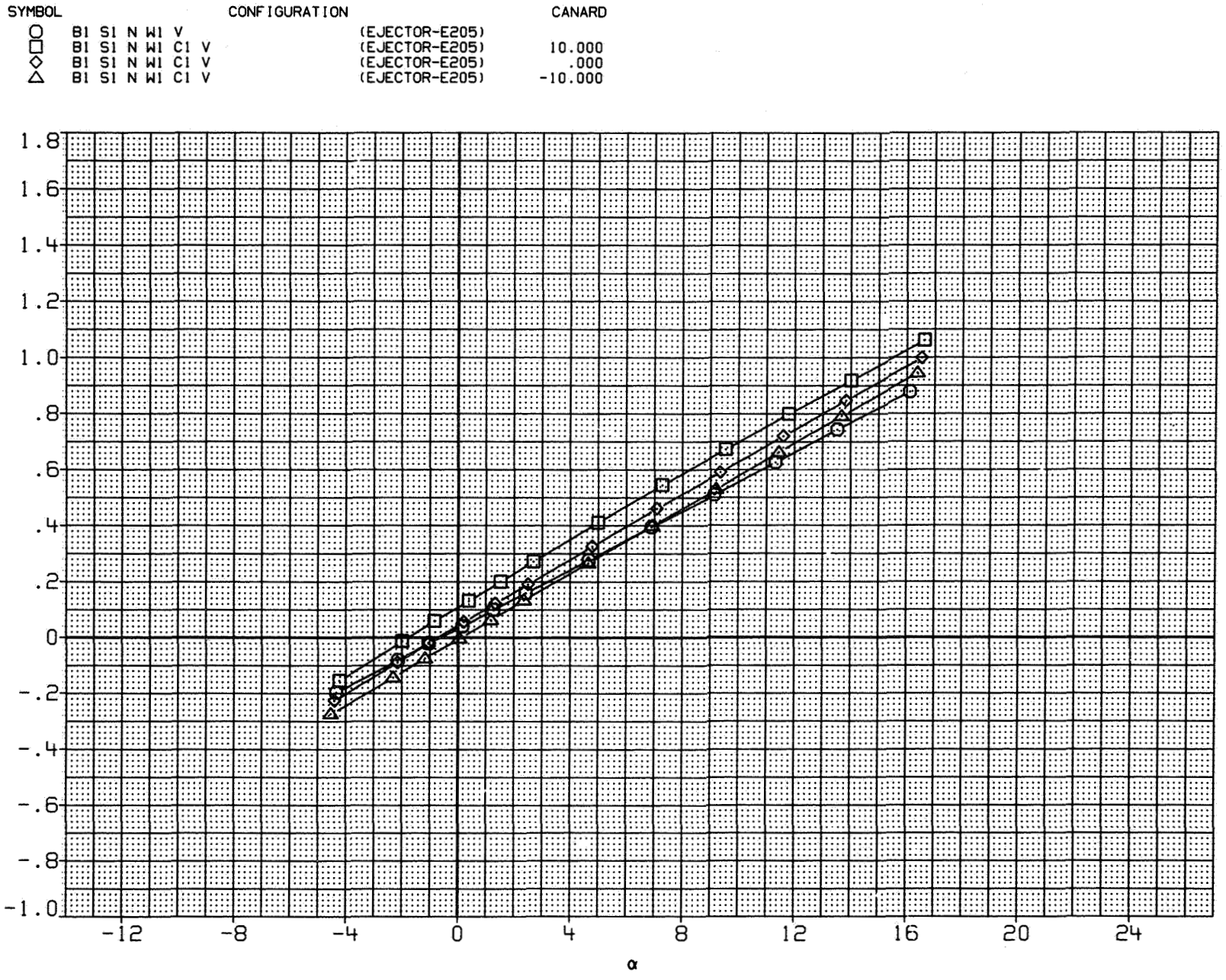


FIG. 20 CANARD INCIDENCE EFFECTS, TE-W = 10 DEGREES

MACH = 2.00

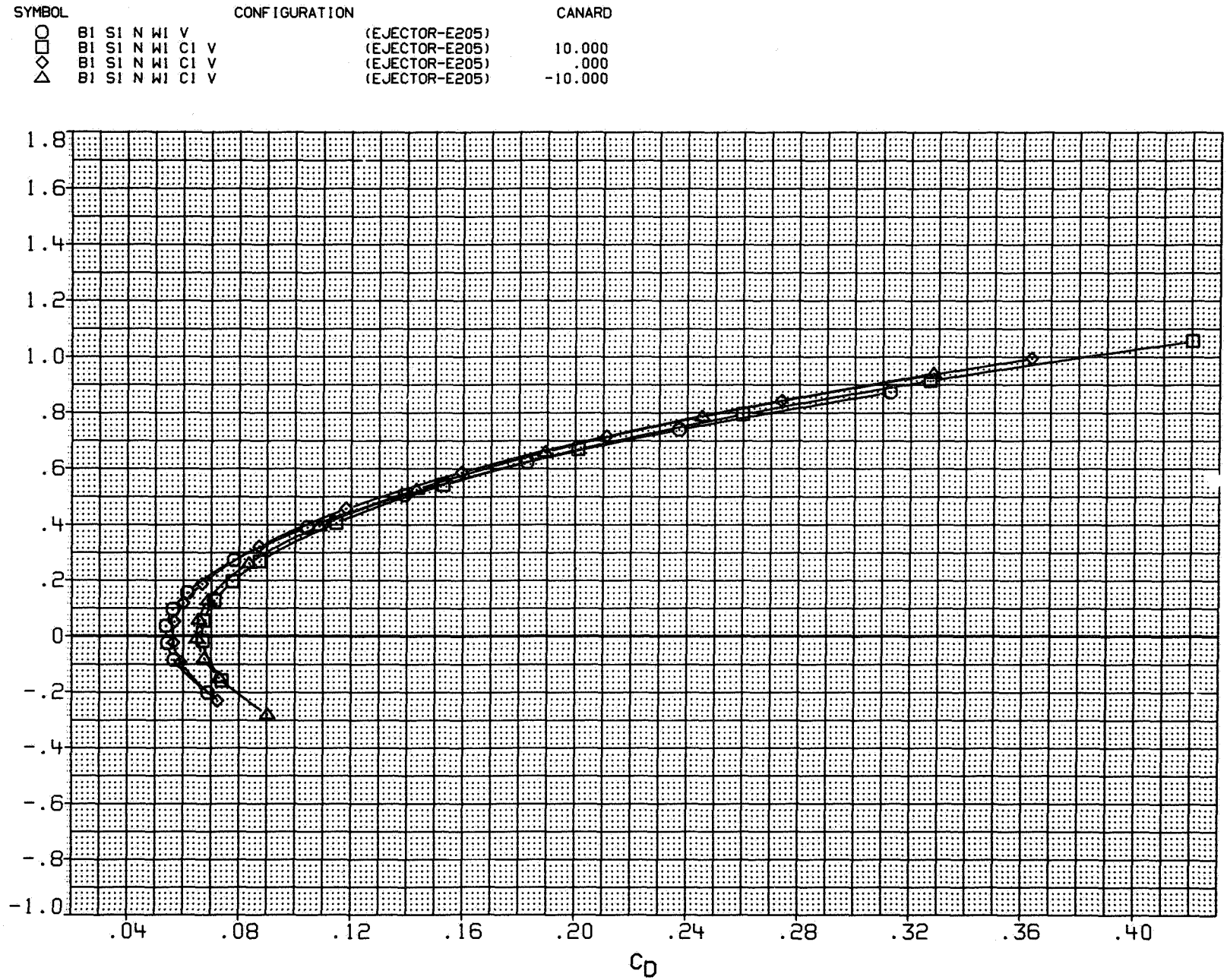


FIG. 20 CANARD INCIDENCE EFFECTS, TE-W = 10 DEGREES

MACH = 2.00

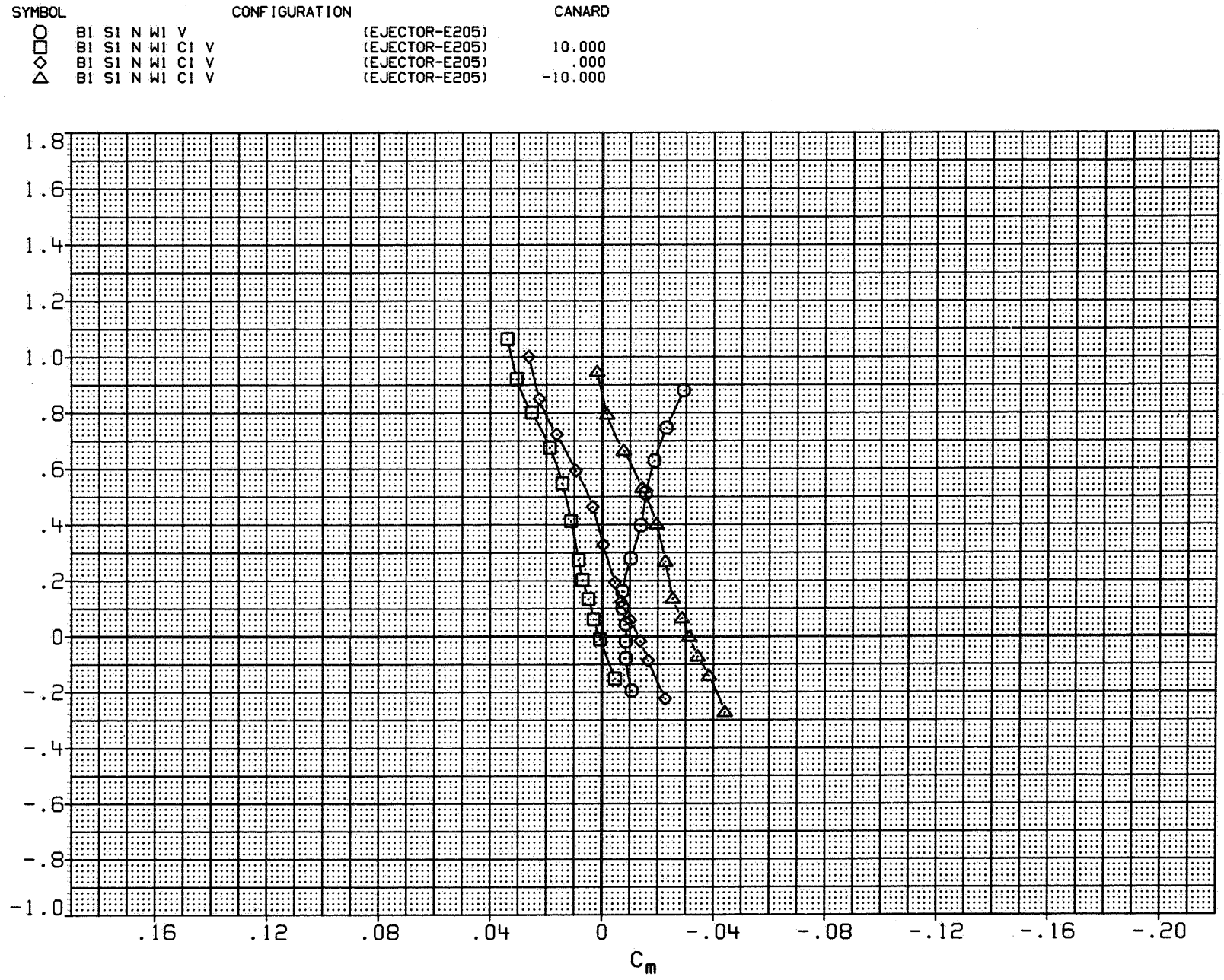


FIG. 20 CANARD INCIDENCE EFFECTS, TE-W = 10 DEGREES

MACH = 2.00

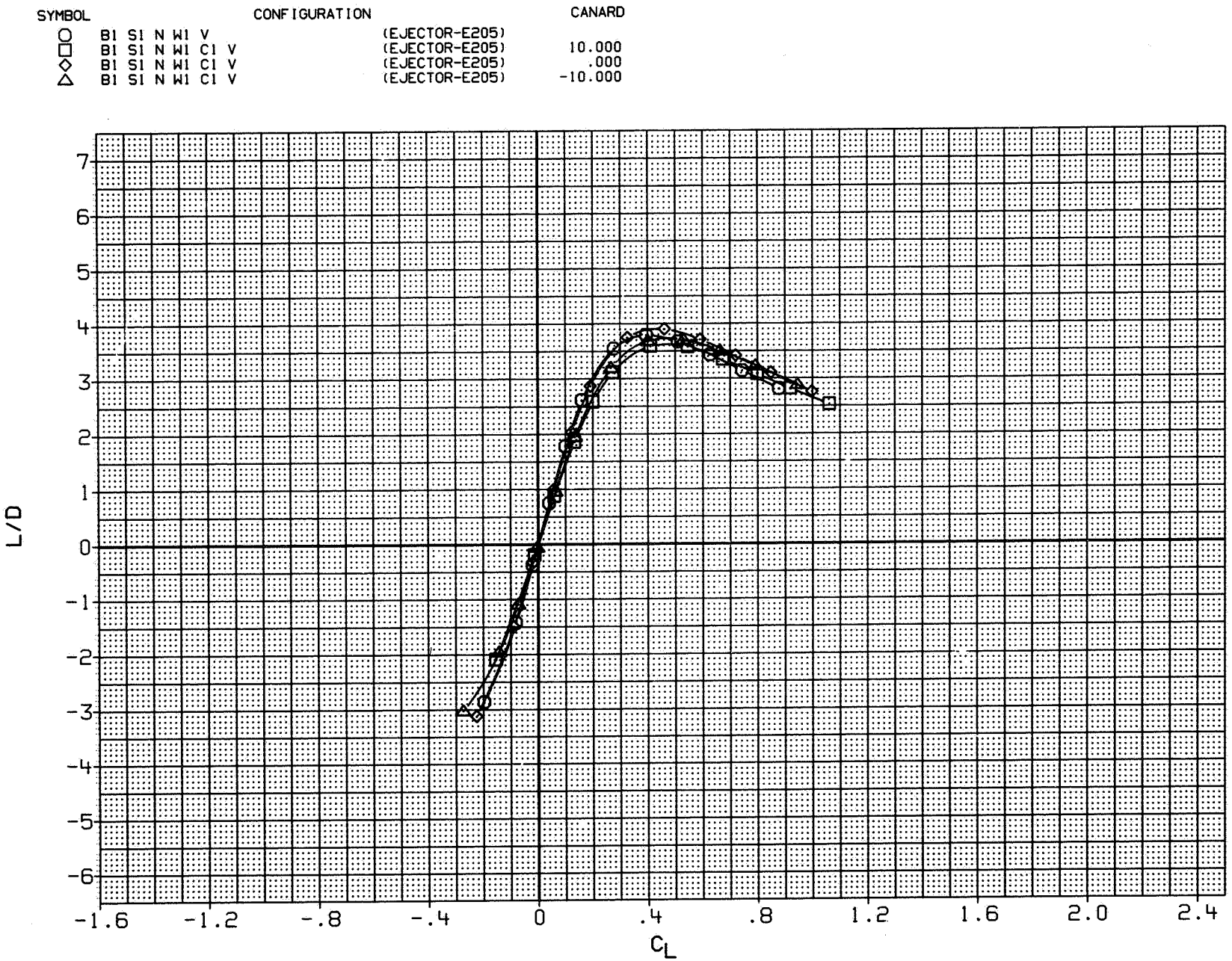


FIG. 20 CANARD INCIDENCE EFFECTS, TE-W = 10 DEGREES

MACH = 2.00

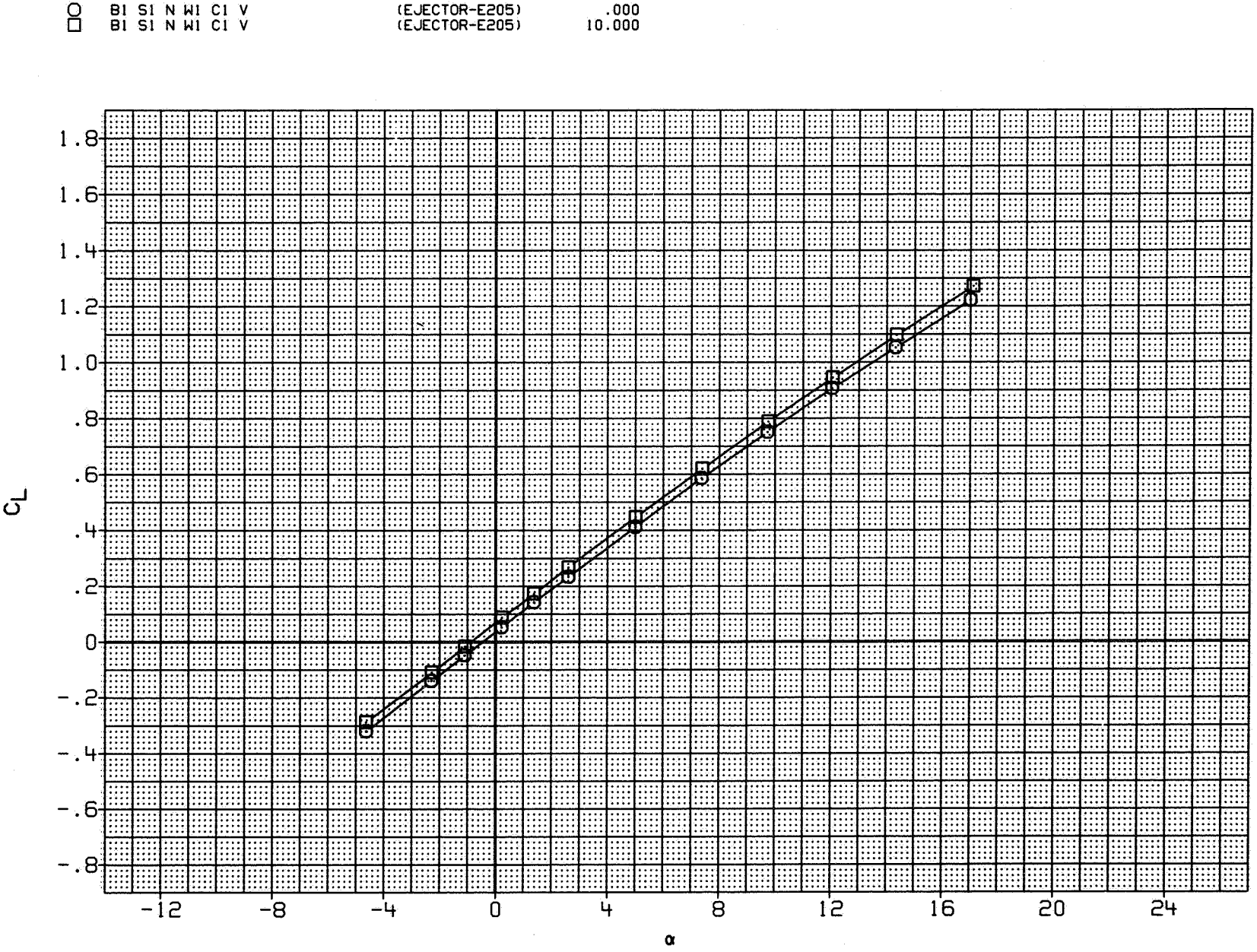


FIG. 21 FLAP DEFLECTION EFFECTS, CANARD = 0 DEGREES

MACH = 1.60

| SYMBOL | CONFIGURATION | TE-W |
|---|---|---|
| ○ | B1 S1 N W1 C1 V (EJECTOR-E205) | .000 |
| □ | B1 S1 N W1 C1 V (EJECTOR-E205) | 10.000 |

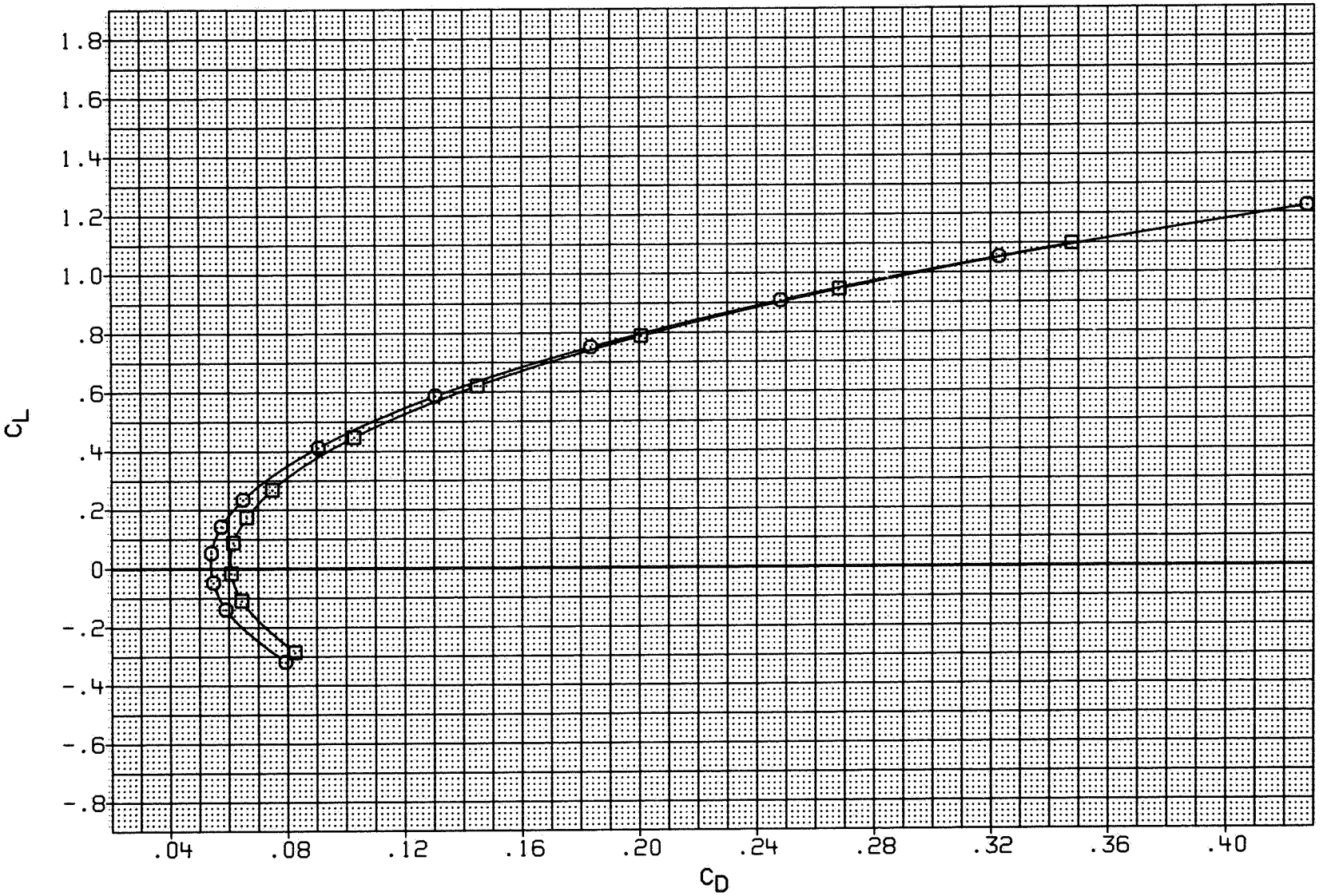


FIG. 21 FLAP DEFLECTION EFFECTS, CANARD = 0 DEGREES

MACH = 1.60

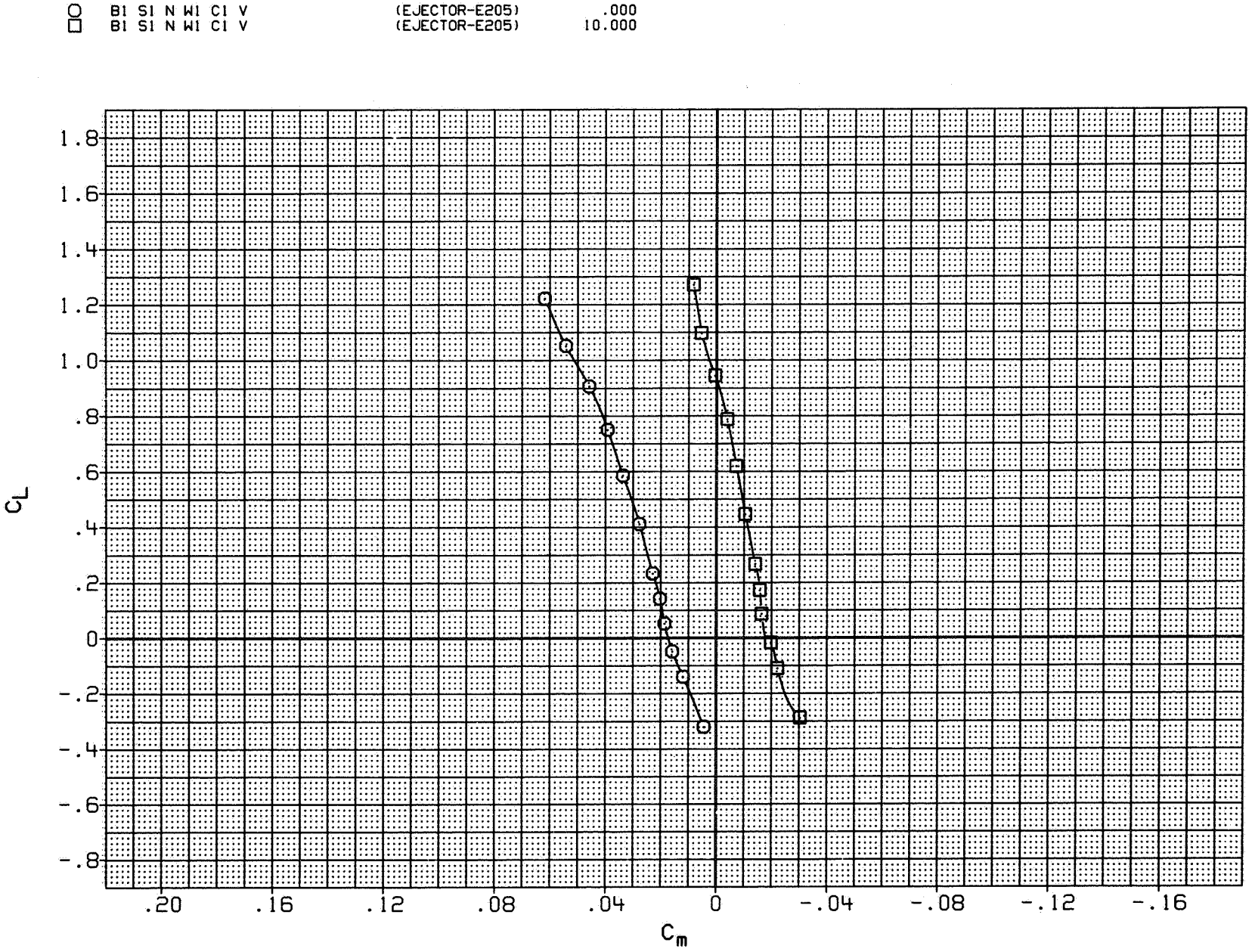


FIG. 21 FLAP DEFLECTION EFFECTS, CANARD = 0 DEGREES

MACH = 1.60

| SYMBOL | CONFIGURATION | TE-W |
|---|---|---|
| ○ | B1 S1 N W1 C1 V (EJECTOR-E205) | .000 |
| □ | B1 S1 N W1 C1 V (EJECTOR-E205) | 10.000 |

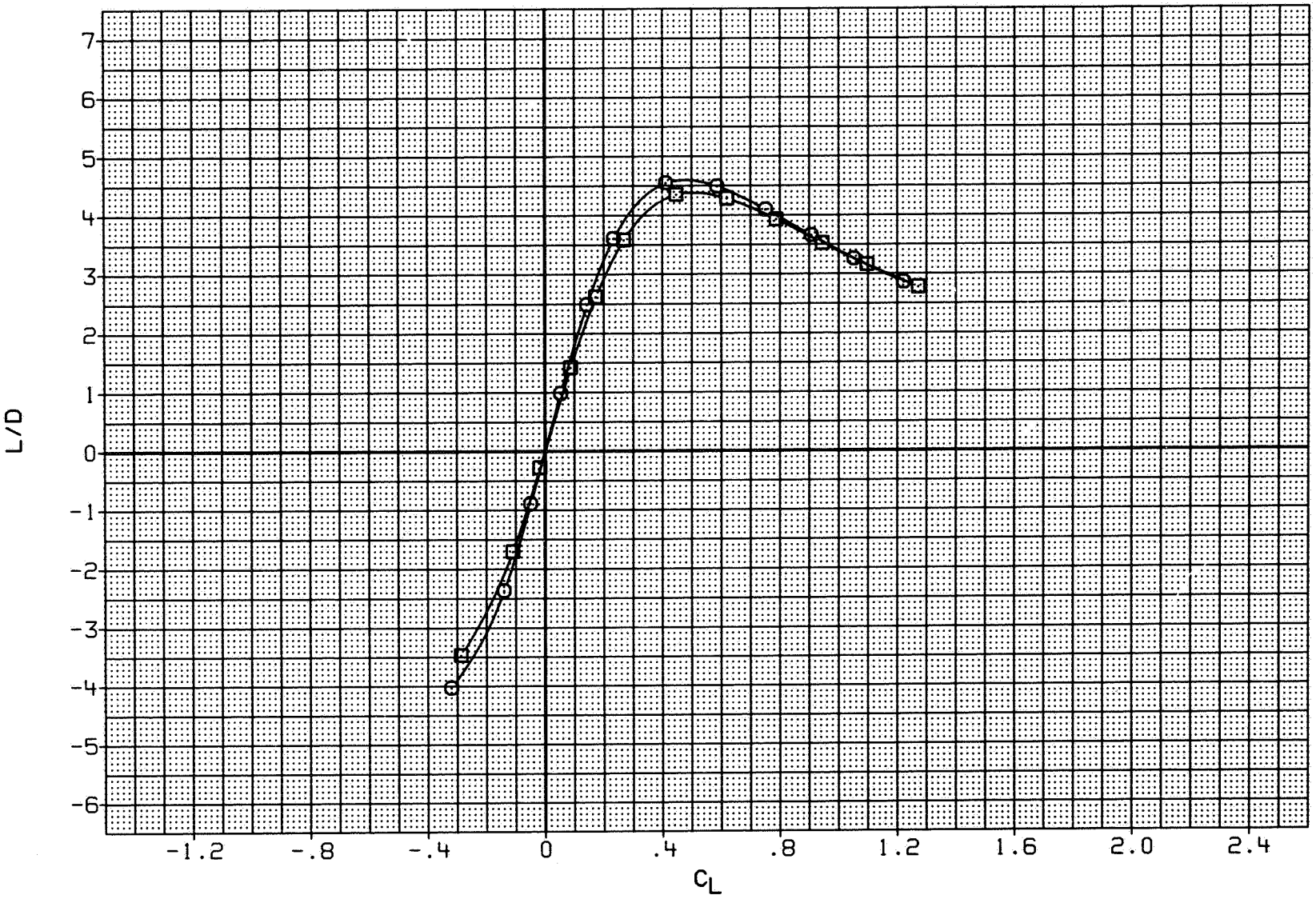


FIG. 21 FLAP DEFLECTION EFFECTS, CANARD = 0 DEGREES

MACH = 1.60

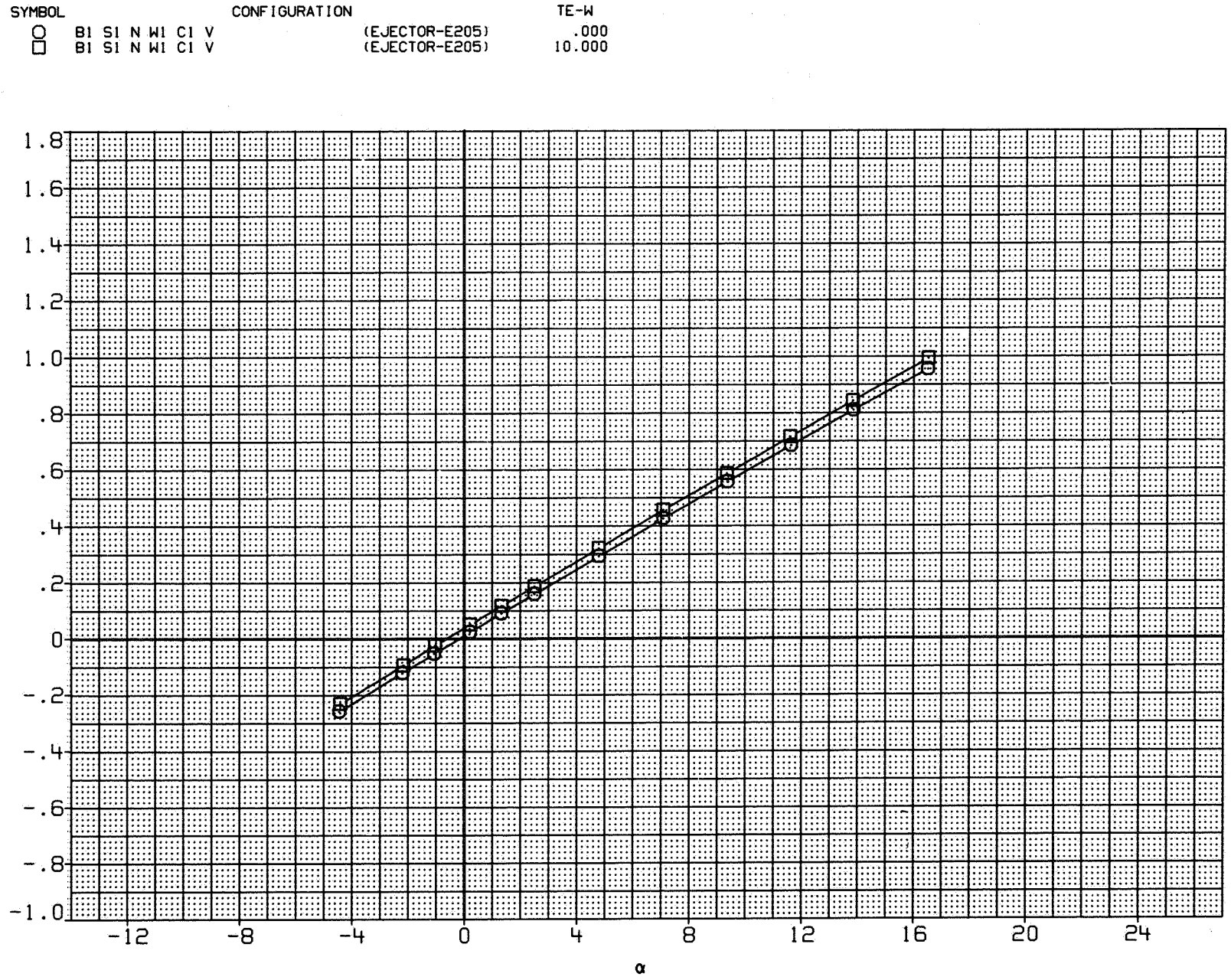


FIG. 22 FLAP DEFLECTION EFFECTS, CANARD = 0 DEGREES

MACH = 2.00

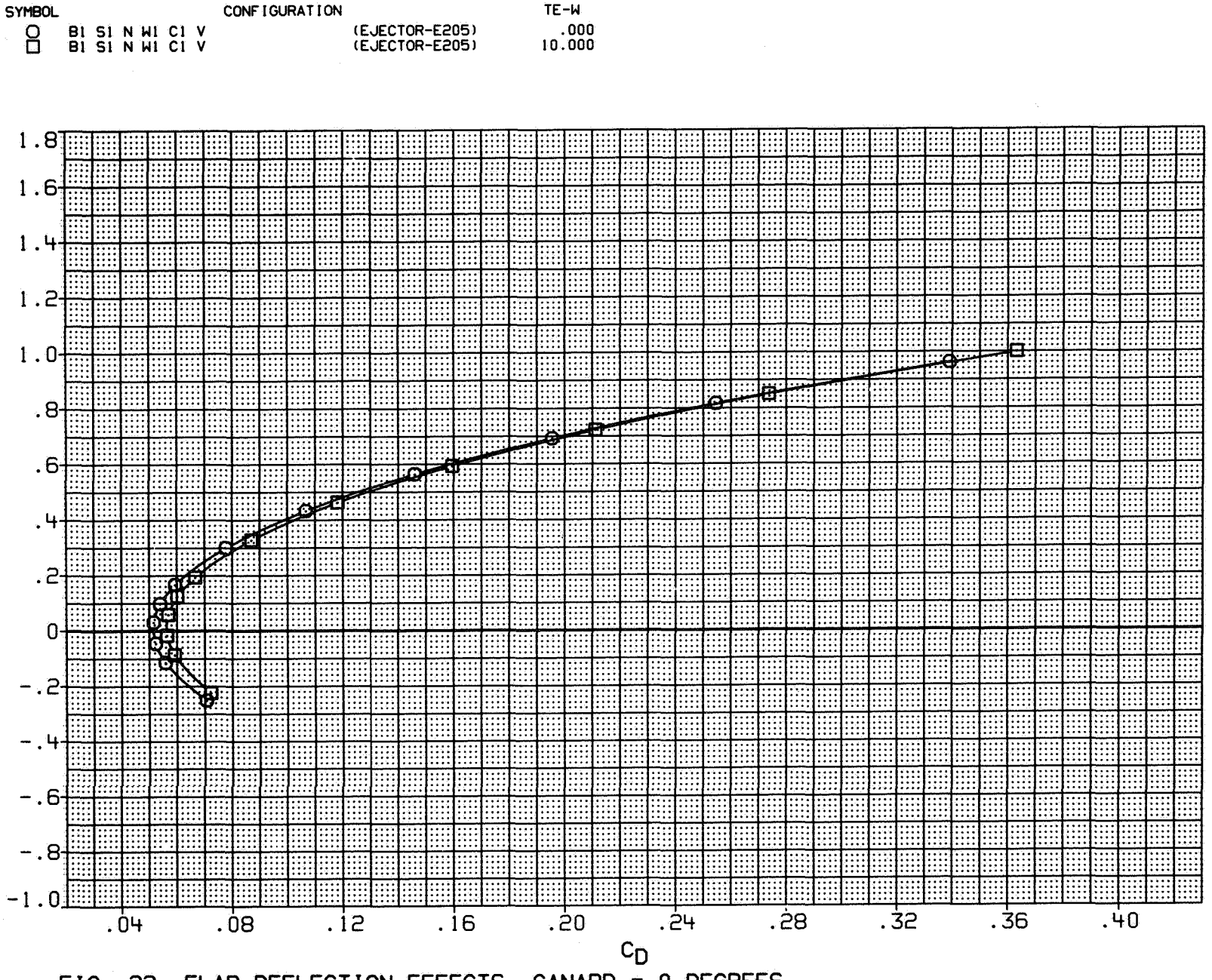


FIG. 22 FLAP DEFLECTION EFFECTS, CANARD = 0 DEGREES

MACH = 2.00

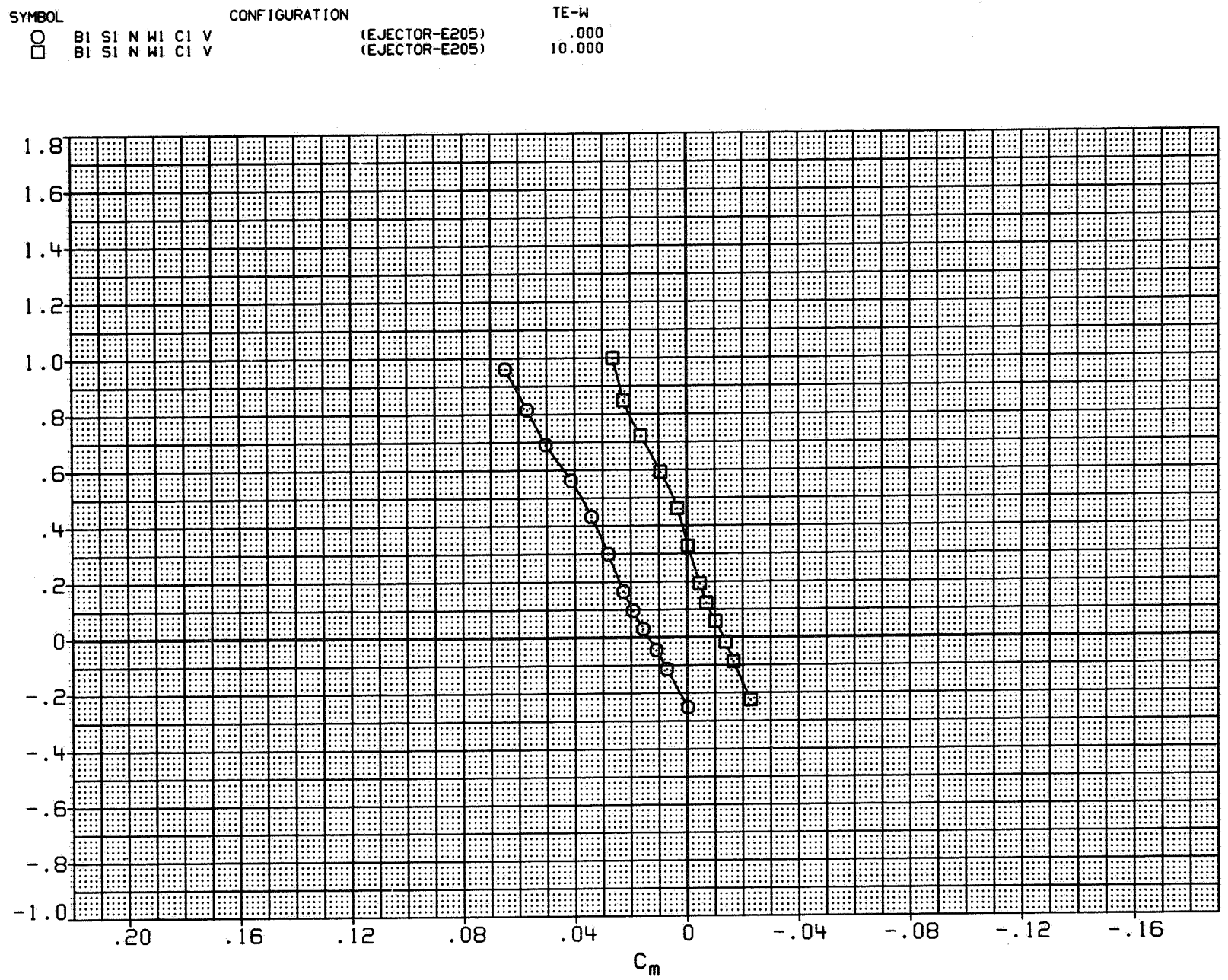


FIG. 22 FLAP DEFLECTION EFFECTS, CANARD = 0 DEGREES

MACH = 2.00

| SYMBOL | CONFIGURATION | TE-W |
|---|---|---|
| ○ B1 S1 N W1 C1 V | (EJECTOR-E205) | .000 |
| □ B1 S1 N W1 C1 V | (EJECTOR-E205) | 10.000 |

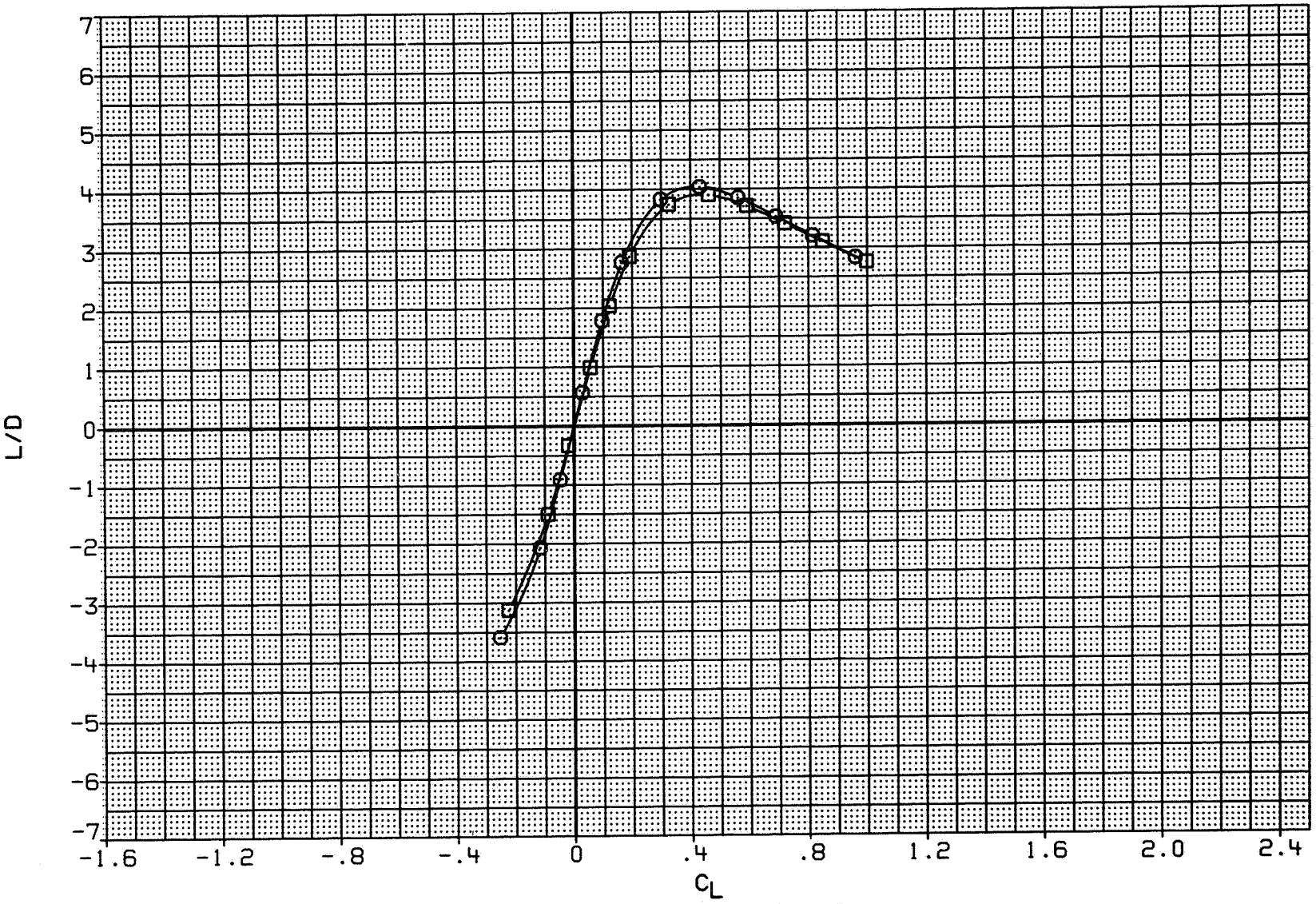


FIG. 22 FLAP DEFLECTION EFFECTS, CANARD = 0 DEGREES

MACH = 2.00

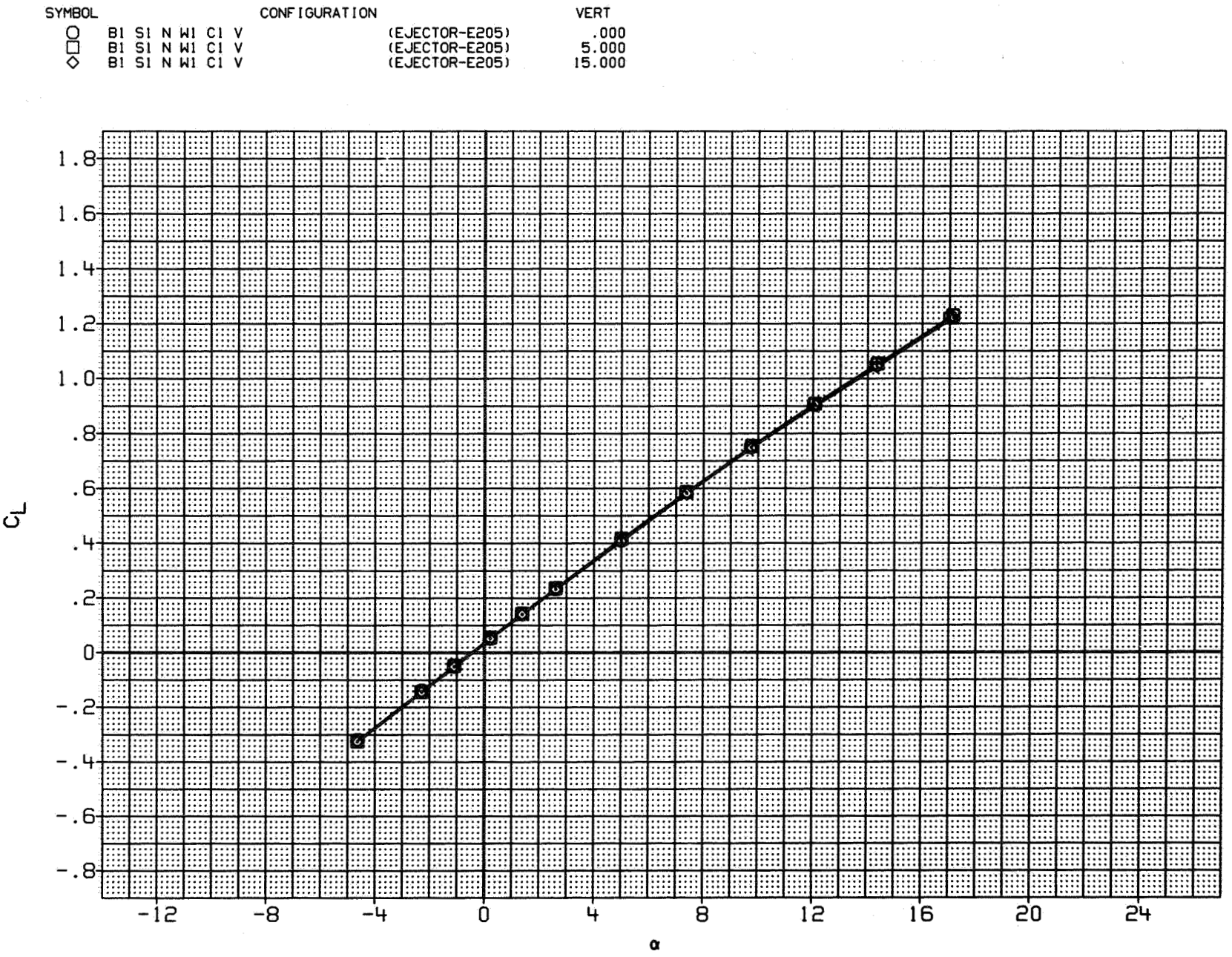


FIG. 23 VERTICAL TAIL DEFLECTION EFFECTS, LONGITUDINAL CHARACTERISTICS

MACH = 1.60

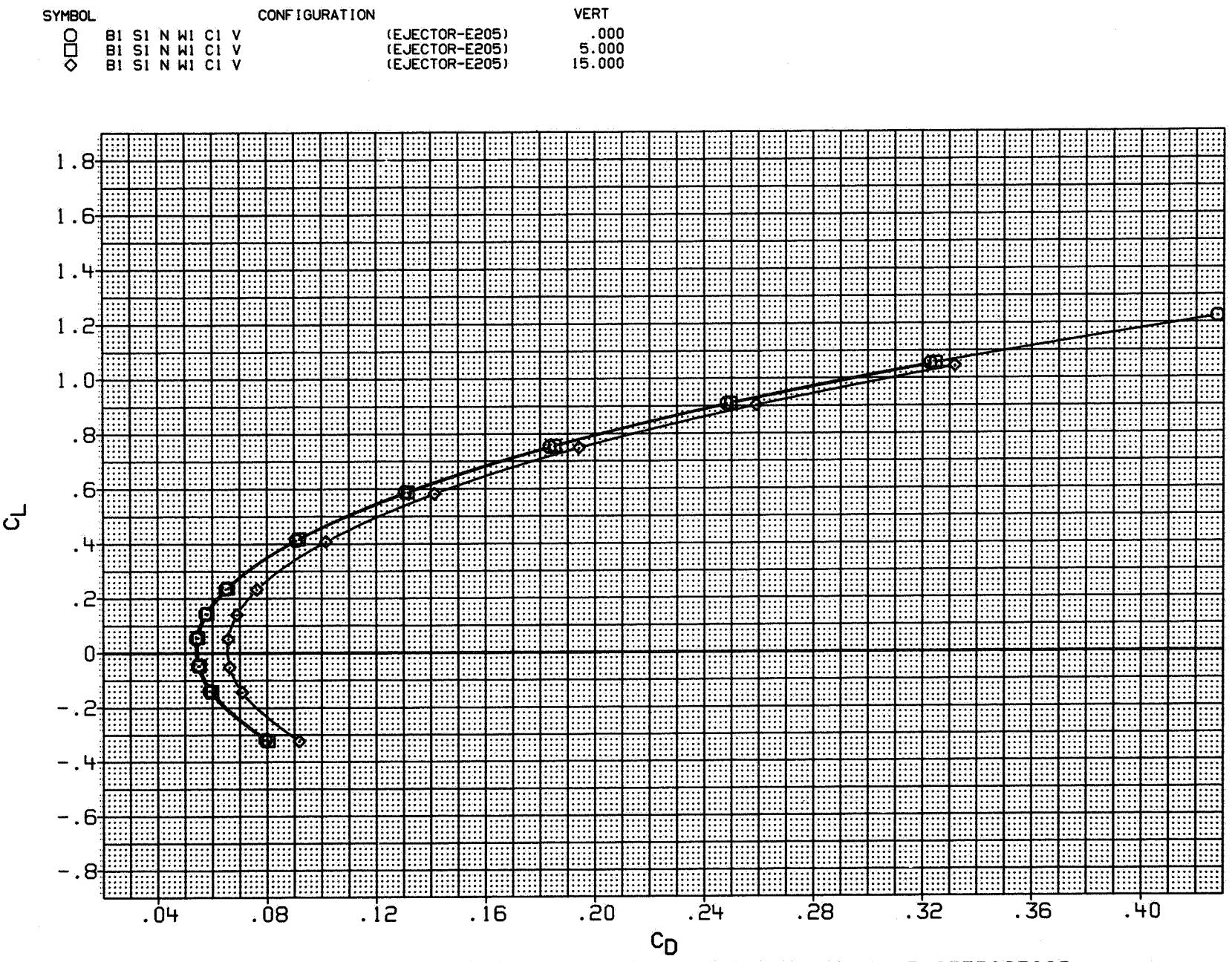


FIG. 23 VERTICAL TAIL DEFLECTION EFFECTS, LONGITUDINAL CHARACTERISTICS

MACH = 1.60

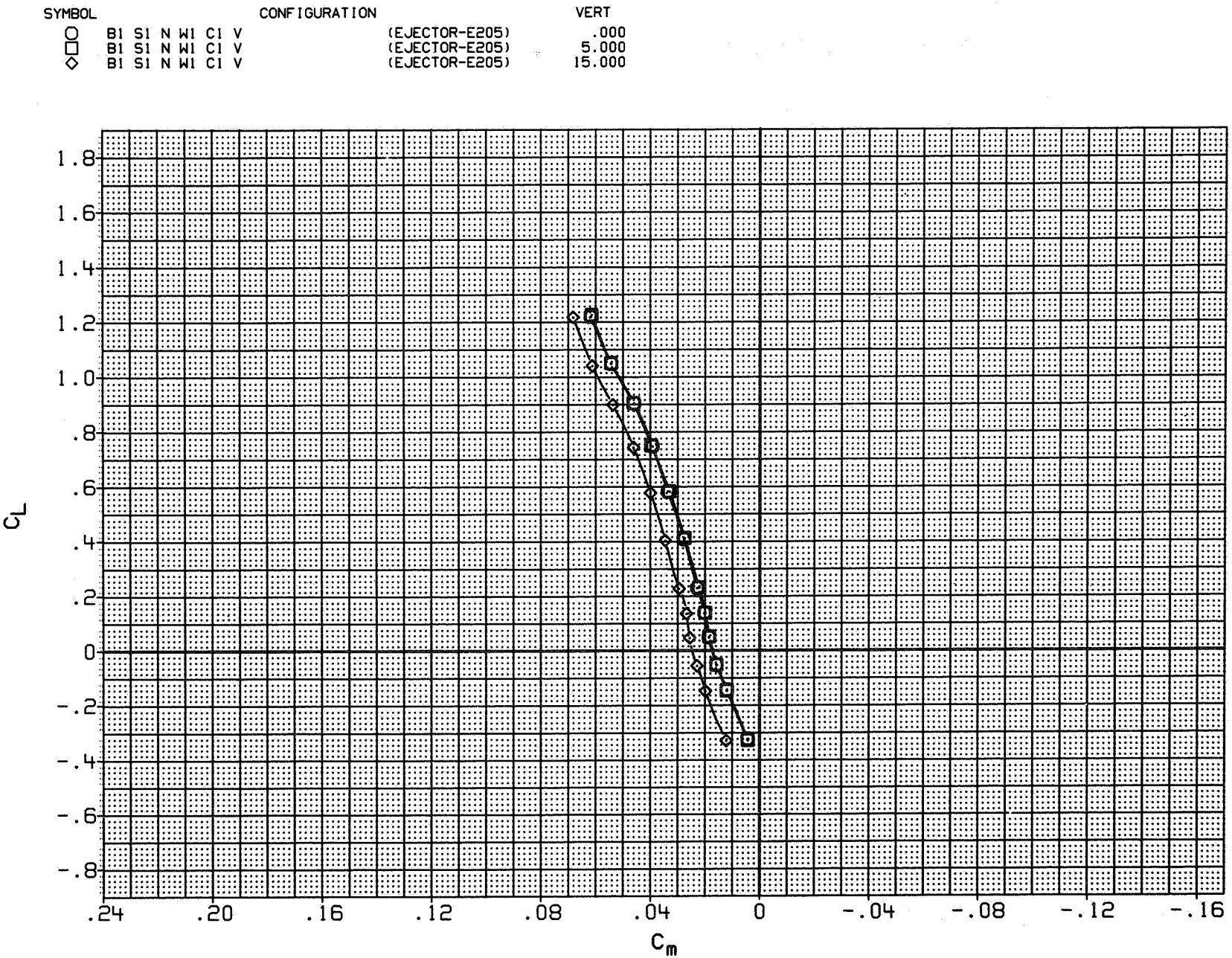


FIG. 23 VERTICAL TAIL DEFLECTION EFFECTS, LONGITUDINAL CHARACTERISTICS

MACH = 1.60

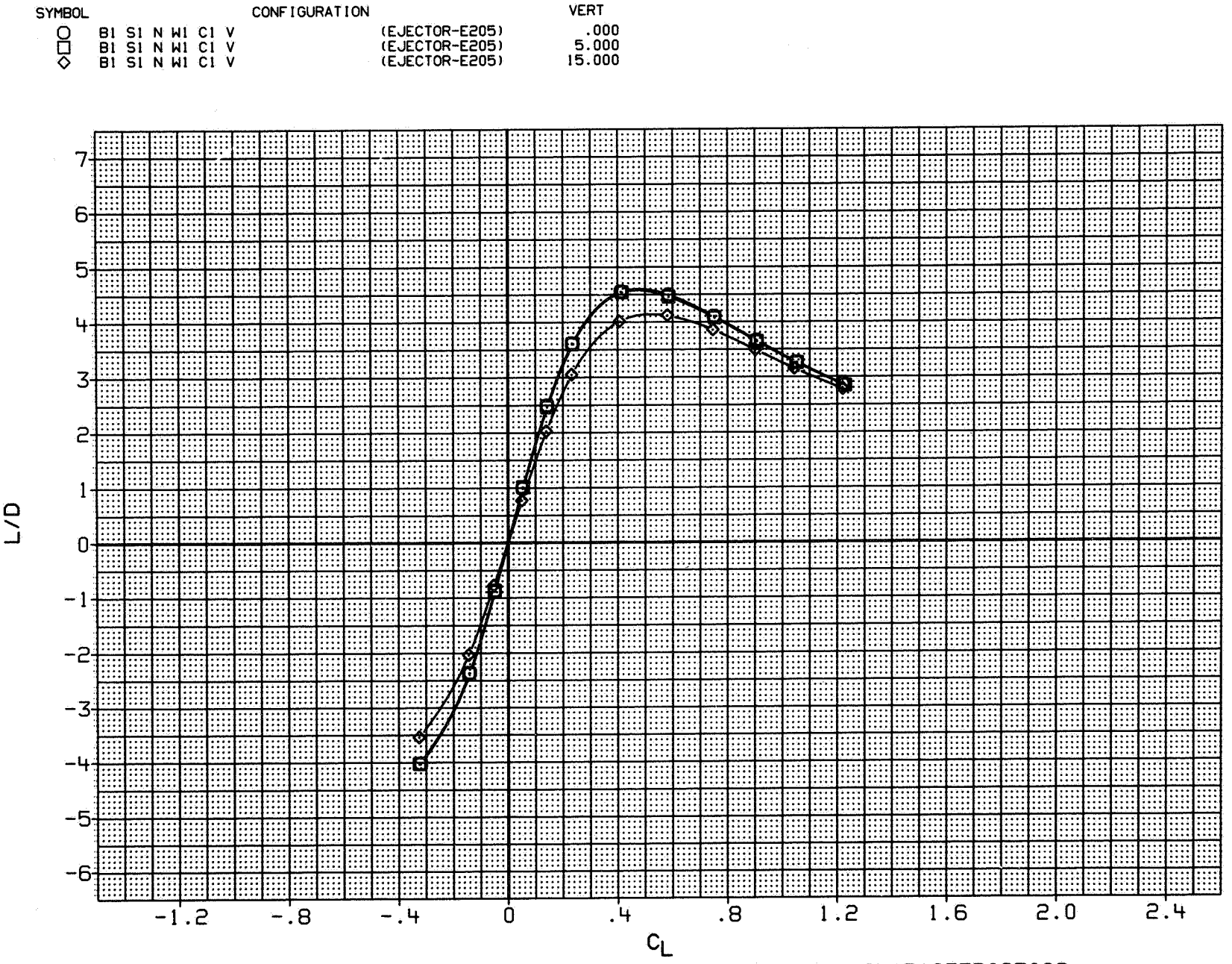


FIG. 23 VERTICAL TAIL DEFLECTION EFFECTS, LONGITUDINAL CHARACTERISTICS

MACH = 1.60

| SYMBOL | CONFIGURATION | | VERT |
|---|---|---|---|
| ○ | B1 S1 N W1 C1 V | (EJECTOR-E205) | .000 |
| □ | B1 S1 N W1 C1 V | (EJECTOR-E205) | 5.000 |
| ◇ | B1 S1 N W1 C1 V | (EJECTOR-E205) | 15.000 |

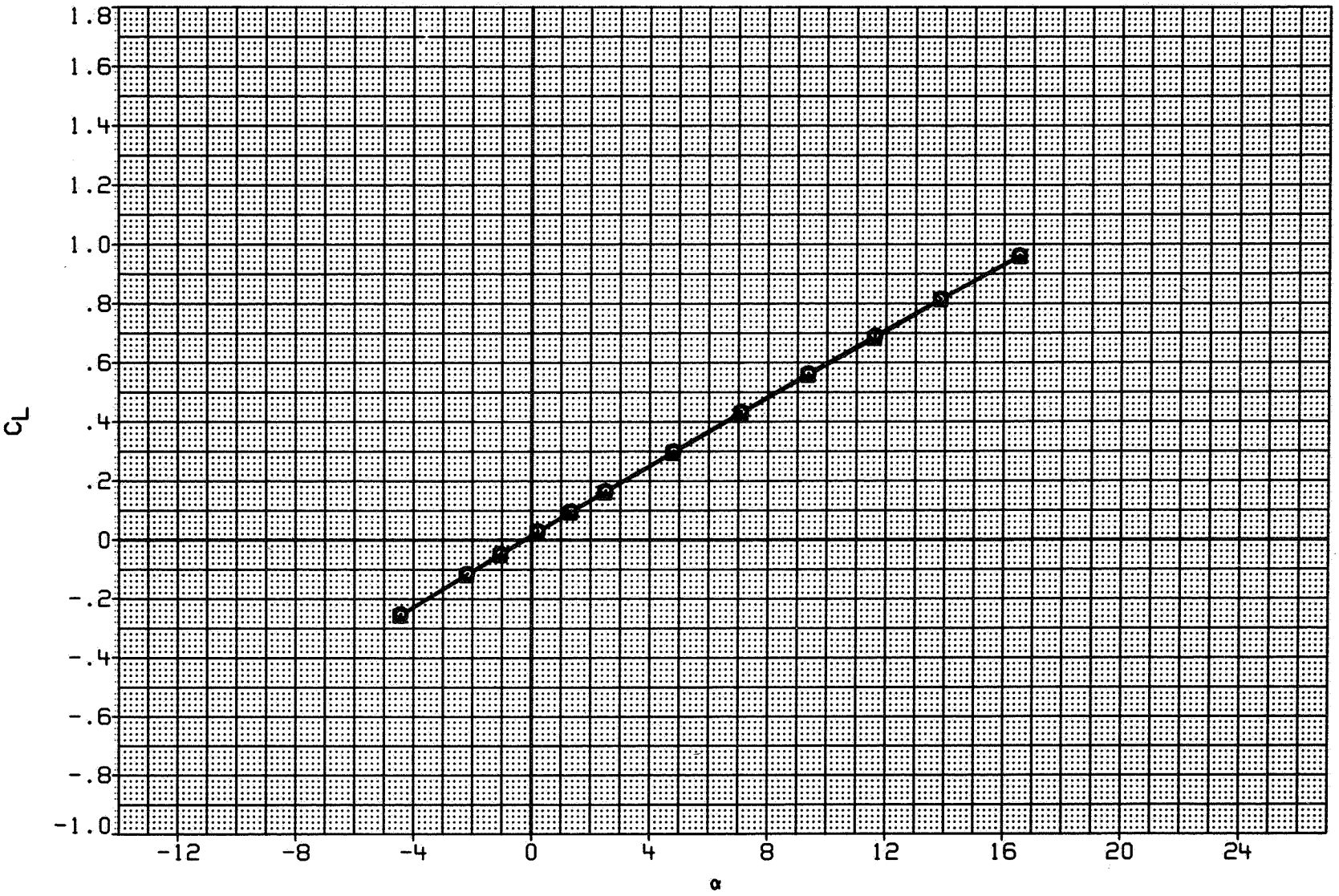


FIG. 24 VERTICAL TAIL DEFLECTION EFFECTS, LONGITUDINAL CHARACTERISTICS

MACH = 2.00

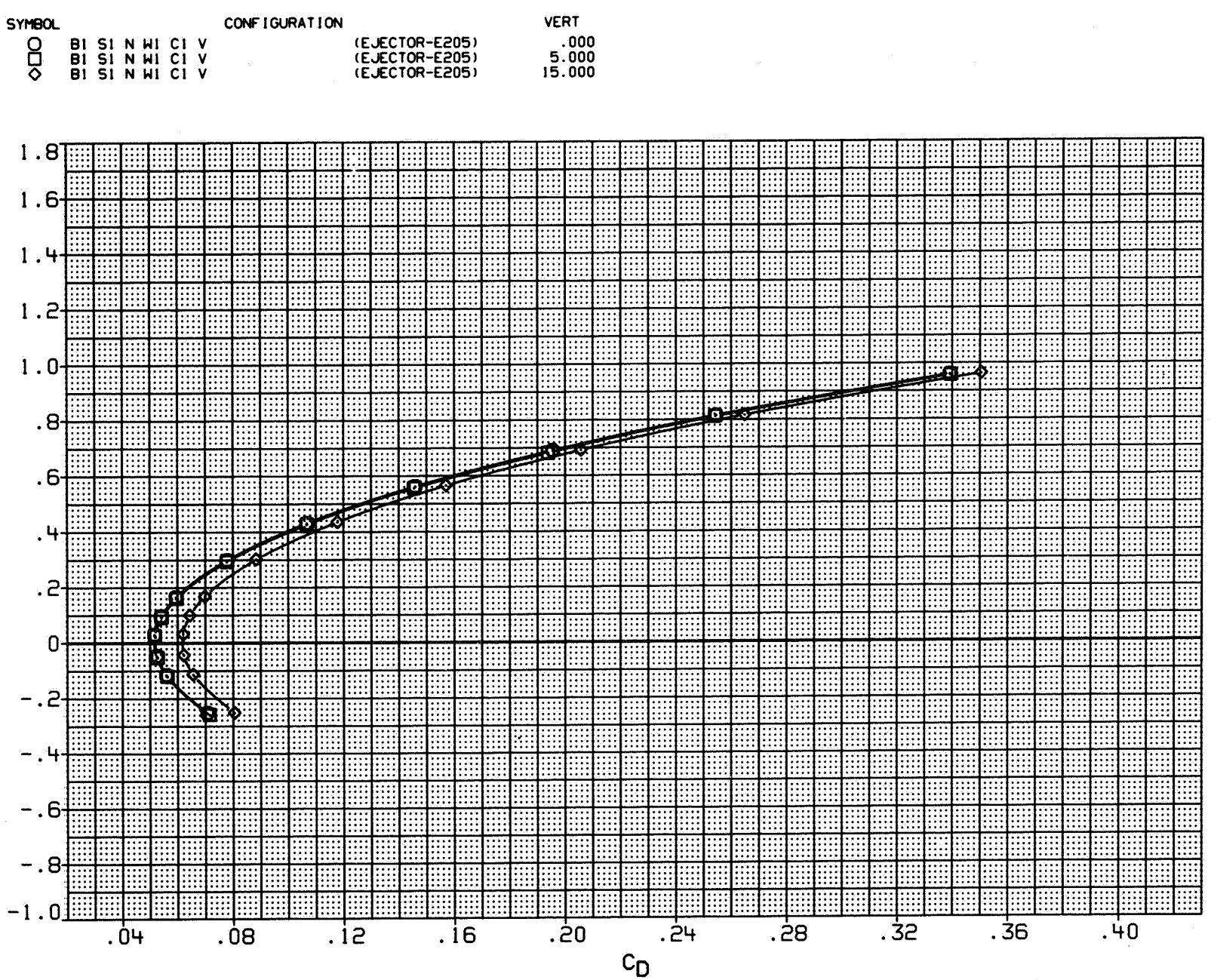


FIG. 24 VERTICAL TAIL DEFLECTION EFFECTS, LONGITUDINAL CHARACTERISTICS

MACH = 2.00

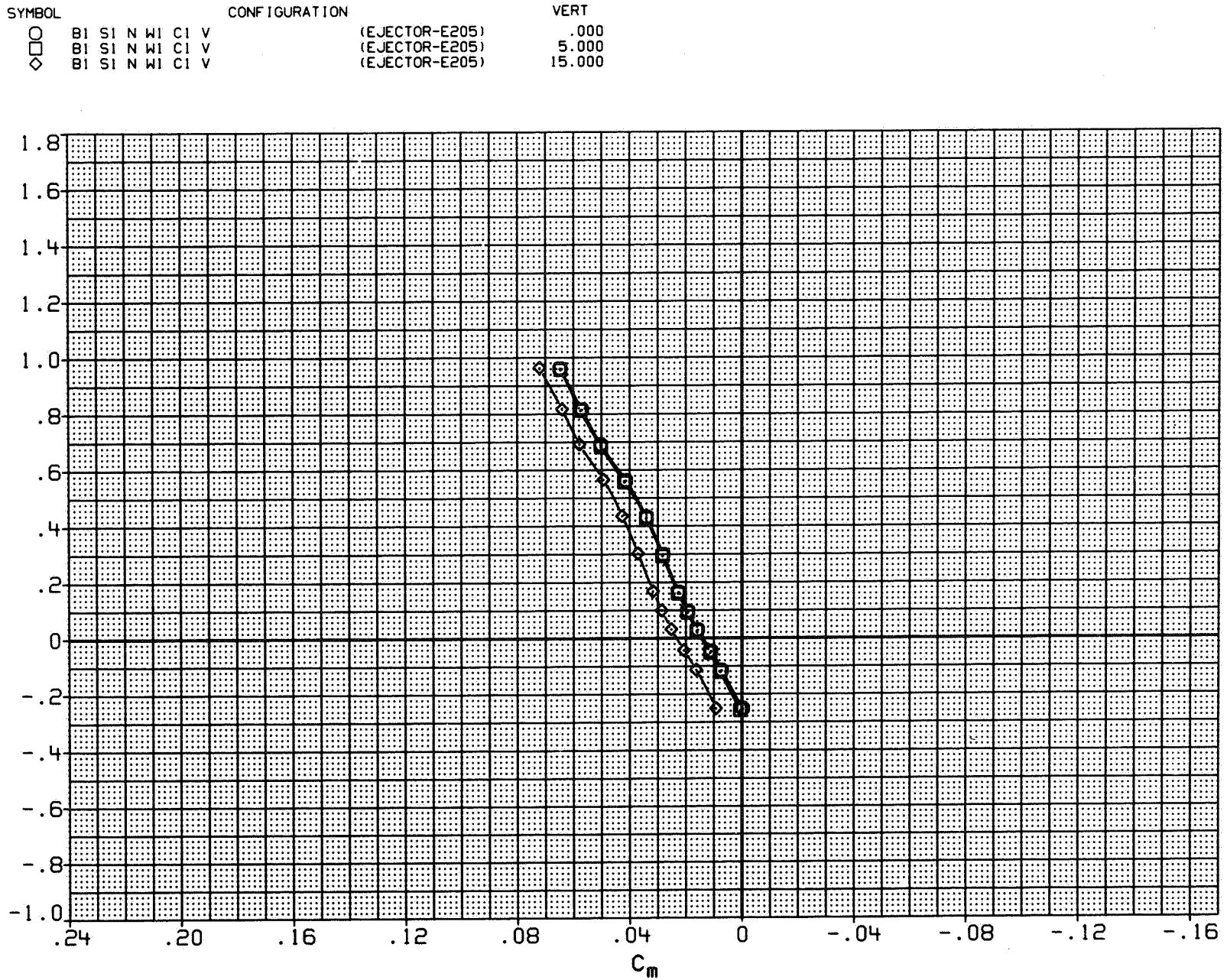


FIG. 24 VERTICAL TAIL DEFLECTION EFFECTS, LONGITUDINAL CHARACTERISTICS

MACH = 2.00

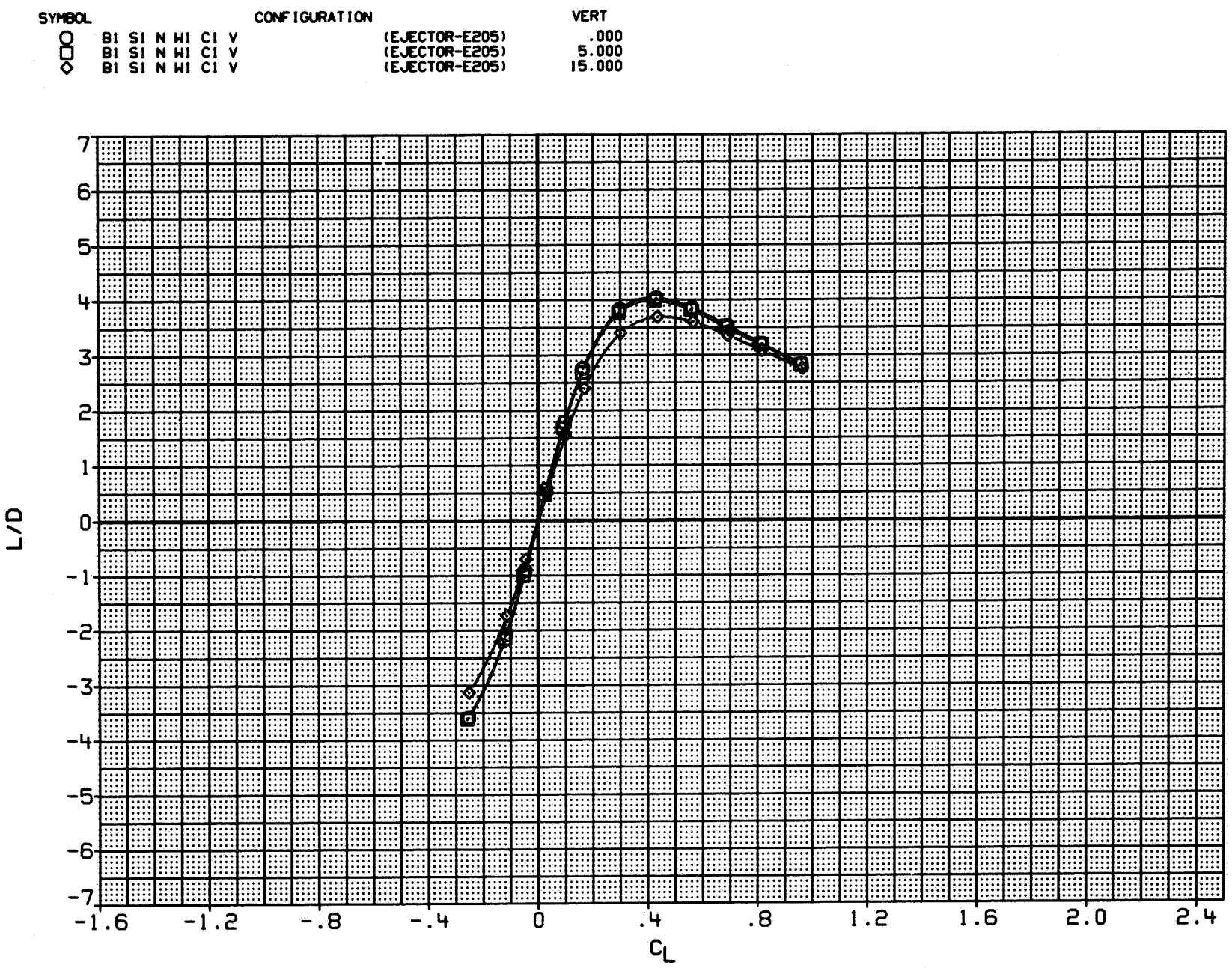


FIG. 24 VERTICAL TAIL DEFLECTION EFFECTS, LONGITUDINAL CHARACTERISTICS

MACH = 2.00

| SYMBOL | CONFIGURATION | | VERT | ALPHA |
|---|---|---|---|---|
| ○ | B1 S1 N W1 C1 | (EJECTOR-E205) | | .000 |
| □ | B1 S1 N W1 C1 V | (EJECTOR-E205) | .000 | .000 |
| ◇ | B1 S1 N W1 C1 V | (EJECTOR-E205) | 5.000 | .000 |
| △ | B1 S1 N W1 C1 V | (EJECTOR-E205) | 15.000 | .000 |

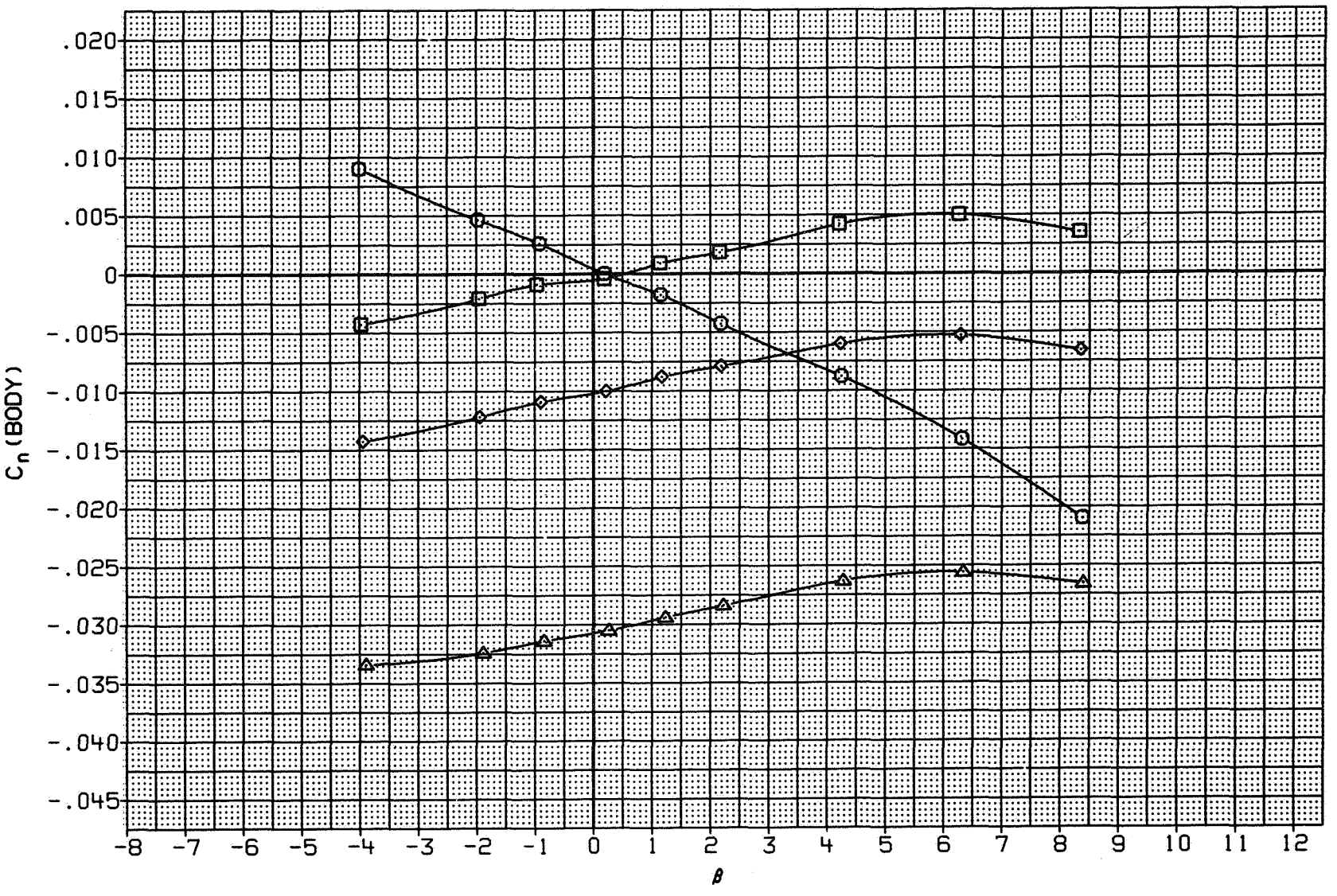


FIG. 25 VERTICAL TAIL DEFLECTION EFFECTS, LATERAL/DIRECTIONAL CHARACTERISTICS
ALPHA = 0 DEGREES

MACH = 1.60

| SYMBOL | CONFIGURATION | | VERT | ALPHA |
|---|---|---|---|---|
| ○ | B1 S1 N W1 C1 | (EJECTOR-E205) | | .000 |
| □ | B1 S1 N W1 C1 V | (EJECTOR-E205) | .000 | .000 |
| ◇ | B1 S1 N W1 C1 V | (EJECTOR-E205) | 5.000 | .000 |
| △ | B1 S1 N W1 C1 V | (EJECTOR-E205) | 15.000 | .000 |

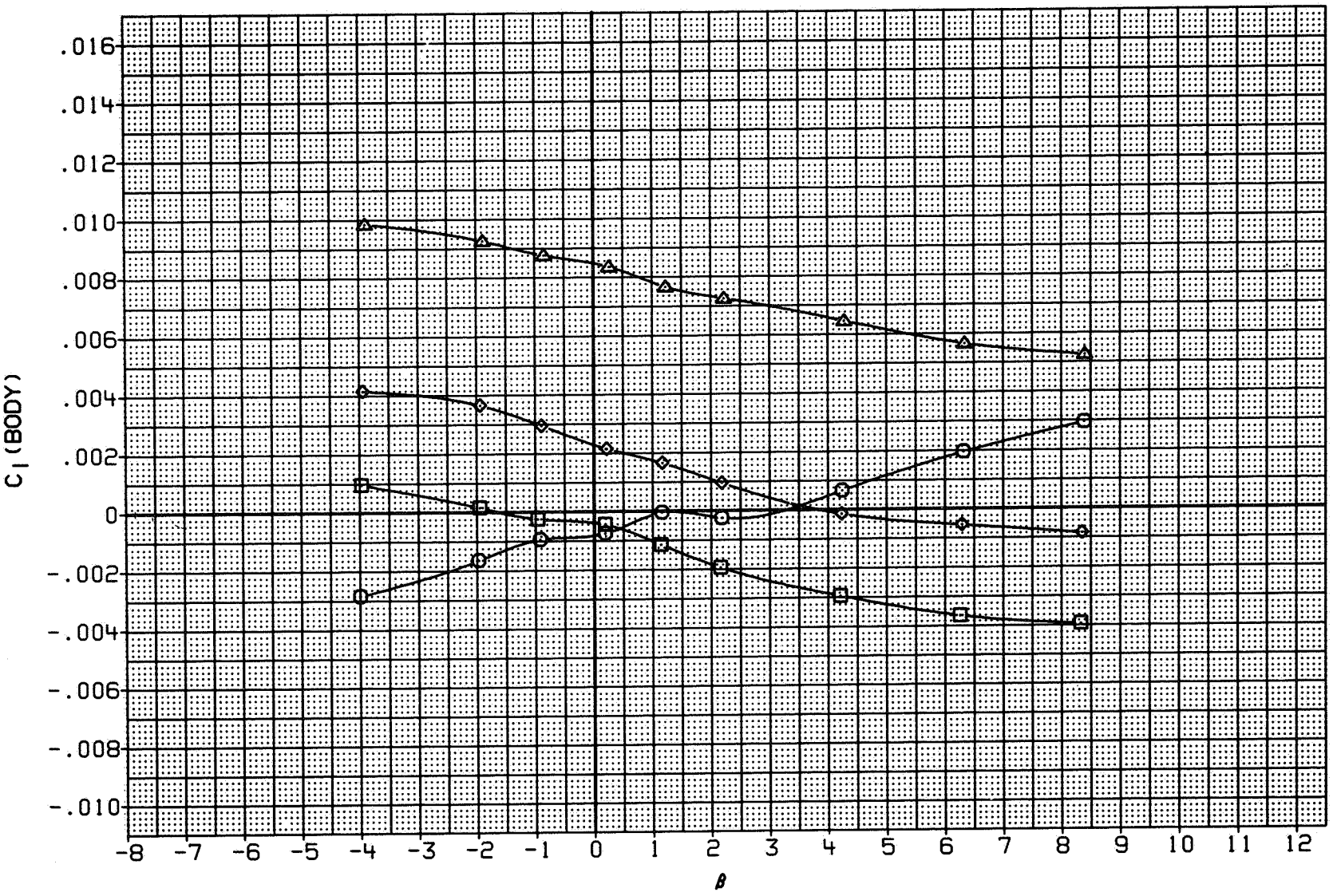


FIG. 25 VERTICAL TAIL DEFLECTION EFFECTS, LATERAL/DIRECTIONAL CHARACTERISTICS
ALPHA = 0 DEGREES

MACH = 1.60

| SYMBOL | CONFIGURATION | | VERT | ALPHA |
|---|---|---|---|---|
| ○ | B1 S1 N W1 C1 | (EJECTOR-E205) | | .000 |
| □ | B1 S1 N W1 C1 V | (EJECTOR-E205) | .000 | .000 |
| ◇ | B1 S1 N W1 C1 V | (EJECTOR-E205) | 5.000 | .000 |
| △ | B1 S1 N W1 C1 V | (EJECTOR-E205) | 15.000 | .000 |

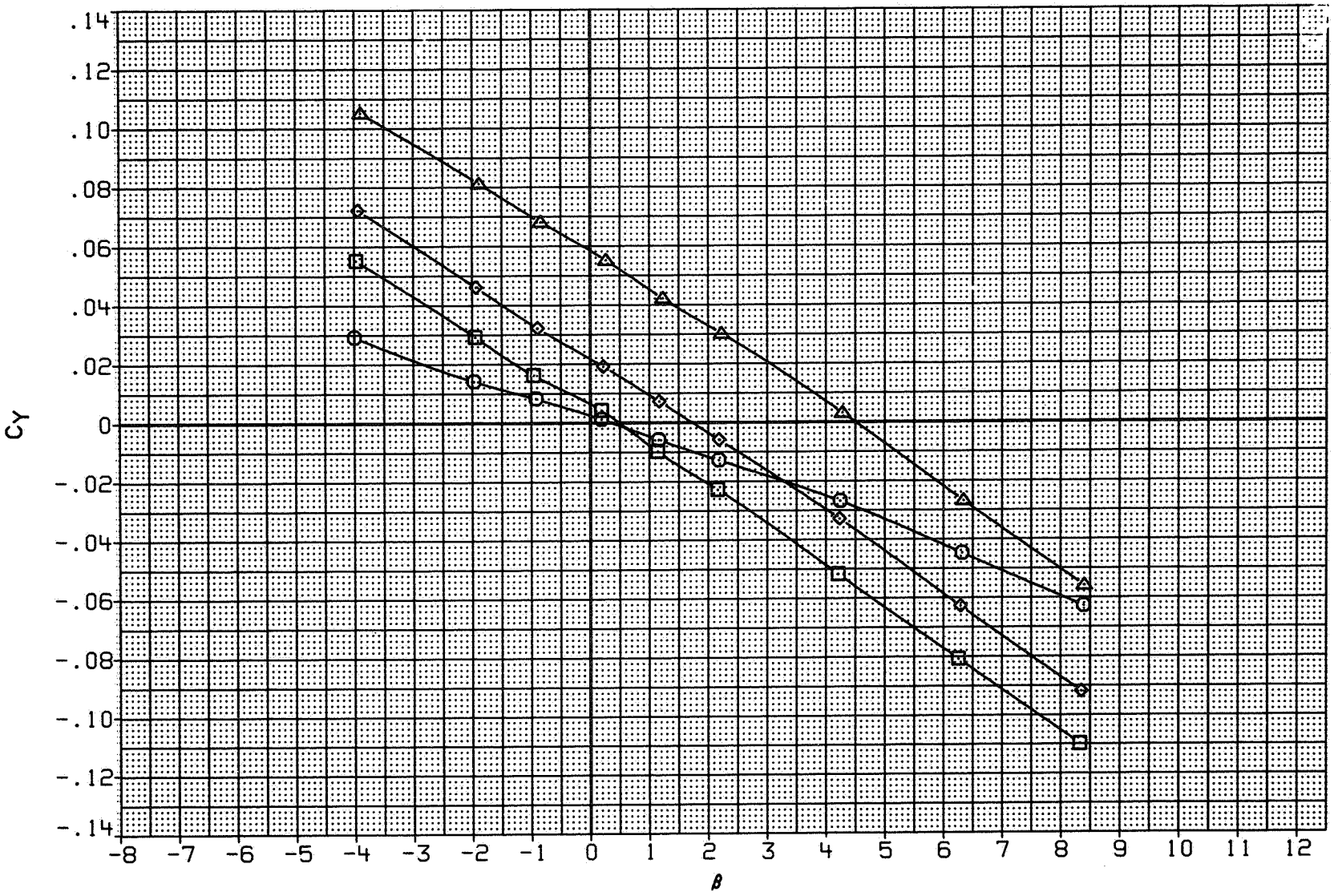


FIG. 25 VERTICAL TAIL DEFLECTION EFFECTS, LATERAL/DIRECTIONAL CHARACTERISTICS
ALPHA = 0 DEGREES

MACH = 1.60

| SYMBOL | CONFIGURATION | | VERT | ALPHA |
|---|---|---|---|---|
| ○ | B1 S1 N W1 C1 | (EJECTOR-E205) | | 9.500 |
| □ | B1 S1 N W1 C1 V | (EJECTOR-E205) | .000 | 9.500 |
| ◇ | B1 S1 N W1 C1 V | (EJECTOR-E205) | 5.000 | 9.500 |
| △ | B1 S1 N W1 C1 V | (EJECTOR-E205) | 15.000 | 9.500 |

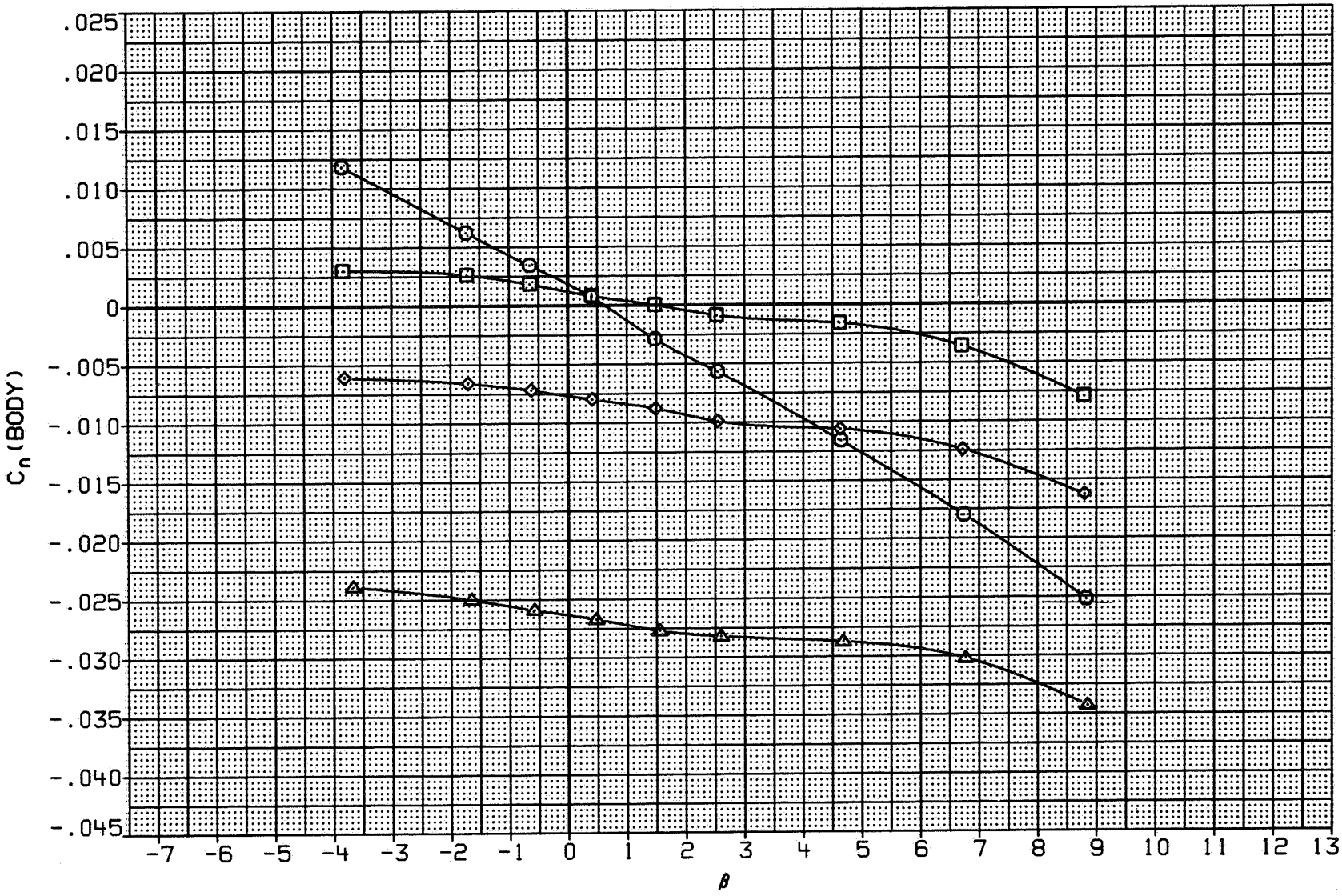


FIG. 26 VERTICAL TAIL DEFLECTION EFFECTS, LATERAL/DIRECTIONAL CHARACTERISTICS
ALPHA = 8 DEGREES

MACH = 1.60

| SYMBOL | CONFIGURATION | | VERT | ALPHA |
|---|---|---|---|---|
| ○ | B1 S1 N W1 C1 | (EJECTOR-E205) | | 9.500 |
| □ | B1 S1 N W1 C1 V | (EJECTOR-E205) | .000 | 9.500 |
| ◇ | B1 S1 N W1 C1 V | (EJECTOR-E205) | 5.000 | 9.500 |
| △ | B1 S1 N W1 C1 V | (EJECTOR-E205) | 15.000 | 9.500 |

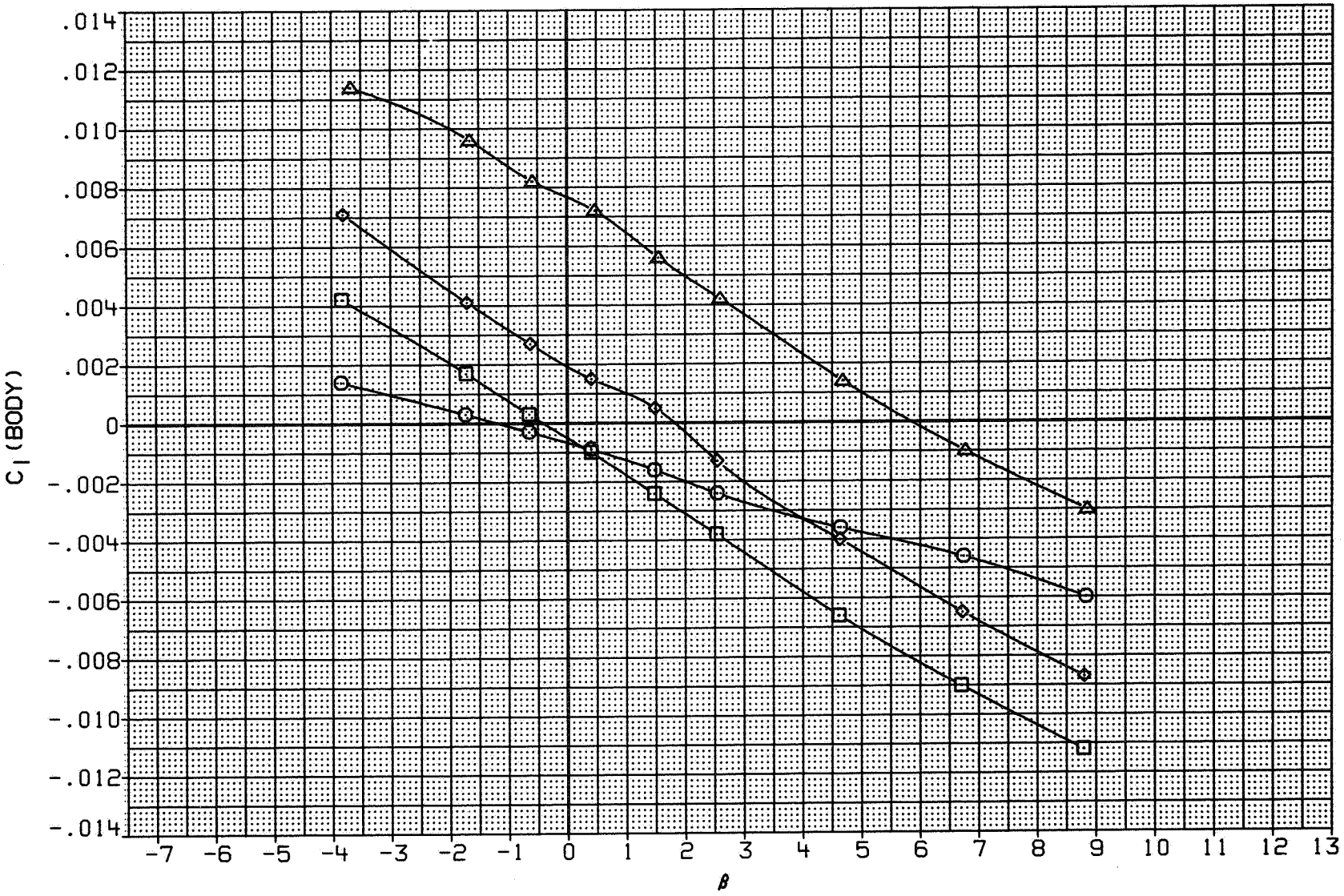


FIG. 26 VERTICAL TAIL DEFLECTION EFFECTS, LATERAL/DIRECTIONAL CHARACTERISTICS
ALPHA = 8 DEGREES

MACH = 1.60

| SYMBOL | CONFIGURATION | | VERT | ALPHA |
|---|---|---|---|---|
| ○ | B1 S1 N W1 C1 | (EJECTOR-E205) | | 9.500 |
| □ | B1 S1 N W1 C1 V | (EJECTOR-E205) | .000 | 9.500 |
| ◇ | B1 S1 N W1 C1 V | (EJECTOR-E205) | 5.000 | 9.500 |
| △ | B1 S1 N W1 C1 V | (EJECTOR-E205) | 15.000 | 9.500 |

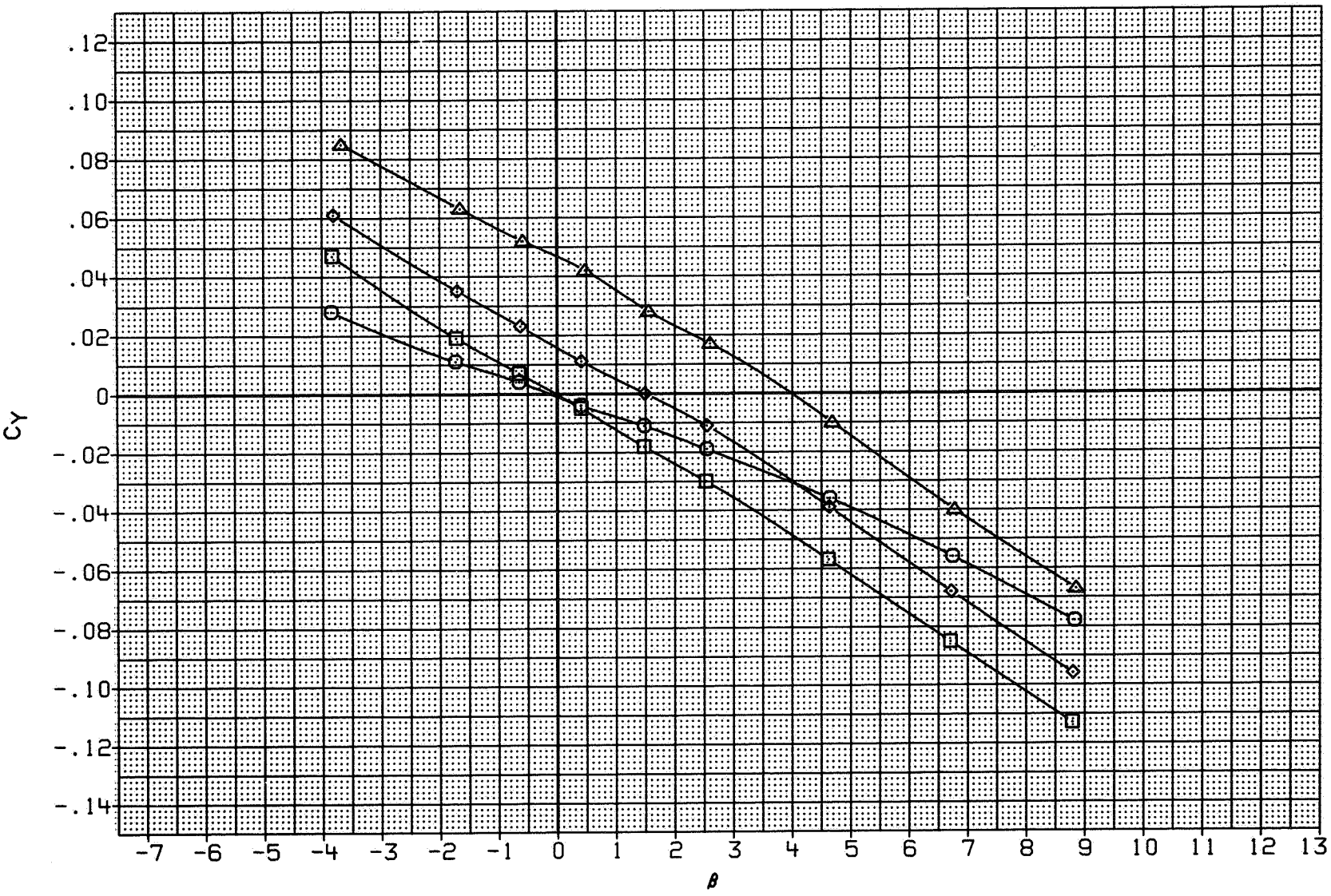


FIG. 26 VERTICAL TAIL DEFLECTION EFFECTS, LATERAL/DIRECTIONAL CHARACTERISTICS
ALPHA = 8 DEGREES

MACH = 1.60

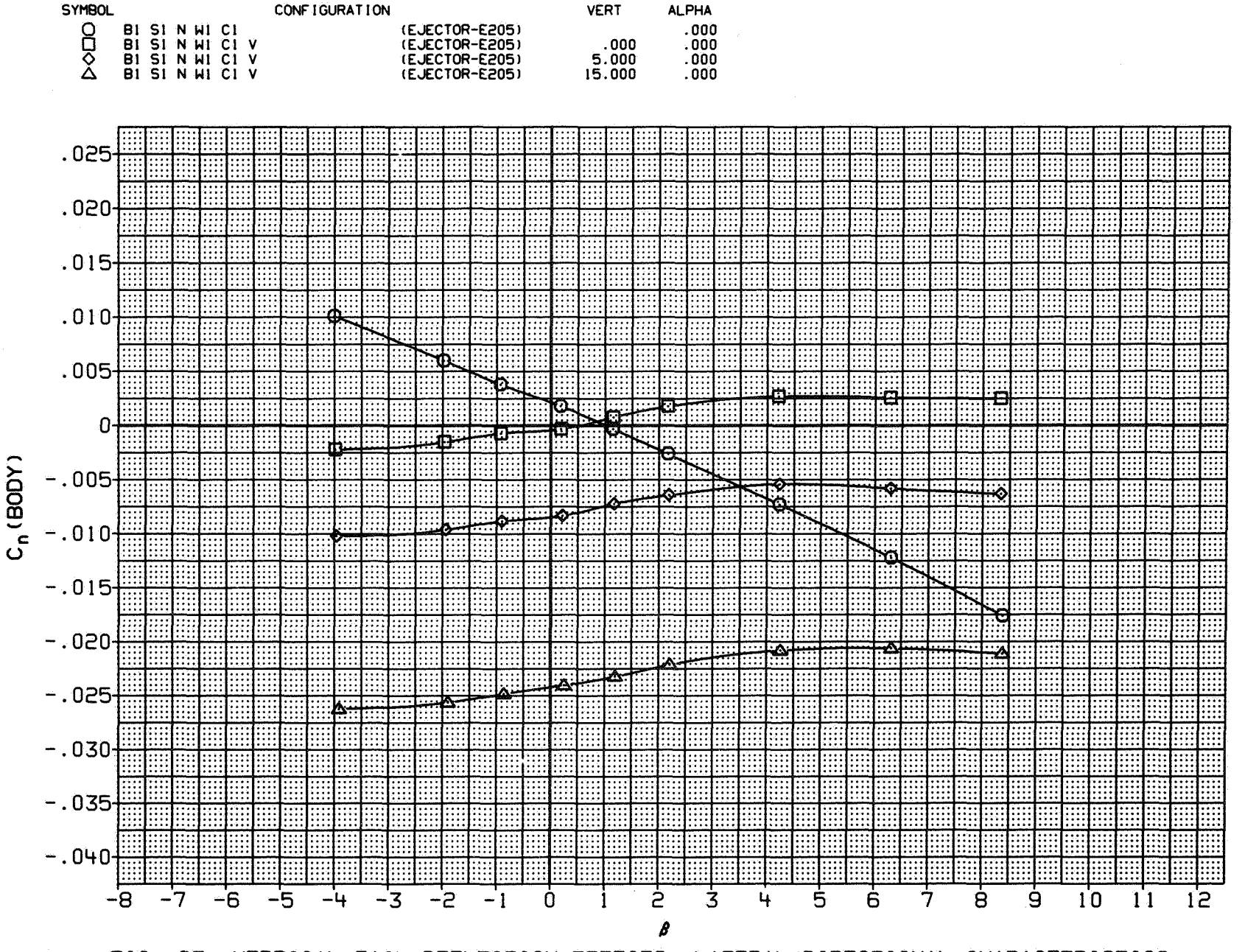


FIG. 27 VERTICAL TAIL DEFLECTION EFFECTS, LATERAL/DIRECTIONAL CHARACTERISTICS
ALPHA = 0 DEGREES

MACH = 2.00

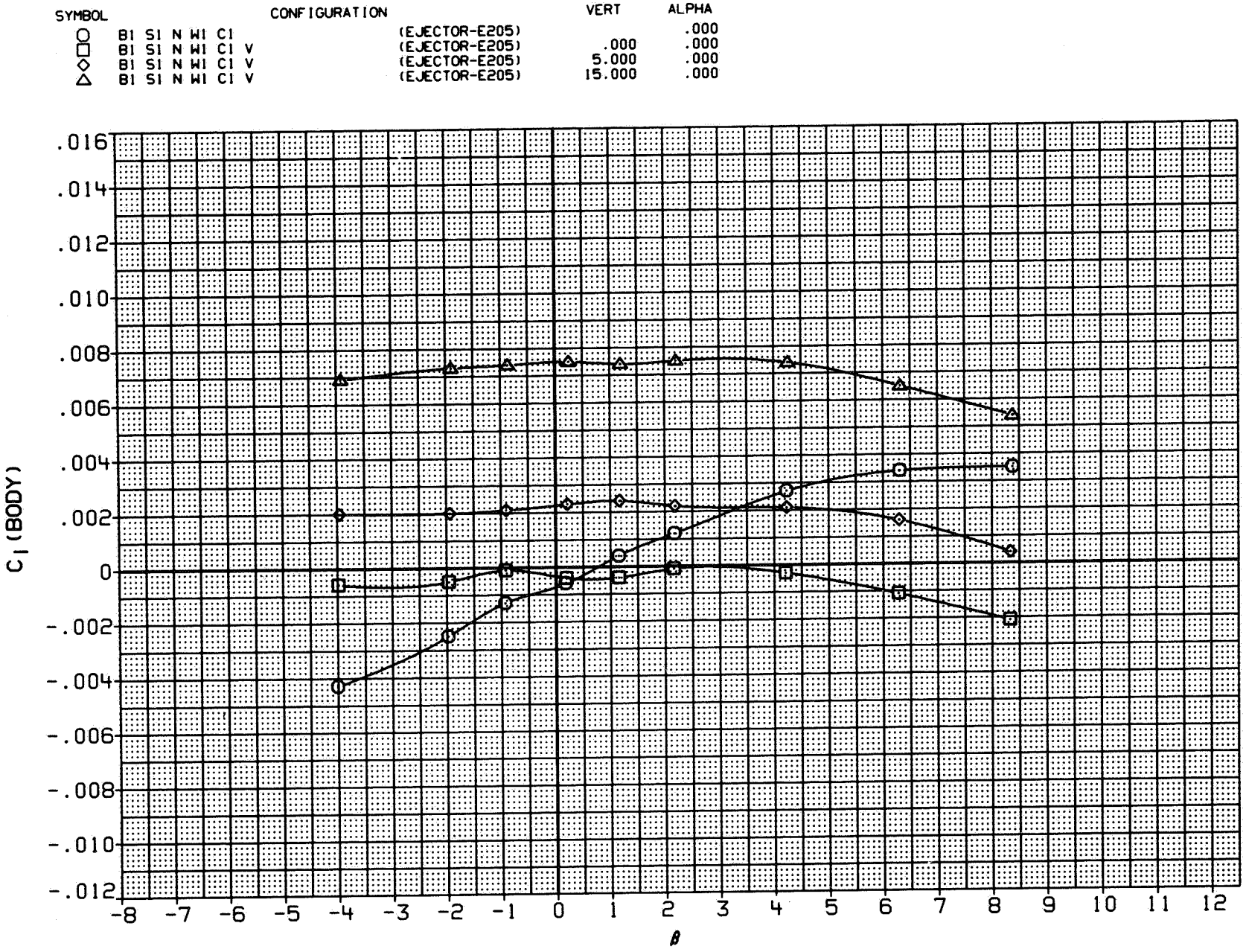


FIG. 27 VERTICAL TAIL DEFLECTION EFFECTS, LATERAL/DIRECTIONAL CHARACTERISTICS
ALPHA = 0 DEGREES

MACH = 2.00

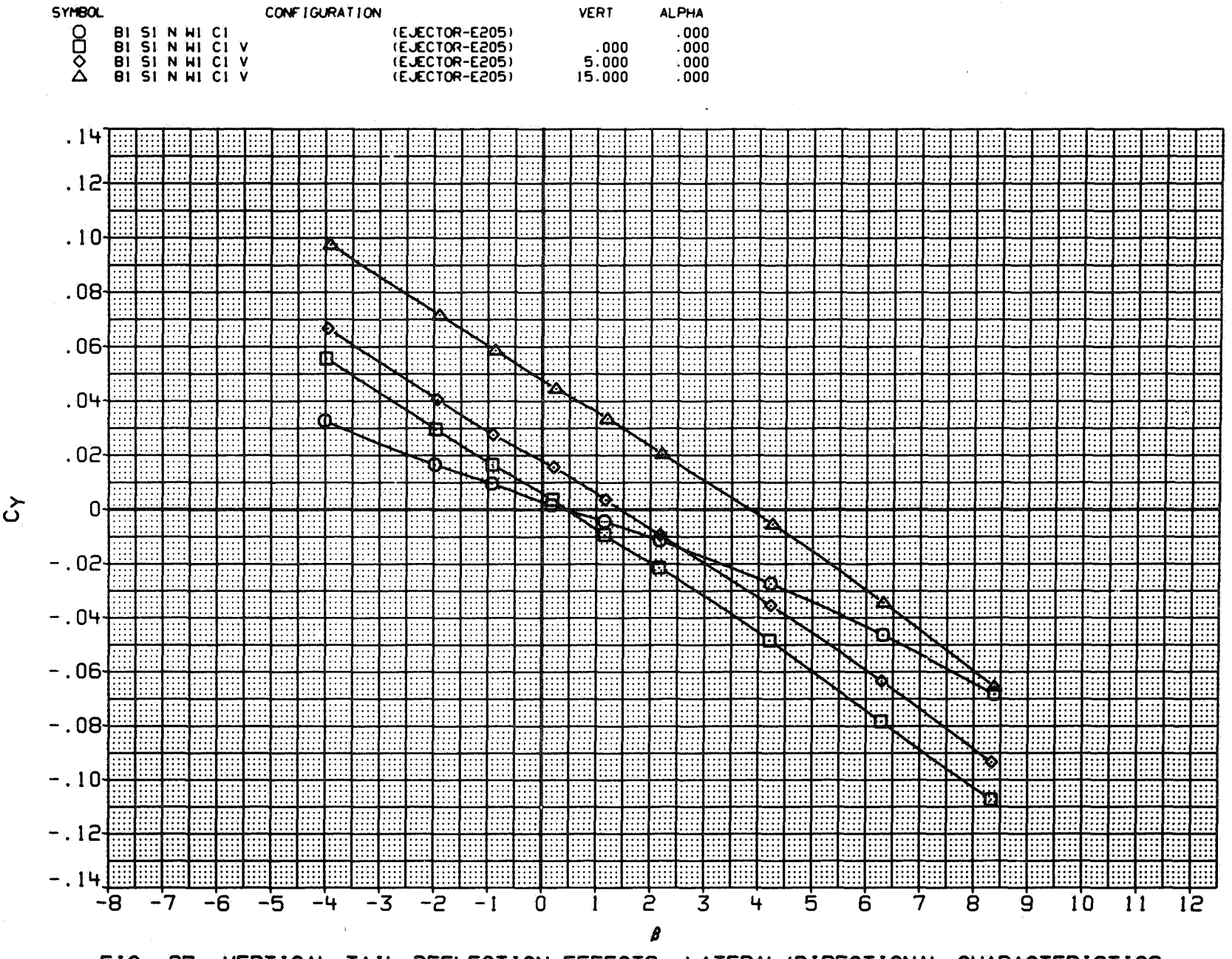


FIG. 27 VERTICAL TAIL DEFLECTION EFFECTS, LATERAL/DIRECTIONAL CHARACTERISTICS
ALPHA = 0 DEGREES

MACH = 2.00

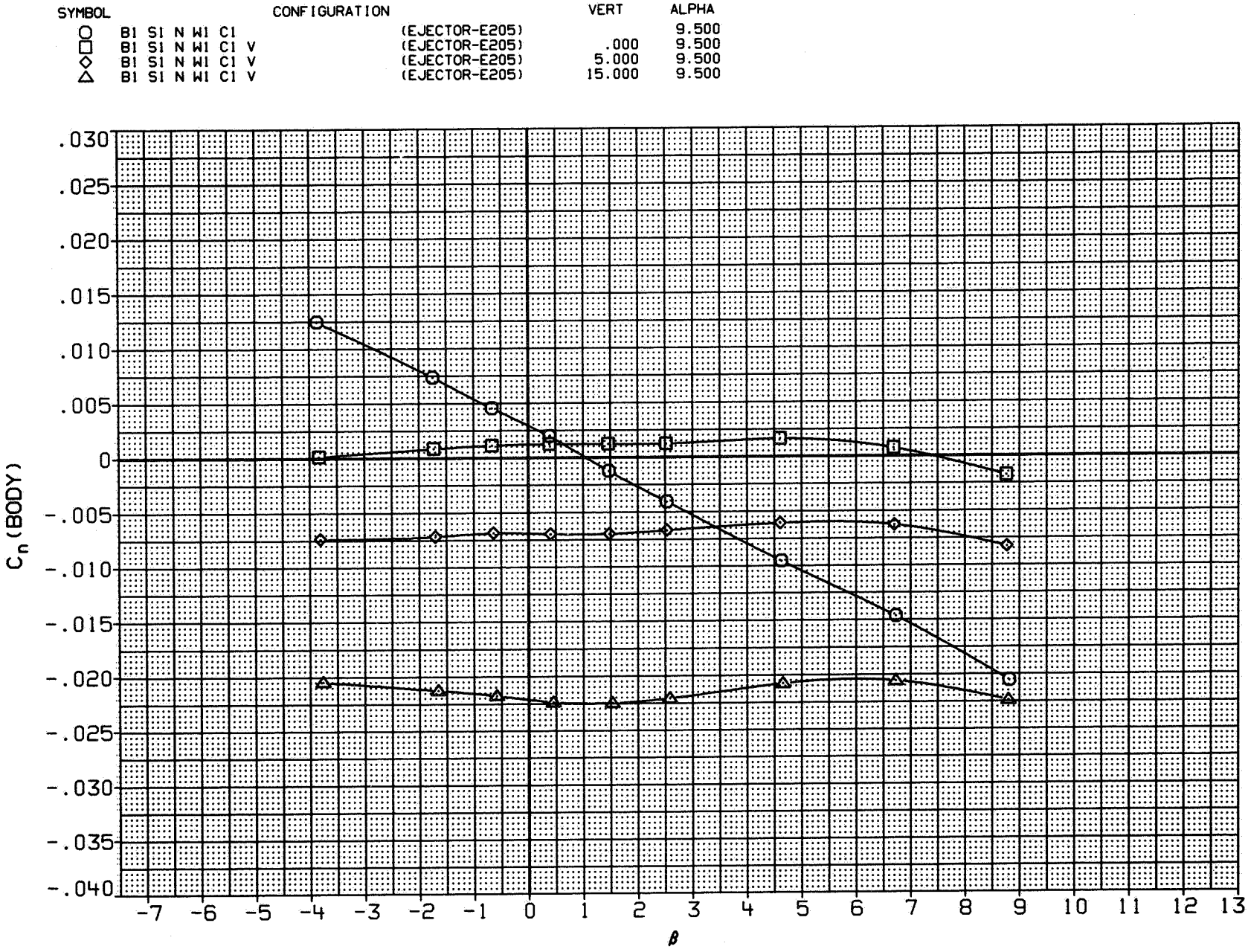


FIG. 28 VERTICAL TAIL DEFLECTION EFFECTS, LATERAL/DIRECTIONAL CHARACTERISTICS
ALPHA = 8 DEGREES

MACH = 2.00

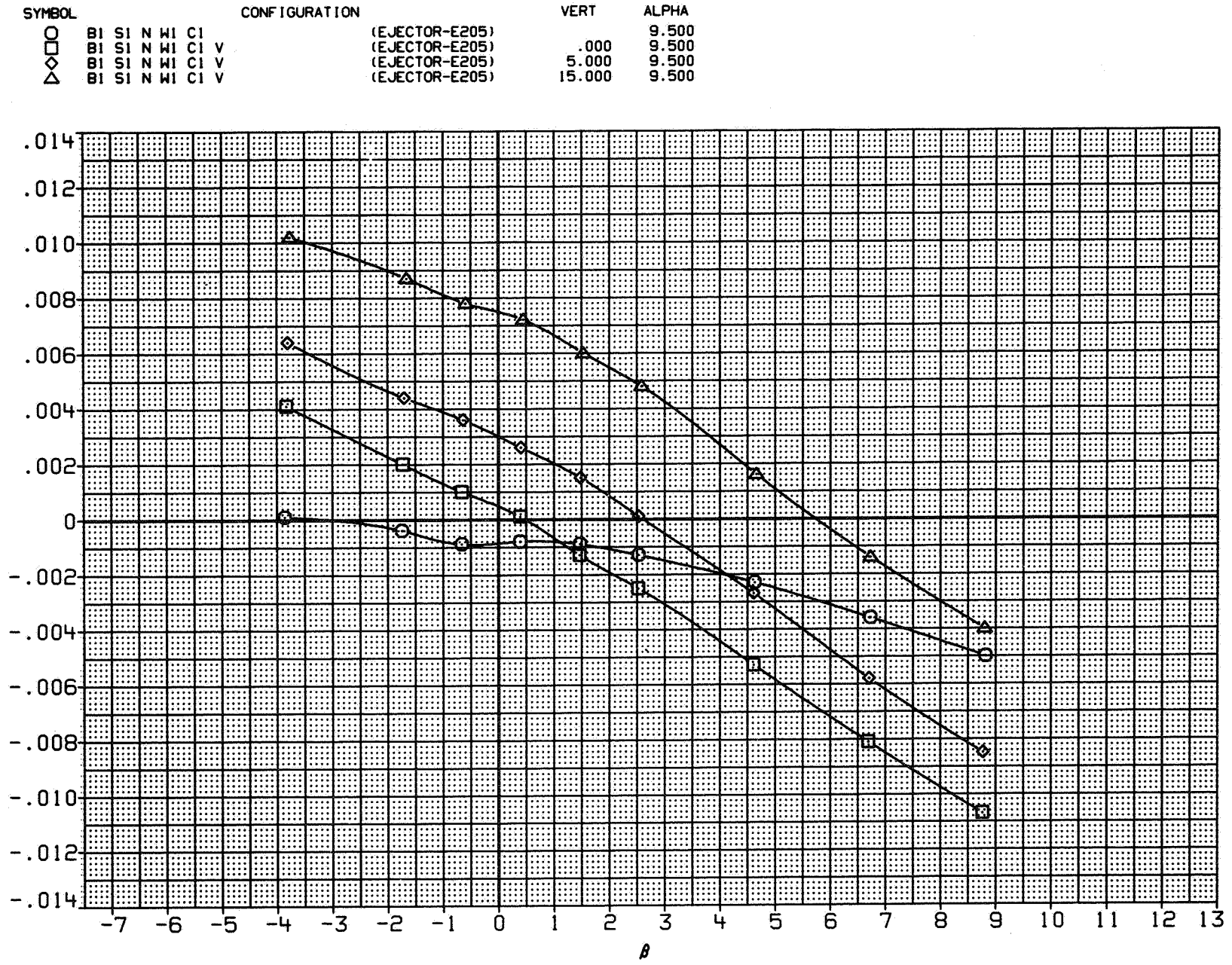


FIG. 28 VERTICAL TAIL DEFLECTION EFFECTS, LATERAL/DIRECTIONAL CHARACTERISTICS
ALPHA = 8 DEGREES

MACH = 2.00

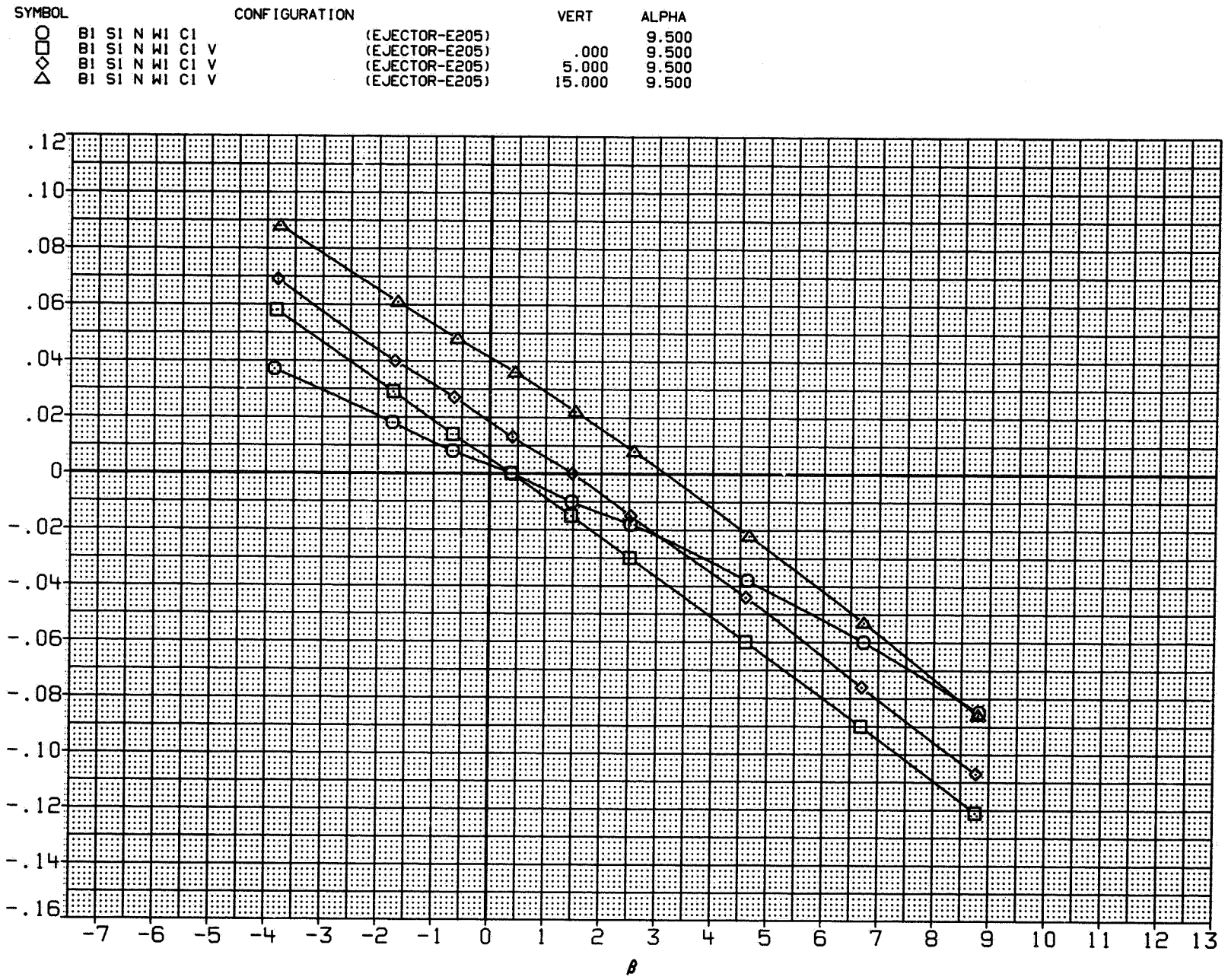


FIG. 28 VERTICAL TAIL DEFLECTION EFFECTS, LATERAL/DIRECTIONAL CHARACTERISTICS
ALPHA = 8 DEGREES

MACH = 2.00

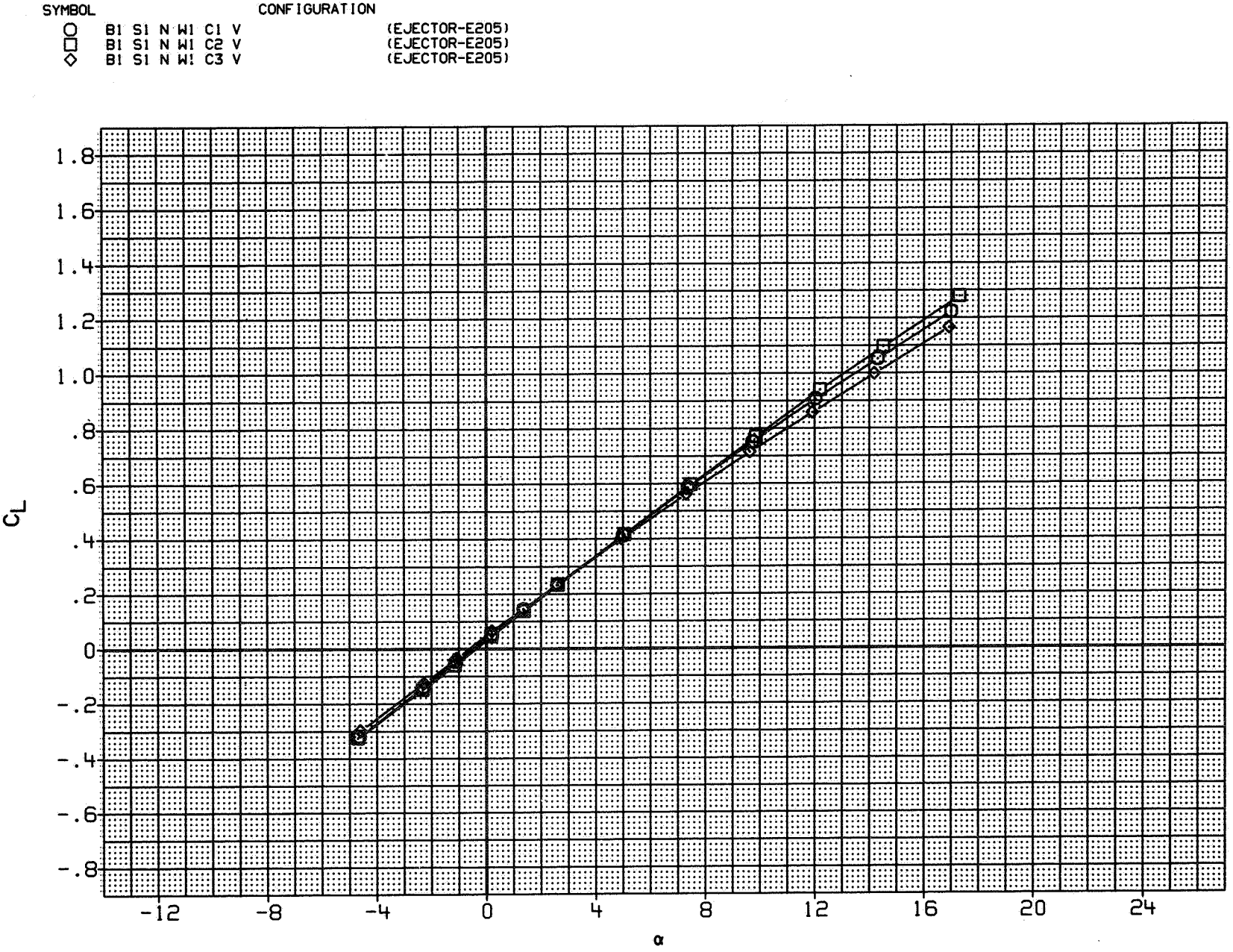


FIG. 29 CANARD LOCATION EFFECTS, LONGITUDINAL CHARACTERISTICS
CANARD = 0 DEGREES, STRAKE S1

MACH = 1.60

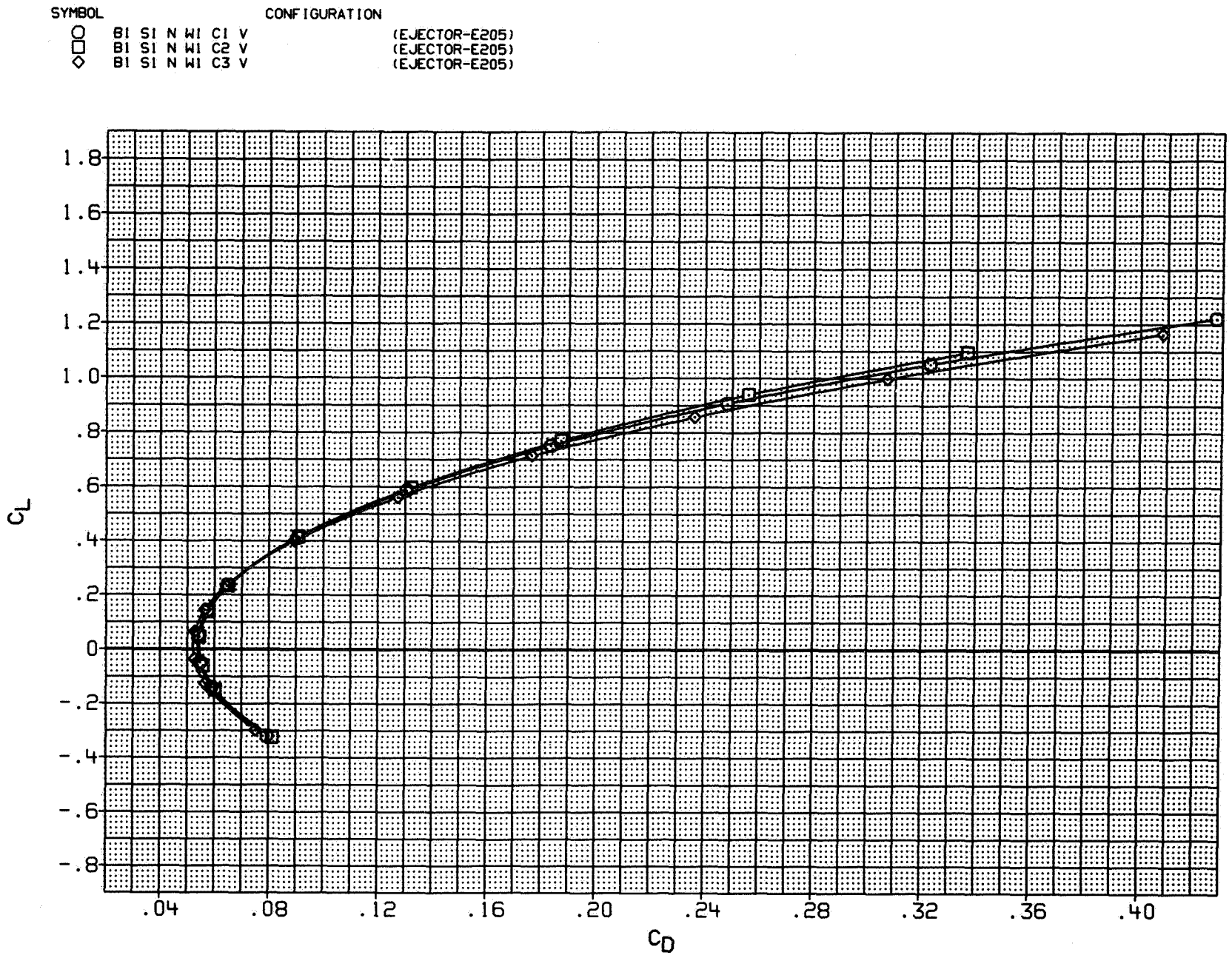


FIG. 29 CANARD LOCATION EFFECTS, LONGITUDINAL CHARACTERISTICS
CANARD = 0 DEGREES, STRAKE S1

MACH = 1.60

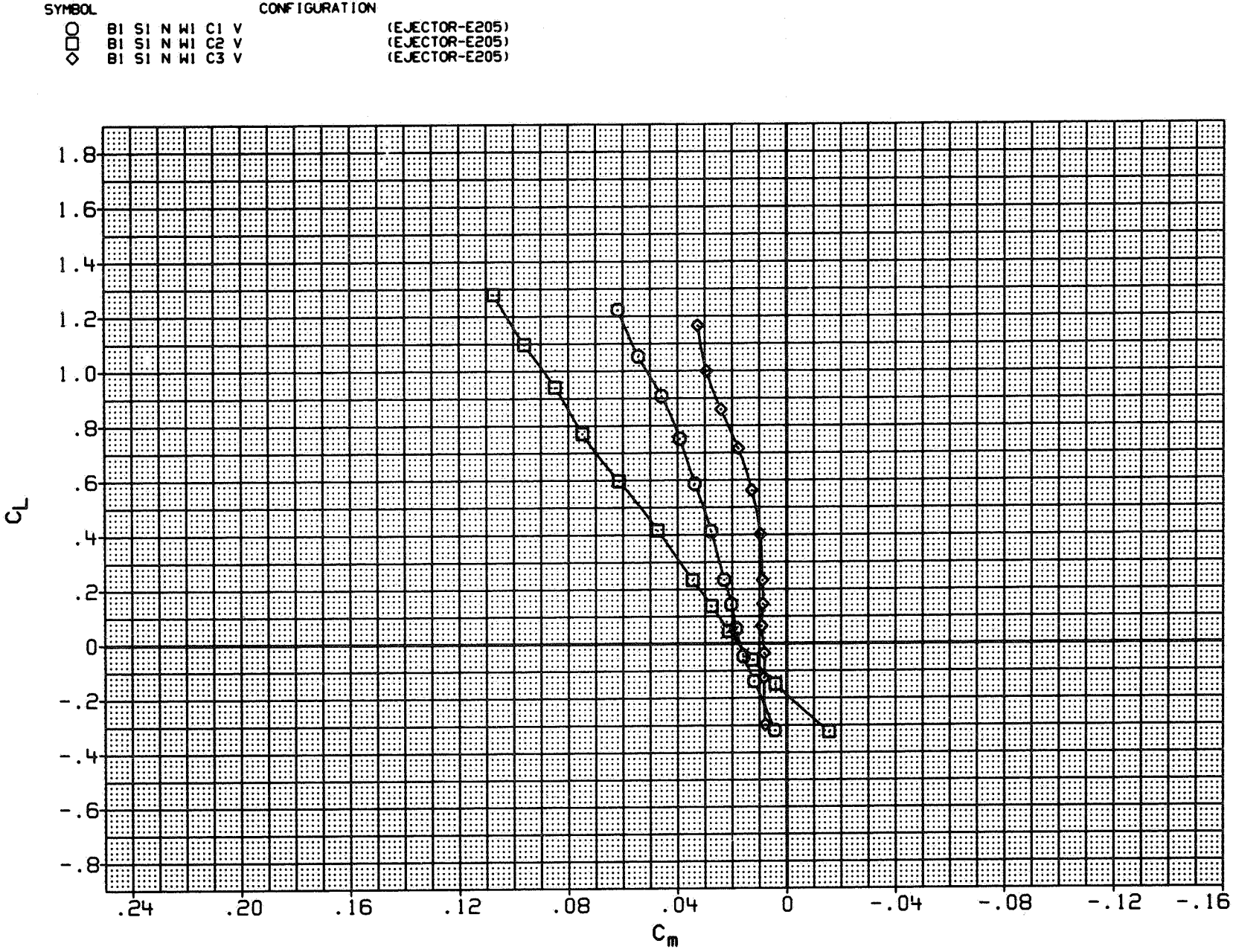


FIG. 29 CANARD LOCATION EFFECTS, LONGITUDINAL CHARACTERISTICS
CANARD = 0 DEGREES, STRAKE S1

MACH = 1.60

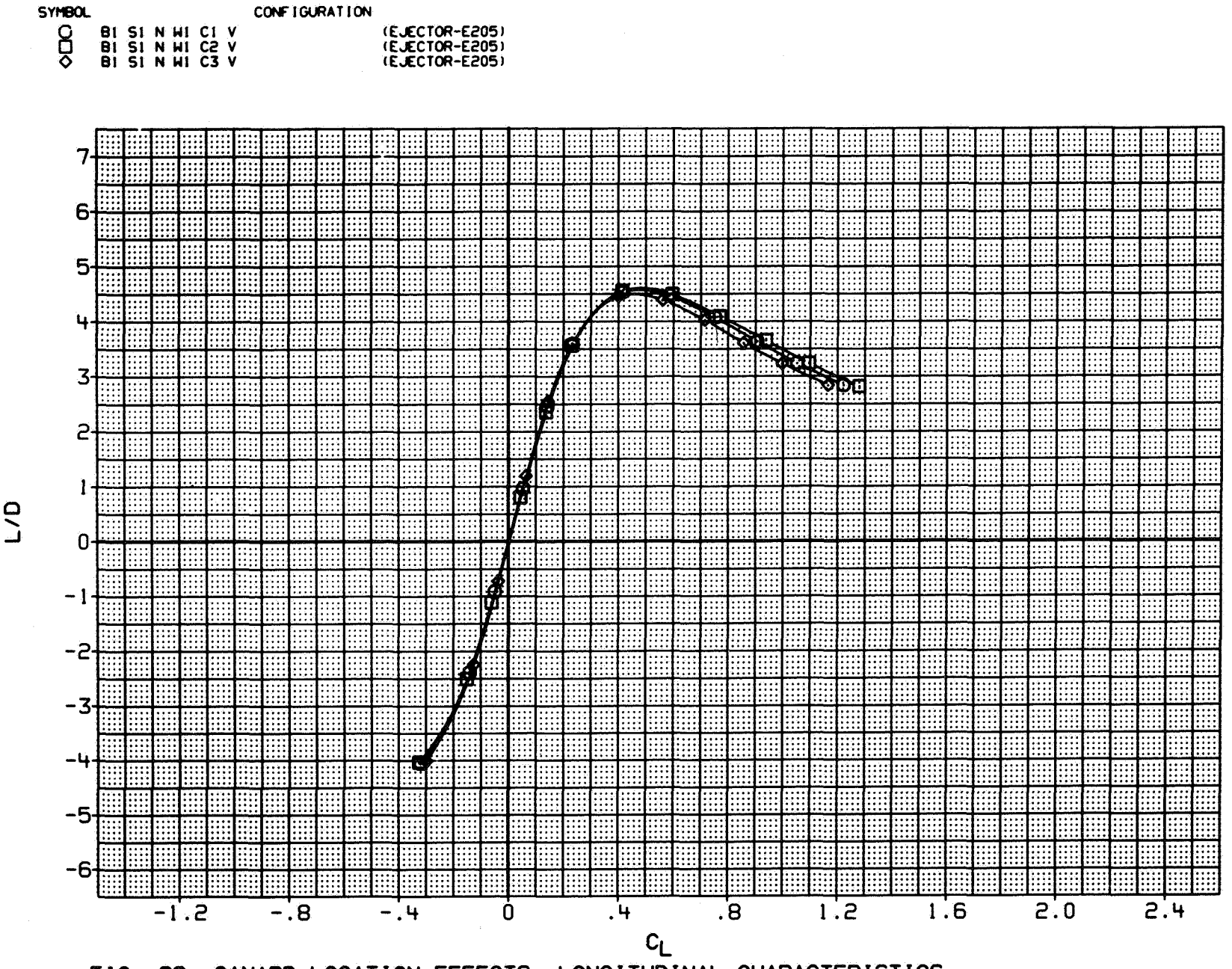


FIG. 29 CANARD LOCATION EFFECTS, LONGITUDINAL CHARACTERISTICS
CANARD = 0 DEGREES, STRAKE S1

MACH = 1.60

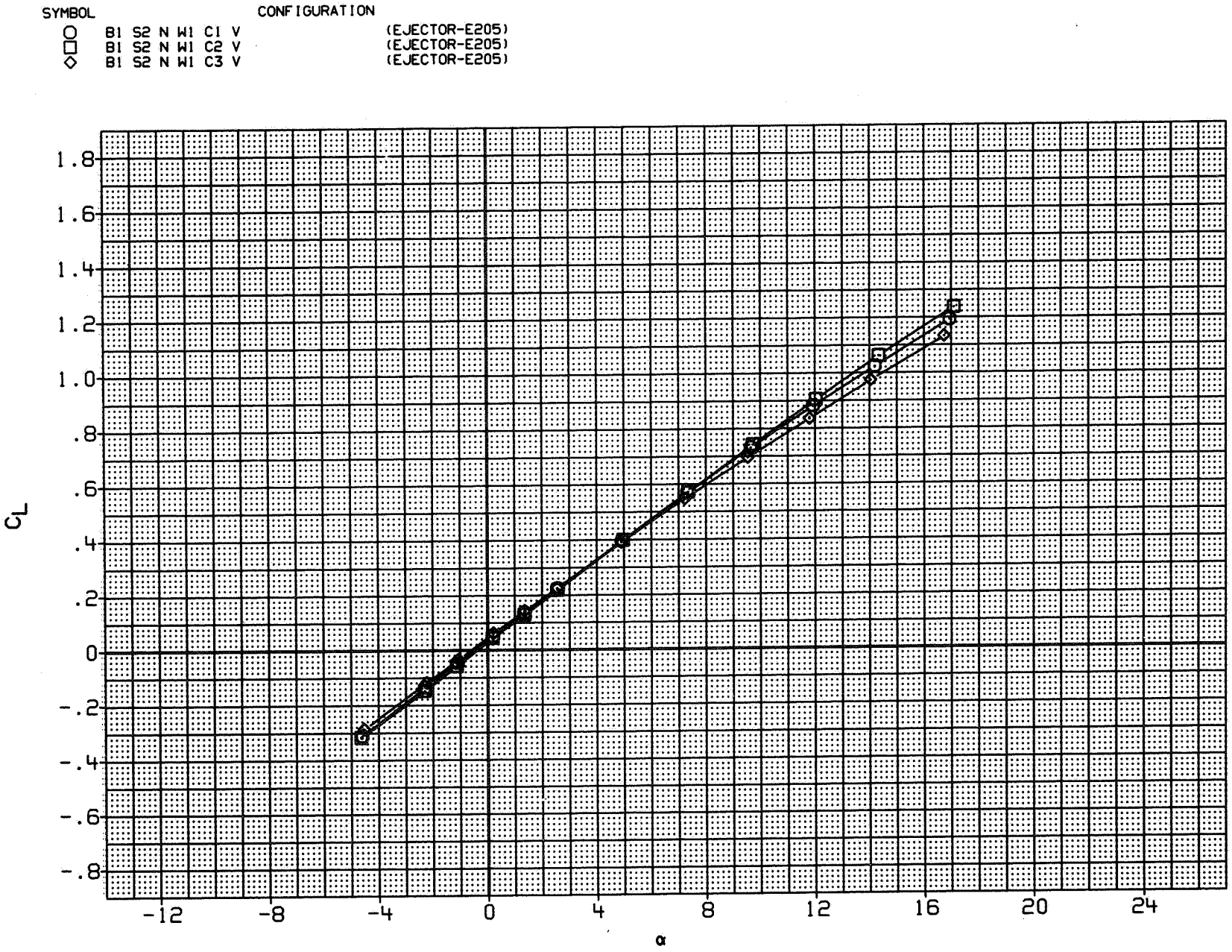


FIG. 30 CANARD LOCATION EFFECTS, LONGITUDINAL CHARACTERISTICS
CANARD = 0 DEGREES, STRAKE S2

MACH = 1.60

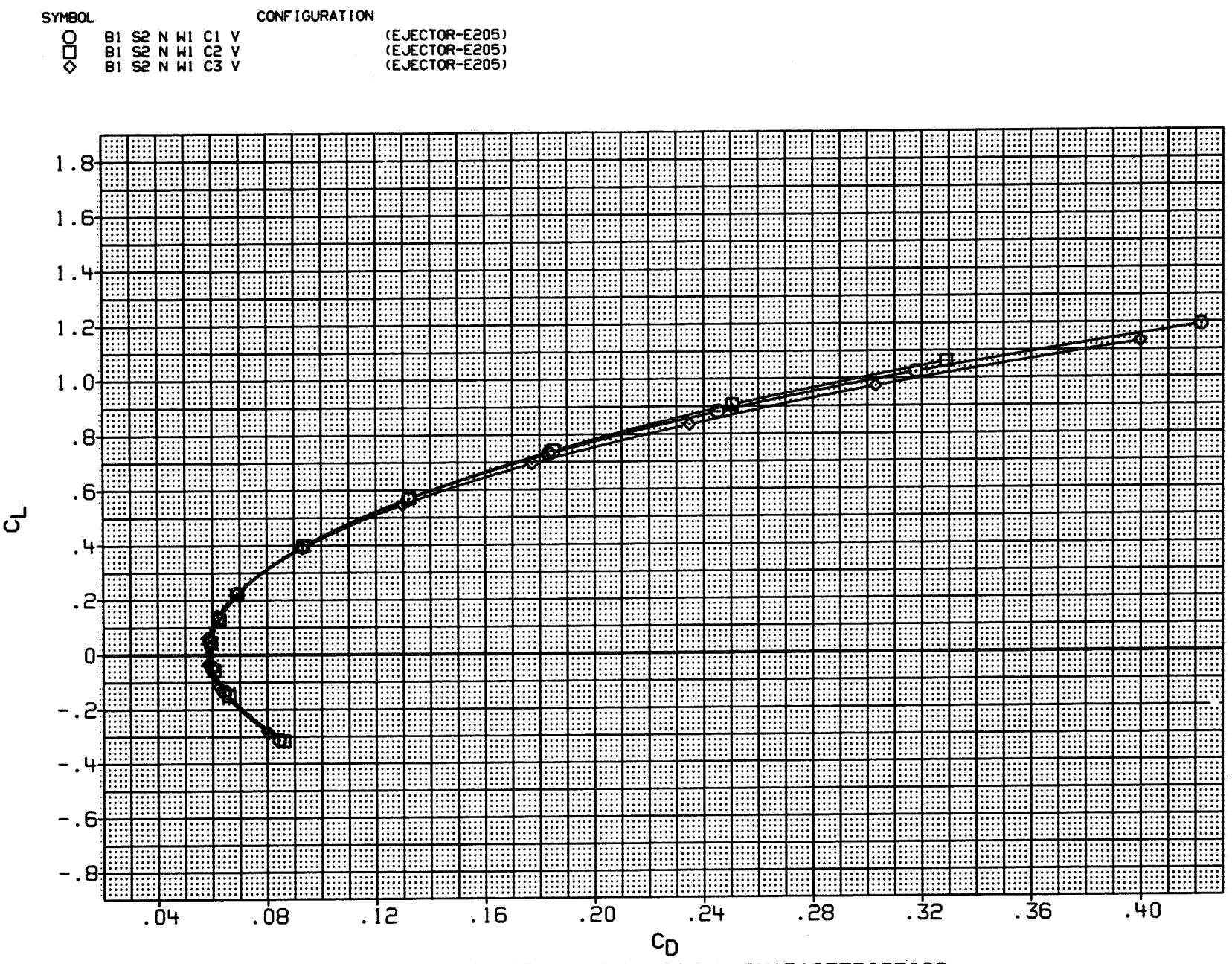


FIG. 30 CANARD LOCATION EFFECTS, LONGITUDINAL CHARACTERISTICS
CANARD = 0 DEGREES, STRAKE S2

MACH = 1.60

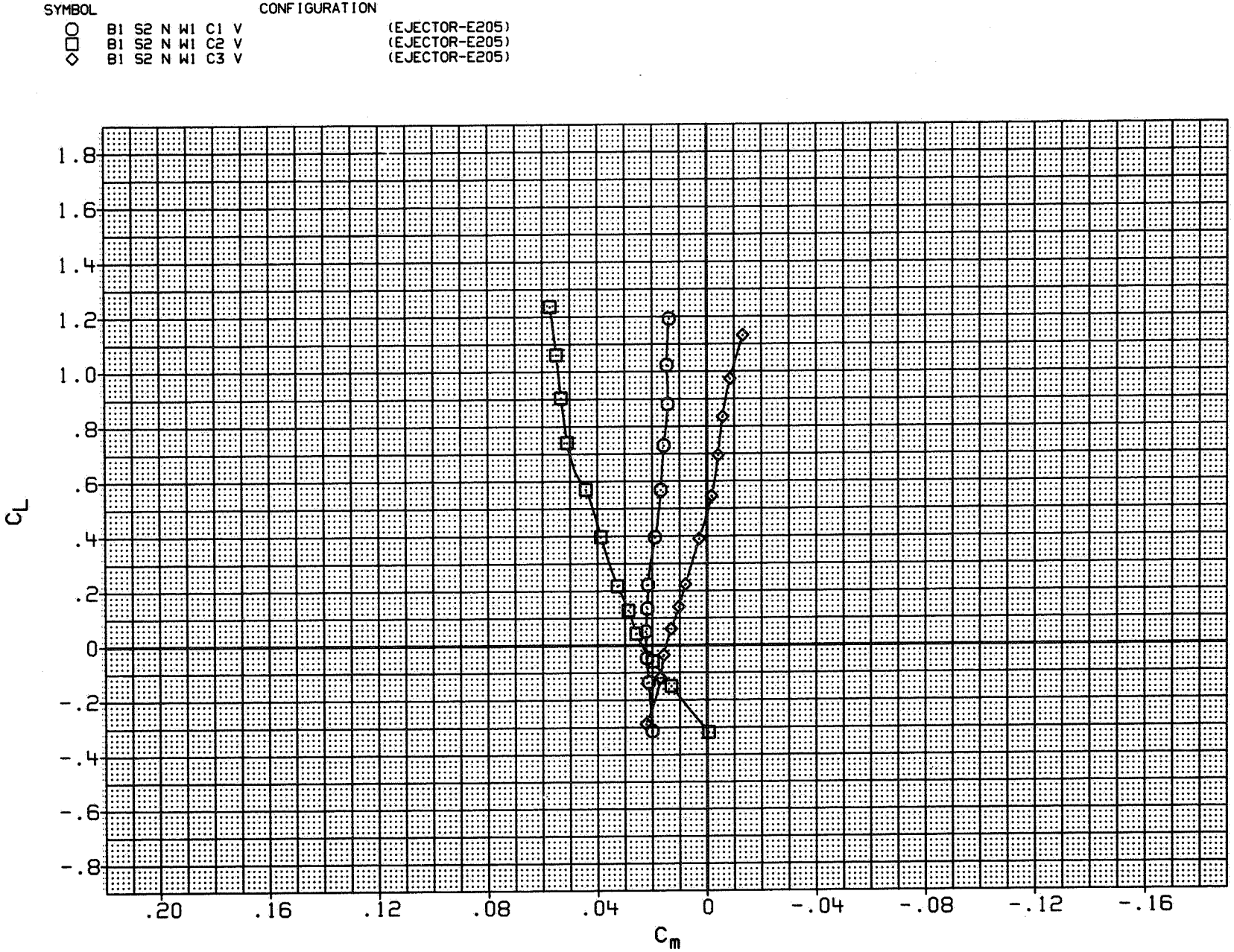


FIG. 30 CANARD LOCATION EFFECTS, LONGITUDINAL CHARACTERISTICS
CANARD = 0 DEGREES, STRAKE S2

MACH = 1.60

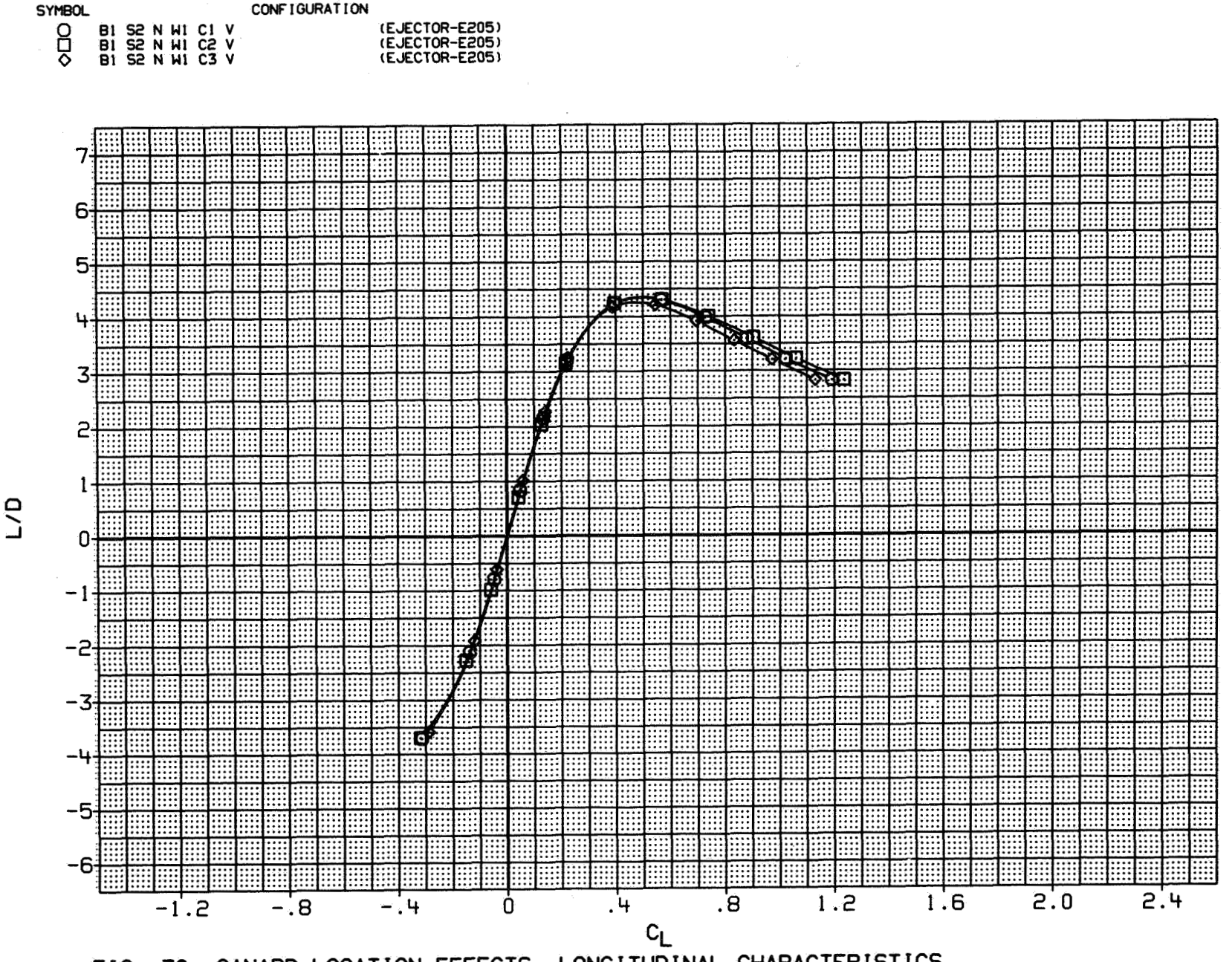


FIG. 30 CANARD LOCATION EFFECTS, LONGITUDINAL CHARACTERISTICS
CANARD = 0 DEGREES, STRAKE S2

MACH = 1.60

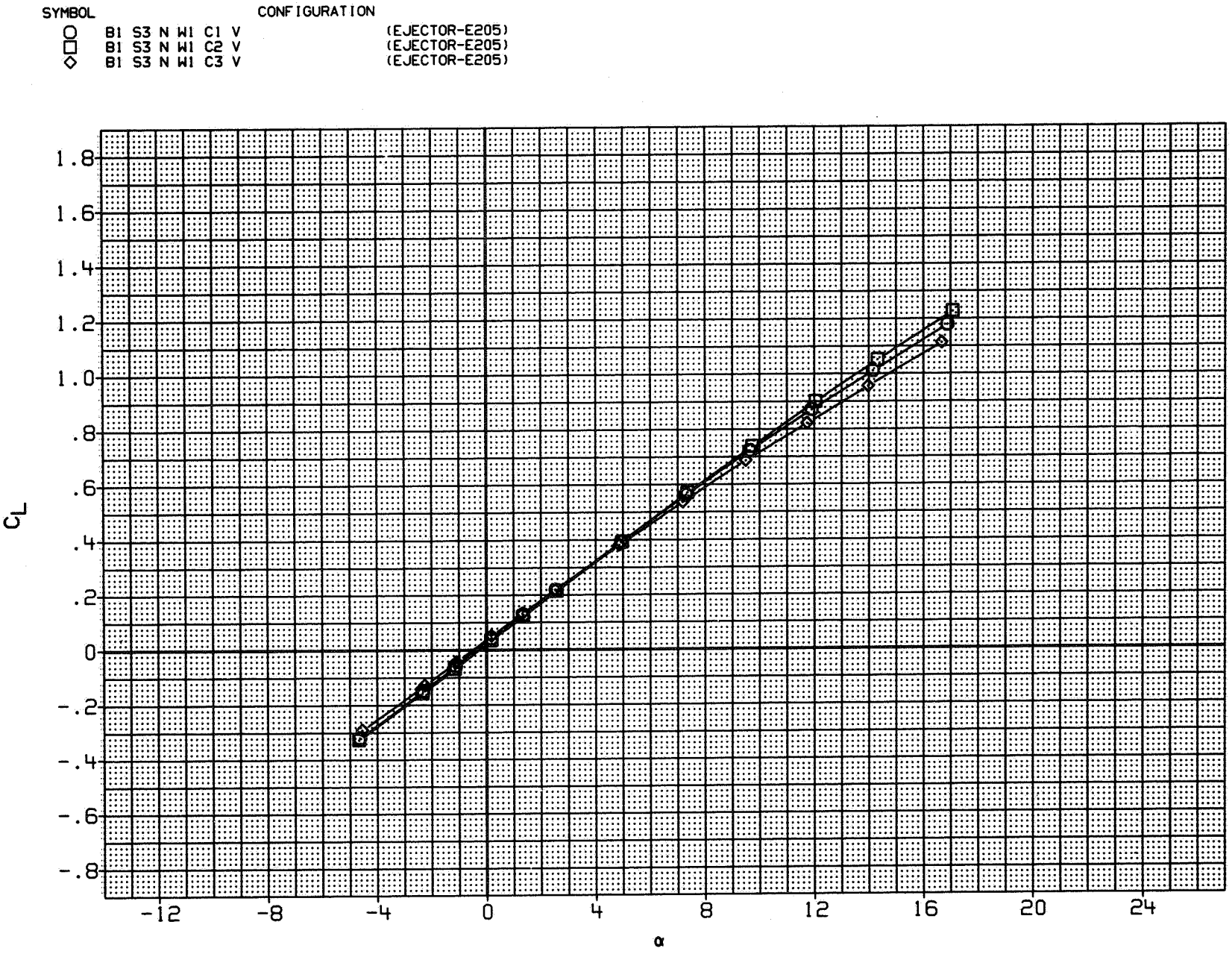


FIG. 31 CANARD LOCATION EFFECTS, LONGITUDINAL CHARACTERISTICS
CANARD = 0 DEGREES, STRAKE S3

MACH = 1.60

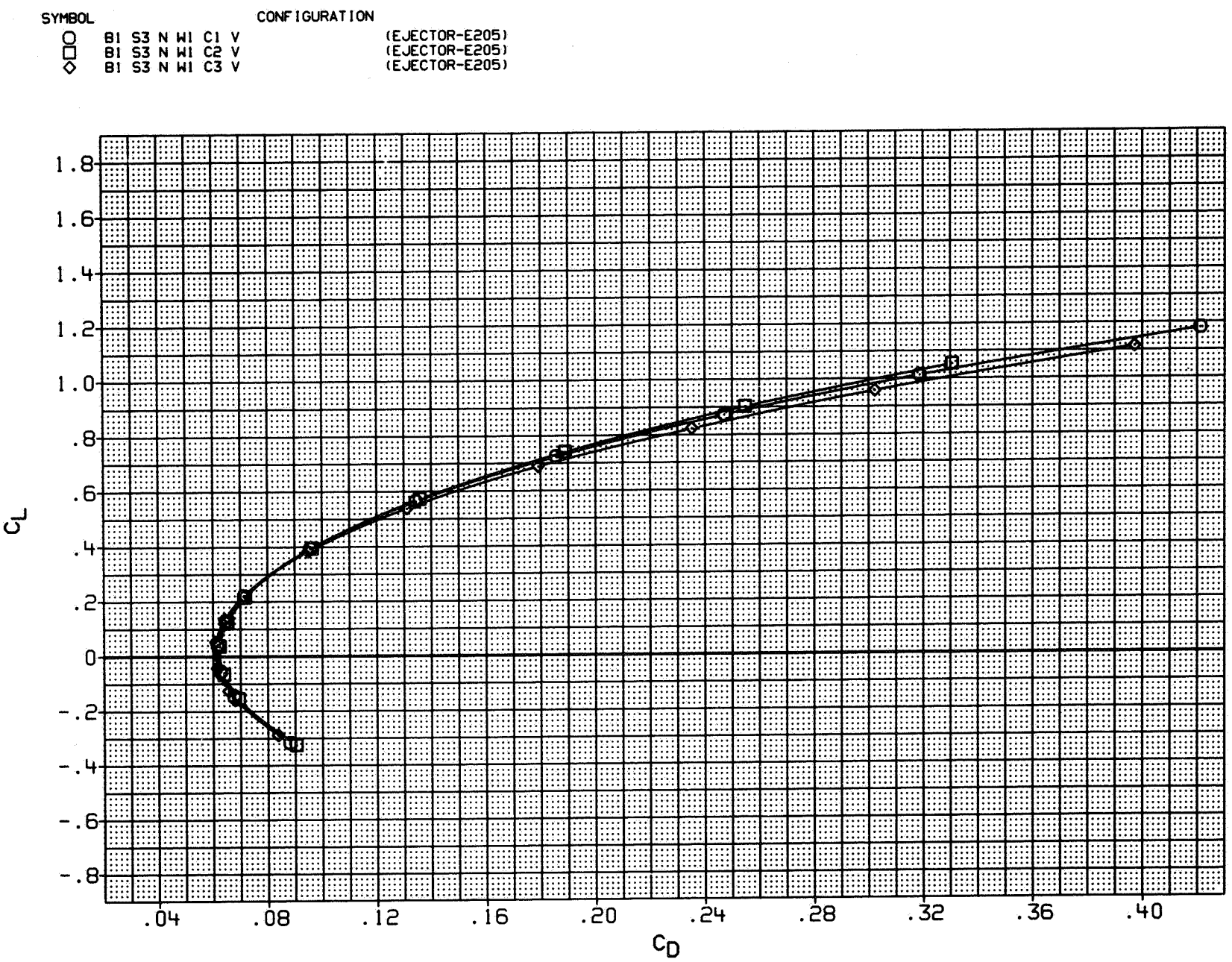


FIG. 31 CANARD LOCATION EFFECTS, LONGITUDINAL CHARACTERISTICS
CANARD = 0 DEGREES, STRAKE S3

MACH = 1.60

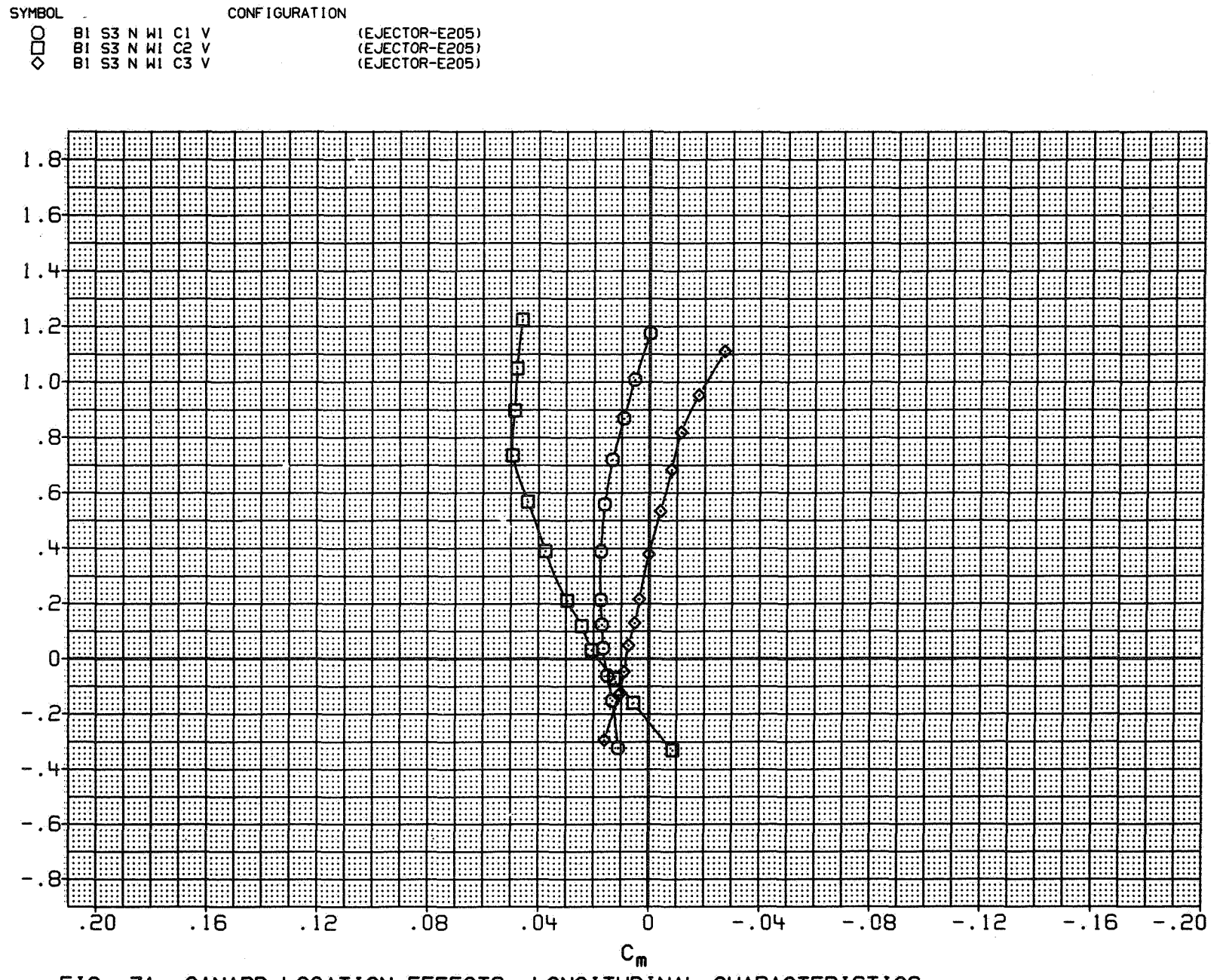


FIG. 31 CANARD LOCATION EFFECTS, LONGITUDINAL CHARACTERISTICS
CANARD = 0 DEGREES, STRAKE S3

MACH = 1.60

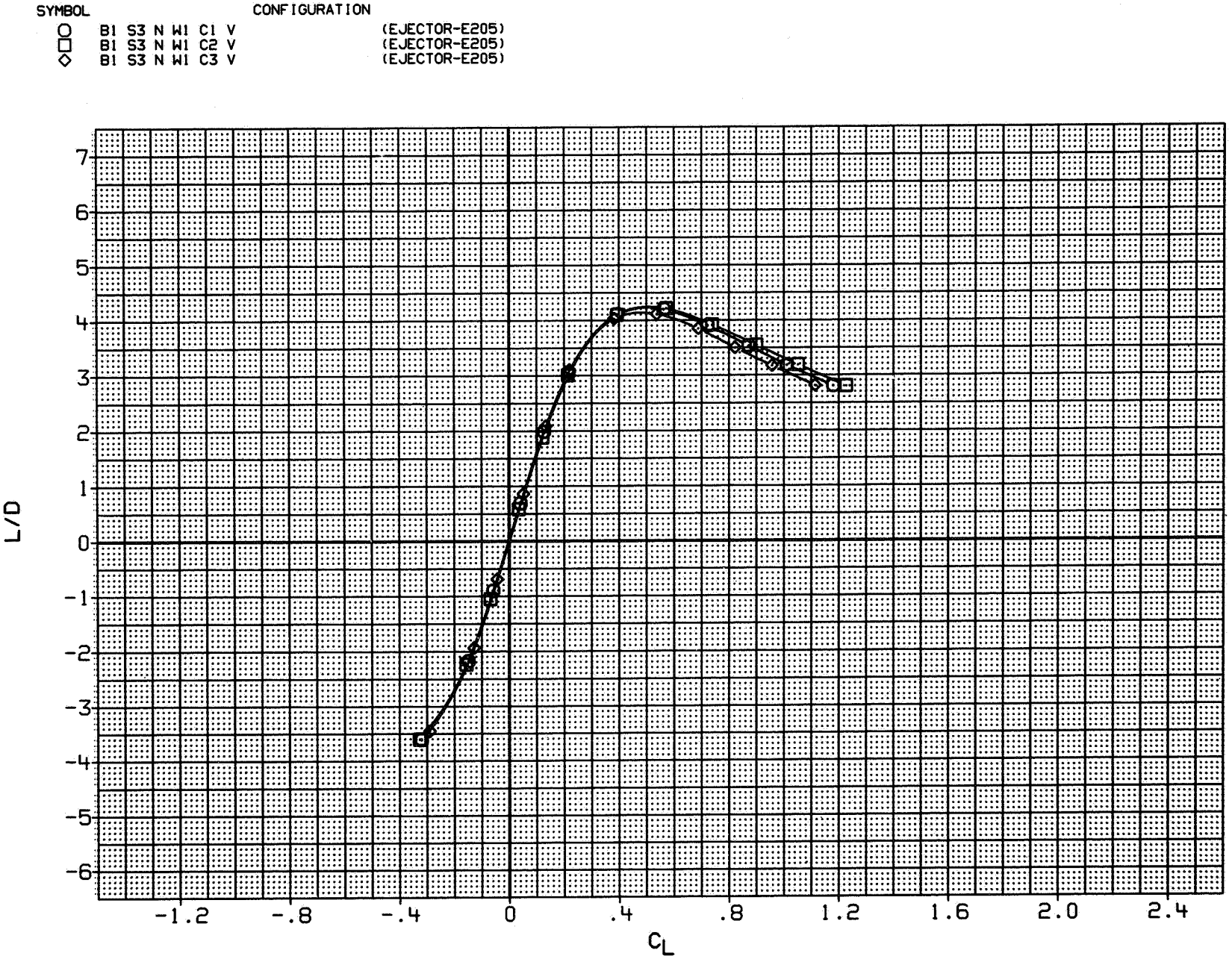


FIG. 31 CANARD LOCATION EFFECTS, LONGITUDINAL CHARACTERISTICS
CANARD = 0 DEGREES, STRAKE S3

MACH = 1.60

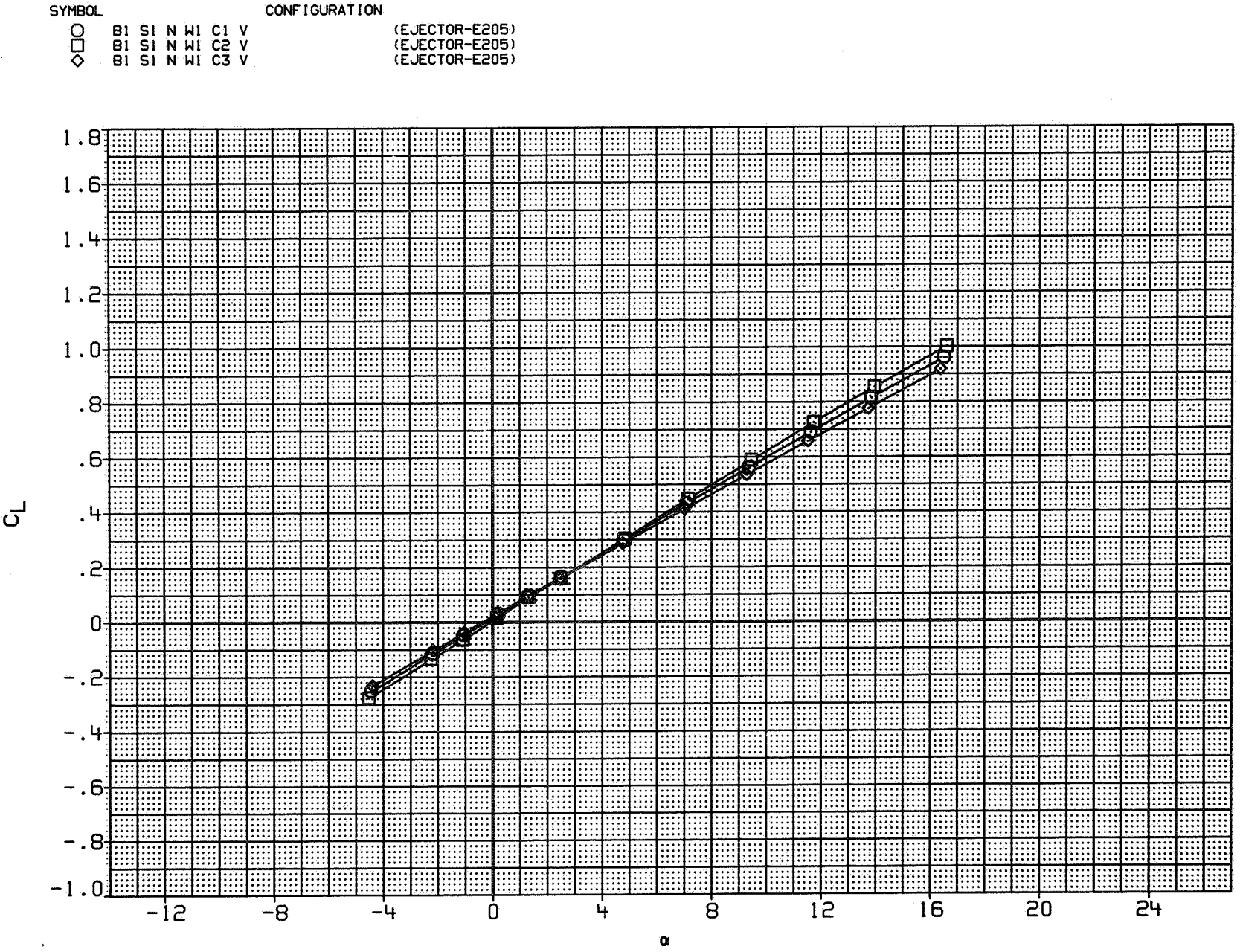


FIG. 32 CANARD LOCATION EFFECTS, LONGITUDINAL CHARACTERISTICS
CANARD = 0 DEGREES, STRAKE S1
MACH = 2.00

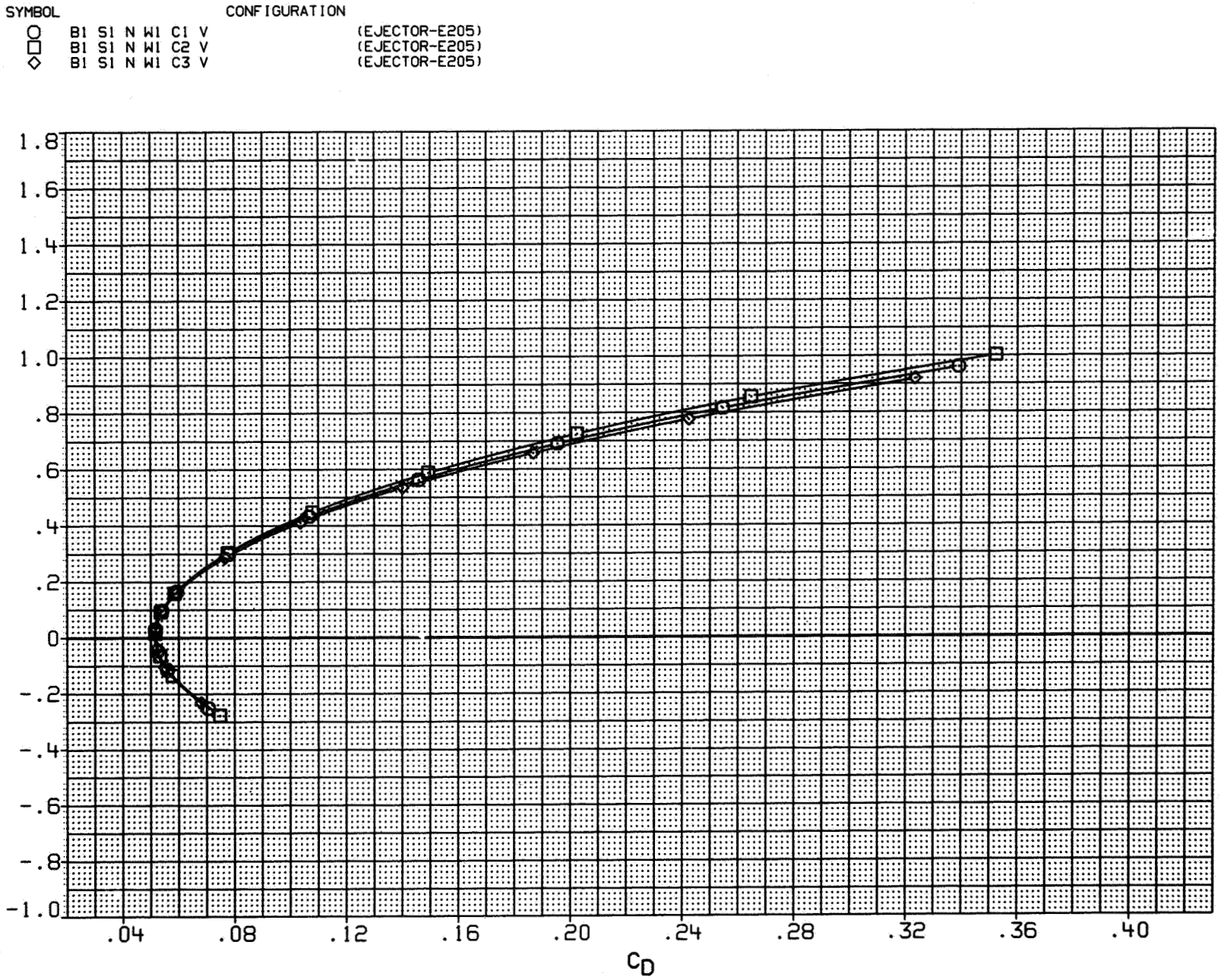


FIG. 32 CANARD LOCATION EFFECTS, LONGITUDINAL CHARACTERISTICS
CANARD = 0 DEGREES, STRAKE S1

MACH = 2.00

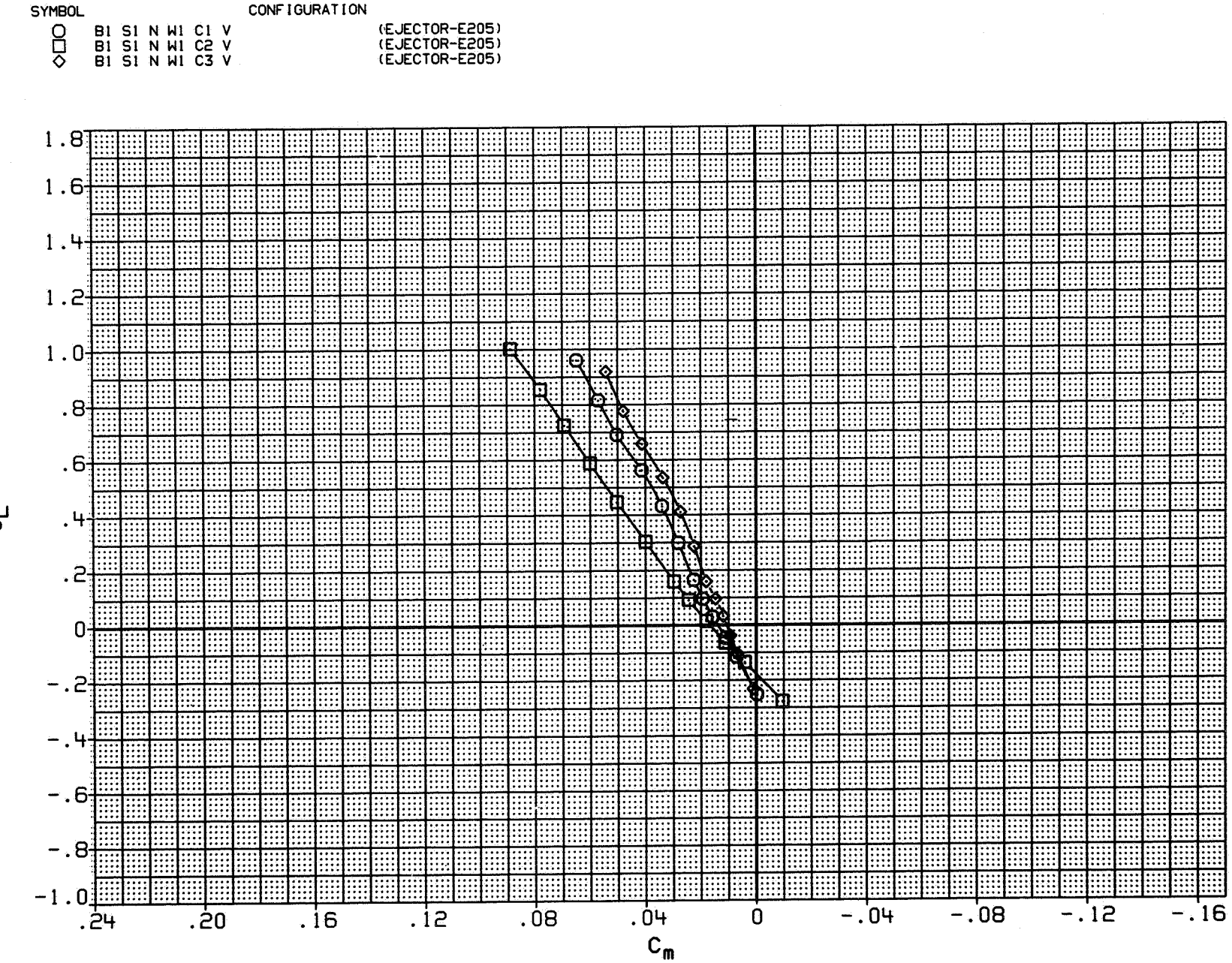


FIG. 32 CANARD LOCATION EFFECTS, LONGITUDINAL CHARACTERISTICS
CANARD = 0 DEGREES, STRAKE S1

MACH = 2.00

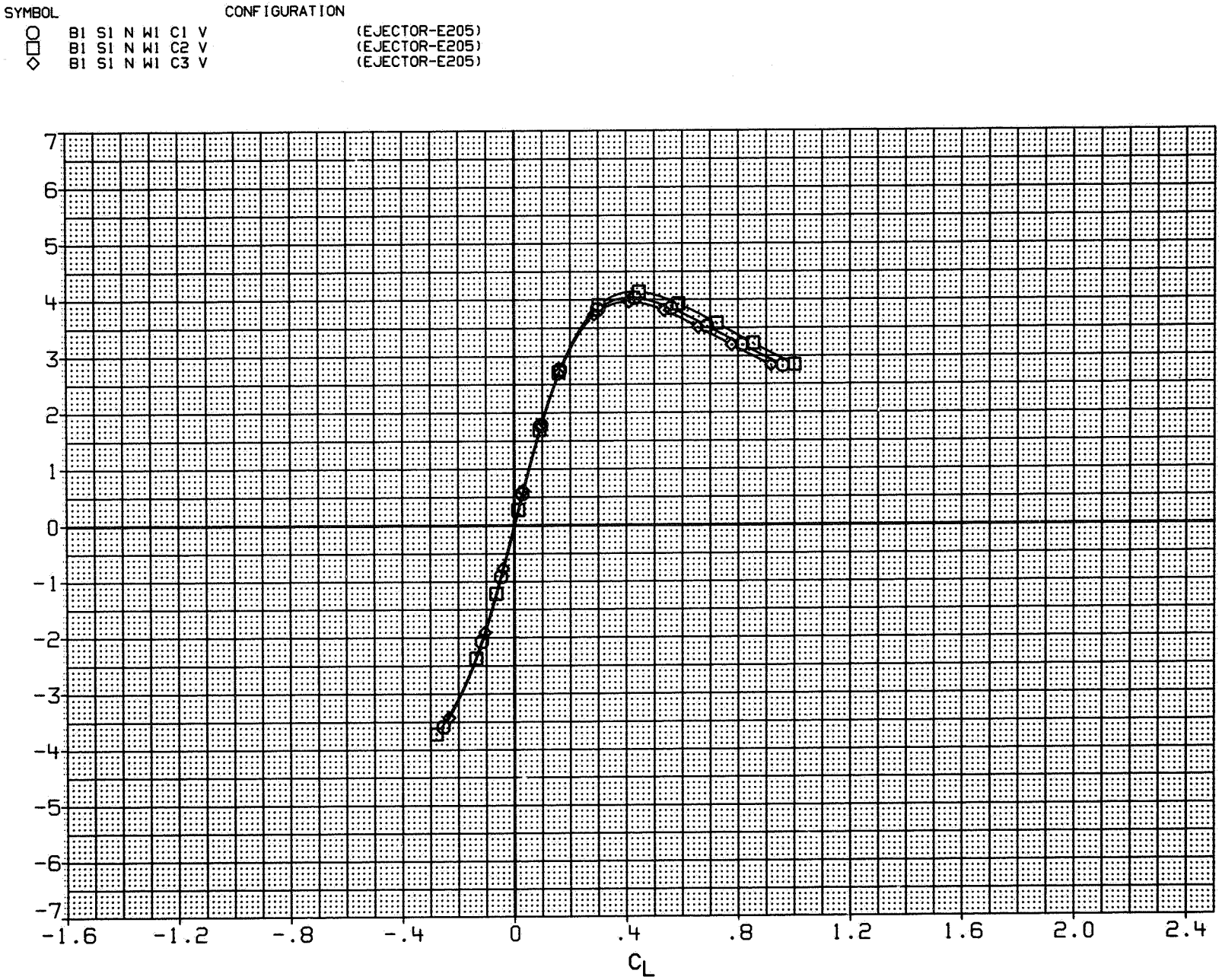


FIG. 32 CANARD LOCATION EFFECTS, LONGITUDINAL CHARACTERISTICS
CANARD = 0 DEGREES, STRAKE S1

MACH = 2.00

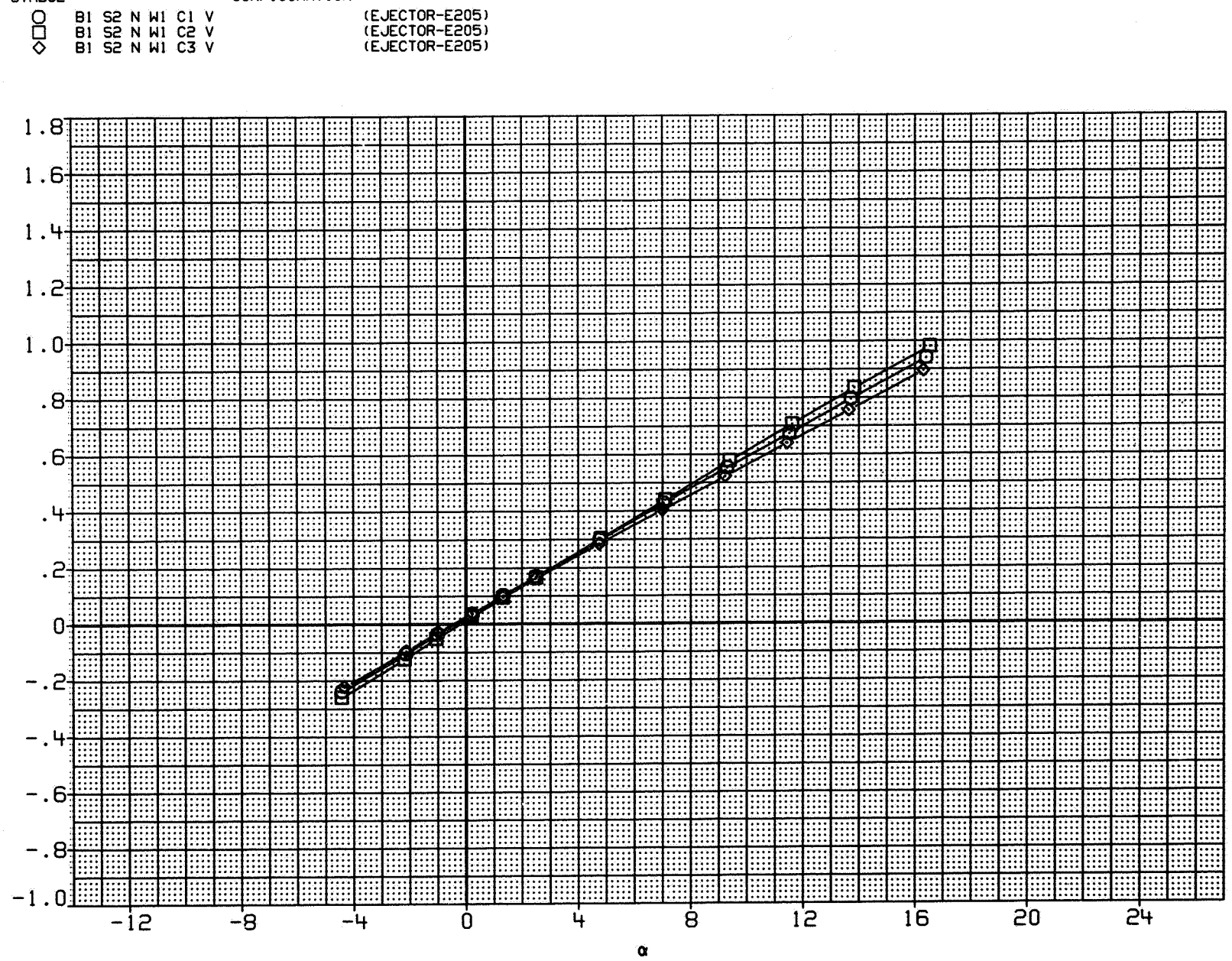


FIG. 33 CANARD LOCATION EFFECTS, LONGITUDINAL CHARACTERISTICS
CANARD = 0 DEGREES, STRAKE S2

MACH = 2.00

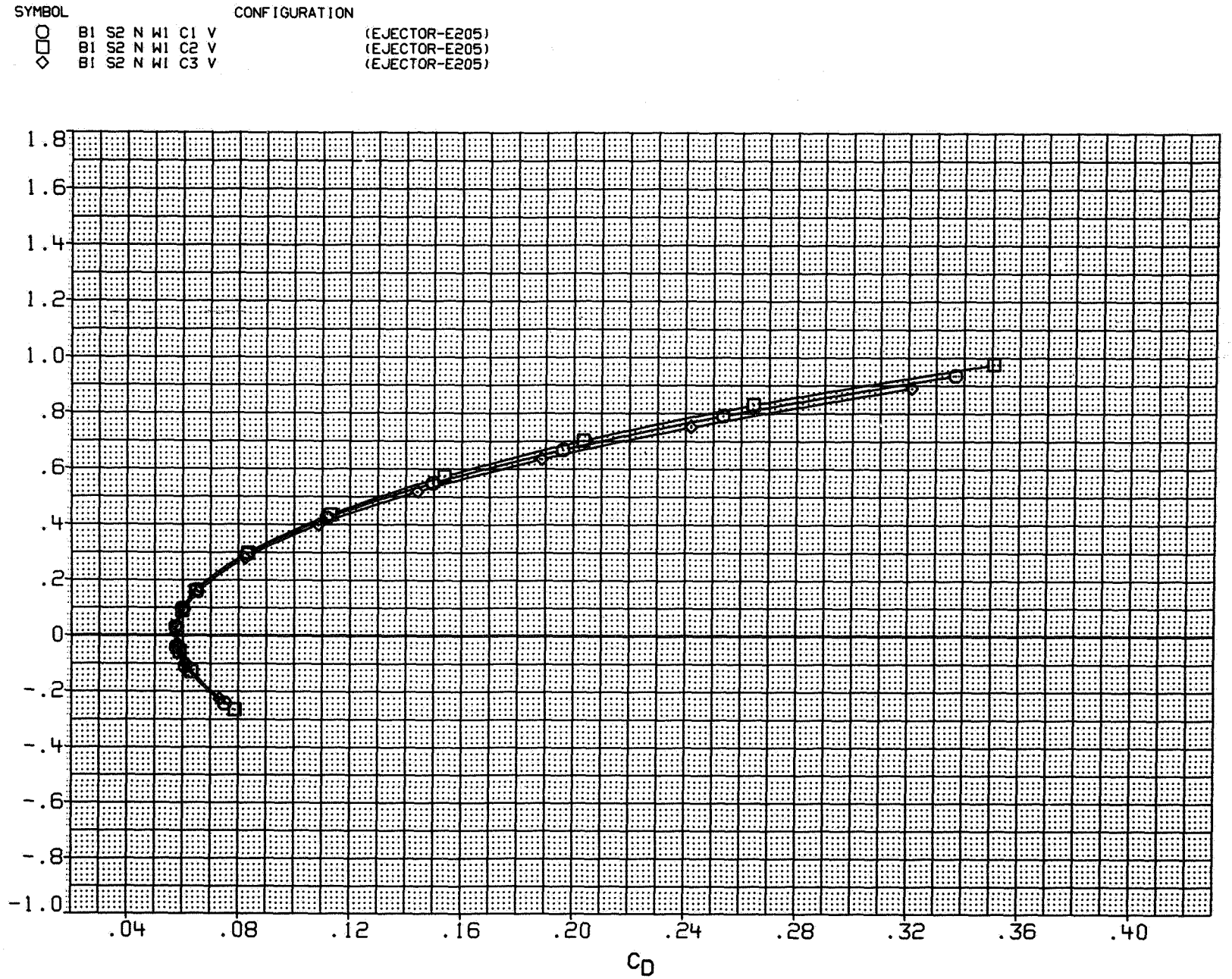


FIG. 33 CANARD LOCATION EFFECTS, LONGITUDINAL CHARACTERISTICS
CANARD = 0 DEGREES, STRAKE S2
MACH = 2.00

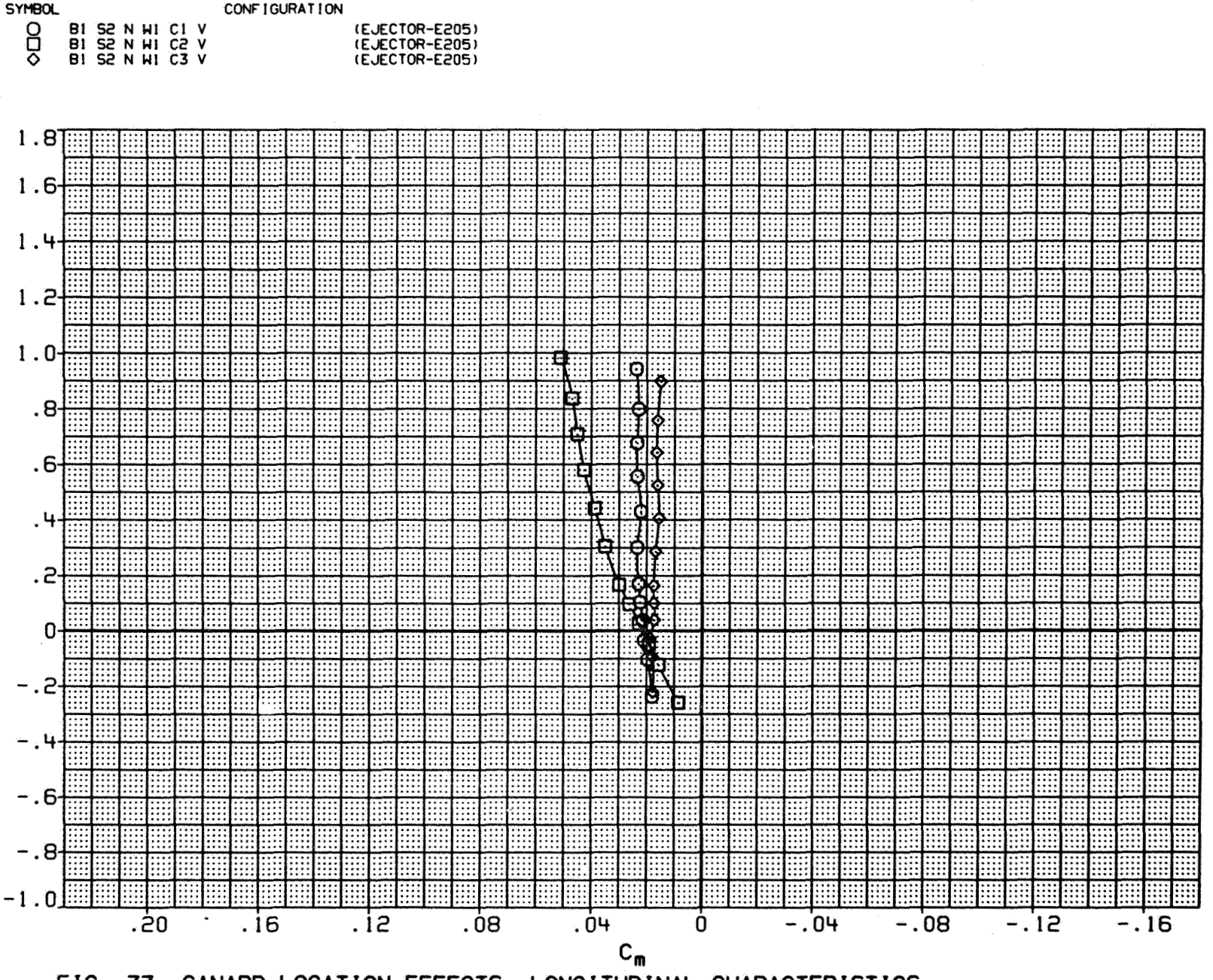


FIG. 33 CANARD LOCATION EFFECTS, LONGITUDINAL CHARACTERISTICS
CANARD = 0 DEGREES, STRAKE S2

MACH = 2.00

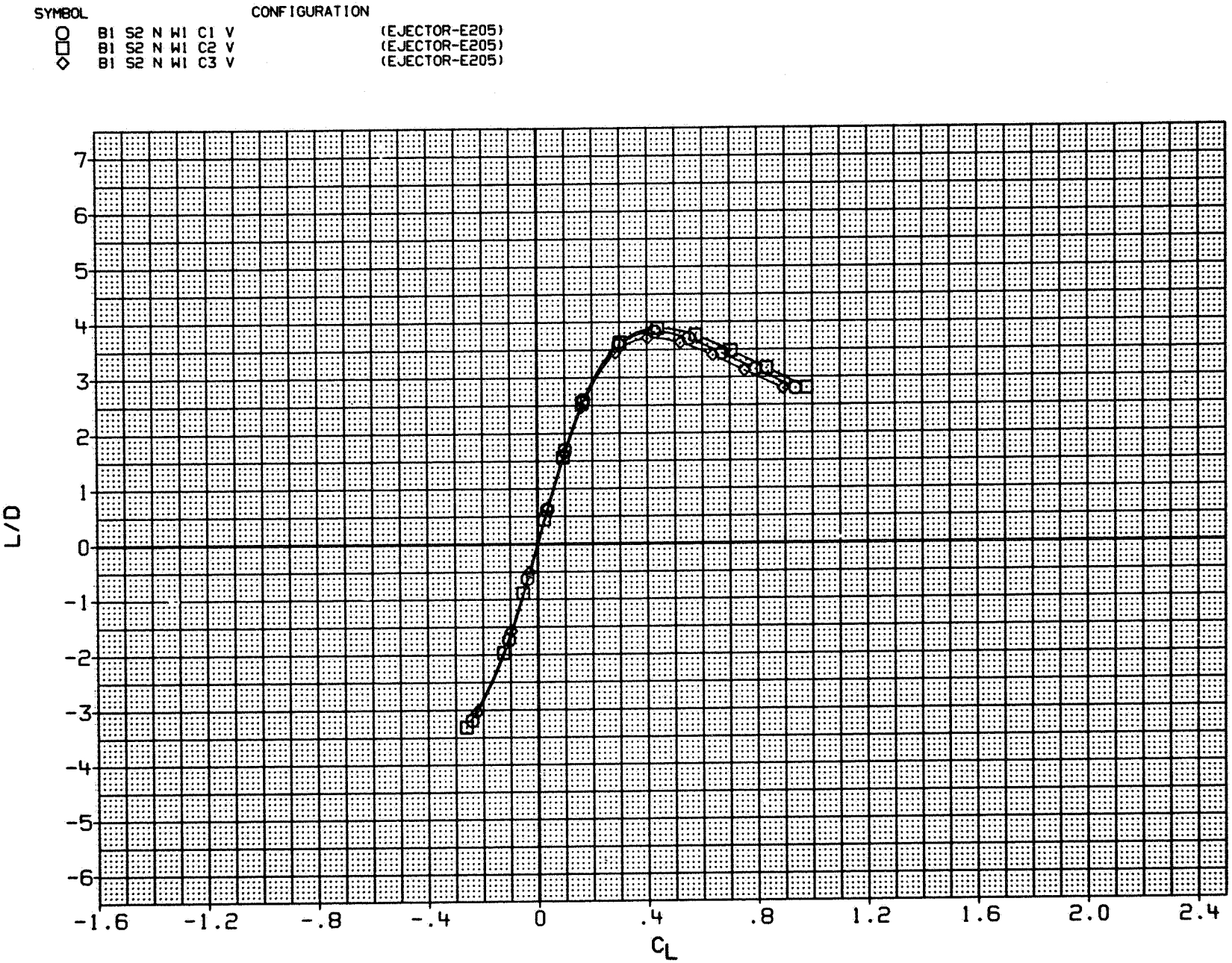


FIG. 33 CANARD LOCATION EFFECTS, LONGITUDINAL CHARACTERISTICS
CANARD = 0 DEGREES, STRAKE S2

MACH = 2.00

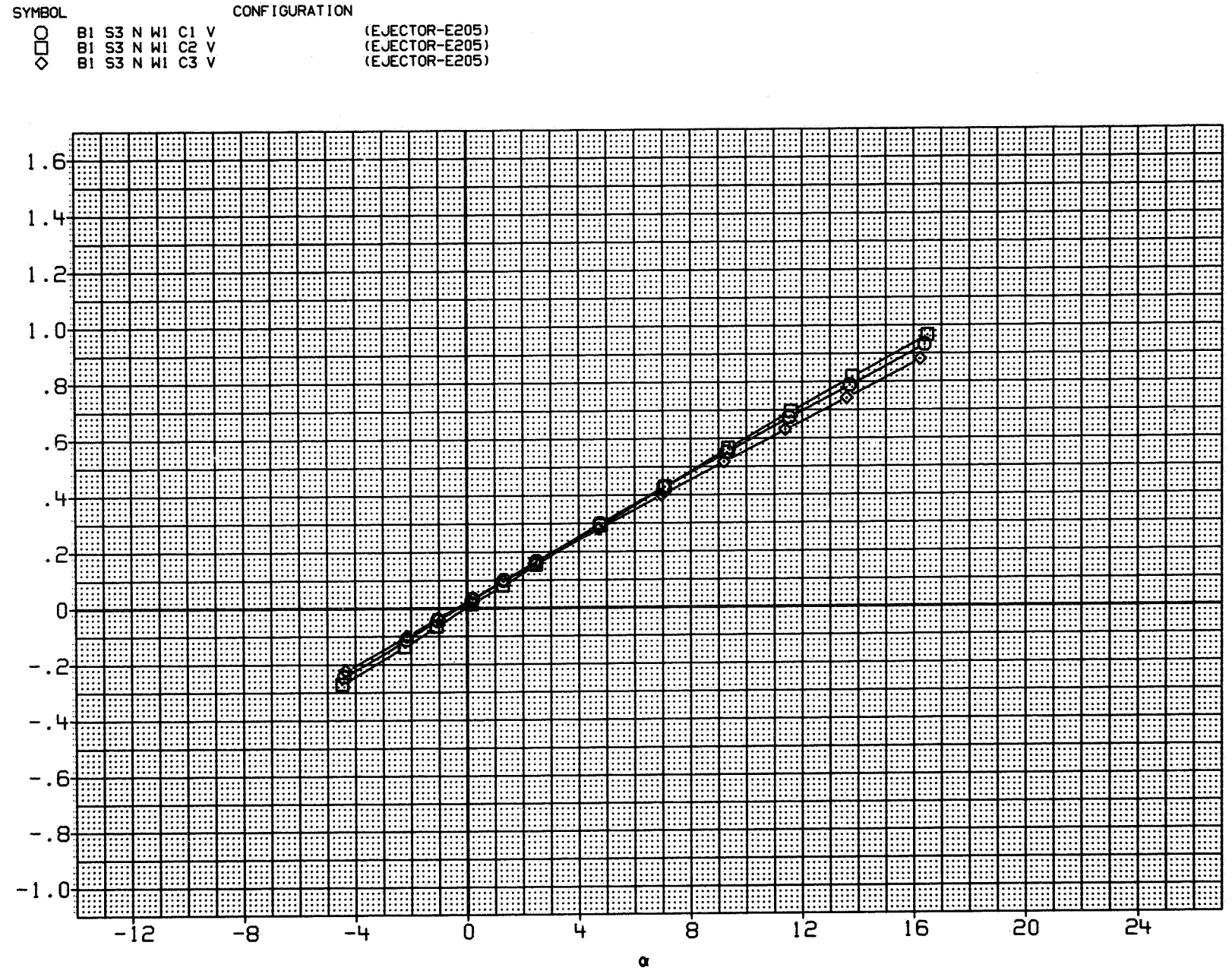


FIG. 34 CANARD LOCATION EFFECTS, LONGITUDINAL CHARACTERISTICS
CANARD = 0 DEGREES, STRAKE S3

MACH = 2.00

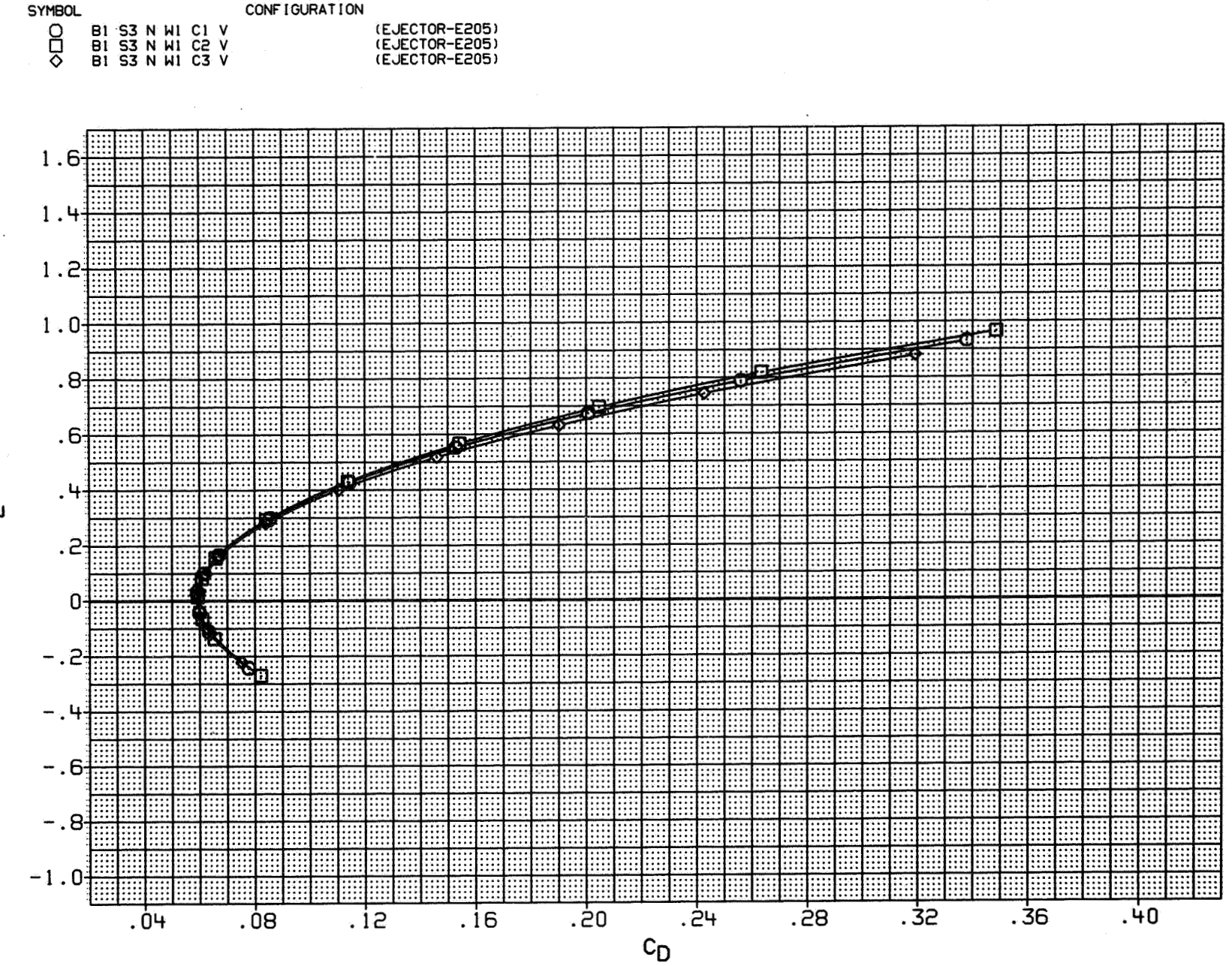


FIG. 34 CANARD LOCATION EFFECTS, LONGITUDINAL CHARACTERISTICS
CANARD = 0 DEGREES, STRAKE S3

MACH = 2.00

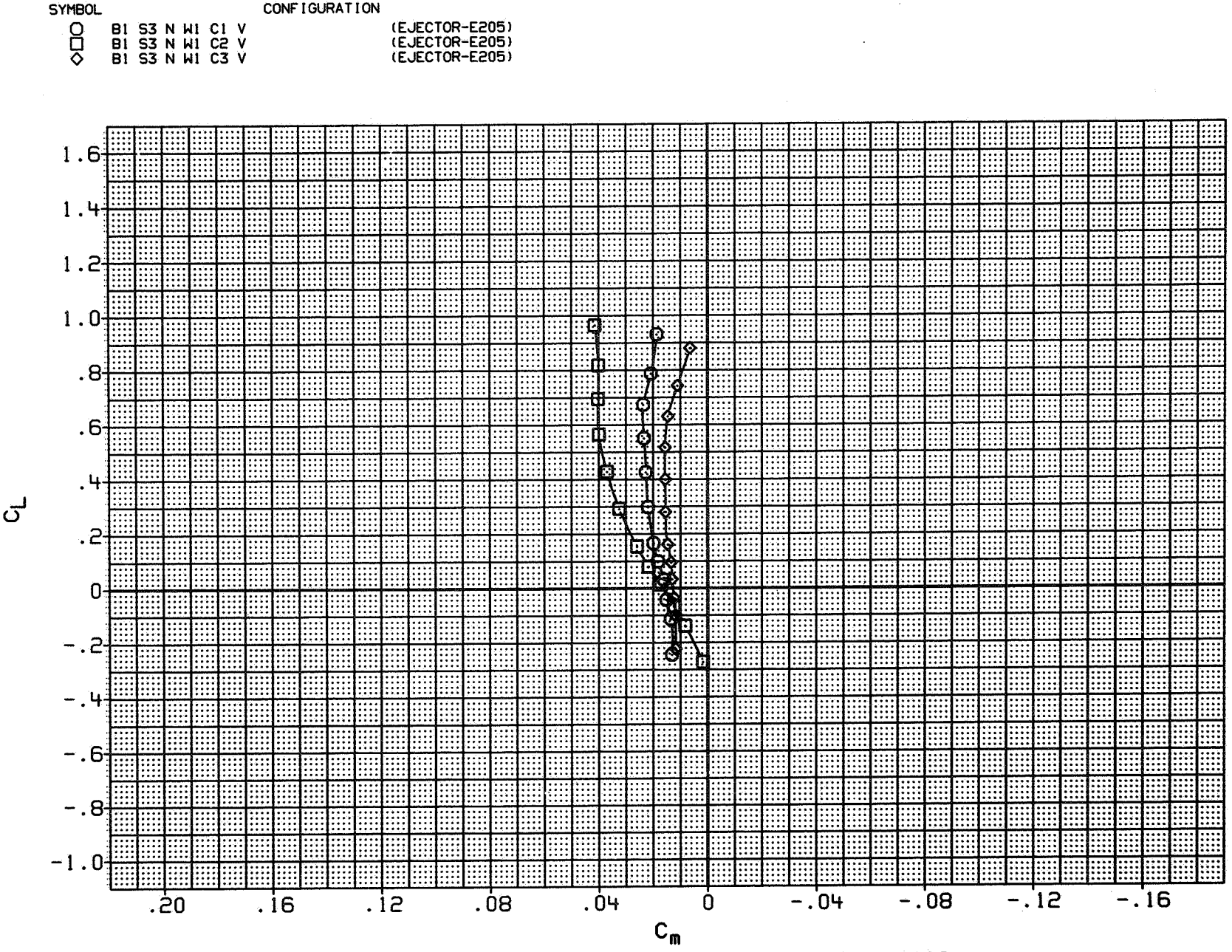


FIG. 34 CANARD LOCATION EFFECTS, LONGITUDINAL CHARACTERISTICS
CANARD = 0 DEGREES, STRAKE S3

MACH = 2.00

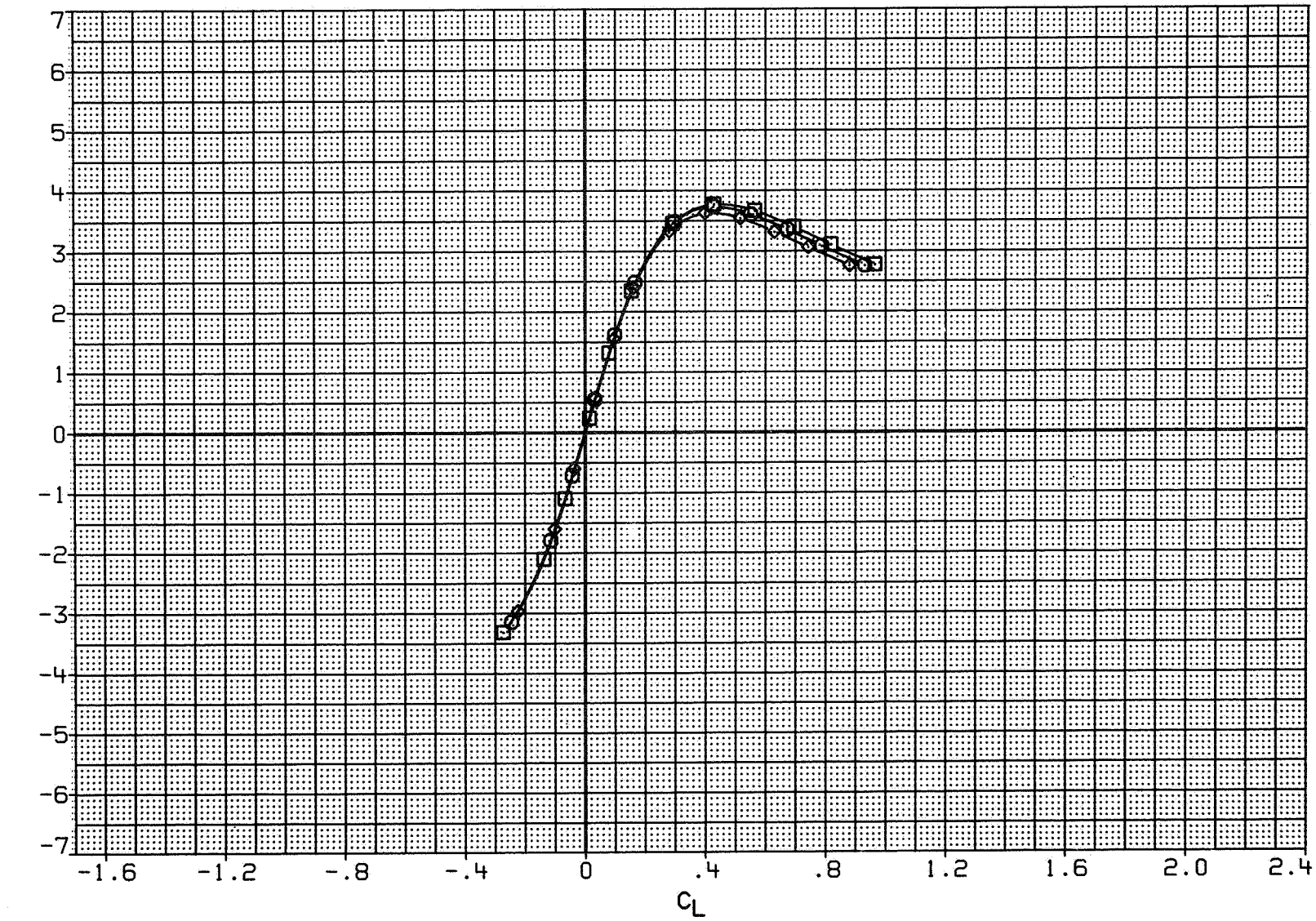


FIG. 34 CANARD LOCATION EFFECTS, LONGITUDINAL CHARACTERISTICS
CANARD = 0 DEGREES, STRAKE S3

MACH = 2.00

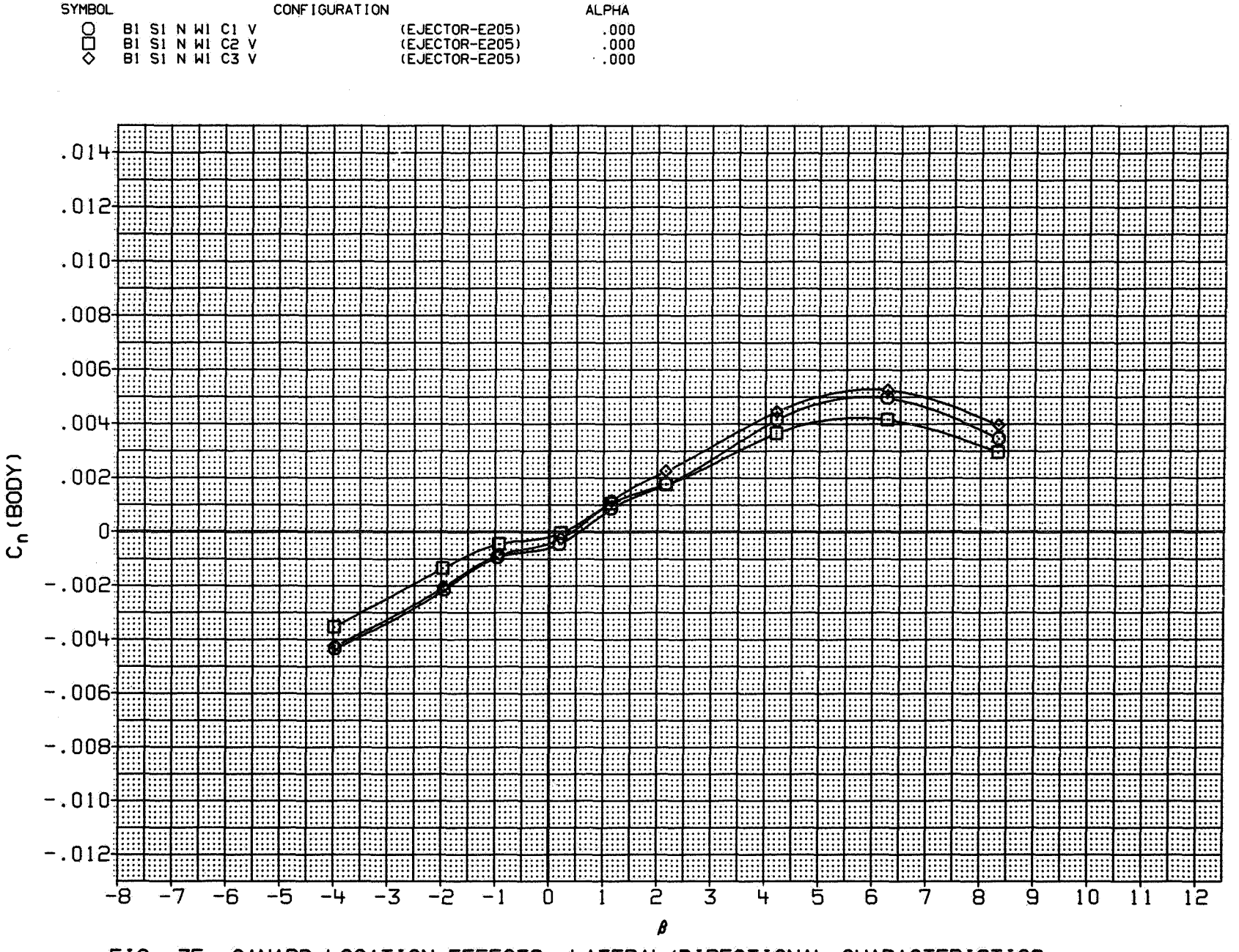


FIG. 35 CANARD LOCATION EFFECTS, LATERAL/DIRECTIONAL CHARACTERISTICS
ALPHA = 0 DEGREES

MACH = 1.60

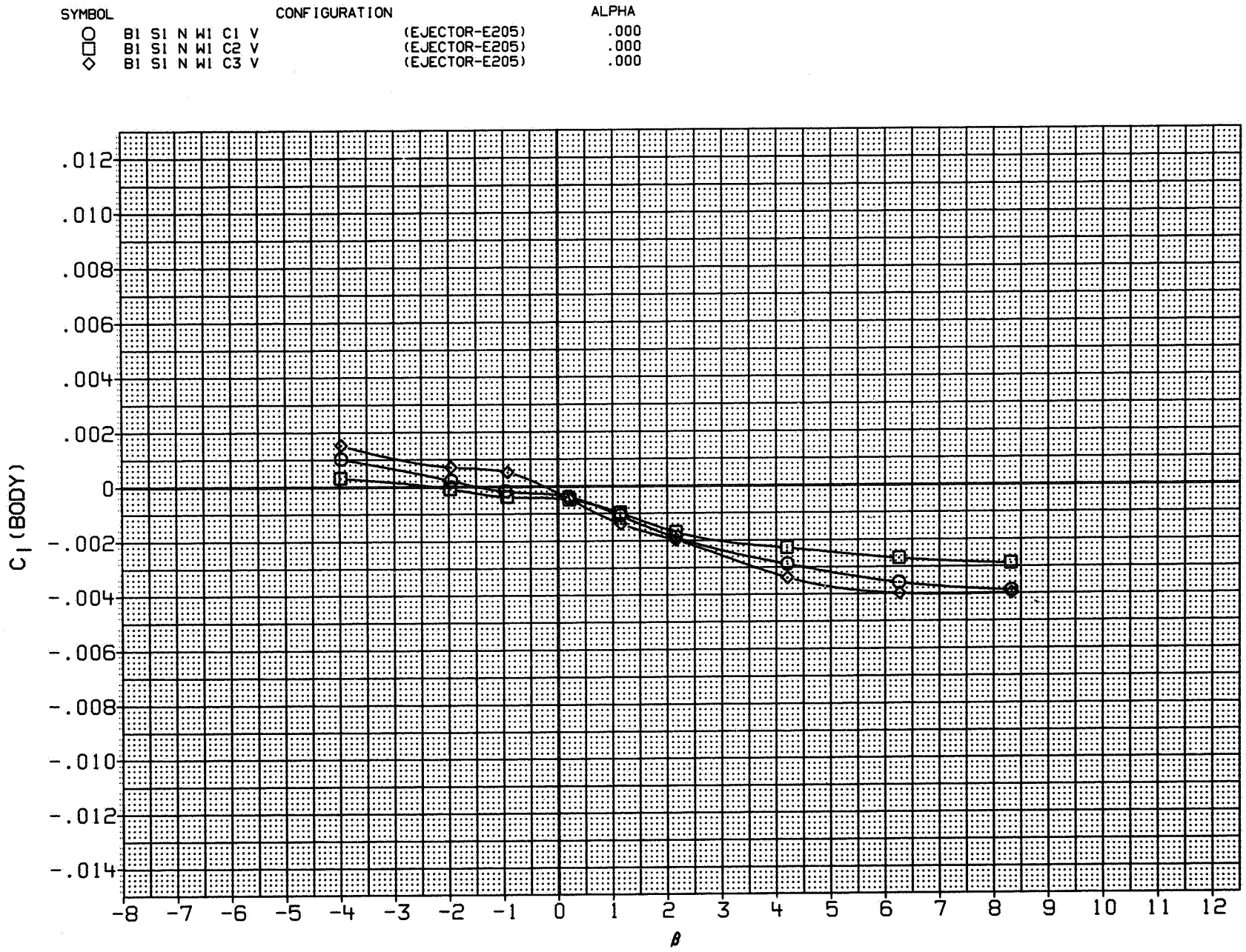


FIG. 35 CANARD LOCATION EFFECTS, LATERAL/DIRECTIONAL CHARACTERISTICS
ALPHA = 0 DEGREES
MACH = 1.60

| SYMBOL | CONFIGURATION | | ALPHA |
|---|---|---|---|
| ○ | B1 S1 N W1 C1 V | (EJECTOR-E205) | .000 |
| □ | B1 S1 N W1 C2 V | (EJECTOR-E205) | .000 |
| ◇ | B1 S1 N W1 C3 V | (EJECTOR-E205) | .000 |

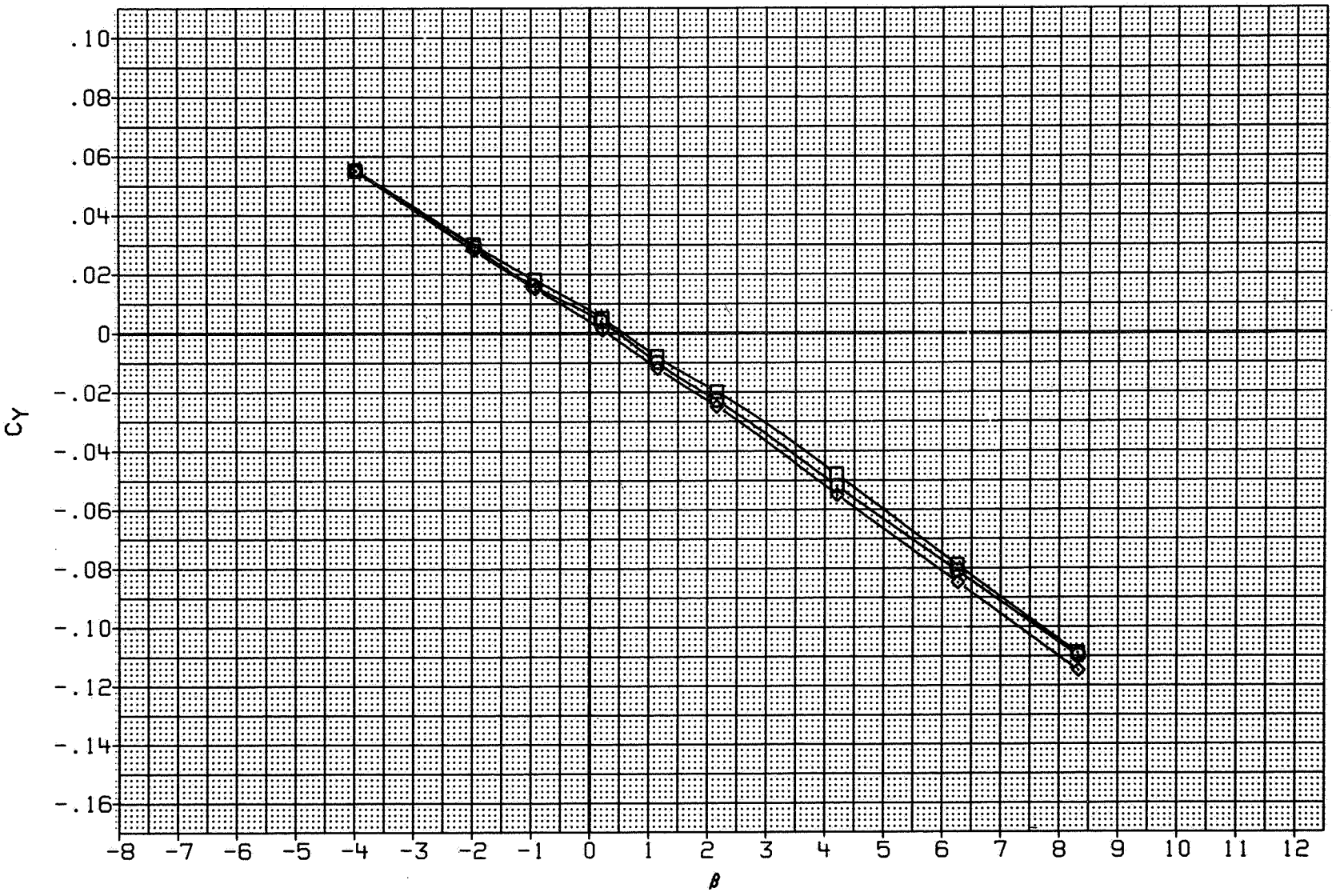


FIG. 35 CANARD LOCATION EFFECTS, LATERAL/DIRECTIONAL CHARACTERISTICS
ALPHA = 0 DEGREES

MACH = 1.60

| SYMBOL | CONFIGURATION | ALPHA |
|---|---|---|
| ○ | B1 S1 N W1 C1 V (EJECTOR-E205) | 9.500 |
| □ | B1 S1 N W1 C2 V (EJECTOR-E205) | 9.500 |
| ◇ | B1 S1 N W1 C3 V (EJECTOR-E205) | 9.500 |

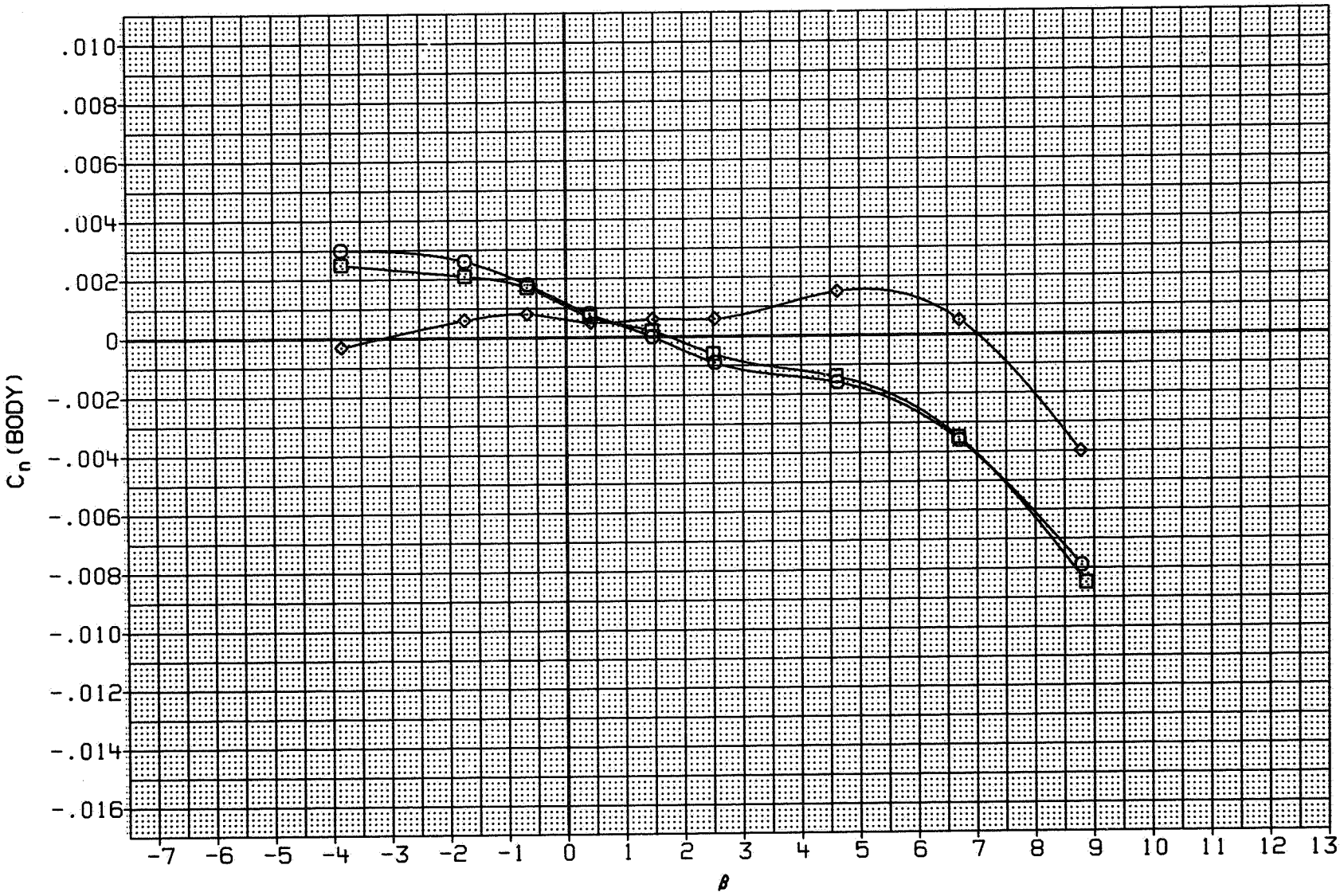


FIG. 36 CANARD LOCATION EFFECTS, LATERAL/DIRECTIONAL CHARACTERISTICS
ALPHA = 8 DEGREES

MACH = 1.60

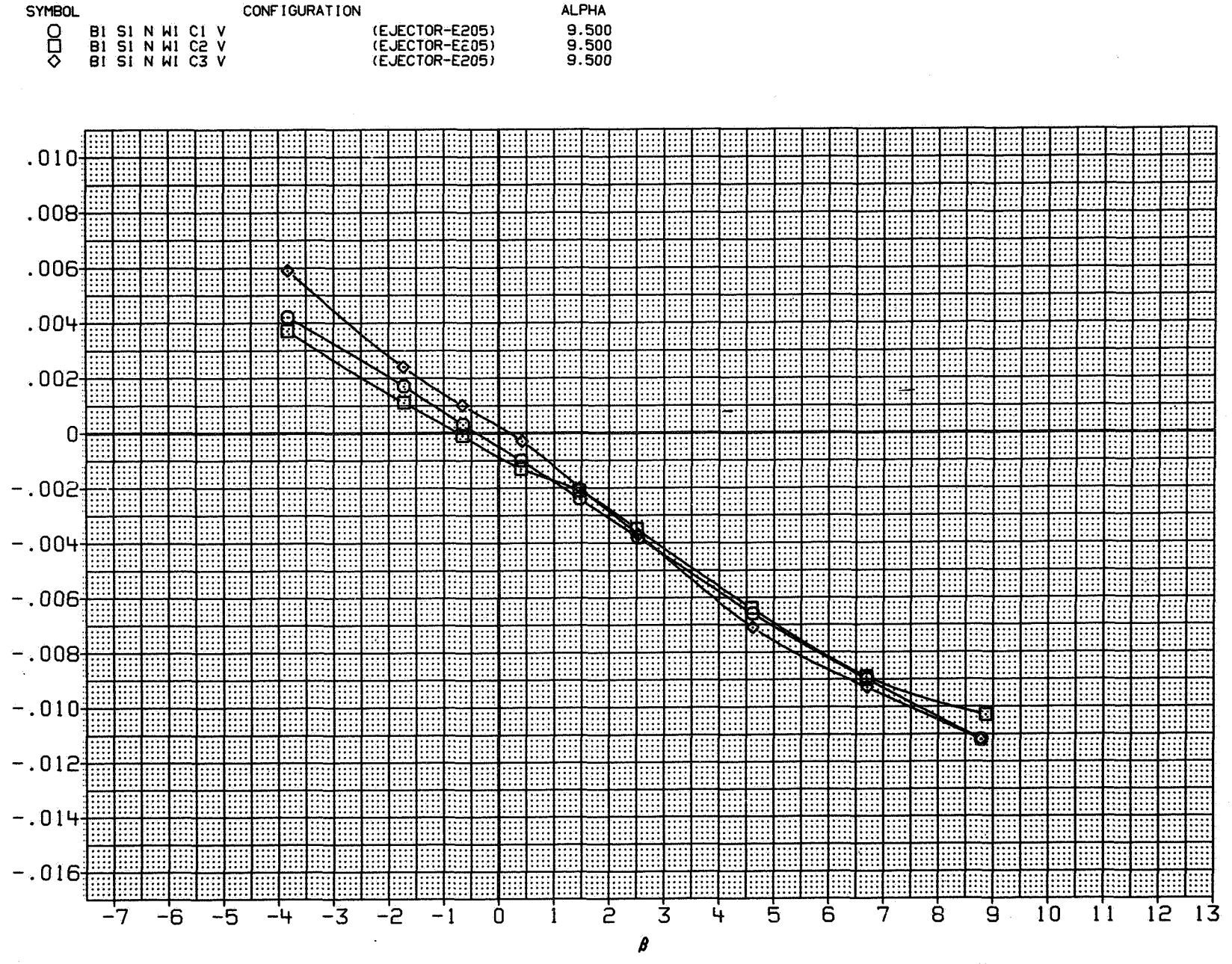


FIG. 36 CANARD LOCATION EFFECTS, LATERAL/DIRECTIONAL CHARACTERISTICS
ALPHA = 8 DEGREES

MACH = 1.60

| SYMBOL | CONFIGURATION | | ALPHA |
|---|---|---|---|
| ○ | B1 S1 N W1 C1 V | (EJECTOR-E205) | 9.500 |
| □ | B1 S1 N W1 C2 V | (EJECTOR-E205) | 9.500 |
| ◇ | B1 S1 N W1 C3 V | (EJECTOR-E205) | 9.500 |

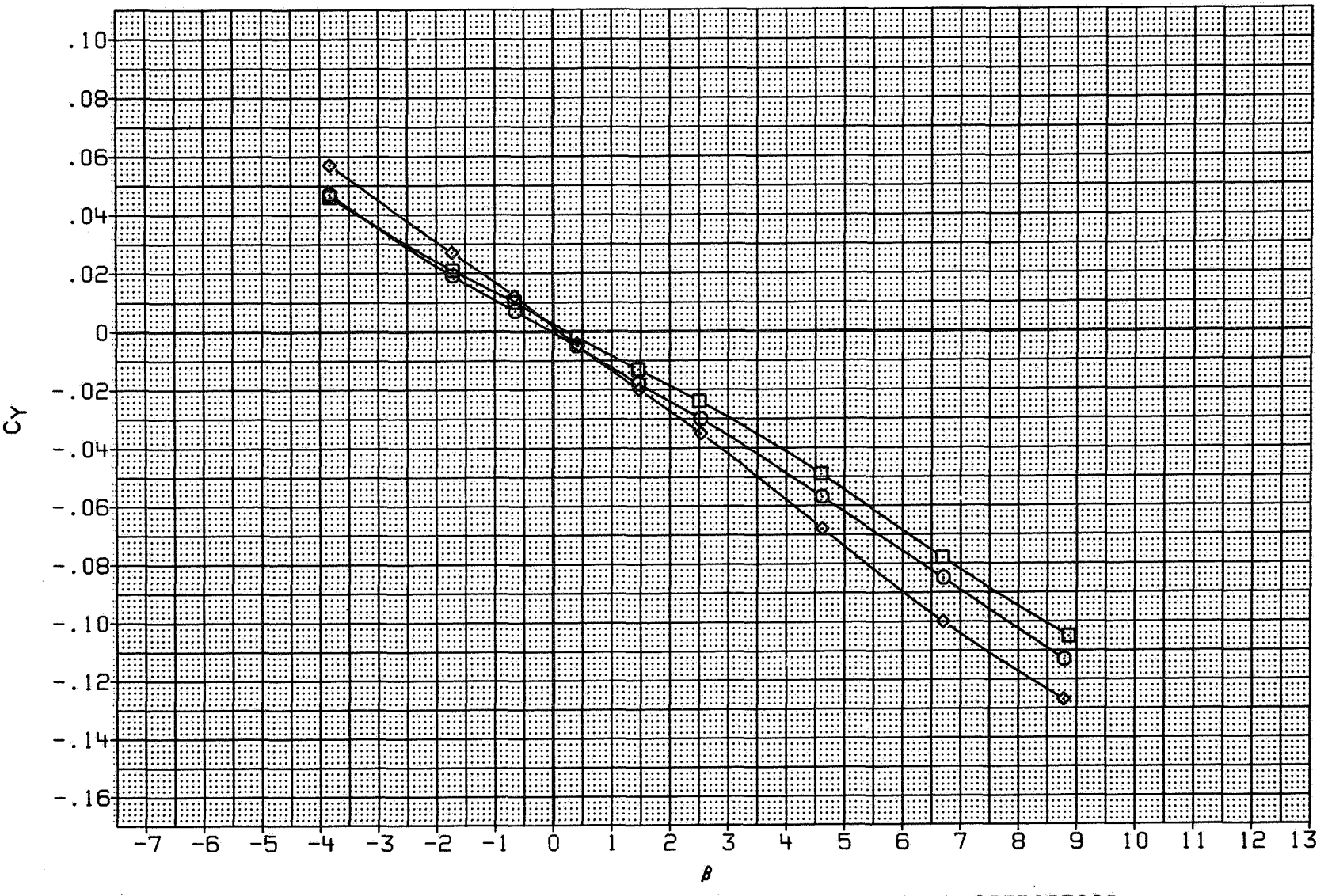


FIG. 36 CANARD LOCATION EFFECTS, LATERAL/DIRECTIONAL CHARACTERISTICS
ALPHA = 8 DEGREES

MACH = 1.60

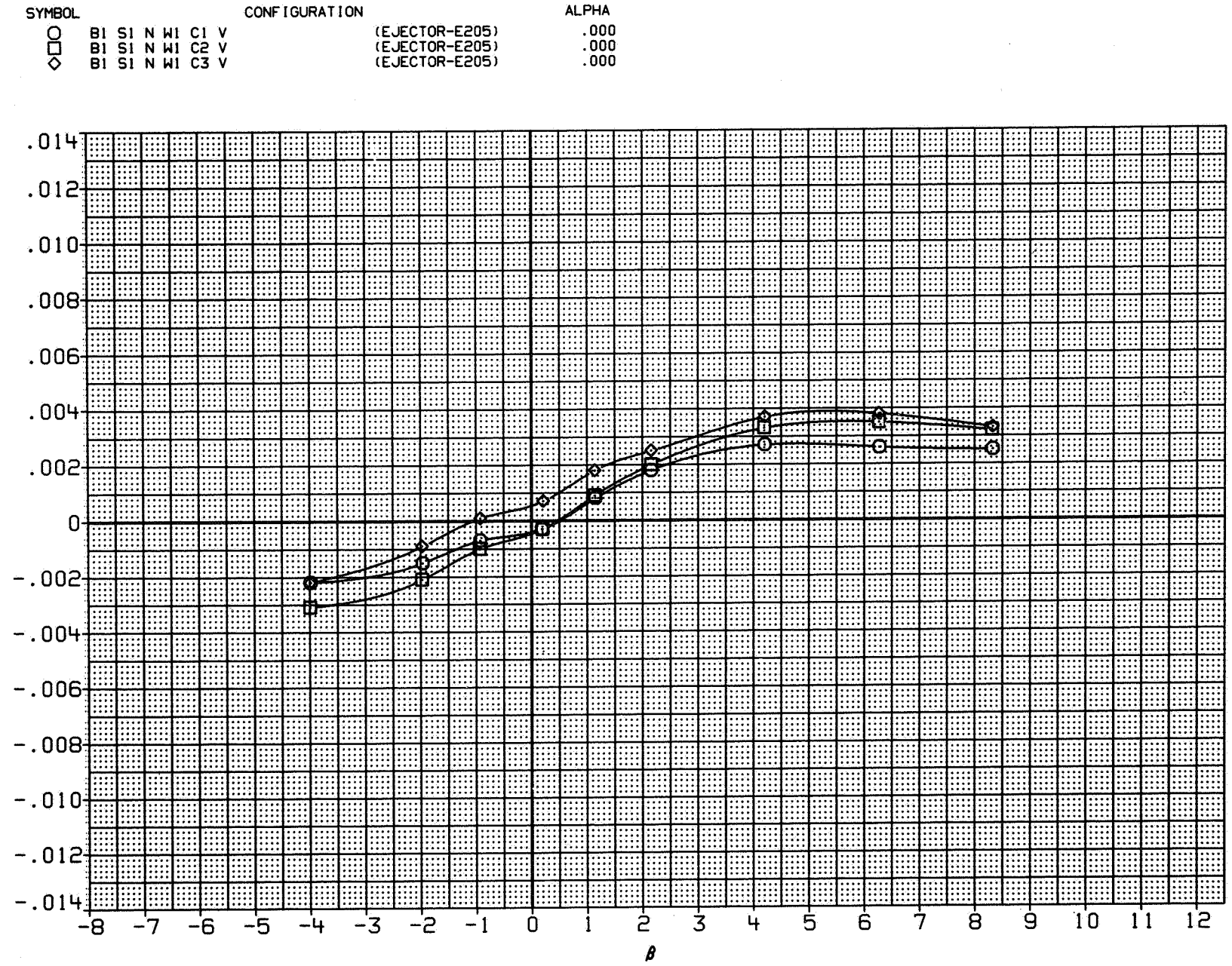


FIG. 37 CANARD LOCATION EFFECTS, LATERAL/DIRECTIONAL CHARACTERISTICS
ALPHA = 0 DEGREES
MACH = 2.00

| SYMBOL | CONFIGURATION | ALPHA |
|---|---|---|
| ○ | B1 S1 N W1 C1 V (EJECTOR-E205) | .000 |
| □ | B1 S1 N W1 C2 V (EJECTOR-E205) | .000 |
| ◇ | B1 S1 N W1 C3 V (EJECTOR-E205) | .000 |

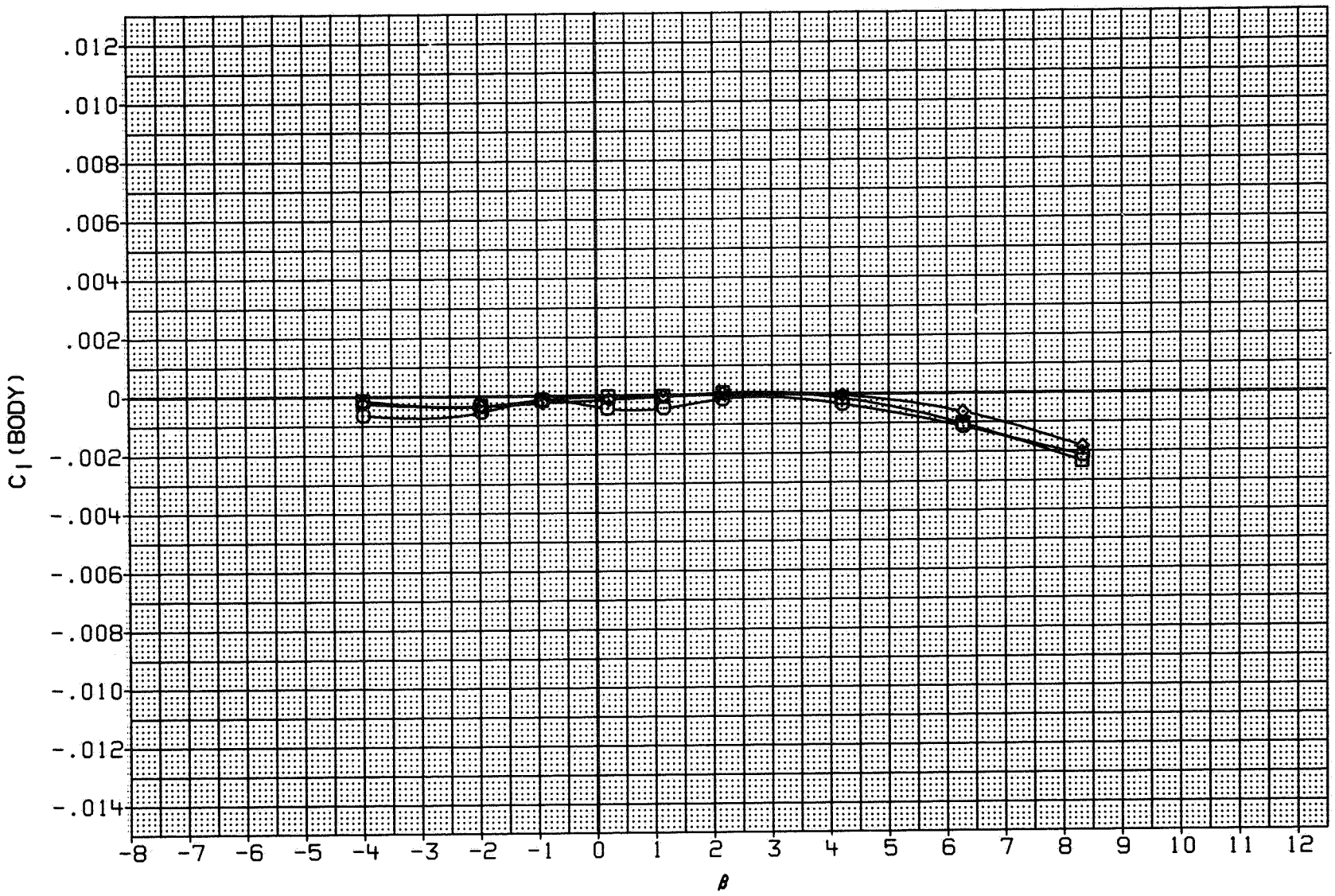


FIG. 37 CANARD LOCATION EFFECTS, LATERAL/DIRECTIONAL CHARACTERISTICS
ALPHA = 0 DEGREES

MACH = 2.00

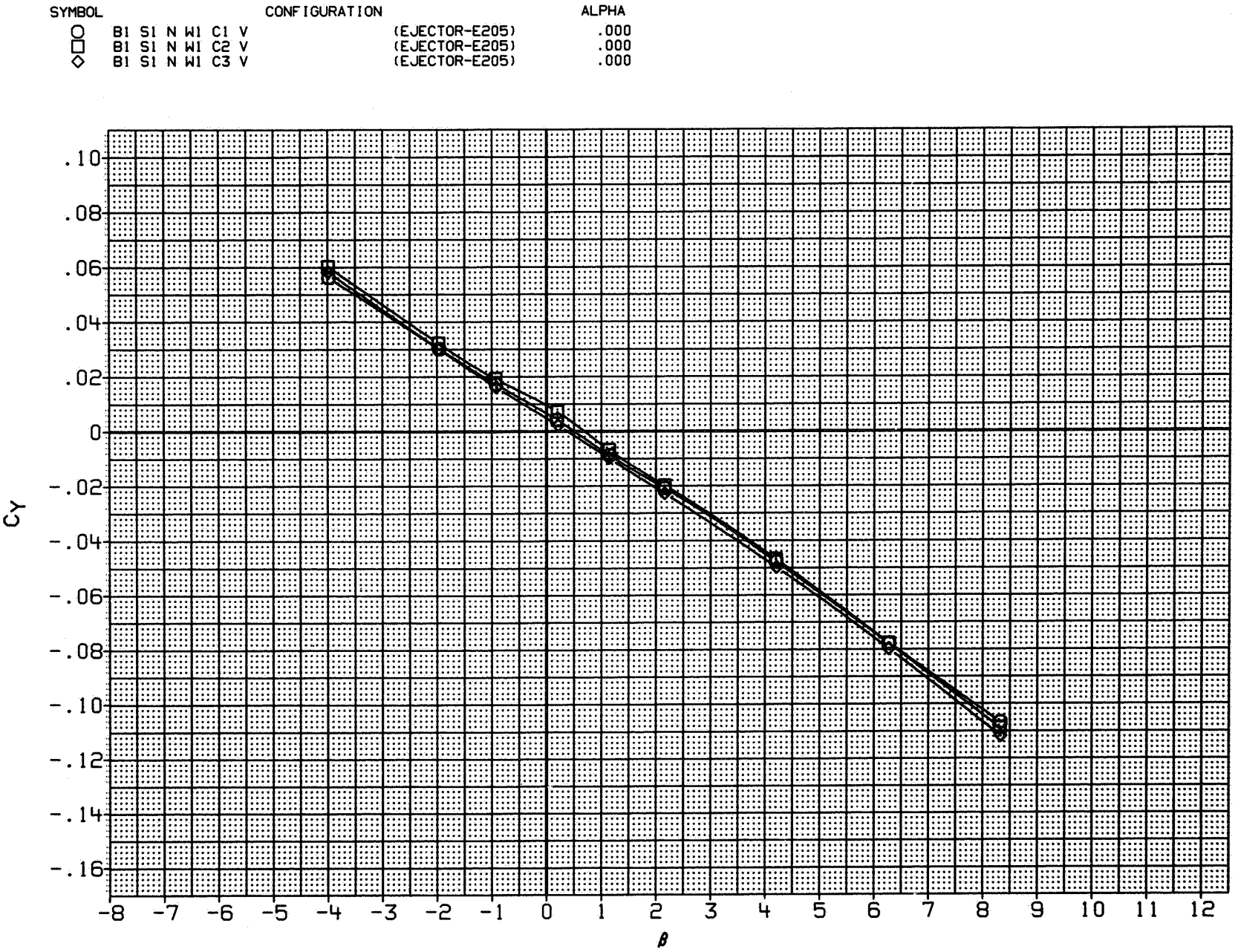


FIG. 37 CANARD LOCATION EFFECTS, LATERAL/DIRECTIONAL CHARACTERISTICS
ALPHA = 0 DEGREES

MACH = 2.00

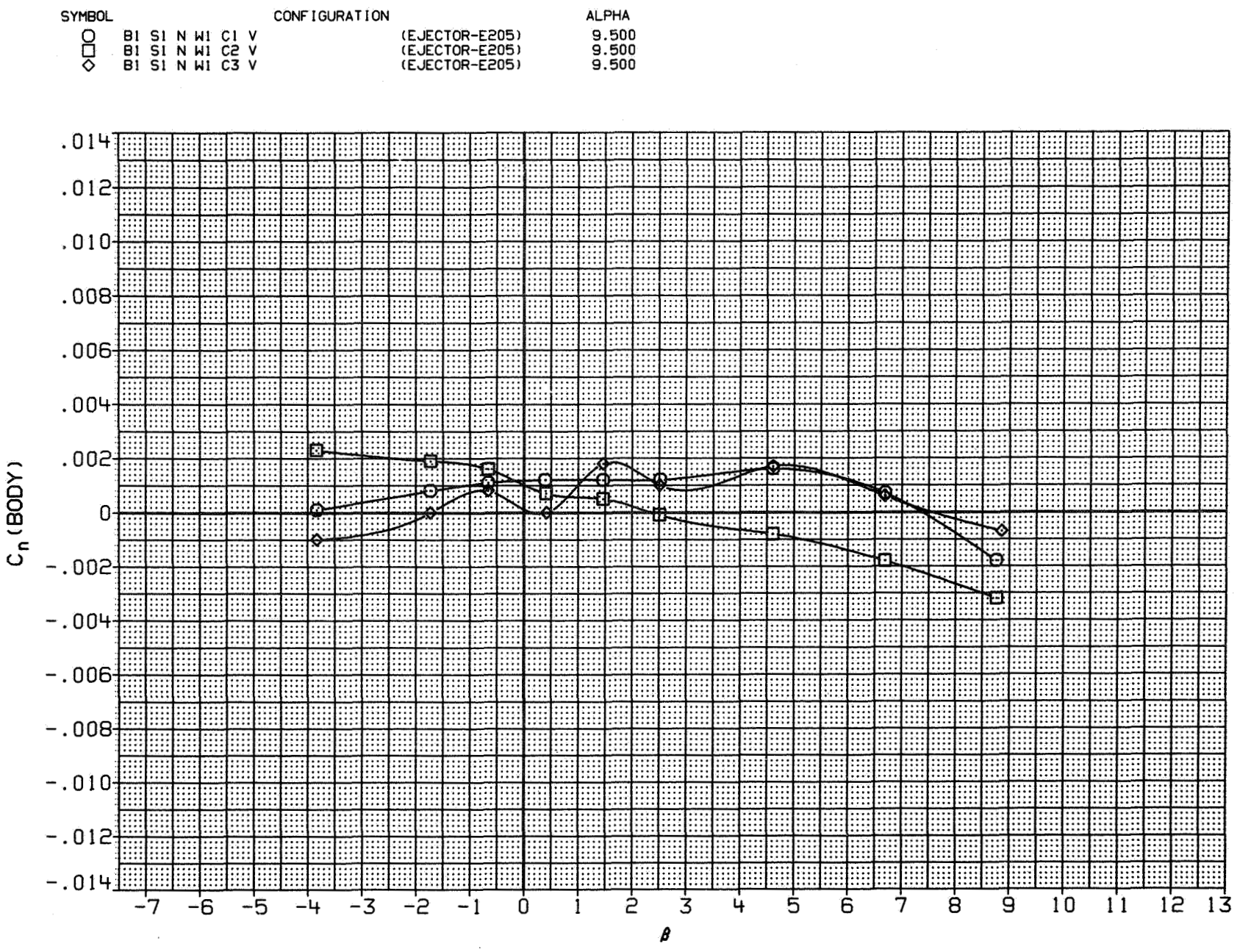


FIG. 38 CANARD LOCATION EFFECTS, LATERAL/DIRECTIONAL CHARACTERISTICS
ALPHA = 8 DEGREES

MACH = 2.00

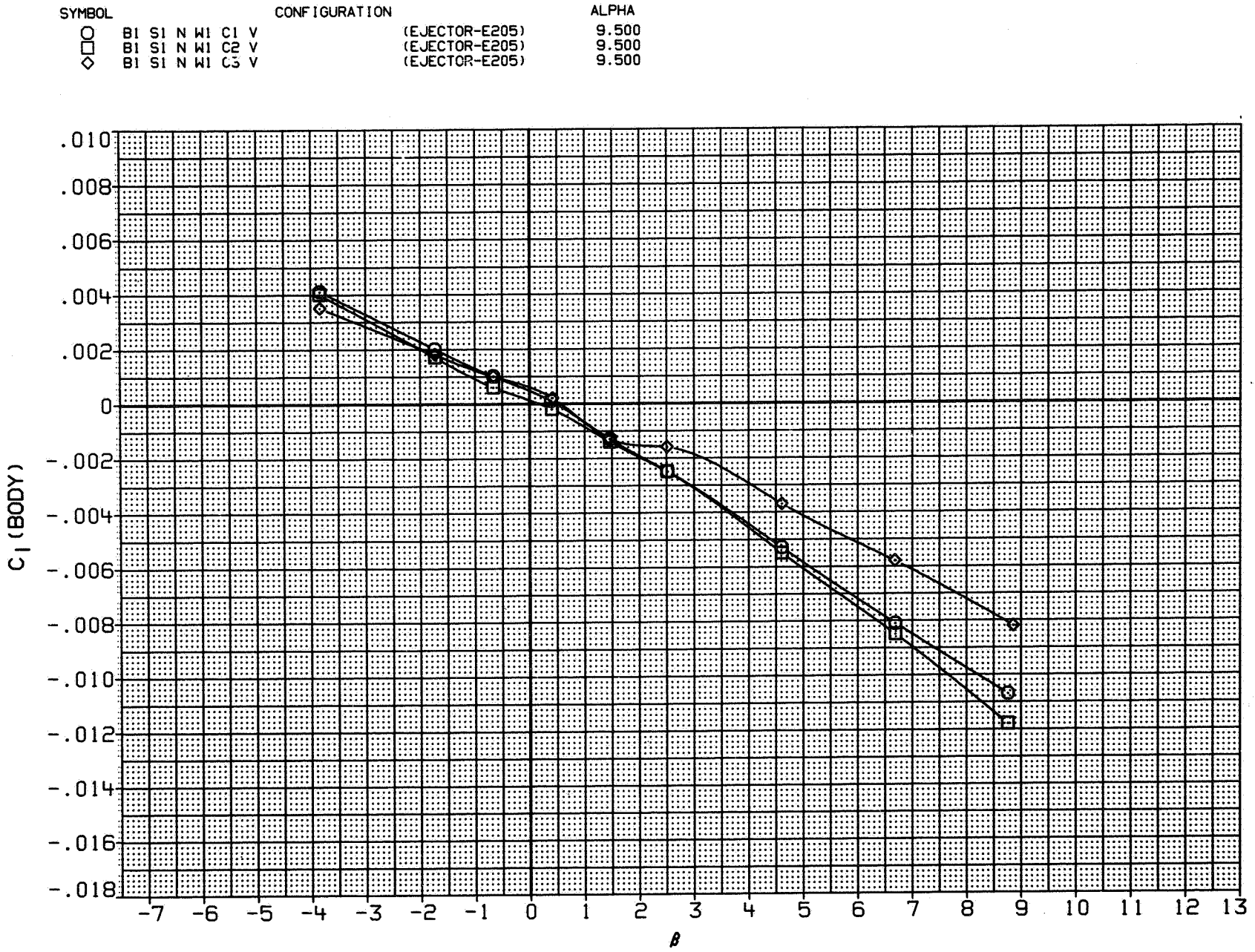


FIG. 38 CANARD LOCATION EFFECTS, LATERAL/DIRECTIONAL CHARACTERISTICS
ALPHA = 8 DEGREES
MACH = 2.00

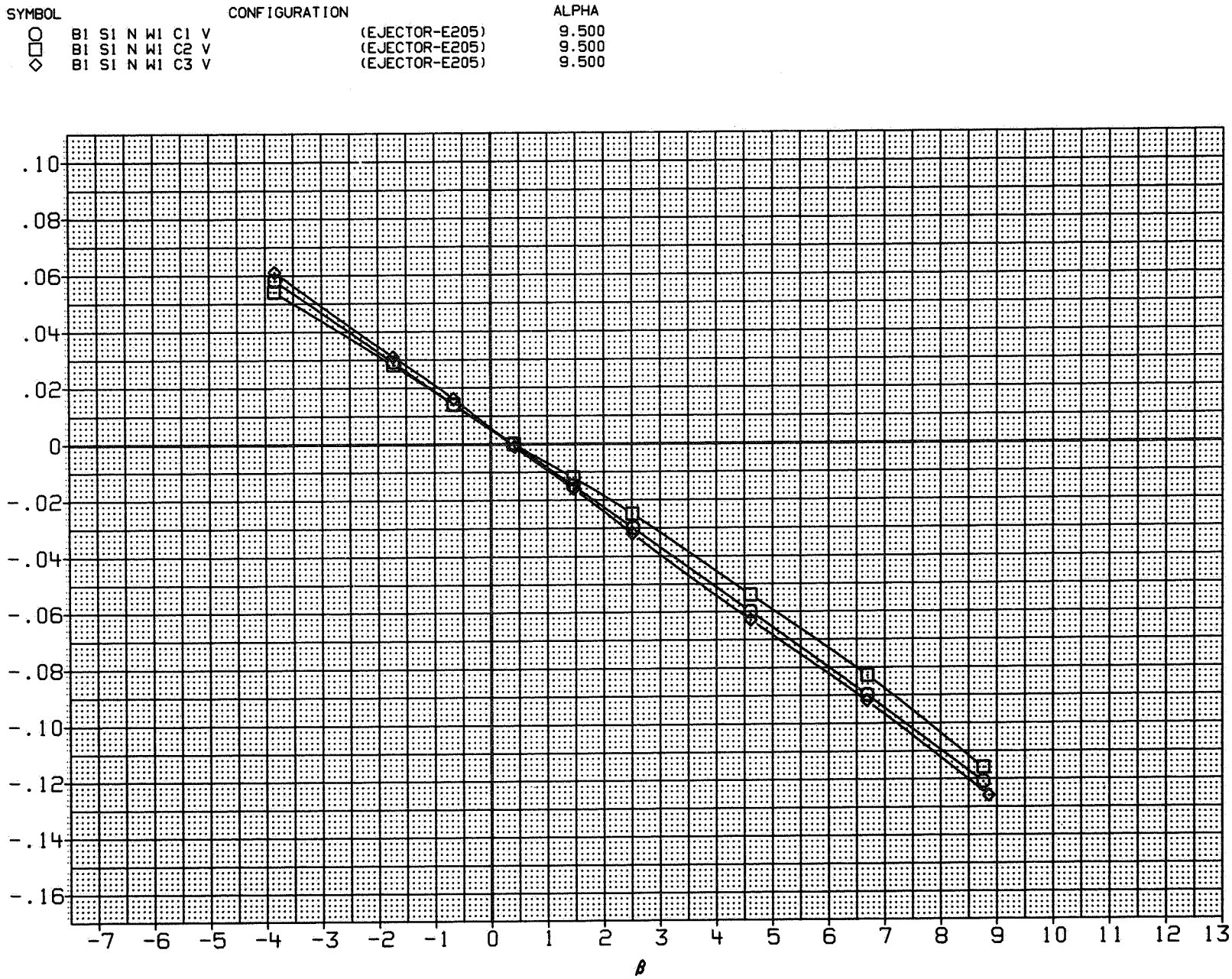


FIG. 38 CANARD LOCATION EFFECTS, LATERAL/DIRECTIONAL CHARACTERISTICS
ALPHA = 8 DEGREES

MACH = 2.00

| SYMBOL | CONFIGURATION | CANARD |
|---|---|---|
| ○ | B1 S1 N W1 C1 V (EJECTOR-E205) | .000 |
| □ | B1 S2 N W1 C1 V (EJECTOR-E205) | .000 |
| ◇ | B1 S3 N W1 C1 V (EJECTOR-E205) | .000 |

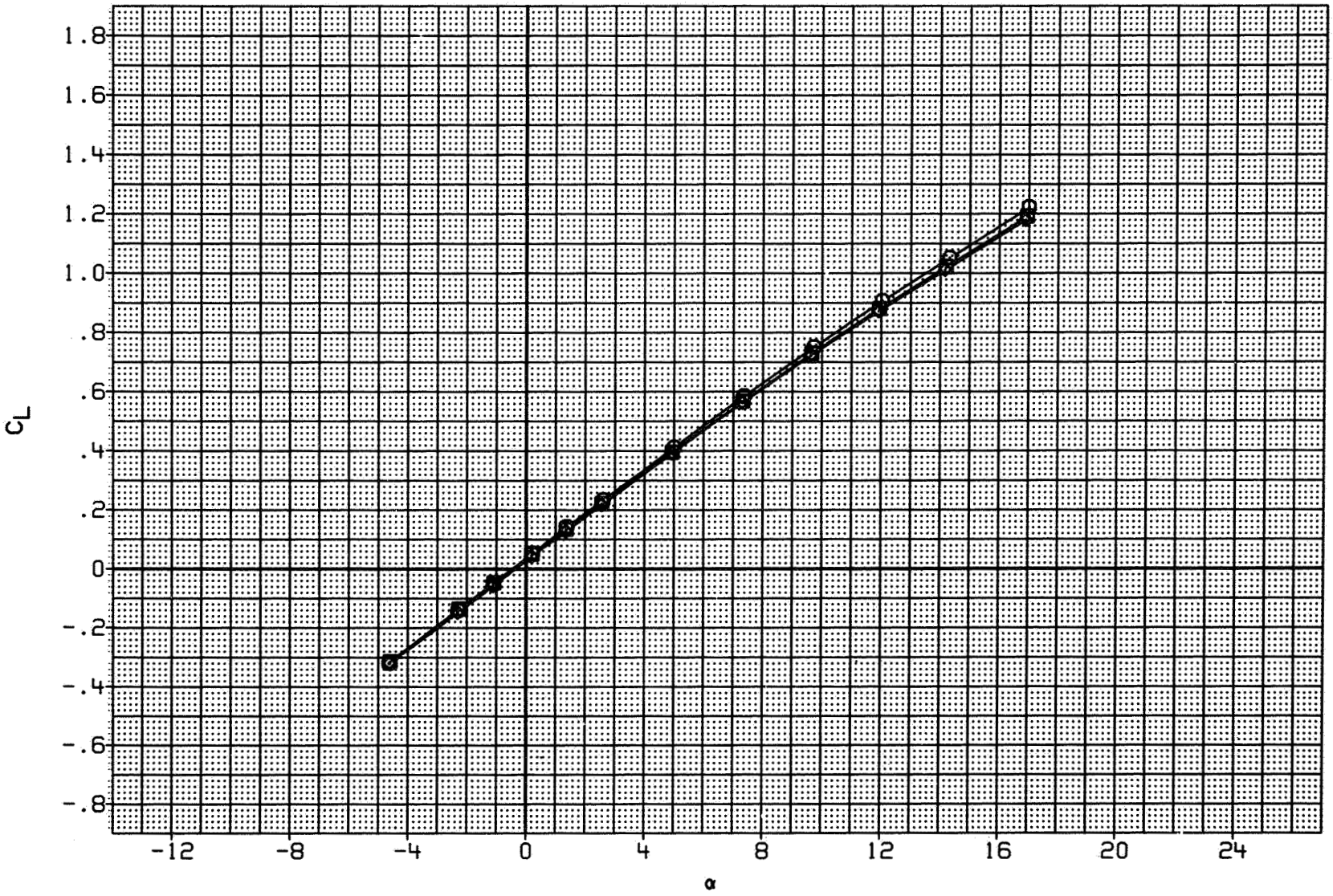


FIG. 39 STRAKE VARIATIONS, LONGITUDINAL CHARACTERISTICS

MACH = 1.60

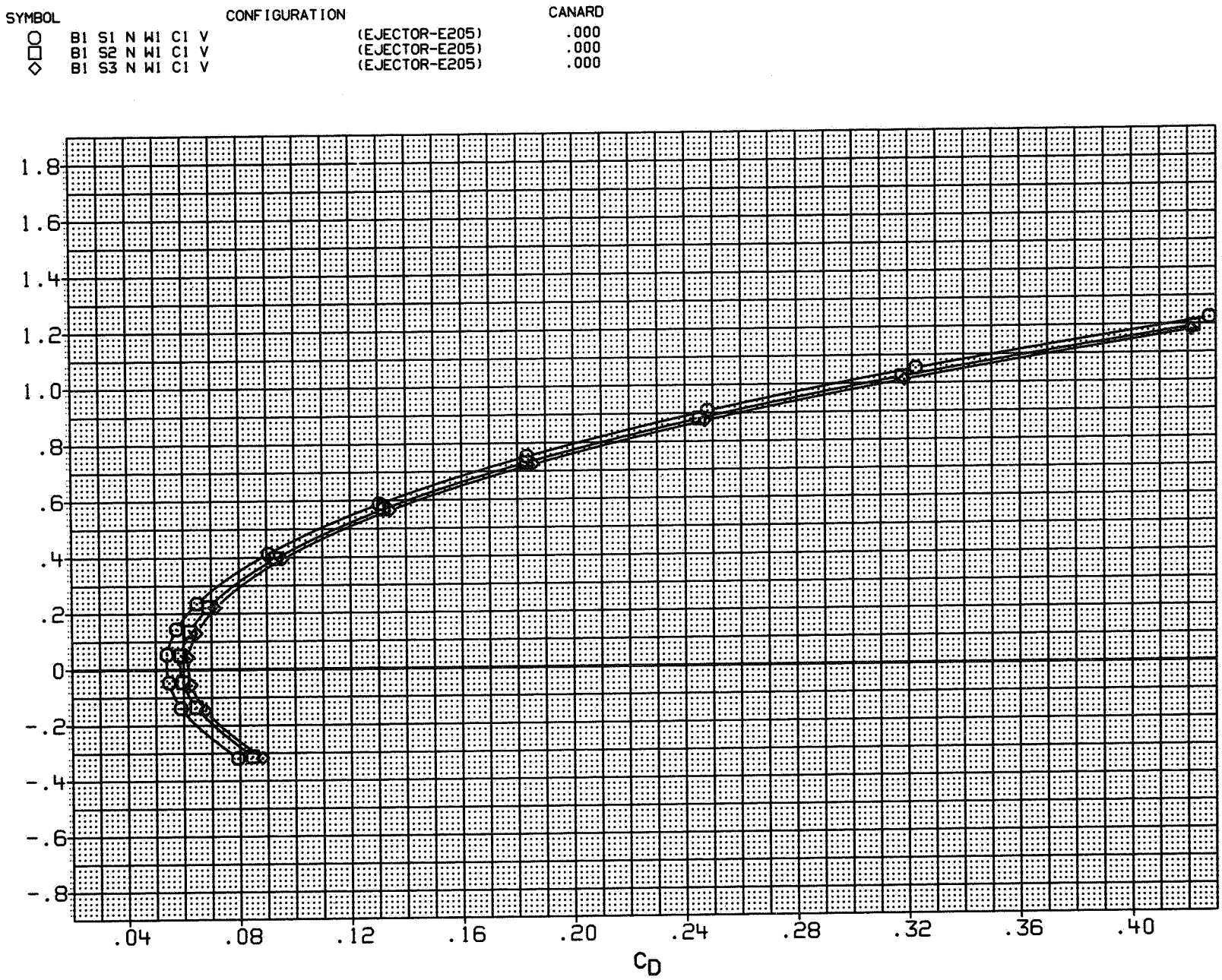


FIG. 39 STRAKE VARIATIONS, LONGITUDINAL CHARACTERISTICS

MACH = 1.60

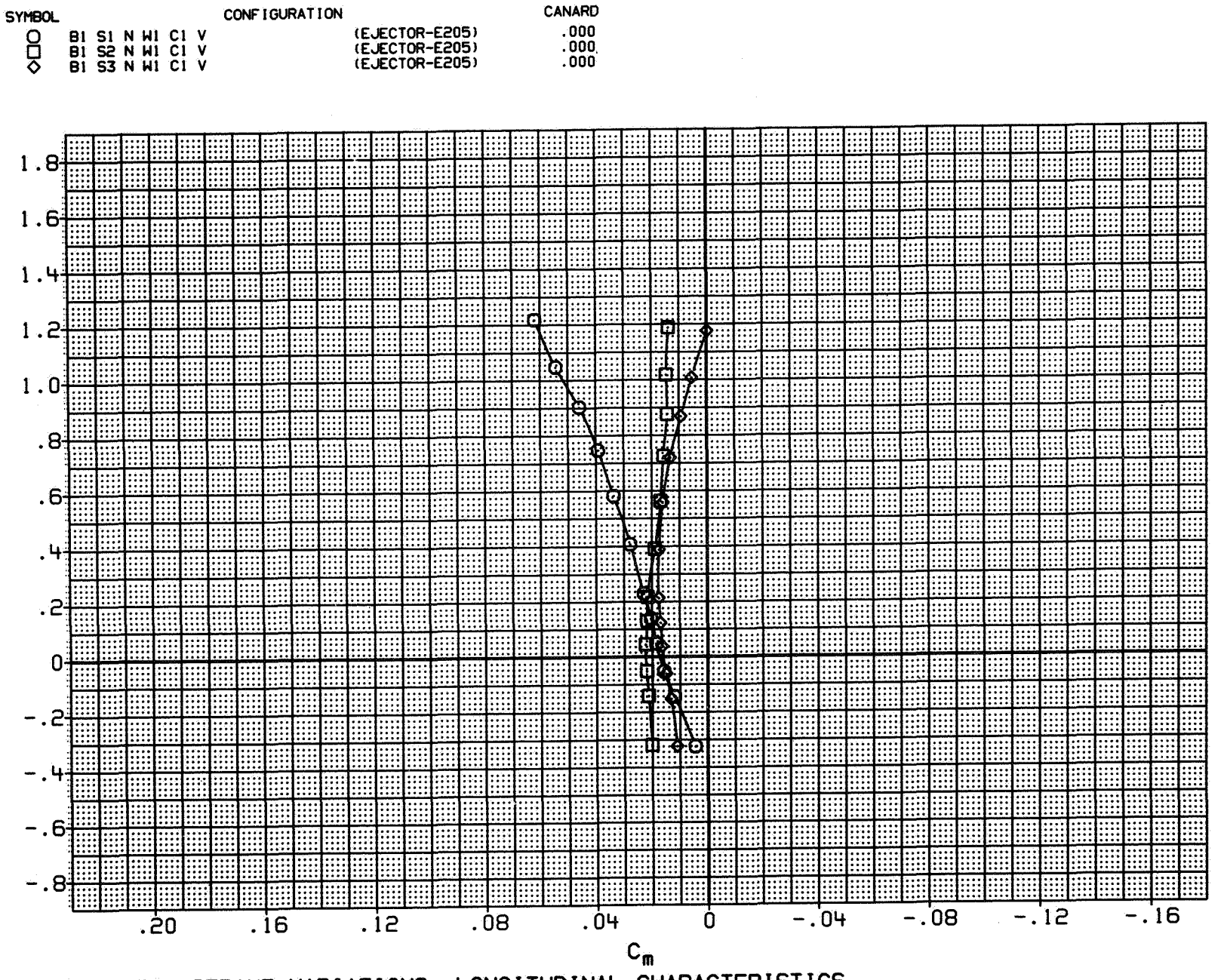


FIG. 39 STRAKE VARIATIONS, LONGITUDINAL CHARACTERISTICS

MACH = 1.60

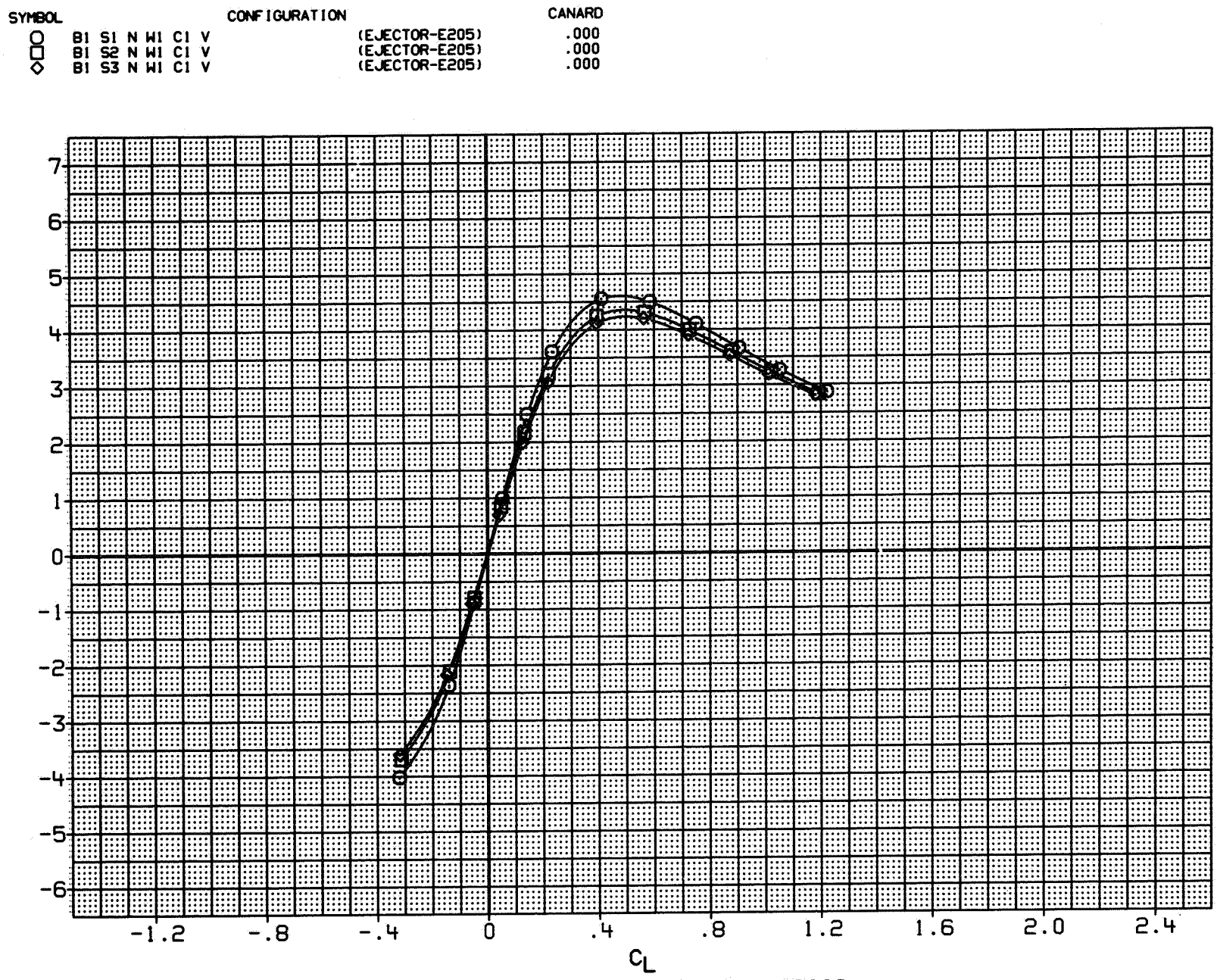


FIG. 39 STRAKE VARIATIONS, LONGITUDINAL CHARACTERISTICS

MACH = 1.60

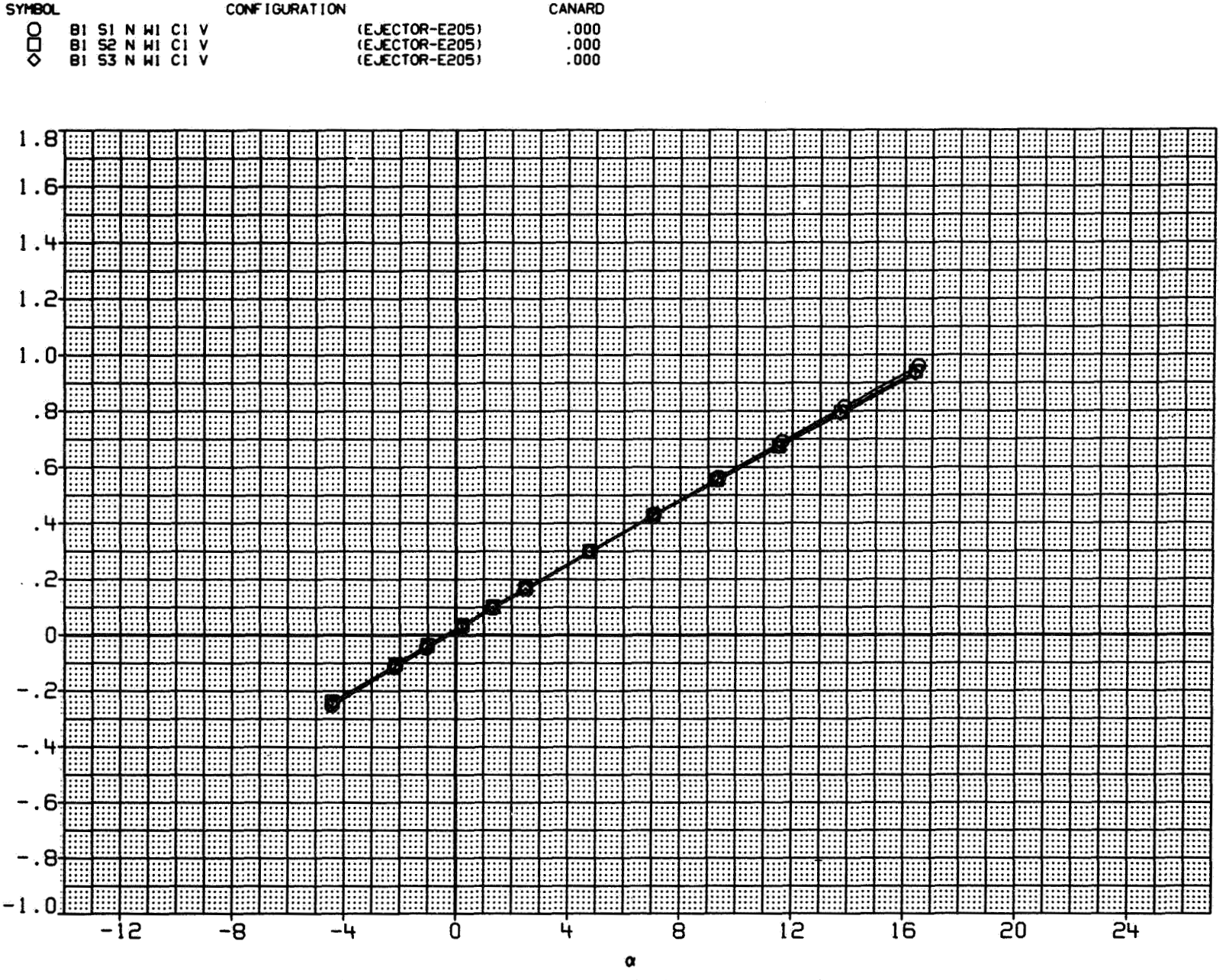


FIG. 40 STRAKE VARIATIONS, LONGITUDINAL CHARACTERISTICS

MACH = 2.00

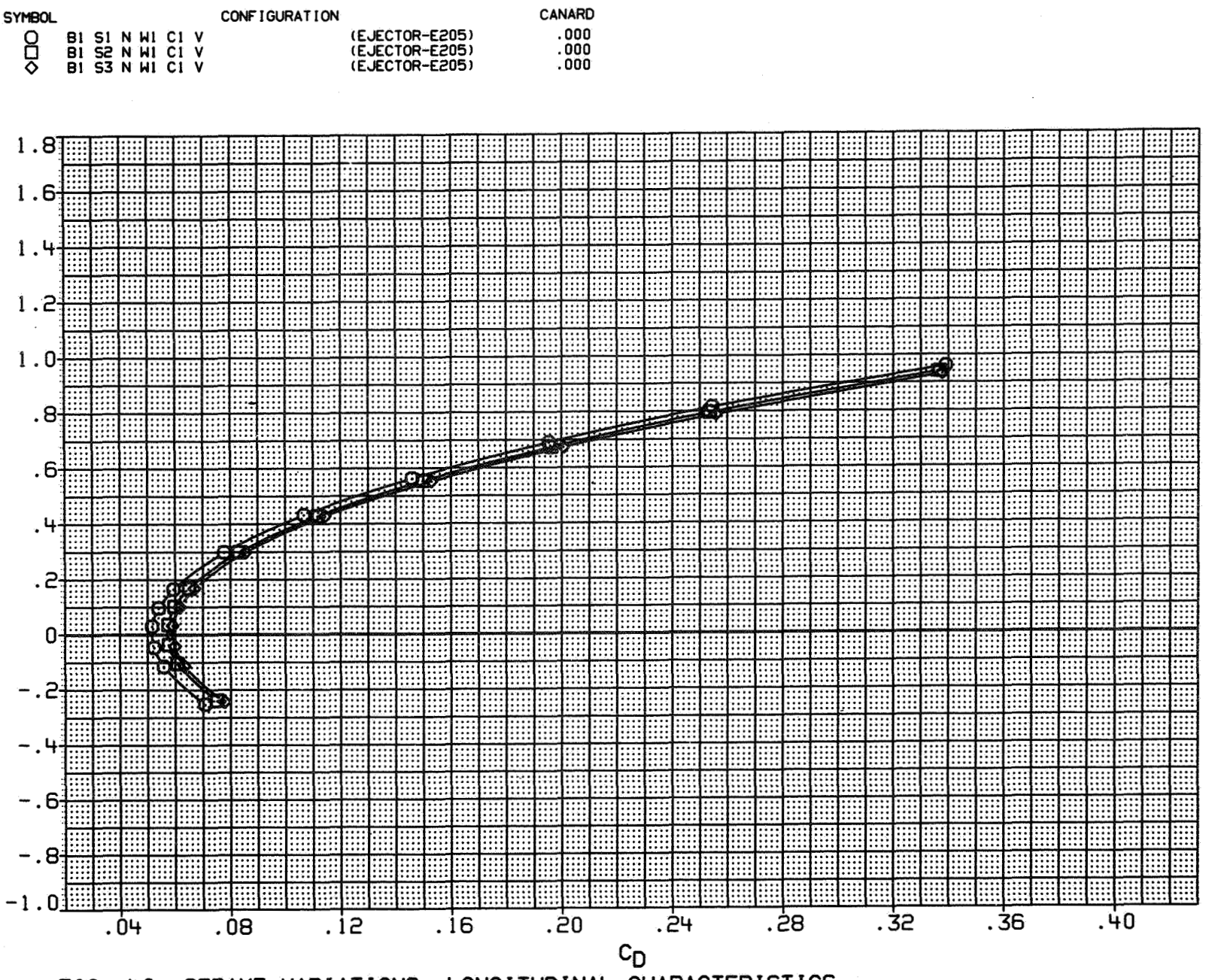


FIG. 40 STRAKE VARIATIONS, LONGITUDINAL CHARACTERISTICS

MACH = 2.00

| SYMBOL | CONFIGURATION | CANARD |
|---|---|---|
| ○ | B1 S1 N W1 C1 V (EJECTOR-E205) | .000 |
| □ | B1 S2 N W1 C1 V (EJECTOR-E205) | .000 |
| ◇ | B1 S3 N W1 C1 V (EJECTOR-E205) | .000 |

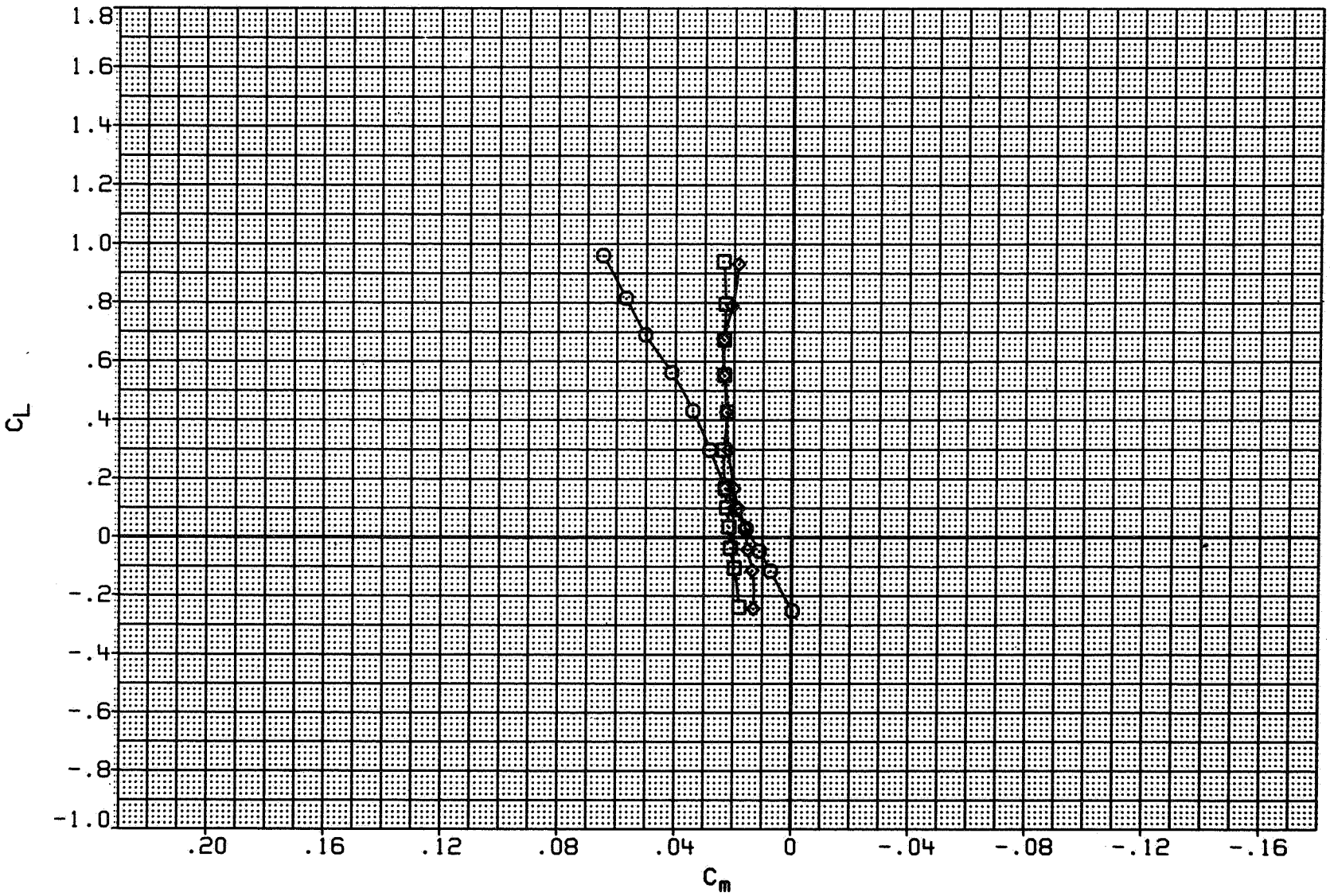


FIG. 40 STRAKE VARIATIONS, LONGITUDINAL CHARACTERISTICS

MACH = 2.00

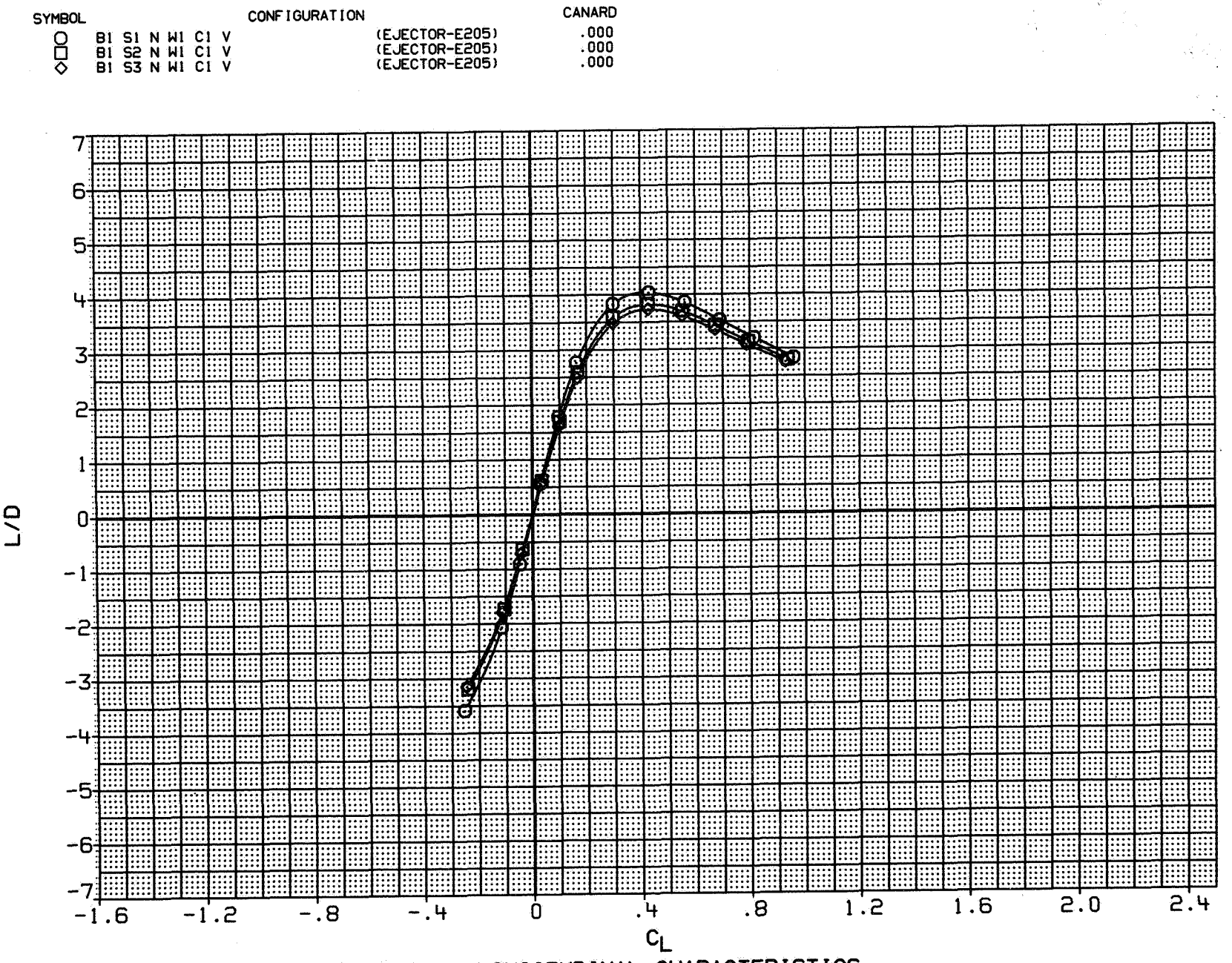


FIG. 40 STRAKE VARIATIONS, LONGITUDINAL CHARACTERISTICS

MACH = 2.00

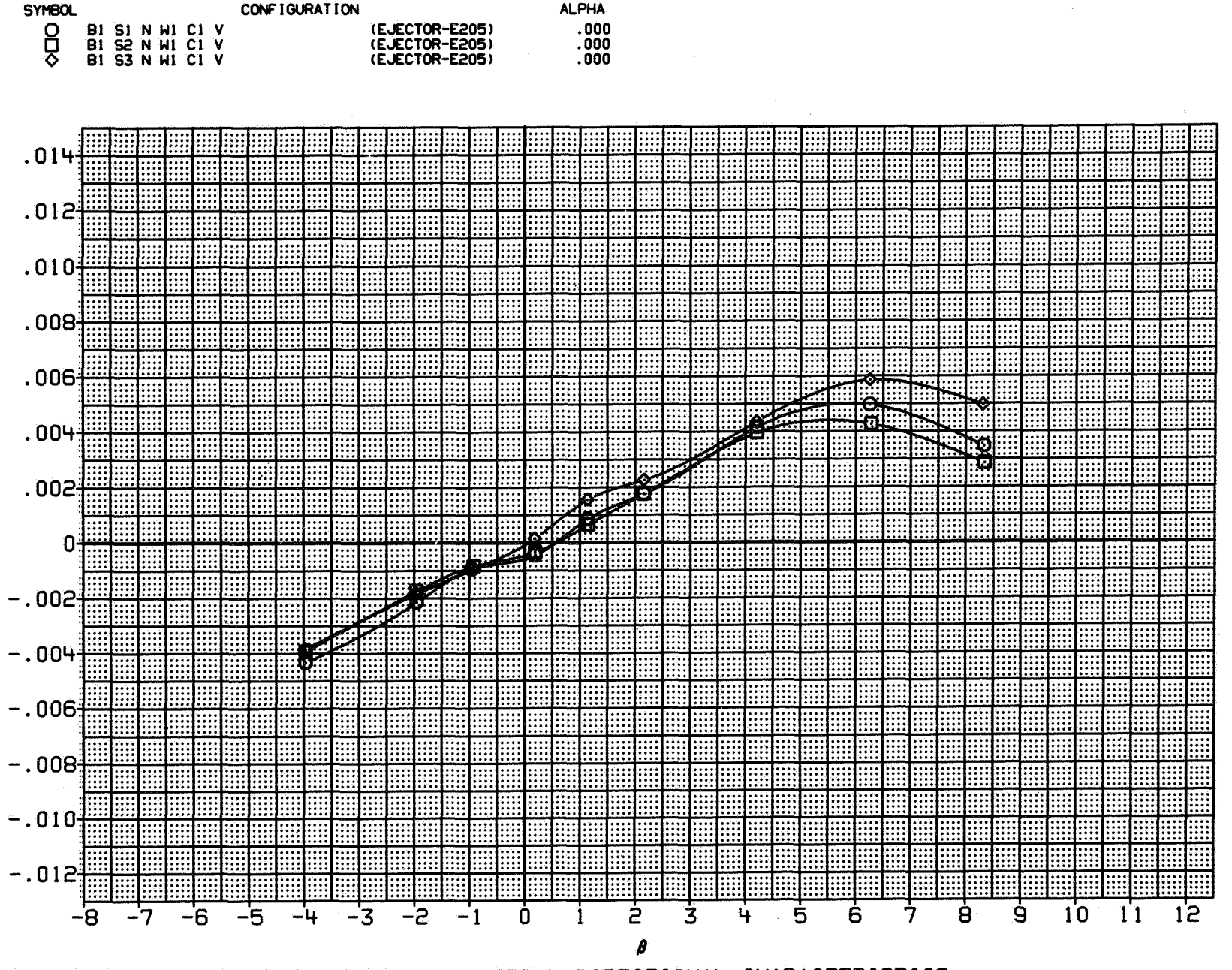


FIG. 41 STRAKE VARIATIONS, LATERAL/DIRECTIONAL CHARACTERISTICS
ALPHA = 0 DEGREES

MACH = 1.60

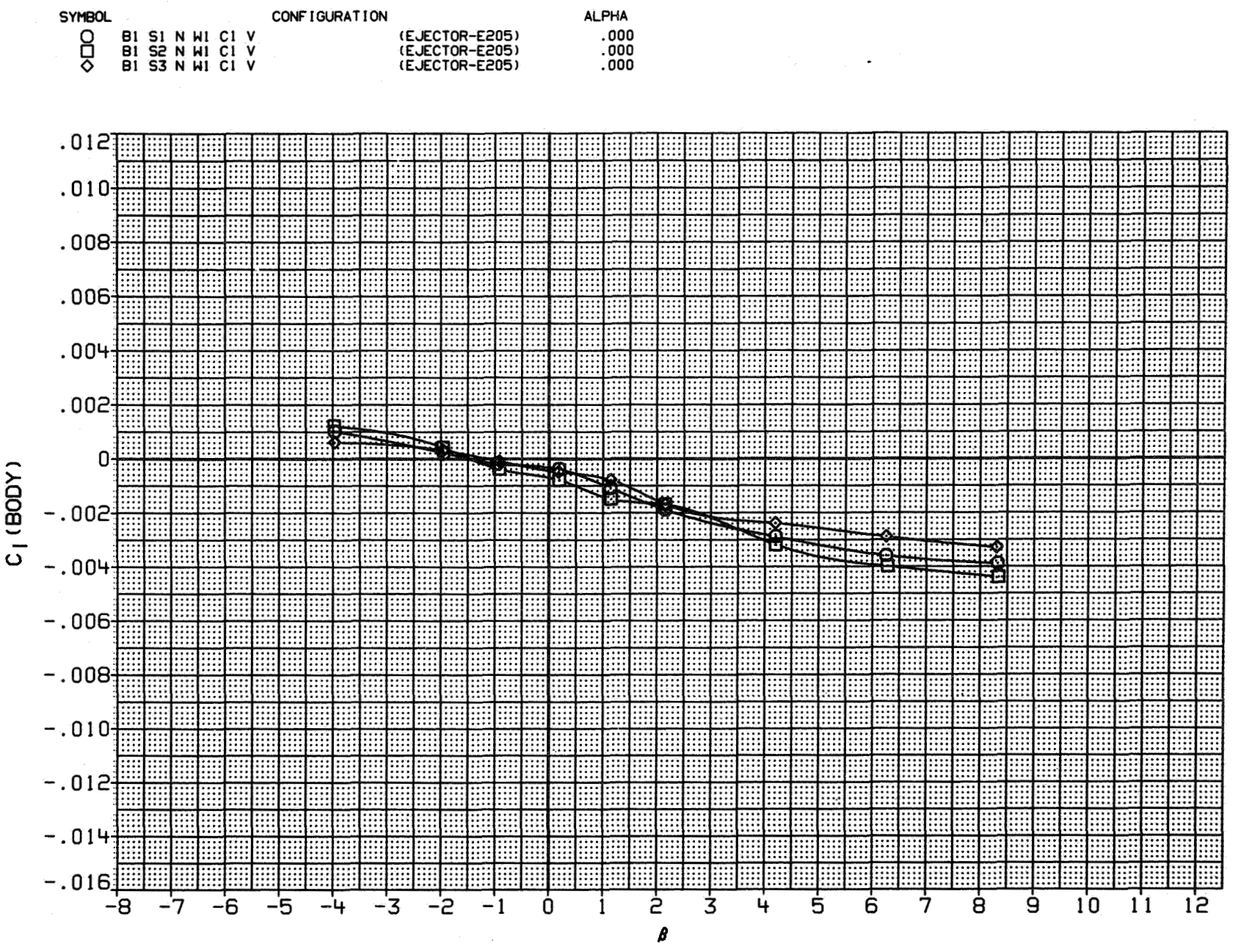


FIG. 41 STRAKE VARIATIONS, LATERAL/DIRECTIONAL CHARACTERISTICS
ALPHA = 0 DEGREES

MACH = 1.60

| SYMBOL | CONFIGURATION | ALPHA |
|---|---|---|
| ○ | B1 S1 N W1 C1 V (EJECTOR-E205) | .000 |
| □ | B1 S2 N W1 C1 V (EJECTOR-E205) | .000 |
| ◇ | B1 S3 N W1 C1 V (EJECTOR-E205) | .000 |

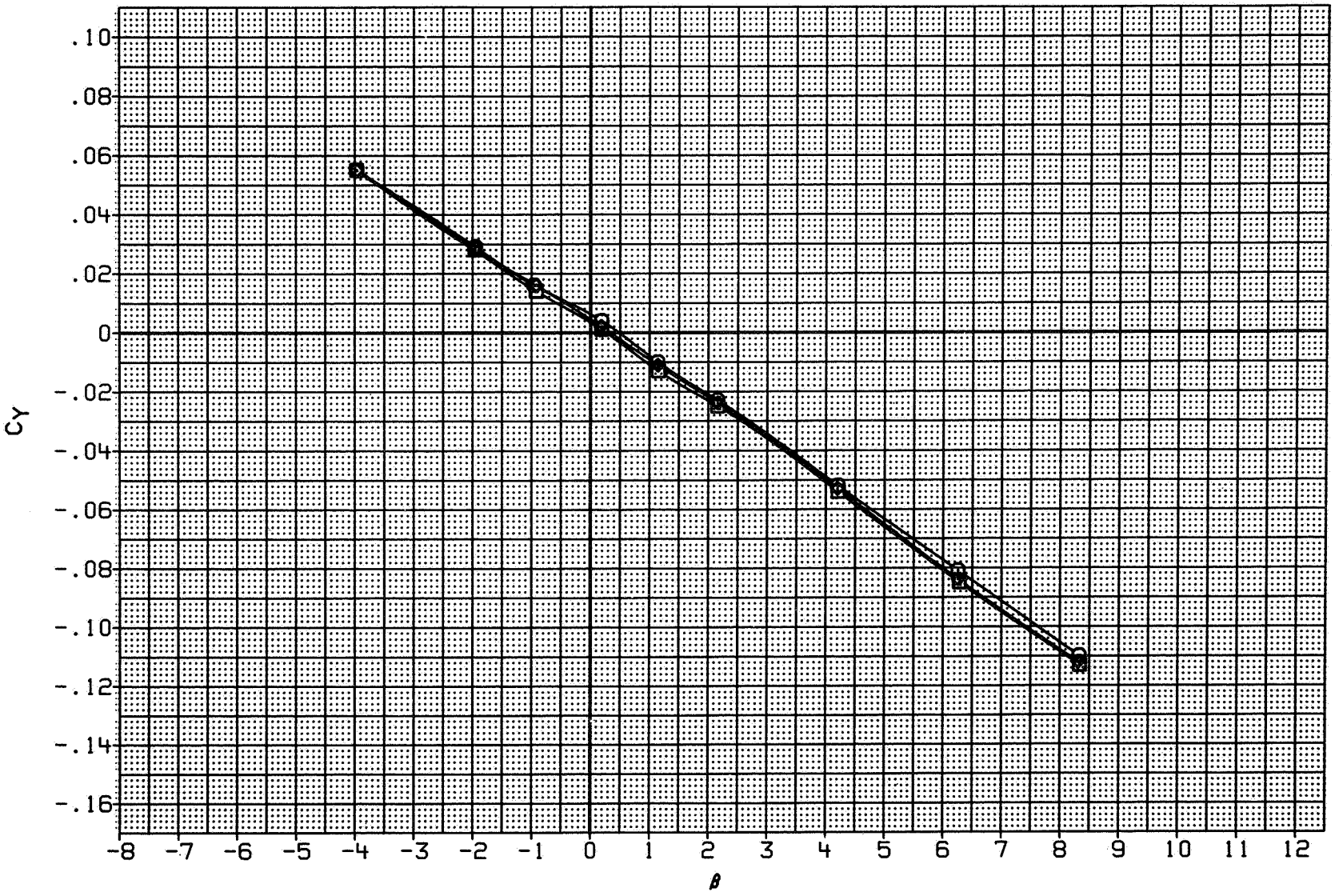


FIG. 41 STRAKE VARIATIONS, LATERAL/DIRECTIONAL CHARACTERISTICS
ALPHA = 0 DEGREES

MACH = 1.60

| SYMBOL | CONFIGURATION | | ALPHA |
|---|---|---|---|
| ○ | B1 S1 N W1 C1 V | (EJECTOR-E205) | 9.500 |
| □ | B1 S2 N W1 C1 V | (EJECTOR-E205) | 9.500 |
| ◇ | B1 S3 N W1 C1 V | (EJECTOR-E205) | 9.500 |

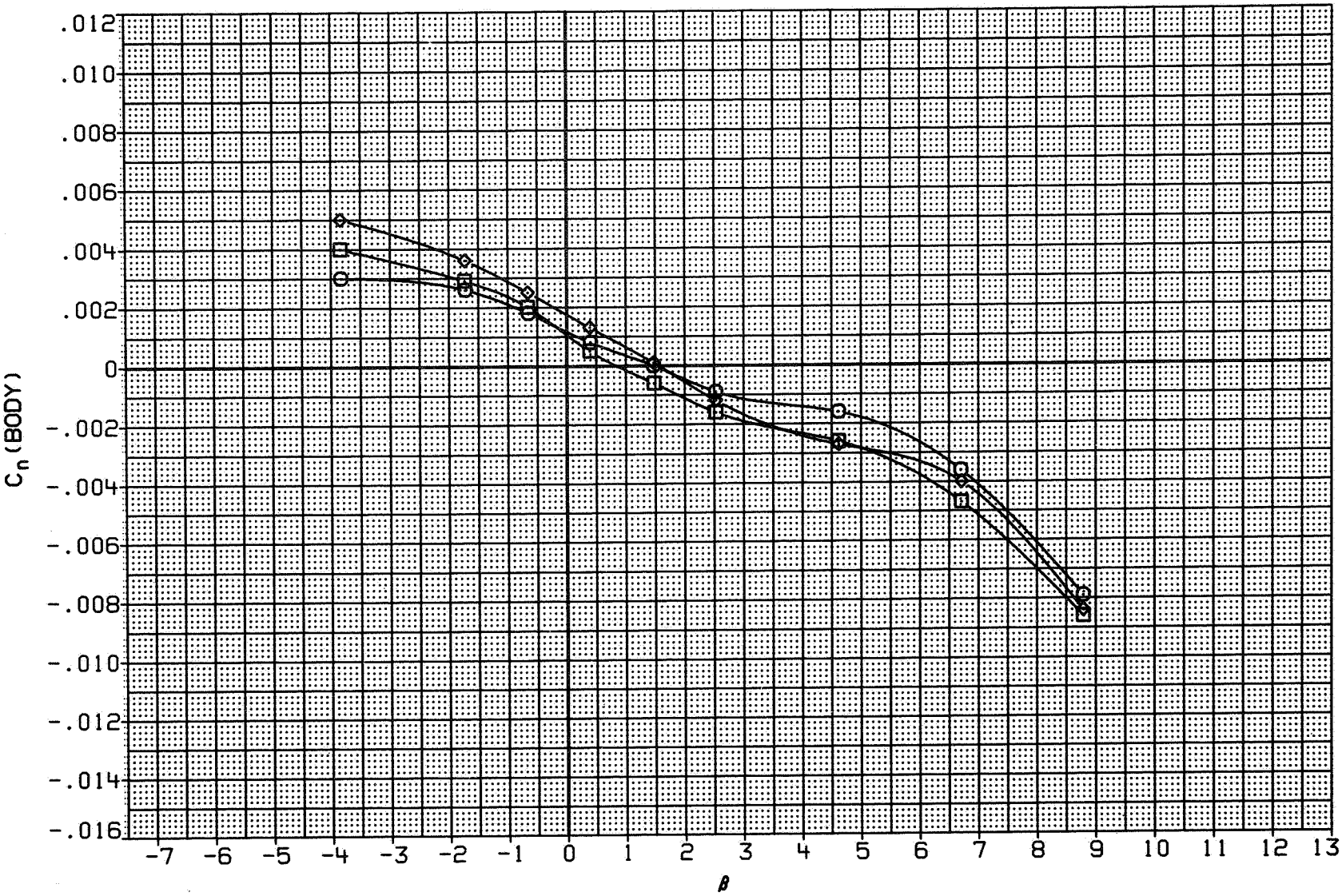


FIG. 42 STRAKE VARIATIONS, LATERAL/DIRECTIONAL CHARACTERISTICS
ALPHA = 8 DEGREES

MACH = 1.60

| SYMBOL | CONFIGURATION | | ALPHA |
|---|---|---|---|
| ○ | B1 S1 N W1 C1 V | (EJECTOR-E205) | 9.500 |
| □ | B1 S2 N W1 C1 V | (EJECTOR-E205) | 9.500 |
| ◇ | B1 S3 N W1 C1 V | (EJECTOR-E205) | 9.500 |

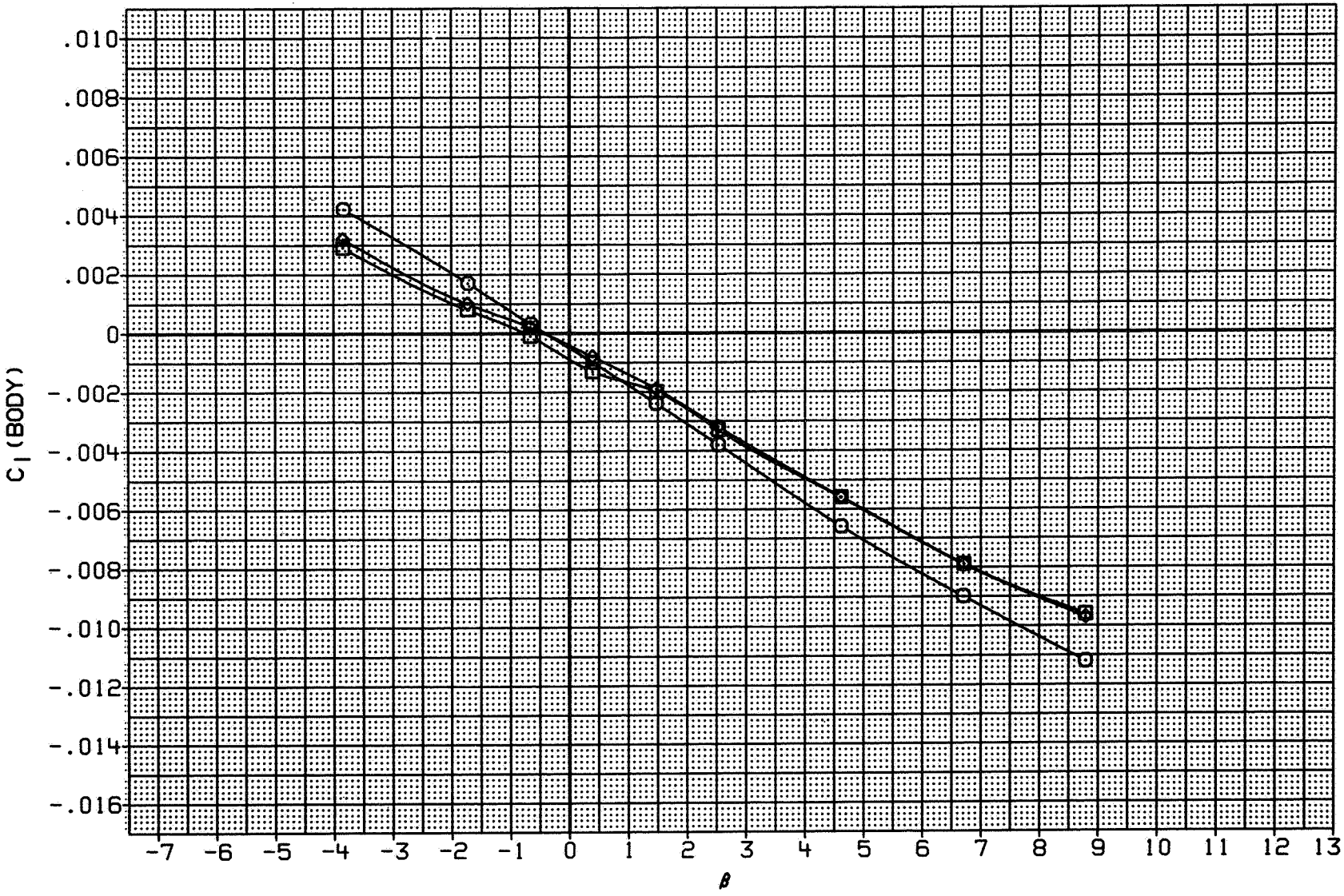


FIG. 42 STRAKE VARIATIONS, LATERAL/DIRECTIONAL CHARACTERISTICS
ALPHA = 8 DEGREES

MACH = 1.60

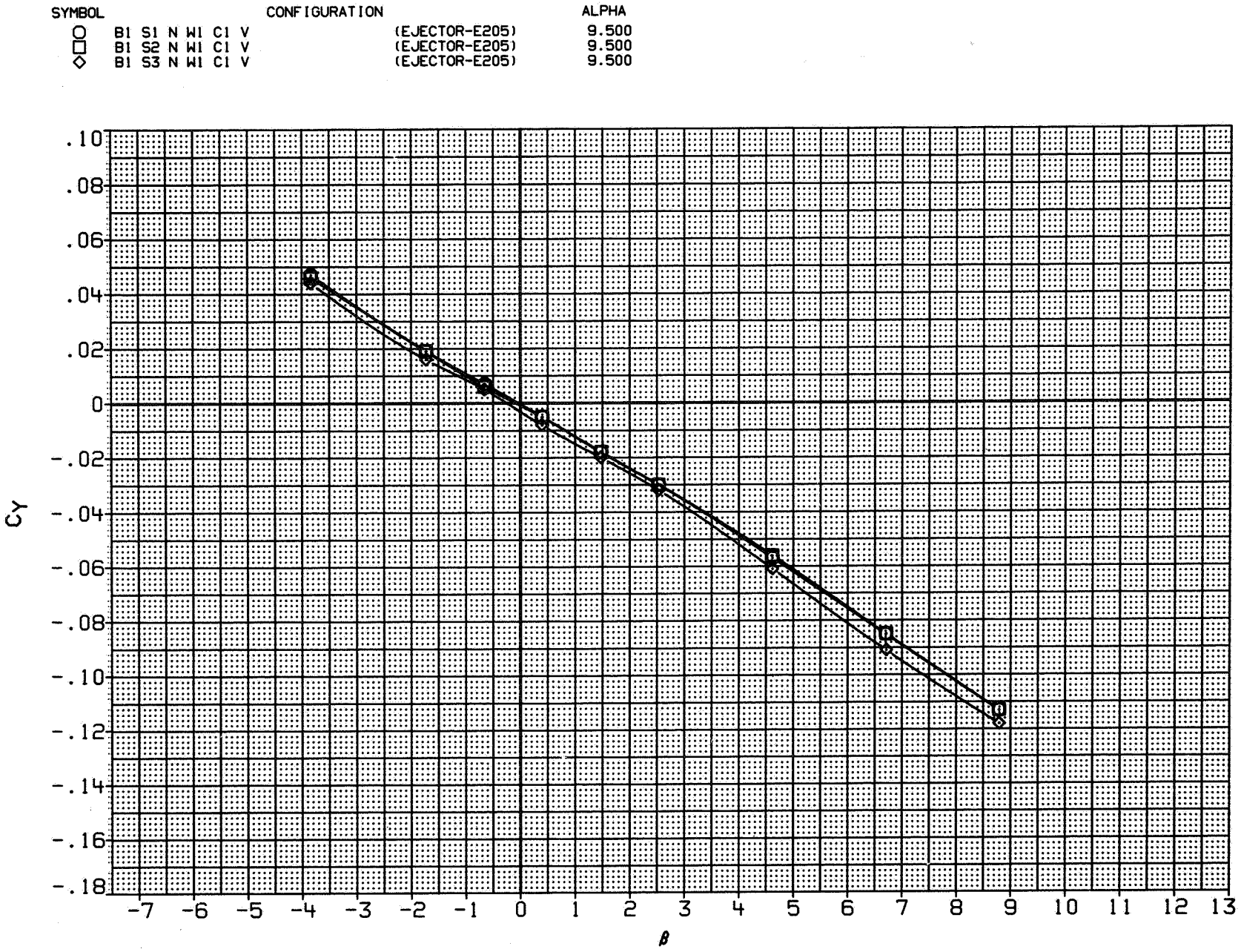


FIG. 42 STRAKE VARIATIONS, LATERAL/DIRECTIONAL CHARACTERISTICS
ALPHA = 8 DEGREES
MACH = 1.60

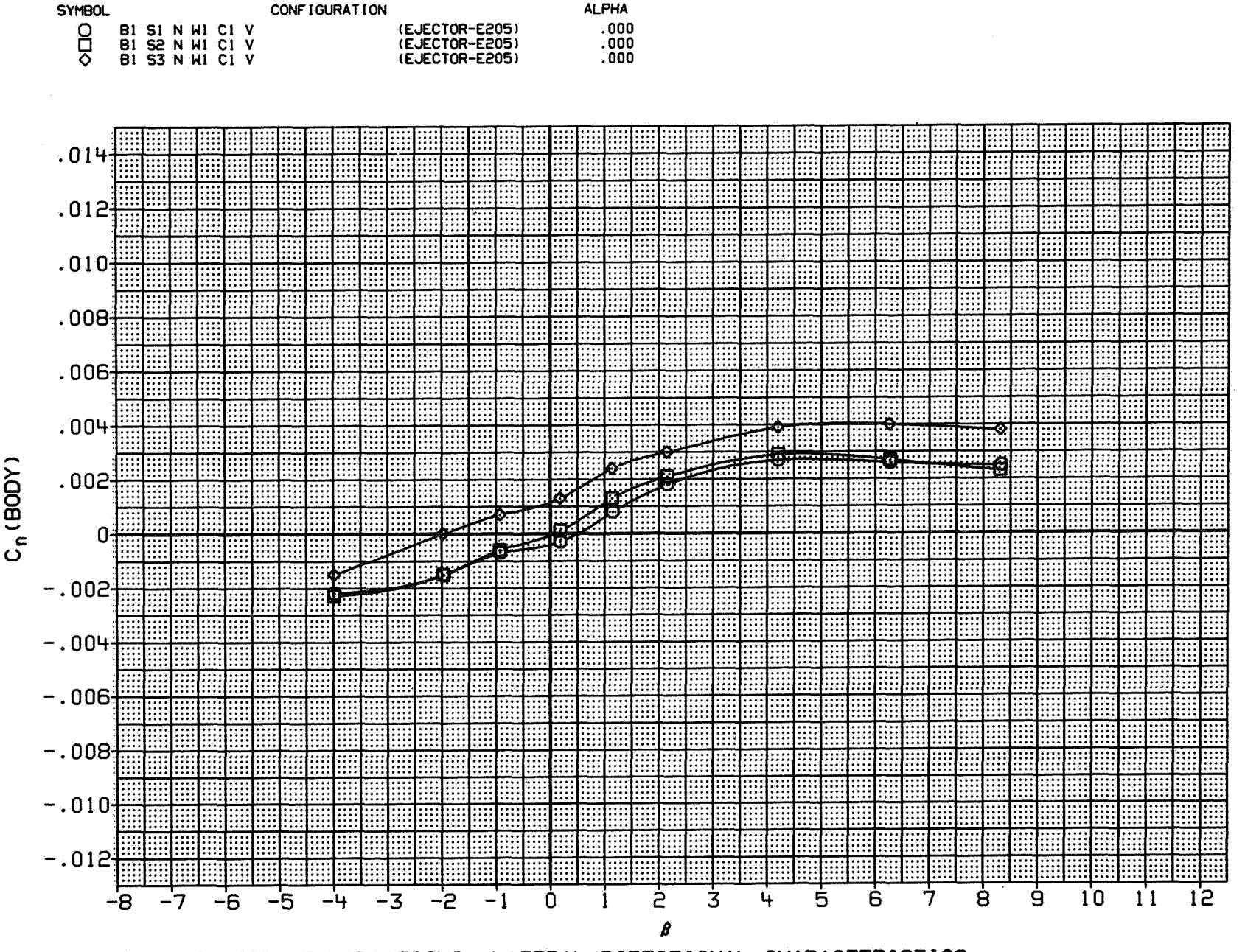


FIG. 43 STRAKE VARIATIONS, LATERAL/DIRECTIONAL CHARACTERISTICS
ALPHA = 0 DEGREES
MACH = 2.00

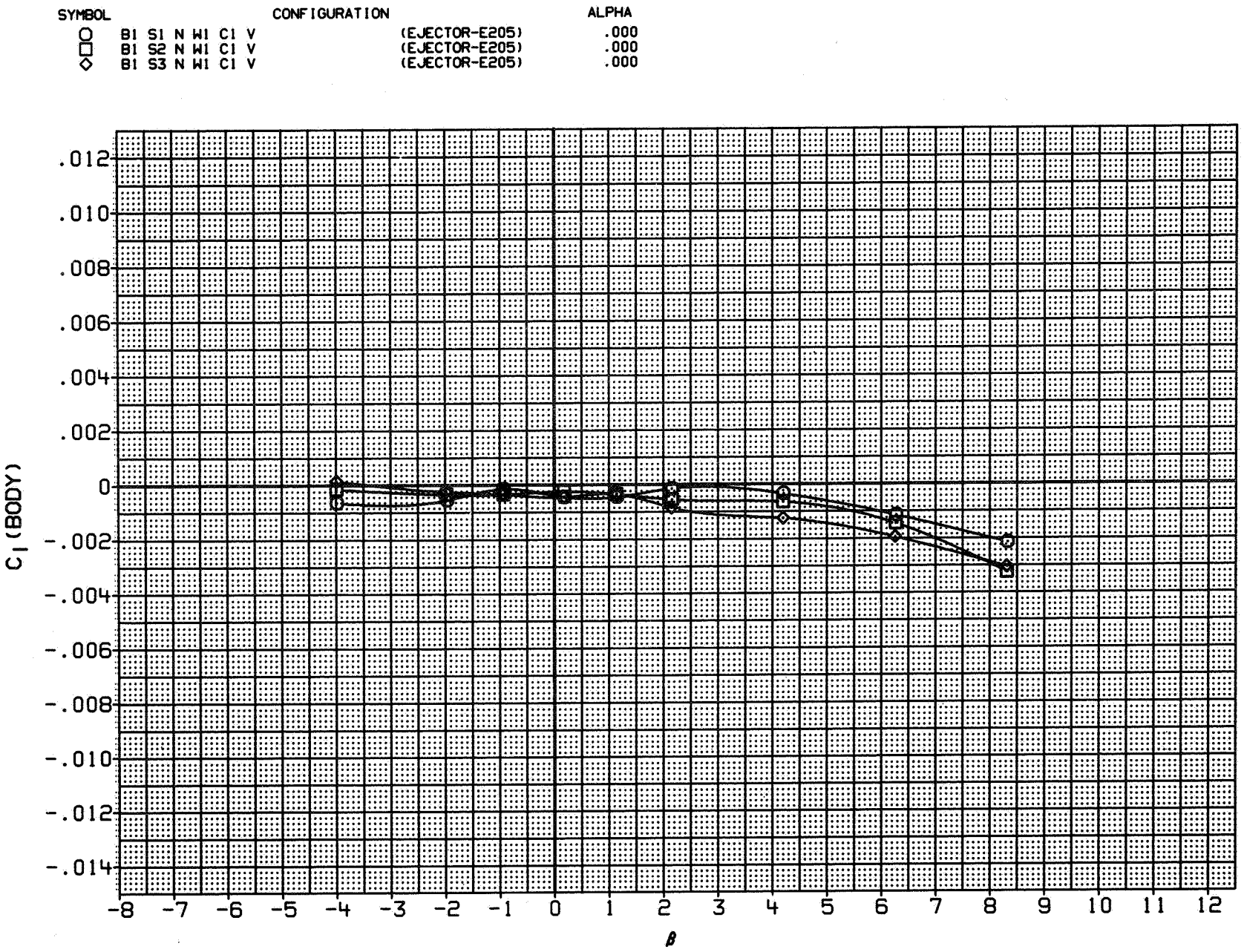


FIG. 43 STRAKE VARIATIONS, LATERAL/DIRECTIONAL CHARACTERISTICS
ALPHA = 0 DEGREES
MACH = 2.00

| SYMBOL | CONFIGURATION | ALPHA |
|---|---|---|
| ○ | B1 S1 N W1 C1 V (EJECTOR-E205) | .000 |
| □ | B1 S2 N W1 C1 V (EJECTOR-E205) | .000 |
| ◇ | B1 S3 N W1 C1 V (EJECTOR-E205) | .000 |

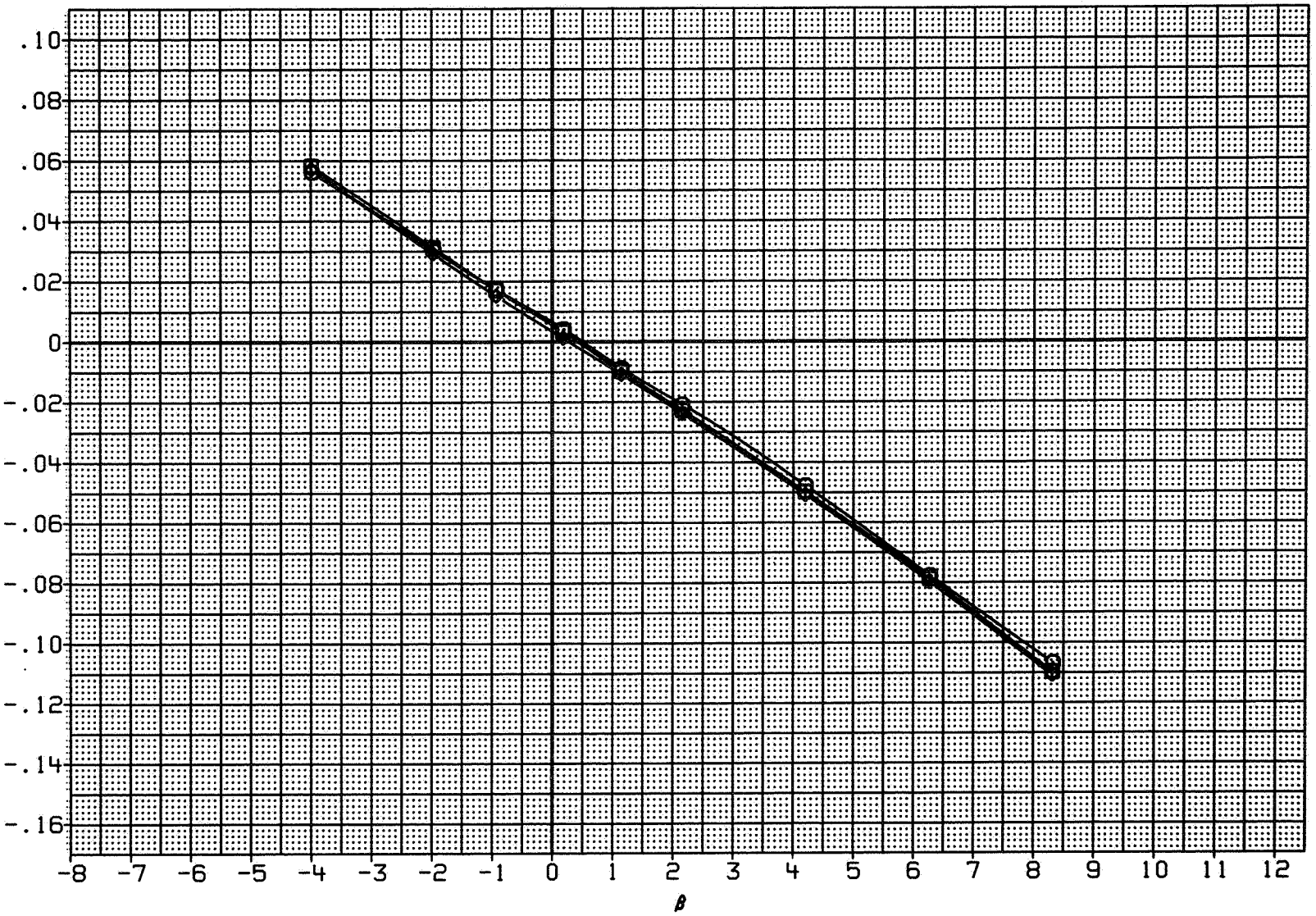


FIG. 43 STRAKE VARIATIONS, LATERAL/DIRECTIONAL CHARACTERISTICS
ALPHA = 0 DEGREES
MACH = 2.00

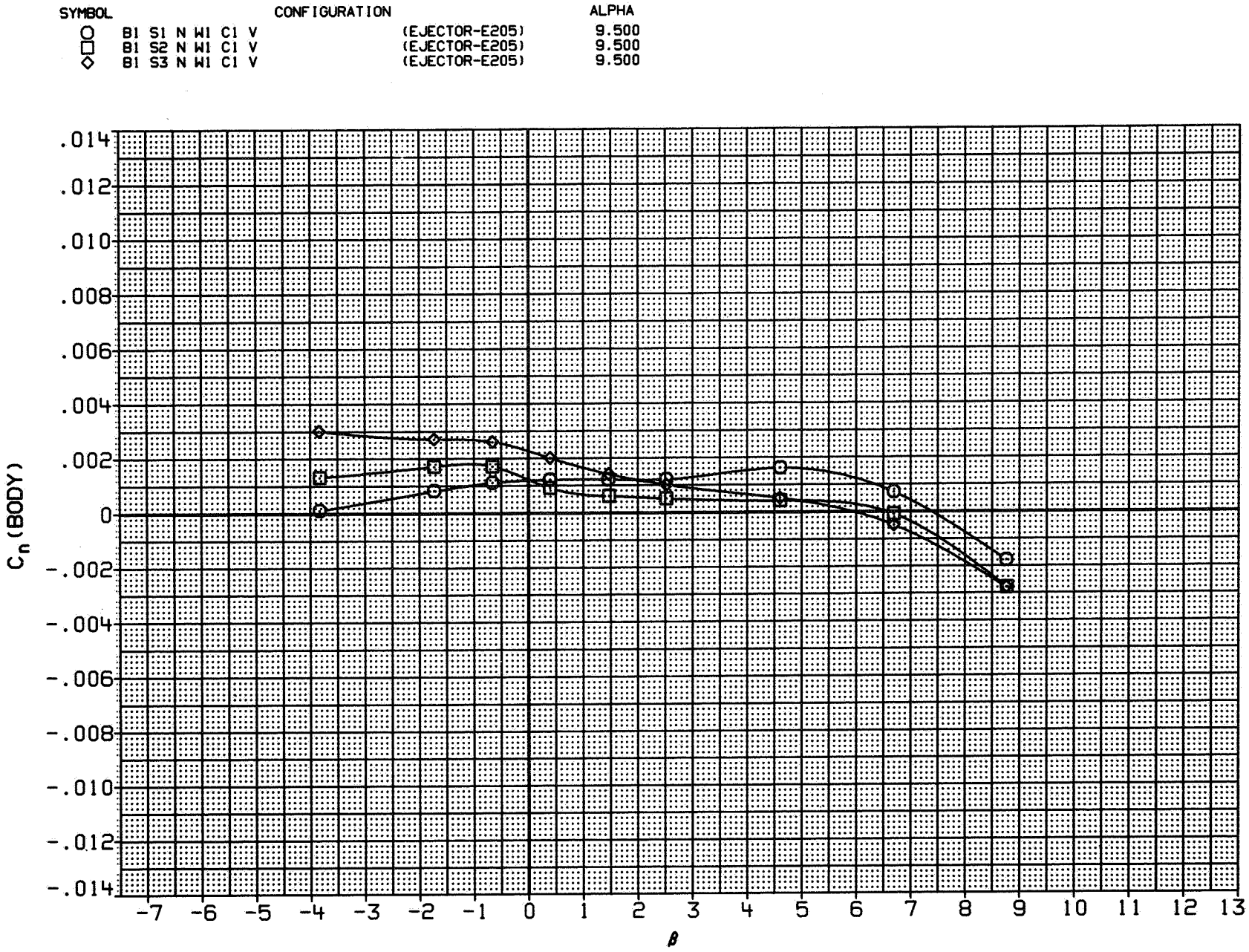


FIG. 44 STRAKE VARIATIONS, LATERAL/DIRECTIONAL CHARACTERISTICS
ALPHA = 8 DEGREES
MACH = 2.00

| SYMBOL | CONFIGURATION | | ALPHA |
|---|---|---|---|
| ○ | B1 S1 N W1 C1 V | (EJECTOR-E205) | 9.500 |
| □ | B1 S2 N W1 C1 V | (EJECTOR-E205) | 9.500 |
| ◇ | B1 S3 N W1 C1 V | (EJECTOR-E205) | 9.500 |

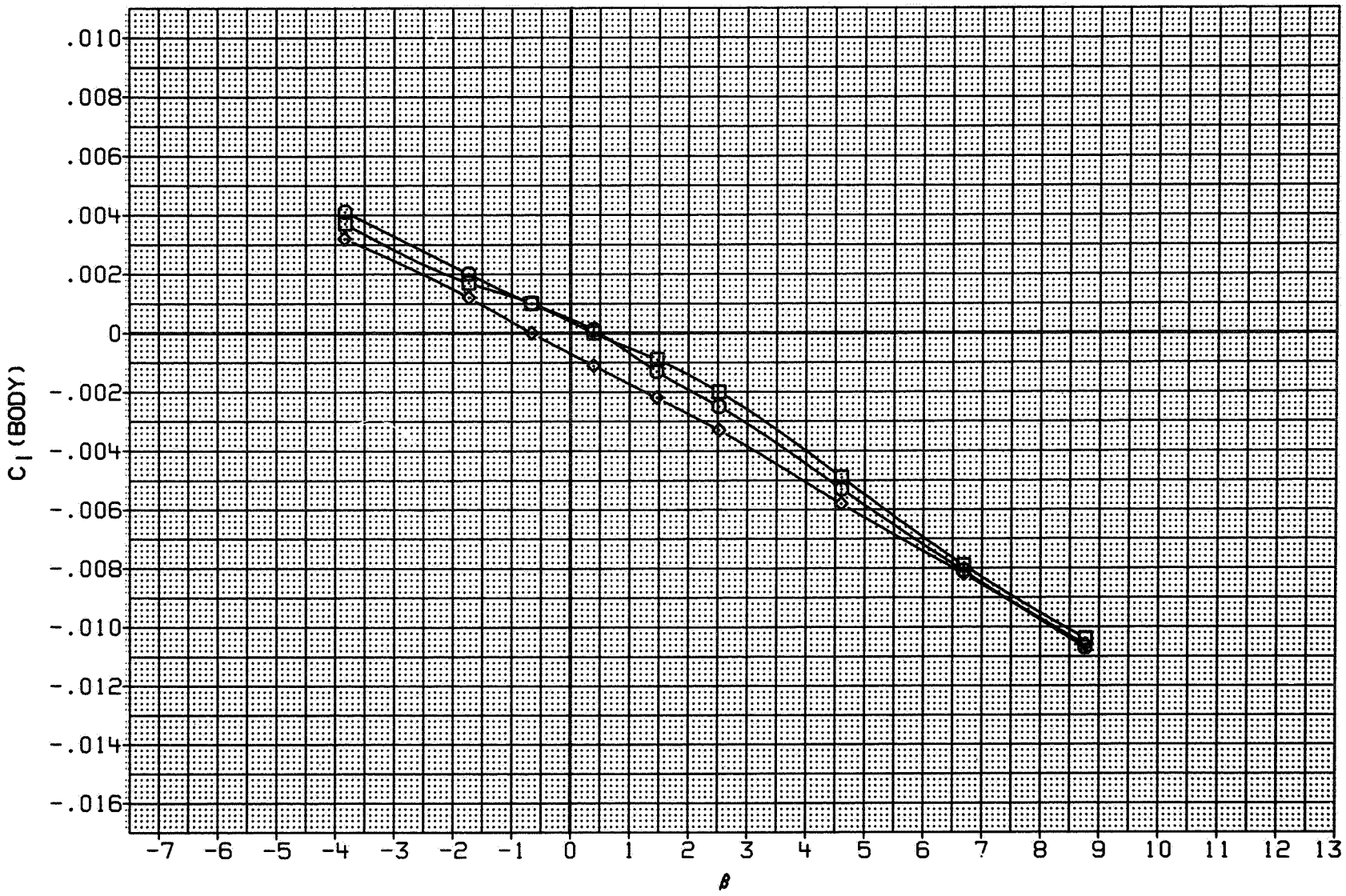


FIG. 44 STRAKE VARIATIONS, LATERAL/DIRECTIONAL CHARACTERISTICS
ALPHA = 8 DEGREES

MACH = 2.00

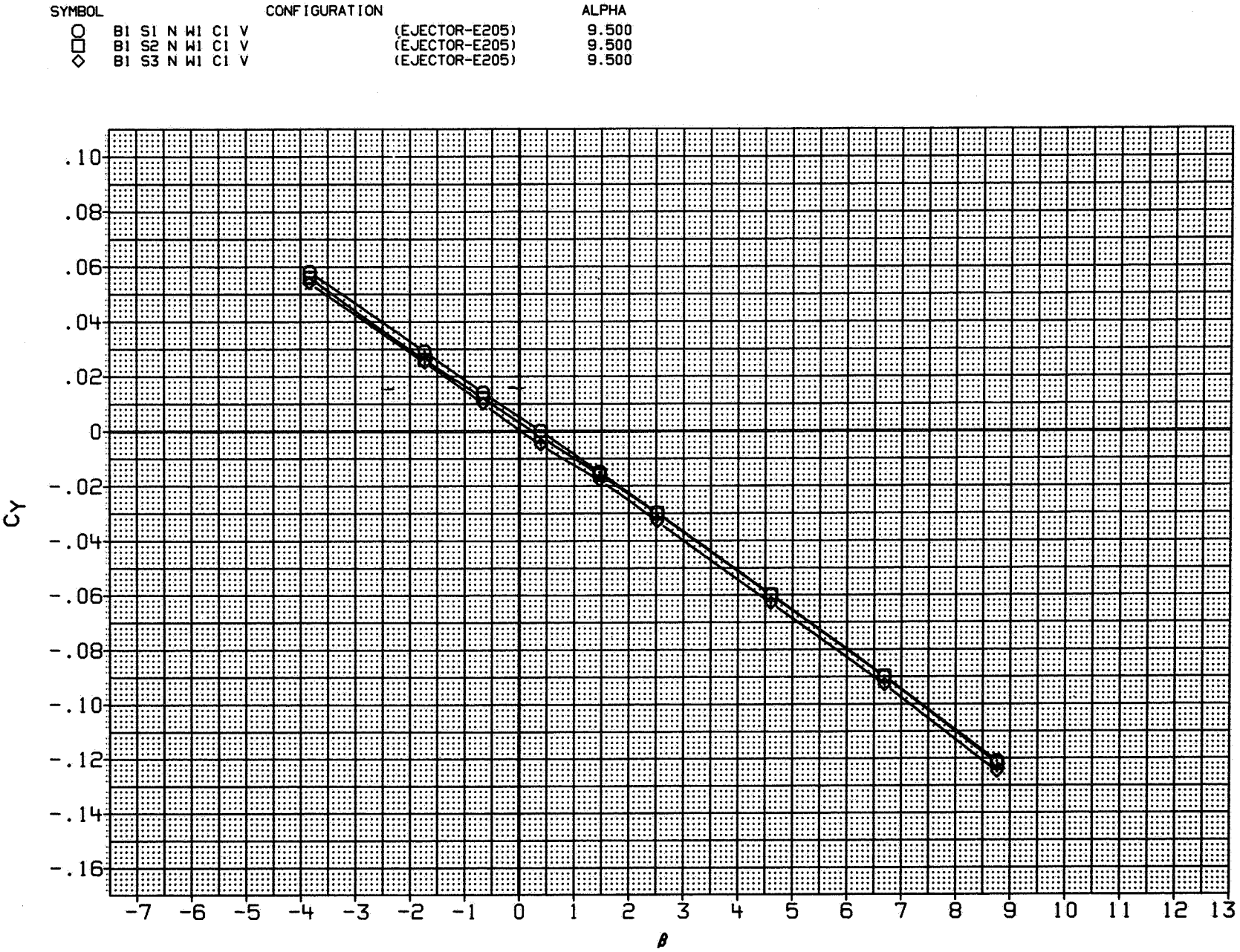


FIG. 44 STRAKE VARIATIONS, LATERAL/DIRECTIONAL CHARACTERISTICS
ALPHA = 8 DEGREES
MACH = 2.00

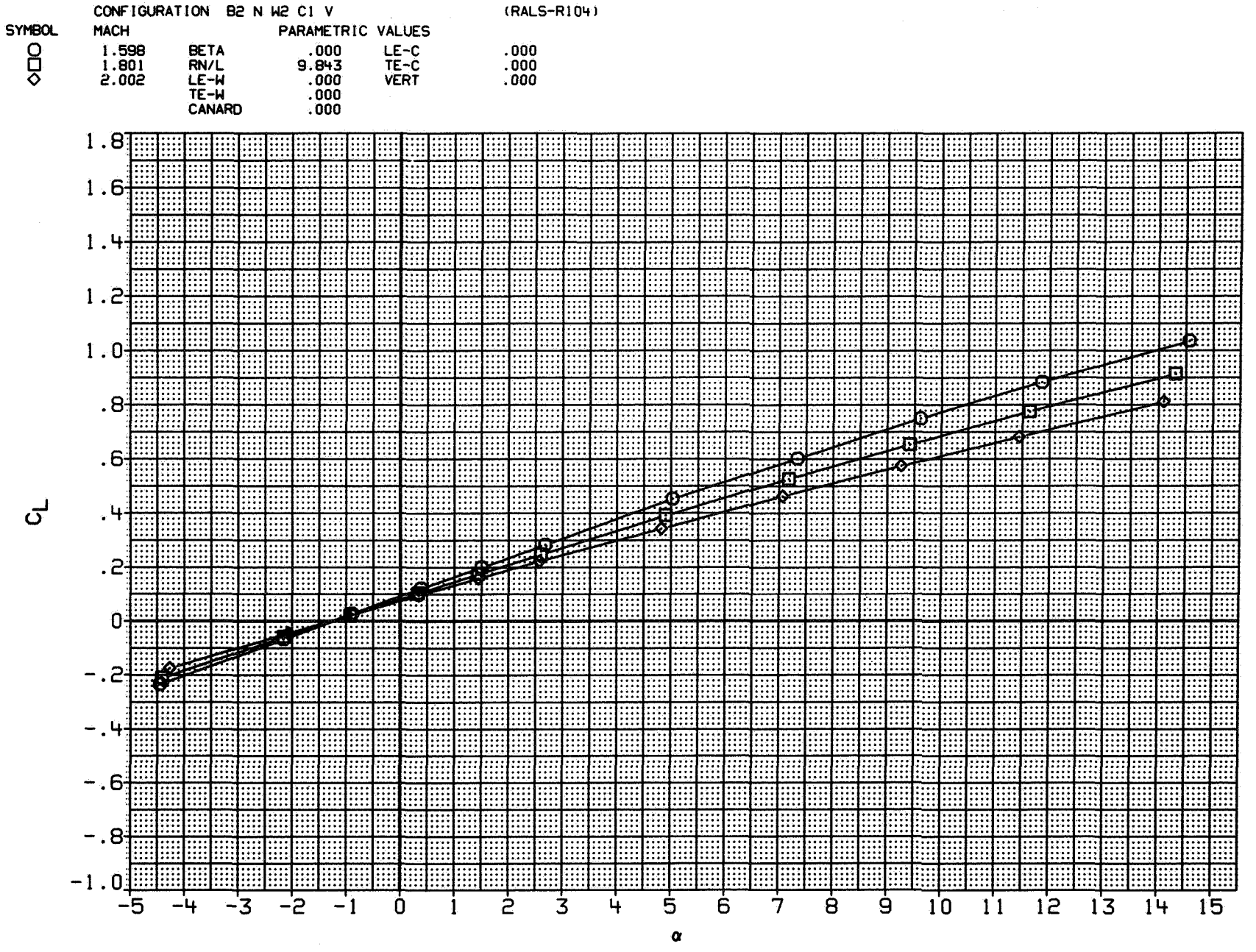


FIG. 45 BASIC LONGITUDINAL CHARACTERISTICS FOR VARIOUS MACH NUMBERS

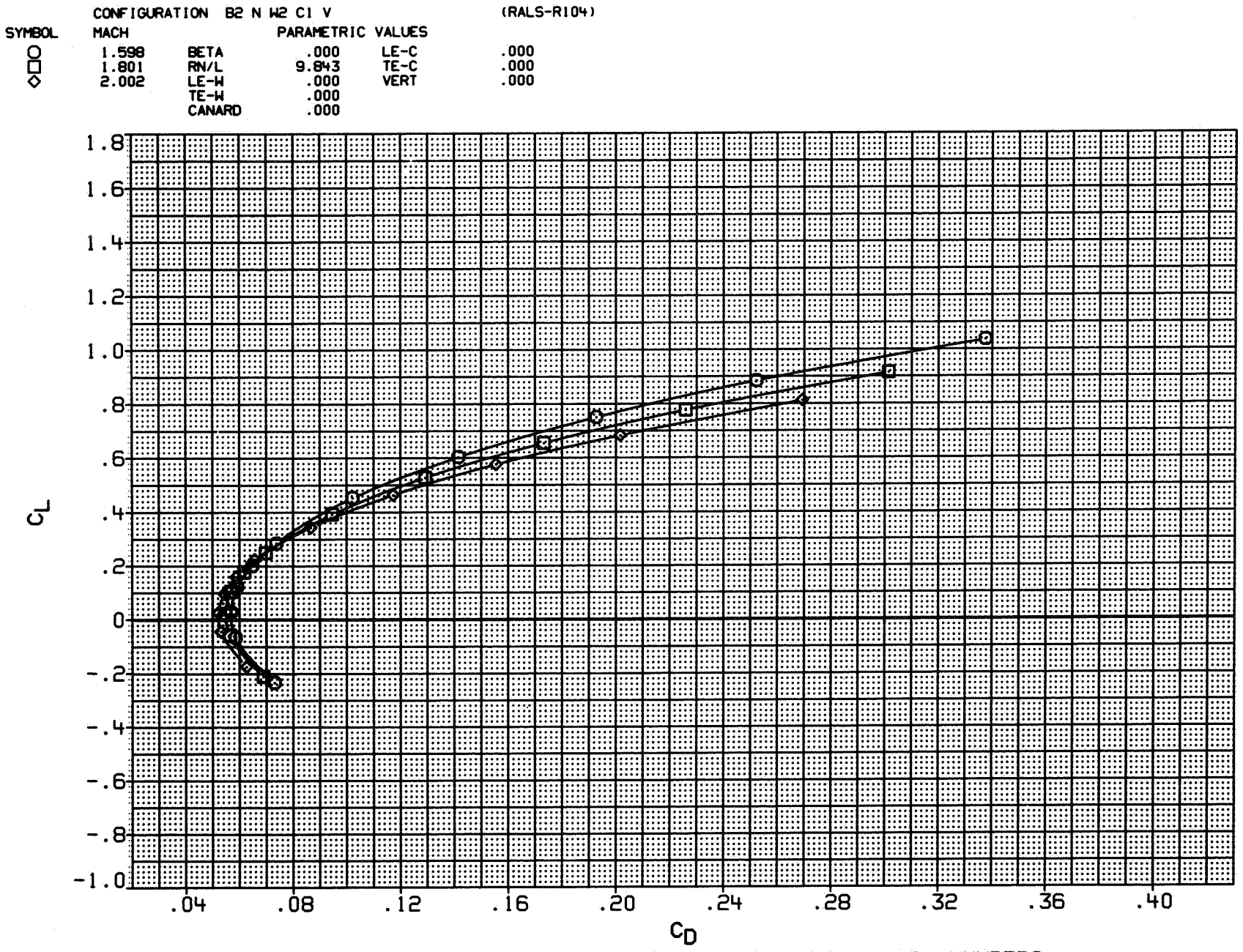


FIG. 45 BASIC LONGITUDINAL CHARACTERISTICS FOR VARIOUS MACH NUMBERS

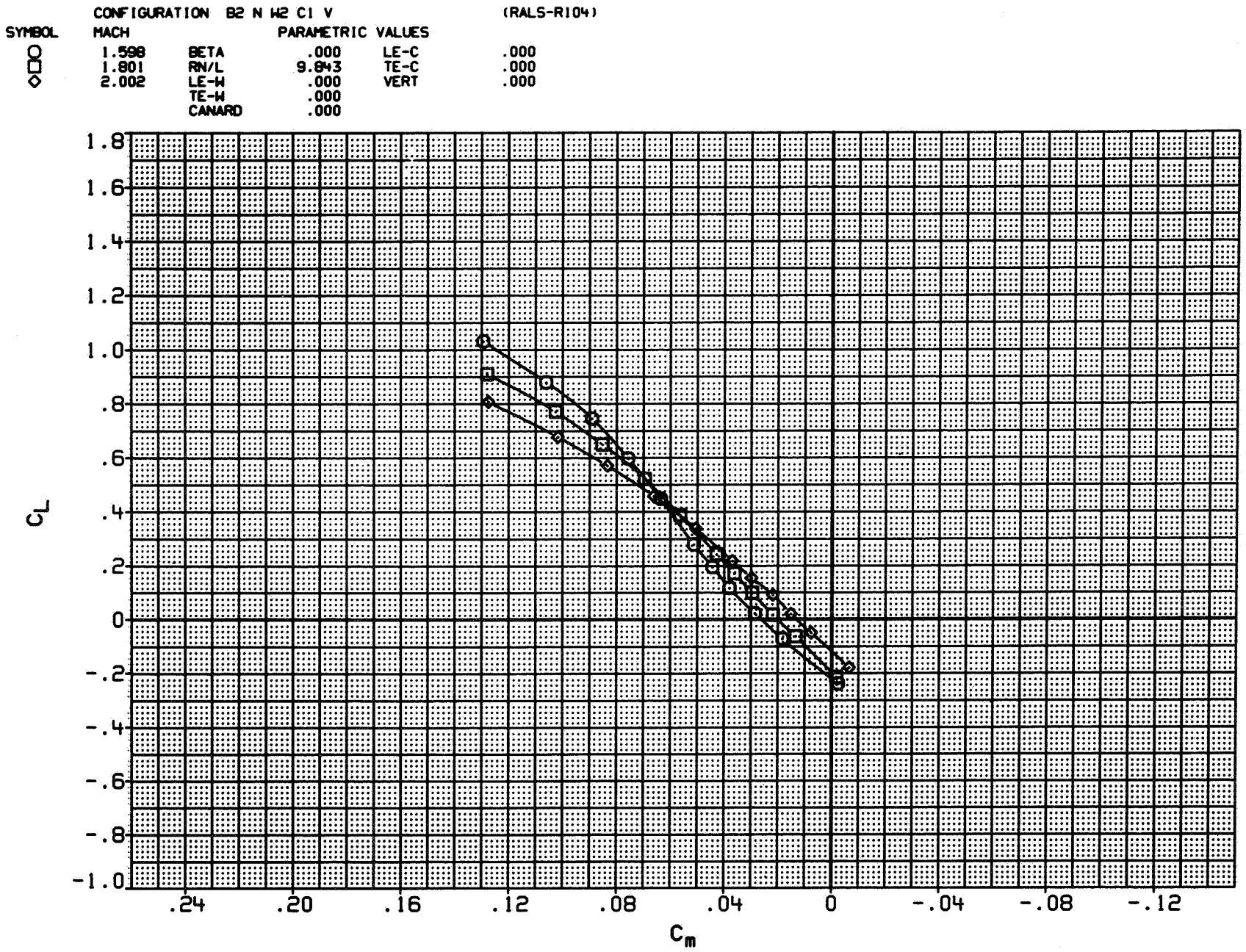


FIG. 45 BASIC LONGITUDINAL CHARACTERISTICS FOR VARIOUS MACH NUMBERS

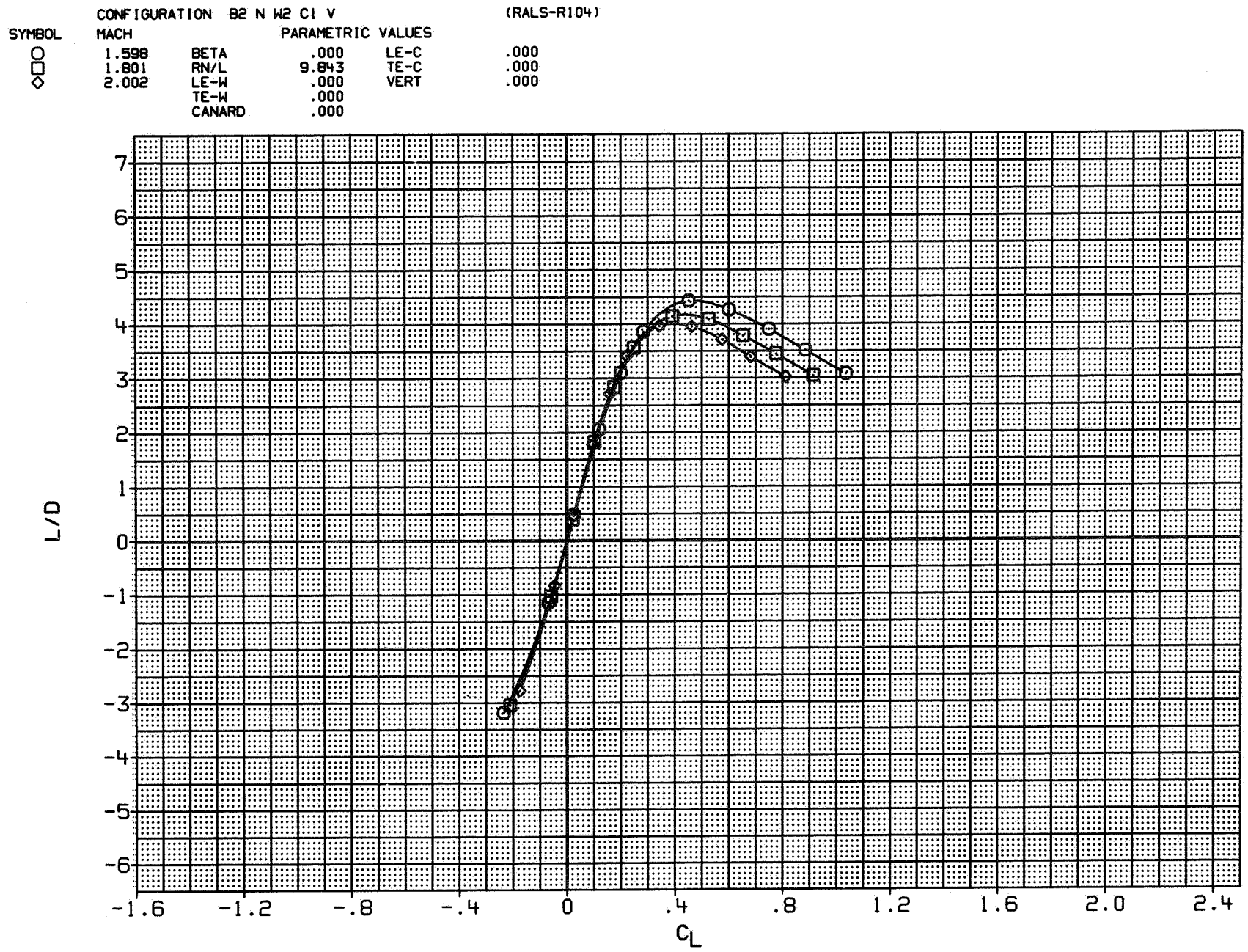


FIG. 45 BASIC LONGITUDINAL CHARACTERISTICS FOR VARIOUS MACH NUMBERS

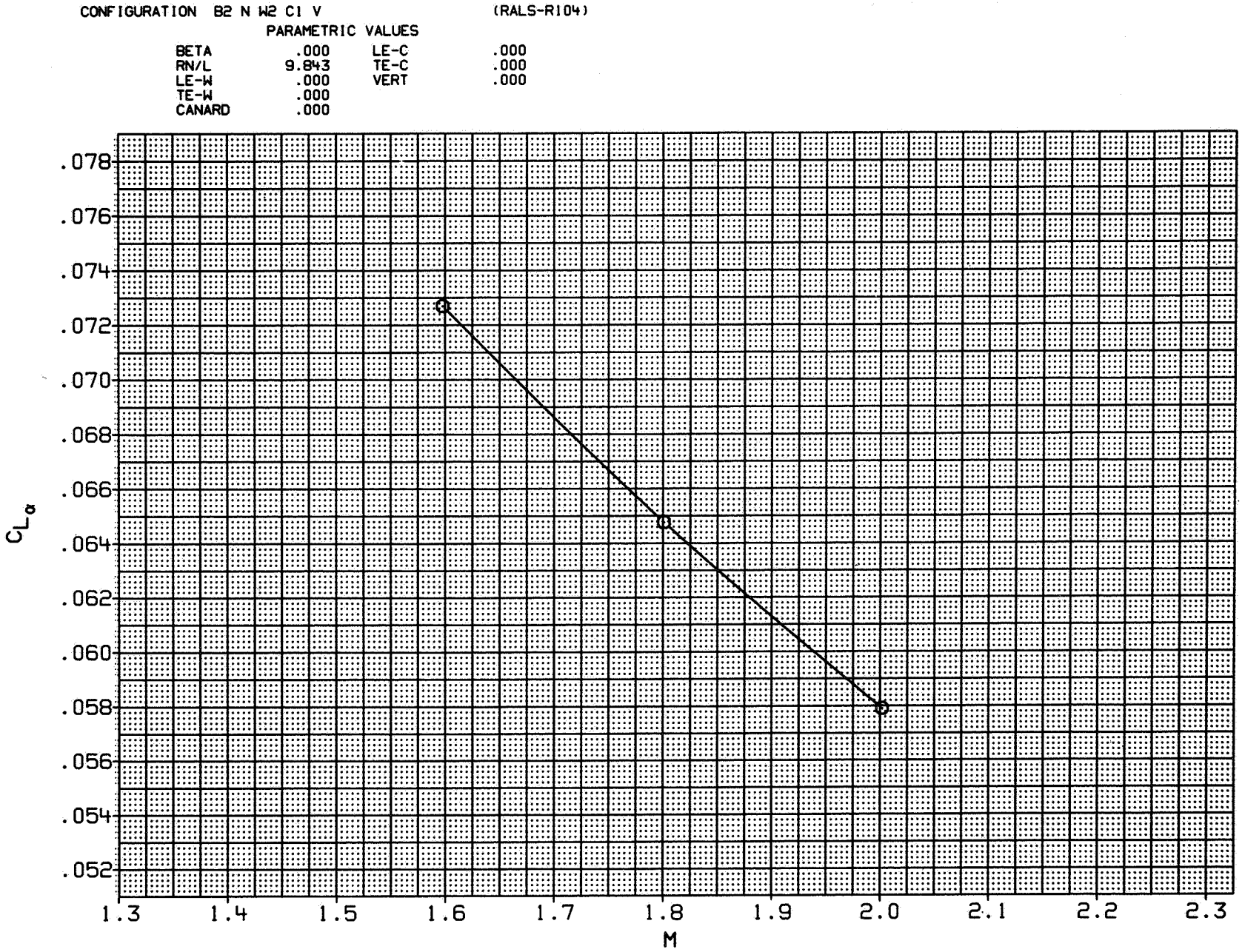


FIG. 46 SUMMARY OF BASIC LONGITUDINAL CHARACTERISTICS WITH MACH NUMBER

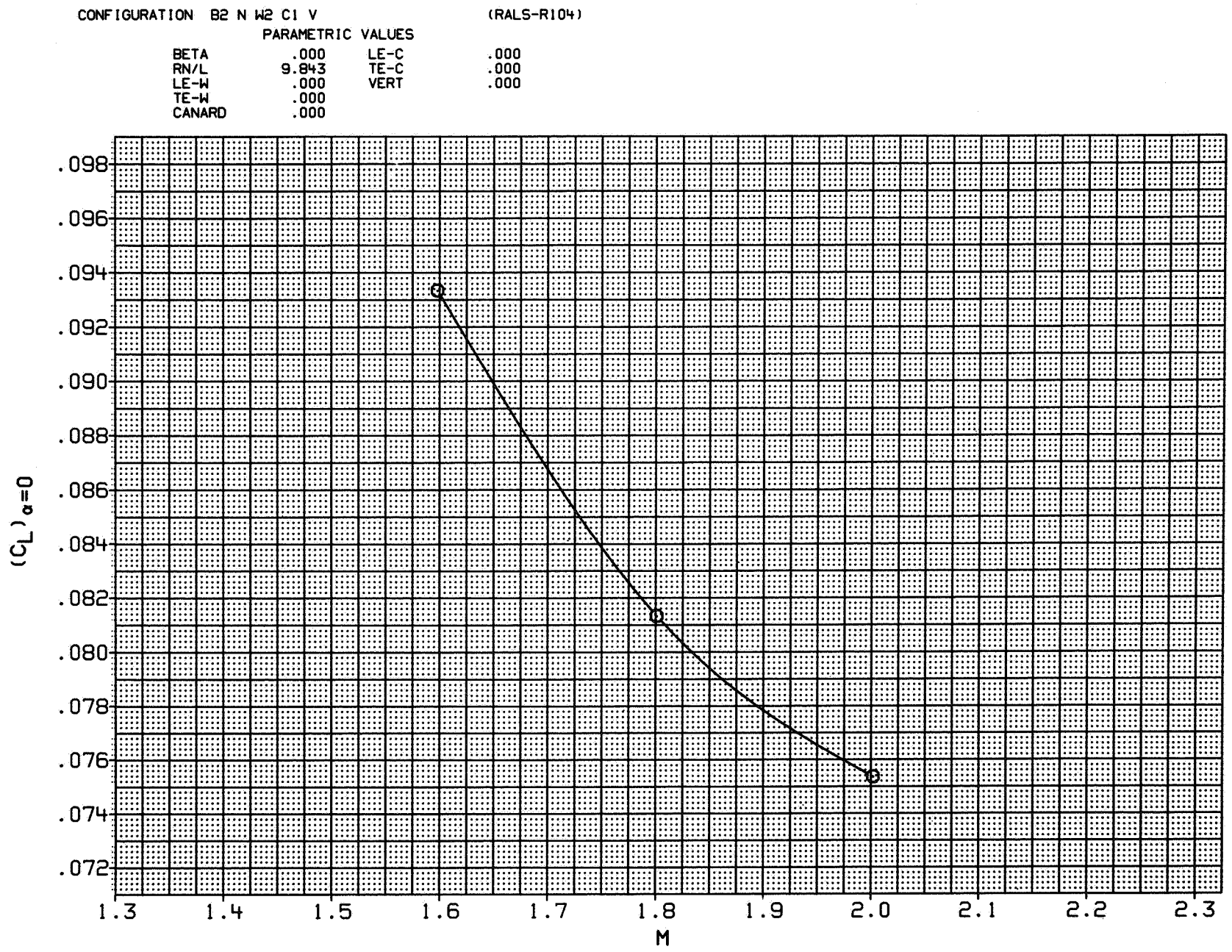


FIG. 46 SUMMARY OF BASIC LONGITUDINAL CHARACTERISTICS WITH MACH NUMBER

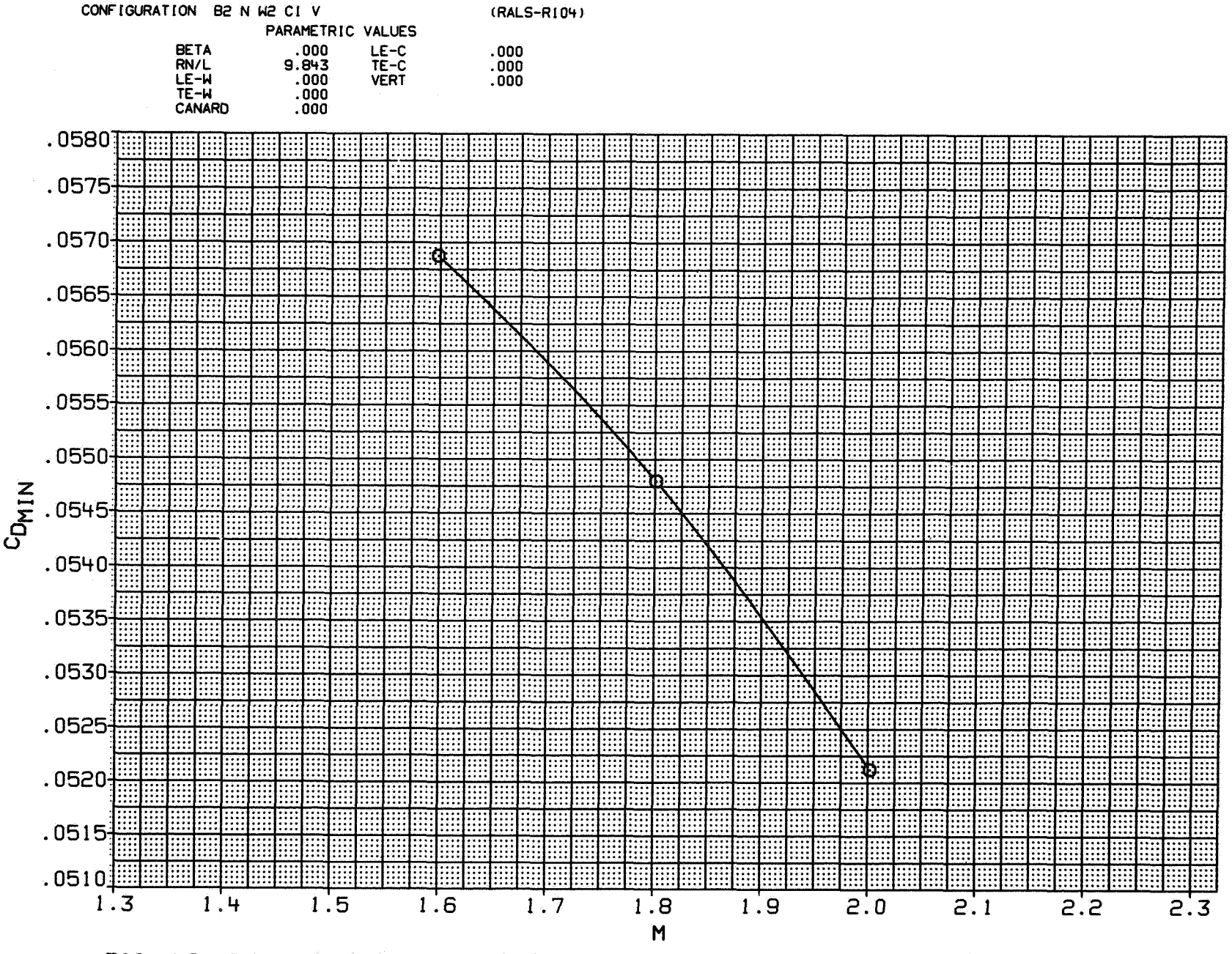


FIG. 46 SUMMARY OF BASIC LONGITUDINAL CHARACTERISTICS WITH MACH NUMBER

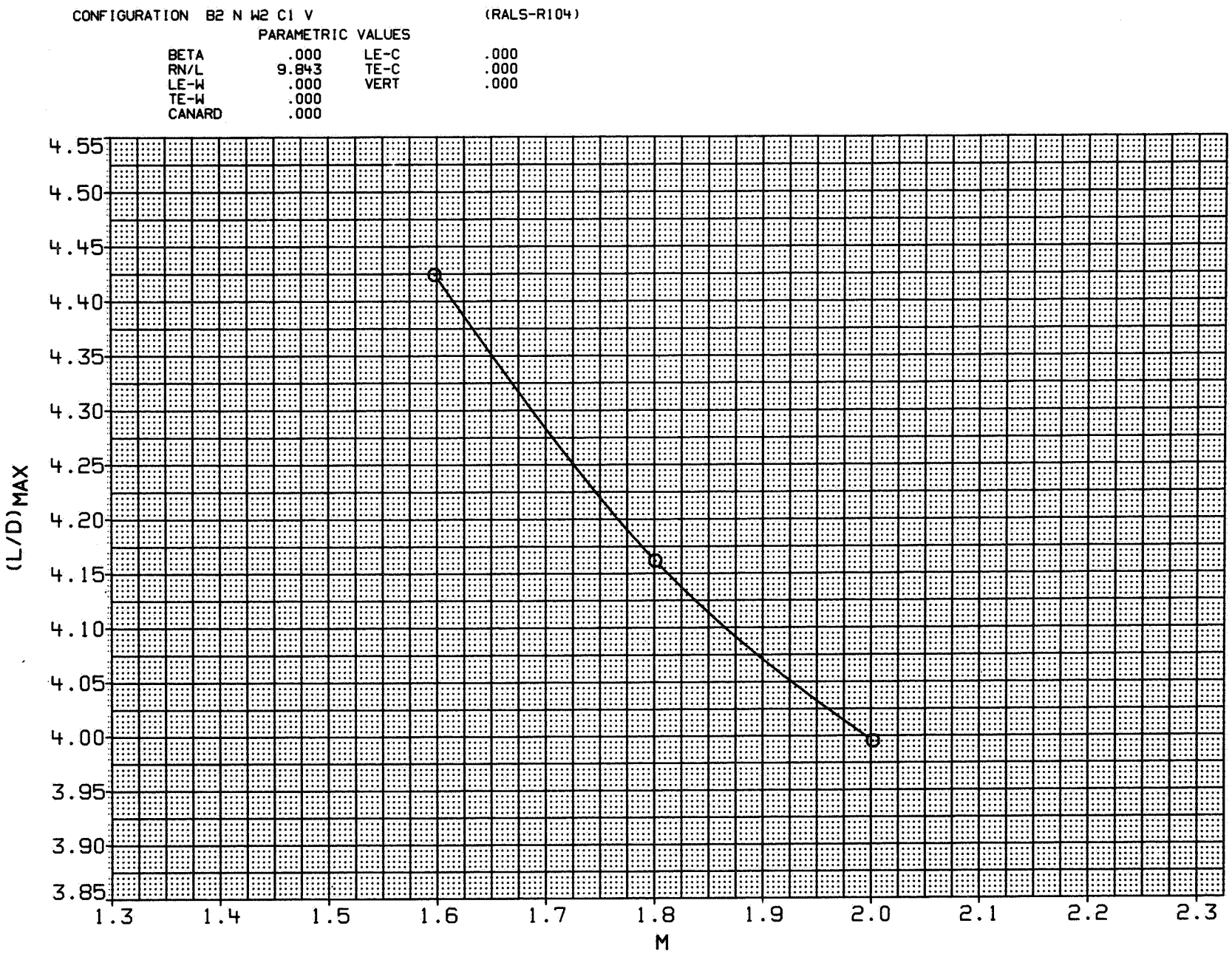


FIG. 46 SUMMARY OF BASIC LONGITUDINAL CHARACTERISTICS WITH MACH NUMBER

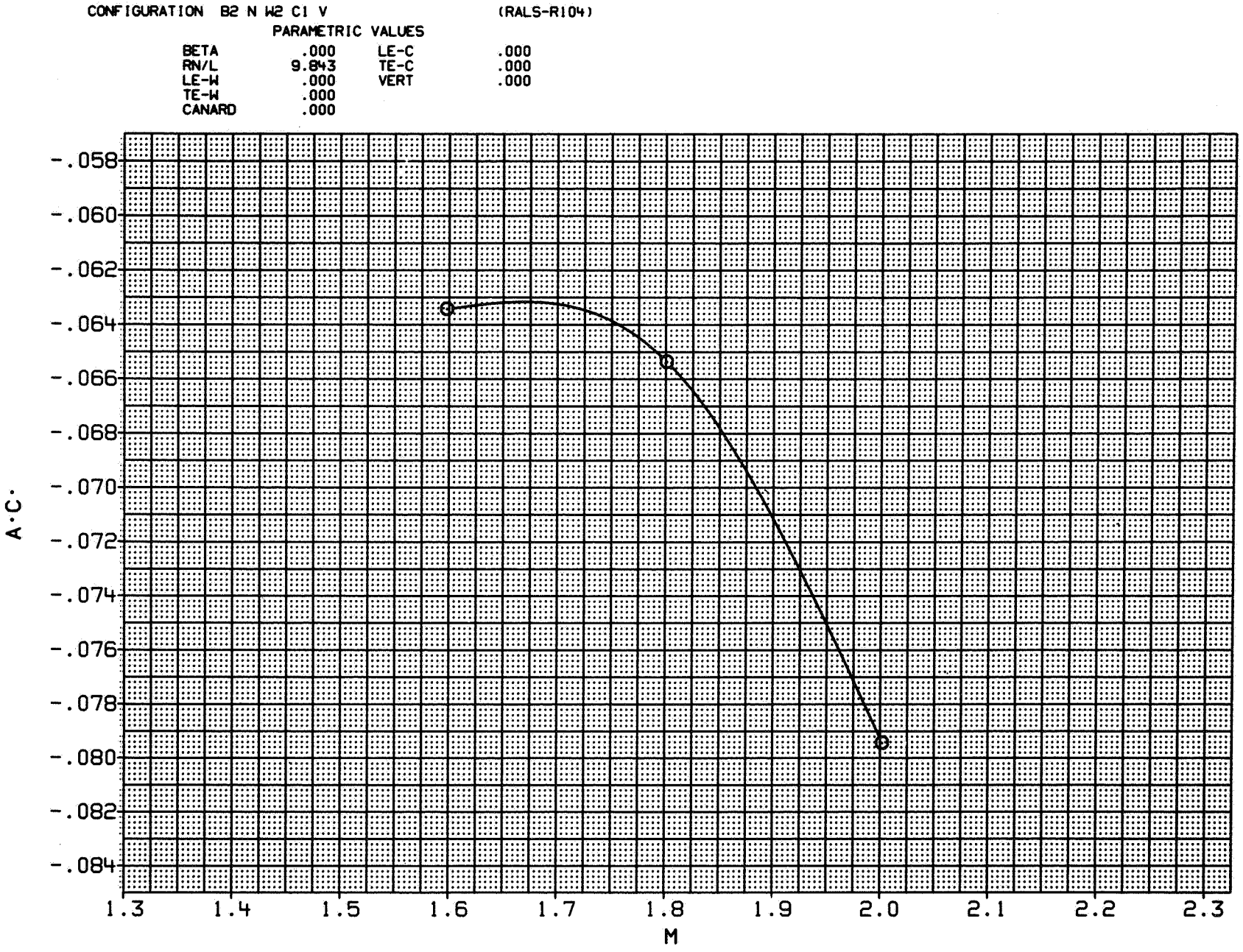


FIG. 46 SUMMARY OF BASIC LONGITUDINAL CHARACTERISTICS WITH MACH NUMBER

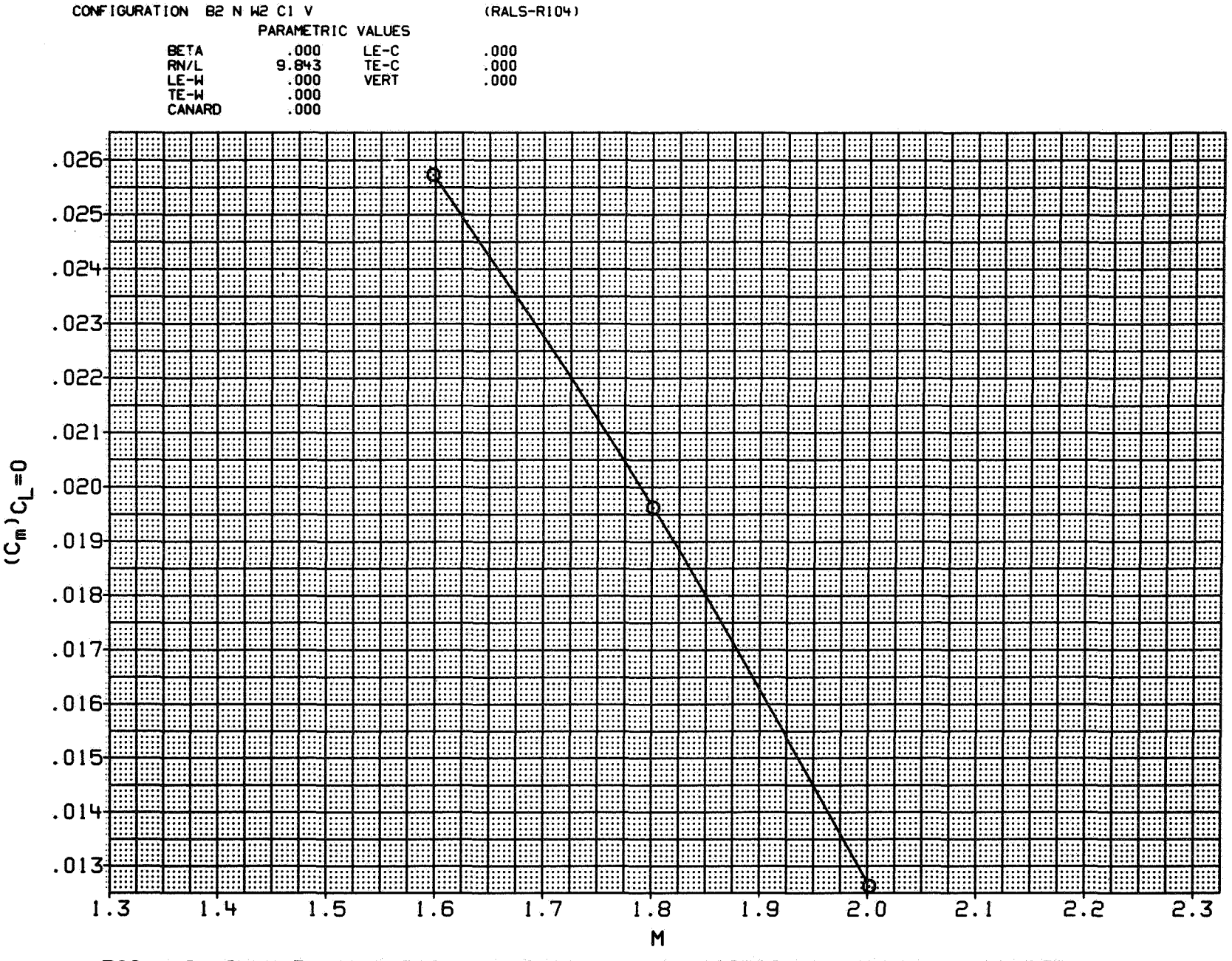


FIG. 46 SUMMARY OF BASIC LONGITUDINAL CHARACTERISTICS WITH MACH NUMBER

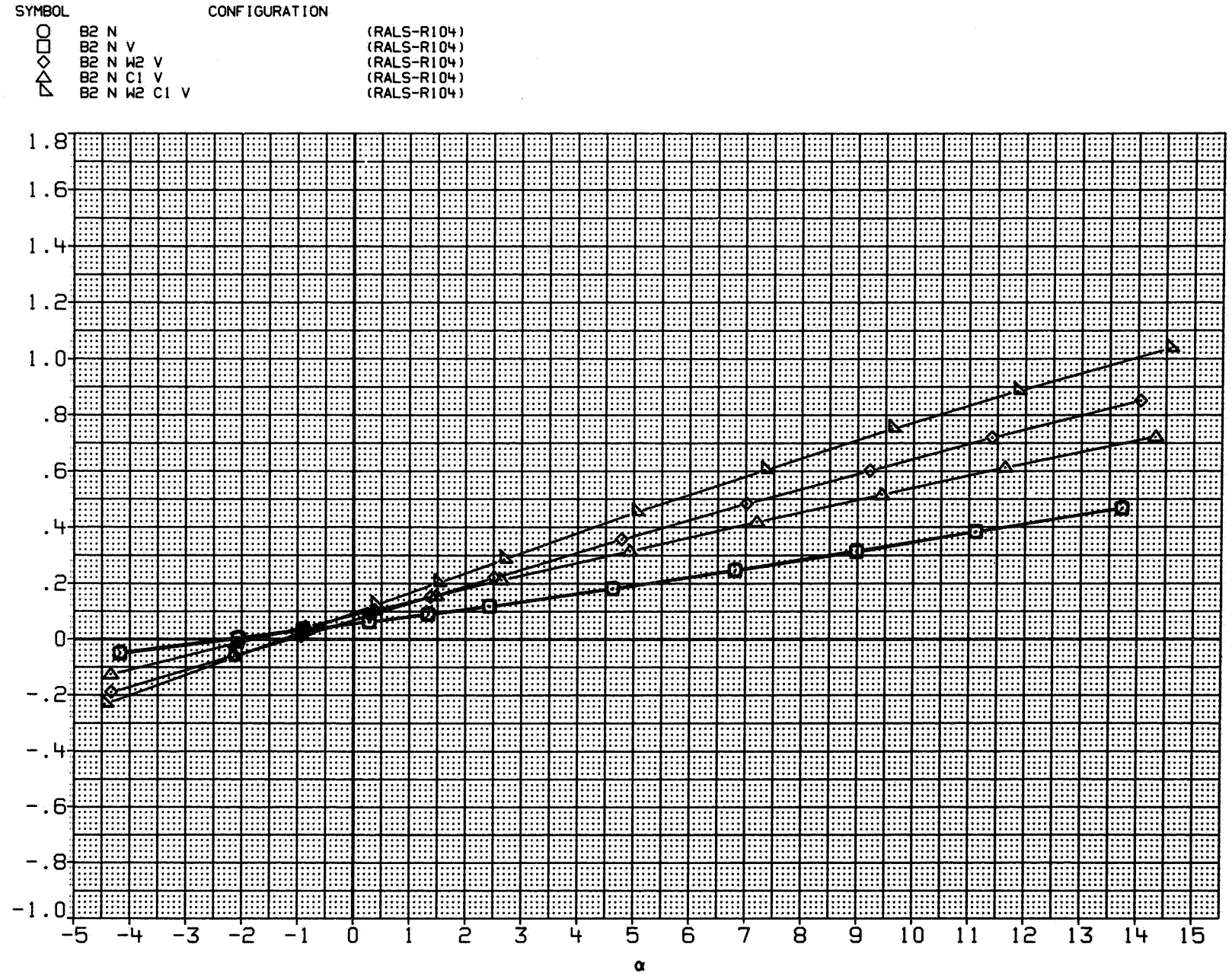


FIG. 47 COMPONENT BUILDUP, LONGITUDINAL CHARACTERISTICS

MACH = 1.60

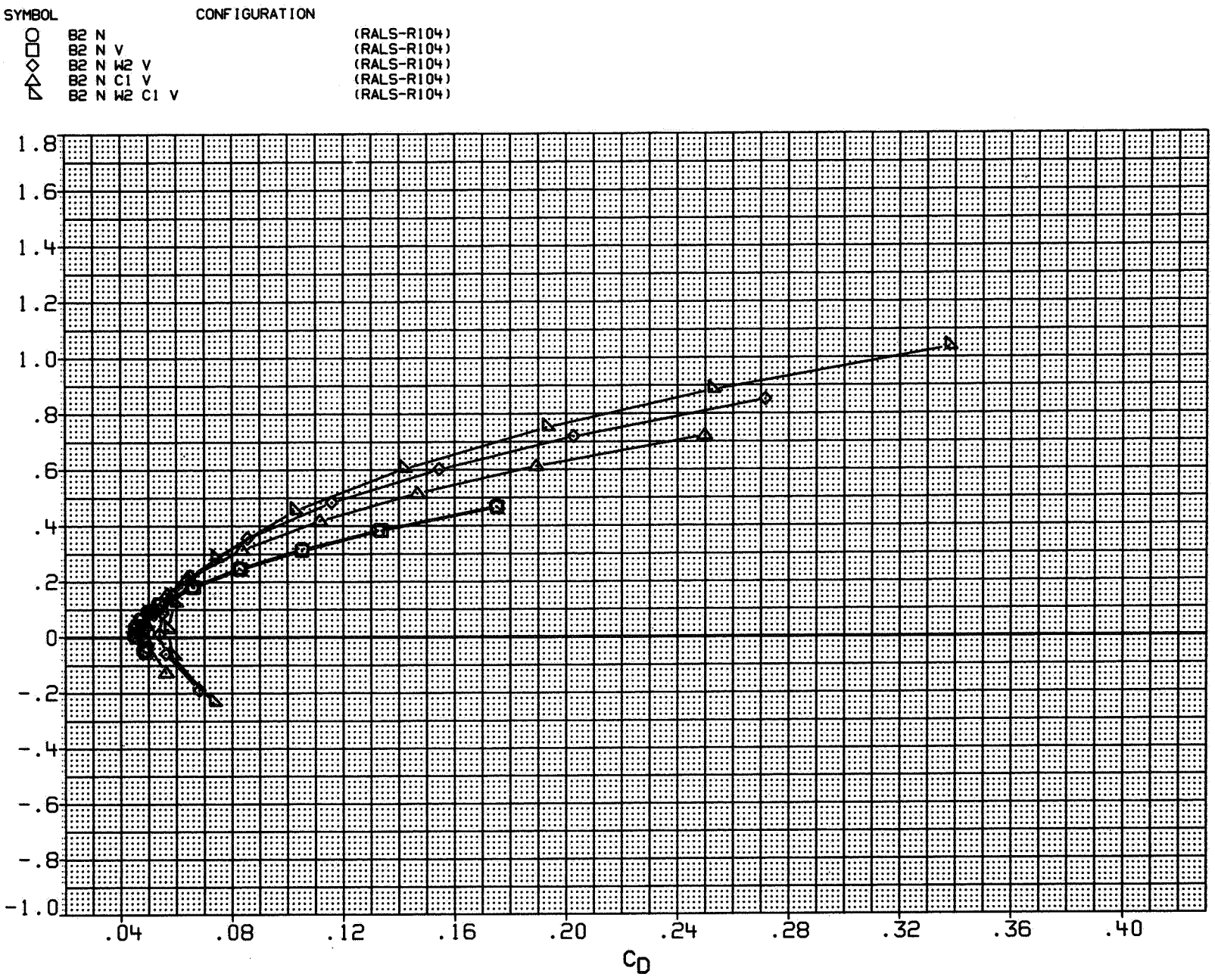


FIG. 47 COMPONENT BUILDUP, LONGITUDINAL CHARACTERISTICS

MACH = 1.60

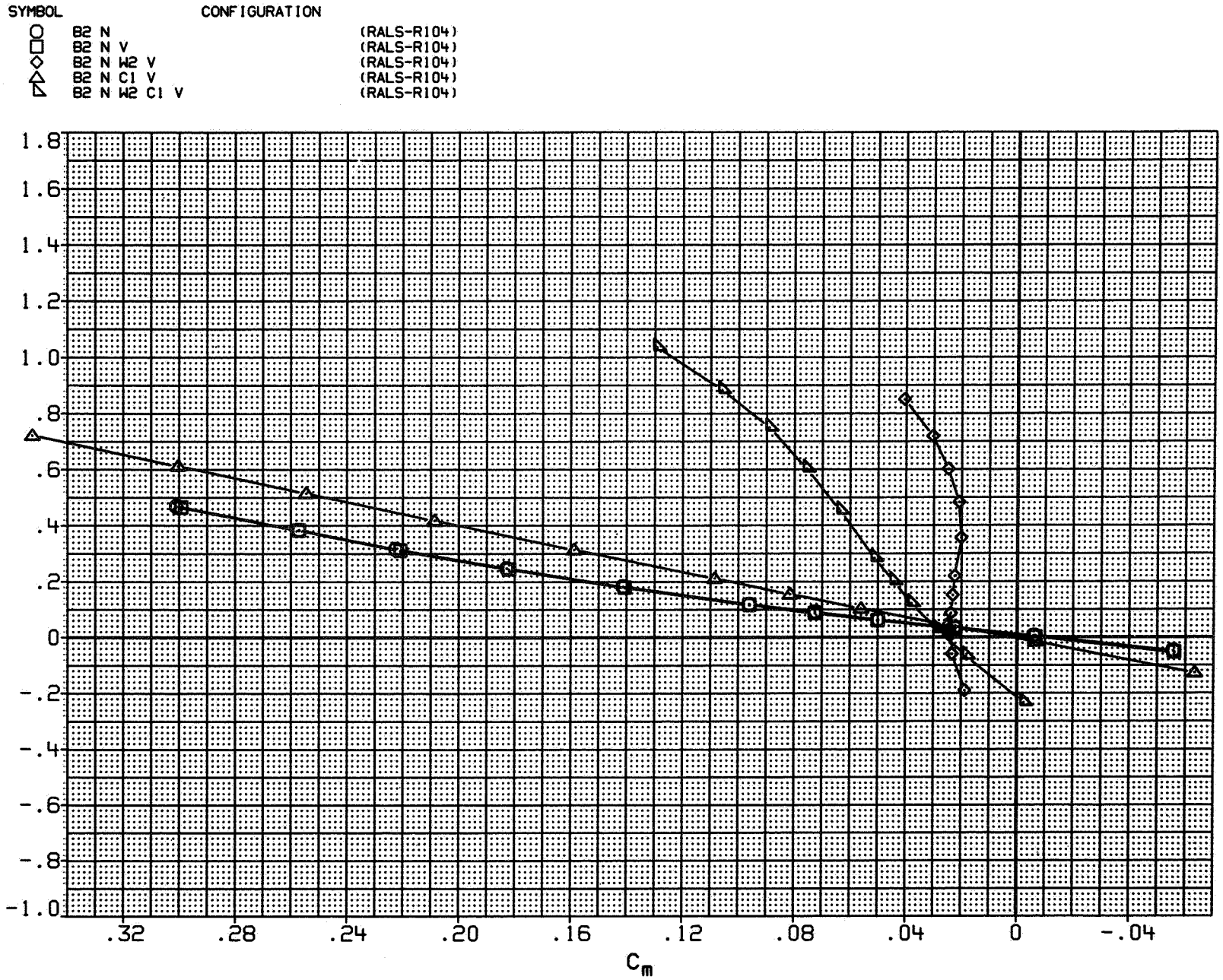


FIG. 47 COMPONENT BUILDUP, LONGITUDINAL CHARACTERISTICS

MACH = 1.60

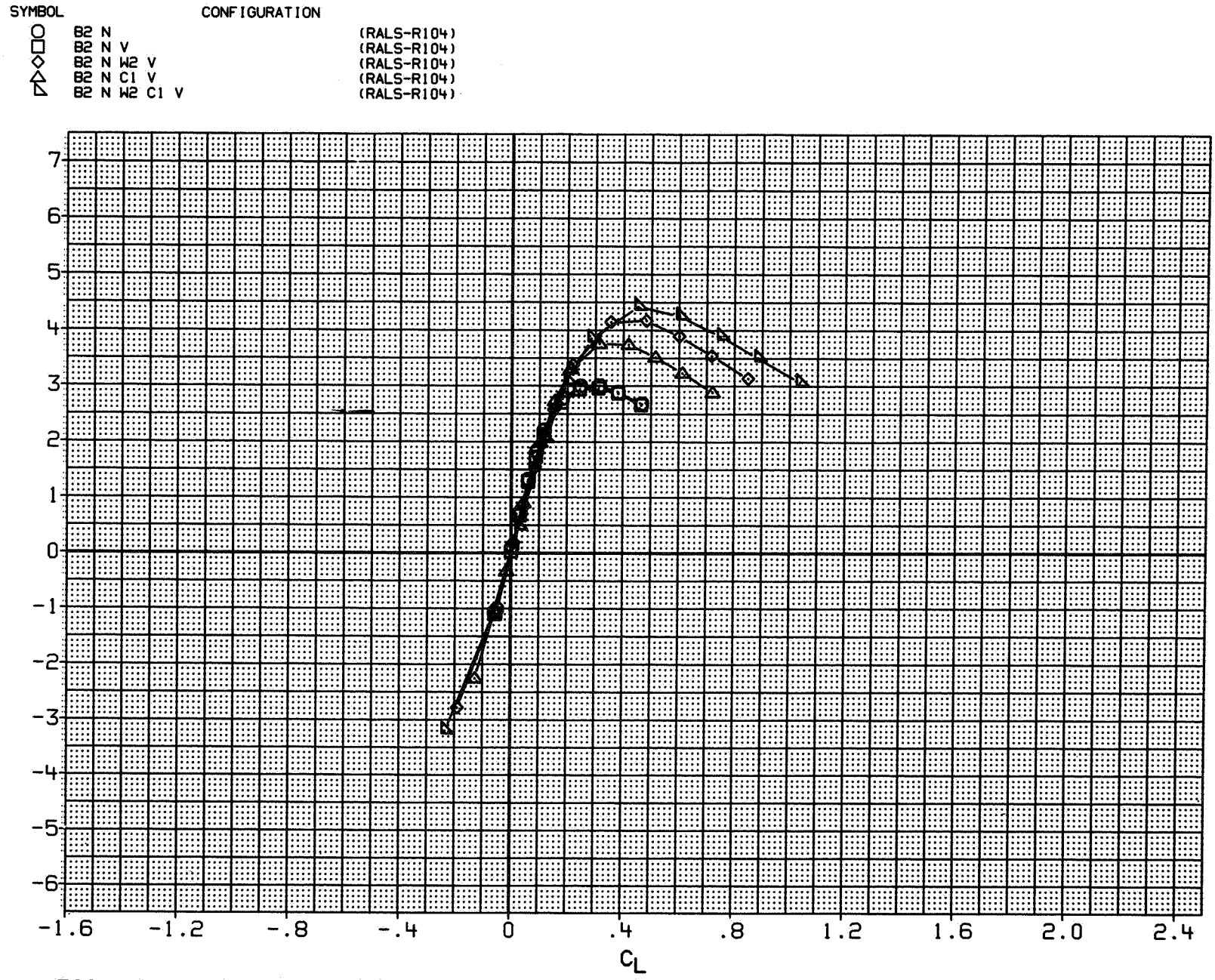


FIG. 47 COMPONENT BUILDUP, LONGITUDINAL CHARACTERISTICS

MACH = 1.60

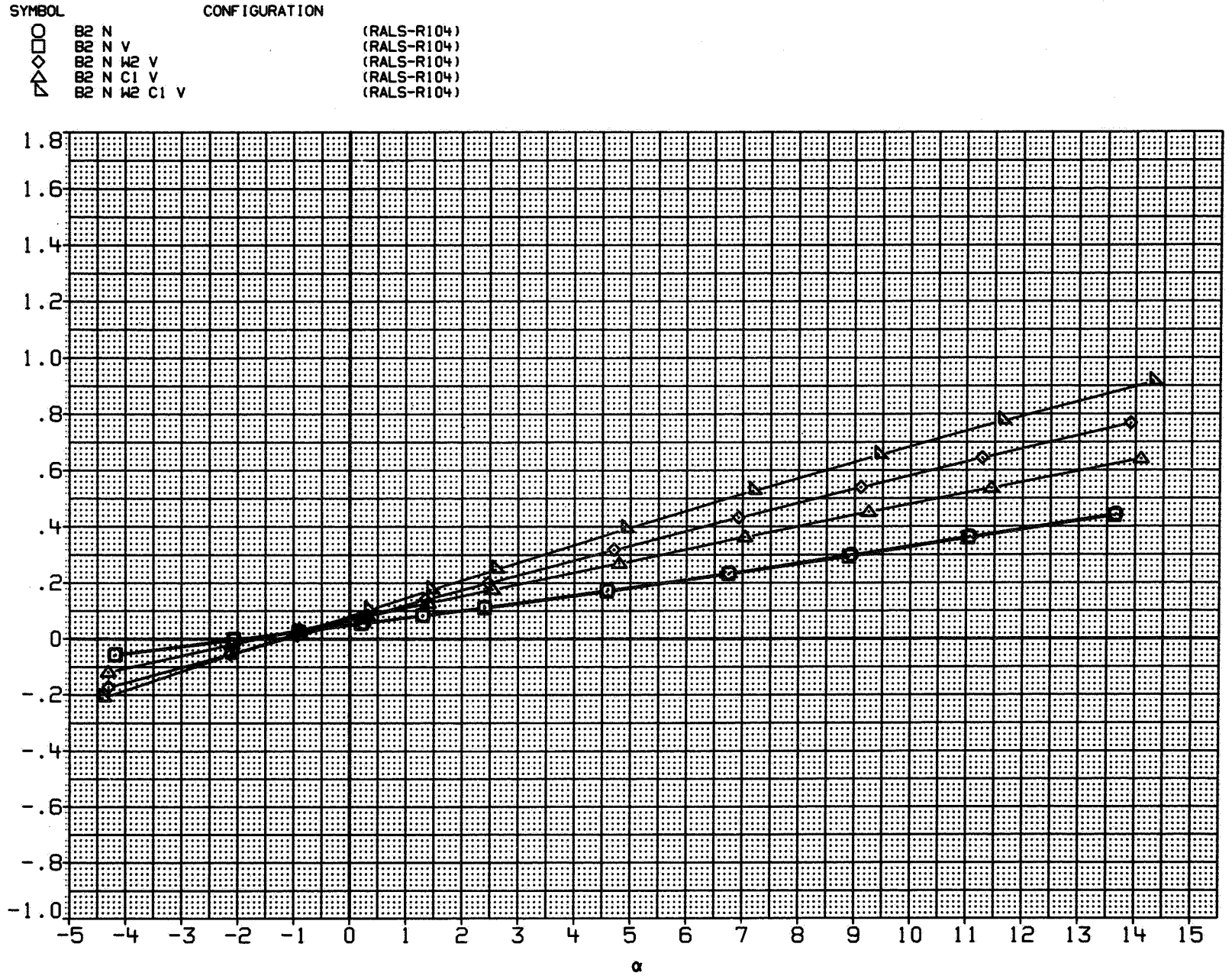


FIG. 48 COMPONENT BUILDUP, LONGITUDINAL CHARACTERISTICS

MACH = 1.80

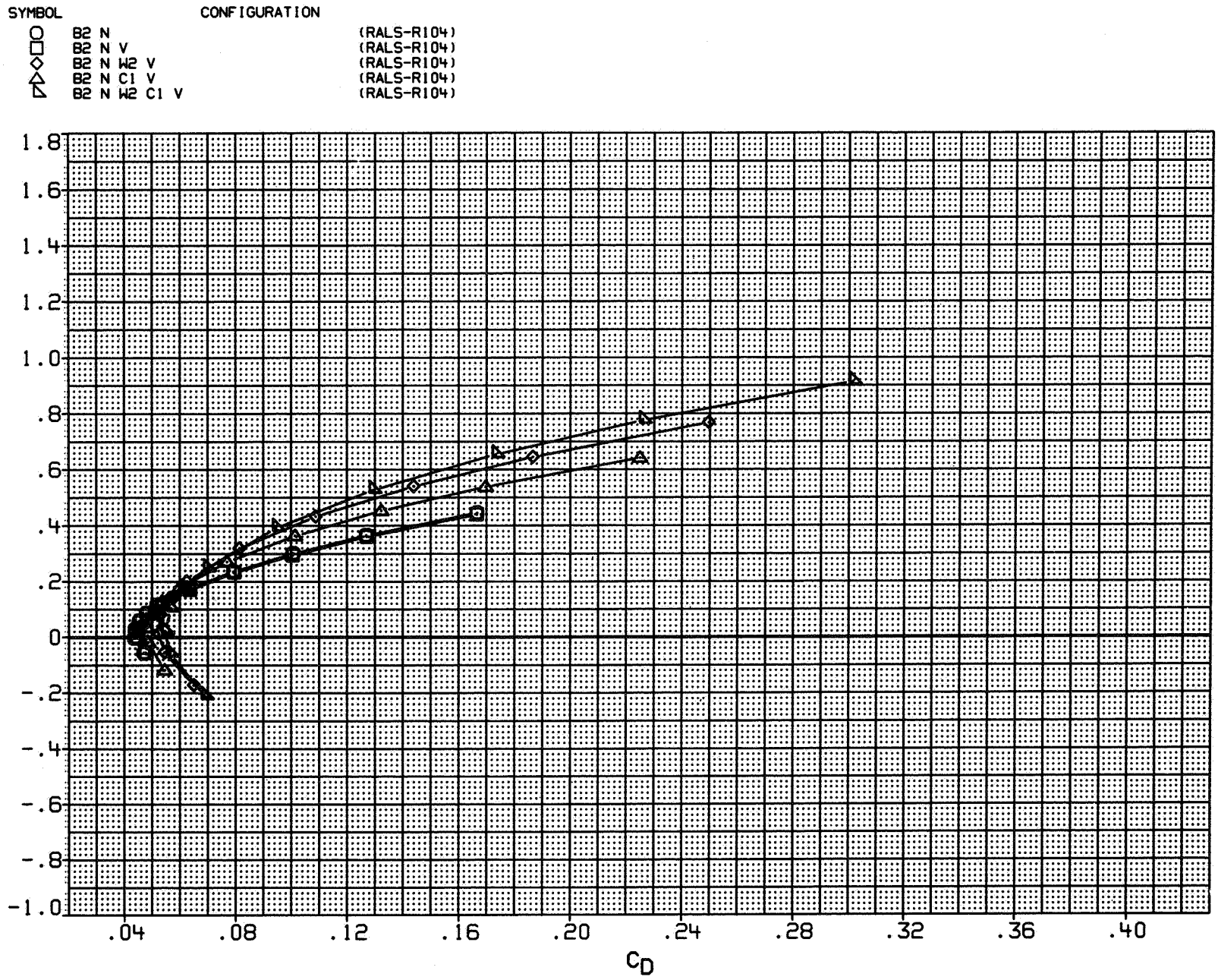


FIG. 48 COMPONENT BUILDUP, LONGITUDINAL CHARACTERISTICS

MACH = 1.80

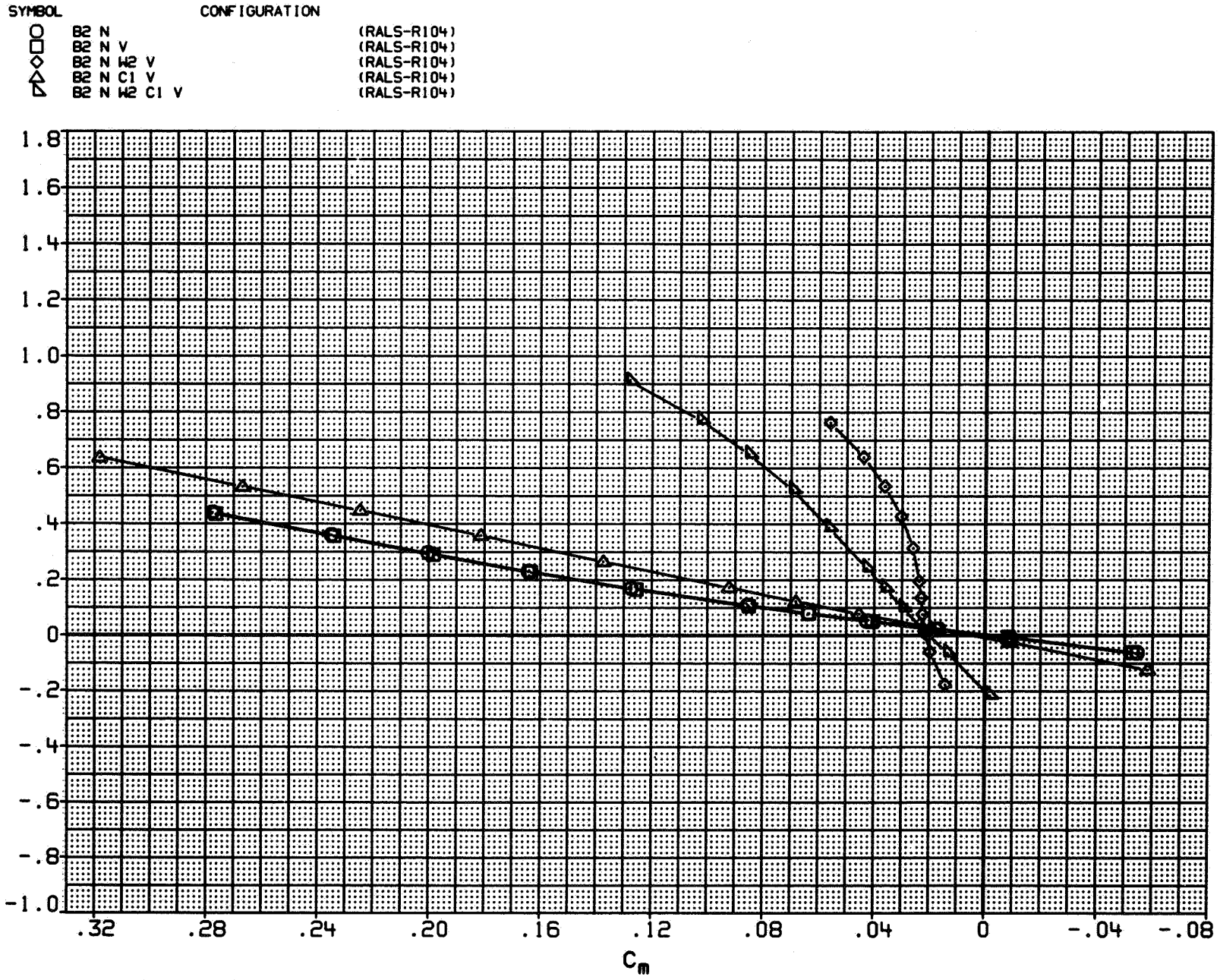


FIG. 48 COMPONENT BUILDUP, LONGITUDINAL CHARACTERISTICS

MACH = 1.80

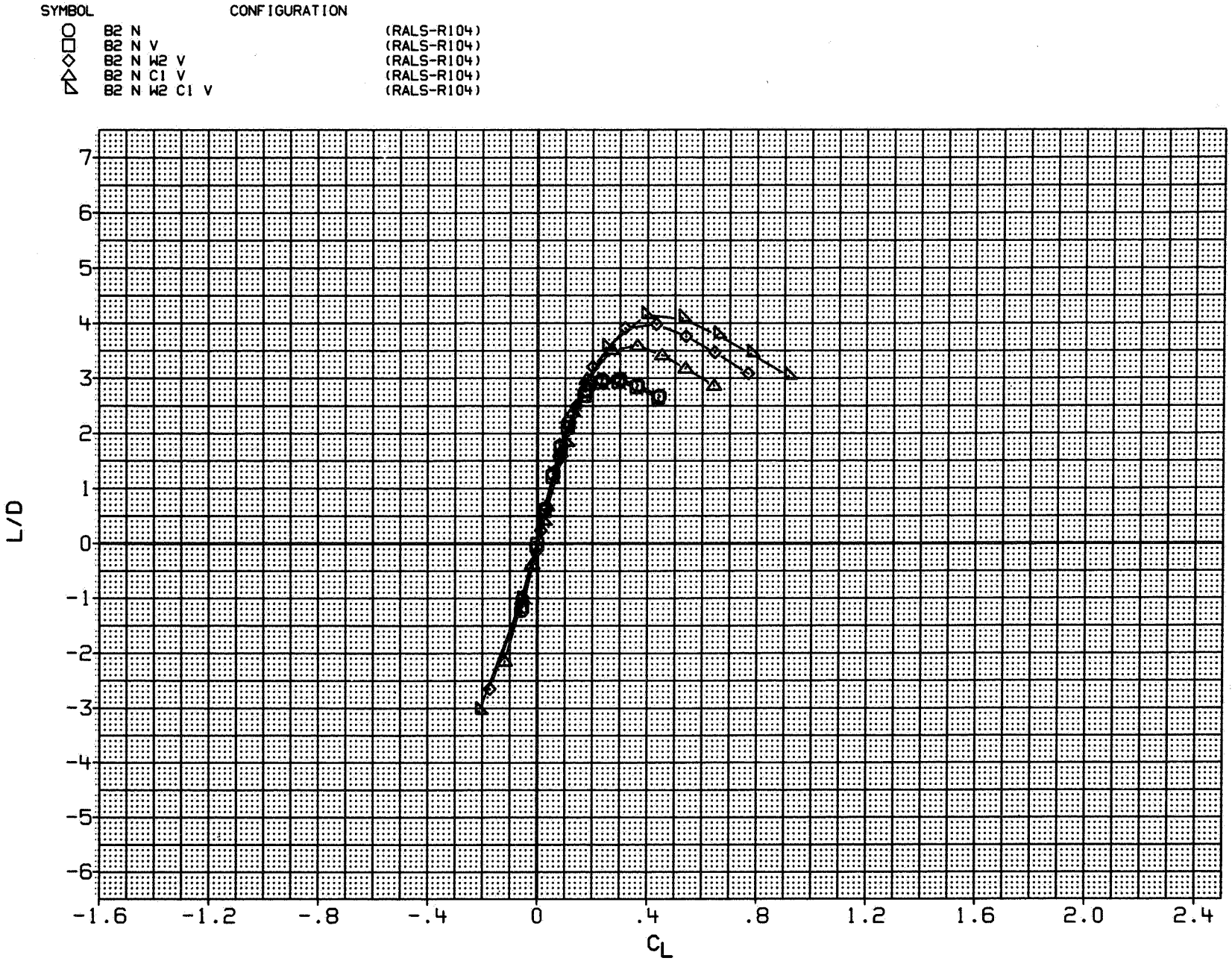


FIG. 48 COMPONENT BUILDUP, LONGITUDINAL CHARACTERISTICS

MACH = 1.80

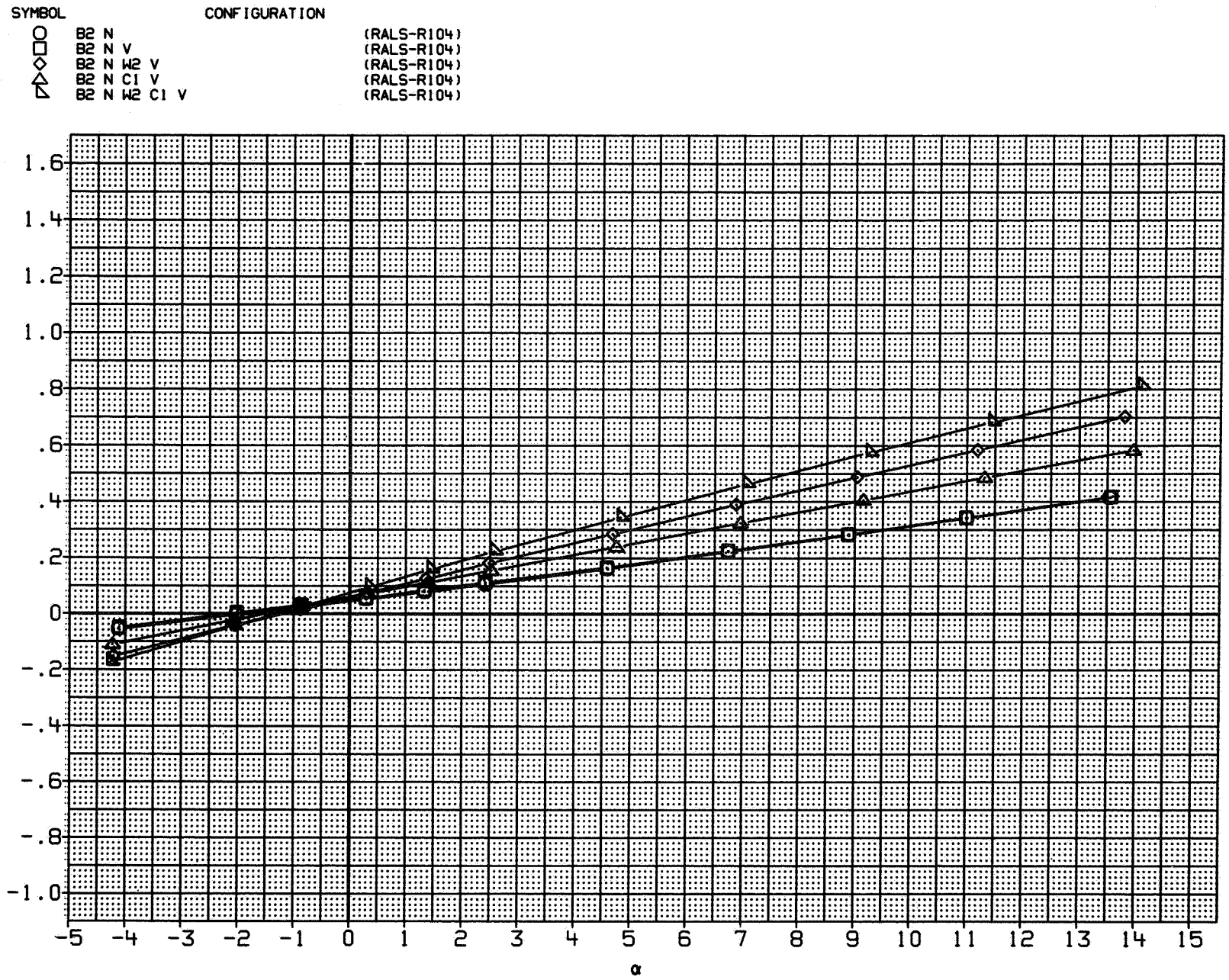


FIG. 49 COMPONENT BUILDUP, LONGITUDINAL CHARACTERISTICS

MACH = 2.00

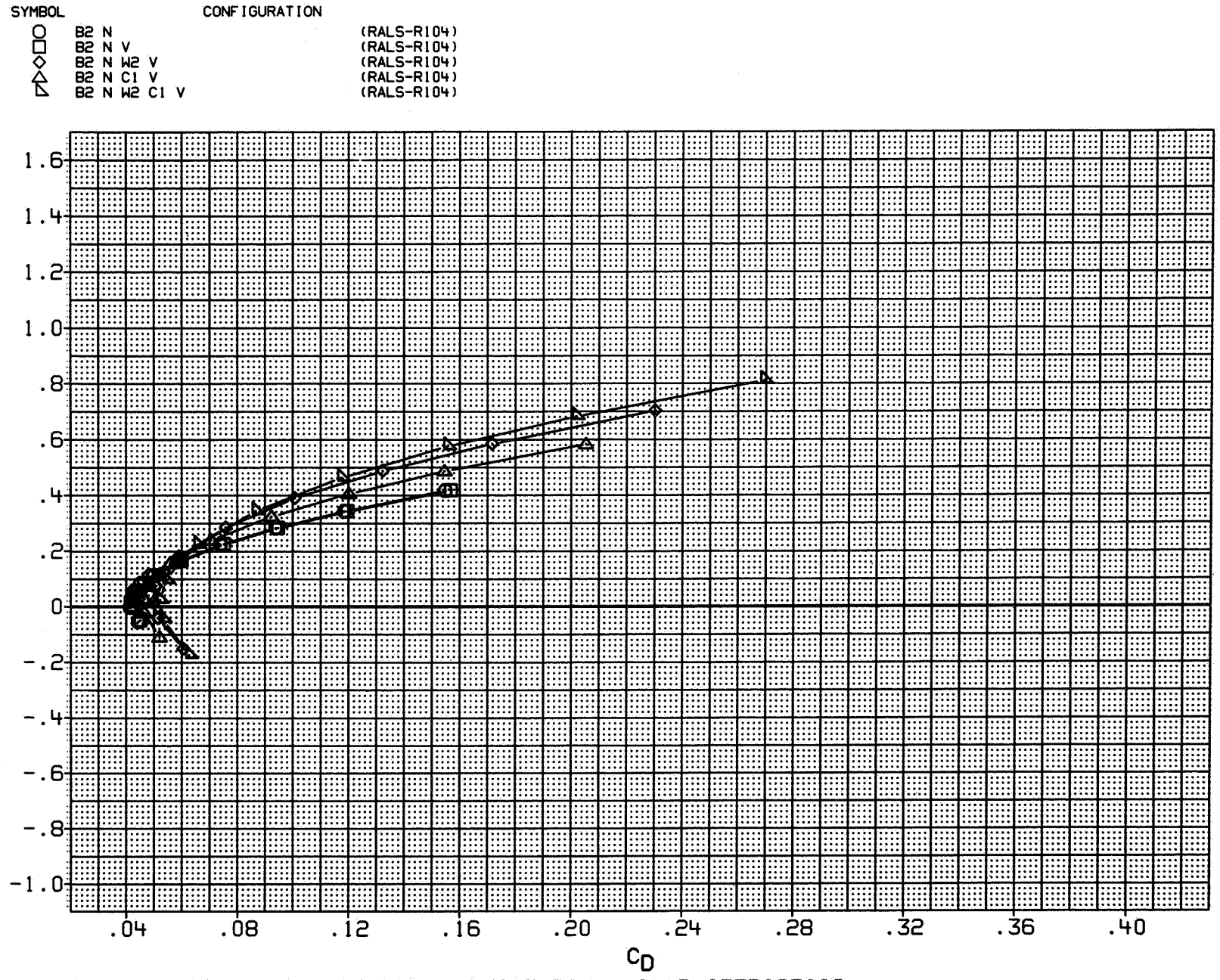


FIG. 49 COMPONENT BUILDUP, LONGITUDINAL CHARACTERISTICS

MACH = 2.00

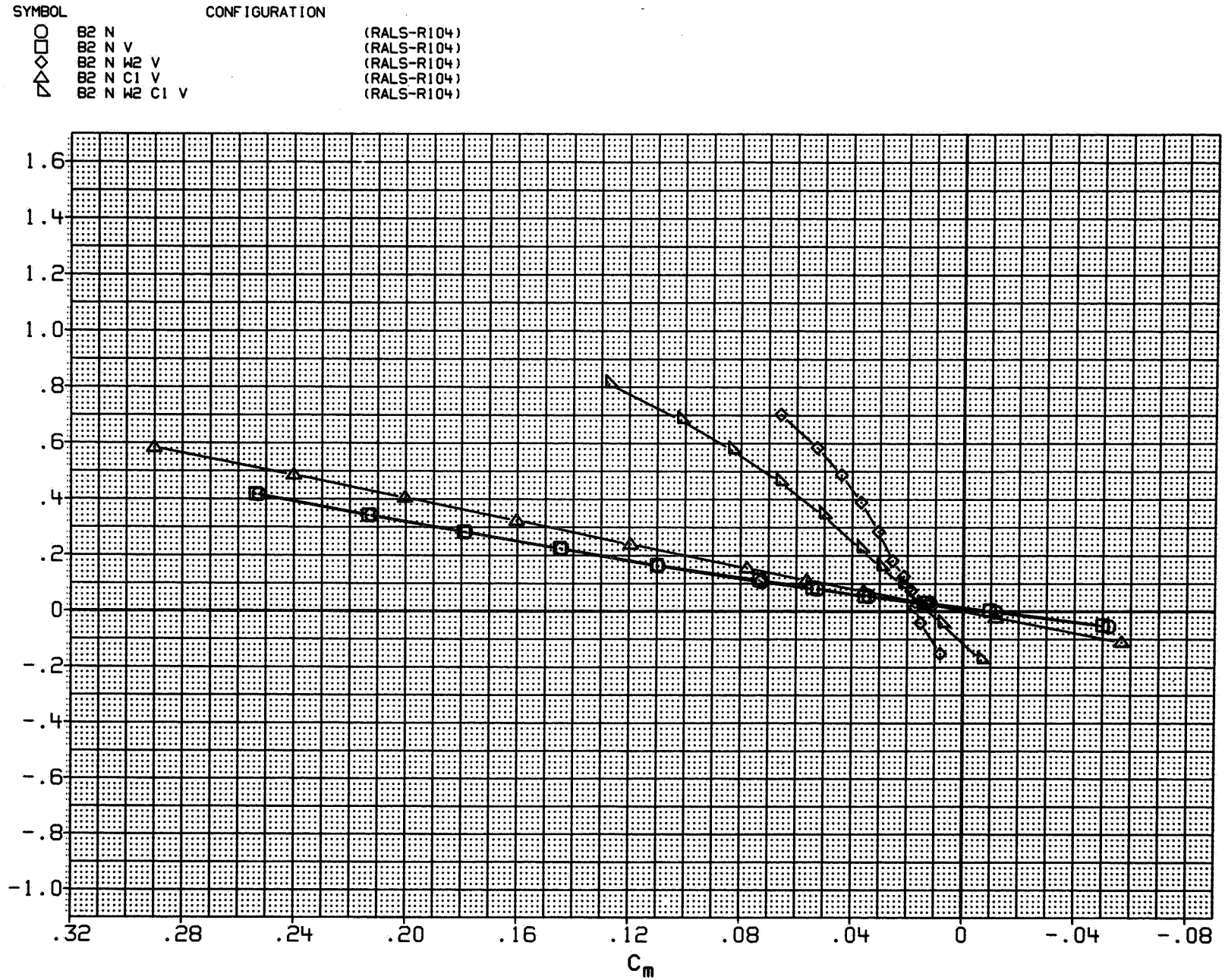


FIG. 49 COMPONENT BUILDUP, LONGITUDINAL CHARACTERISTICS

MACH = 2.00

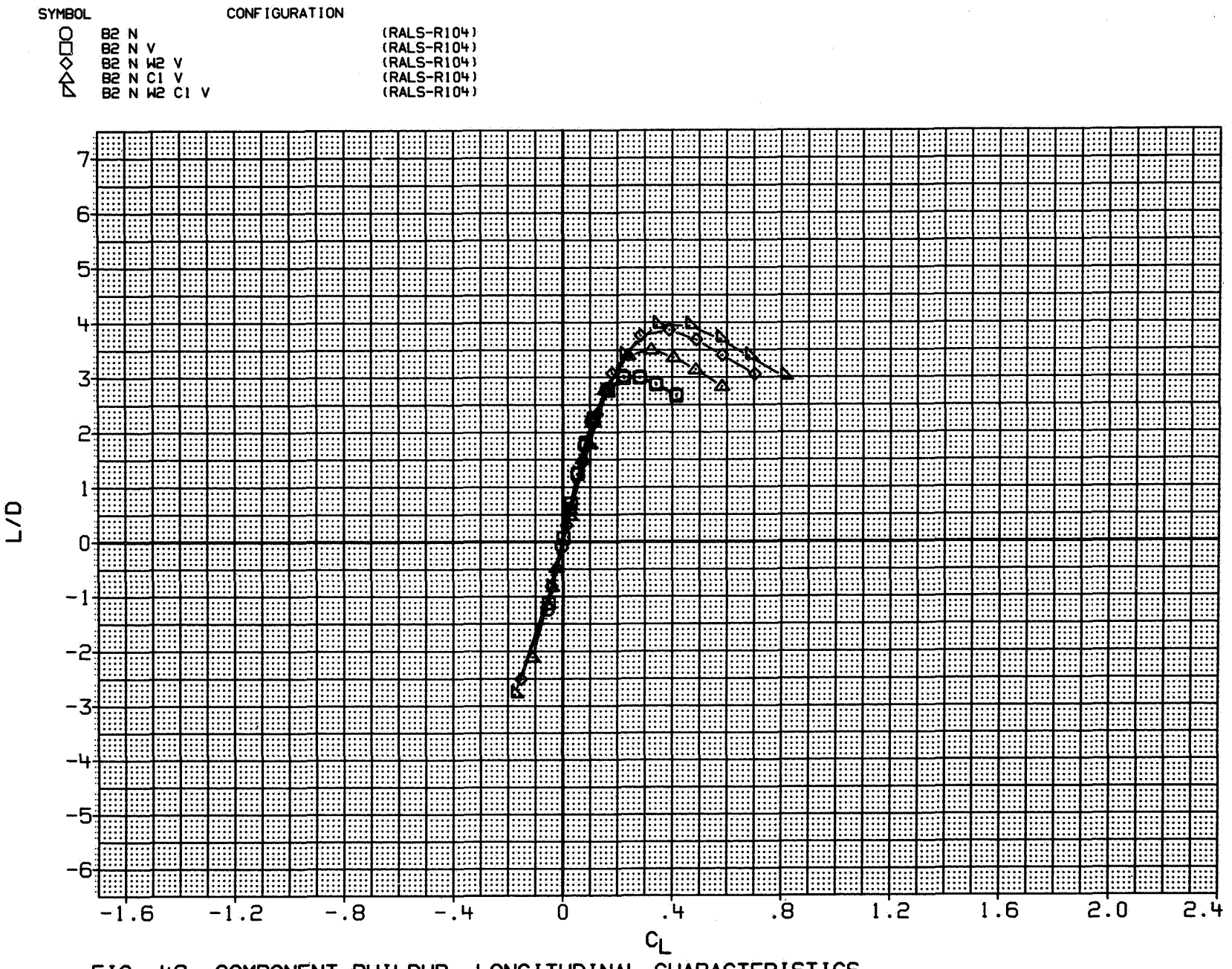


FIG. 49 COMPONENT BUILDUP, LONGITUDINAL CHARACTERISTICS

MACH = 2.00

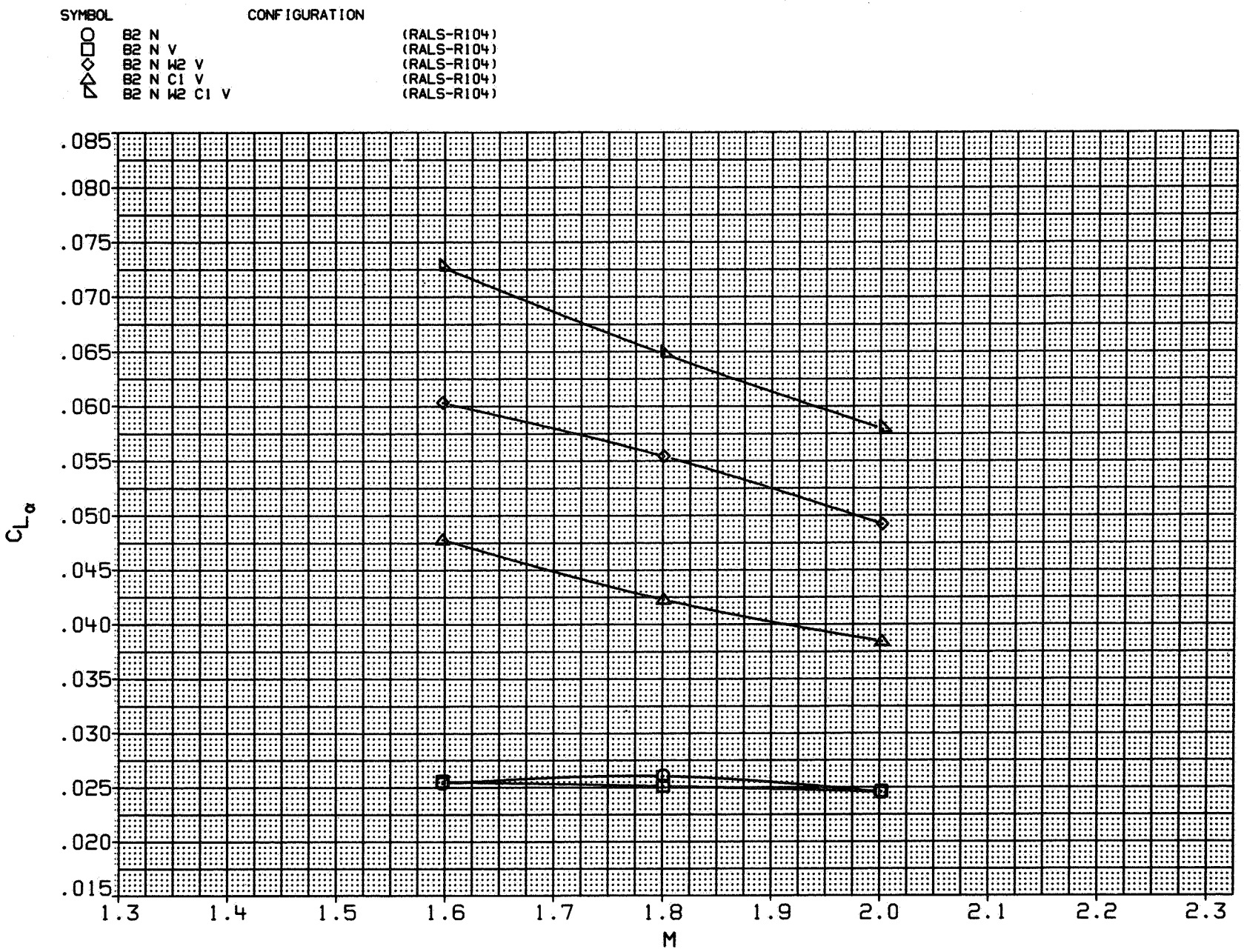


FIG. 50 SUMMARY OF COMPONENT BUILDUP WITH MACH NUMBER

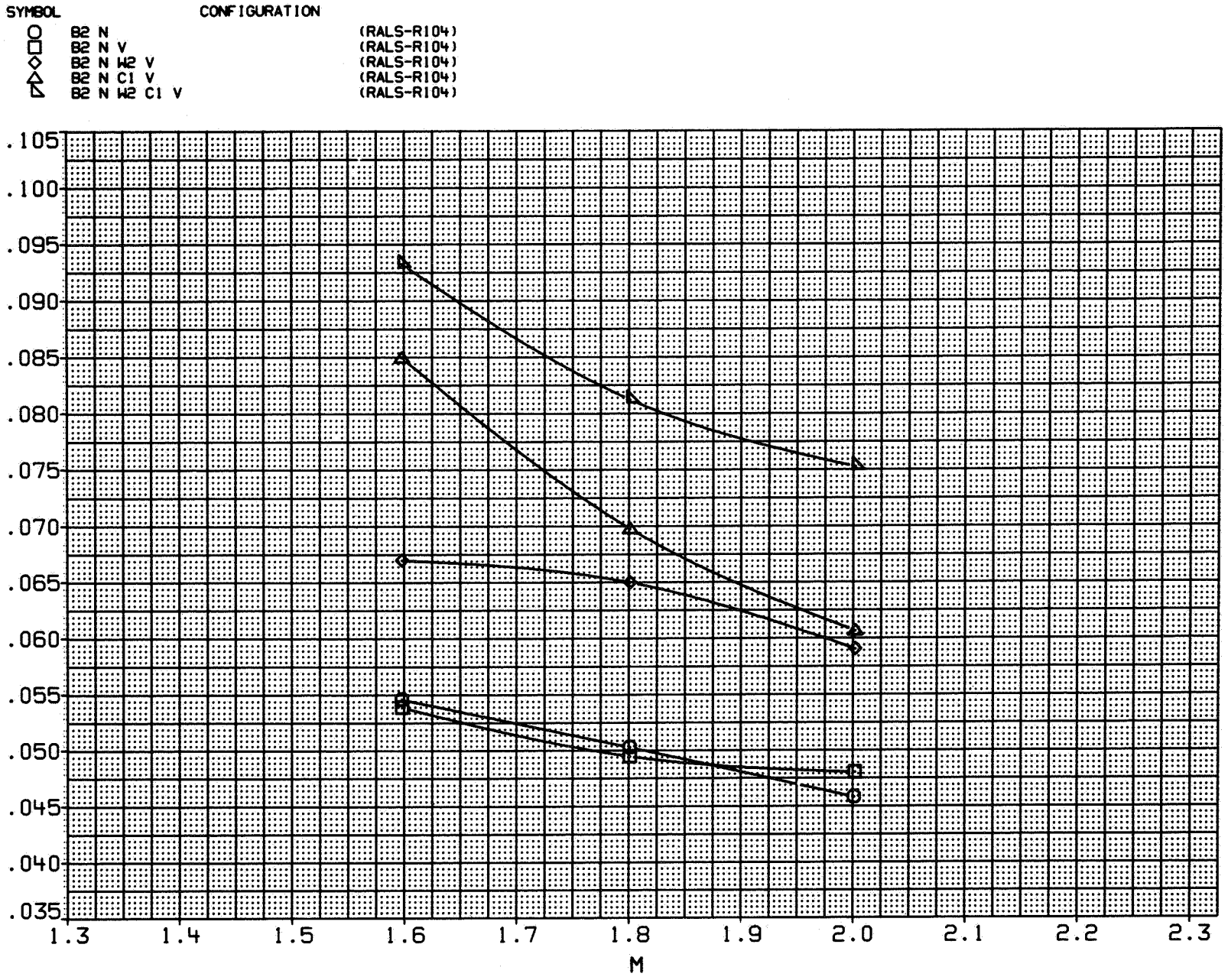


FIG. 50 SUMMARY OF COMPONENT BUILDUP WITH MACH NUMBER

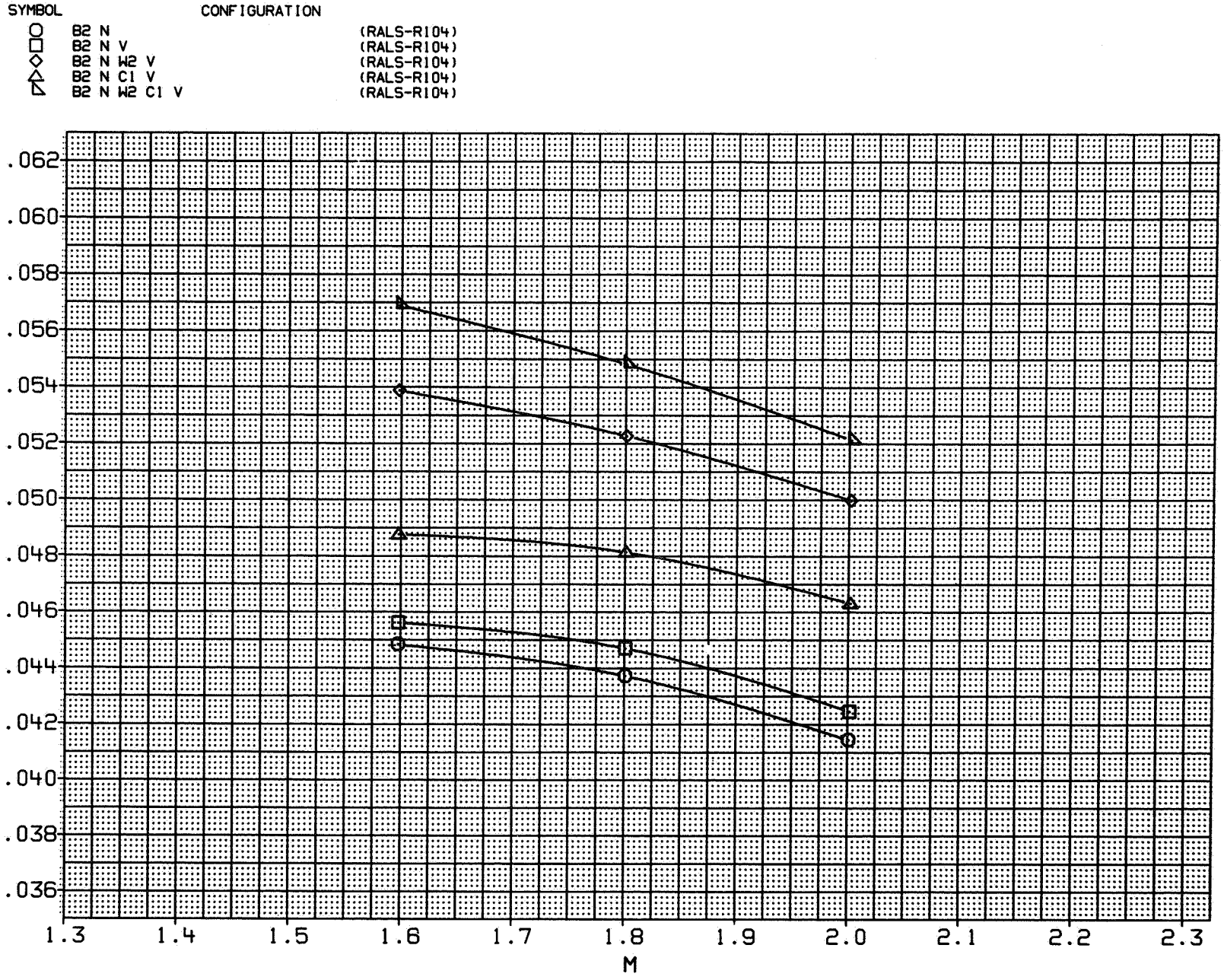


FIG. 50 SUMMARY OF COMPONENT BUILDUP WITH MACH NUMBER

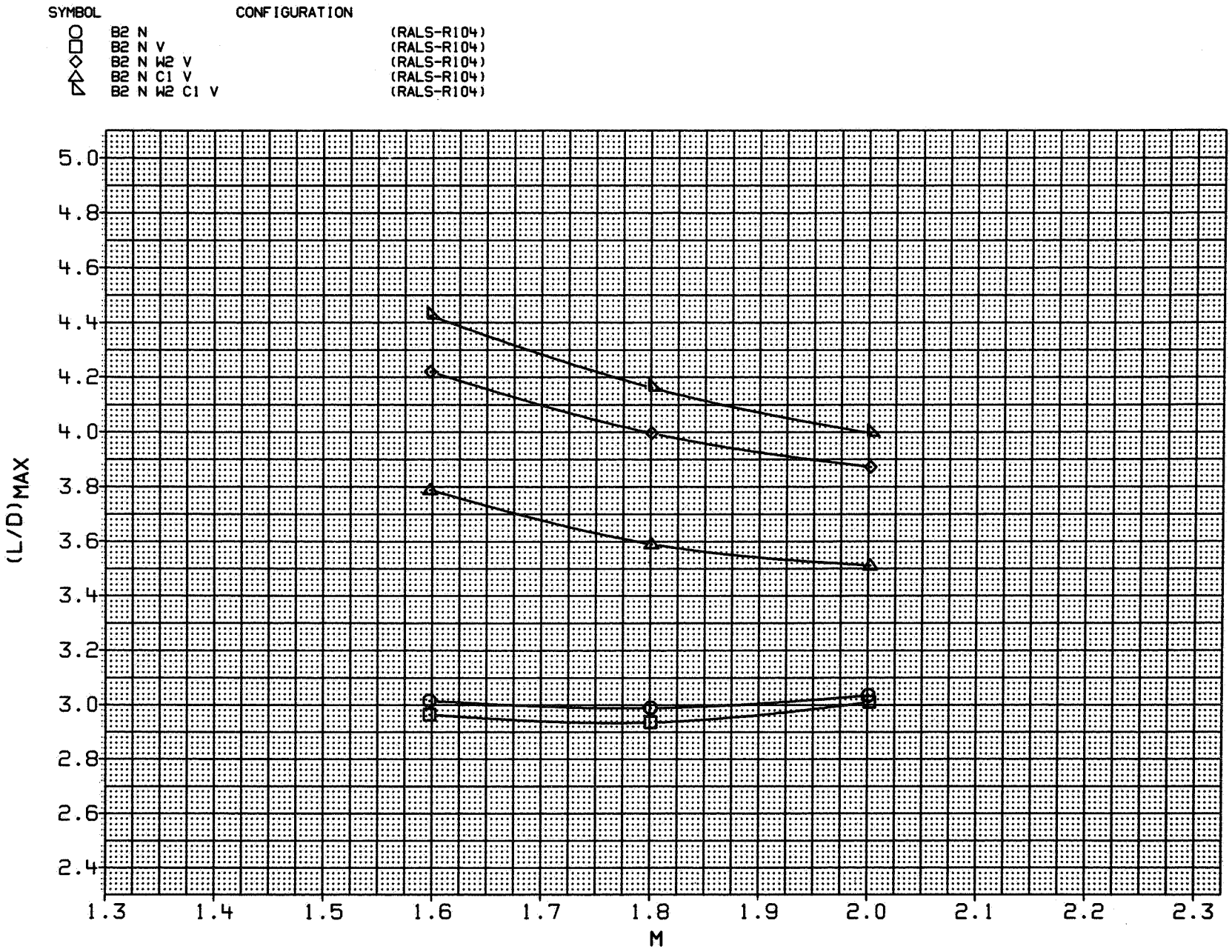


FIG. 50 SUMMARY OF COMPONENT BUILDUP WITH MACH NUMBER

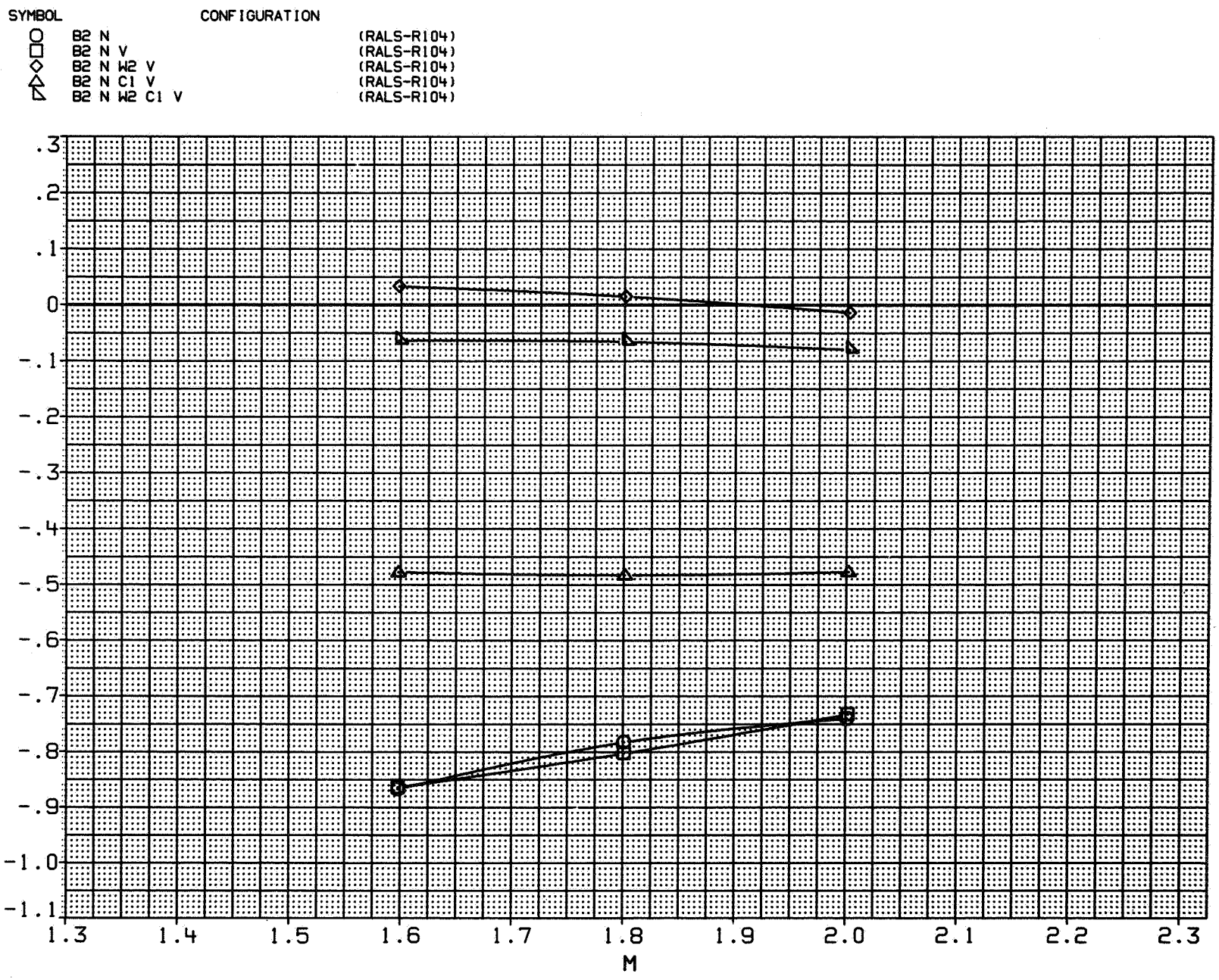


FIG. 50 SUMMARY OF COMPONENT BUILDUP WITH MACH NUMBER

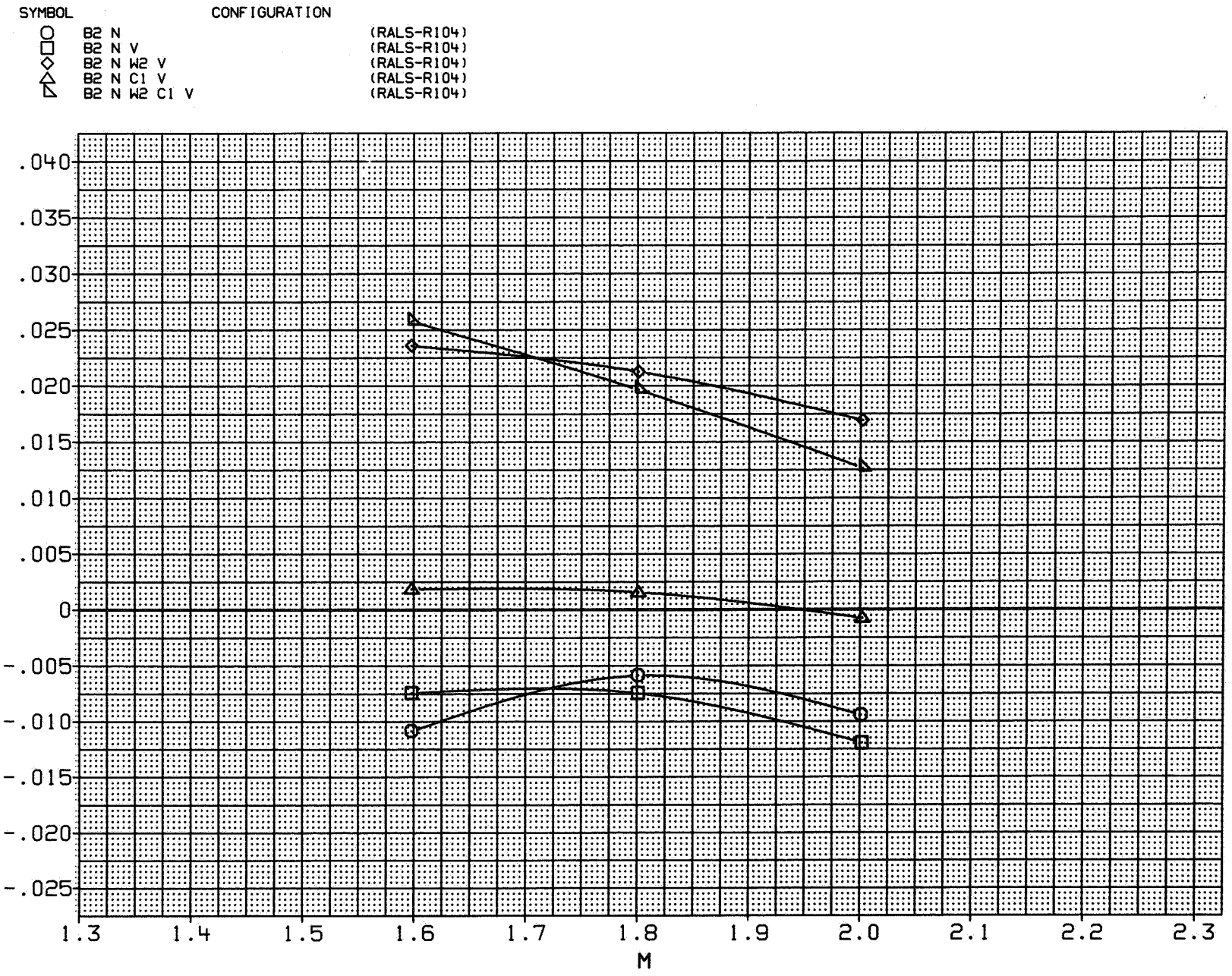


FIG. 50 SUMMARY OF COMPONENT BUILDUP WITH MACH NUMBER

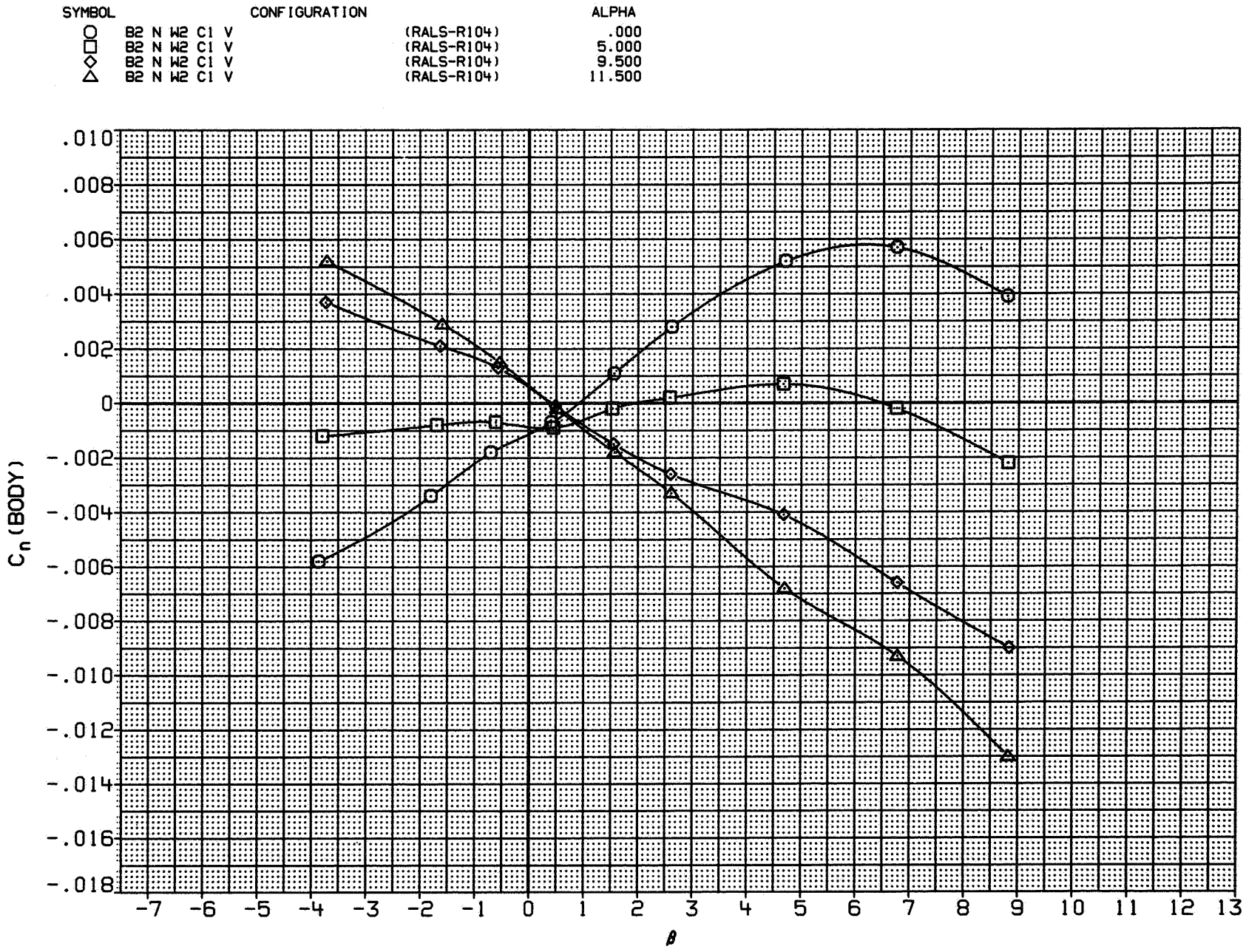


FIG. 51 BASIC LATERAL/DIRECTIONAL CHARACTERISTICS FOR VARIOUS ALPHA

MACH = 1.60

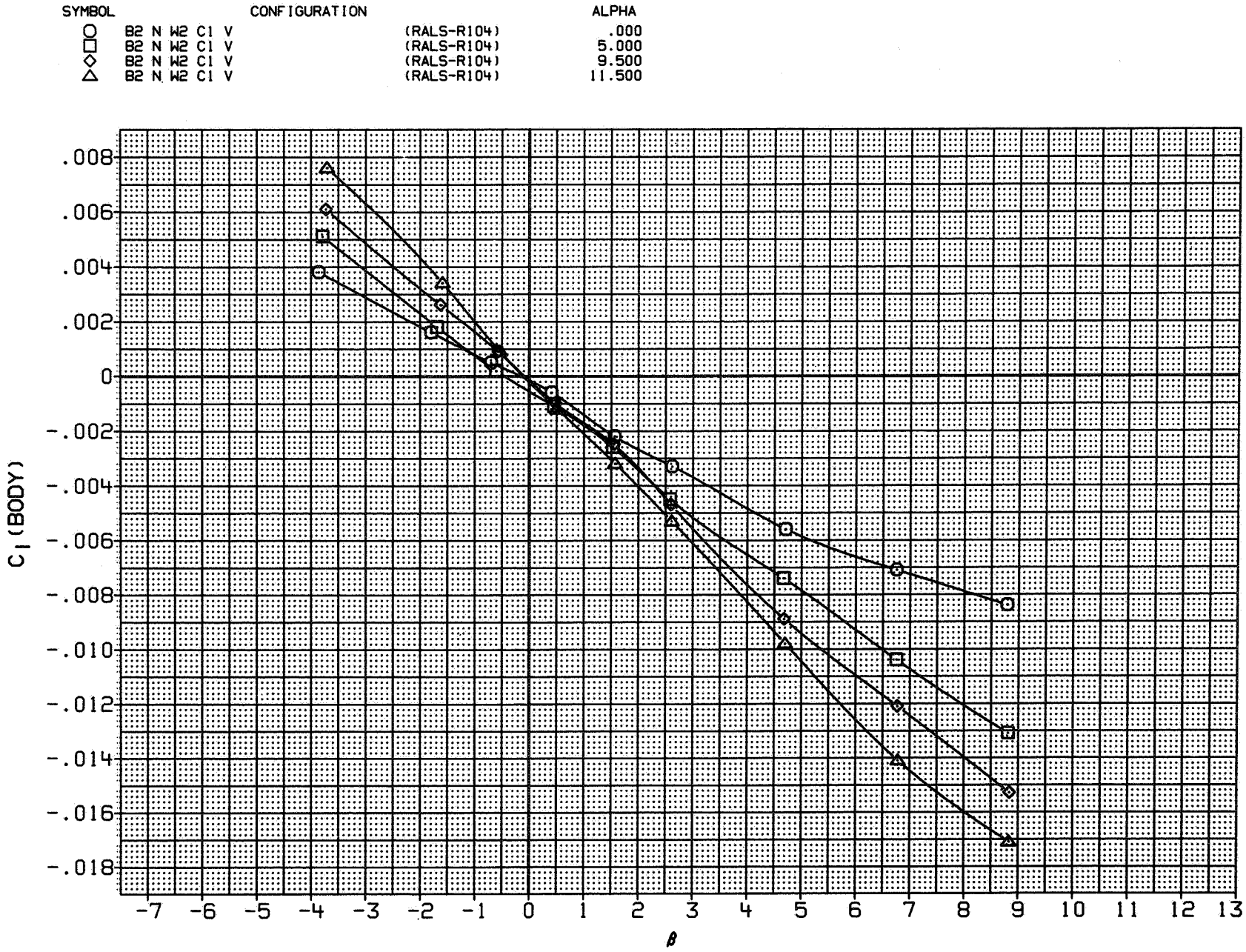


FIG. 51 BASIC LATERAL/DIRECTIONAL CHARACTERISTICS FOR VARIOUS ALPHA

MACH = 1.60

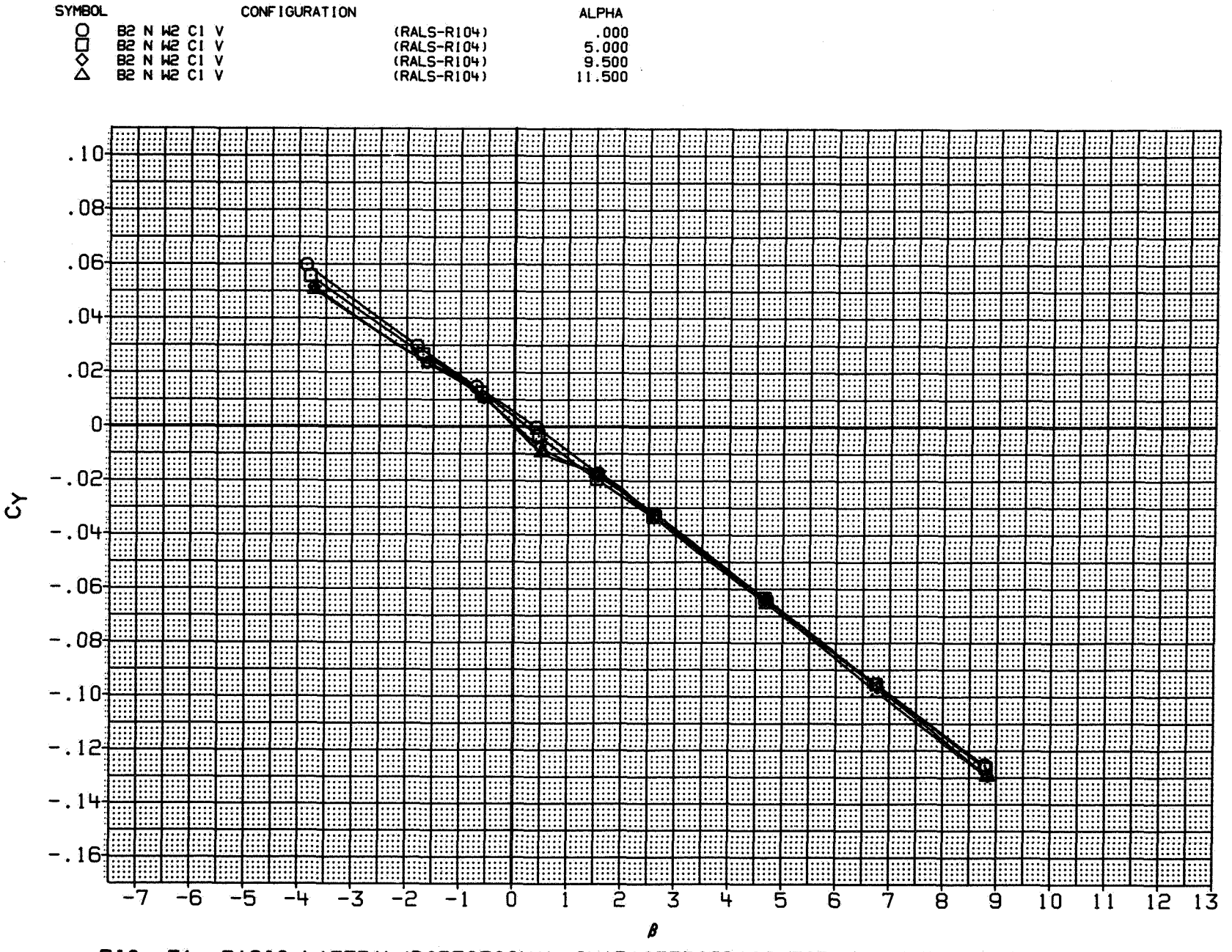


FIG. 51 BASIC LATERAL/DIRECTIONAL CHARACTERISTICS FOR VARIOUS ALPHA

MACH = 1.60

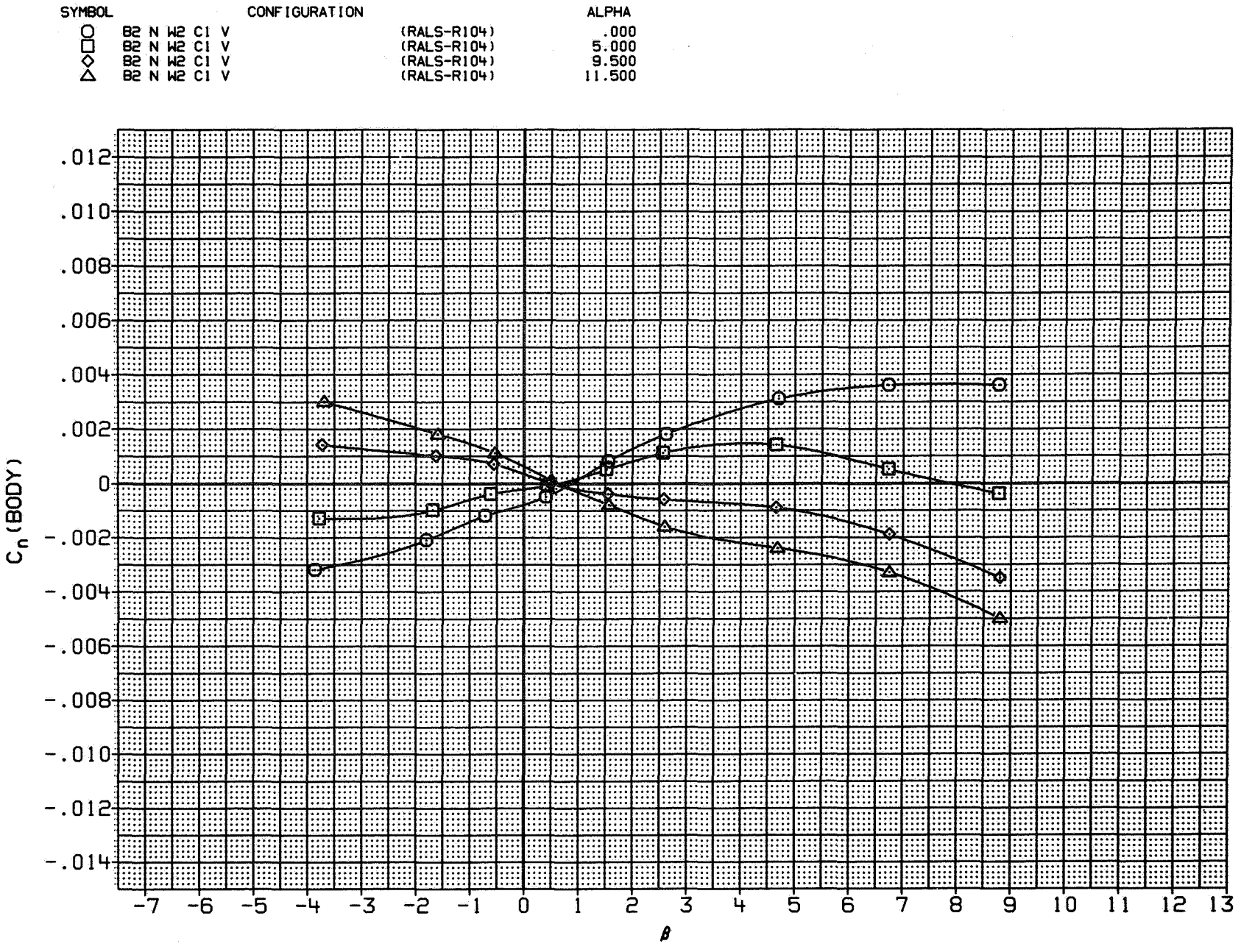


FIG. 52 BASIC LATERAL/DIRECTIONAL CHARACTERISTICS FOR VARIOUS ALPHA

MACH = 2.00

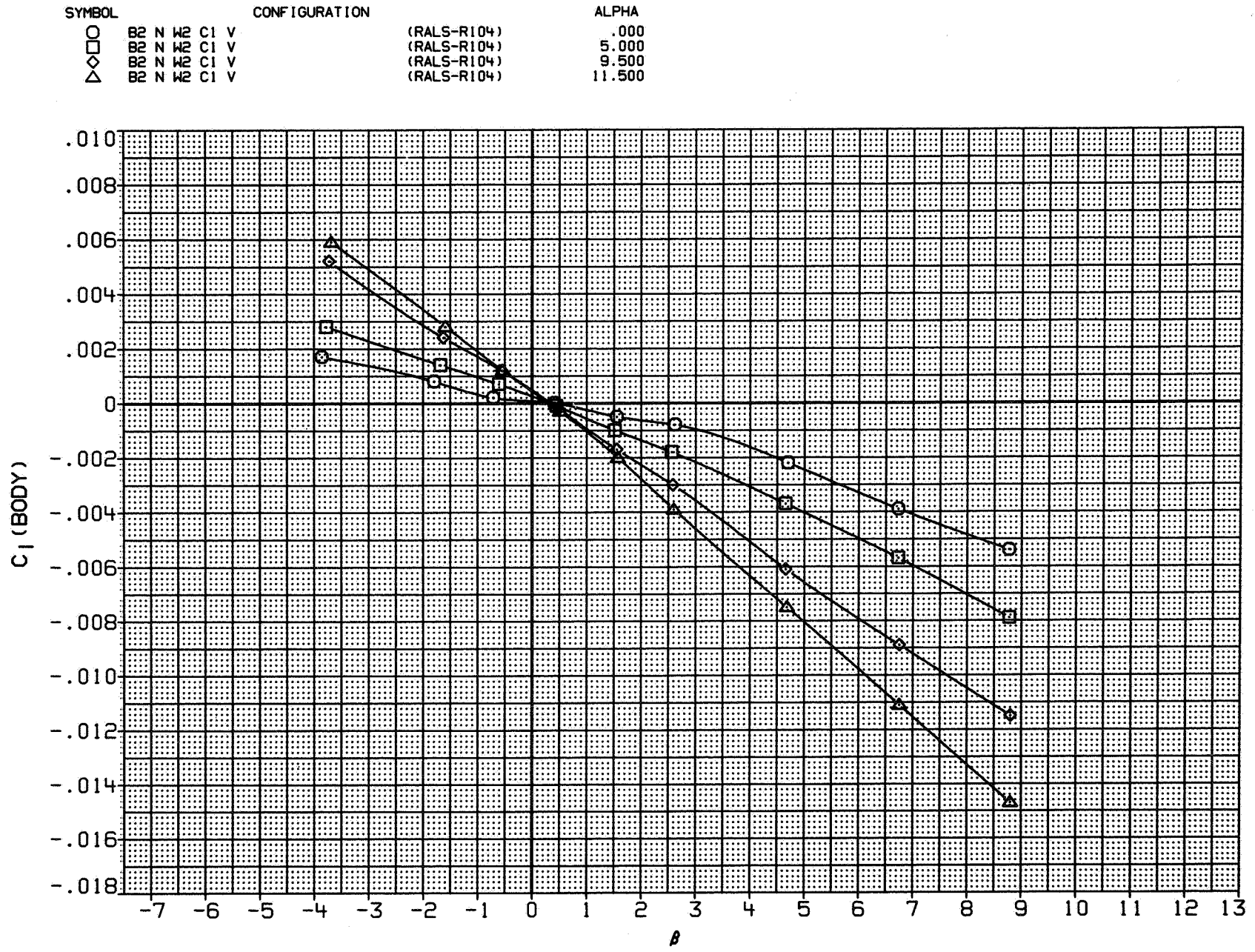


FIG. 52 BASIC LATERAL/DIRECTIONAL CHARACTERISTICS FOR VARIOUS ALPHA

MACH = 2.00

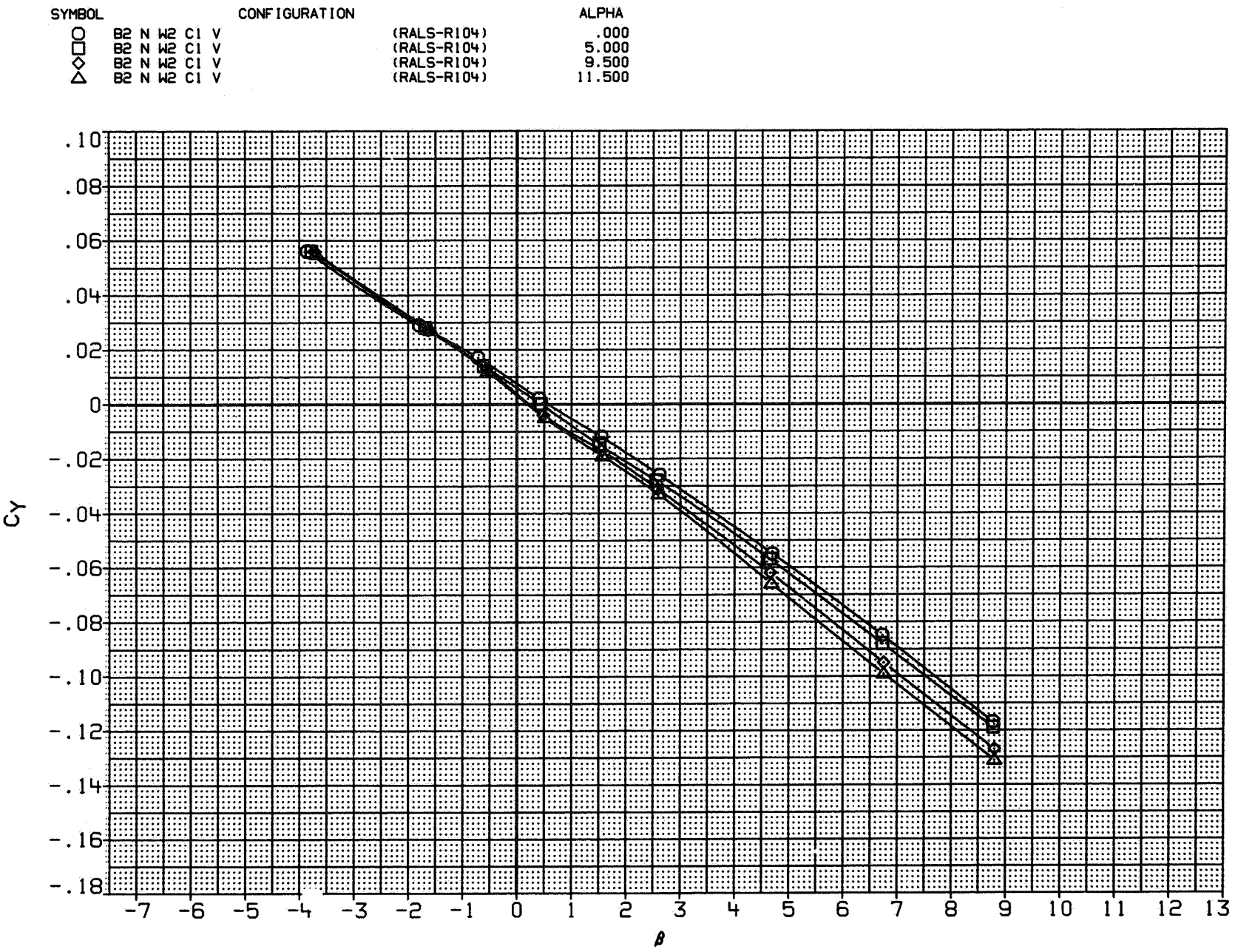


FIG. 52 BASIC LATERAL/DIRECTIONAL CHARACTERISTICS FOR VARIOUS ALPHA

MACH = 2.00

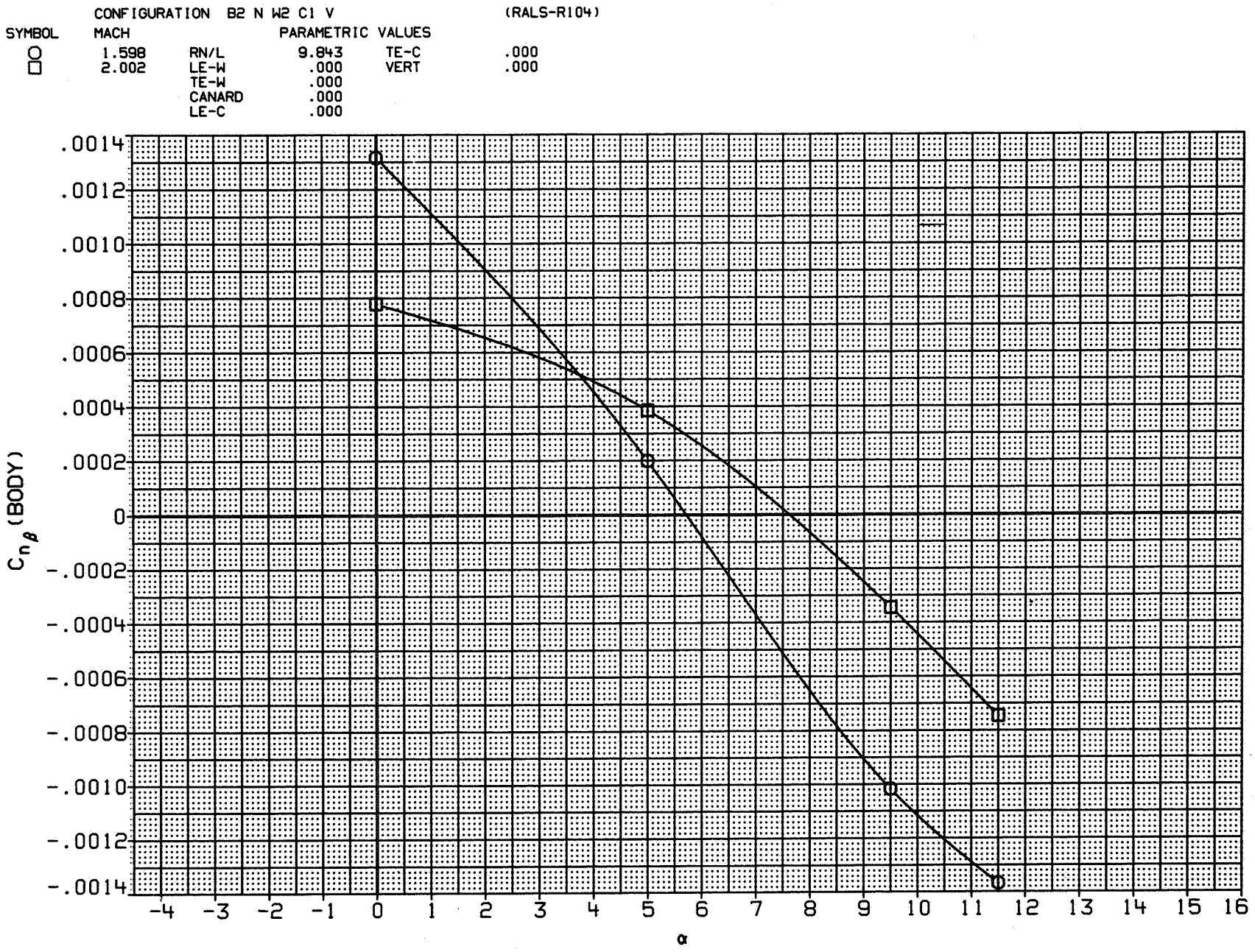


FIG. 53 SUMMARY OF BASIC LATERAL/DIRECTIONAL CHARACTERISTICS WITH ALPHA

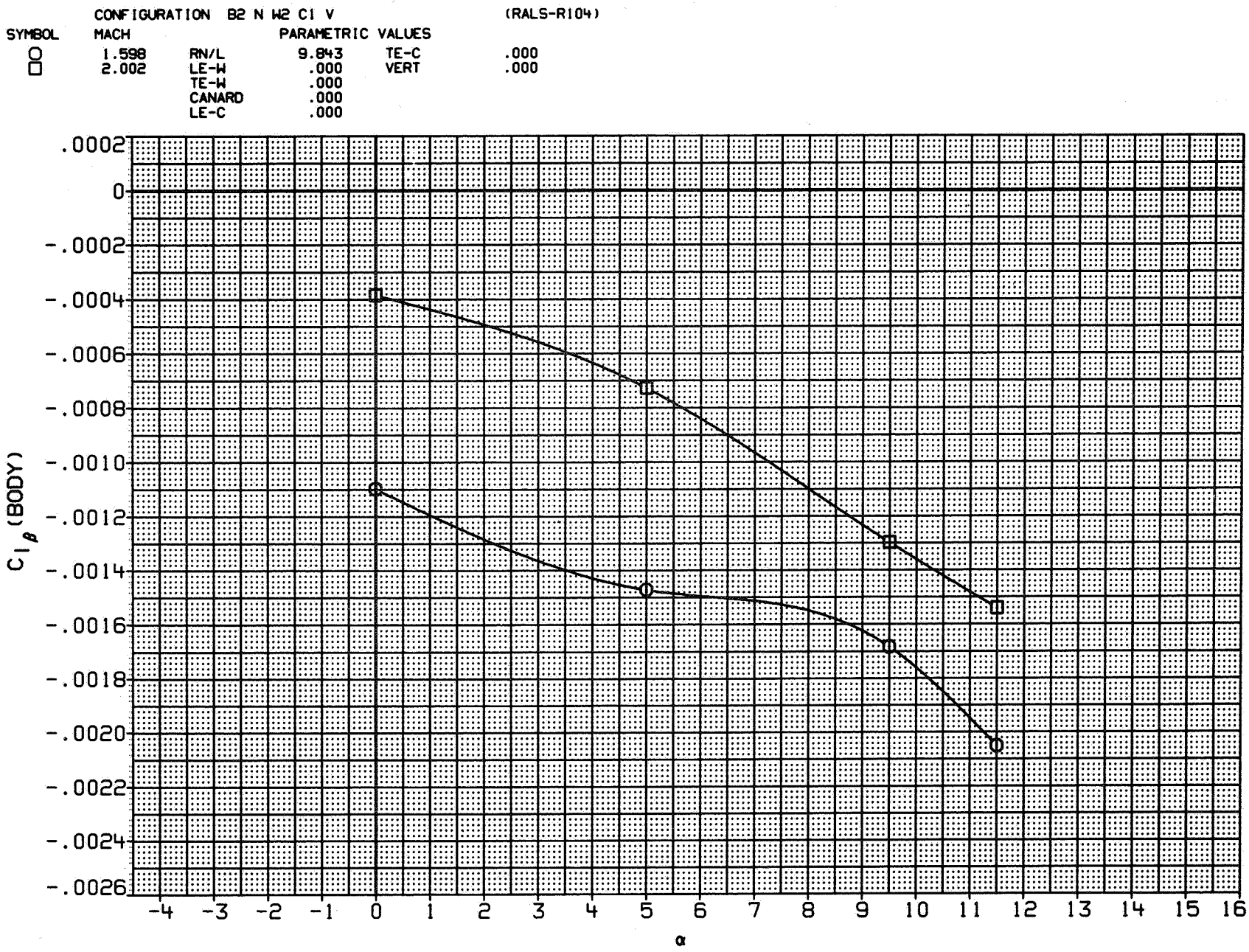


FIG. 53 SUMMARY OF BASIC LATERAL/DIRECTIONAL CHARACTERISTICS WITH ALPHA

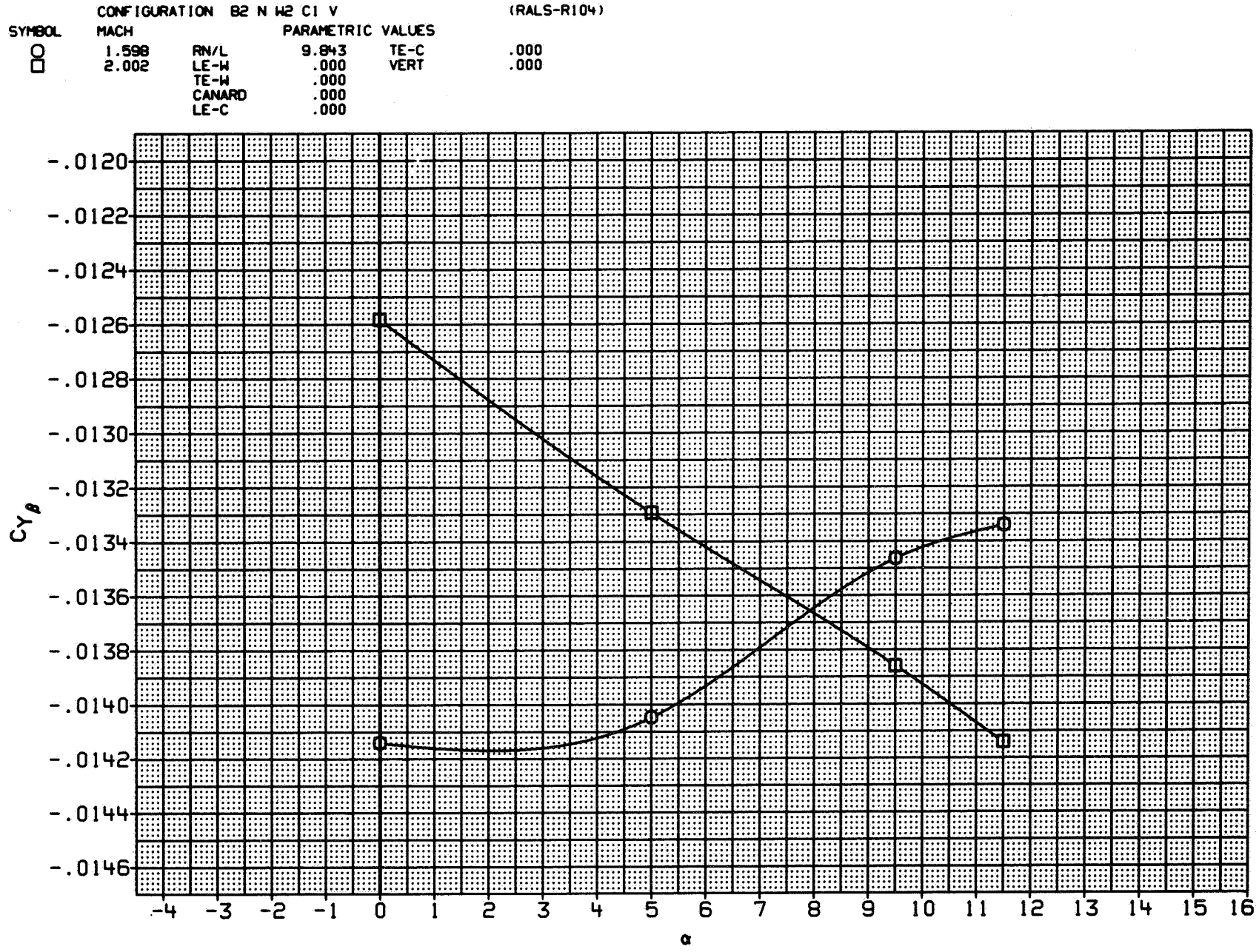


FIG. 53 SUMMARY OF BASIC LATERAL/DIRECTIONAL CHARACTERISTICS WITH ALPHA

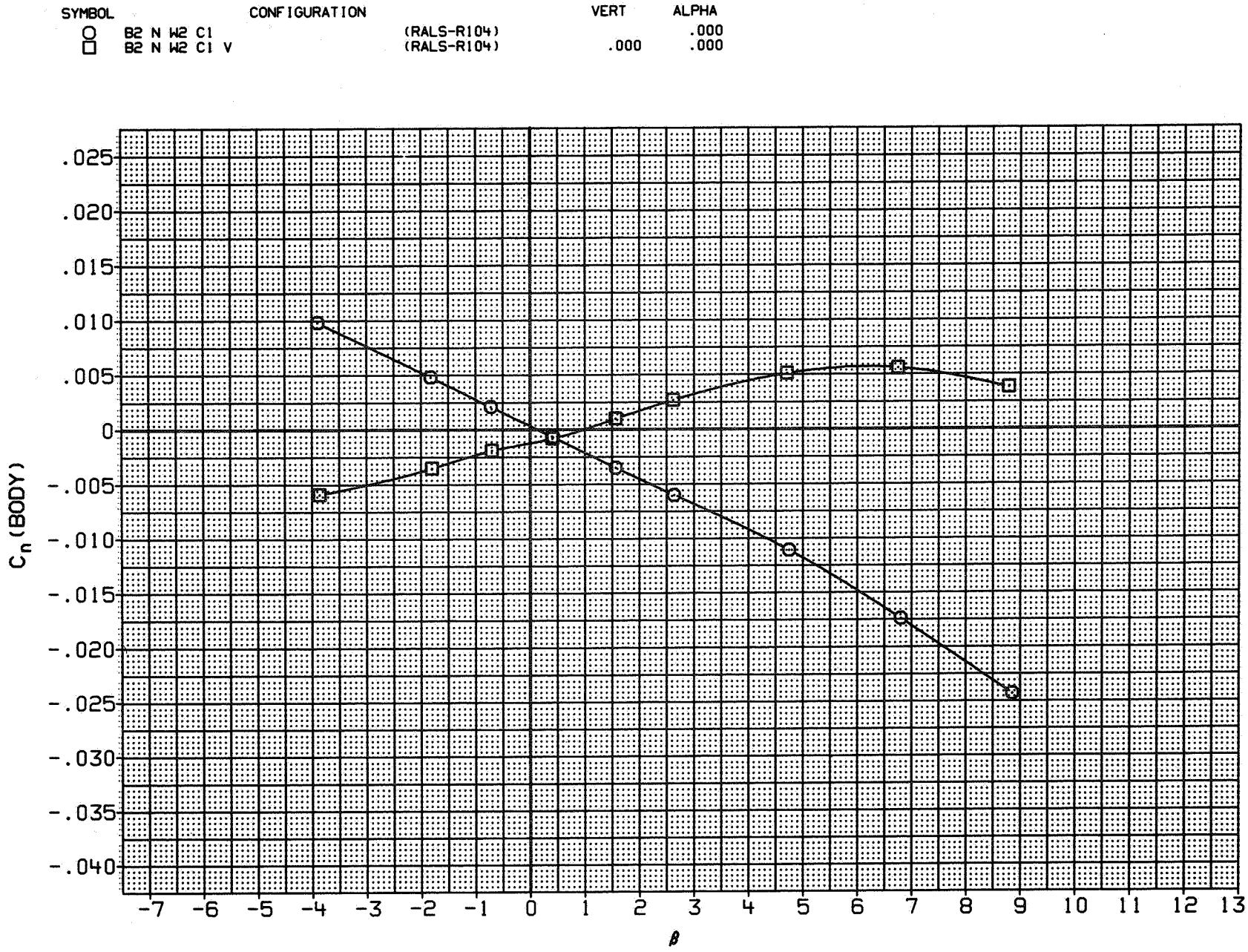


FIG. 54 VERTICAL TAIL ON/OFF, LATERAL/DIRECTIONAL CHARACTERISTICS
ALPHA = 0 DEGREES

MACH = 1.60

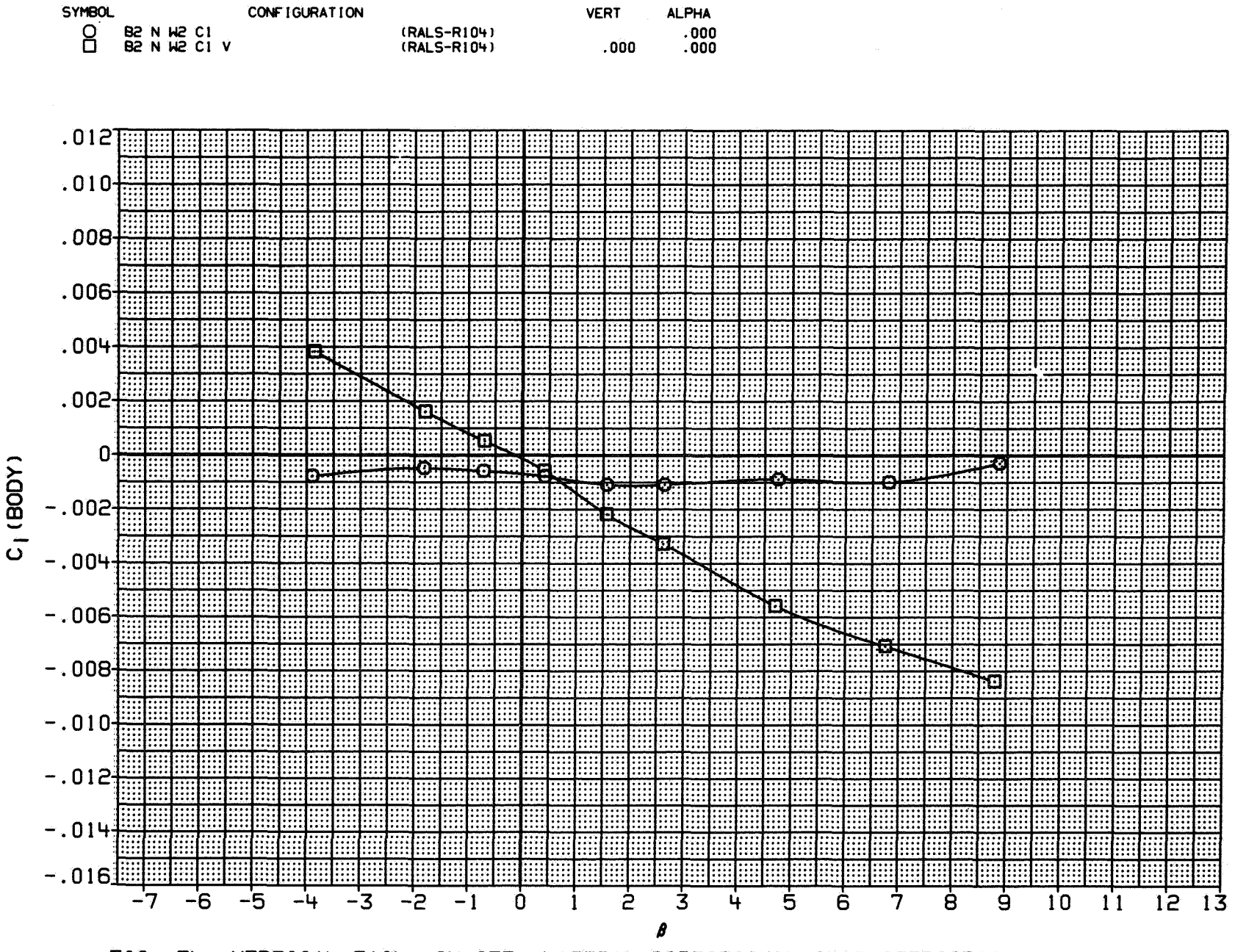


FIG. 54 VERTICAL TAIL ON/OFF, LATERAL/DIRECTIONAL CHARACTERISTICS
ALPHA = 0 DEGREES
MACH = 1.60

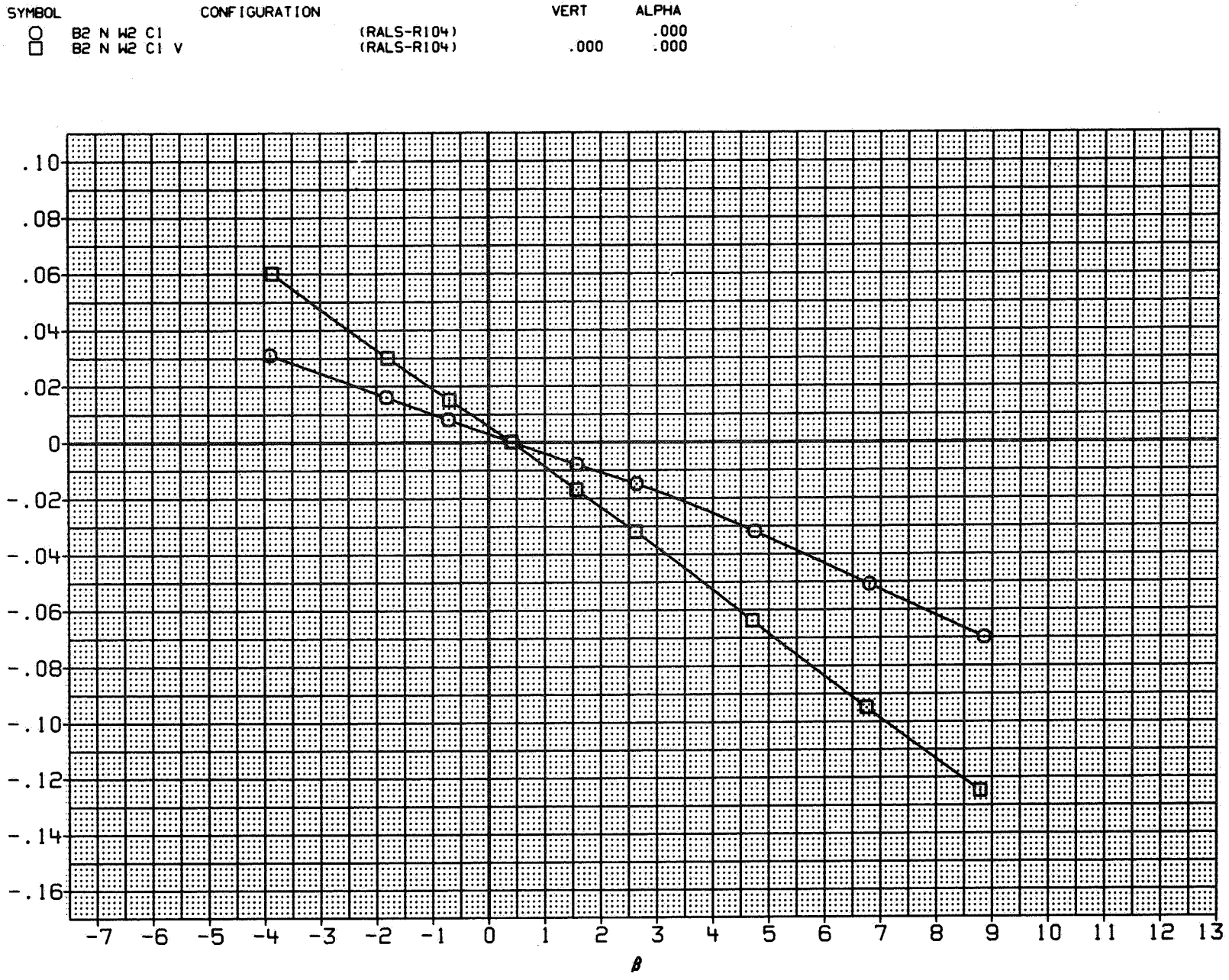


FIG. 54 VERTICAL TAIL ON/OFF, LATERAL/DIRECTIONAL CHARACTERISTICS
ALPHA = 0 DEGREES
MACH = 1.60

| SYMBOL | CONFIGURATION | | VERT | ALPHA |
|---|---|---|---|---|
| ○ | B2 N W2 C1 | (RALS-R104) | | 9.500 |
| □ | B2 N W2 C1 V | (RALS-R104) | .000 | 9.500 |

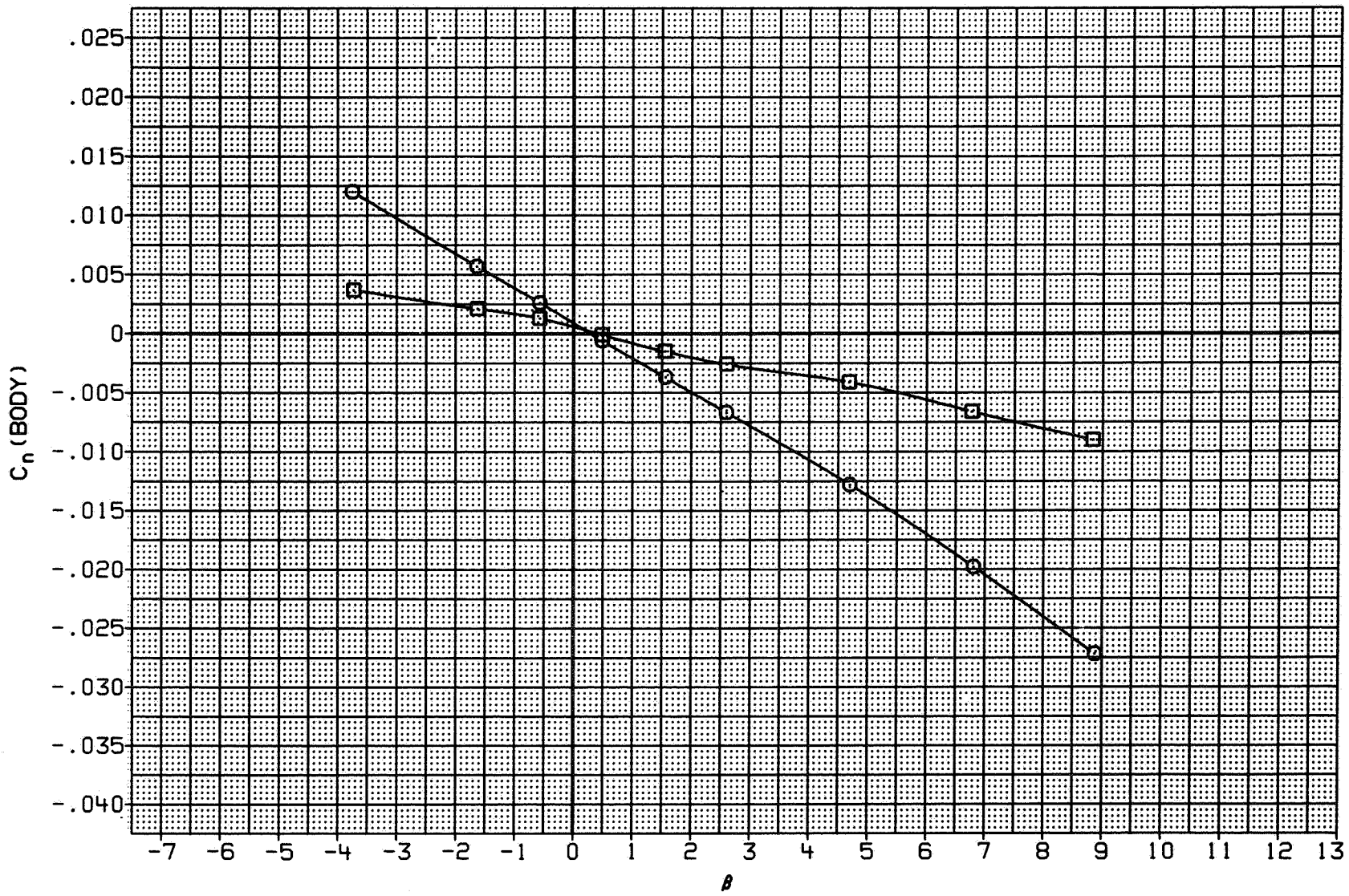


FIG. 55 VERTICAL TAIL ON/OFF, LATERAL/DIRECTIONAL CHARACTERISTICS
ALPHA = 8 DEGREES

MACH = 1.60

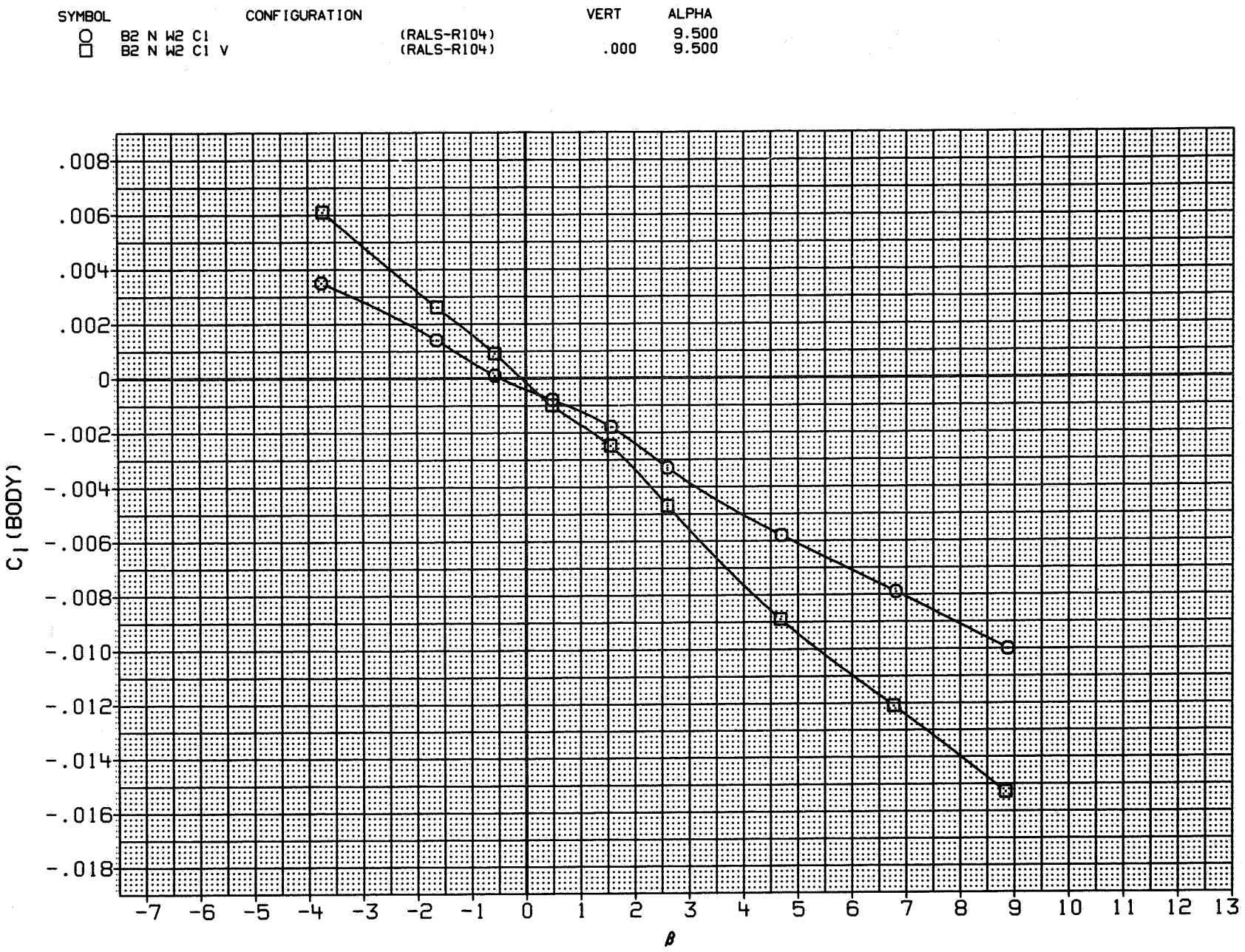


FIG. 55 VERTICAL TAIL ON/OFF, LATERAL/DIRECTIONAL CHARACTERISTICS
ALPHA = 8 DEGREES
MACH = 1.60

| SYMBOL | CONFIGURATION | | VERT | ALPHA |
|---|---|---|---|---|
| ○ | B2 N W2 C1 | (RALS-R104) | | 9.500 |
| □ | B2 N W2 C1 V | (RALS-R104) | .000 | 9.500 |

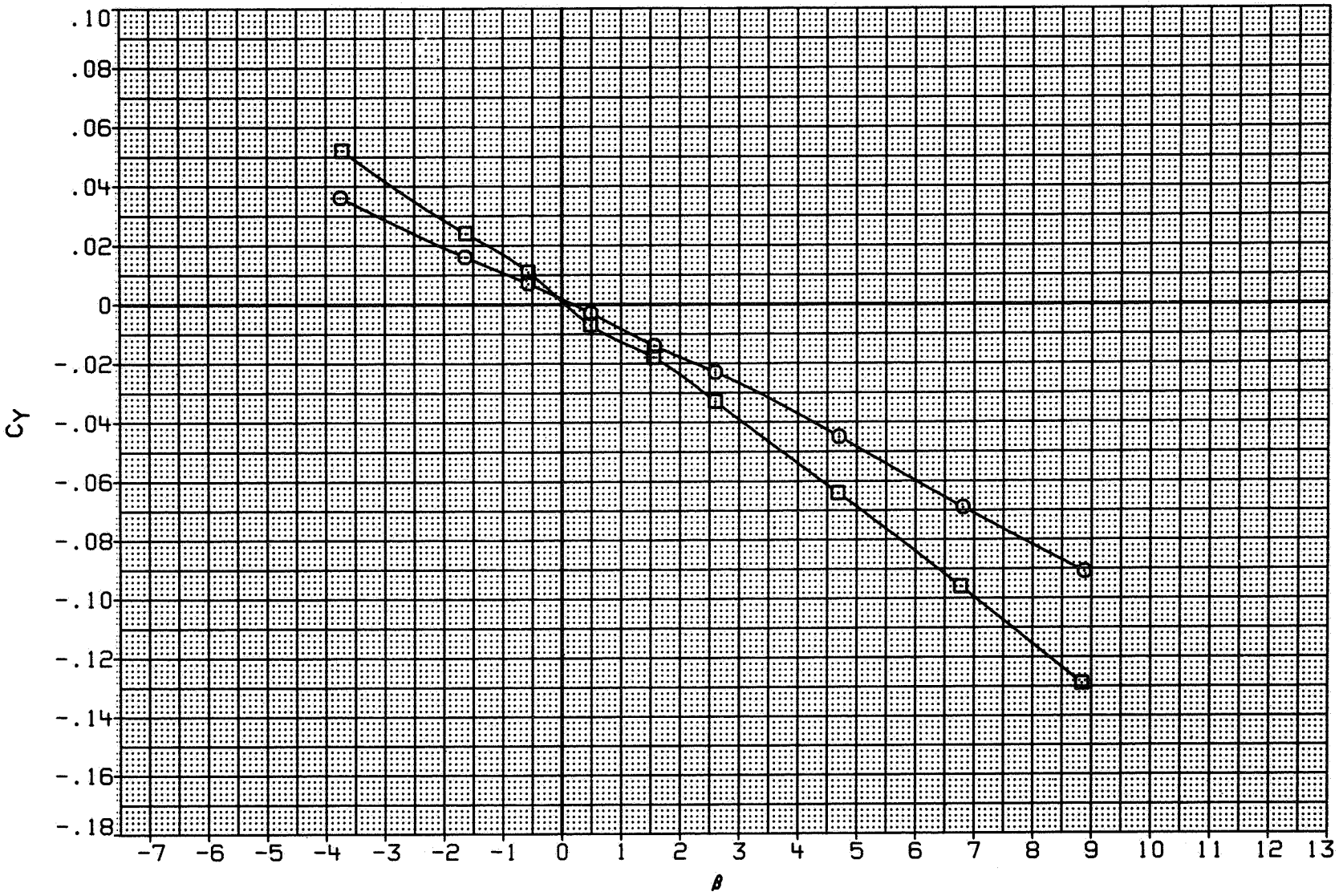


FIG. 55 VERTICAL TAIL ON/OFF, LATERAL/DIRECTIONAL CHARACTERISTICS
ALPHA = 8 DEGREES
MACH = 1.60

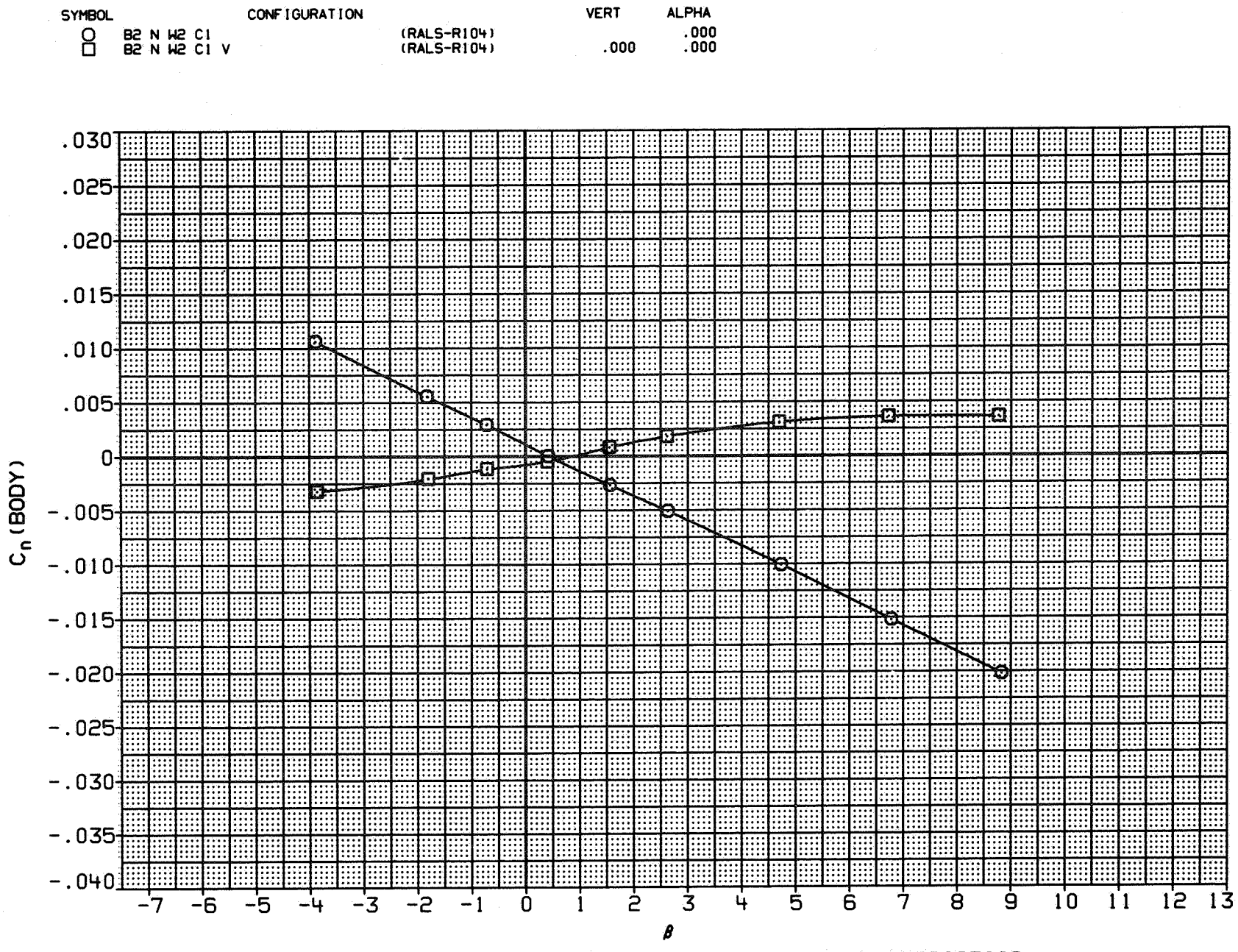


FIG. 56 VERTICAL TAIL ON/OFF, LATERAL/DIRECTIONAL CHARACTERISTICS
ALPHA = 0 DEGREES
MACH = 2.00

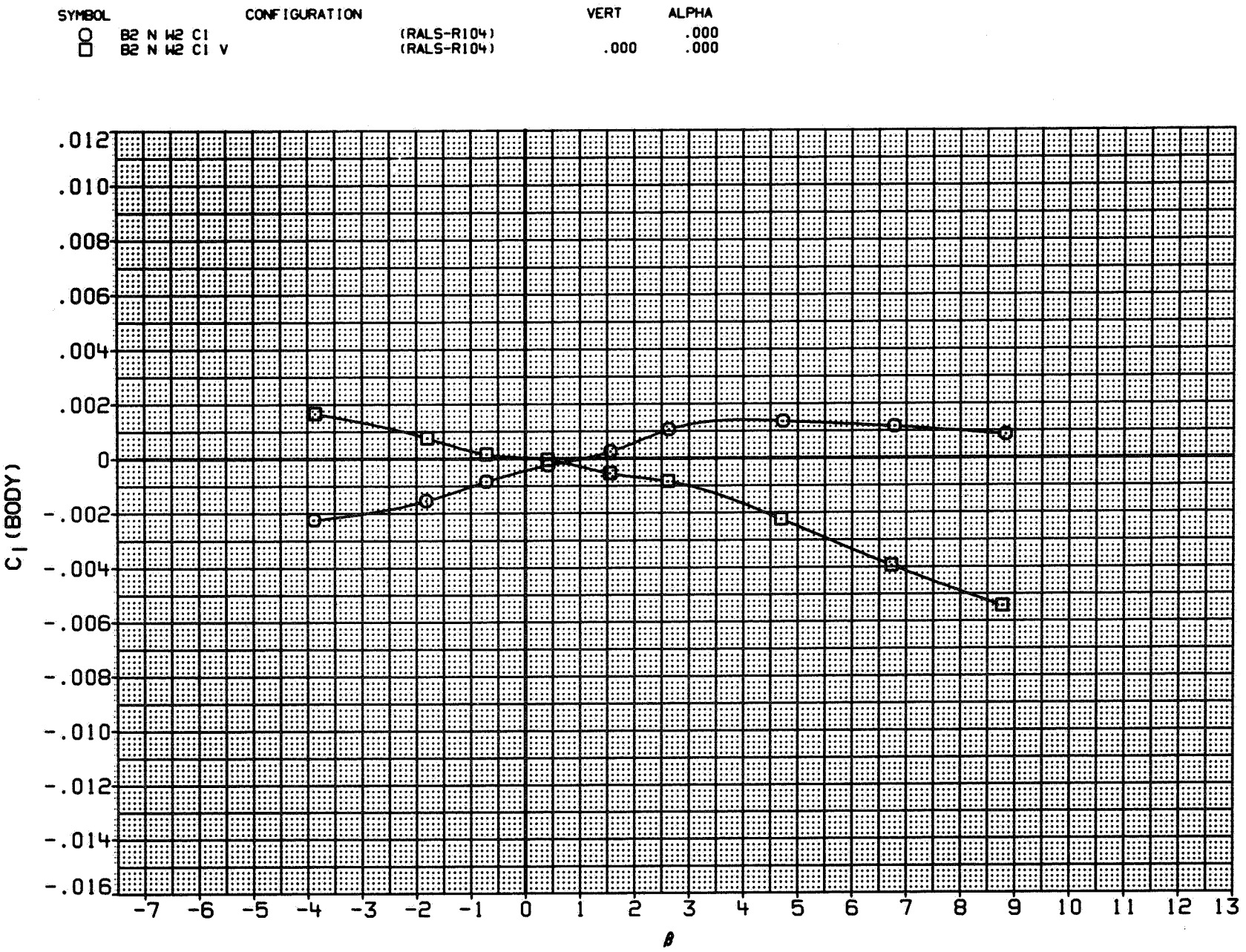


FIG. 56 VERTICAL TAIL ON/OFF, LATERAL/DIRECTIONAL CHARACTERISTICS
ALPHA = 0 DEGREES
MACH = 2.00

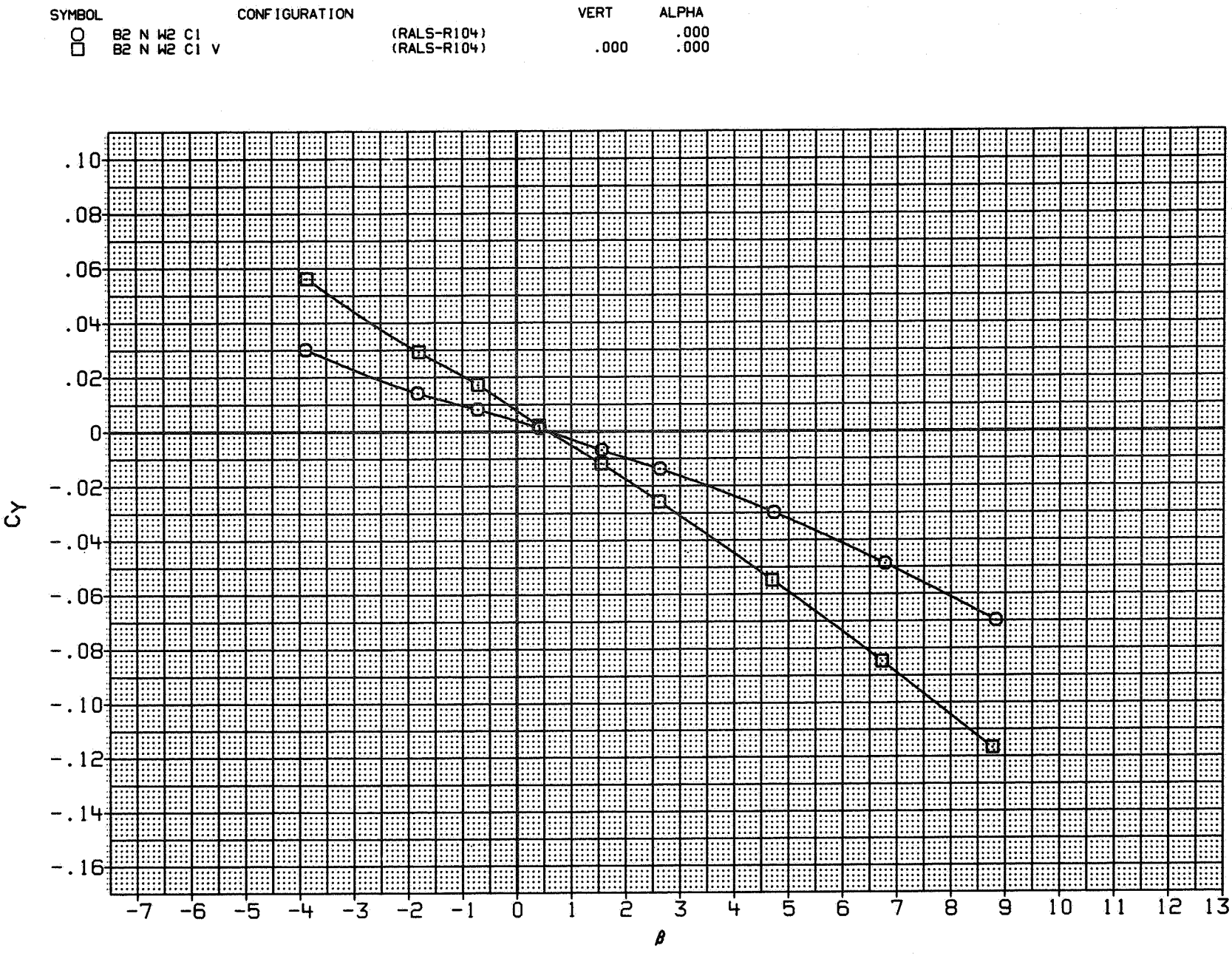


FIG. 56 VERTICAL TAIL ON/OFF, LATERAL/DIRECTIONAL CHARACTERISTICS
ALPHA = 0 DEGREES
MACH = 2.00

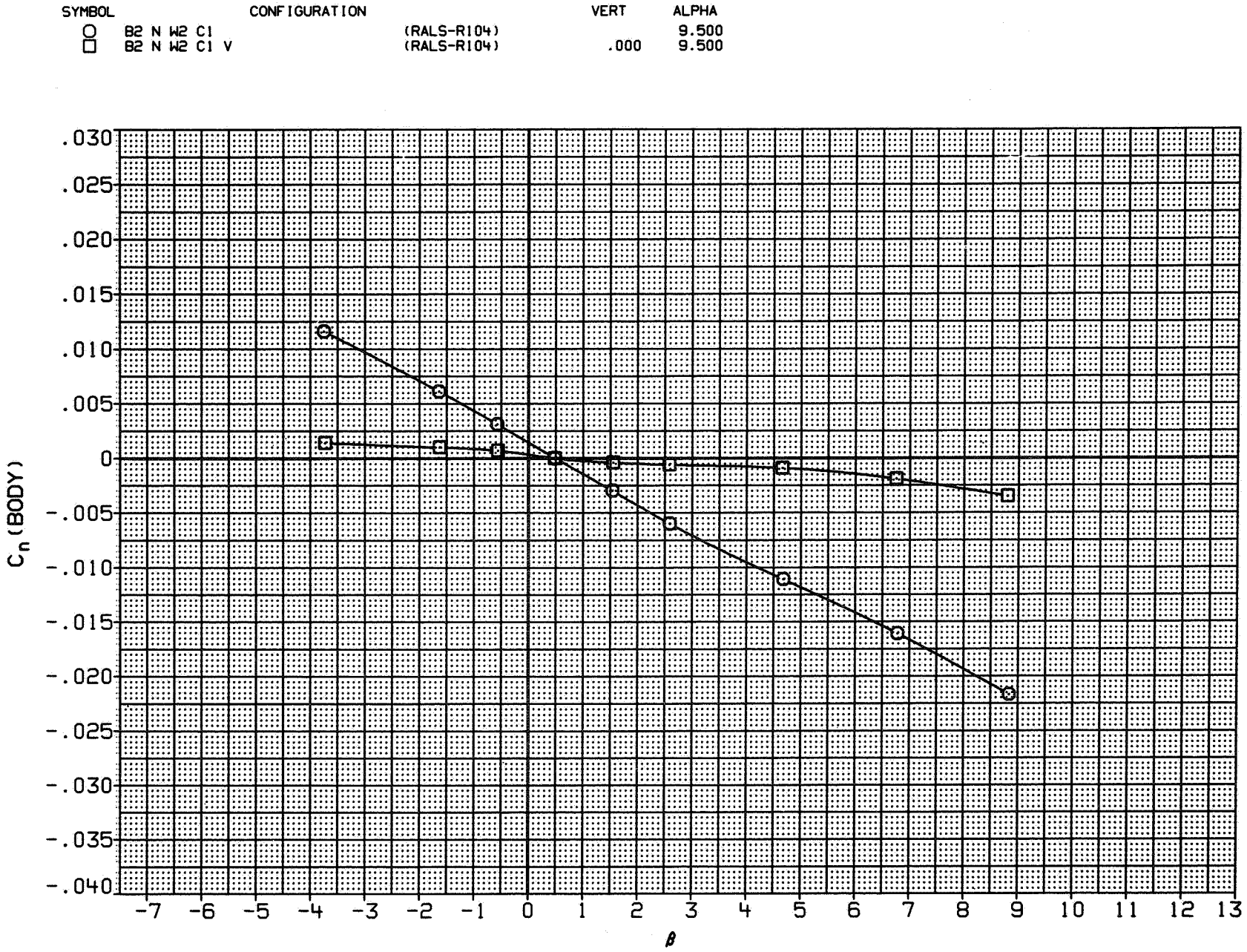


FIG. 57 VERTICAL TAIL ON/OFF, LATERAL/DIRECTIONAL CHARACTERISTICS
ALPHA = 8 DEGREES
MACH = 2.00

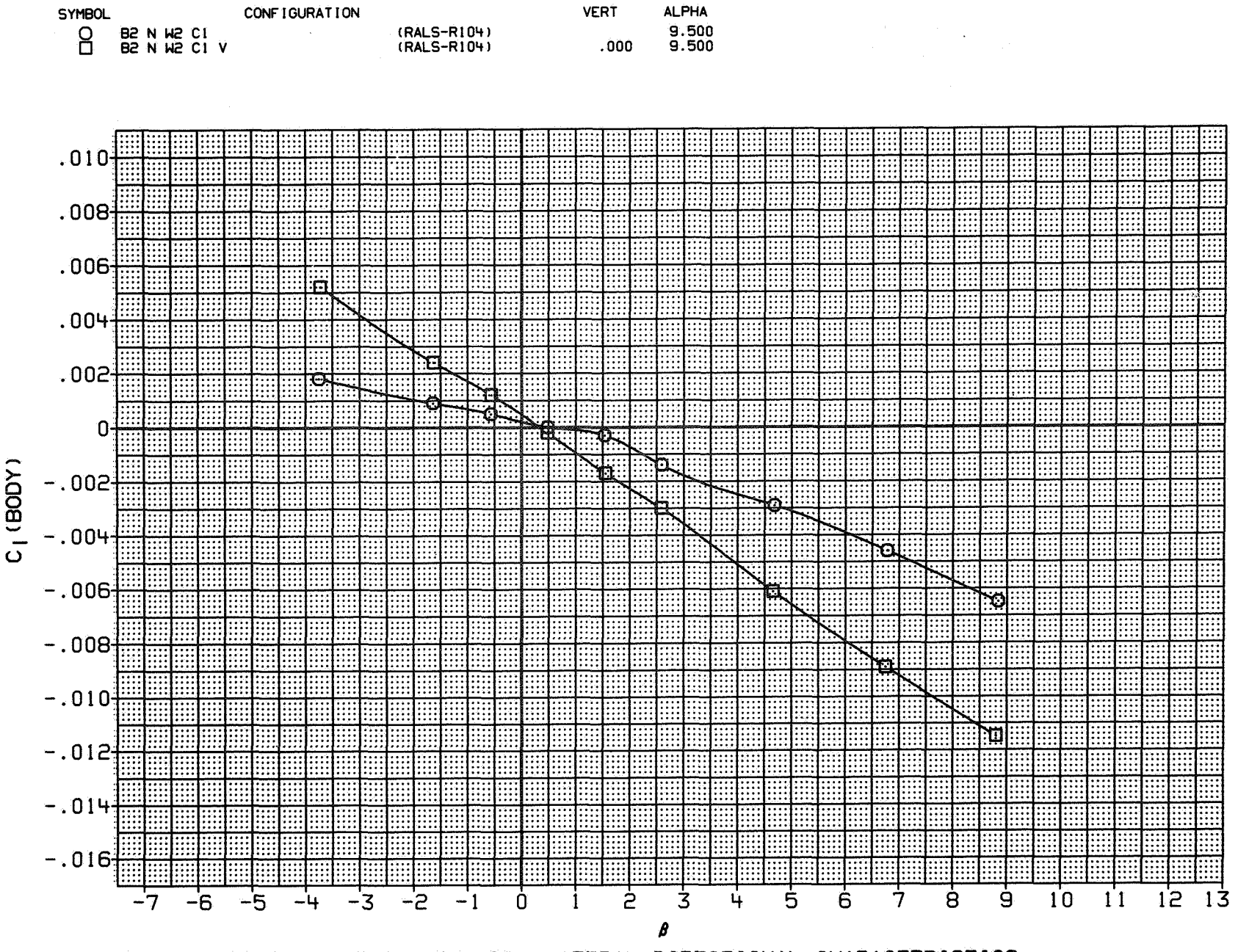


FIG. 57 VERTICAL TAIL ON/OFF, LATERAL/DIRECTIONAL CHARACTERISTICS
ALPHA = 8 DEGREES
MACH = 2.00

| SYMBOL | CONFIGURATION | | VERT | ALPHA |
|---|---|---|---|---|
| ○ | B2 N W2 C1 | (RALS-R104) | | 9.500 |
| □ | B2 N W2 C1 V | (RALS-R104) | .000 | 9.500 |

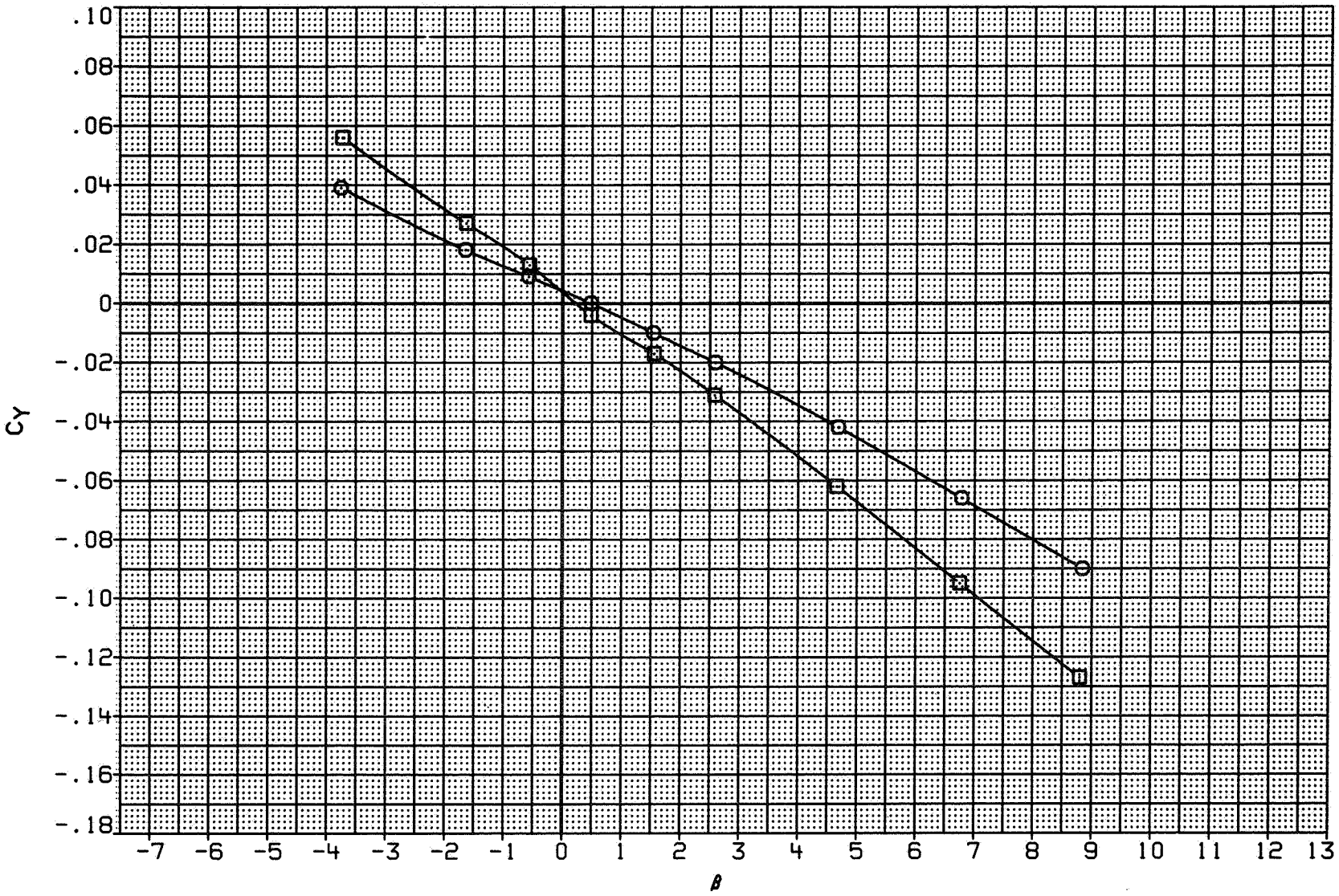


FIG. 57 VERTICAL TAIL ON/OFF, LATERAL/DIRECTIONAL CHARACTERISTICS
ALPHA = 8 DEGREES
MACH = 2.00

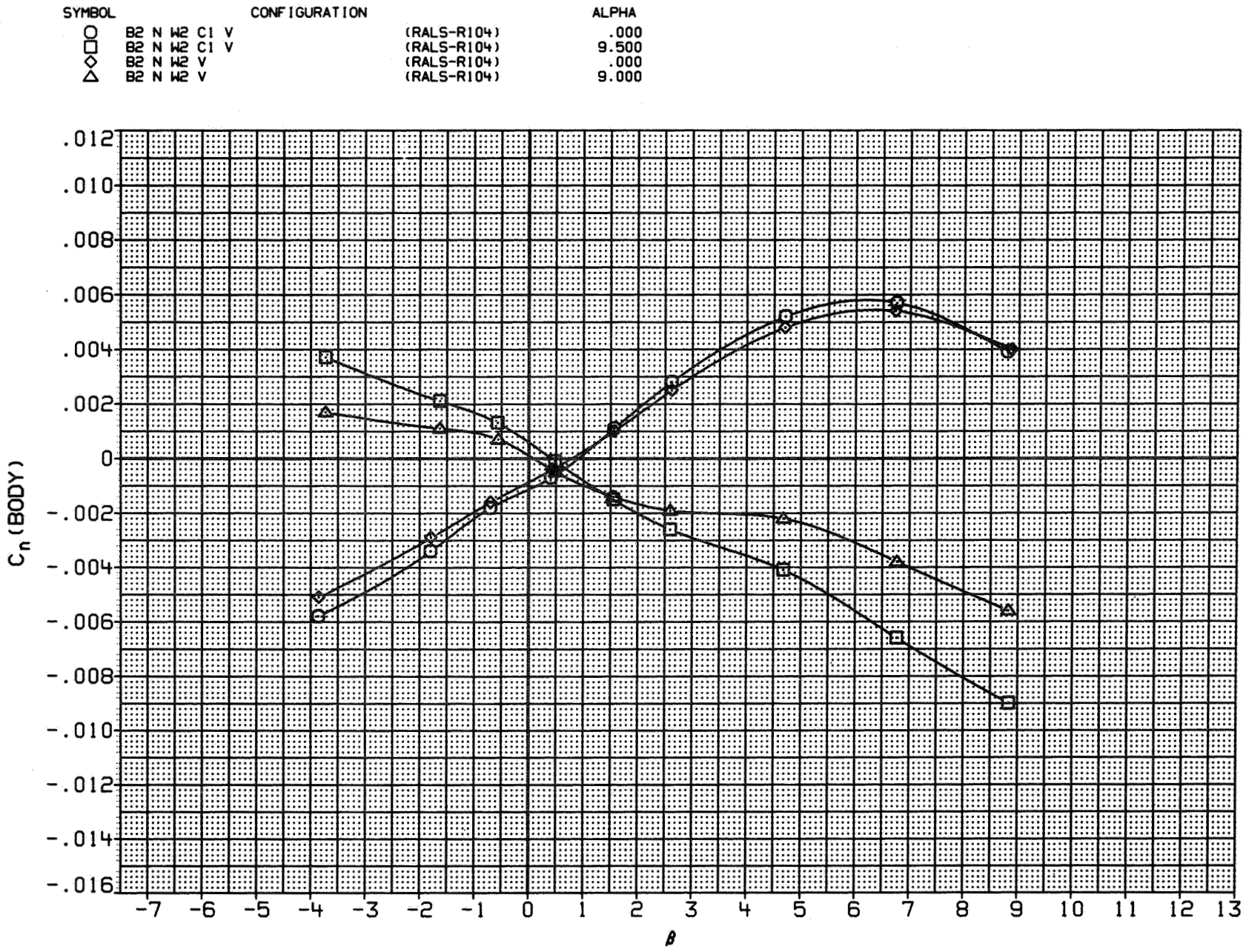


FIG. 58 LATERAL/DIRECTIONAL CHARACTERISTICS, CANARD ON/OFF

MACH = 1.60

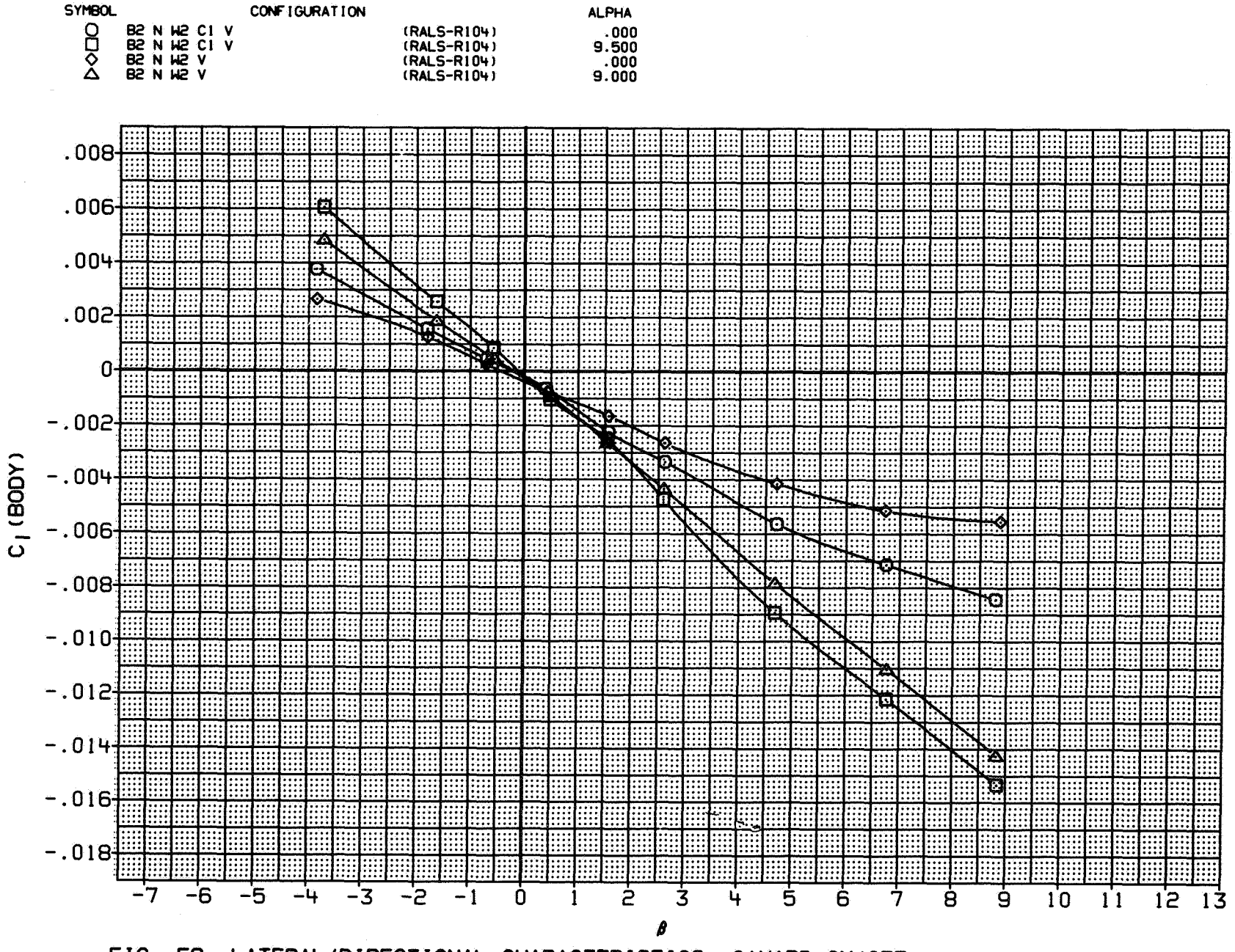


FIG. 58 LATERAL/DIRECTIONAL CHARACTERISTICS, CANARD ON/OFF

MACH = 1.60

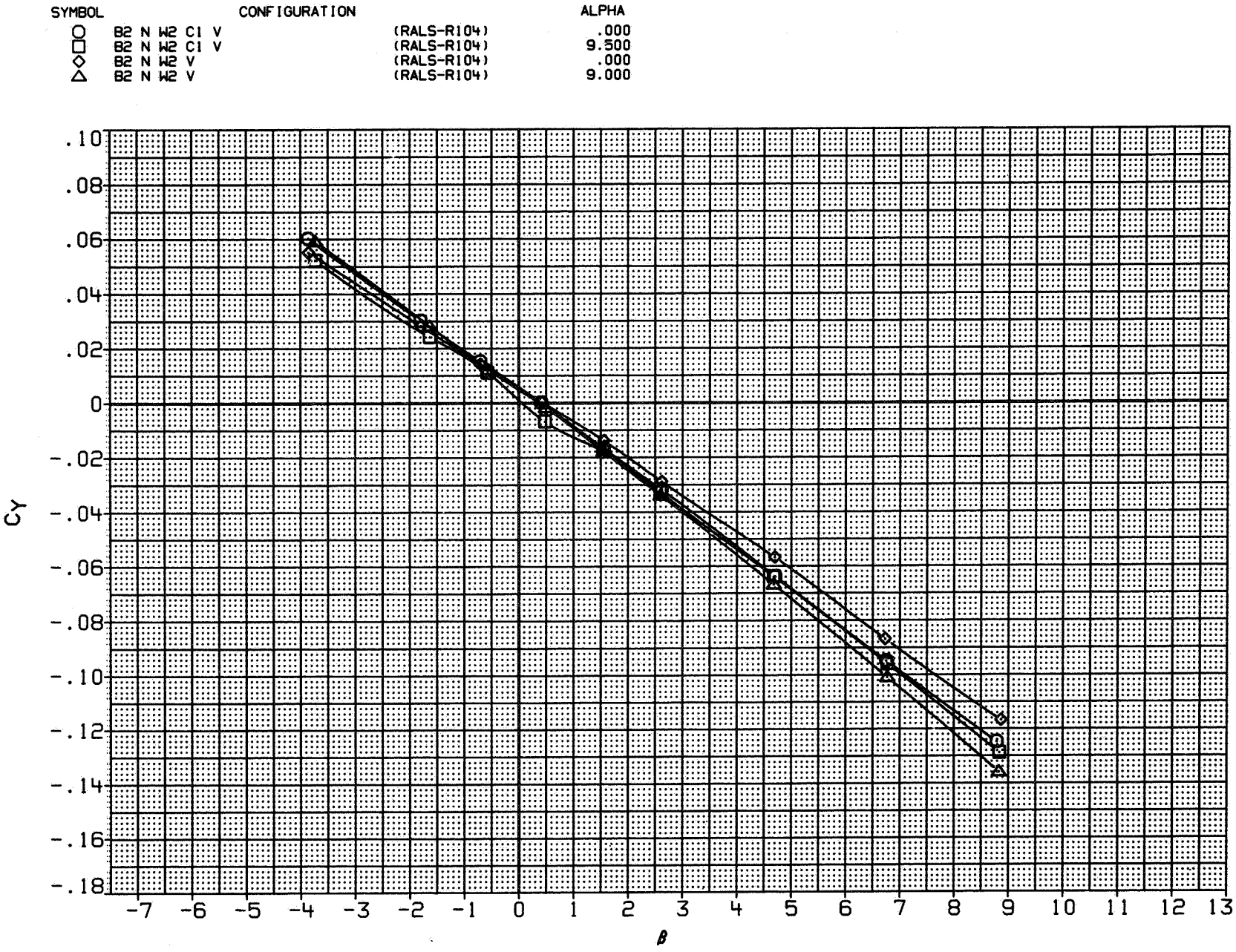


FIG. 58 LATERAL/DIRECTIONAL CHARACTERISTICS, CANARD ON/OFF

MACH = 1.60

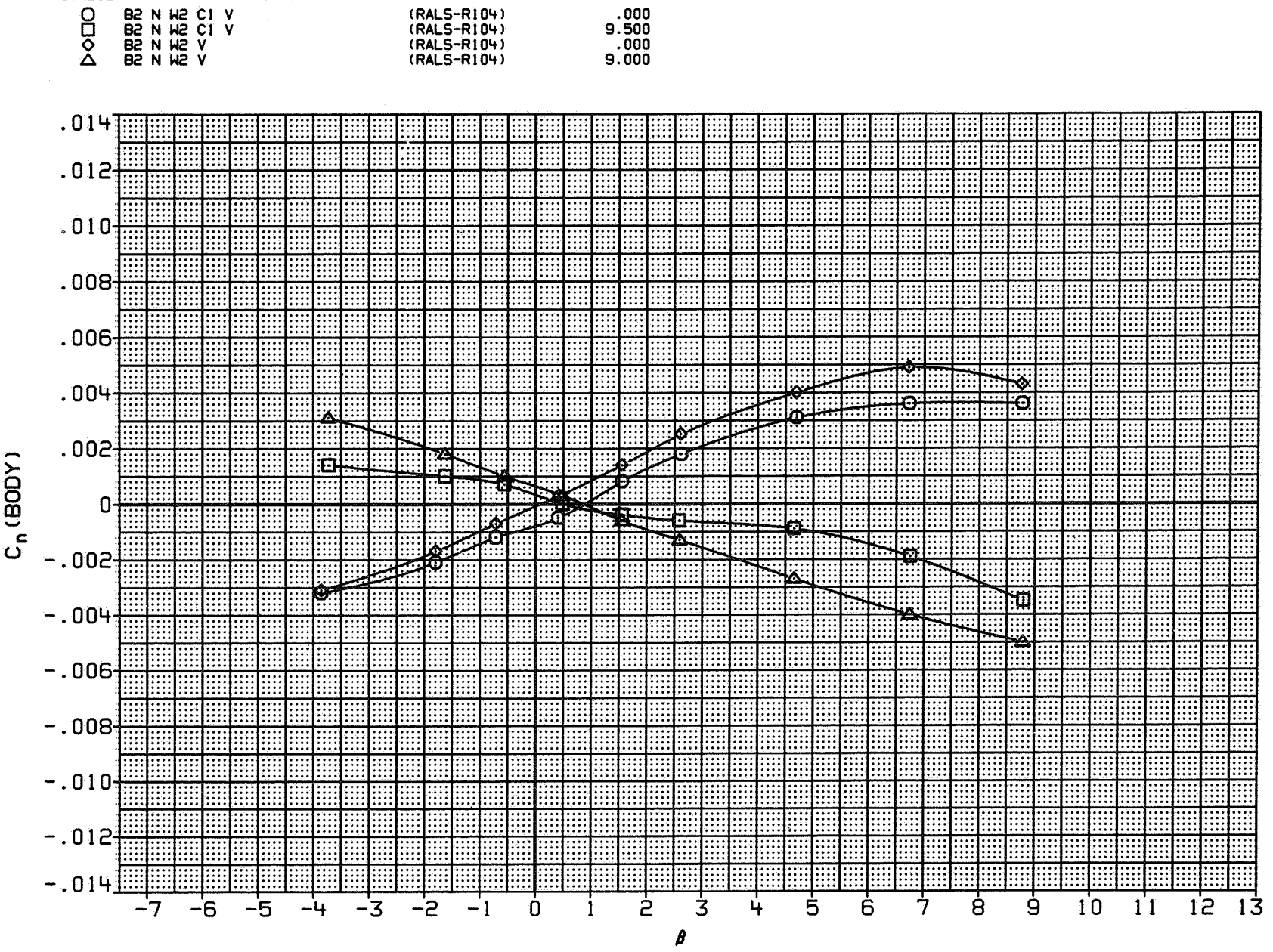


FIG. 59 LATERAL/DIRECTIONAL CHARACTERISTICS, CANARD ON/OFF

MACH = 2.00

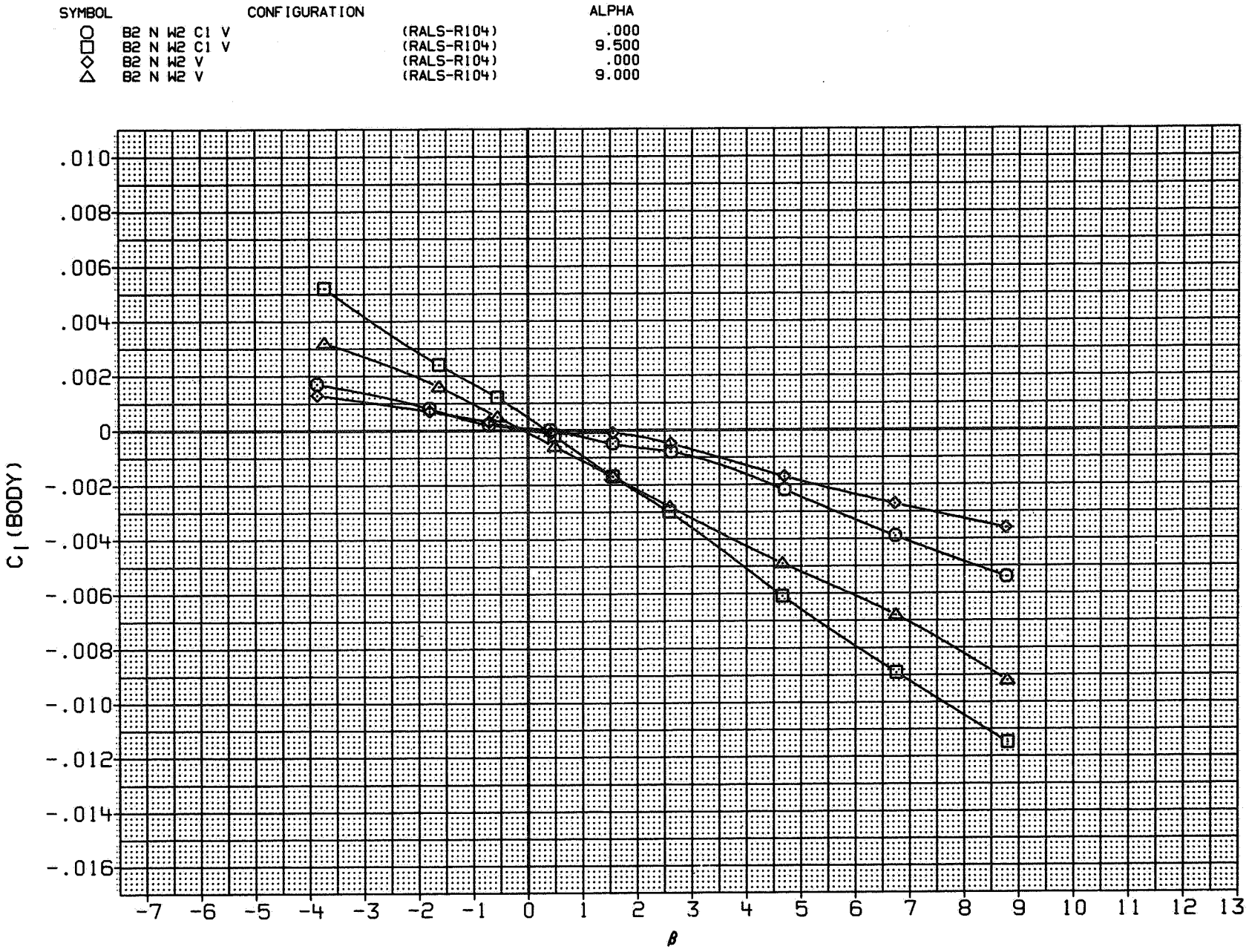


FIG. 59 LATERAL/DIRECTIONAL CHARACTERISTICS, CANARD ON/OFF

MACH = 2.00

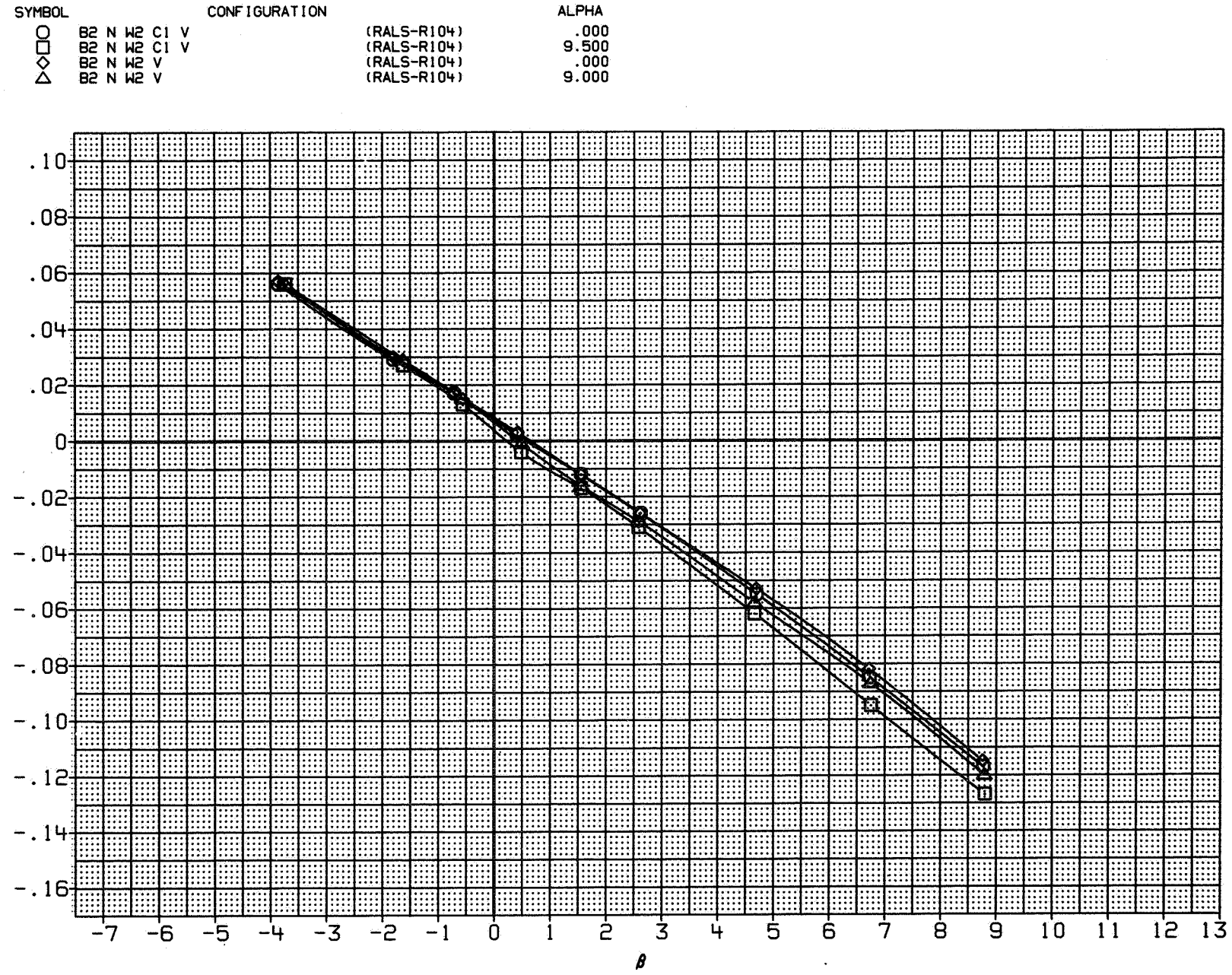


FIG. 59 LATERAL/DIRECTIONAL CHARACTERISTICS, CANARD ON/OFF

MACH = 2.00

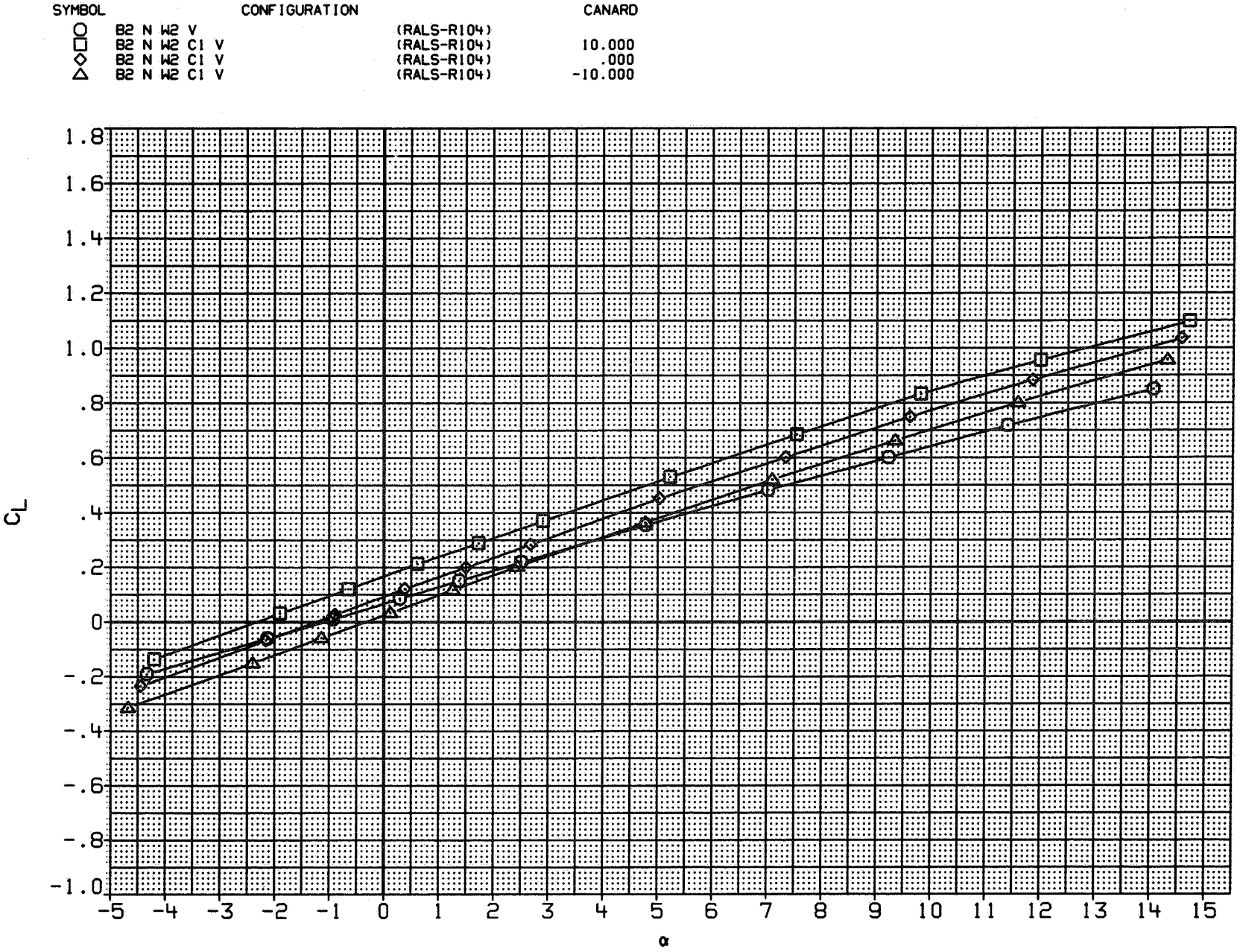


FIG. 60 CANARD INCIDENCE EFFECTS, TE-W = 0 DEGREES

MACH = 1.60

| SYMBOL | CONFIGURATION | | CANARD |
|---|---|---|---|
| ○ | B2 N W2 V | (RALS-R104) | |
| □ | B2 N W2 C1 V | (RALS-R104) | 10.000 |
| ◇ | B2 N W2 C1 V | (RALS-R104) | .000 |
| △ | B2 N W2 C1 V | (RALS-R104) | -10.000 |

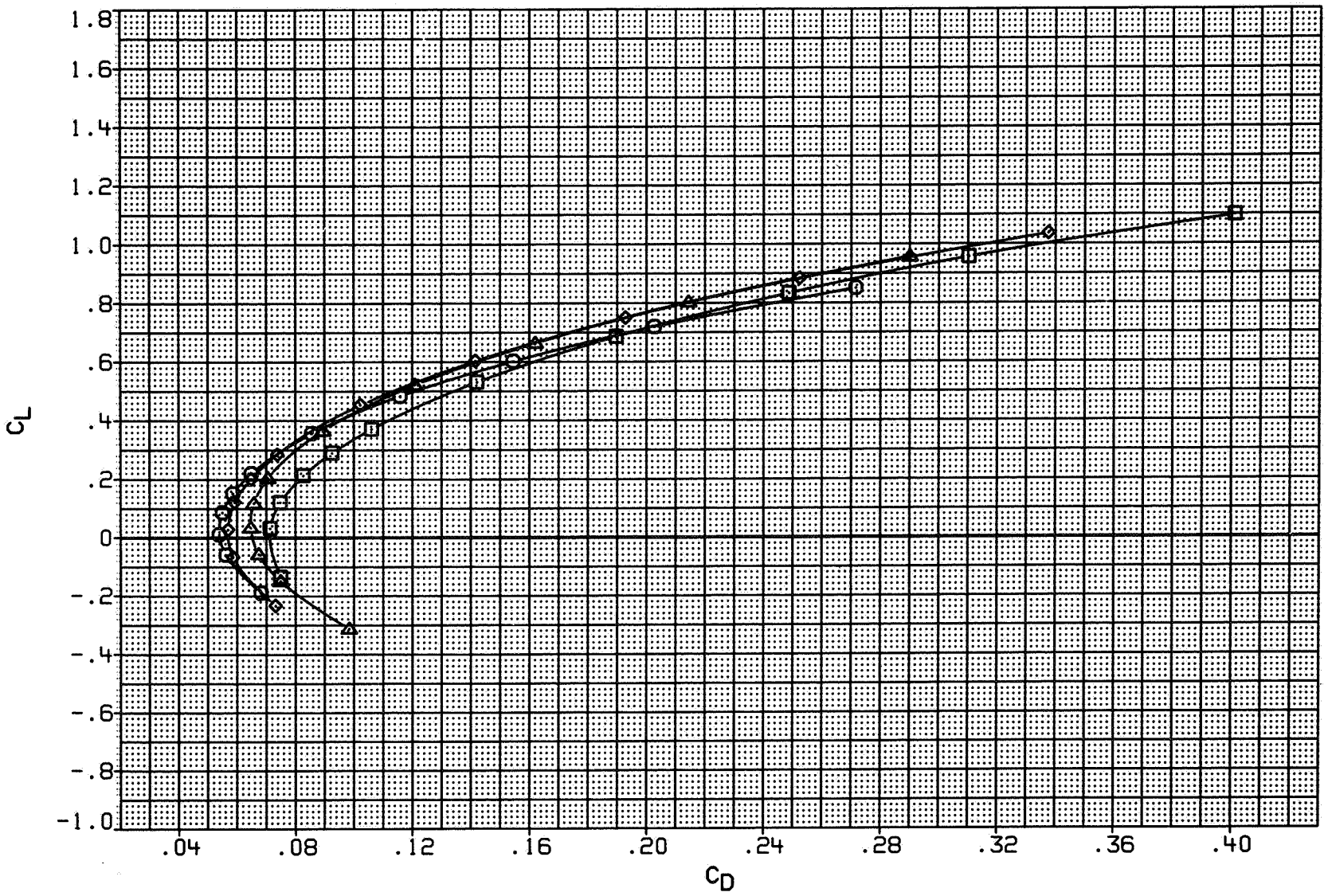


FIG. 60 CANARD INCIDENCE EFFECTS, TE-W = 0 DEGREES

MACH = 1.60

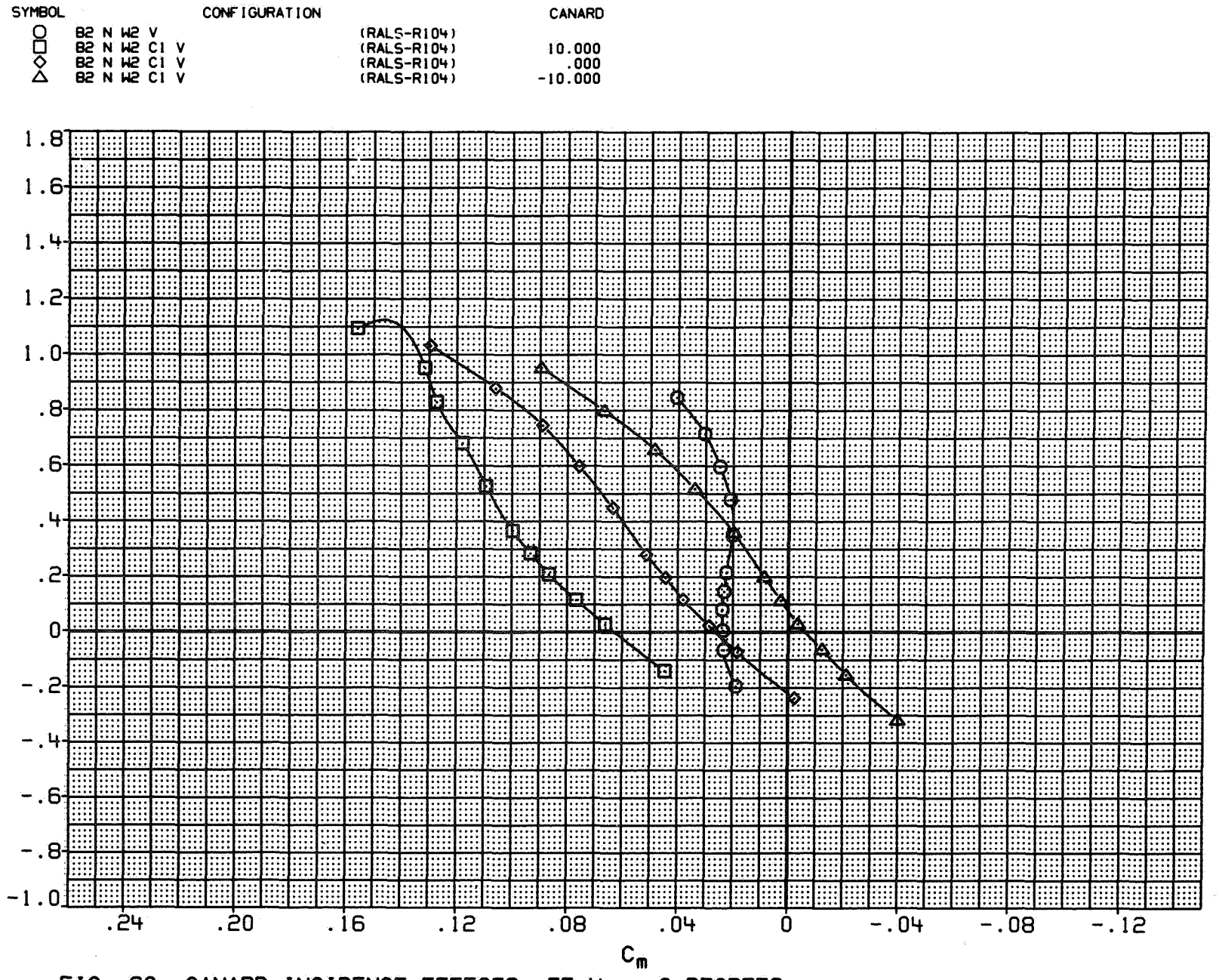


FIG. 60 CANARD INCIDENCE EFFECTS, TE-W = 0 DEGREES

MACH = 1.60

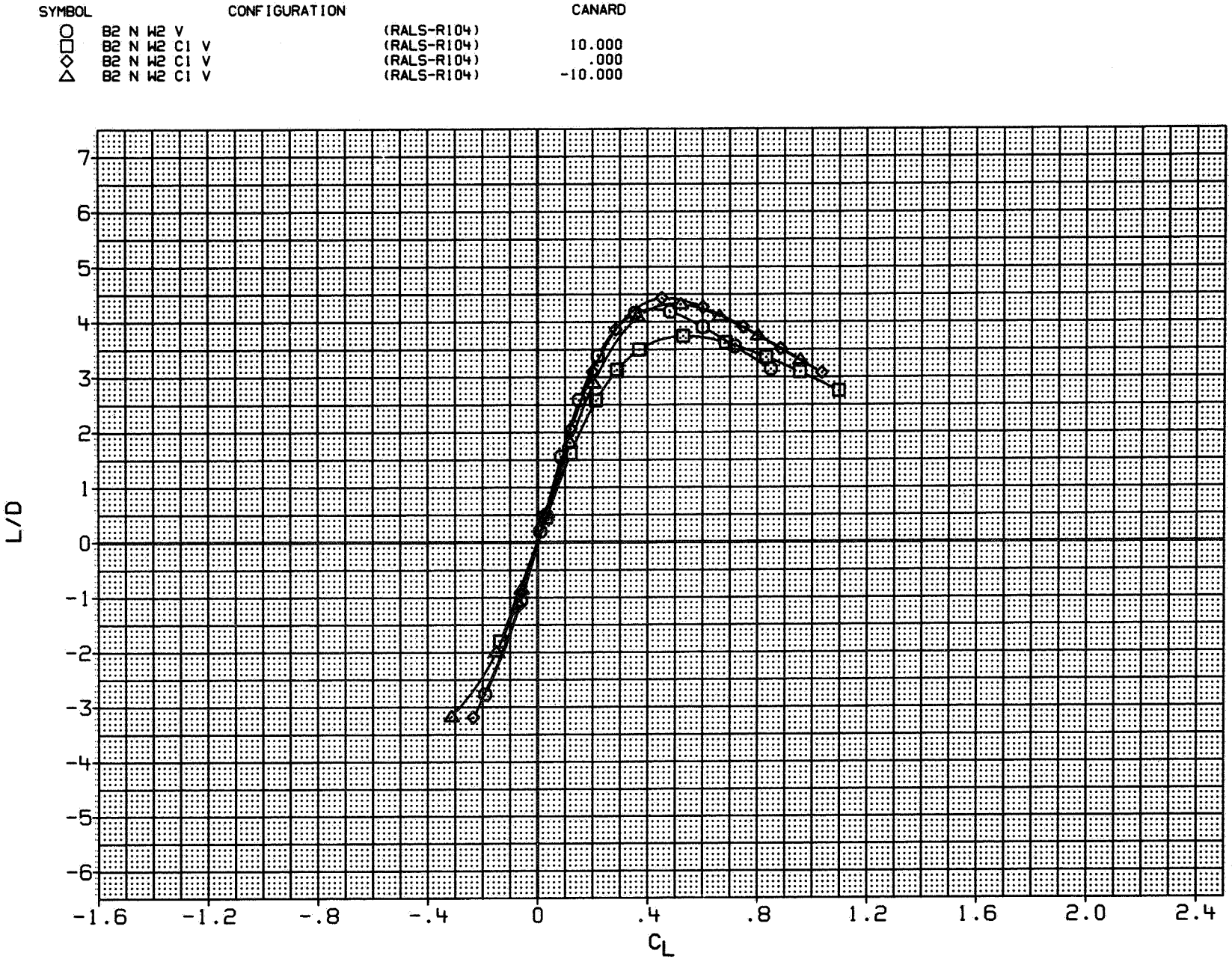


FIG. 60 CANARD INCIDENCE EFFECTS, TE-W = 0 DEGREES

MACH = 1.60

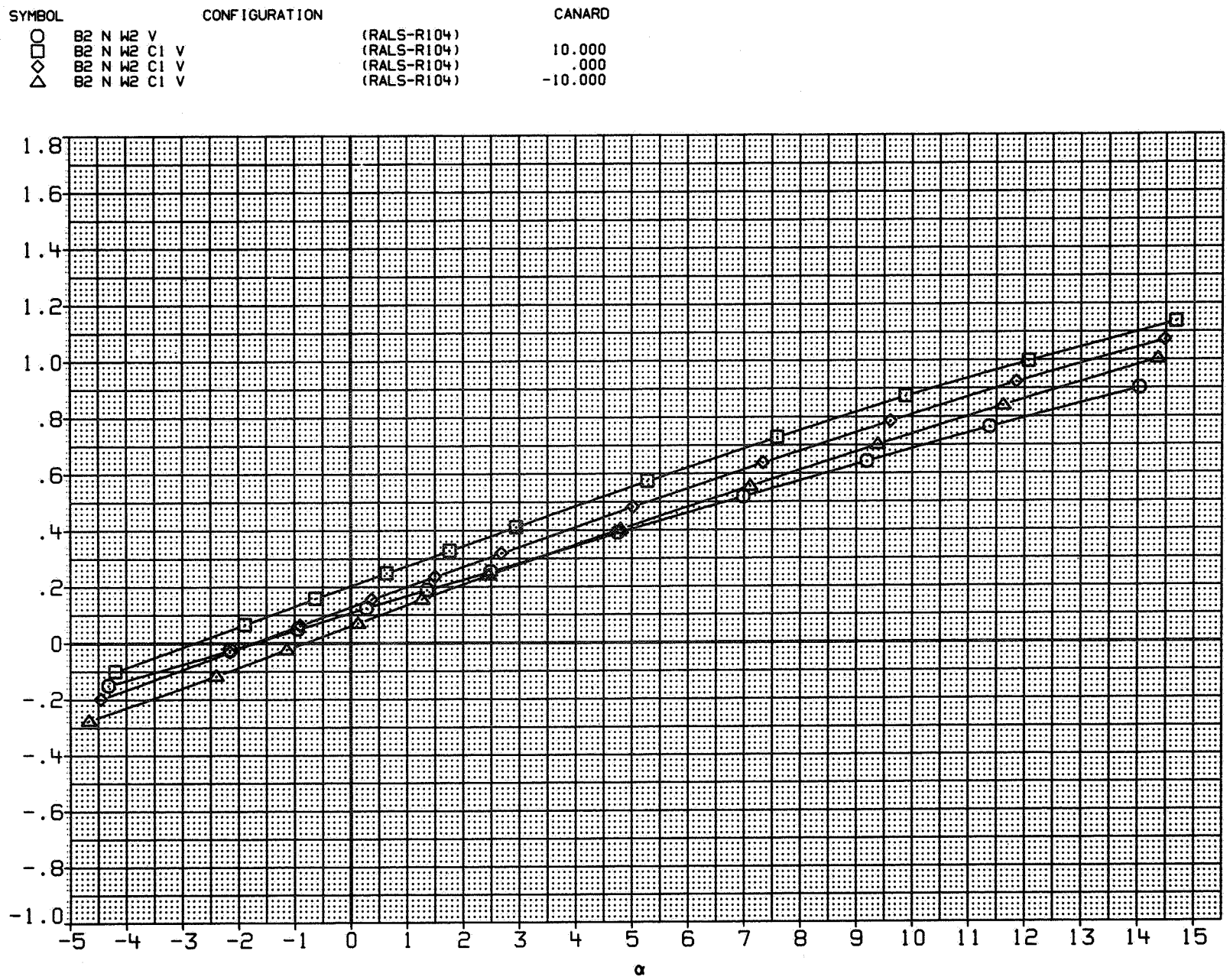


FIG. 61 CANARD INCIDENCE EFFECTS, TE-W = 10 DEGREES

MACH = 1.60

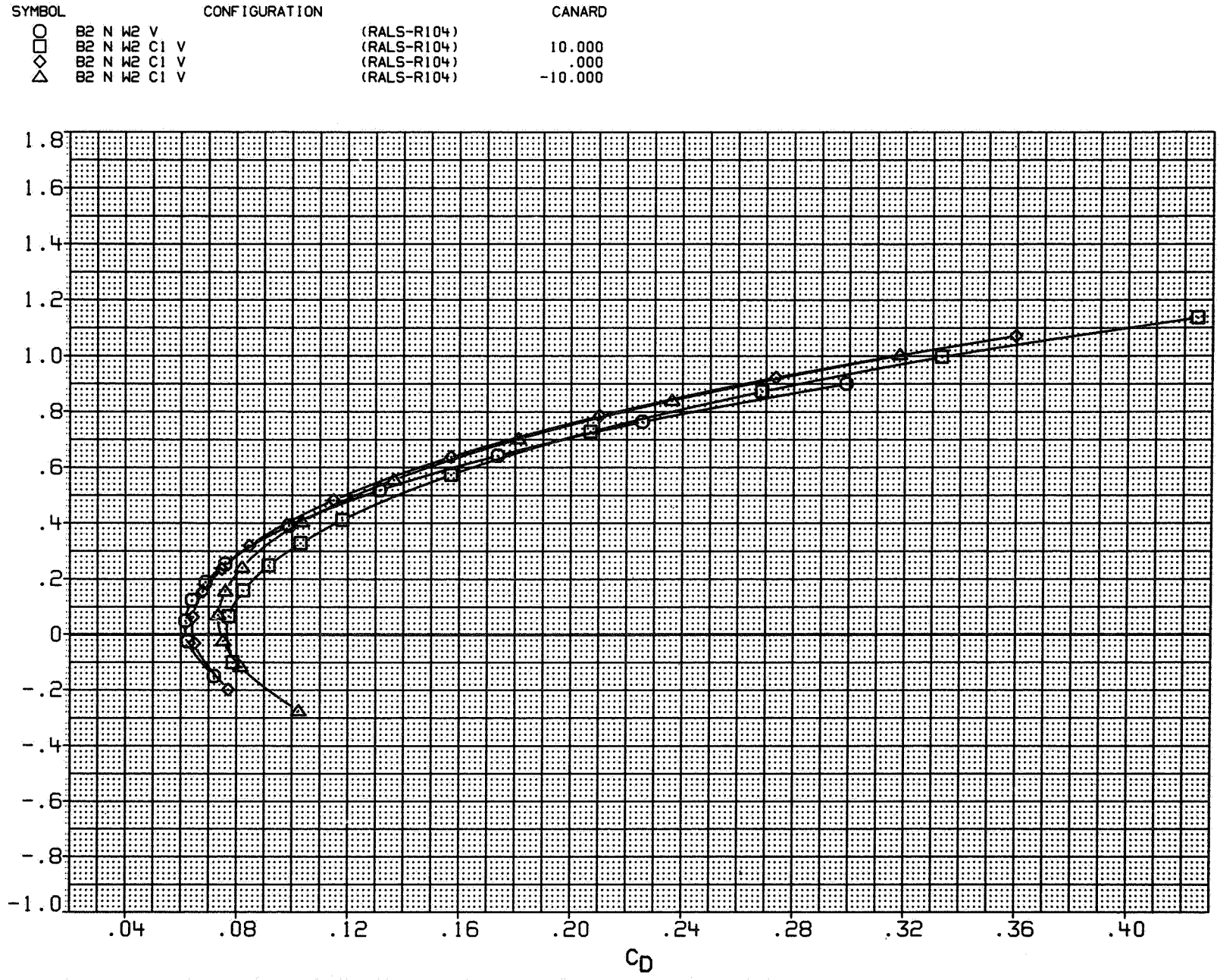


FIG. 61 CANARD INCIDENCE EFFECTS, TE-W = 10 DEGREES

MACH = 1.60

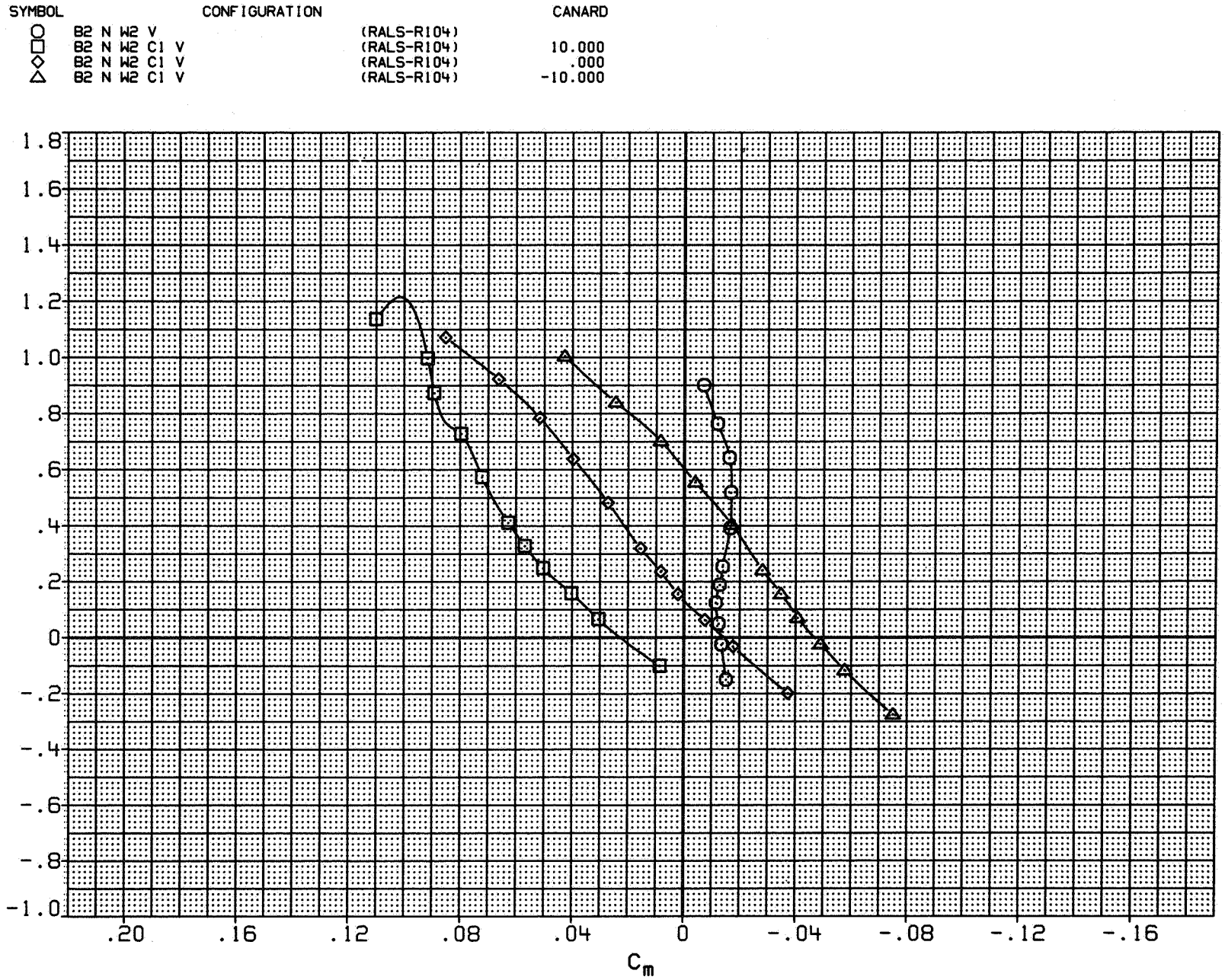


FIG. 61 CANARD INCIDENCE EFFECTS, TE-W = 10 DEGREES

MACH = 1.60

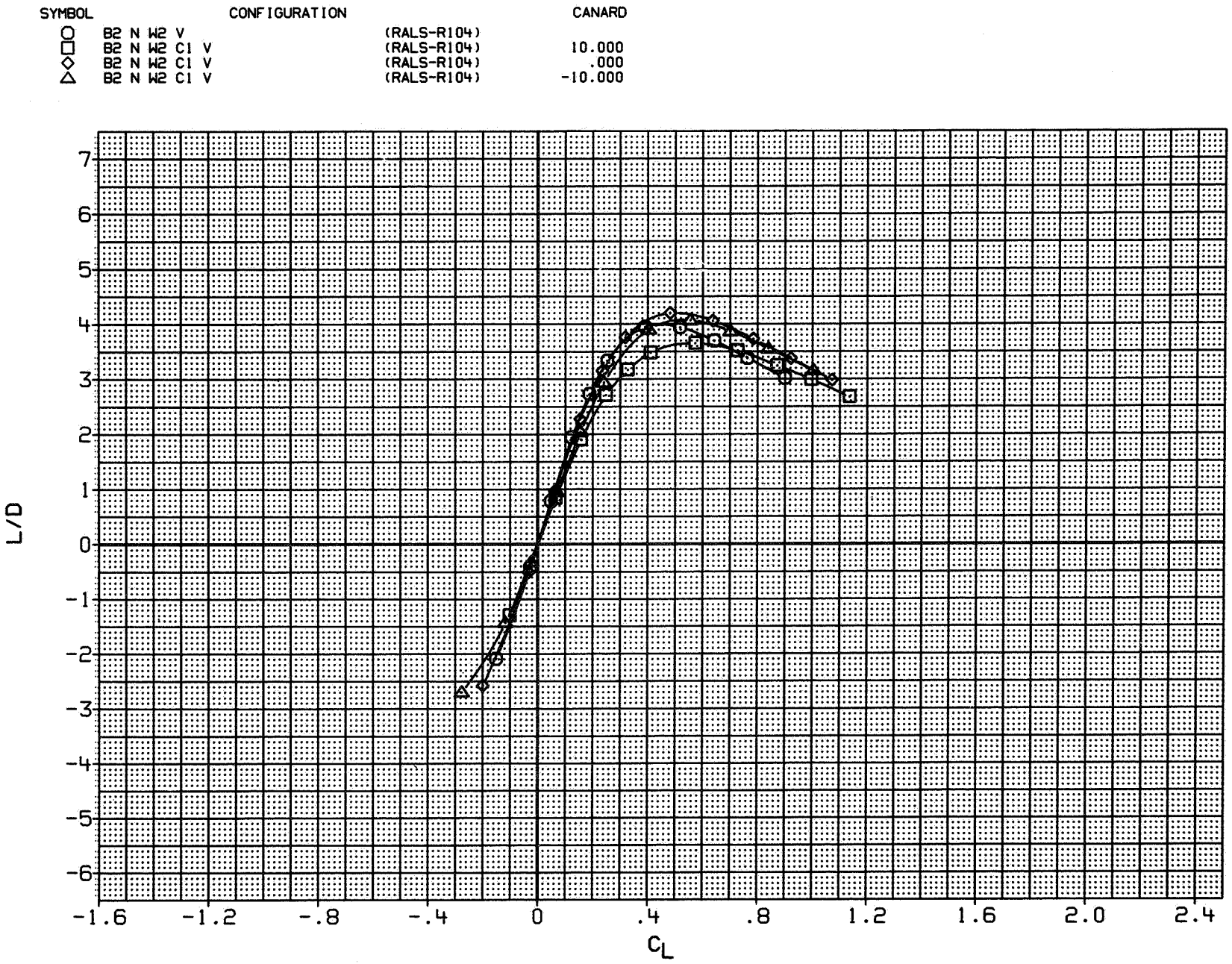


FIG. 61 CANARD INCIDENCE EFFECTS, TE-W = 10 DEGREES

MACH = 1.60

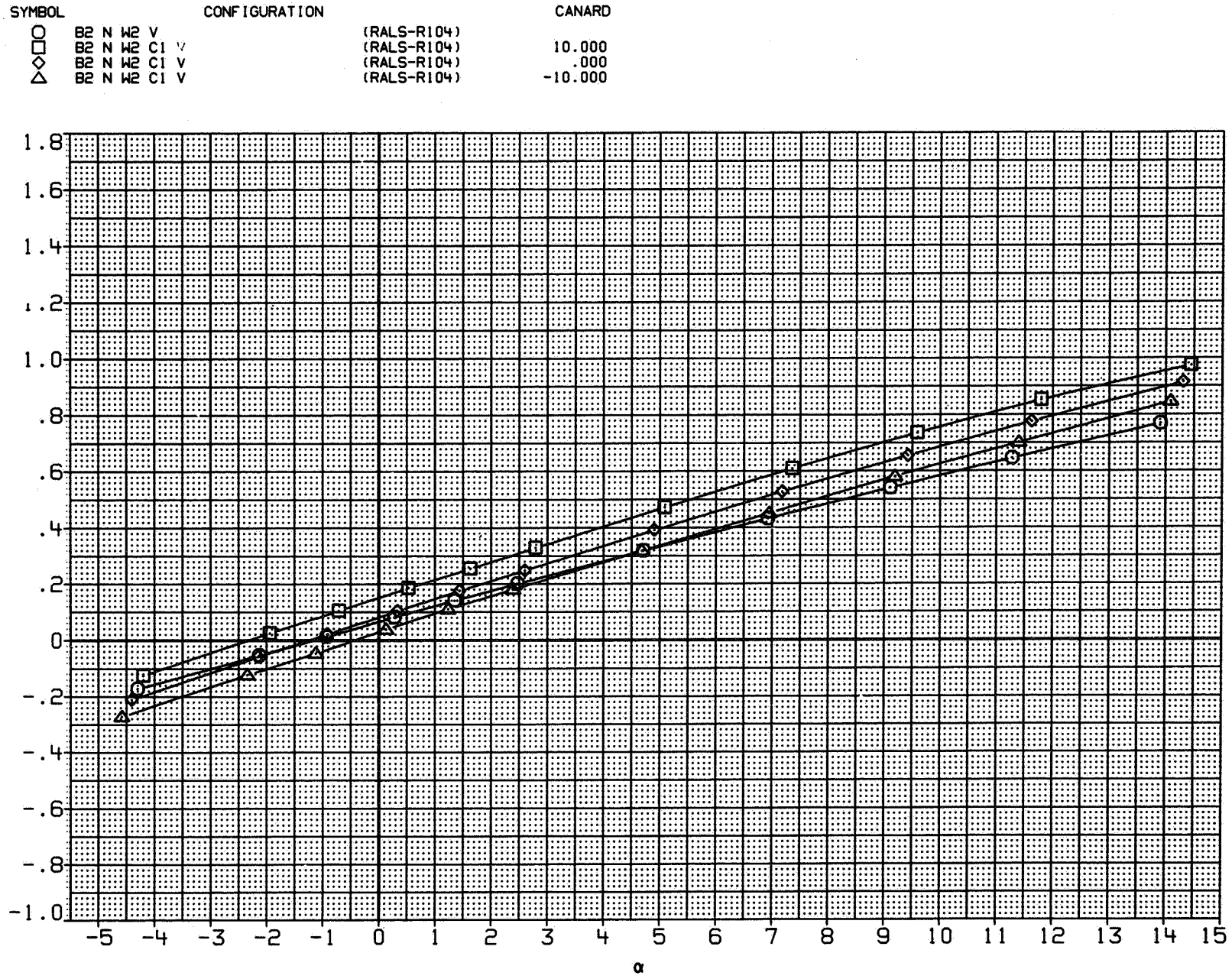


FIG. 62 CANARD INCIDENCE EFFECTS, TE-W = 0 DEGREES

MACH = 1.80

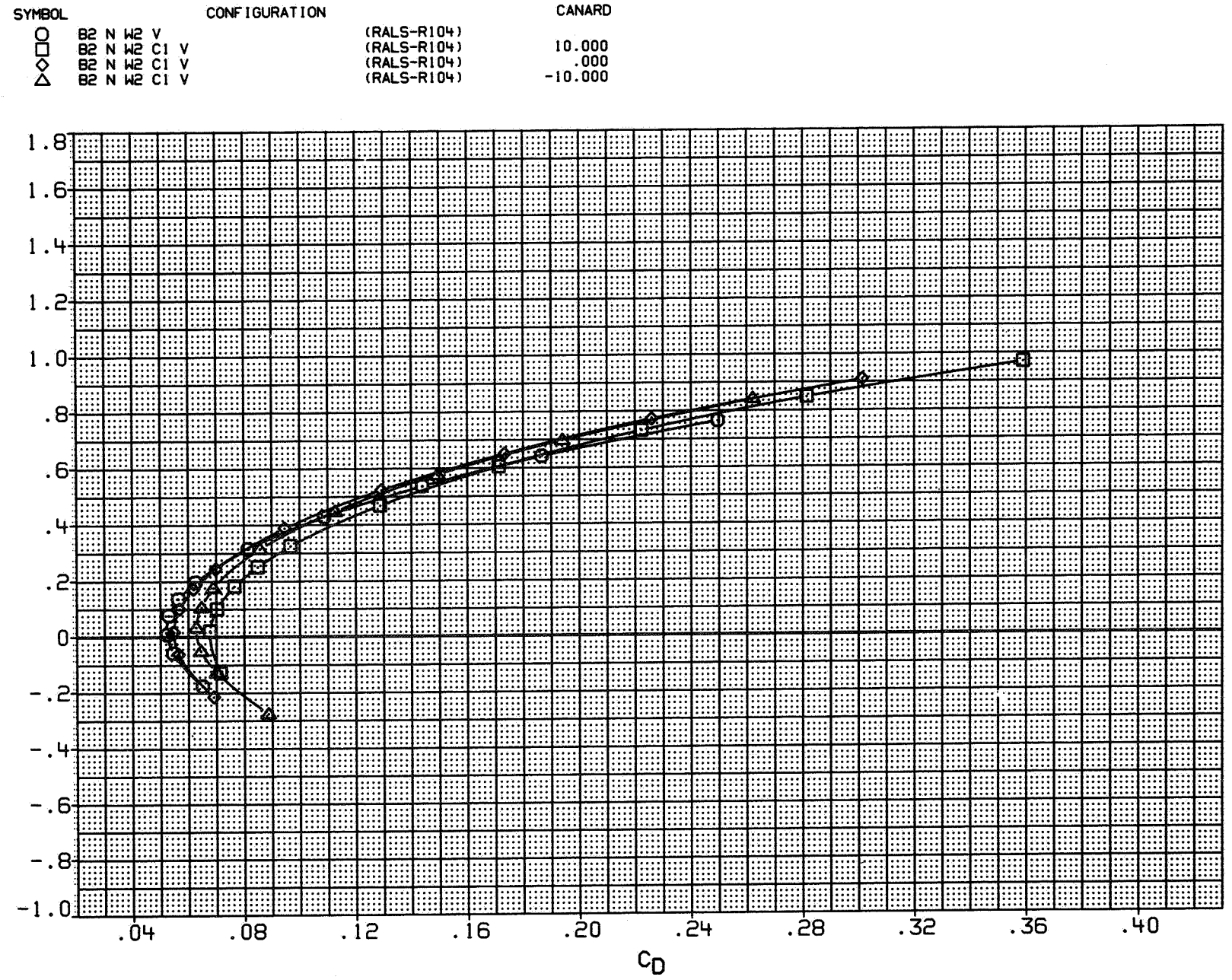


FIG. 62 CANARD INCIDENCE EFFECTS, TE-W = 0 DEGREES

MACH = 1.80

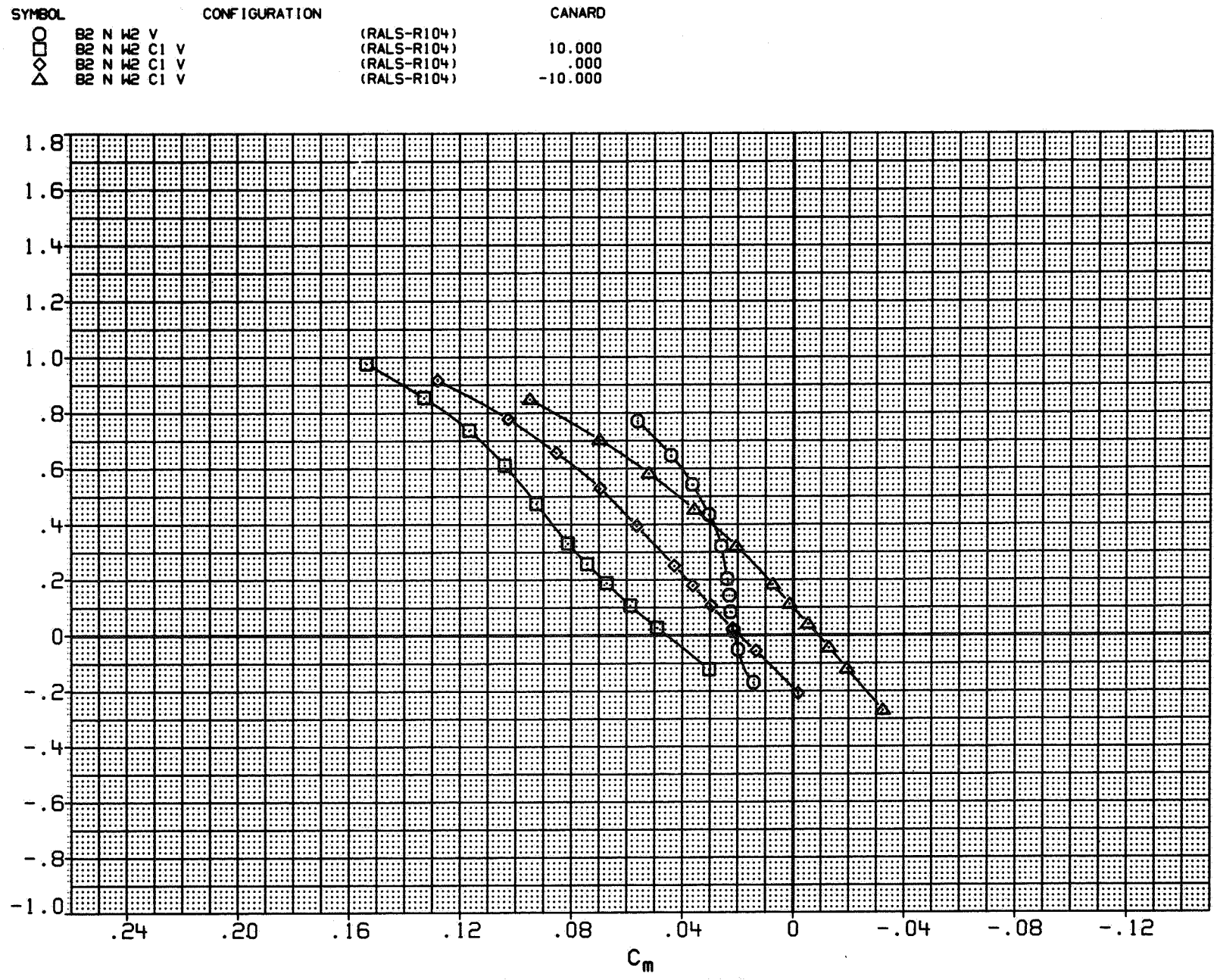


FIG. 62 CANARD INCIDENCE EFFECTS, TE-W = 0 DEGREES

MACH = 1.80

| SYMBOL | CONFIGURATION | | CANARD |
|---|---|---|---|
| ○ | B2 N W2 V | (RALS-R104) | |
| □ | B2 N W2 C1 V | (RALS-R104) | 10.000 |
| ◇ | B2 N W2 C1 V | (RALS-R104) | .000 |
| △ | B2 N W2 C1 V | (RALS-R104) | -10.000 |

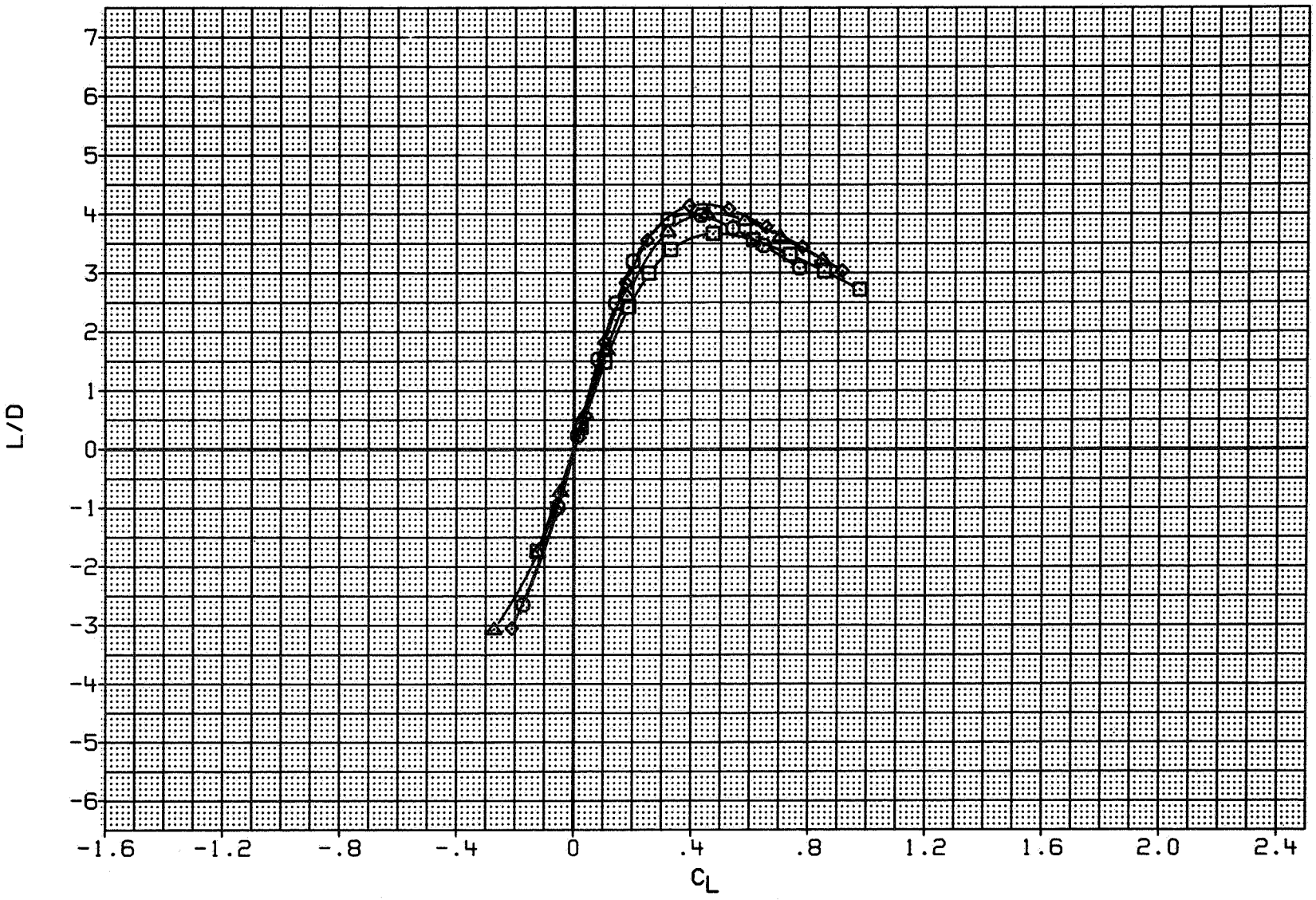


FIG. 62 CANARD INCIDENCE EFFECTS, TE-W = 0 DEGREES

MACH = 1.80

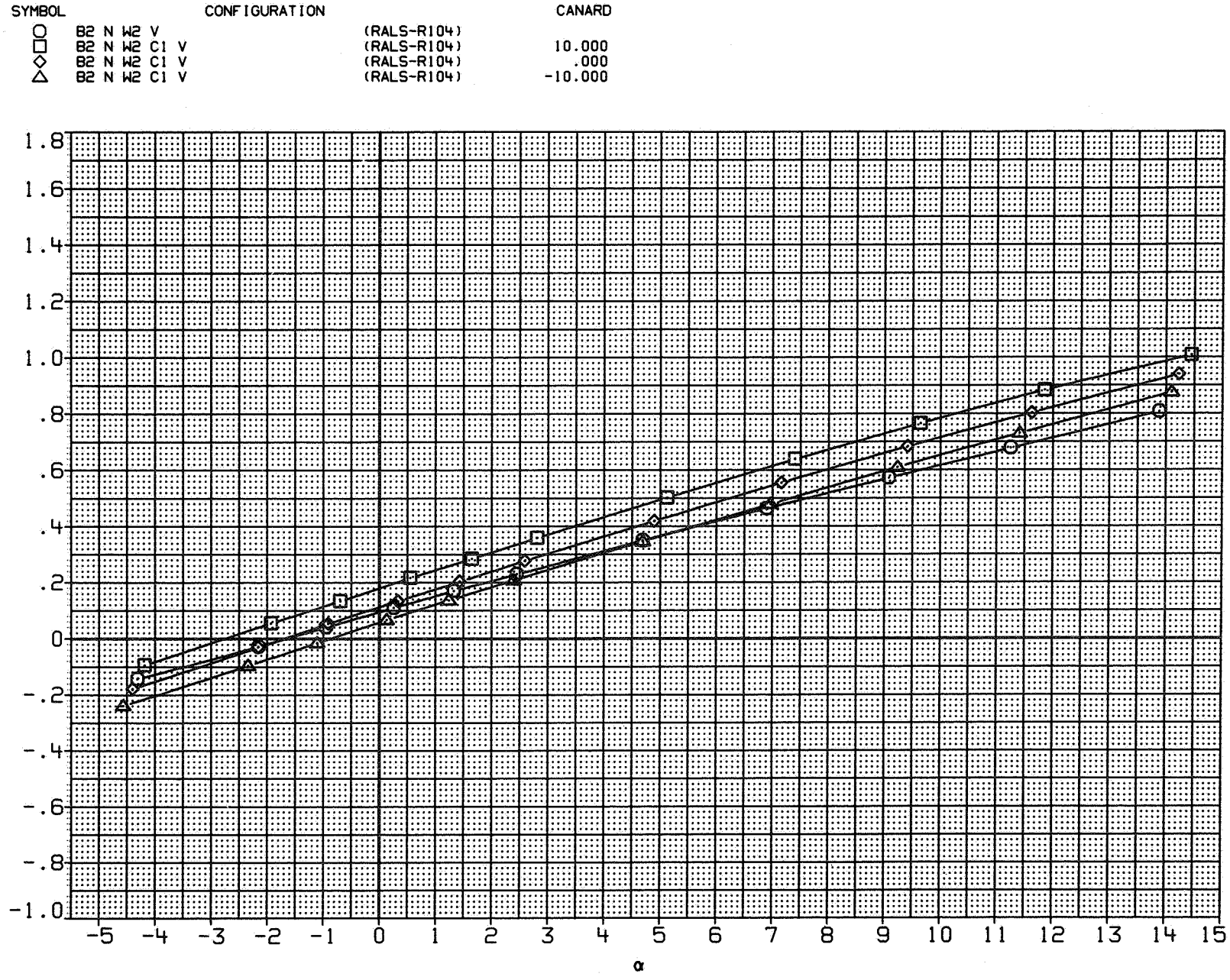


FIG. 63 CANARD INCIDENCE EFFECTS, TE-W = 10 DEGREES

MACH = 1.80

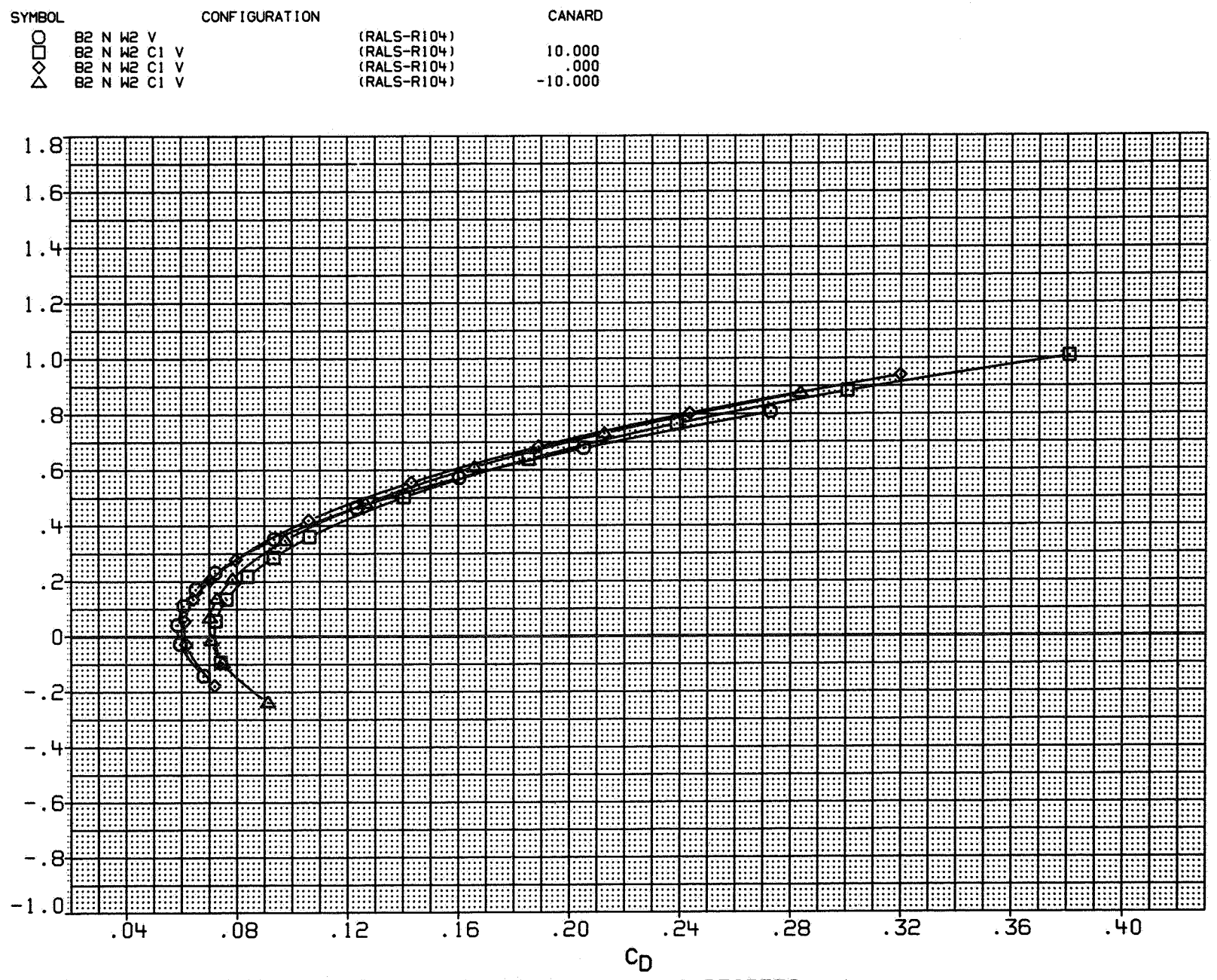


FIG. 63 CANARD INCIDENCE EFFECTS, TE-W = 10 DEGREES

MACH = 1.80

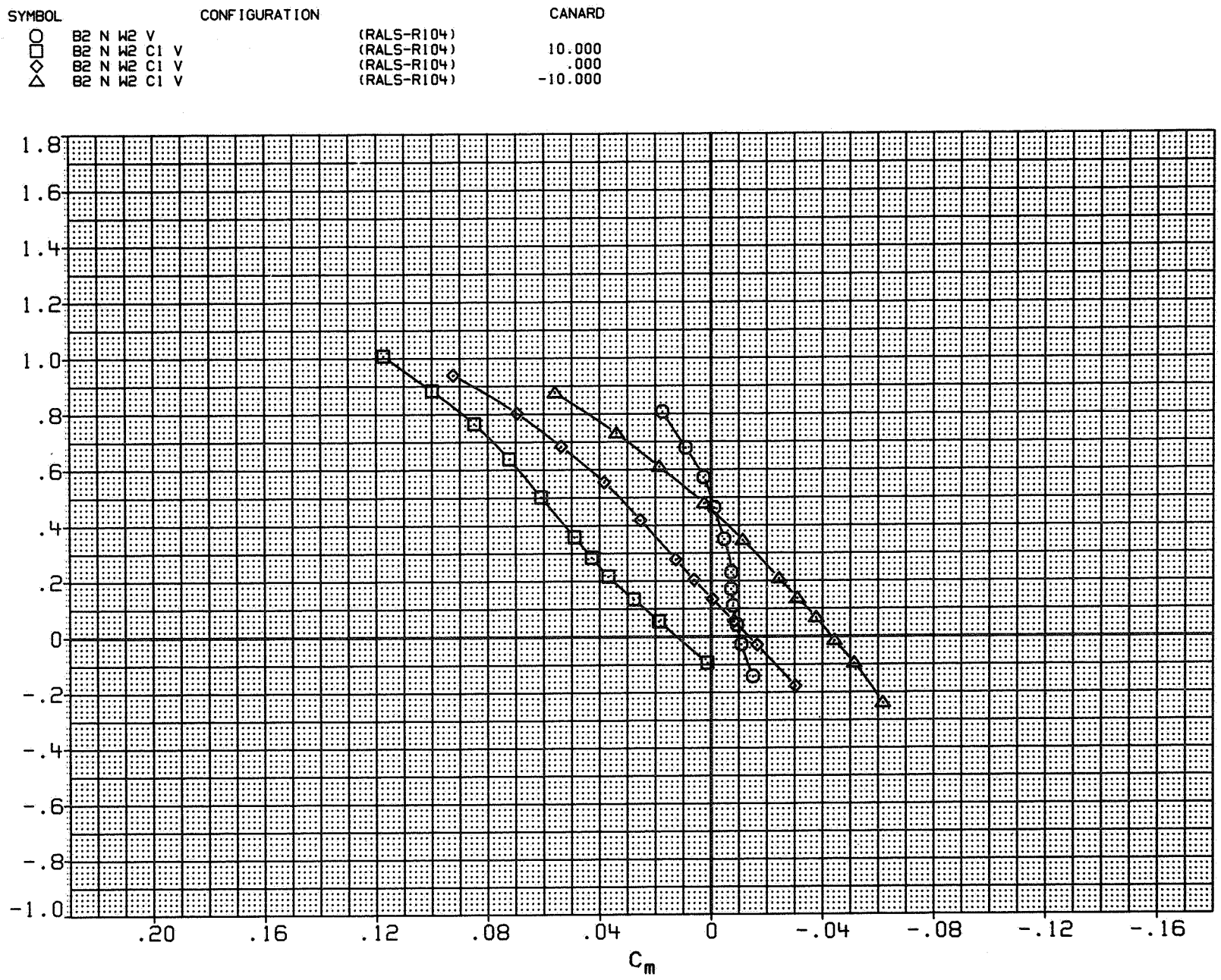


FIG. 63 CANARD INCIDENCE EFFECTS, TE-W = 10 DEGREES

MACH = 1.80

| SYMBOL | CONFIGURATION | | CANARD |
|---|---|---|---|
| ○ | B2 N W2 V | (RALS-R104) | |
| □ | B2 N W2 C1 V | (RALS-R104) | 10.000 |
| ◇ | B2 N W2 C1 V | (RALS-R104) | .000 |
| △ | B2 N W2 C1 V | (RALS-R104) | -10.000 |

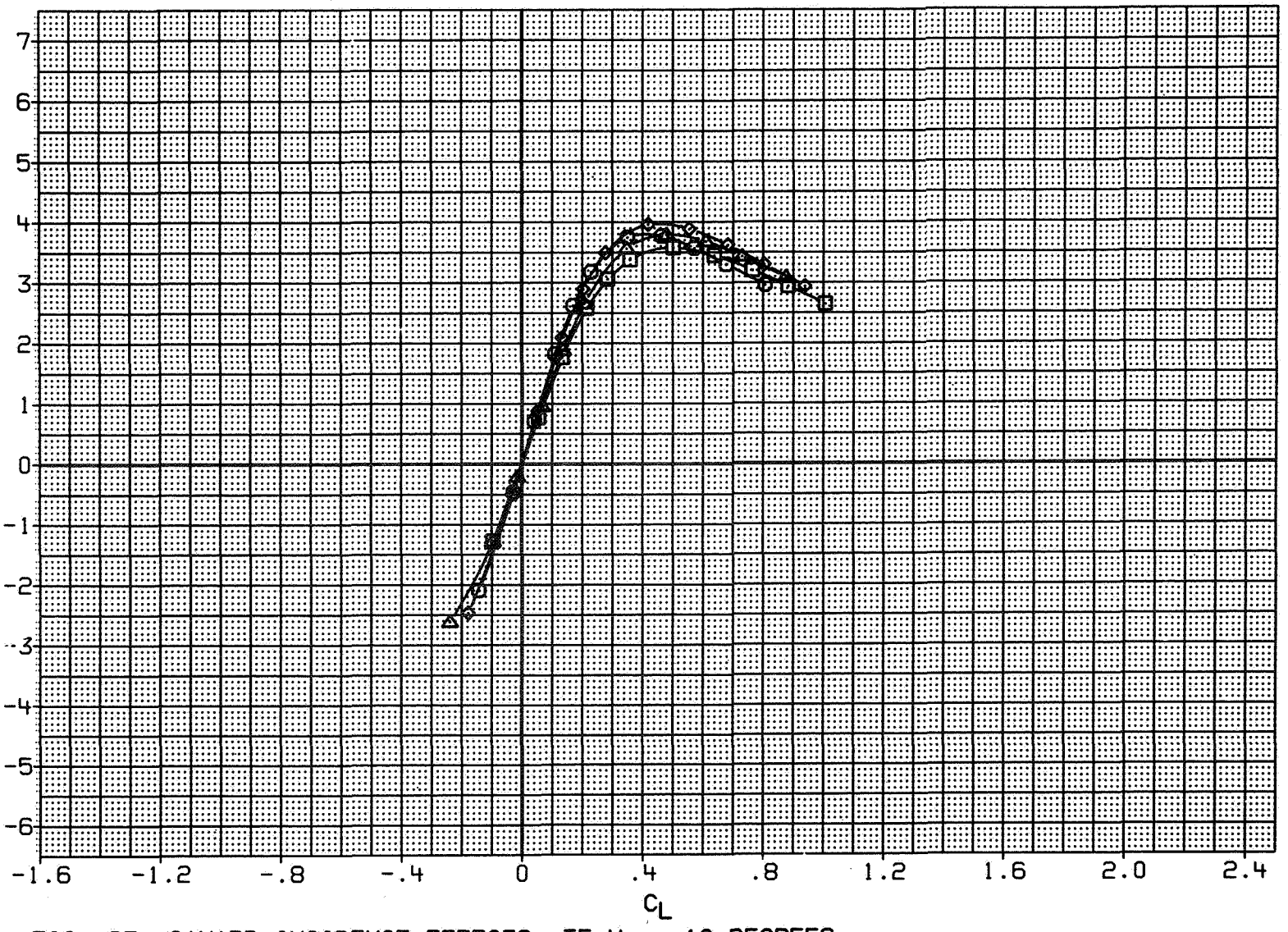


FIG. 63 CANARD INCIDENCE EFFECTS, TE-W = 10 DEGREES

MACH = 1.80

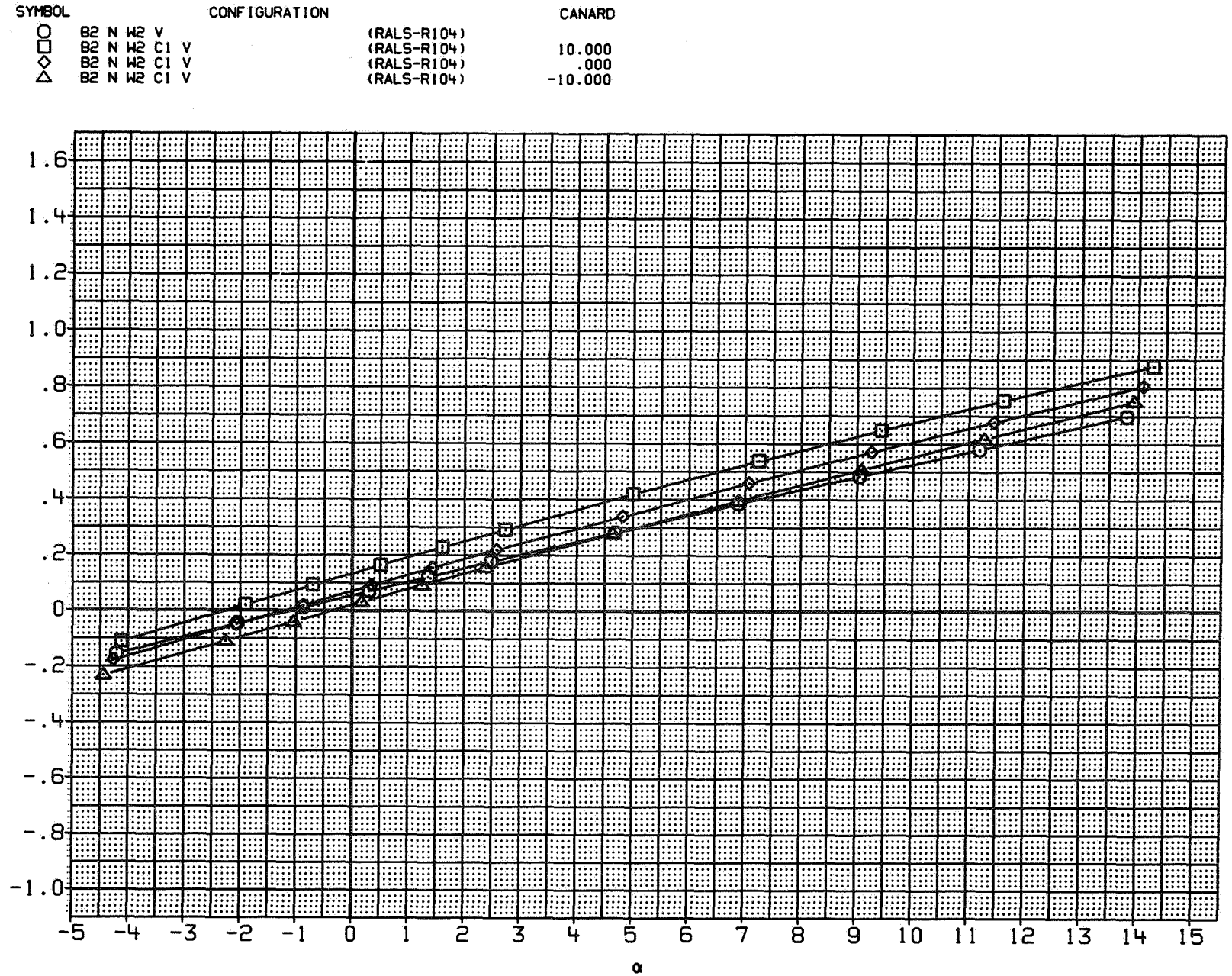


FIG. 64 CANARD INCIDENCE EFFECTS, TE-W = 0 DEGREES

MACH = 2.00

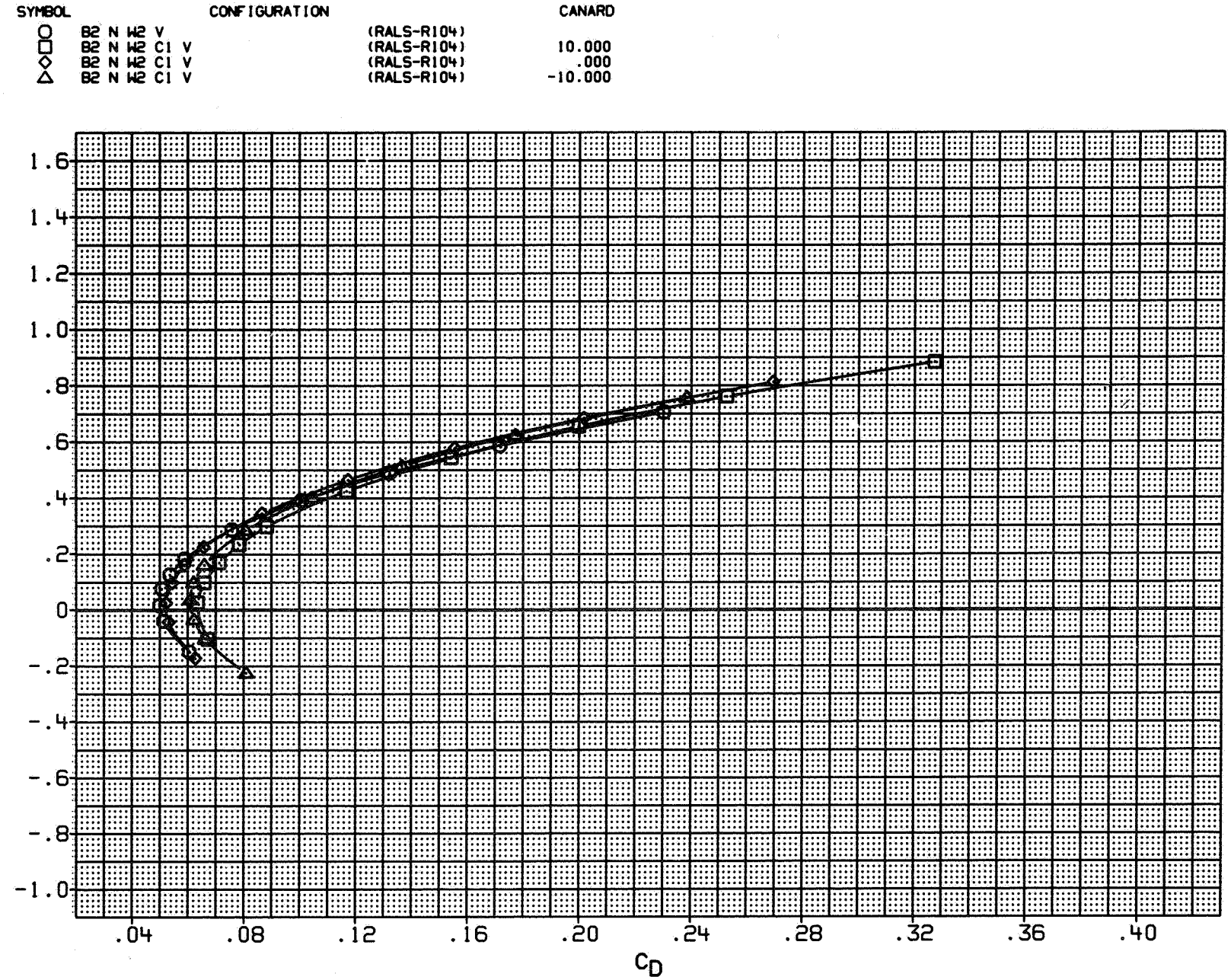


FIG. 64 CANARD INCIDENCE EFFECTS, TE-W = 0 DEGREES

MACH = 2.00

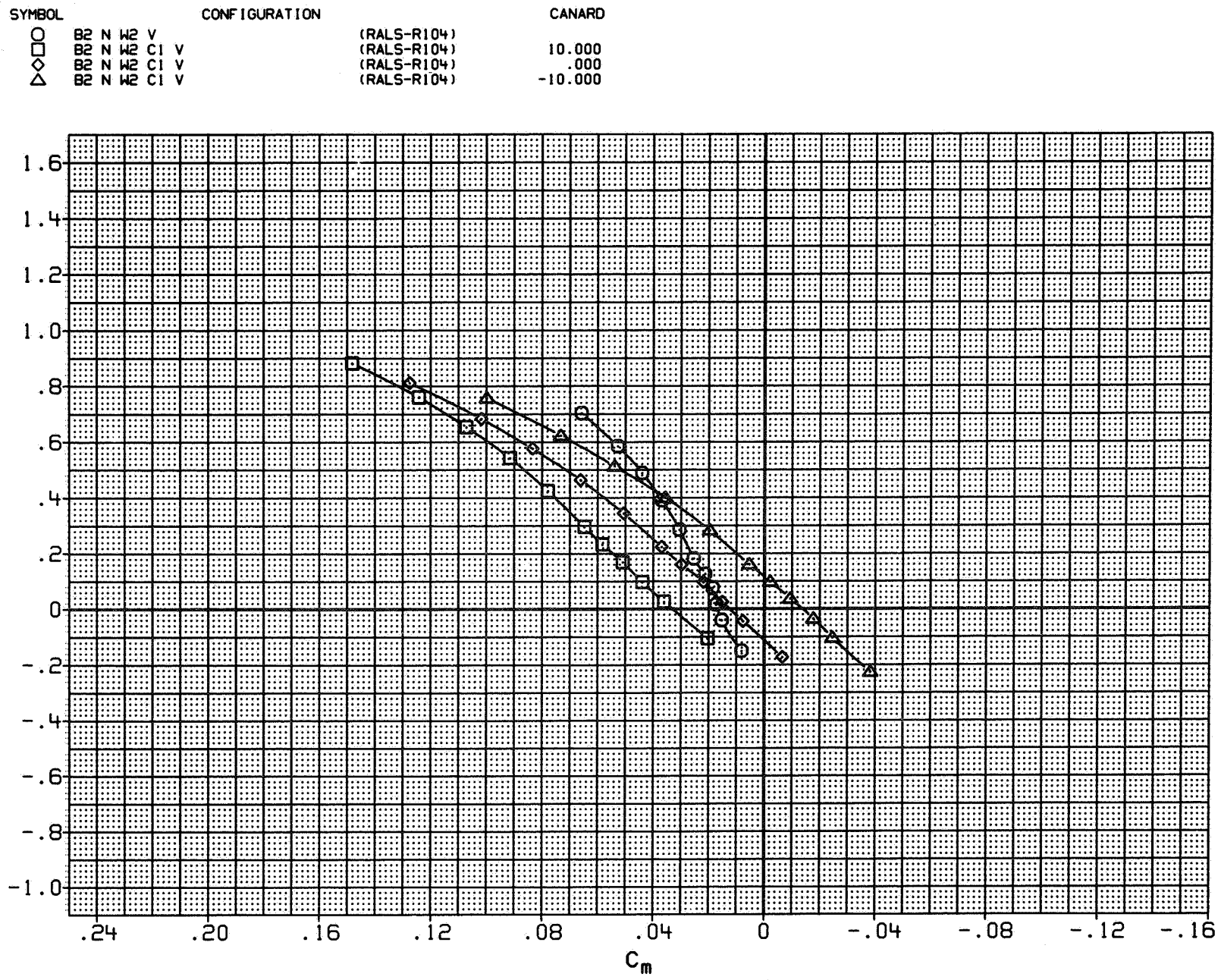


FIG. 64 CANARD INCIDENCE EFFECTS, TE-W = 0 DEGREES

MACH = 2.00

| SYMBOL | CONFIGURATION | | CANARD |
|---|---|---|---|
| ○ | B2 N W2 V | (RALS-R104) | |
| □ | B2 N W2 C1 V | (RALS-R104) | 10.000 |
| ◇ | B2 N W2 C1 V | (RALS-R104) | .000 |
| △ | B2 N W2 C1 V | (RALS-R104) | -10.000 |

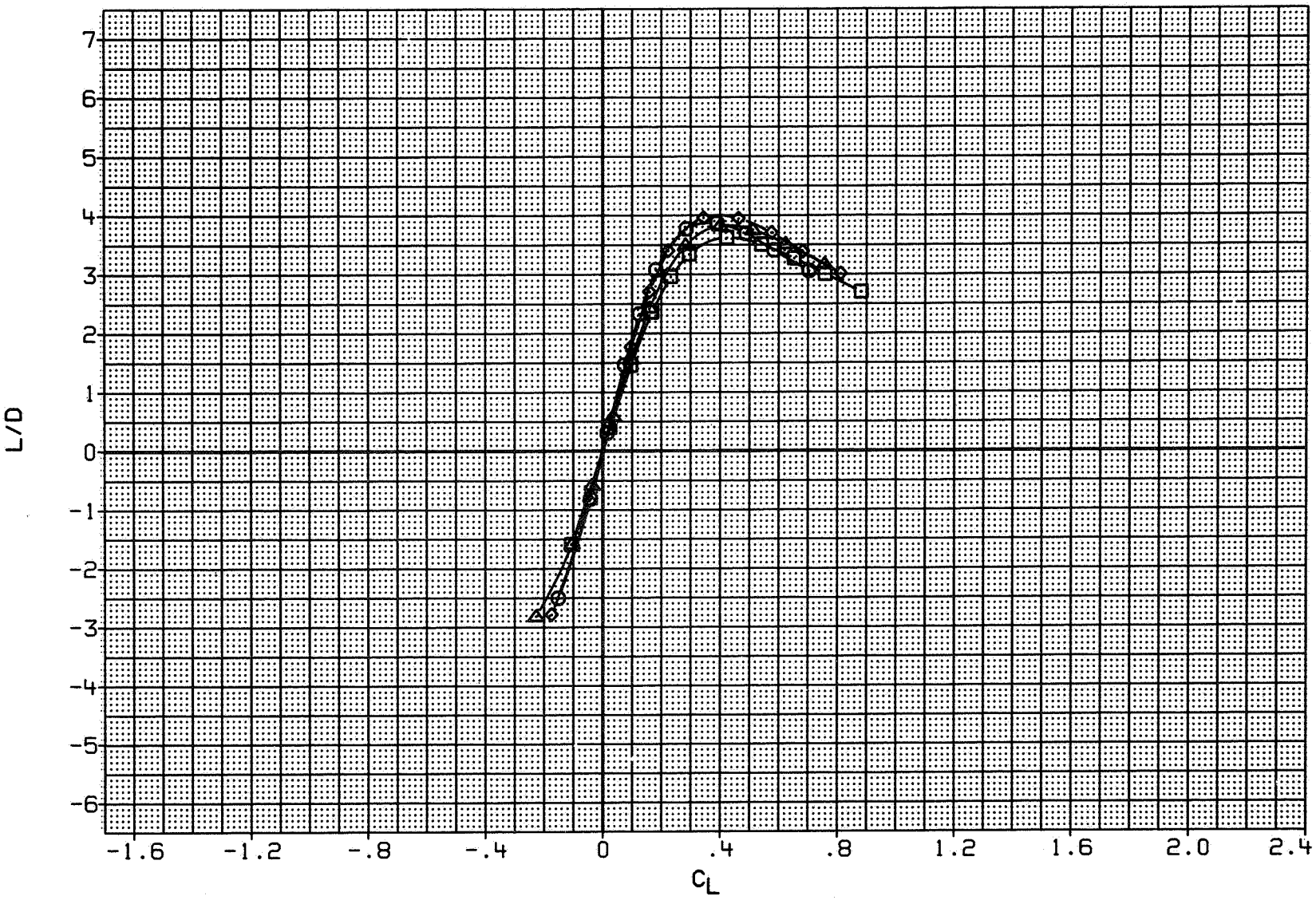


FIG. 64 CANARD INCIDENCE EFFECTS, TE-W = 0 DEGREES

MACH = 2.00

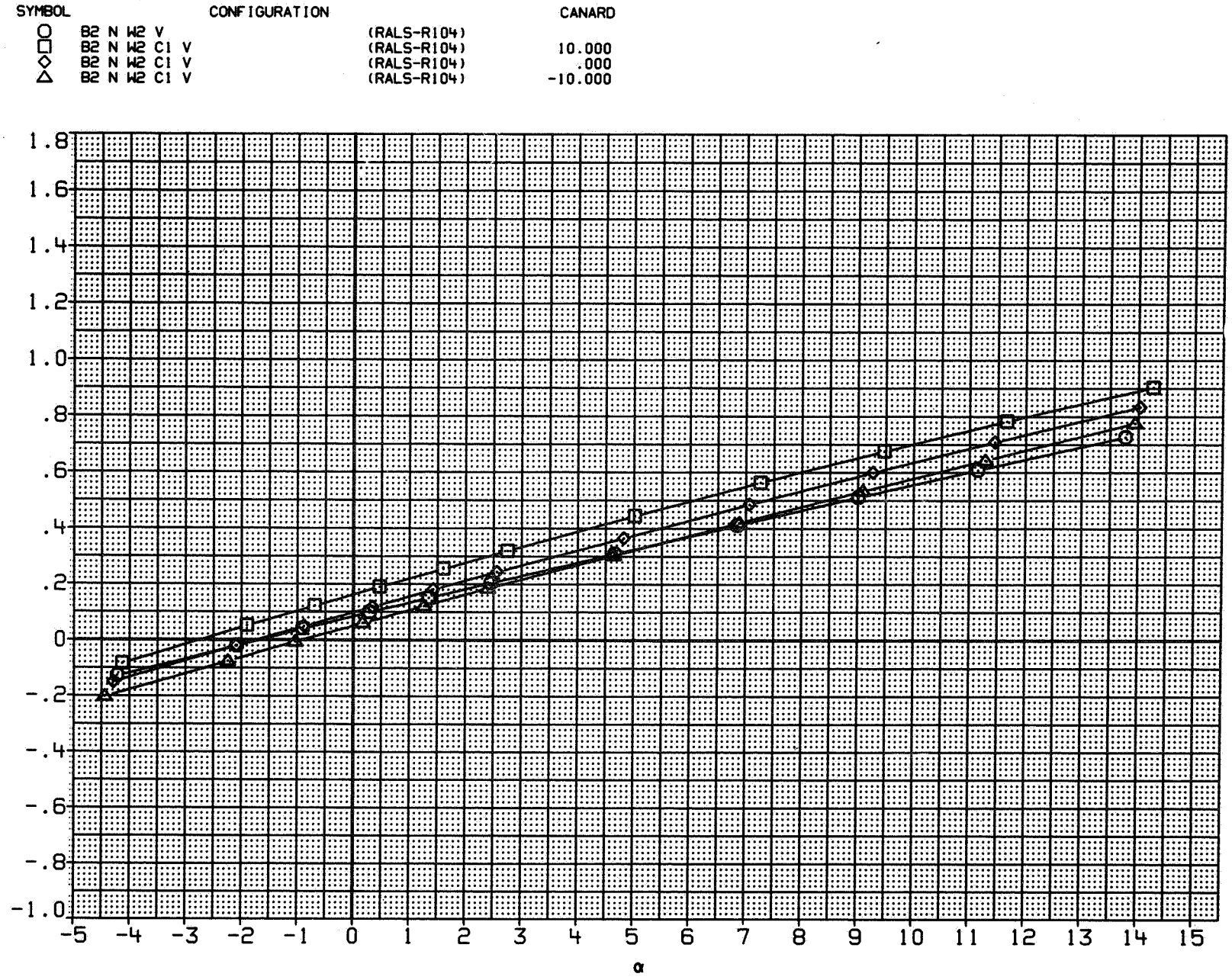


FIG. 65 CANARD INCIDENCE EFFECTS, TE-W = 10 DEGREES

MACH = 2.00

| SYMBOL | CONFIGURATION | | CANARD |
|---|---|---|---|
| ○ | B2 N W2 V | (RALS-R104) | |
| □ | B2 N W2 C1 V | (RALS-R104) | 10.000 |
| ◇ | B2 N W2 C1 V | (RALS-R104) | .000 |
| △ | B2 N W2 C1 V | (RALS-R104) | -10.000 |

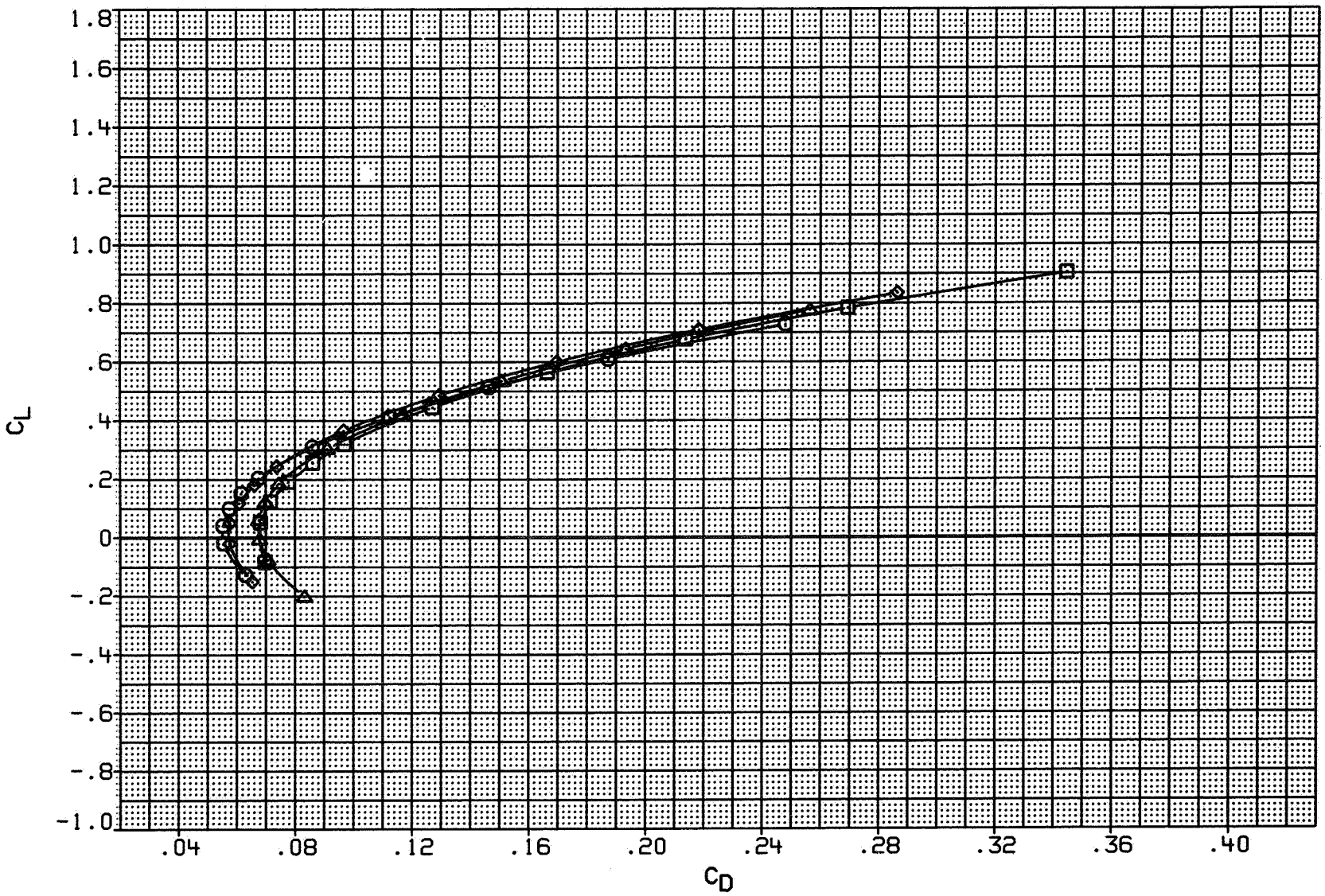


FIG. 65 CANARD INCIDENCE EFFECTS, TE-W = 10 DEGREES

MACH = 2.00

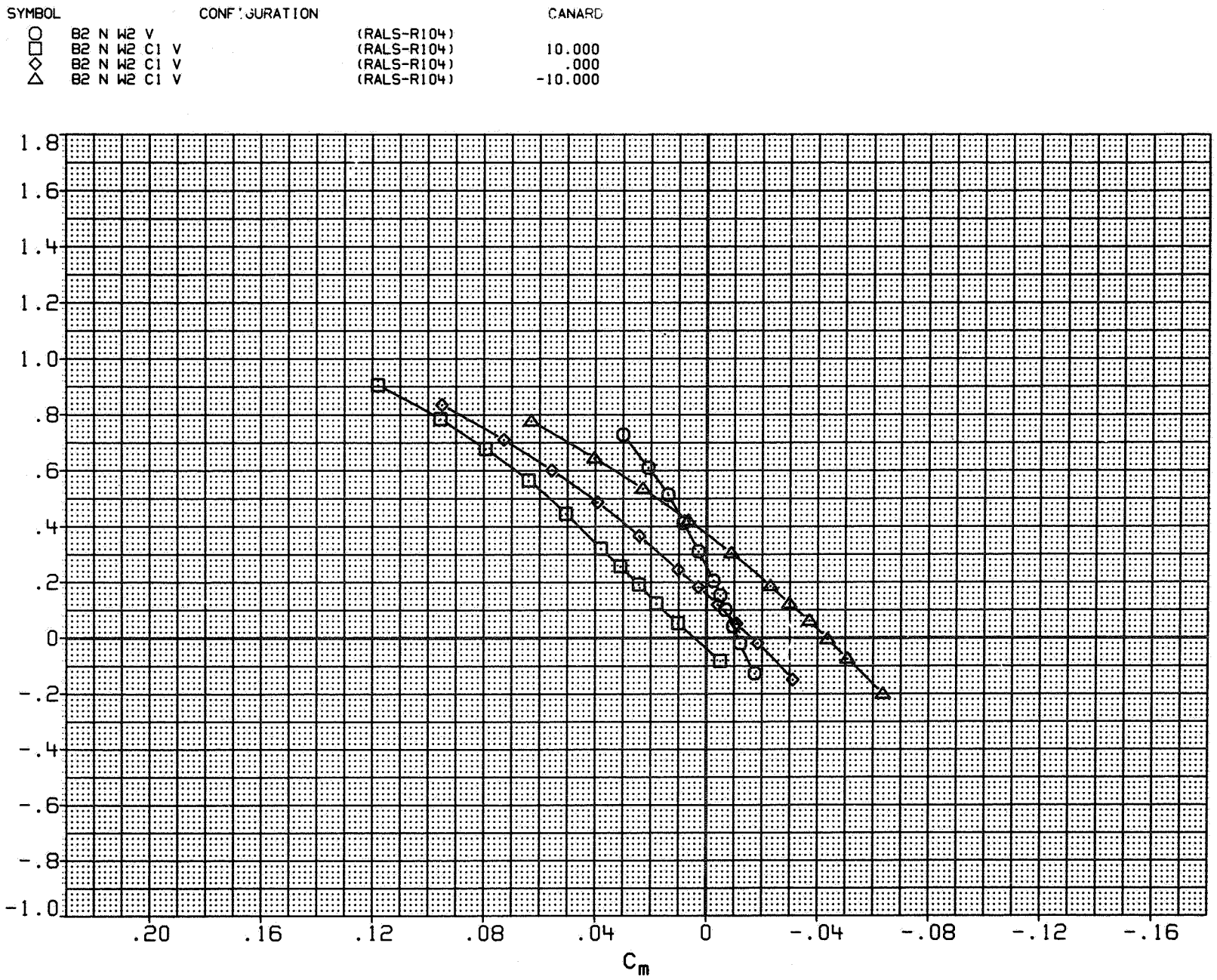


FIG. 65 CANARD INCIDENCE EFFECTS, TE-W = 10 DEGREES

MACH = 2.00

| SYMBOL | CONFIGURATION | | CANARD |
|---|---|---|---|
| ○ | B2 N W2 V | (RALS-R104) | |
| □ | B2 N W2 C1 V | (RALS-R104) | 10.000 |
| ◇ | B2 N W2 C1 V | (RALS-R104) | .000 |
| △ | B2 N W2 C1 V | (RALS-R104) | -10.000 |

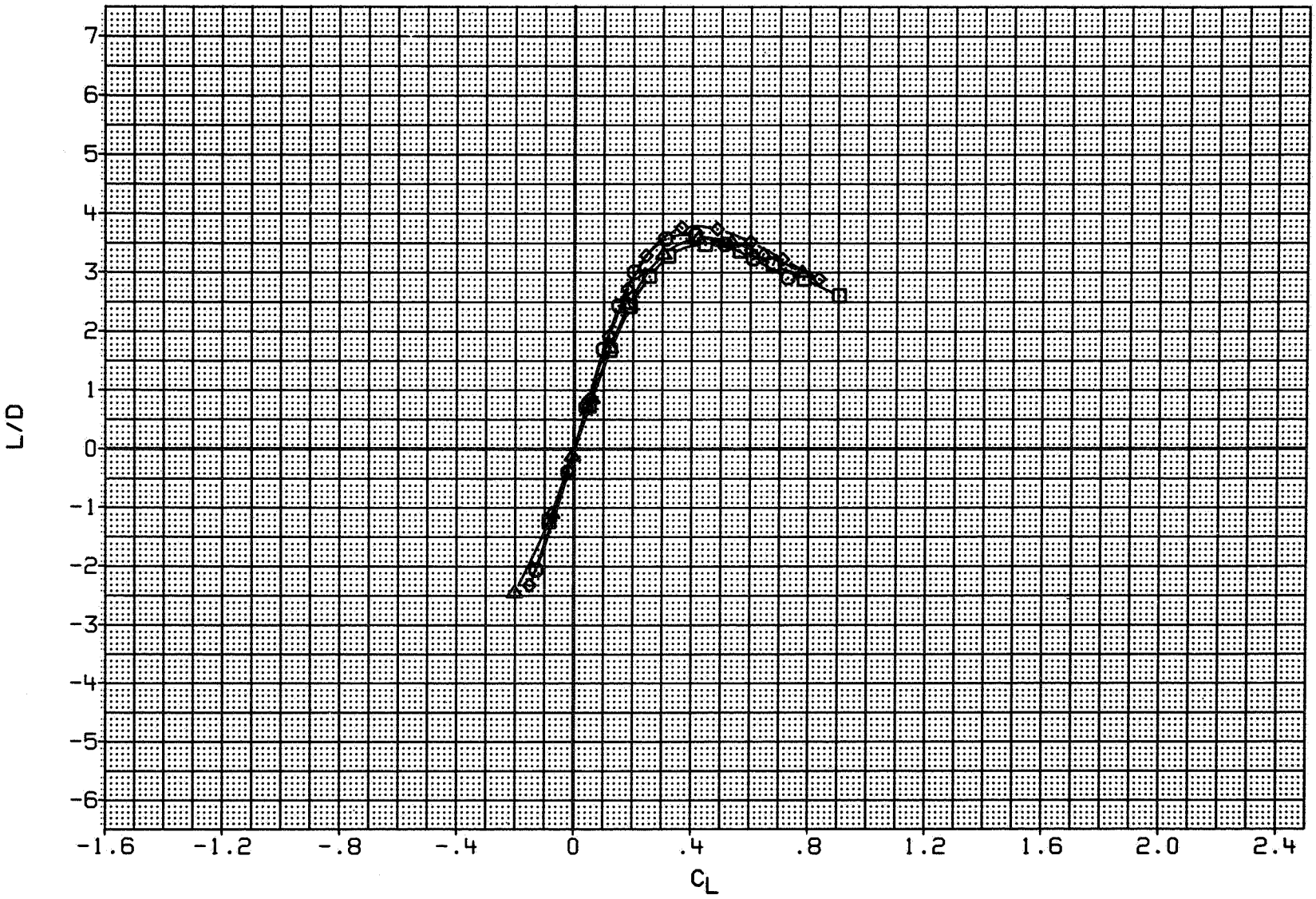


FIG. 65 CANARD INCIDENCE EFFECTS, TE-W = 10 DEGREES

MACH = 2.00

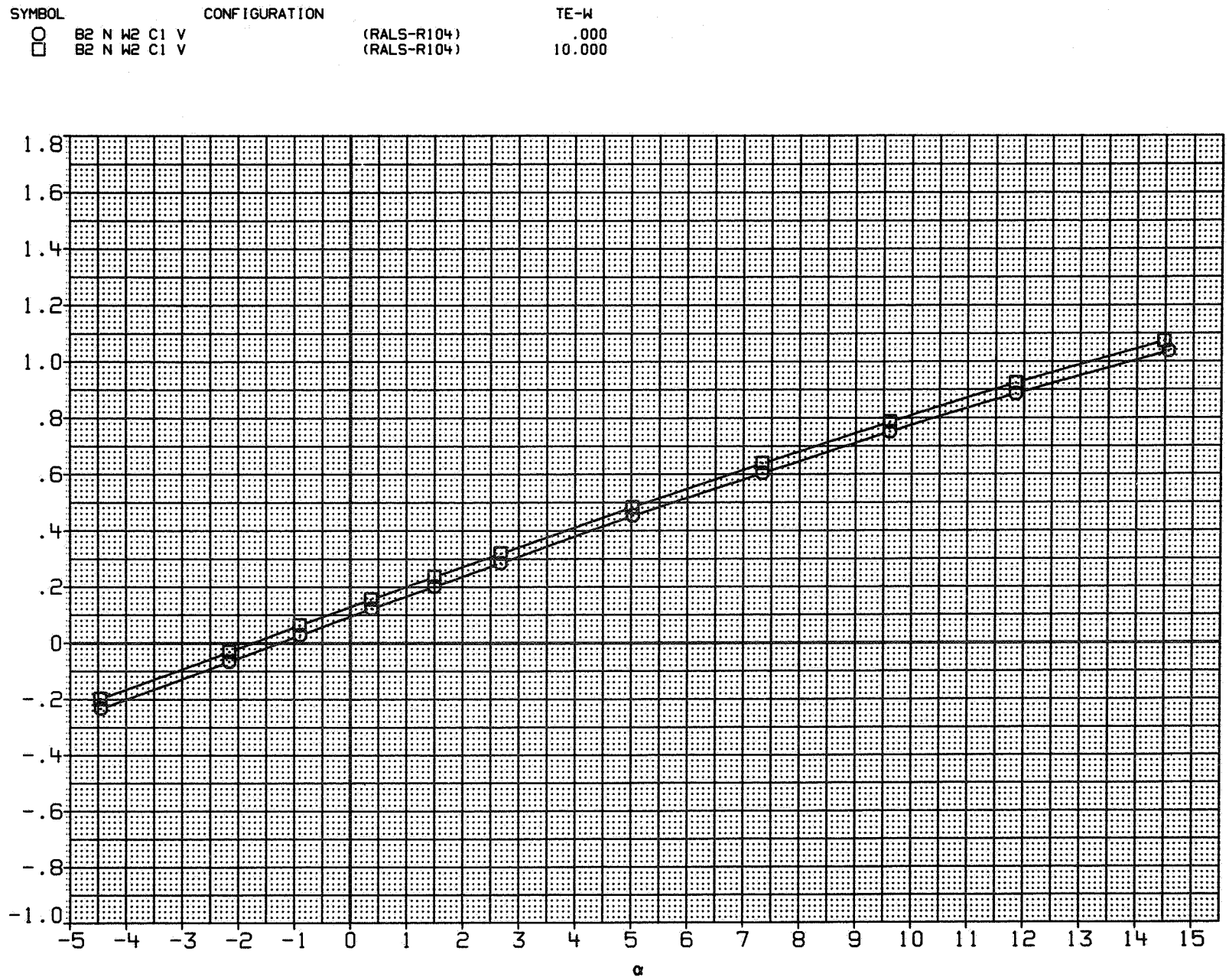


FIG. 66 FLAP DEFLECTION EFFECTS, CANARD = 0 DEGREES

MACH = 1.60

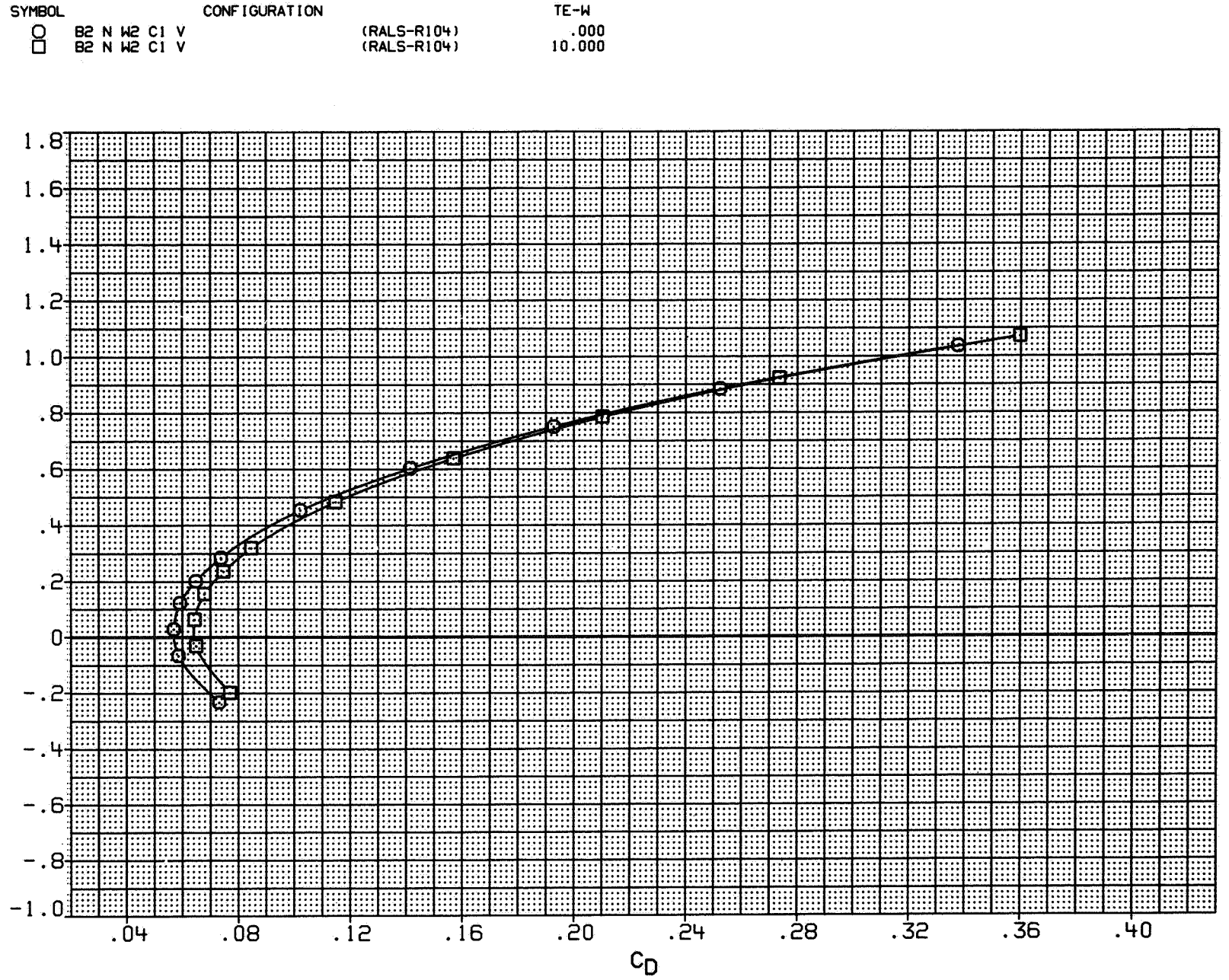


FIG. 66 FLAP DEFLECTION EFFECTS, CANARD = 0 DEGREES

MACH = 1.60

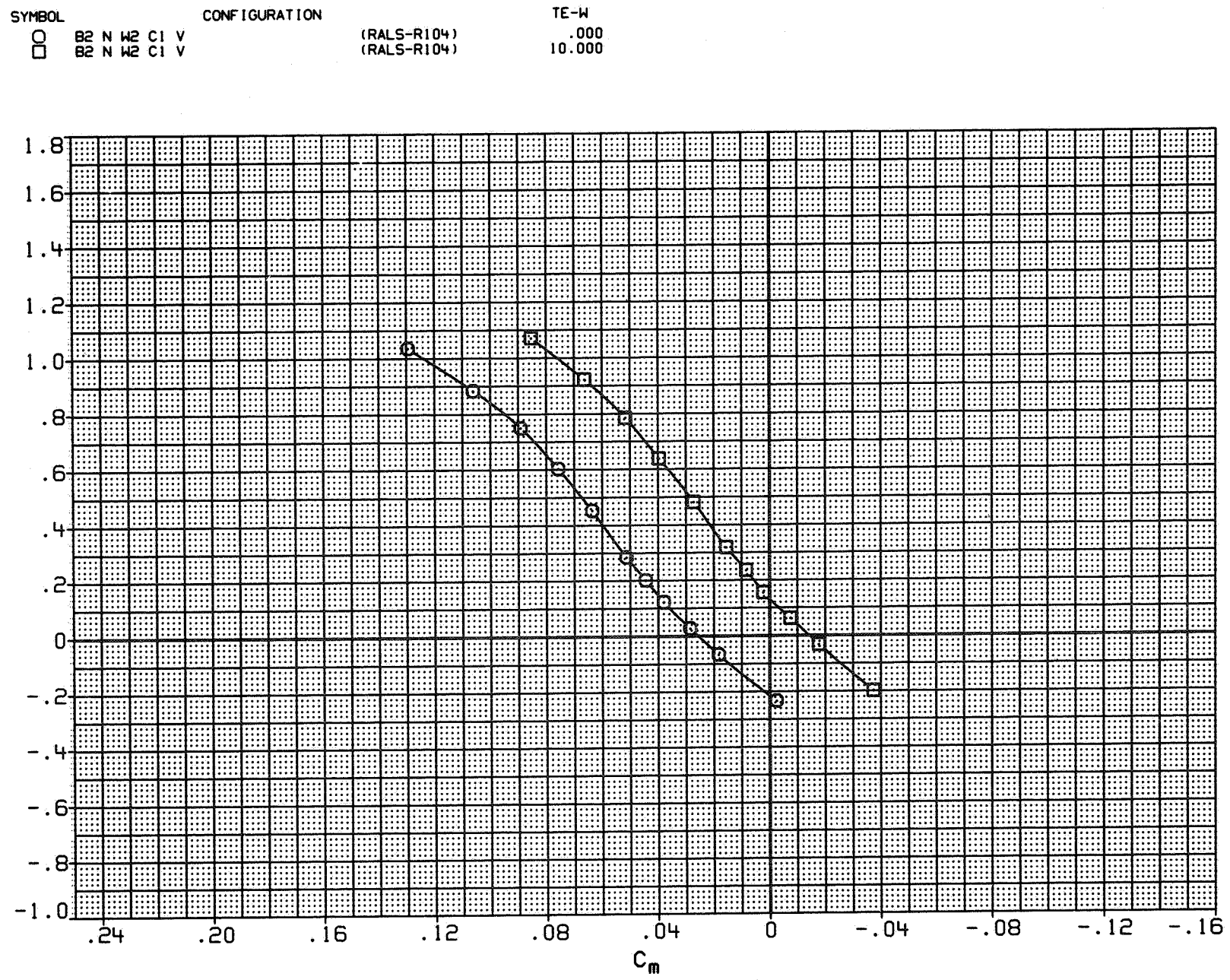


FIG. 66 FLAP DEFLECTION EFFECTS, CANARD = 0 DEGREES

MACH = 1.60

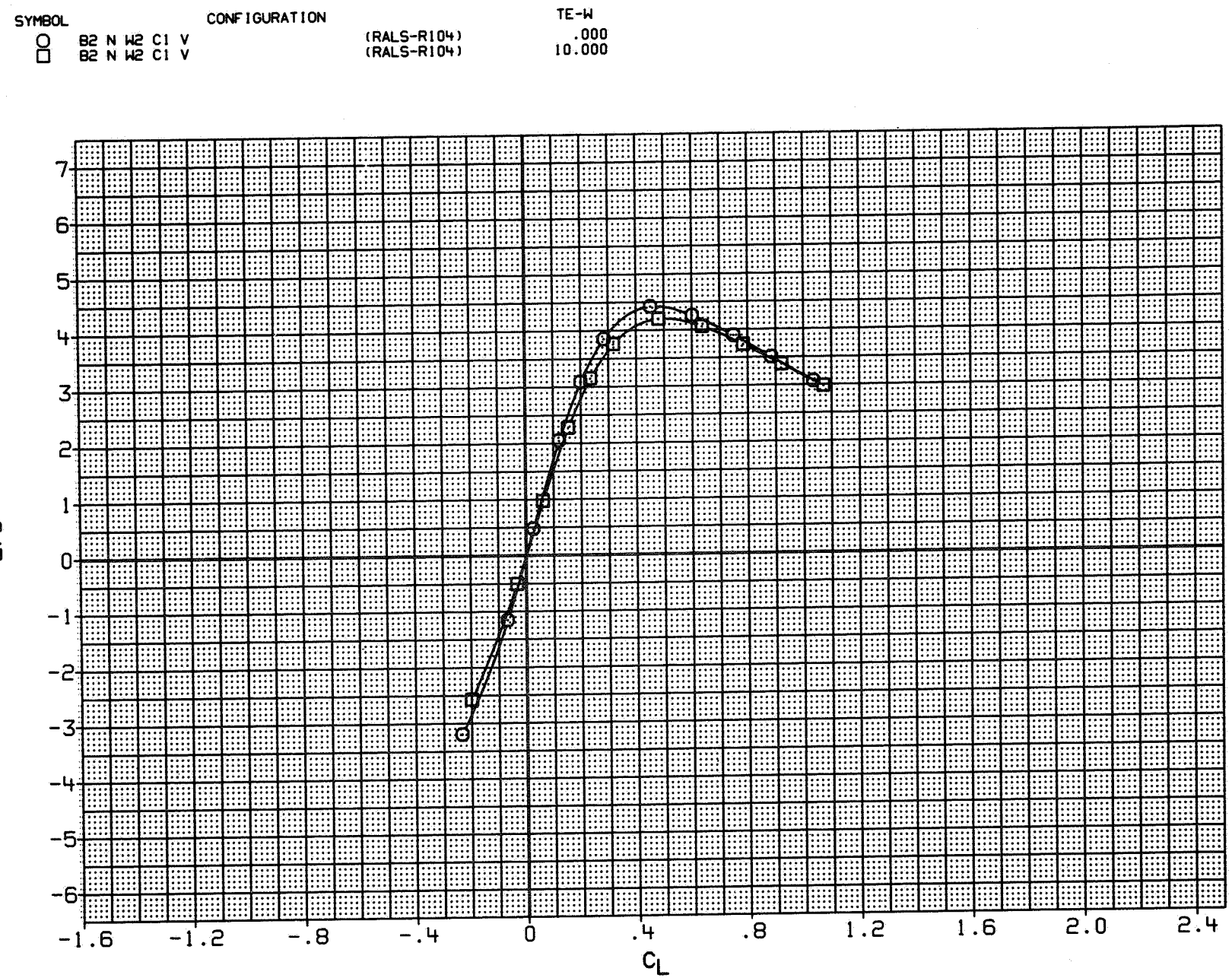


FIG. 66 FLAP DEFLECTION EFFECTS, CANARD = 0 DEGREES

MACH = 1.60

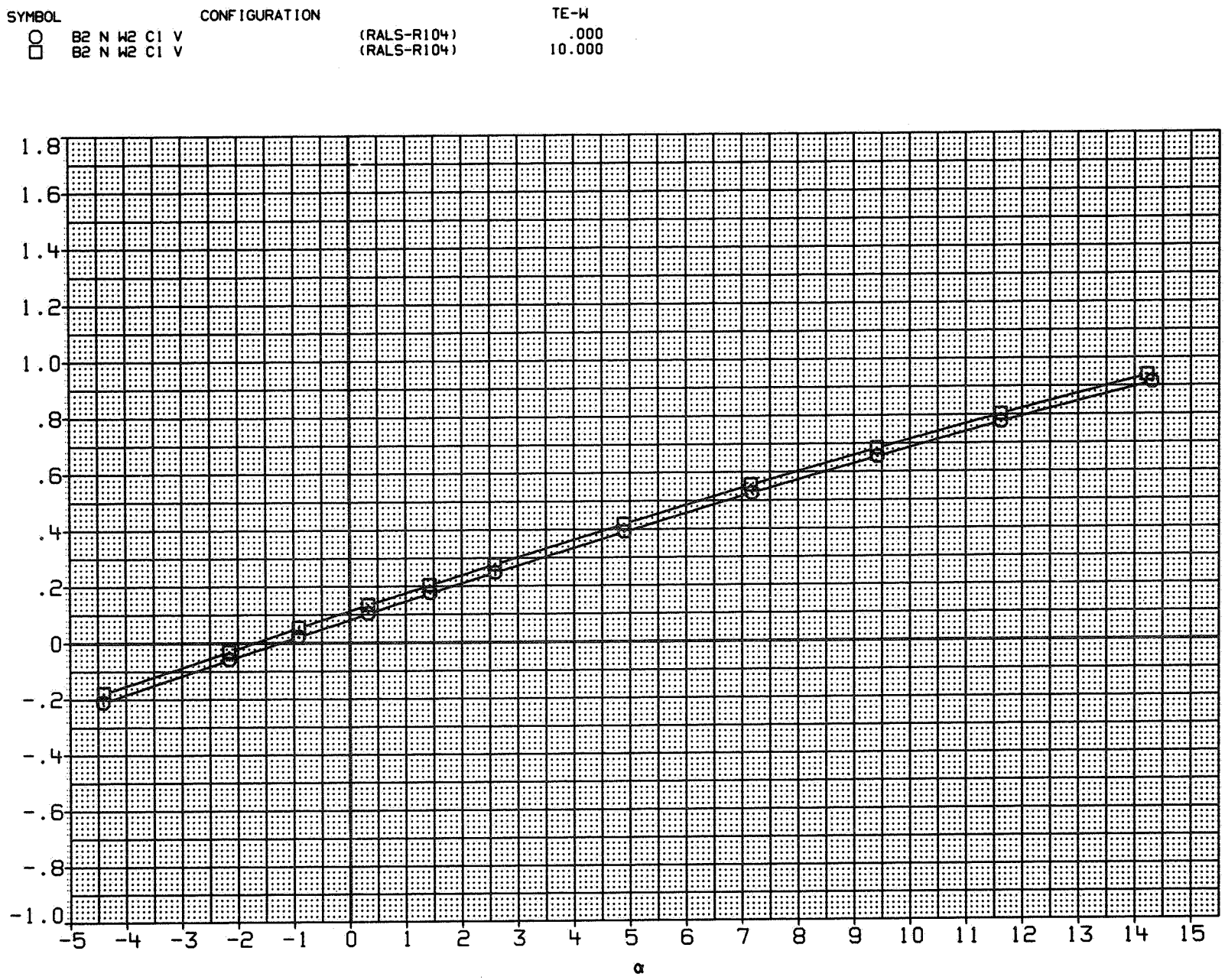


FIG. 67 FLAP DEFLECTION EFFECTS, CANARD = 0 DEGREES

MACH = 1.80

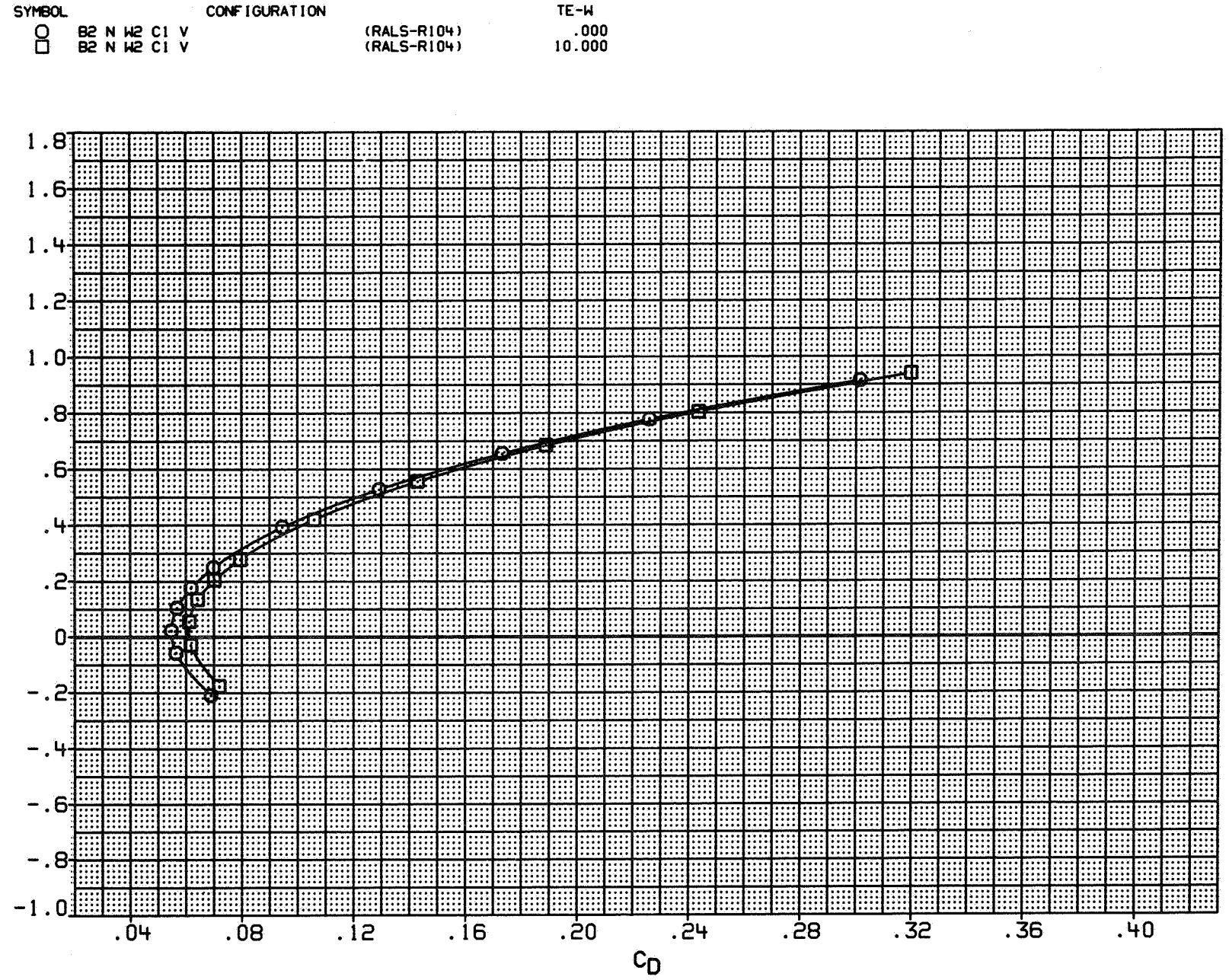


FIG. 67 FLAP DEFLECTION EFFECTS, CANARD = 0 DEGREES

MACH = 1.80

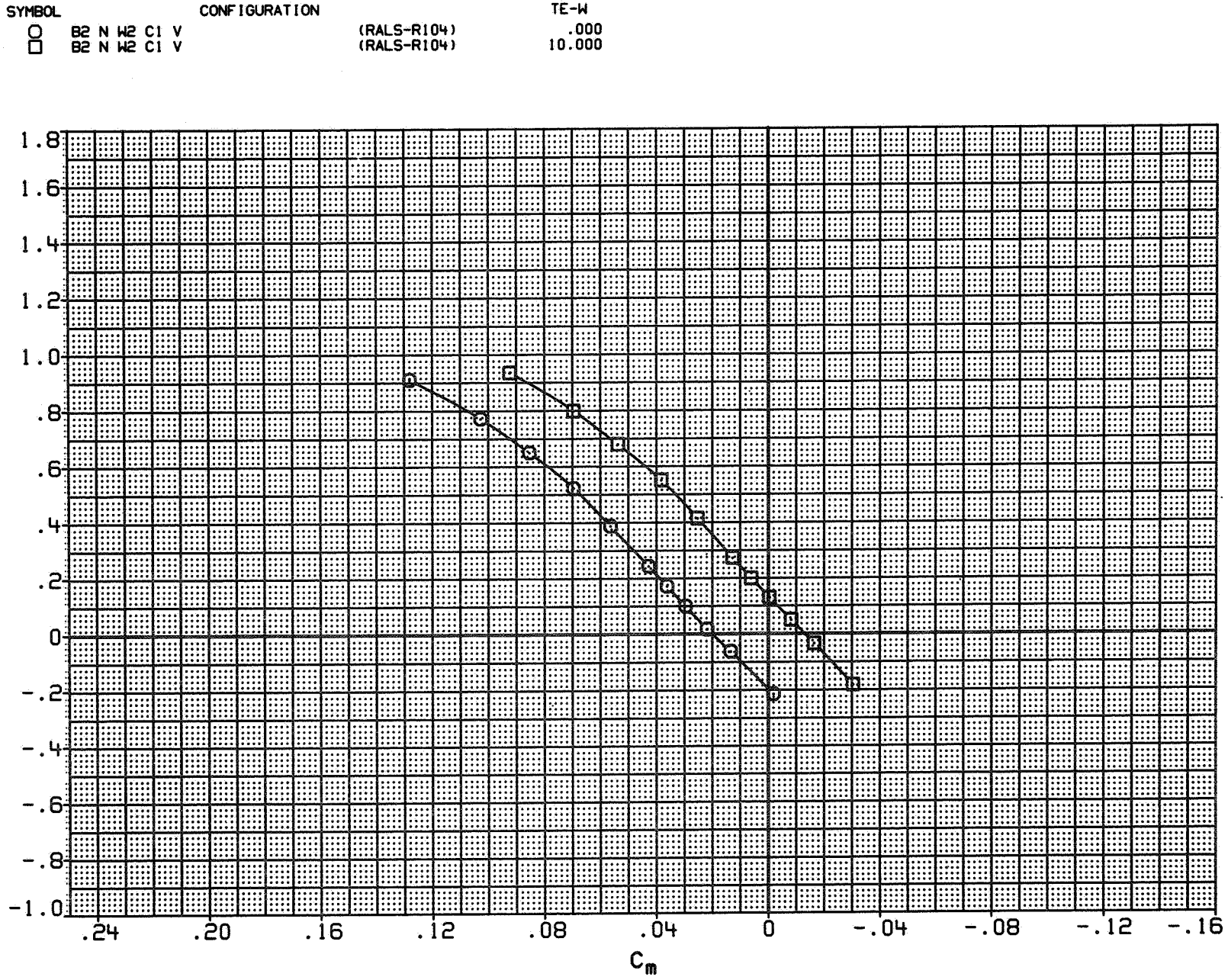


FIG. 67 FLAP DEFLECTION EFFECTS, CANARD = 0 DEGREES

MACH = 1.80

| SYMBOL | CONFIGURATION | | TE-W |
|---|---|---|---|
| ○ | B2 N W2 C1 V | (RALS-R104) | .000 |
| □ | B2 N W2 C1 V | (RALS-R104) | 10.000 |

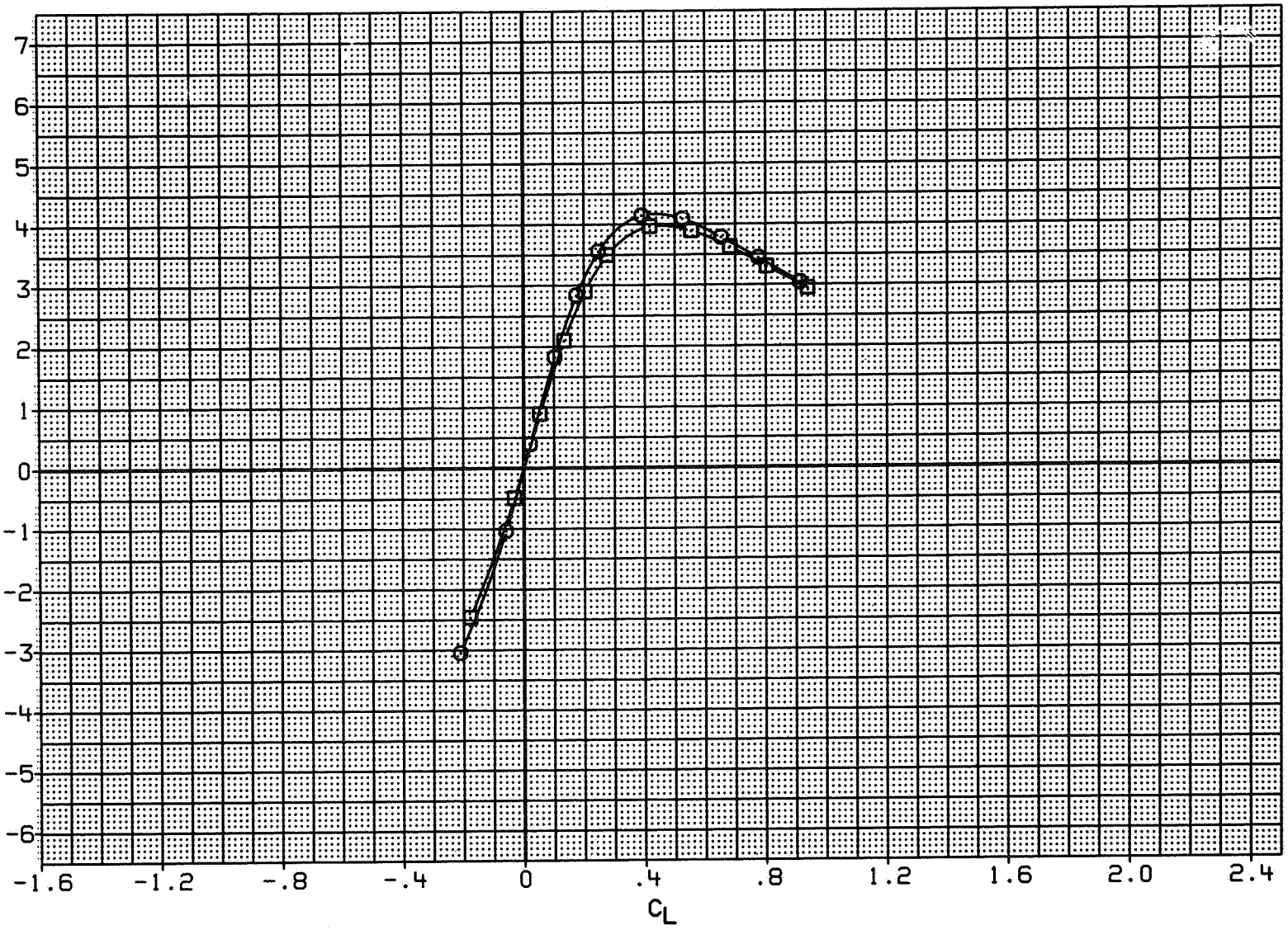


FIG. 67 FLAP DEFLECTION EFFECTS, CANARD = 0 DEGREES

MACH = 1.80

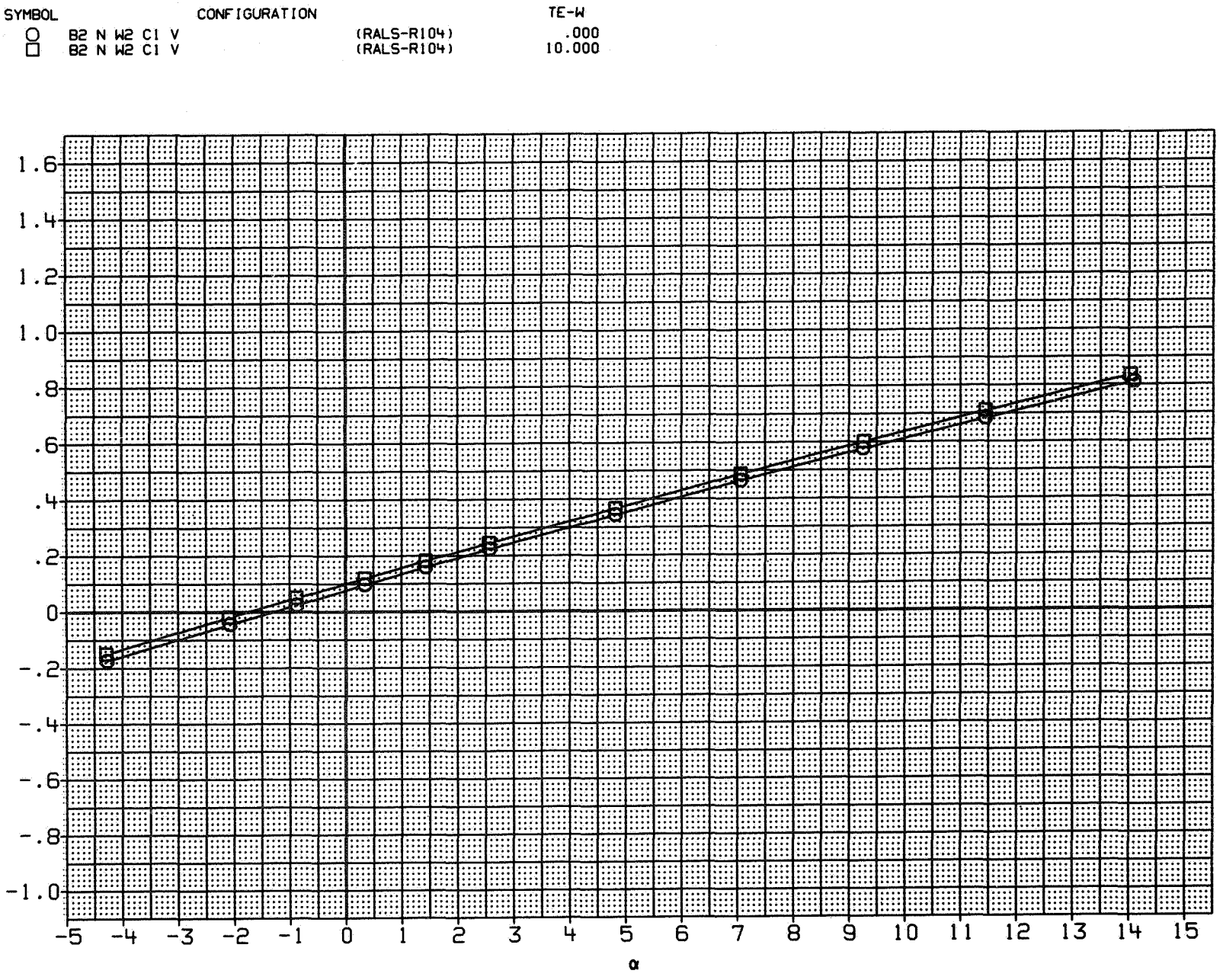


FIG. 68 FLAP DEFLECTION EFFECTS, CANARD - 0 DEGREES

MACH = 2.00

| SYMBOL | CONFIGURATION | | TE-W |
|---|---|---|---|
| ○ | B2 N W2 C1 V | (RALS-R104) | .000 |
| □ | B2 N W2 C1 V | (RALS-R104) | 10.000 |

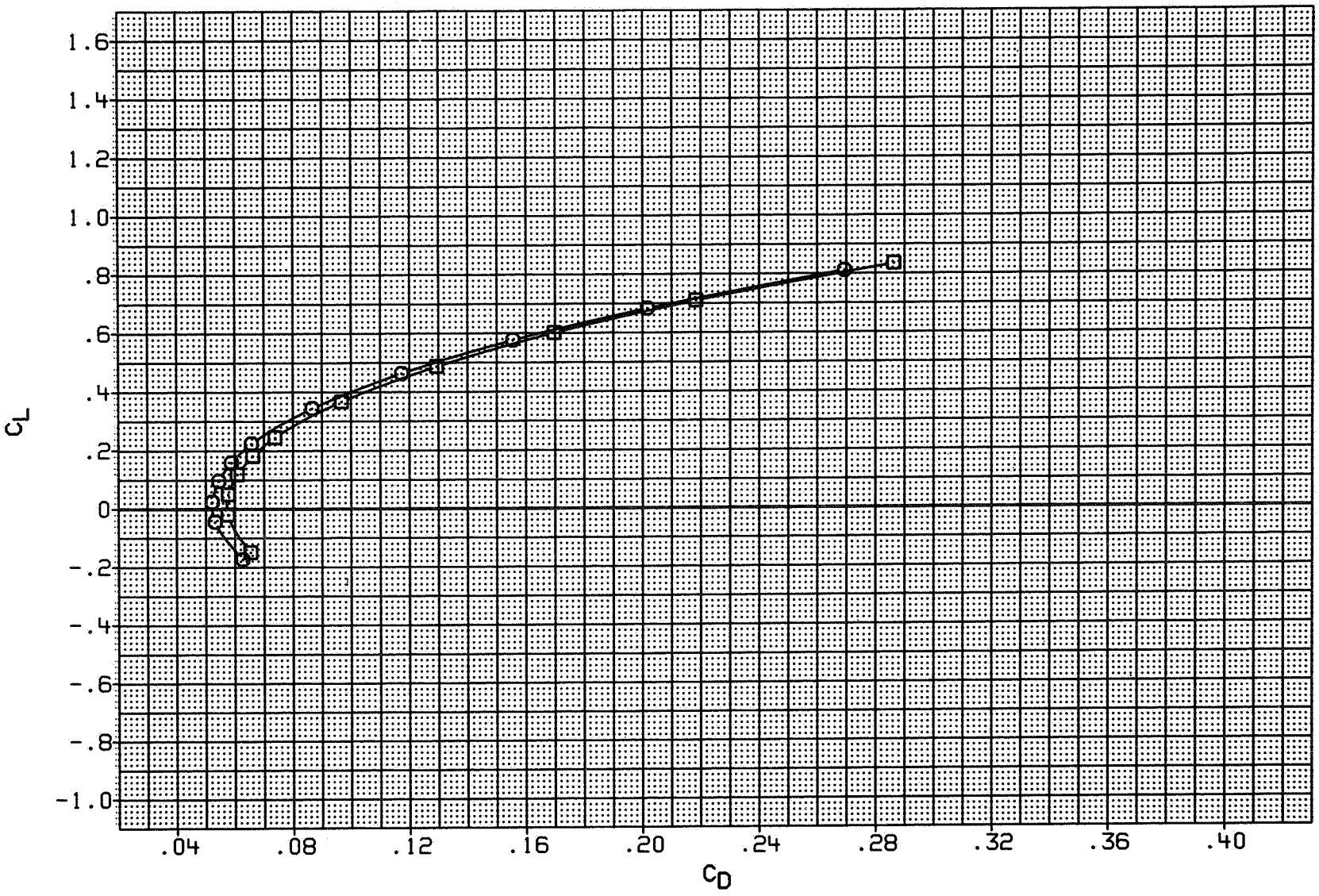


FIG. 68 FLAP DEFLECTION EFFECTS, CANARD = 0 DEGREES

MACH = 2.00

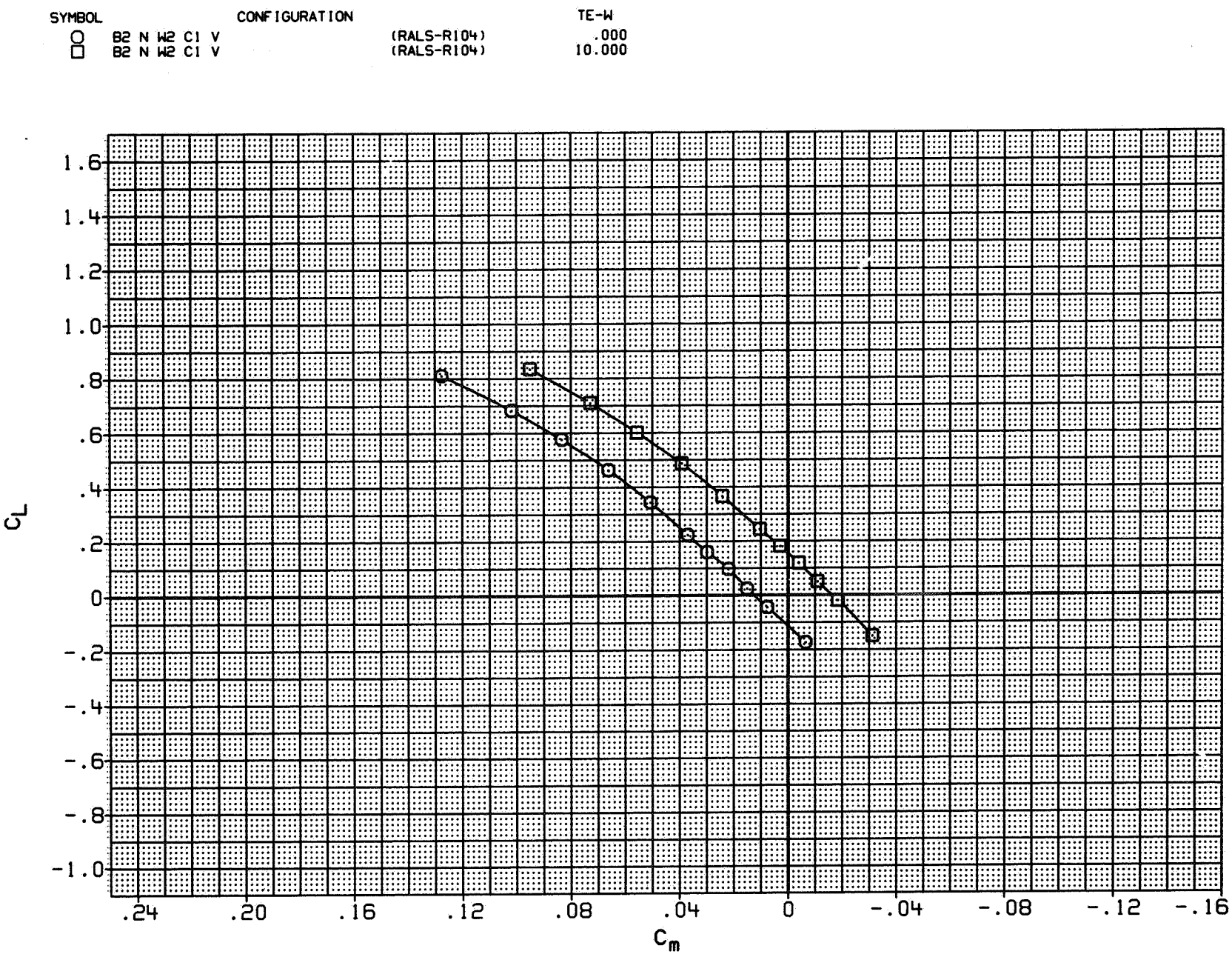


FIG. 68 FLAP DEFLECTION EFFECTS, CANARD = 0 DEGREES

MACH = 2.00

| SYMBOL | CONFIGURATION | | TE-W |
|---|---|---|---|
| ○ | B2 N W2 C1 V | (RALS-R104) | .000 |
| □ | B2 N W2 C1 V | (RALS-R104) | 10.000 |

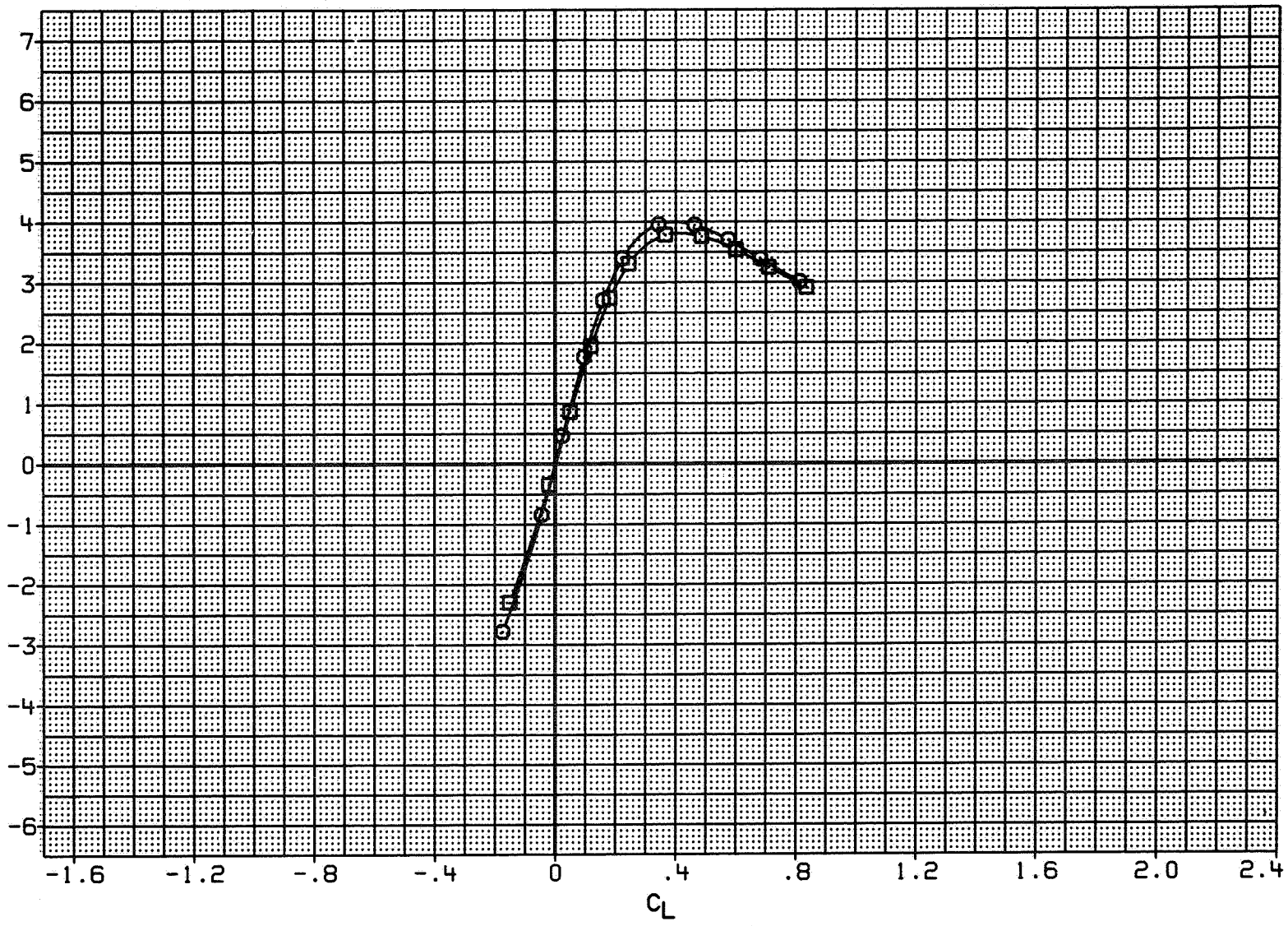


FIG. 68 FLAP DEFLECTION EFFECTS, CANARD = 0 DEGREES

MACH = 2.00

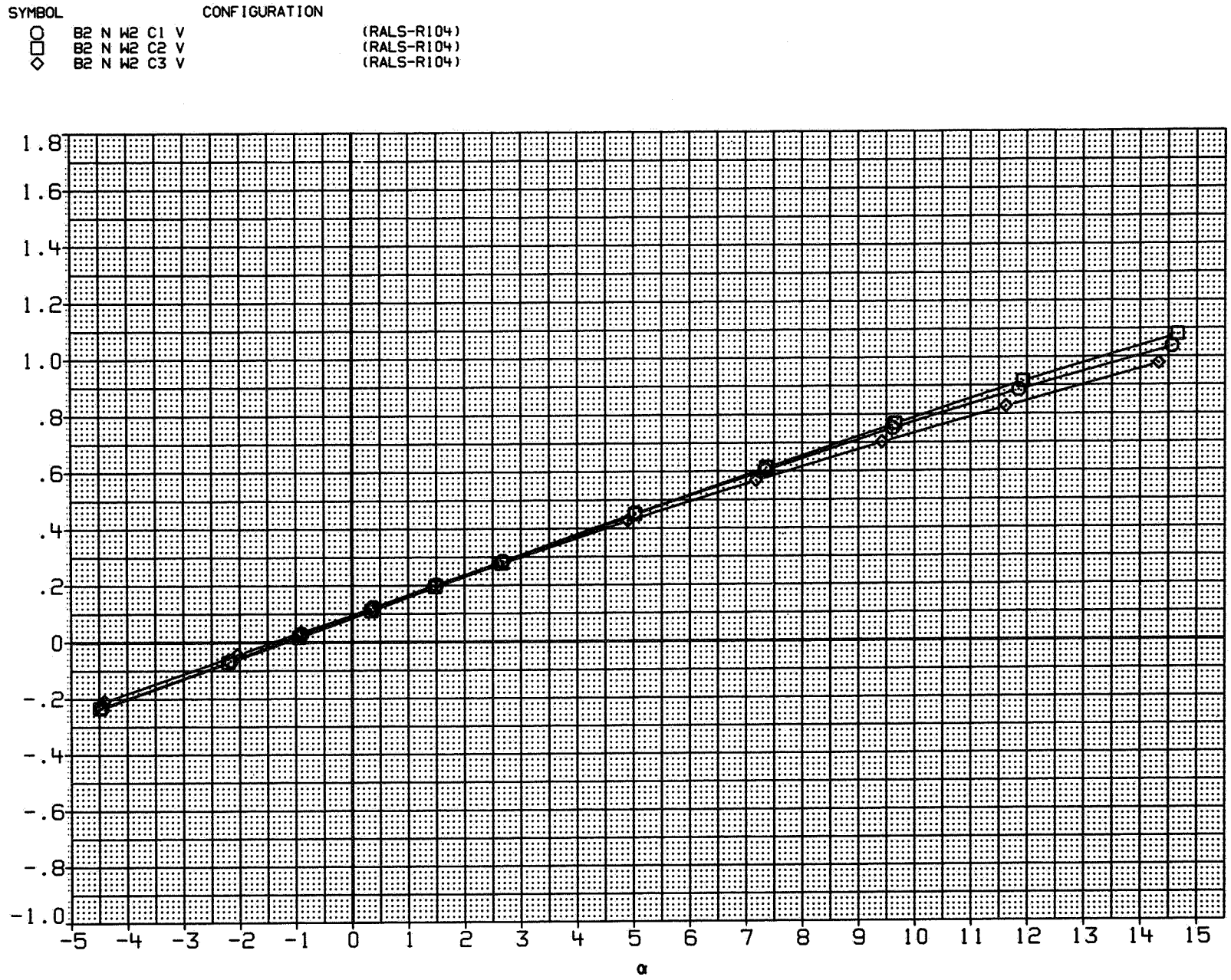


FIG. 69 CANARD LOCATION EFFECTS, LONGITUDINAL CHARACTERISTICS

MACH = 1.60

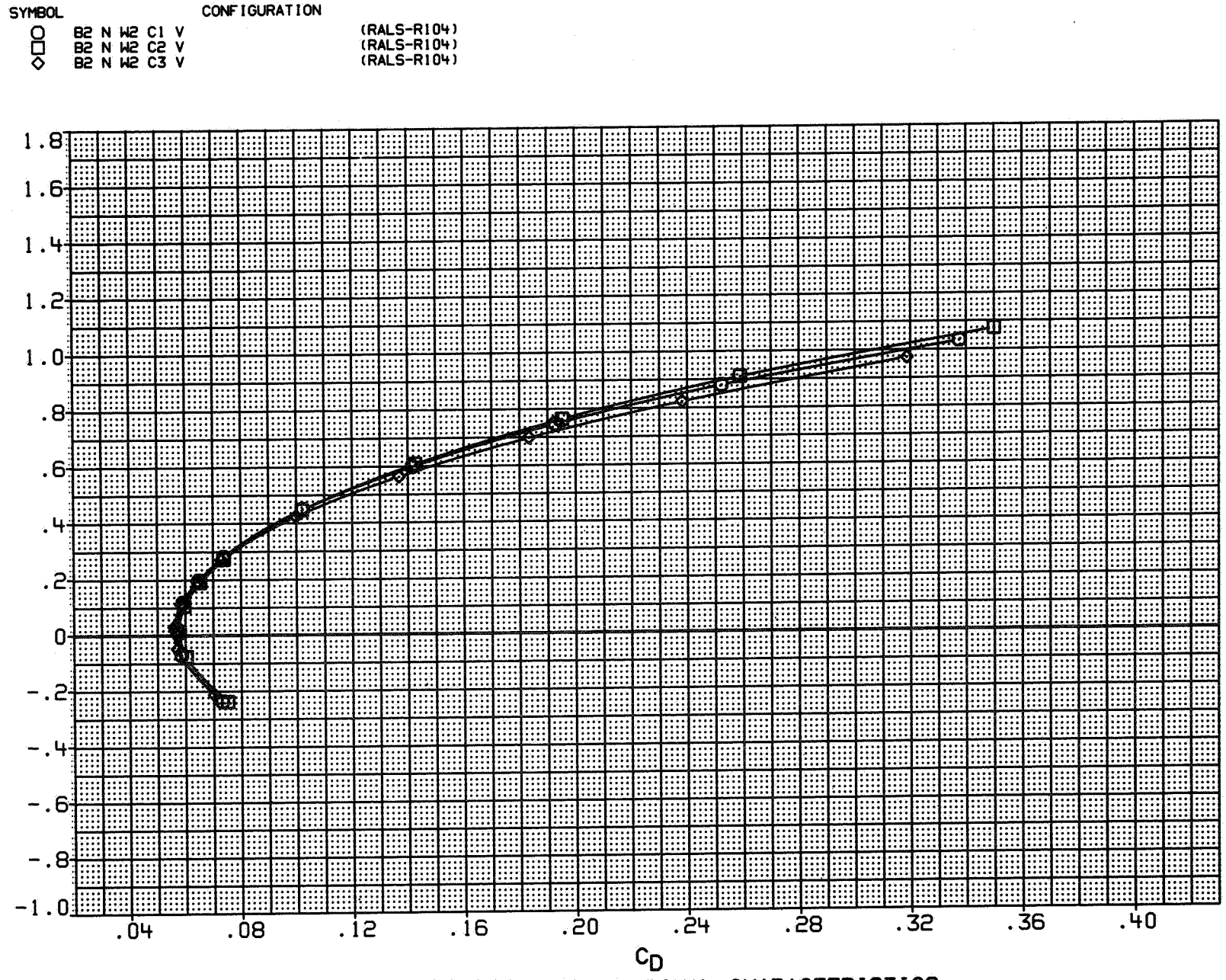


FIG. 69 CANARD LOCATION EFFECTS, LONGITUDINAL CHARACTERISTICS

MACH = 1.60

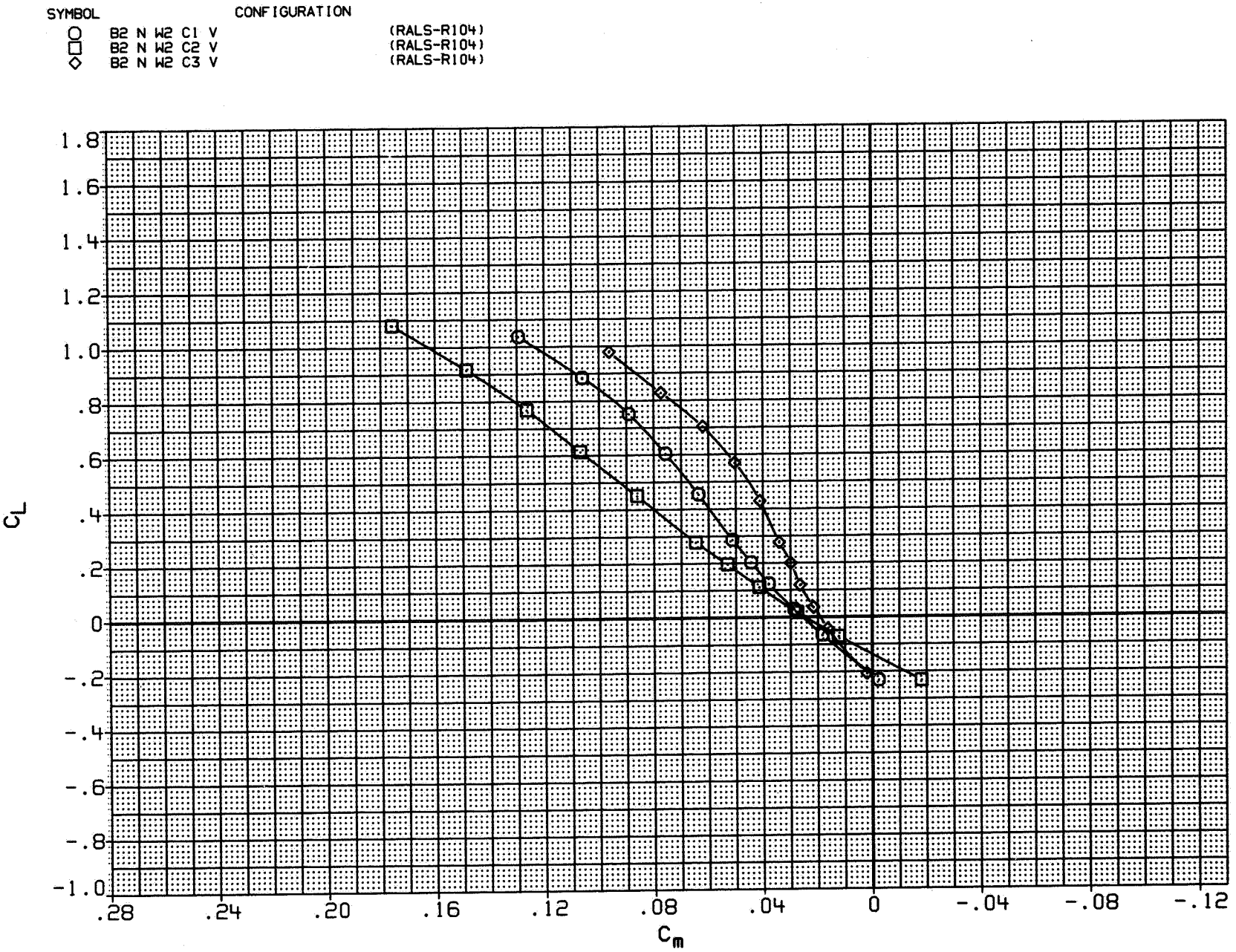


FIG. 69 CANARD LOCATION EFFECTS, LONGITUDINAL CHARACTERISTICS

MACH = 1.60

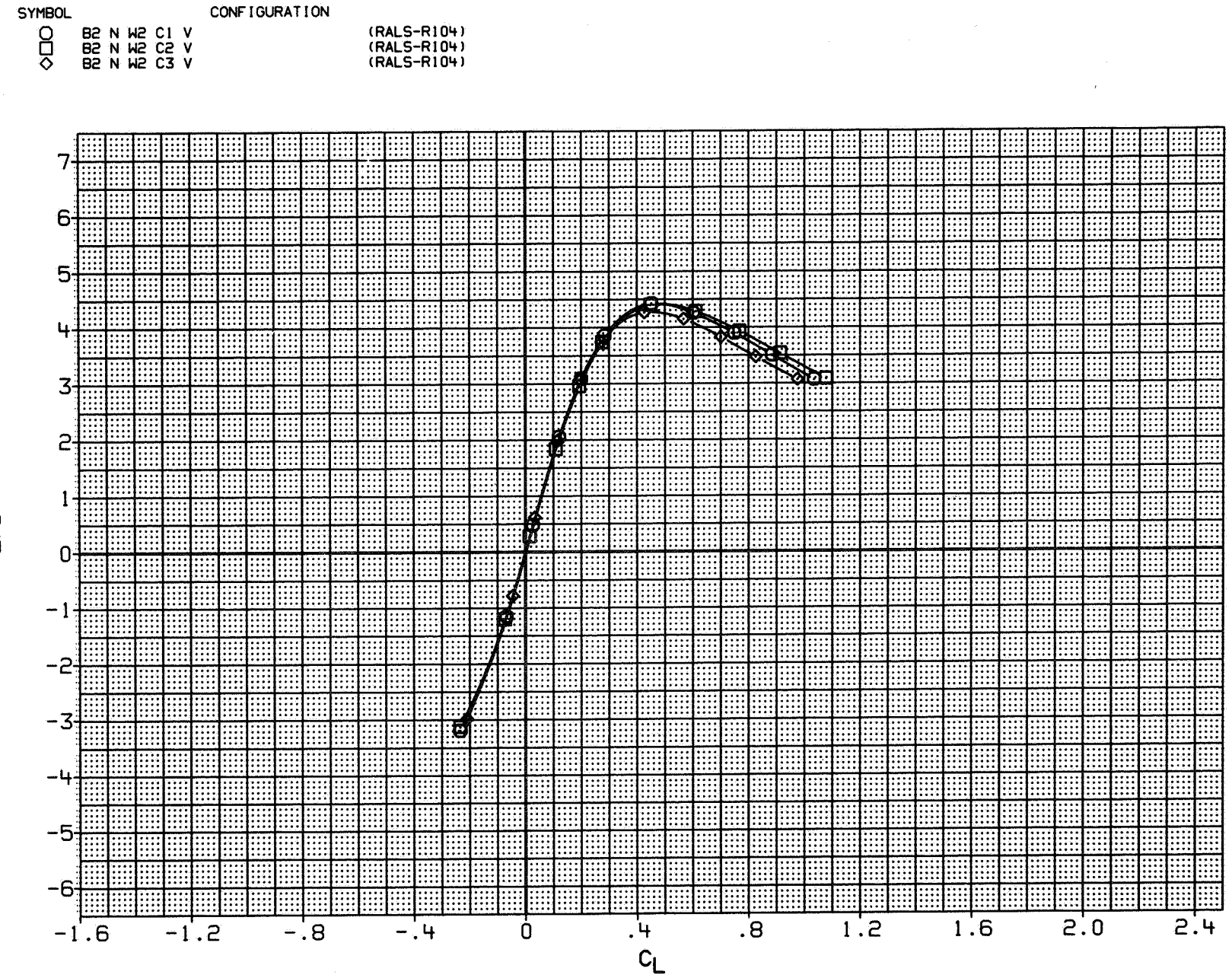


FIG. 69 CANARD LOCATION EFFECTS, LONGITUDINAL CHARACTERISTICS

MACH = 1.60

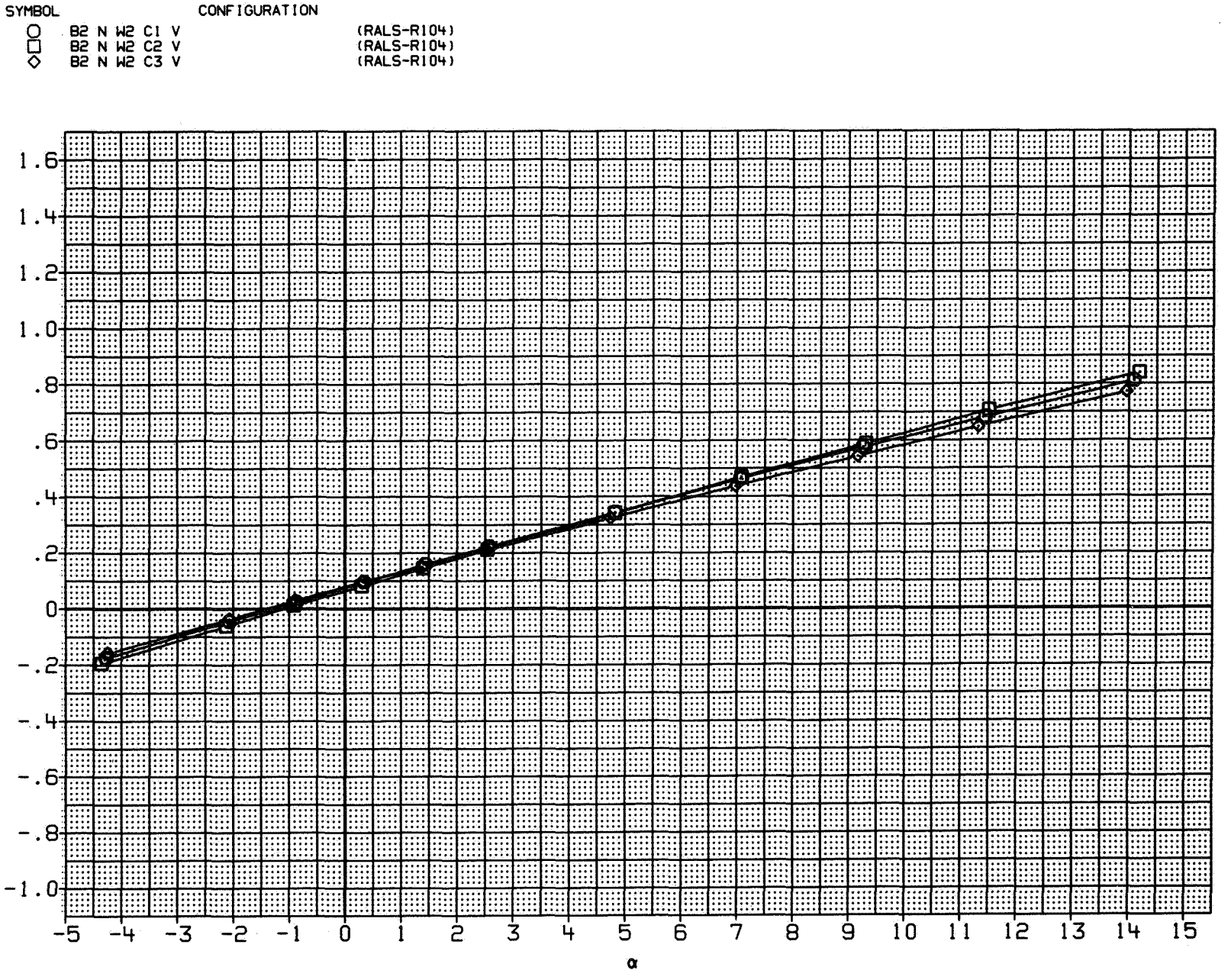


FIG. 70 CANARD LOCATION EFFECTS, LONGITUDINAL CHARACTERISTICS

MACH = 2.00

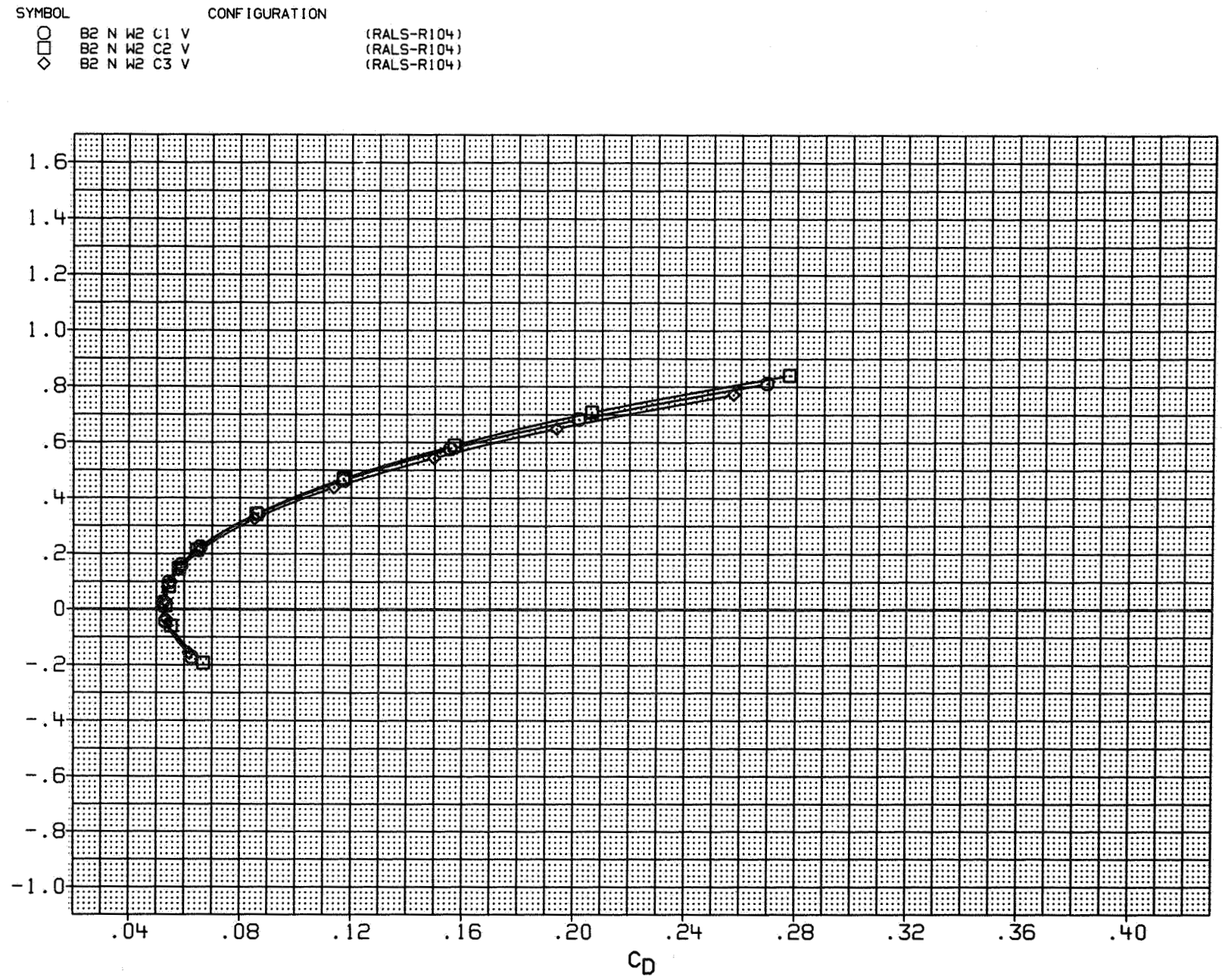


FIG. 70 CANARD LOCATION EFFECTS, LONGITUDINAL CHARACTERISTICS

MACH = 2.00

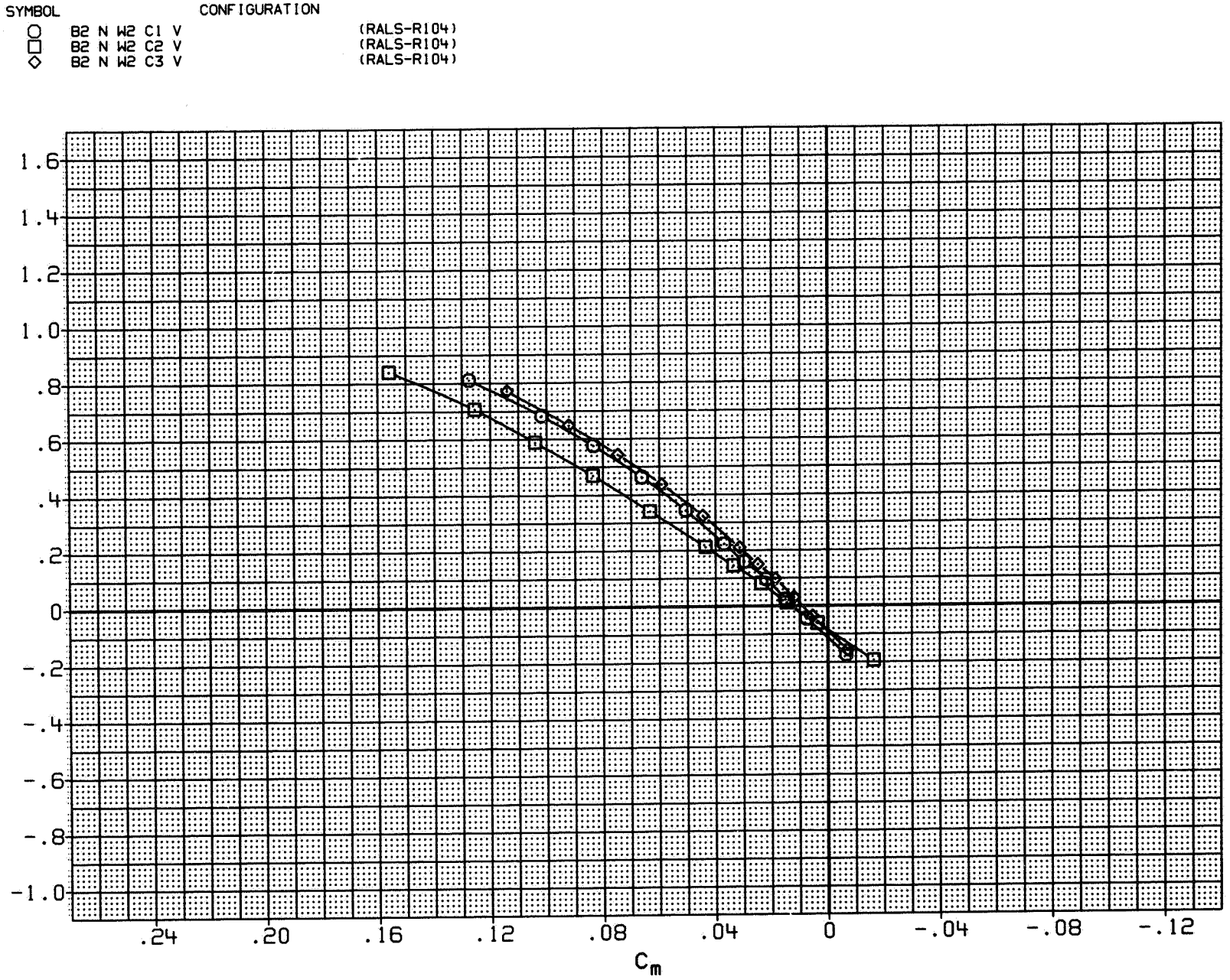


FIG. 70 CANARD LOCATION EFFECTS, LONGITUDINAL CHARACTERISTICS

MACH = 2.00

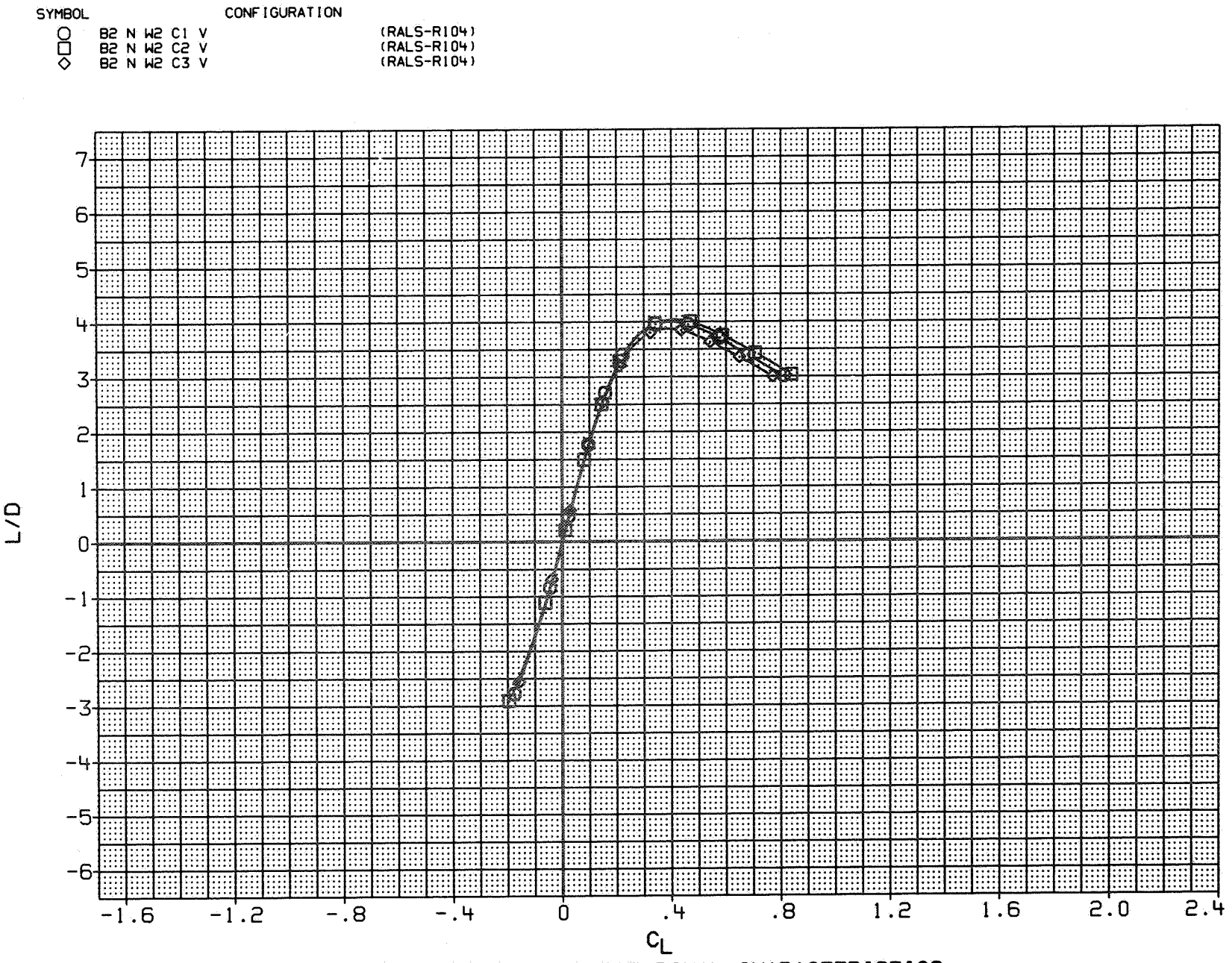


FIG. 70 CANARD LOCATION EFFECTS, LONGITUDINAL CHARACTERISTICS

MACH = 2.00

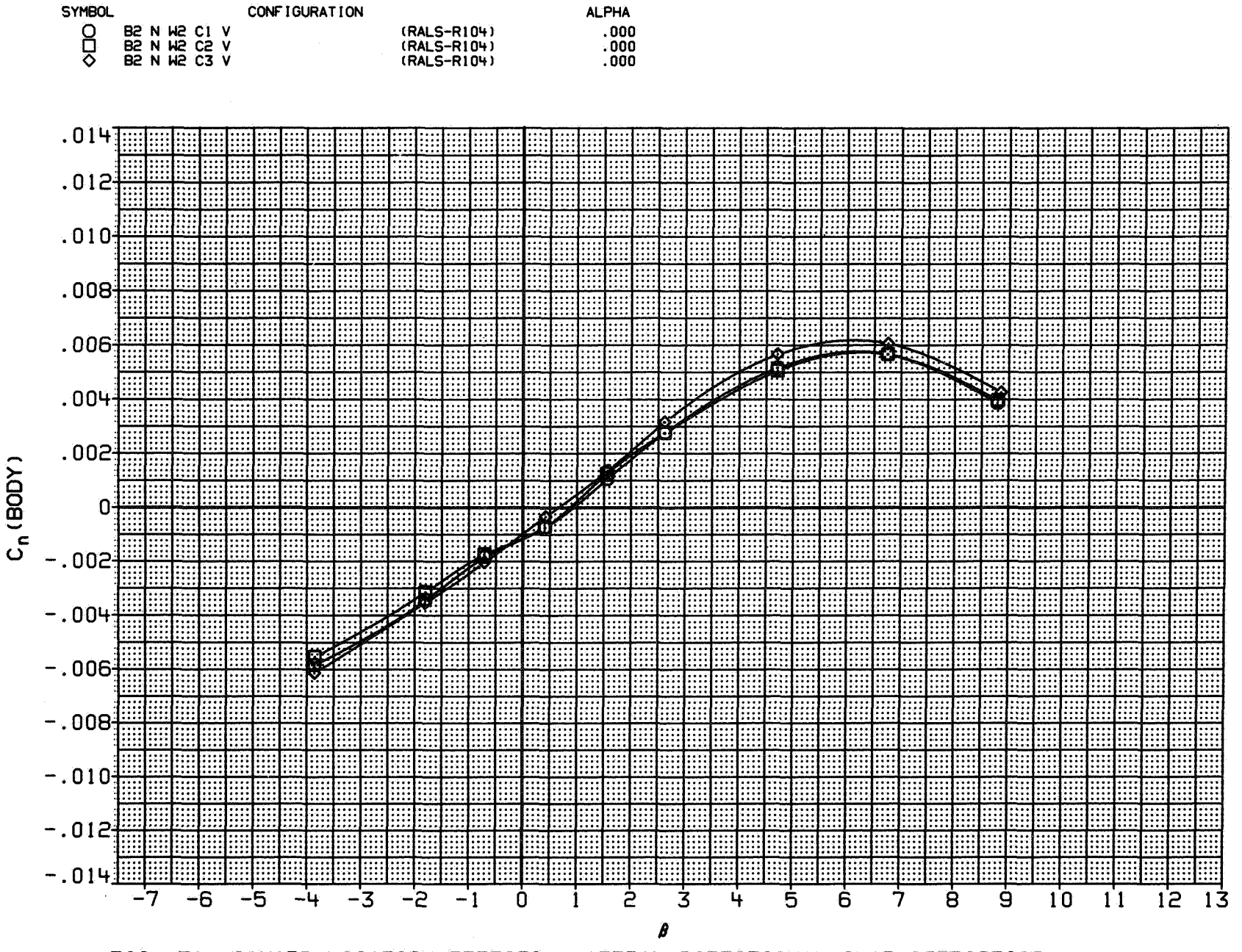


FIG. 71 CANARD LOCATION EFFECTS, LATERAL/DIRECTIONAL CHARACTERISTICS
ALPHA = 0 DEGREES
MACH = 1.60

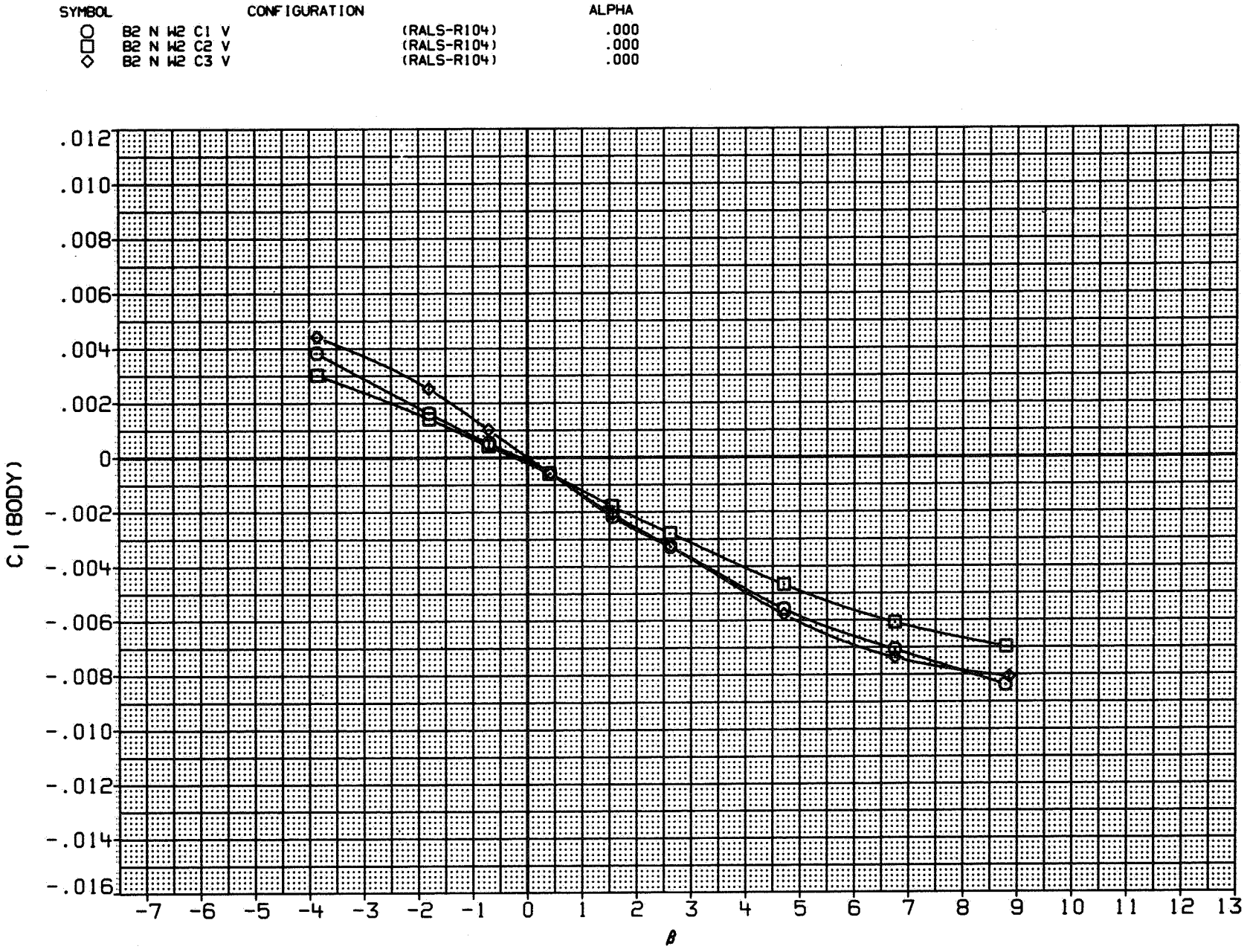


FIG. 71 CANARD LOCATION EFFECTS, LATERAL/DIRECTIONAL CHARACTERISTICS
ALPHA = 0 DEGREES

MACH = 1.60

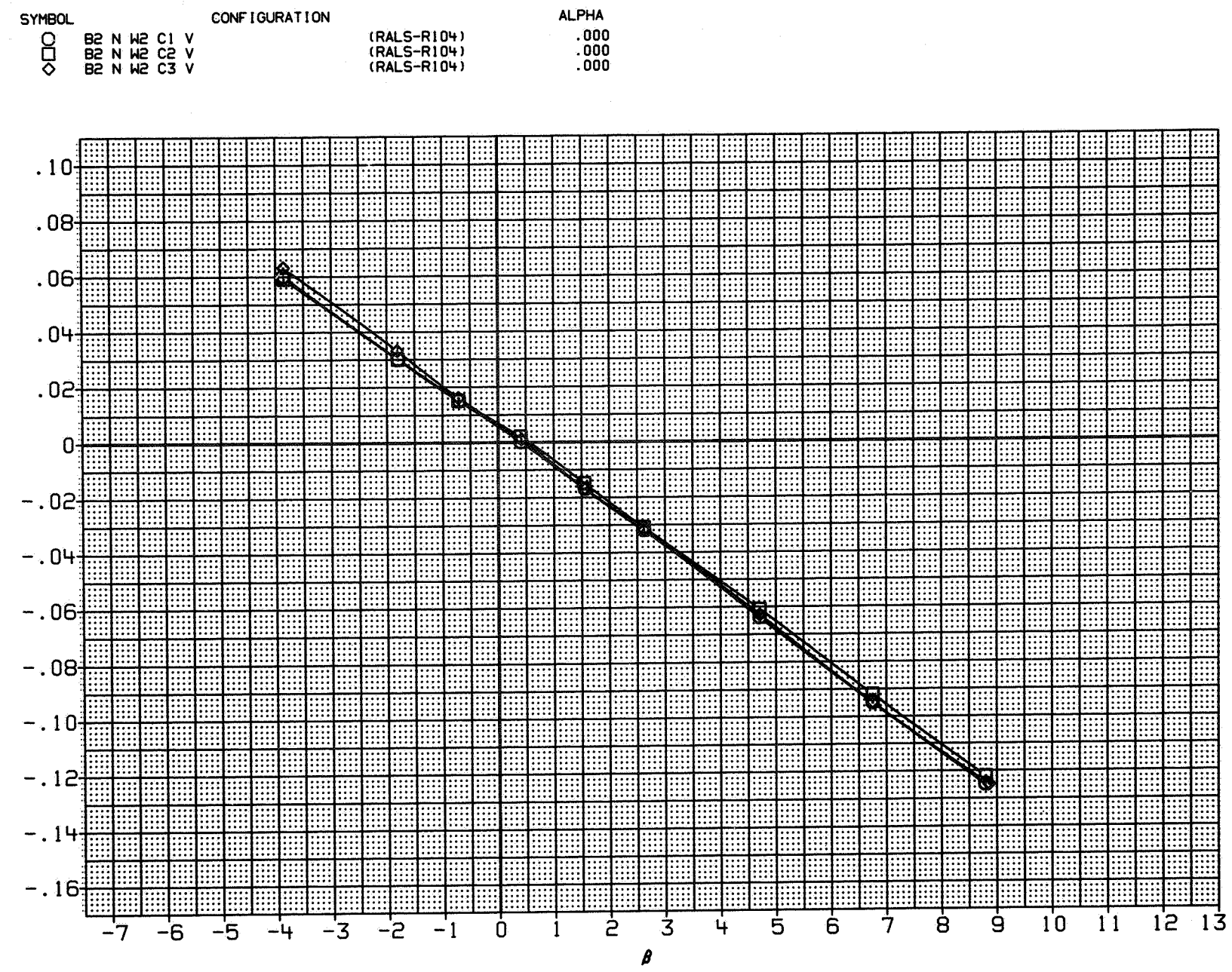


FIG. 71 CANARD LOCATION EFFECTS, LATERAL/DIRECTIONAL CHARACTERISTICS
ALPHA = 0 DEGREES

MACH = 1.60

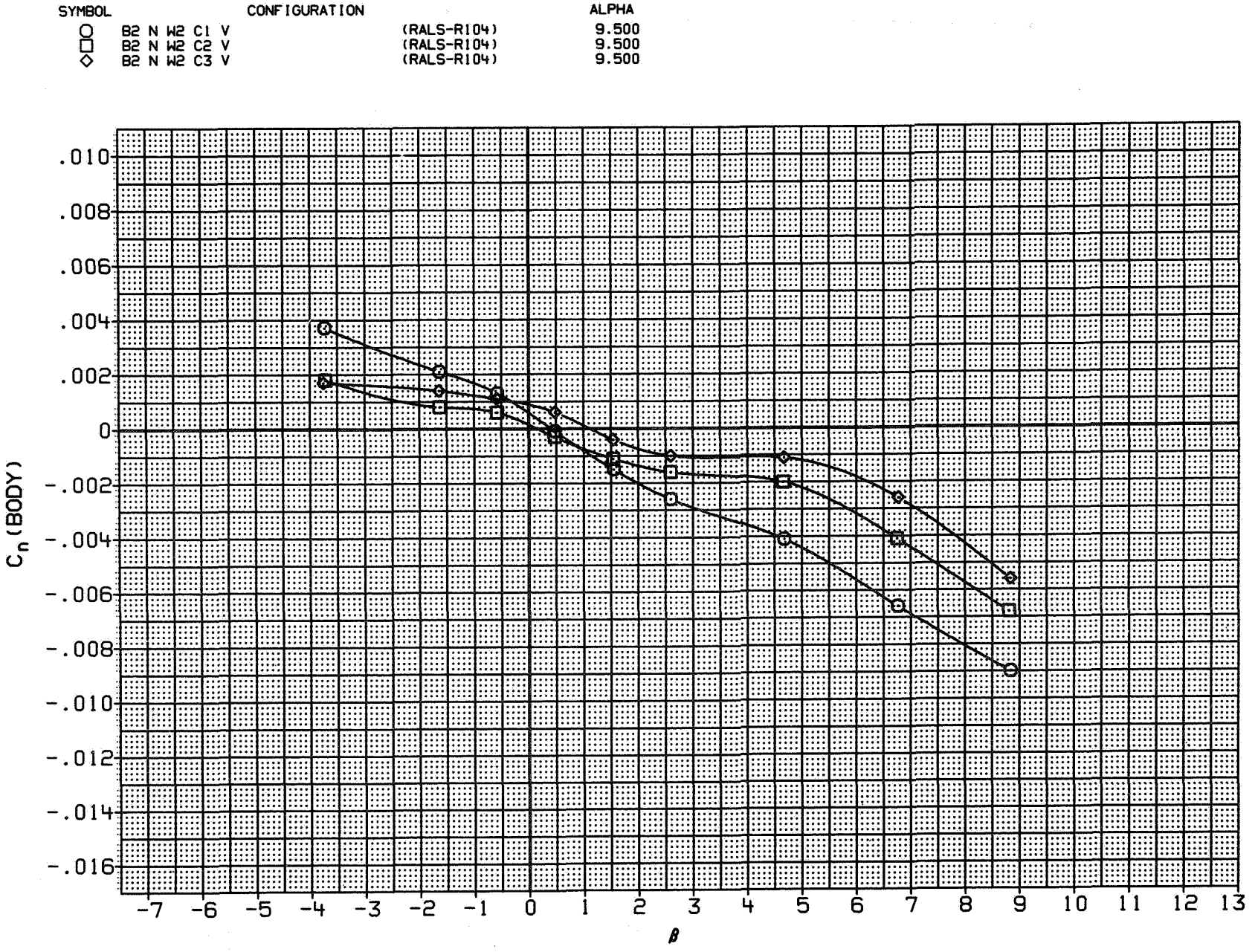


FIG. 72 CANARD LOCATION EFFECTS, LATERAL/DIRECTIONAL CHARACTERISTICS
ALPHA = 8 DEGREES
MACH = 1.60

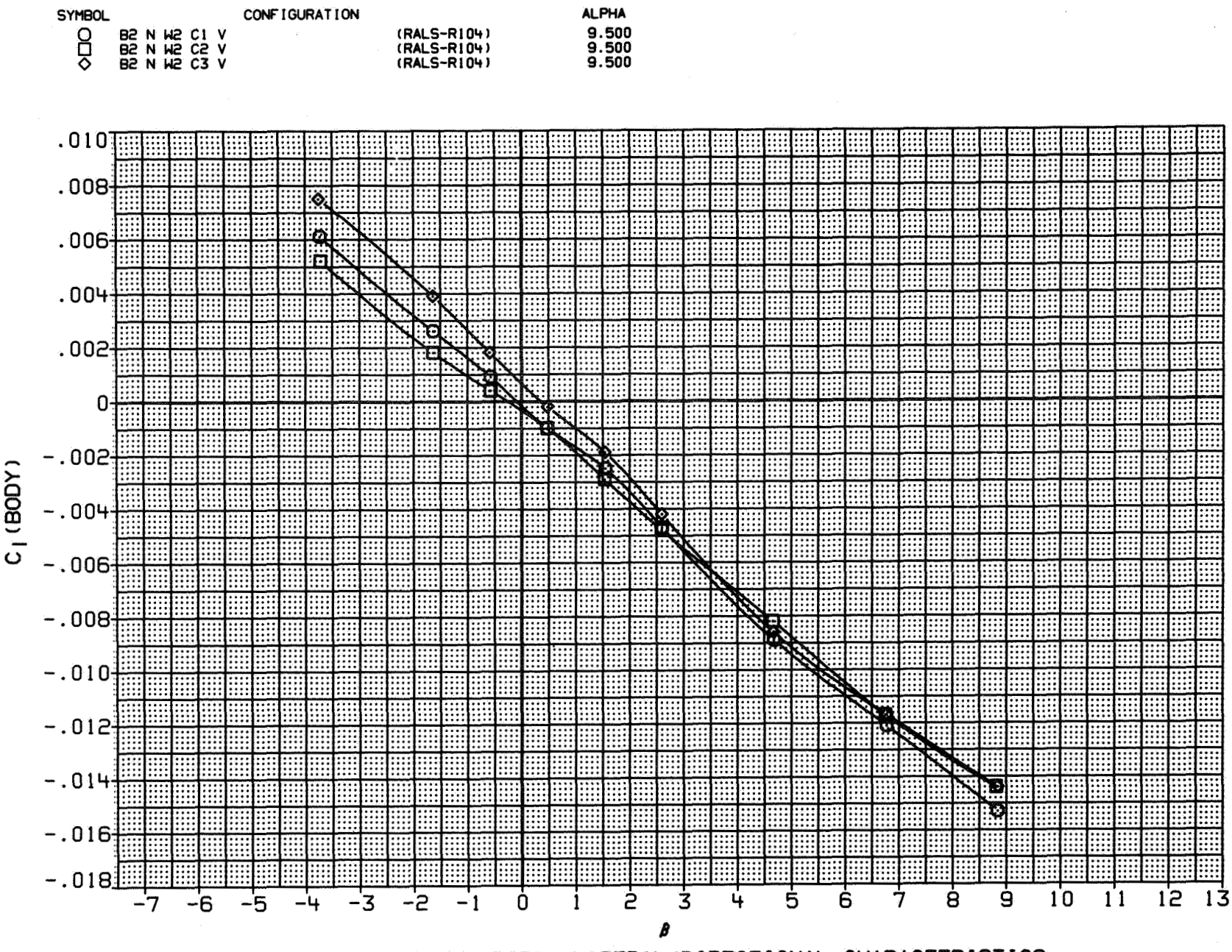


FIG. 72 CANARD LOCATION EFFECTS, LATERAL/DIRECTIONAL CHARACTERISTICS
ALPHA = 8 DEGREES
MACH = 1.60

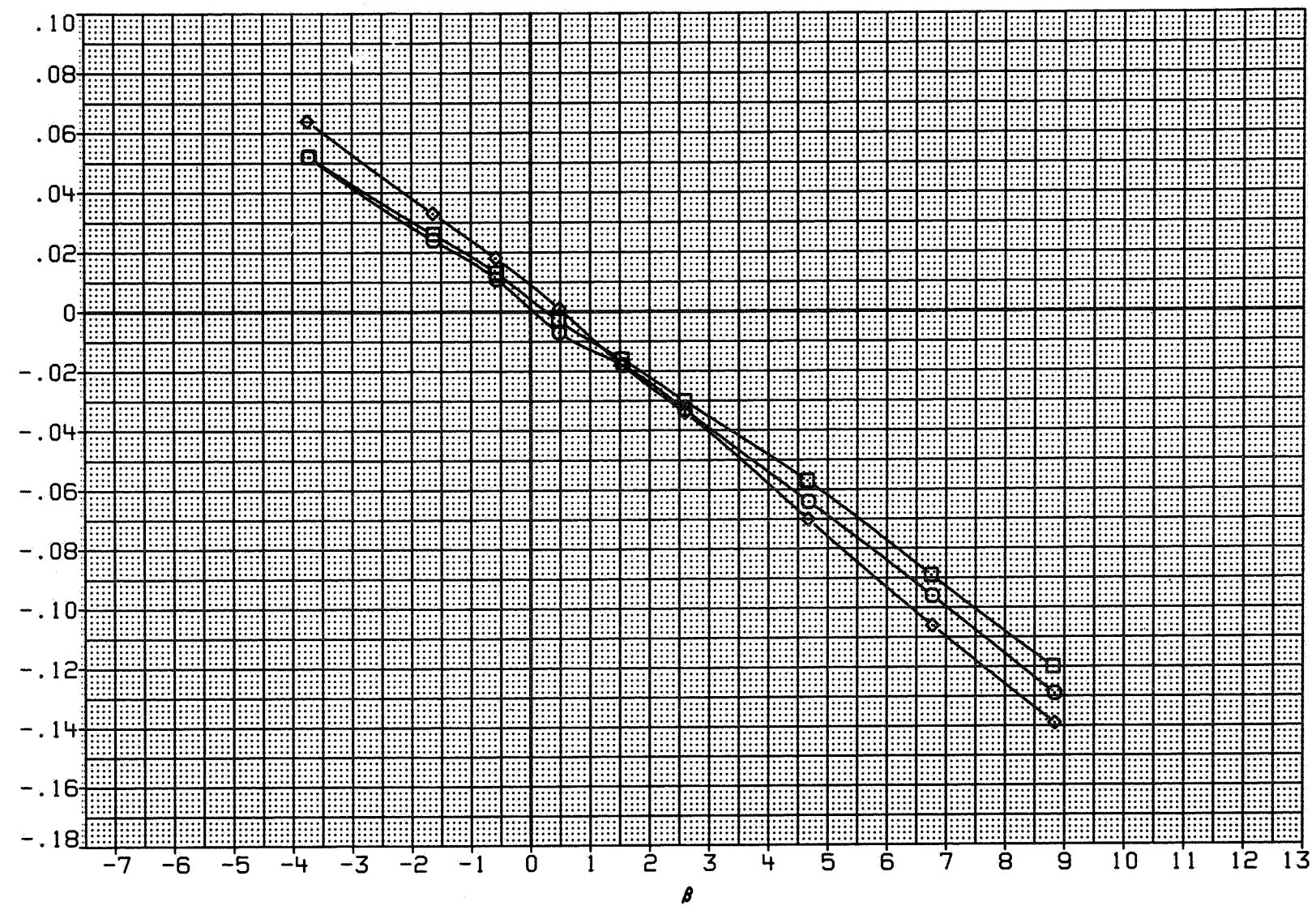


FIG. 72 CANARD LOCATION EFFECTS, LATERAL/DIRECTIONAL CHARACTERISTICS
ALPHA = 8 DEGREES
MACH = 1.60

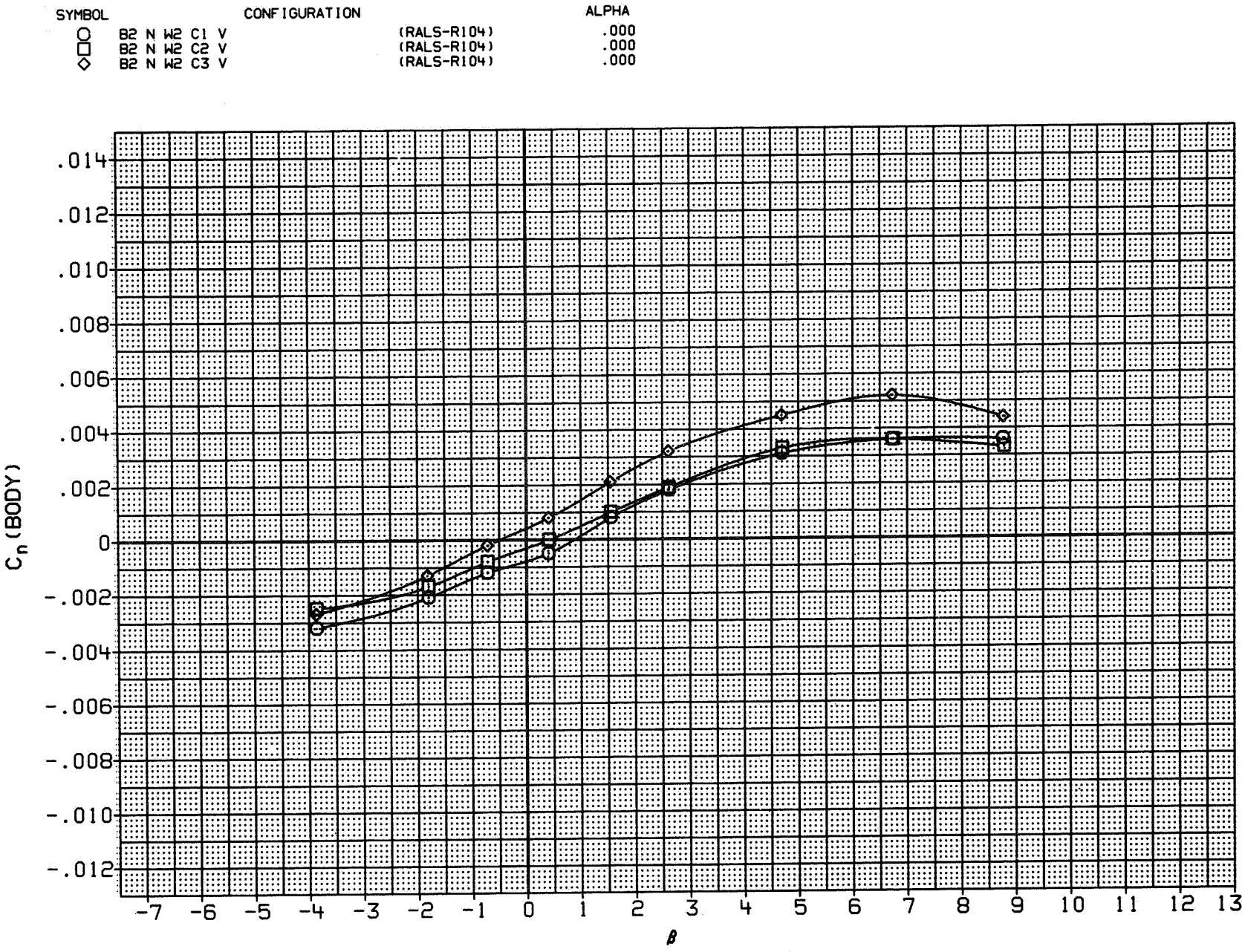


FIG. 73 CANARD LOCATION EFFECTS, LATERAL/DIRECTIONAL CHARACTERISTICS
ALPHA = 0 DEGREES
MACH = 2.00

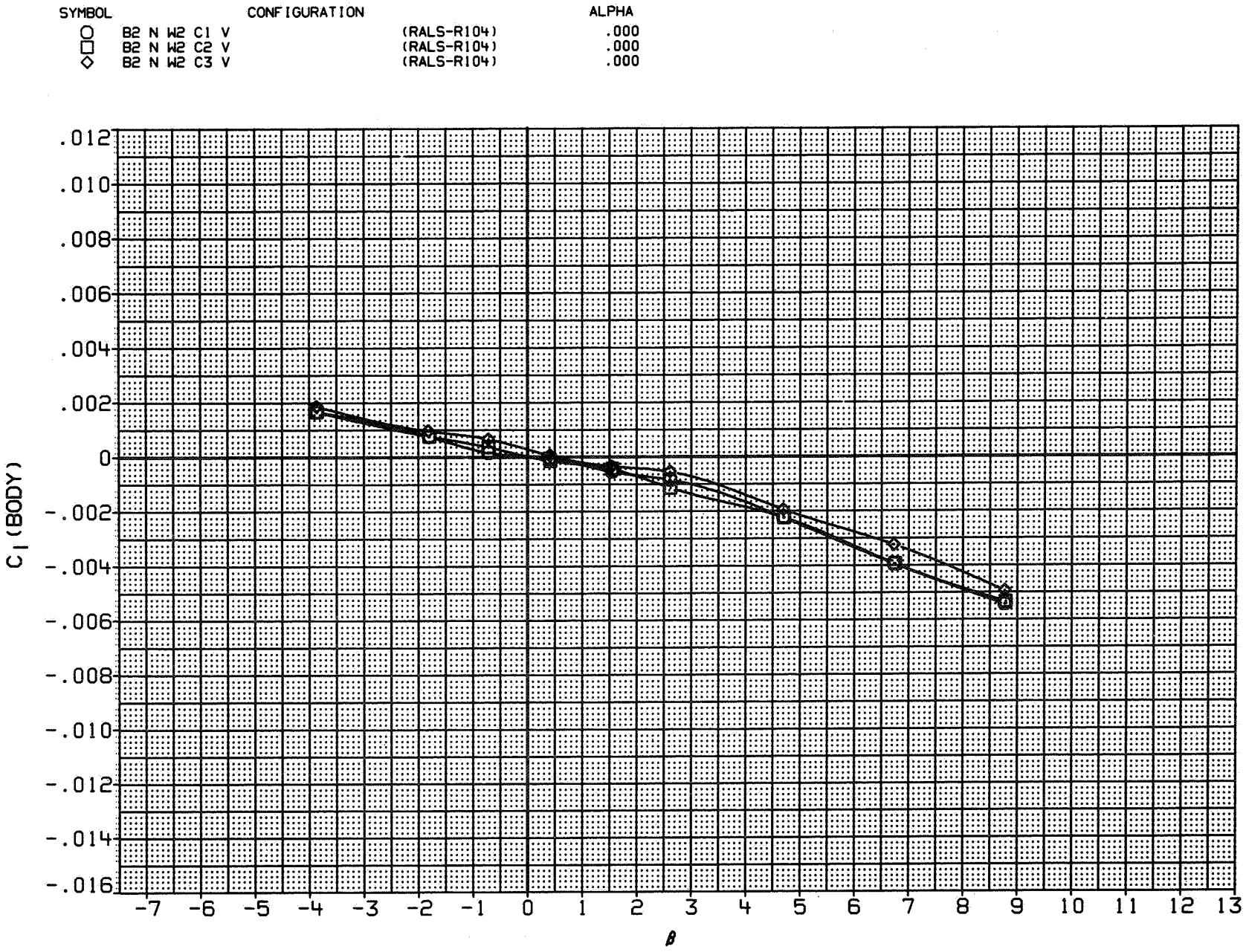


FIG. 73 CANARD LOCATION EFFECTS, LATERAL/DIRECTIONAL CHARACTERISTICS
ALPHA = 0 DEGREES
MACH = 2.00

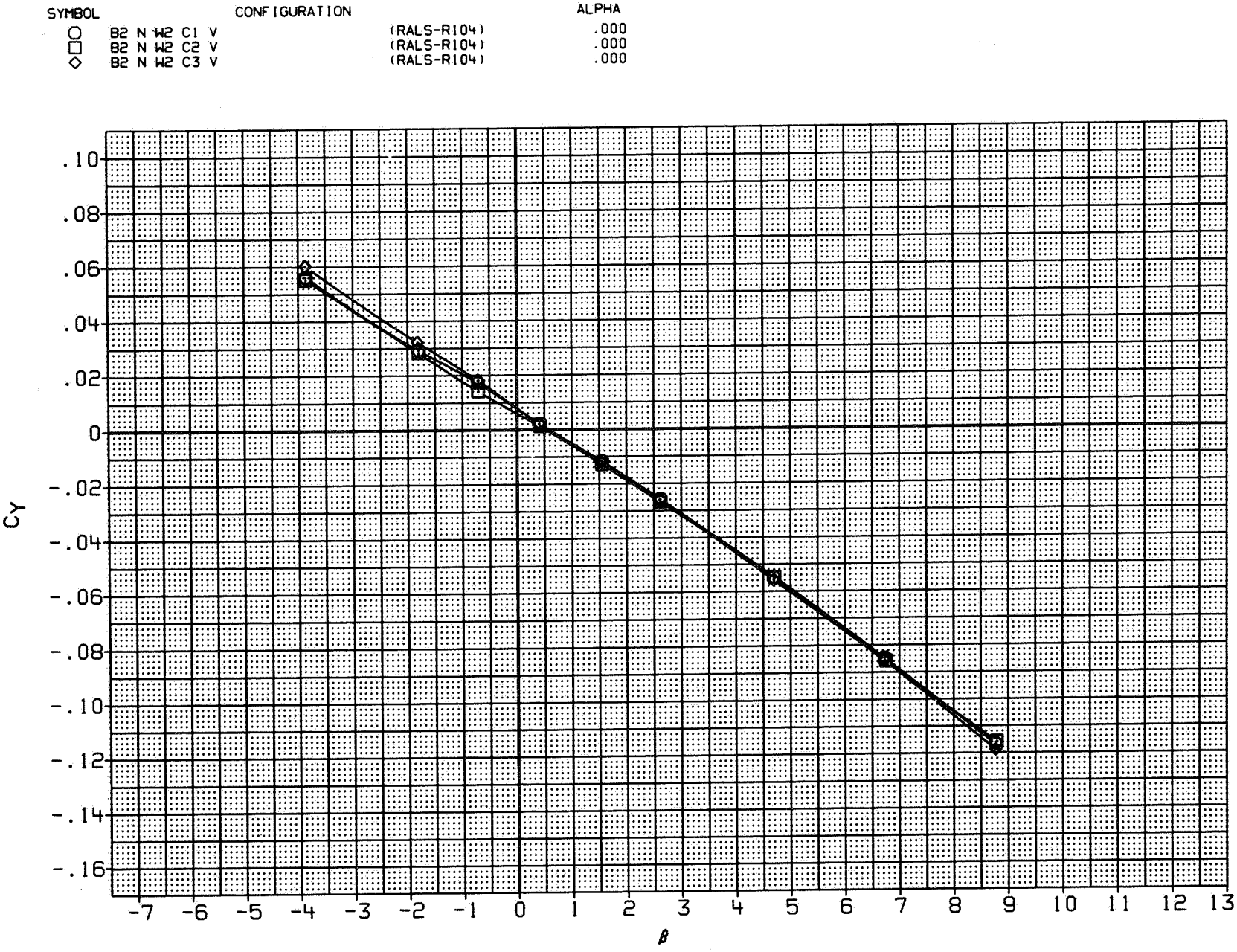


FIG. 73 CANARD LOCATION EFFECTS, LATERAL/DIRECTIONAL CHARACTERISTICS
ALPHA = 0 DEGREES

MACH = 2.00

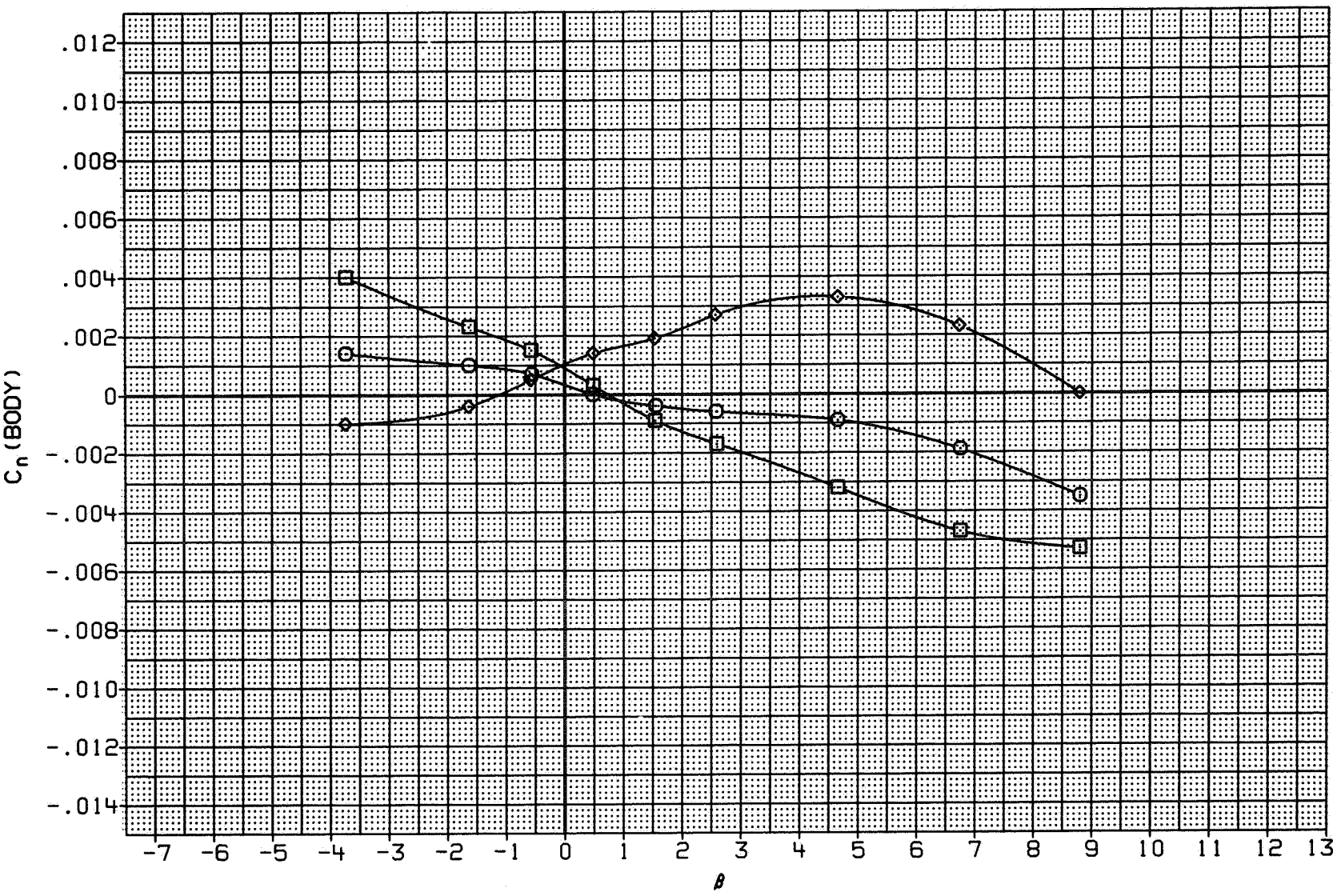


FIG. 74 CANARD LOCATION EFFECTS, LATERAL/DIRECTIONAL CHARACTERISTICS
ALPHA = 8 DEGREES
MACH = 2.00

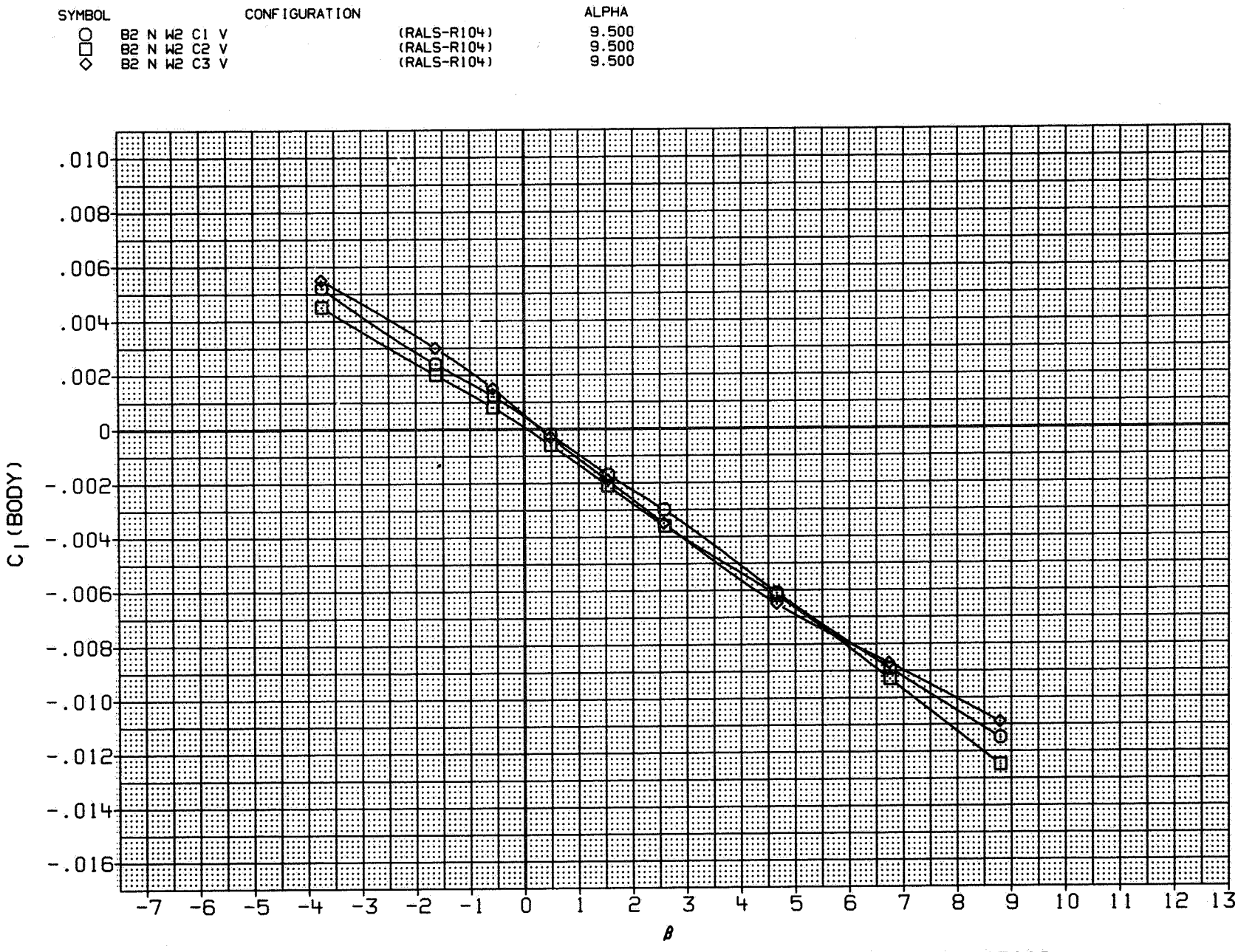


FIG. 74 CANARD LOCATION EFFECTS, LATERAL/DIRECTIONAL CHARACTERISTICS
ALPHA = 8 DEGREES
MACH = 2.00

| SYMBOL | CONFIGURATION | | ALPHA |
|---|---|---|---|
| ○ | B2 N W2 C1 V | (RALS-R104) | 9.500 |
| □ | B2 N W2 C2 V | (RALS-R104) | 9.500 |
| ◇ | B2 N W2 C3 V | (RALS-R104) | 9.500 |

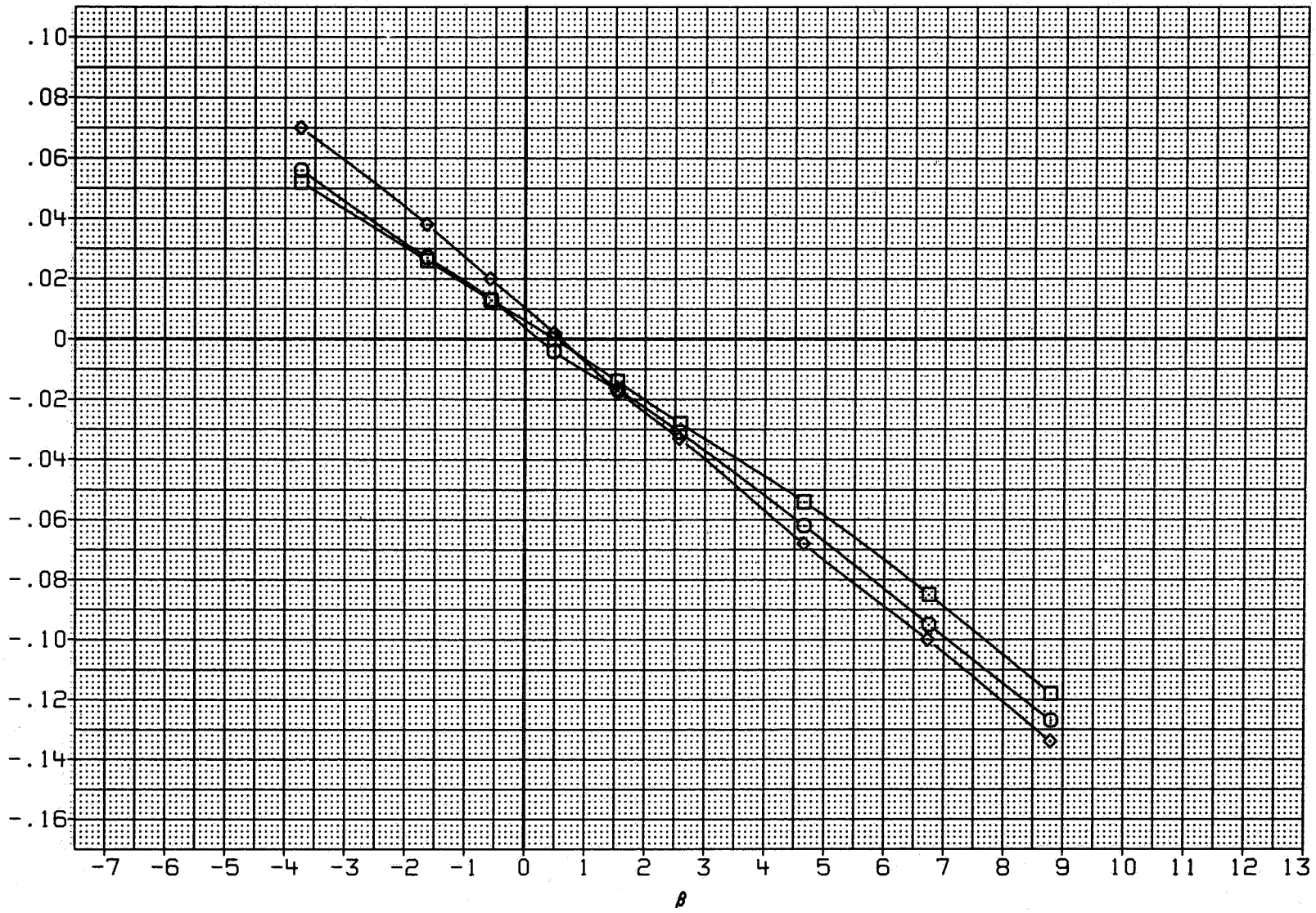


FIG. 74 CANARD LOCATION EFFECTS, LATERAL/DIRECTIONAL CHARACTERISTICS
ALPHA = 8 DEGREES
MACH = 2.00

| 1. Report No. | 2. Government Accession No. | 3. Recipient's Catalog No. |
|---|---|---|
| NASA TM-81286 | | |

| 4. Title and Subtitle | 5. Report Date |
|---|---|
| EXPERIMENTAL AERODYNAMIC CHARACTERISTICS OF TWO V/STOL FIGHTER/ ATTACK AIRCRAFT CONFIGURATIONS AT MACH NUMBERS FROM 1.6 TO 2.0* | May 1981 |
| | 6. Performing Organization Code |

| 7. Author(s) | 8. Performing Organization Report No. |
|---|---|
| Walter P. Nelms,† Donald A. Durston,† and J. R. Lummus‡ | A-8559 |
| | 10. Work Unit No. 505-42-71 |

| 9. Performing Organization Name and Address | 11. Contract or Grant No. |
|---|---|
| †Ames Research Center, NASA, Moffett Field, Calif. 94035 and ‡General Dynamics Corp., Fort Worth Division, Fort Worth, Texas | |

| 12. Sponsoring Agency Name and Address | 13. Type of Report and Period Covered |
|---|---|
| National Aeronautics and Space Administration Washington, D.C. 20546 | Technical Memorandum |
| | 14. Sponsoring Agency Code |

15. Supplementary Notes

*Joint agreement work co-sponsored by David Taylor Naval Ship Research and Development Center. Points of contact: C. Joseph Martin and James H. Nichols.

16. Abstract

A wind-tunnel test was conducted at Ames Research Center to measure the aerodynamic characteristics of two horizontal-attitude takeoff and landing V/STOL fighter/attack aircraft concepts. The concepts were developed by the General Dynamics Corporation, Fort Worth Division, in a contracted study for Ames and the David Taylor Naval Ship Research and Development Center (DTNSRDC). One concept featured a jet diffuser ejector for its vertical-lift system and the other employed a remote augmentation lift system (RALS). Wind-tunnel tests to investigate the aerodynamic uncertainties and to establish a data base for these types of concepts have been conducted at Ames for a Mach number range from 0.2 to 2.0. The present report covers tests conducted in the Ames 9- by 7-Foot Supersonic Wind Tunnel for Mach numbers from 1.6 to 2.0.

Detailed effects of varying the angle of attack (-4 to +17°), angle of sideslip (-4 to +8°), Mach number, and configuration buildup were investigated. In addition, the effects of wing trailing-edge flap deflections, canard incidence, and vertical tail deflections were explored. The effects of varying the canard longitudinal location and shapes of the inboard nacelle-body strakes were also investigated.

| 17. Key Words (Suggested by Author(s)) | 18. Distribution Statement |
|---|---|
| Fighter/attack aircraft<br>Aerodynamic technology<br>Vectored-engine-over-wing (VEO-wing)<br>Remote augmentation lift system (RALS)<br>Propulsive lift; VSTOL; Ejector | Unlimited<br><br>STAR Category — 02 |

| 19. Security Classif. (of this report) | 20. Security Classif. (of this page) | 21. No. of Pages | 22. Price* |
|---|---|---|---|
| Unclassified | Unclassified | 296 | $21.50 |

*For sale by the National Technical Information Service, Springfield, Virginia 22161